NASA Technical Memorandum 108802

Final Reports of the U.S. Experiments Flown on the Soviet Biosatellite Cosmos 2044

Volume I: Mission Description, Experiments K-7-01 – K-7-15

James P. Connolly, Richard E. Grindeland, and Rodney W. Ballard, Editors
Ames Research Center, Moffett Field, California

September 1994

National Aeronautics and
Space Administration

Ames Research Center
Moffett Field, California 94035-1000

PREFACE

On September 15, 1989, the Soviet Union launched Cosmos 2044, an unmanned spacecraft carrying biological and radiation physics experiments from several countries. Those participating included countries from the InterCosmos Council (U.S.S.R., Czechoslovakia, etc.), along with the United States, France, Great Britain, Canada, and the European Space Agency. This mission included 29 U.S./U.S.S.R. joint experiments and involved more than 80 American scientists.

Cosmos 2044 represents the seventh consecutive Soviet biosatellite mission involving U.S./U.S.S.R. joint experiments. Earlier flights included Cosmos 782 in November 1975, Cosmos 936 in August 1977, Cosmos 1129 in September 1979, Cosmos 1514 in December 1983, Cosmos 1667 in July 1985, and Cosmos 1887 in September 1987. These Cosmos Biosatellite missions, involving experiments with monkeys, rats, plants, and insects, have provided scientists with valuable information on how the basic biology of living organisms is affected by the space environment.

The Cosmos 1887 mission had two problems which complicated interpretation of some experiment results. First, a feeder failure within one of the primate capsules on day 5 resulted in reduced food intake by the monkey, requiring termination of the mission at 12.5 days. Second, the biosatellite landed significantly off-course, delaying post-landing processing of the biospecimens by more than 40 hours. For these reasons, Soviet specialists recommended a reflight of the Cosmos 1887 experiments on Cosmos 2044. In addition to these experiments, several new experiments were added for Cosmos 2044, some involving extensive preflight and postflight testing of the flight pool of rhesus monkeys. The Cosmos 2044 mission was conducted according to plan and produced a significant body of scientific and technical results which are described in this report.

Cosmos 2044 was a very successful mission. It was a complex mission, requiring the utmost dedication and cooperation by all participants to achieve this success. Throughout the preparations for this mission, there was a great deal of trust displayed between the Soviet and American teams; the outstanding results of the Cosmos 2044 mission serve as a tribute to this mutual trust.

On behalf of all American participants, I wish to thank the Institute of Biomedical Problems, SKTB Biophyspribor, and the many fine Soviet scientists, engineers and other specialists who supported these joint experiments.

James P. Connolly
Cosmos Project Manager
NASA Ames Research Center

Technical Memorandum 108802 consists of two volumes.

Volume I contains:

- The Mission Description
- U.S. Flight and Ground-Support Hardware
- Rat Studies, Science Reports K-7-01 through K-7-15. (Rat Studies are continued in Volume II).

Volume II contains:

- Rat Studies, Science Reports K-7-16 through K-7-29
- A Comparison of The Physiology of the Spaceflight and the Suspended Rat
- Primate Studies, Science Reports K-7-30 through K-7-35
- Radiation Studies, Science Report K-7-41

TABLE OF CONTENTS—VOLUME 1

TABLE OF CONTENTS—VOLUME 2

LIST OF TABLES

SECTION I

SECTION II

LIST OF FIGURES

SECTION I

SECTION II

SUMMARY

Cosmos 2044 was launched on September 15, 1989, containing radiation dosimetry experiments and a biological payload including two young male rhesus monkeys, ten adult male Wistar rats, insects, amphibians, protozoa, cell cultures, worms, plants and fish.

The biosatellite was launched from the Plesetsk Cosmodrome in the Soviet Union for a mission duration of 14 days, as planned. The major research objectives were:

- Study adaptive response mechanisms of mammals during flight
- Study physiological mechanisms underlying vestibular, motor system and brain function in primates during early and later adaptation phases
- Study the tissue regeneration processes of mammals
- Study the development of single-celled organisms, cell cultures and embryos in microgravity
- Study radiation characteristics during the mission and investigate doses, fluxes and spectra of cosmic radiation for various types of shielding

American and Soviet specialists jointly conducted 29 experiments on this mission including extensive preflight and postflight studies with rhesus monkeys, and tissue processing and cell culturing postflight. Biosamples and data were subsequently transferred to the United States. The U.S. responsibilities for this flight included development of flight and ground-based hardware, the preparation of rat tissue sample procedures, the verification testing of hardware and experiment procedures, and the postflight analysis of biospecimens and data for the joint experiments. The U.S. investigations included four primate experiments, 24 rat experiments, and one radiation dosimetry experiment. Three scientists investigated tissue repair during flight for a subgroup of rats injured preflight by surgical intervention.

A description of the Cosmos 2044 mission is presented in this report including preflight, on-orbit and postflight activities. The flight and ground-based bioinstrumentation which was developed by the U.S. and U.S.S.R. is also described, along with the associated preflight testing of the U.S. hardware. The major hardware components for this mission (Bios systems and major instrumentation systems) were developed by SKTB Biophyspribor in St. Petersburg, Russia. Final Science Reports for each of the U.S./U.S.S.R. joint experiments are also included.

Richard Mains, Gretchen Gold and the staff of Mains Associates expended a great deal of effort on the compilation and organization of materials for this Cosmos 2044 report. Their assistance in the preparation of this document is greatly appreciated.

I. COSMOS 2044 MISSION DESCRIPTION

A. INTRODUCTION

The Cosmos 2044 biosatellite was launched from Plesetsk on September 15, 1989, at 0930 hours Moscow time. Recovery was at 0550 hours on September 29, 1989. Total mission duration was 14 days. More than 80 U.S. investigators were involved in conducting the 29 joint U.S./U.S.S.R. flight experiments. Cosmos 2044 was the seventh consecutive Soviet biosatellite mission to include the participation of U.S. scientists. Table 1 lists all Cosmos missions with joint U.S./U.S.S.R. experiments and summarizes mission parameters for each. Other countries that participated in the Cosmos 2044 mission were Canada, Czechoslovakia, German Democratic Republic, Great Britain, Hungary, France, Poland, and Rumania. The European Space Agency also sponsored some experiments. Table 2 provides a complete listing of the investigations flown aboard Cosmos 2044.

The Cosmos 2044 biosatellite carried two male rhesus monkeys, ten male Specific type Pathogen Free Wistar rats, and an assortment of fish, amphibians, insects, worms, protozoans, cell cultures and plants. Many of the experiments conducted on the Cosmos 2044 mission were repeats of studies carried out on Cosmos 1887. (Difficulties during the recovery of the Cosmos 1887 biosatellite resulted in inconclusive results for many of these experiments.) The U.S./U.S.S.R. joint experiments conducted on Cosmos 2044 included: twenty-four rat experiments (including repeats of Cosmos 1887 experiments and several new or enhanced experiments); one radiation physics experiment; and four primate experiments studying neurovestibular, muscular, circadian rhythm and metabolic responses.

B. MISSION OVERVIEW

V. Korolkov, Ye. A. Ilyin
Institute of Biomedical Problems (IMBP), Moscow

U.S.S.R. EXPERIMENTS

1. Introduction

On September 15, 1989, at 0930 hours Moscow daylight savings time, the Cosmos 2044 biological satellite was launched from the Plesetsk cosmodrome in the Soviet Union. The total duration of the biosatellite's flight was 14 days, the period scheduled to allow completion of the planned scientific program.

The descent module of the Cosmos-2044 biosatellite landed on September 29, 1989, 160 km southwest of the city of Kustanai, Kazakhstan, at 5:30 a.m., Moscow daylight savings time.

The major objectives of the research performed on the biosatellite were:

- to study the mechanisms underlying development of adaptive responses to microgravity at various states of flight;
- to study the physiological mechanism underlying changes in the vestibular and motor systems and in brain function in primates during the early and transitional periods of adaptation to weightlessness;
- to investigate tissue regeneration processes of mammals in weightlessness;
- to study the effects of weightlessness on embryonal development of fish and invertebrates, cellular proliferation processes, and the structure and functioning of one-celled organisms;
- to investigate doses, fluxes, and spectra of cosmic radiation with various types and thickness of shielding.

The biosatellite carried two male rhesus monkeys and ten male Wistar rats, along with insects, amphibians, protozoa, cell cultures, worms, plants and fish. The majority of investigations and experiments were conducted as stipulated by the planned scientific program. It should be noted that the launch of the biosatellite was delayed by one week for technical reasons. This necessitated replacement of virtually all of the biological subjects with new ones.

During the 14-day flight, the biosatellite completed 224 orbits around the Earth. The orbital parameters were: apogee - 294 km; perigee - 216 km; angle of inclination - 82.3°; initial rotation period - 89.3 minutes.

Environmental parameters within the biological module were:

- total barometric pressure: 730-770 mm Hg
- partial O_2 pressure: 140-180 mm Hg
- partial CO_2 pressure: up to 2 mm Hg
- relative humidity: approximately 60%
- ambient temperature during the first 11 days: 23-26.5°C
- ambient temperature during days 12-13: in cabin as high as 29.4°C,in primate capsules as high as 31.4°C due to technical malfunction
- light cycle: 16 hours light, 8 hours dark, illumination level in the Primate-Bios: approximately 60 ± 10 lux during light phase and less than 1 lux during dark phase
- illumination level was 4-8 lux at the rodent cage floor.

In a total of 103 telemetric communication sessions, information was down-linked on a number of primate physiological parameters, the status of several other biological subjects, environmental parameters in the satellite, and also on the functioning of scientific research apparatus and spacecraft hardware.

Scientists from countries participating in the InterCosmos program, and also from the U.S., France, Great Britain, Canada and the European Space Agency, worked with Soviet scientists to achieve the scientific objectives of the flight.

2. Rodent Experiments

Wistar Specific Pathogen Free (SPF) rats were provided by specialists of the Institute of Endocrinology, of the Slovak Academy of Science, Bratislava, Czechoslovakia. The birth date of the animals was May 29, 1989. The animals entered the vivarium of the Institute of Biomedical Problems on July 11 and were maintained on special rations including fresh fruits and vegetables until August 24, after which they were switched to a paste-like diet until the end of the experiment.

Five groups of ten subjects each were studied in the rat experiments:

- a flight group
- a synchronous control group which experienced environmental conditions profiling those on board the satellite
- a vivarium control group
- a basal control group sacrificed on the day of launch
- a group subjected to tail suspension on the ground as a flight simulation model

As stipulated by the experiment design, each group included five untreated animals and five rats that had been surgically treated. In this operation, the skin, lateral head of the gastrocnemius, and the soleus muscles of both hindlimbs were sectioned, and the fibula bones were fractured (wounds were sutured after the operation). No basal control rats were surgically treated.

Surgical intervention took place on September 12 at 1000 - 1100 hours and the rats were placed in the capsule on September 13 at 1500 hours. The flight experiment was completed on September 29 at 0600 hours, and dissection of the rats began at 1100 hours (Moscow time), five hours post-recovery. During the flight, the animals were maintained in a group (10 rats) in a common cage in the "Bios-Vivaria" unit. The paste-like diet, 55 g per rat per day, was made available in four equal portions in the course of a day, at six-hour intervals; access to water was *ad libitum* via a sipping tube. Actual consumption of food averaged 45 g per day.

The synchronous control group, begun on September 20, using five intact and five surgically treated rats (operated upon on September 17), reproduced the maintenance and feeding conditions of flight animals on board the biosatellite, as well as the light-dark cycle and temperature dynamics that occurred throughout the flight. At the start of the experiment, synchronous animals were exposed to the vibration and linear acceleration similar to that occurring during biosatellite lift-off, and at the end of the experiment, to the linear acceleration similar to that occurring on reentry.

The ten rats of the vivarium control group spent the entire period of the study in the vivarium, where they were maintained in a cage similar in size to that in the Bios-Vivaria flight unit. Surgery was performed on five animals of the vivarium control group on September 22. Vivarium animals received the same food ration as the flight group: 55 g per day per rat in the form of a single portion, placed in the cage each morning. Water was provided *ad libitum* . The animals were sacrificed on October 5 at 1100 hours, the same time of day as the rats of the other groups.

Along with the above conditions, a "tail-suspension" simulation was performed on five intact and five surgically treated rats (operated upon on September 21). From September 24 to October 8, these animals were suspended by their tails in a head-down position to remove static loads from the hindlimbs and to simulate fluid redistribution. They were placed in individual transparent stalls and also received 55 g of food in the form of a single portion in the morning and water *ad libitum.*

Animals of the flight, synchronous and vivarium control, and tail-suspension conditions were decapitated at the same time of the day on September 29 and October 4, 6 and 8, 1989, respectively. In addition, on the day the flight experiment began (September 15) ten basal control rats were sacrificed, and muscle and bone samples were prepared for study.

When the flight Bios-Vivaria unit was opened at the recovery site, it was observed that all the rats were alive, active and in satisfactory condition. Their coats were soiled with dried food. By the time of sacrifice, which occurred five hours after landing, the animals became inactive and had reddish chaffing on the tips of their noses (this is thought to be a result of the gravitational stress which developed after transition from weightlessness to Earth's gravity). During dissection it was noted that their blood had thickened, and consequently the total blood volume of the flown rats was smaller than expected. No pathological changes were detected in the flown rats upon dissection.

As compared to vivarium controls, the flown rats showed a smaller body weight gain, lower spleen and thymus weight, a slight increase of the adrenal weigh and no changes in the weight of liver, kidneys or testes. The strength and size of bone callus was lower in treated flight rats compared to all controls except the suspended rats.

Biospecimens from the flight rats, synchronous, vivarium and suspended controls were obtained and shared with co-investigators from Hungary, East Germany, Poland, Rumania, Czechoslovakia, Canada, France and the U.S., in accordance with previous agreements.

3. Primate Experiments

Primate experiments utilized rhesus (*Macaca mulatta*) monkeys, raised in the Institute of Experimental Pathology and Therapy of the U.S.S.R. Academy of Medicine in the city of Sukhumi. The flight candidate group of 16 primates was brought to the Primate Center of the Institute of Biomedical Problems in October-December 1988.

Biosatellite Cosmos-2044 carried two monkeys given the names Zhakonya (#782) and Zabiyaka (#2483). The animals underwent a complete course of preflight training for the experiment, including habituation in a mock-up of the descent module and clinical physiological examinations. The two monkeys chosen had been recommended by a special biomedical primate selection committee for participation in the flight experiment.

Throughout the entire period of preparations for the flight experiment, animal health was kept under clinical/physiological observation. This included a special evaluation of the condition of the skin and pelt; morphometric investigation of the status of the skeletal and muscle systems; observation of changes in body weight; study of parameters of peripheral blood and hemodynamics (heart rate, blood pressure, EKG); and study of biochemical and hormonal parameters of blood, parameters of natural immunity and microbial status of the intestines and body temperature.

The animals' tolerance of +Gz acceleration was investigated by means of a centrifuge to simulate launch and reentry phases. At the same time these observations were being conducted, the animals were trained to perform motor tasks in accordance with special programs. During the final stage of conditioning, the operator performance of each animal was tested in a session lasting several hours after confinement in the Primate-Bios flight capsule for several days.

After completion of general and specialized training, the animals underwent surgery to implant various electrodes and sensors (Table 3).

The final flight candidate primates were selected for the spaceflight experiments in August 1989..The major final selection criteria were clinical state, level of adaptability and training, functioning of the implanted electrodes and sensors, and tolerance of prolonged acceleration (+Gz) and prolonged confinement in a biosatellite mock-up.

Zhakonya and Zabiyaka tolerated the flight well. No deviations of physiological parameters from normal values were noted at any time during the flight. Both animals adapted well to the conditions of a two-week flight, as confirmed by the fact that their mean daily values of body temperature and heart rate were normal and stable.

Zabiyaka's mean daily values of heart rate ranged from 112-141 beats/minute; body temperature ranged from 37.1-38.5°C. Zhakonya's mean daily values of heart rate ranged from 106-121 beats/minute; body temperature ranged from 37.6-37.9°C (Zhakonya's body temperature was analyzed only during the first seven days of flight due to breakdown of the temperature measurement channel). There was no tendency for change in temperature or pulse rate in either animal as flight duration increased, as compared with preflight data.

Inflight food and juice consumption for Zabiyaka and Zhakonya are shown in Figures 1-4. The monkeys consumed an average of 65% of the mean daily amount of paste-like food that had been consumed during the preflight period, which may be associated with a general decrease in energy expenditure in weightlessness. Both monkeys utilized only one quarter of the time period allotted for eating (the first half hour after the food dispenser was made available).

Both animals demonstrated a high level of performance of the behavioral tasks they had been taught, as indexed by level and rate of responding, as well as performance stability throughout the flight.

A specific characteristic of this flight was the low level of behavioral activity displayed by the monkeys during daytime (as compared to the three preceding flights). As a rule, during the intervals between performance of the sequence of operator responses and eating, the monkeys were inactive or slept. They made virtually no attempts to free themselves from the restraint system. Zabiyaka , however, was slightly more active, especially during the second week of flight. On the average, Zabiyaka worked at a higher pace than Zhakonya, but the latter worked in a more regular and meaningful manner, as determined from TV observations. This suggests that Zabiyaka made a greater number of mistakes. From the beginning of flight, Zhakonya showed distinct diurnal (day:night) variations of heart rate and body temperature and a good correlation between heart rate and body temperature changes. Zabiyaka, on the other hand, displayed a correlation between heart rate and body temperature variations only during the second flight week. These differences point to individual variations of adaptive reactions in animals to microgravity.

Their low activity level was evidently due to their particular type of organization of higher nervous activity and was not an indicator of poor adaptation to spaceflight conditions. On the contrary, in conjunction with their good performance of the operator tasks, this phenomenon may serve as an indicator of the animals' high level of conditioning — an optimal behavior pattern given their confinement, while under restraint, in a pressurized cabin. The good duration and rate of performance of the operator sequence (for an average of 10-15 minutes) may also indicate that they were highly motivated by thirst since fluid losses typically occur in microgravity, i.e., performance was reinforced by juice. Under conditions of increased temperature in the cabin on days 12-13 of flight, heart rate and body temperature values remained stable and within the boundaries of

(previous) mean daily values. This also supports the conclusion that the animals' level of adaptation was good.

Data from the telecommunications sessions show a clear temporal pattern in the adaptation of the monkeys to conditions of weightlessness. During the first day of the flight the animals were tense and immobile. Beginning on day two of flight, both animals displayed marked edema of the soft tissues of the face and neck, which persisted through day five. During the fourth and fifth day of flight, head movements were low in amplitude and speed, which are characteristic of the initial stage of adaptation of the vestibular apparatus to conditions of weightlessness. The amount of paste-like diet they consumed was evidently adequate to their physiological requirements related to low energy expenditures. The descent module of the Cosmos-2044 biosatellite landed on September 29, in the scheduled area (160 km southeast of the city of Kustanai, Kazakhstan) at 0550 hours Moscow daylight savings time.

A field laboratory was deployed at the landing site of the descent module. The module was opened and the primate capsules were removed from the descent module and transferred to the field laboratory. After removal of the scientific apparatus from the descent module, the primates were active and responded appropriately to the experimenters. After the primates were extracted from the Primate-Bios, they underwent clinical physiological examinations at the landing site.

Examination of the monkeys immediately after touchdown showed the animals to be in satisfactory condition, active and responsive. No disorders of the musculoskeletal system were observed. Only Zhakonya lost weight overall (200 g). Zabiyaka's body weight was virtually unchanged. The visible mucous membranes were light pink in color.

In accordance with the scientific program, microbiological smears (rinses) were taken of the mucous membranes of the nose and mouth, and of the skin after external examination of the monkeys at the landing site. Blood samples were taken for biochemical studies and to obtain a profile of peripheral blood. Analysis of the hemogram revealed the presence of a stress response pattern and hemoconcentration, as manifest in changes in the quantity of leukocytes and increased value of the hematocrit and hemoglobin. (Table 4).

Twelve hours after landing the monkeys arrived in Moscow. As stipulated by the postflight research program, the monkeys were subjected to experimental procedures directed primarily at study of the mechanisms of development of space motion sickness ("Axon and Amor" joint experiments sponsored by the Institute of Biomedical Problems and NASA) and the function of the psychomotor response apparatus. After physiological testing of the motor apparatus, muscle biopsies were performed to evaluate the structure of changes recorded in the skeletal musculature.

In addition, a wide range of other primate studies were conducted on metabolism, circulation, hematology, attention, and biorhythms.

4. General Biology Experiments

The subjects of the general biology experiments were removed from the descent module and sent to the appropriate investigators within 12 hours of recovery.

- Beetle-2 Experiment

  Darkling beetles *(Trigonoscelis gigas)* eight flight and eight in a control group, were all found to be in good condition and active. The beetles displayed a clear depression in general motor activity in weightlessness, beginning immediately after launch and recovering immediately after landing.

- Chlamydomonas Experiment

  Cultures of *(Chlamydomonas reinhardii)* which were grown on a solid substrate in Petri dishes and secured in the in the aquarium unit, were recovered in good condition and manifested adequate growth. Cultures were fixed postflight. Electron microscopy revealed some changes in distribution of the main cell organelles.

- Bacterial Metabolism Experiment

  E. coli cultures in the Cytos unit were recovered in satisfactory condition overall. Biosamples were processed postflight with the aid of molecular engineering and gene engineering methods. No significant changes were detected in cultures of bacteria infected by K 12 fag. The manifestation of SOS reaction confirmed that prokaryotic cells are not sensitive to microgravity.

- Immunocytos Experiment

  Cultured human T-lymphocytes exposed to weightlessness in the Cytos unit were returned in good condition. Biosamples were shared by U.S.S.R. and French co-investigators for postflight analysis. It was shown, that the synthesis of interleukins in microgravity is surpressed when lymphoid and monocyte cells are artificially activated. Intercellular interactions are not involved in these effects.

- Protoplast Experiment

  Cultures of *Brassika napus* and *Daucus carota* protoplasts were recovered in good condition. Biosamples were shared by U.S.S.R. and ESA co-investigators. Preliminary analysis suggested a tendency for the rate of cell aggregation to be depressed in weightlessness. It appeared that microgravity did not prevent cell wall regeneration. But cell walls grown in spaceflight contained less structural components (cellulose, hemicellulose).

- Drosophila Mutagenesis Experiment

  Fruitflies *(Drosophila melanogaster)* of the Oregon-R strain and the mutant Minute line were recovered in satisfactory condition. The embryological portion of the experiment was completed although a significant portion of the imago died due to liquefaction of the nutrient medium, presumably due to the rise in air temperature at the end of flight. Larvae and eggs were used for postflight studies. A 100% death rate of Oregon-R male fruitflies, due to medium contamination with mold, precluded the gerontological portion of the experiment.

- "Stick Insect" Experiment

  Examination of the eggs of the Indian stick insect *(Carausius morosus Br.)* showed that the biomaterial had been well preserved. The chorion of a small number of the eggs was found by U.S.S.R. specialists to be damaged when biomaterial was prepared in West Germany. The plates containing the eggs were photographed and biomaterial distributed between U.S.S.R. and ESA co-investigators. Results are rather contradictory; they do not support the hypothesis about a detremental effect of microgravity on embryogenesis.

- Worm Regeneration Experiment

  Planaria worms *(Dugesia tugrina)* were cut preflight and regenerated sections were all found to be in good condition. Untreated (intact) worms, maintained for postflight sectioning, died. Annelid (earth) worms *(Lumbricus terrestris)* died possibly due to overheating.

- Ant-Hill Experiment

  Ants*(Formic rufa)* did not survive flight evidently due to the sealing of the container to meet engineering requirements.

- Newt Experiment

  The experiment on caudate amphibia (Spanish tritons - *Pleurodeles waltlii*) is a comprehensive study aimed at investigating: the regenerative process, oogenesis, fluid-electrolyte metabolism, red blood cell structure, and physiological parameters with respect to growth rate. At L - 24 days , forelimbs were removed (at the level of the forearm proximal third) and at L - 13 days the corneas of both eyes were extirpated.

  Flight, synchronous and laboratory control groups included 14 animals each (at the age of two months after metamorphosis with the average weight of 5.7 g and an average length of 10.6 cm). Laboratory controls were kept at ambient temperature.

  Animals were found to be alive and active when container was opened at the recovery site. The moisture-retaining padding remained wet and fluoroplastic membranes clean. The condition of the animals permitted the research program to be completed in full. At R + 0 days, four tritons were dissected and biosamples were fixed for histological study of the cornea, retina, limb regeneration, oogenetic development, red blood cell structure and ultimobranchial gland (a calcium metabolism regulator). Animals from the control groups were treated analogously.

  Ten animals from each group were allowed to survive for three months until limb morphogenesis was complete. Once a week the stage of limb regeneration was identified, the size and weight of the animals and of the regenerating limb were measured. The speed of regeneration in newts was not influenced by spaceflight conditions. No changes in newly-regenerated tissues were detected in space samples compared to control ones. On the other hand, investigation of the ultimobranchial gland revealed its hypertrophy after spaceflight.

- Aquarium-2 and Bokoplav Experiments

  The objective of this experiment was to investigate spaceflight effects on separate biological subjects, as well as on the stability of "fish-*Chlorella*- microorganism" and "*Hyalella-Chlorella*" systems as a whole. The fish-*Chlorella*- microorganism ecosystem was maintained under hermetically-sealed conditions for 18 days, including 14 days at 0 g.

  Postflight analysis showed that algal cells were alive and green. The proportion of cells with a low viability in the population was 3.0%. Cells were of a regular spherical shape with a mean size of 3.7 μm (1.5 times less than laboratory controls). The cells were not granularized but were filled throughout with chromatophore. The cell population consisted of: 3.0% cells with autospore, 36% autospores, and 61% actively photosynthesizing cells. The modal number of autospores forming in each cell was four.

During flight, the algal biomass increased by 0.200 g/l suspension which was close to the value recorded in preflight and control experiments. Preliminary analysis of the environmental parameters (concentration of the basic biogenic elements, pH, total water hardness, concentration of dissolved oxygen, concentration of gaseous oxygen) demonstrated that the algobacterial cenosis that formed during flight supported stabilization of environmental parameters at optimal levels for the fish and algae.

Cultures of *Chlorella* prepared for flight and for ground control were grown in the laboratory following recovery. Cultures were evaluated for the effects of 0 g on the basis of the rate increase in biomass and cell number.

Aquarium data were processed postflight in terms of algal biochemistry, quantity and quality of cell pigments, ultrastructure of algal cells, morphology and biochemistry of fish organs and tissues, bacteriocenosis and constituent species.

The U.S.S.R.-British experiment "AMPHIPOD" yielded data to clarify the effect of microgravity on the biotic and abiotic components of the amphipod-*Chlorella*-microorganism system.

At R + 0 days, the fish *(Poecilia poecilia)* that had been maintained in the aquarium were alive and in good condition on the day of reentry, enabling the research program to be completed fully. Biosamples were obtained and fixed for subsequent study of the effects of microgravity on early stages of embryonic development of fish (histological and electron microscopic examinations of ovaries), structure and metabolism of skeletal muscles, and for the study of the vestibular apparatus, neuron ultrastructure and synapses of the central nervous system.

5. Radiation Dosimetry

The goal of radiation studies was to measure various parameters of cosmic rays inside and outside the biosatellite, as well as temperature variations outside the biosatellite which might influence the measurements. With the aid of a U.S. temperature recorder, it became possible to measure temperature variations in two containers outside the biosatellite for the first time. Temperature was recorded at four sites within each of the two containers where different detectors and bio-objects were located. The temperature range was from -30 ° C to +60 ° C and higher, depending on the orientation of containers towards the Sun.

6. Radiation Biology Experiments

The purpose of these studies was to accumulate data concerning the combined effect of cosmic radiation and sunlight (including UV radiation).

The objectives were as follows:

- to evaluate the biological effects of the sunlight with different spectral parameters in outer space;
- to assess the effect of heavy ions on bio-objects shielded by foils of different thicknesses;
- to obtain data describing the absorbed dose and fluence of heavy ions, U.S.-radiation and sunlight spectral characteristics and temperature variations.

The following bio-objects were used in the experiment: *Lactuca sativa* seeds, *Crepis capillaris* seeds, dry nucleotides, and dry uracyl films. Dry nucleotides were employed to investigate potential abiogenic synthesis of nucleic acid components under the influence of various energy sources. Dry uracyl films were used to measure UV-radiation outside the biosatellite.

The goal of the Biodose experiment was to measure integrated doses of cosmic radiation in seeds as a function of the shielding thickness. One mm thick thermoluminescent detectors were used and seeds were located behind screens of 0.00114 and 0.026 g/cm^2 thickness.

The goal of the Dosicos experiment was to study the effect of single heavy ions on seeds located behind varying thicknesses. In this experiment, a biostack consisting of three layers of bio-objects and physical detectors as well as two plates with seeds outside the biostack were used.

Dielectric tracking detectors (DTD) which simultaneously served as seed holders were applied to measure heavy ion fluence and to detect seeds hit with single ions.

The goal of the Seeds experiment was to study the combined effect of cosmic radiation and microgravity on *Arabidopsis* seeds. The experiment will help assess the effect of heavy ions and microgravity on the status of meristematic initial cells in the dormant germs of *Arabidopsis* seeds, on the initiation of tumors, and on the genetic lesions in the seed genotypes.

C. U.S.S.R. HARDWARE SUPPORT OF EXPERIMENTS

V. K. Golov, V. S. Magedov, V. I. Korolkov
IMBP, Moscow

The Cosmos 2044 biosatellite was traditional in design and consisted of three modules: a descent module, an equipment module, and a pressurized module with auxiliary chemical energy sources.

The descent module was the most complex autonomous module. Approximately 2 m in diameter, the spherically shaped body was made of aluminum alloy and treated with a thermal protective coating. The scientific equipment and auxiliary systems rest inside, with the most accessible areas reserved for instruments and modules containing animals and other biological subjects.

The equipment module contained systems for measuring spacecraft orbital parameters, automated control of the apparatus, and radio devices for transmitting commands from Earth. This same module also contained the radiotelemetric system, which allowed transmission of information concerning the status of major satellite systems, as well as data on the functioning of scientific apparatus and operational parameters from monitoring the condition of biological subjects.

The scientific research apparatus included devices to maintain appropriate living conditions for the two primates, ten rats, and other biological subjects, and instruments for collecting, recording, and preliminary processing of physiological information.

One of the most complex pieces of scientific apparatus was the "Primate-Bios," designed to maintain requisite conditions for maintenance and experimentation on the monkeys. It included the capsule in which the animals were housed, the life support system, and apparatus for testing the animals and recording physiological data.

In the capsule, the monkeys were restrained in special chairs with contoured backs and an impact attenuation layer of polyurethane. The animals' position and location within the pressurized module were selected to minimize adverse effects of preflight technological operations and dynamic factors associated with entry into orbit.

The primates were fed a paste-like diet delivered by a pump into the food dispenser twice a day. The maximum portion of food delivered to this dispenser at any one time was 250 grams.

An analogous system was used to provide the animals with juice. The sole difference was that the delivery system was turned off when the animal performed the learned test responses incorrectly. The animals could also be provided with juice even when they were not performing their "operator tasks." The major purpose of this design feature was to allow juice to be delivered immediately before descent.

Removal of animal waste, food fragments, bits of hair, etc. was accomplished through continuous purging of the capsule with air at a rate of no less than 200 l/min. There was a ventilation duct for this purpose in the lower portion of the chair base connected to a waste collector. The ventilation system was equipped with a filter that absorbed harmful trace contaminants and purified the air of bacterial contamination. An auxiliary hot air heater, controlled by the "Thermal Comfort" device developed by the Department of Biophysics of the Czechoslovakian Academy of Sciences supported optimal environmental conditions within the Primate-Bios capsule.

The upper hatch of the capsule contained overhead lamps that provided an illumination level of 60 ± 10 lux during the "day" and 2 ± 1 lux at "night" at the level of the monkeys' heads. During the "day" portion of the light-dark cycle, this illumination enabled television observation of the state and behavior of the animals.

The system for recording physiological information and controlling the experiment included:

- implanted sensors for sensing physiological parameters
- apparatus for transforming and enhancing physiological signals
- on-board apparatus for recording information on magnetic tape
- systems supporting local and joint control of the scientific apparatus

Apparatus for sensing, transforming, and recording physiological information of the primates included:

- blocks for preamplification of electrophysiological signals
- a biotelemetric system for measuring body temperature using an implanted temperature sensor
- an apparatus for amplifying and transforming signals obtained from mechanographic sensors of head movements, oxygen tension in brain tissue, etc
- the post amplifier and commutation blocks supporting output of recorded signals on onboard magnetic tape recorders

All the data obtained from the information measurement system of the scientific apparatus were recorded on low-frequency (Topol'-DR) and high-frequency (SKAT-3) recorders. Operational information on the conditions of the animals and basic data on maintenance conditions (body temperature, heart rate, juice and food consumption, environmental parameters) were telemetered to Earth. A schematic of the data flow is shown in Figure 5.

Equipment for Cosmos 2044 was developed using information about problems and characteristics of the functioning of individual systems from the Cosmos 1887 flight. This was especially important with regard to the primate life support system. A new dispenser nozzle design was used to deliver juice and food. Membrane sensors were eliminated, since their unreliability had created an emergency with regard to the feeding of one of the monkeys on Cosmos 1887. Improvements were also introduced in the animal restraint systems to prevent the animals' upper limbs from being freed.

A set of training equipment was developed for teaching the monkeys the program of instrumental responses and conducting pre- and postflight studies.

This equipment set included:

- self-contained trainers for initial teaching of animals controlled by an "Elektronika BK 0010" or "Algorithm" computer
- a training system for final animal instruction in simulated flight conditions, controlled by a personal computer

An integral part of the biosatellite experimental program was the performance of preflight multifactor biotechnical tests. The performance of all scientific apparatus was checked preflight; the possibility of unintended interactions among individual systems was assessed; and the major atmospheric parameter dynamics in the pressurized module were measured.

The preflight biotechnical tests in the satellite mock-up were also used to evaluate the status of the animals in the flight group and to generate baseline physiological information essential for selecting the primates for flight.

The Bios-Vivaria was developed for spaceflight experiments with small laboratory animals (rats) and has been used on biosatellite experiments starting with Cosmos 1514.

The Bios-Vivaria provides group maintenance of up to ten animals weighing up to 350 grams apiece. The unit is equipped with systems for dispensing a paste-like diet and water, and a device for storing and removing waste products.

The food supply can support an experiment up to 25 days long with food consumption of up to 55 grams per animal per day. On Cosmos 2044, the diet was dispensed in response to an external command four times a day (any delivery schedule can be utilized as needed).

Overhead lamps were installed in the vicinity of the food dispenser; during the "day" portion of the light-dark cycle, illumination was 4 lux.

Waste was removed through continuous purging of the animal module with air at a rate of 200-250 l/min. The waste collector was filled with moisture-absorbing material. Before recirculating into the Bios environment, the air stream was purified of bacterial and harmful gaseous contaminants using special filters.

To implement scientific experiments on cellular and gravitational biology inflight, the biosatellite was equipped with special enclosures to support different small species. This included the Triton (amphibians), Akvarium (fish), and Zhuk,(beetles) enclosures. The "Cytos-4", made in France for the study of cells, was also on board. In addition, there were several small passive containers with a combined volume of 13 cm^3. One of the containers was installed six hours preflight, while the biosatellite was on the launch pad.

The animals were supplied with oxygen and the atmosphere cleansed of carbon dioxide and harmful gaseous contaminants, using traditional methods based on systems with chemically-bound oxygen (in the form of superoxides of alkali metals) and absorbent filters with activated charcoal. For Cosmos 2044 experiments, filter capacity was increased through the addition of a catalytic layer. In addition, measures were taken to increase the capacity of the bacterial contamination filters.

Temperature and humidity conditions in the pressurized module were supported by a system that regulated air temperature by means of a gas-liquid, heat-exchange dehumidifier.

After the flight program was completed, the satellite was prepared for return to Earth. At 04:00 Moscow time, "day" illumination was turned on in the animal cages, and the primates were provided with 40 ml of juice (approximately 1 hour 40 minutes before landing).

The operational-technical group was air-lifted to the landing site, where they set up the equipment for the field laboratory.

The hatch of the spacecraft descent module was opened 35 minutes after landing. A large group of physiologists, biologists, and other specialists then began their work in accordance with the protocol.

A postflight control (synchronous) experiment was conducted on the ground in a full-scale mock-up of the descent module. The major goal of this postflight experiment was to obtain scientific data under conditions simulating all characteristics (except weightlessness) of actual spaceflight. The preflight data and the actual schedule of examinations of biological subjects at the landing site were also taken into account.

Conditions, under which the flight experiment on Cosmos 2044 was performed, were duplicated, with the exception of air temperature in the pressurized module. However, temperature dynamics were fully simulated in synchronous condition, with an accuracy no worse than ±1°C.

The experiment on Cosmos 2044 confirmed the appropriateness of the design decisions made in developing the scientific apparatus, which fully supported the research program. The experience gained will be extremely helpful in designing equipment for future biological experiments.

D. HABITATION CONDITIONS IN THE PRESSURIZED MODULE OF THE BIOSATELLITE

N.N. Lizko, L.N. Petrova, A.K. Burets, I.N. Kornyushenkova, K.D. Rokhlenko, T.I. Kuznetsova, V.P. Savina, V.I. Korolkov, V.K. Golov
IMBP, Moscow

In order to ensure the success of the biosatellite experiments, it was essential that wholesome environmental conditions be maintained for the animals.

One of the most significant parameters influencing the biosatellite environment is dust level, which is determined by the initial state of the spacecraft and the efficiency of its cleansing system. Dust levels were studied in pre- and postflight animal experiments in the ground-based mock-up of Cosmos 2044. These studies involved measurement of the concentration of dust by weight and its dispersion.

Previous data showed that the highest concentration of dust observed in the Cosmos 1887 biosatellite (up to 14 mg/m^3) was associated not only with high initial dust concentration, but also with additional assembly work performed during the course of the experiment.. For this reason, special recommendations were developed to maintain cleanliness within the biosatellite. Thus, the efficiency of the dust filters in the Cosmos 2044 mock-up was increased through the use of "Vion" type chemosorption materials, which reduced dust level to 0.3-0.4 mg/m^3. The results obtained confirmed that initial cleanliness of the interior and equipment, and an effective system of atmospheric purification play a decisive role in creating a clean spacecraft atmosphere.

In addition to studies of the dust level in the biosatellite mock-up, gas chromatography studies were performed to assess the sanitary and chemical conditions of the mock-up atmosphere. Samples were obtained at two points: immediately after emergence from the air purification systems; and in the center of the mock-up interior. The results showed that the atmosphere in the

biosatellite mock-up throughout the pre- and postflight experiments was satisfactory. Traces of methanol and acetone were recorded.

Oher necessary prerequisites for maintaining optimal living conditions for the animals are adequate sanitary and microbiological conditions inside the module. Thus, microbiological studies were conducted to monitor bacterial contamination of interior surfaces of the biosatellite and the interiors of Primate-Bios #1 and #2, and the Bios-Vivaria capsules, pre- and postflight. For surface samples, a section of the surface was wiped with a sterile cotton-gauze pad moistened with sterile normal saline. Next, the pad was placed in a beaker with 2 ml sterile normal saline and shaken well for five minutes; then a 0.1ml aliquot was used to seed a nutritive medium.

As a result of the microbiological studies performed during the postflight period, the following observations were made:

- compared to baseline, the overall microbial contamination of monitored surfaces of the biosatellite decreased by an order of magnitude by the end of the study
- the total microbial contamination of the interior and equipment surfaces of Primate-BIOS #1 increased by four orders of magnitude compared to the baseline, with a marked predominance of gram-negative microflora over gram-positive
- the total microbial contamination of the interior and equipment surfaces of Primate-BIOS #2 increased by four orders of magnitude compared to baseline. The ratio of the quantity of gram-positive to gram-negative microorganisms did not change on the surfaces studied
- the total microbial contamination of the interior of the BIOS-Vivaria capsule increased by two orders of magnitude compared to baseline. The ratio of gram-positive to gram-negative microorganisms on these surfaces also did not change

Analogous results were obtained when the surfaces of the biosatellite mock-up were studied in the control condition. Thus, the results of the sanitary and hygienic studies of the living environment obtained during biomedical ground-based experiments in the mock-up, indicate changes in certain sanitary/chemical and microbiological parameters.

Slight traces of methanol and acetone were observed, and there was an increase in the overall level of microbial contamination (attributable to gram-negative bacteria) on the interior and equipment surfaces.

It may be hypothesized that such shifts in the automicroflora may be induced by intensified emission of microorganisms into the environment from the skin and mucous membranes of the animal subjects' respiratory tracts.

E. PREPARING THE PRIMATES FOR SPACE FLIGHT

V.I. Korolkov, B.A. Lapin, A.N. Truzhennikov, T.G. Urmancheyeva, A.N. Nazin
IMBP, Moscow

By the time preparations for experiments on Cosmos 2044 began, significant experience had been gained in studying the acute period of adaptation to weightlessness in primates. Three experiments previously performed on six primates in studies aboard Cosmos 1514, Cosmos 1667, and Cosmos 1887 confirmed the basic principles used in selecting and preparing primates. The goals of these experiments required that the primates be trained to perform two sets of instrumental responses (hand and foot). Preparation of primates for such a flight experiment takes a mean time of 1.5-2.0 years.

When candidates were selected for the experiments, the most important considerations were the morphometric characteristics of the primates, their capacity for instrumental conditioning and their clinical state.

The first stage of this work was performed at the Institute of Experimental Pathology and Therapy of the U.S.S.R. Academy of Medicine at Sukhumi, where 45 candidates were selected from a group of animals (65-70 individuals), 1.4-2 years of age, on the basis of their state of health and capacity for instrumental conditioning. At this stage the tails of the selected animals were surgically removed. Work was then begun to familiarize them with the primate chairs and to develop instrumental-conditioned responses on training simulators.

Simultaneously, a set of tests was performed to identify tuberculosis carriers, pathogenic and opportunistic intestinal entero-bacteria, and the presence of helminths. The clinical/physiological parameters of the major functional systems of the animals were evaluated. Based on these data, sick animals were eliminated, and suspicious cases were treated and followed up 2-3 times. All animals were treated to eliminate helminths. These measures allowed preparation of a group of 25 primates for the main experiment.

The first group of ten primates entered the primate center of the Institute of Biomedical Problems, U.S.S.R. Ministry of Health, in October 1988. The second group of animals arrived in December 1988. After the primates' arrival at the Institute, their clinical/physiological condition was studied in greater depth. These studies included observation of the state of the animals' health including the following parameters: special evaluation of the skin and coat; status of the musculoskeletal system using morphometry; tracking of body weight dynamics; study of parameters of peripheral blood and hemodynamics (heart rate, blood pressure, EKG); biochemical and hormonal parameters of blood (activity of serum enzymes, hormones, and blood components); homeostasis of the intestine; and body temperature. Meanwhile, the animals were acclimated to confinement in the standard system of constraints (primate chair, contoured base, standard chair, and, ultimately, the Primate-Bios capsule).

One of the selection criteria for the flight group was the animals' tolerance of linear acceleration similar to that occurring during the powered phases of spaceflight. For this reason, from December 1988 to May 1989 studies were performed on the primates' tolerance of peak +Gz acceleration. Based on these studies, the primates were rank-ordered. The degree of linear acceleration tolerance was considered when the primary candidates for the flight group were selected.

Research was performed to evaluate the feeding activity of the animals using a specially developed methodology. The data from these studies were also used in selection. Primates were concurrently acclimated to the special flight diet.

As indicated above, the major parameters of peripheral blood (cellular composition, activity of serum enzymes, hormones and individual components), state of natural immunity and microbiological homeostasis of the intestine were tracked. These data were compared with data from clinical observations of the animals and used to make decisions about the use of complex prophylactic measures.

During the preflight period, the primates' parameters of serum enzymes and protein-carbohydrate metabolism were within the limits of the norm for animals of the appropriate age group. During this period, the microbial status of the intestine did not deviate significantly from the norm.

At the same time, responses were being established within the program of operator performance. These tasks were performed continually throughout the entire period, until the flight and ground-based conditions of the main experiment began. At the final stage, each animal had acquired many hours of experience performing the responses under conditions of multi-day exposure to the Primate-Bios and biosatellite mock-up.

After completion of general and specialized training, the animals were operated on to implant various electrodes and sensors in accordance with the goals for research on Cosmos 2044 (Table

3). Surgical preparation took place in three stages. During the first stage, a framework was mounted on the head for attaching the electrodes and other hardware. In the second stage, cannulae were installed for insertion of NG, ECoG (e.g., EEG), and pO_2 electrodes. Electrodes for EOG, EMG (neck and calf), and EKG, and a body temperature sensor were implanted. During the third stage, two microminiature wire loops were implanted around the eyeball for recording horizontal and vertical position of the eye. A stereotaxic frame was attached to the skull to record activity of vestibular nerve fibers. Wires were run from peripheral electrodes.

The major criteria for the final selection of primates for the Cosmos 2044 experiment were: clinical state of the animals; level of adaptability and training; performance of the implanted sensors and electrodes; and tolerance of long-term exposure to +Gz acceleration and long-term confinement in the biosatellite mock-up.

Basic information about Zhakonya and Zabiyaka, the monkeys flown on Cosmos 2044, is presented in Tables 3 and 4. According to typological characteristics of the data, these animals belonged to the subdominant type, and showed good adaptive capacities and good appetite. Implanted electrodes functioned well and the animals were judged to be clinically healthy.

The program of pre- and postflight clinical examinations was an important element in preparations for and performance of research on the biosatellite. These examinations included:

- neurophysiological studies (testing gaze-fixation reactions)
- study of metabolism (metabolic studies)
- study of gas and energy metabolism
- study of body hydration status of the primates, blood circulation, and cellular composition of bone marrow
- study of biochemical parameters in blood

From June 30 to July 20, three comprehensive biotechnology experiments were conducted in the biosatellite mock-up. The first experiment lasted 14 days, while the second and third lasted three days each. The first experiment used the entire set of equipment, and experiments two and three used only the equipment necessary to support research on the primates.

The experiments performed in the biosatellite mock-up were used to evaluate the function of the the scientific apparatus, obtain baseline data and acclimate the animals to confinement under simulated spaceflight conditions (excluding acceleration and weightlessness).

After completion of clinical physiological examinations, 14 days before the flight, the six best animals were delivered to the launch site. There metabolic studies were performed, special training continued, and the position of the neurographic electrodes in brain structures adjusted.

F. U.S. MISSION MANAGEMENT

U.S. EXPERIMENTS

The joint U.S./U.S.S.R. experiments conducted aboard Cosmos 2044 included four experiments using primates, 24 experiments using rats, and one radiation dosimetry experiment. The primate subjects were rhesus monkeys (*Macaca mulatta*), rats were specific pathogen-free males of Wistar origin (*Rattus norvigicuc*), all provided by the Institute of Biomedical Problems, Moscow.

1. Primate Experiments

The experiments were designed to study physiological responses to microgravity in primates. The specific objectives of the experiments were to study: the effect of microgravity on the

neurovestibular system; electromyographic activity and its relationship to the maintenance of muscle structure and function; the adaptation of optokinetic responses to microgravity; and the functioning of circadian rhythm and thermoregulatory systems. Specific objectives were to:

- Test vestibular primary afferents to obtain information about the dynamic response properties of the horizontal semicircular canals after exposure to microgravity
- Study vestibular ocular reflexes before and after 14 days of spaceflight
- Determine the effect of the absence of weight support on flexor and extensor muscles of the hindlimb. A second objective was to determine the relative importance of activity and force in the adaption of muscle
- Study the circadian rhythms and body temperature regulation systems during exposure to spaceflight and after some postflight readaptation
- Assess doubly-labeled water as a method for determing metabolic rates inflight

2. Rodent Experiments

A main goal of the 24 rodent experiments was to extend studies done on Cosmos 1887 with a shorter post-recovery biospecimen processing time. Sample analysis methodologies from Cosmos 1887 were duplicated so that comparability of results could be maximized. Of the 24 joint U.S./U.S.S.R. rodent experiments conducted, 21 were repeats of those carried out on the Cosmos 1887 mission. These included cell biology and endocrinology experiments, as well as various studies of the morphology, physiology and biochemistry of bone, muscle and organs. One new experiment was designed to study tissue repair in space. The experiment required minor surgical treatment of the rats preflight, to study the healing that occurred primarily during spaceflight.

3. Radiation Dosimetry and Spectrometry Experiment

The objective of this experiment was to study high and low energy neutrons, various flux and energy spectra and the attenuation of space radiation as a function of shielding provided by the spacecraft. Radiation measurements were obtained using passive detectors. Inflight temperature recordings were made for the first time, for radiation dosimeters on the outside of the biosatellite, using two 4-channel portable temperature recorders built by the U.S.

SPACECRAFT DESCRIPTION

The Cosmos 2044 mission was flown aboard a modified Vostok spacecraft, of a design used for previous Cosmos biosatellite flights. The spherical craft, with a diameter of approximately 2.5 meters, had a gross weight of approximately 2250 kg and a 900-kg payload (Figure 6). Spacecraft power was supplied by on-board batteries. A summary of the environmental conditions within the spacecraft during the flight are included in Section B, above. The Soviet animal life support systems (Bios) critical for the U.S. experiments are described below.

1. Primate-Bios

Each Soviet Primate-Bios capsule (Figure 7) included life support and experiment systems. Each monkey was seated in a primate restraint couch equipped with upper and lower arm restraint straps, and a lap-restraint plate with a leg separator, as shown in Figure 8. A waste collection system used unidirectional airflow to direct excreta toward a receptacle underneath the chair. The degree of thoracic restraint could be varied by ground command. The primate chair was designed to provide adequate support to the monkey during the shock experienced on impact with the Earth, following parachute descent. The Primate-Bios also contained separate dispensers for a water/juice mixture and a paste diet which were primate-activated by bite-switches located on the spouts. The dispensers for diet and juice were designed so that presentation of these could be controlled via an uplinked signal from the ground. The orientation of the two primate capsules in the spacecraft

enabled the monkeys to view each other. A television camera mounted in each BIOS allowed inflight video monitoring of the subjects from the ground.

The Primate-Bios capsule was equipped with a Psychomotor Response System as seen in Figure 9. Vestibular measurements were obtained with a light display and an arm response lever; the animal was trained to look at a particular symbol on the display screen, which helped to determine the animal's head position at a particular time. A motorized device attached to the restraint couch provided further vestibular stimulation by elevating the restraint couch, followed by a spring return to its original position. A leg response lever, shown in Figure 8, was used in conjunction with the Psychomotor Response System to obtain limb muscle measurements.

2. Bios-Vivaria (Rodent-Bios)

The ten male rats were housed in a common cage termed the Bios-Vivaria unit. The Bios was equipped with ten nozzles for delivery of a paste diet and ten nozzles for dispensing water. The atmospheric pressure in the cage was 760 mm, the humidity averaged 58%, and the ambient temperature was 22-23°C. On days 12-13, ambient temperature rose as high as 29.4°C due to a technical malfunction. Lights were on from 0800-2400 and off from 2400-0800 hours for a 16:8 light/dark cycle. Light intensity was about 4 lux at the cage floor. An incandescent lamp was placed over each of the ten feeders.

MISSION MANAGEMENT PLAN

The U.S. responsibilities for experiments on the mission were: 1) development of flight and ground-based hardware; 2) completion of flight hardware and experiment verification tests; 3) development, along with Soviet specialists, of procedures and techniques for the collection and preservation of rat tissues; and 4) the postflight transfer of tissues and data to the U.S. for analysis.

1. Hardware Development

The hardware development process and testing of U.S. flight and ground-support hardware for the mission is described in detail in Part II of this document. Flight hardware supplied by the U.S. included two 4-channel temperature recorders for the radiation dosimetry experiment and hardware to support the Circadian Rhythm/Temperature Regulation (CR/T) experiment. Ground-support hardware for the primate experiments and for the shipment of biosamples were also developed by the U.S.

2. Training

Soviet specialists were trained in the use of U.S. flight hardware and associated ground-support hardware. The U.S. investigator for the CR/T experiment and his technical support staff provided training for the attachment of skin temperature sensors and for the postflight downloading of flight data. In addition, Soviet specialists were shown the U.S. muscle biopsy methods for primates and detailed tissue-processing procedures were provided for U.S. rat experiments.

3. Hardware and Experiment Verification Tests

Biotransporters, designed for postflight tissue preservation and shipment to the U.S., were developed and tested at NASA Ames Research Center (ARC). The temperature recorders were tested to ensure that they were operable in a vacuum and in extreme temperatures. Numerous engineering tests were conducted on the CR/T system to confirm its performance to specifications. The CR/T hardware was also tested at ARC with monkeys restrained for the flight duration. The

temperature recorders and CR/T hardware underwent environmental testing to confirm their fabrication to strict spacecraft standards.

4. Data/ Specimen/ Hardware Transfer for Postflight Analysis

CR/T and temperature recorder data stored in solid state memory were transferred to computer disks and printed out. Postflight tissue transfers were carried out in biotransporters. U.S. flight hardware and a large quantity of ground support equipment were shipped to Moscow to support preflight, inflight, and postflight studies.

5. Documentation

The essential information required for conducting each experiment was provided in an Experiment Management Plan (EMP) document. Each EMP included: 1) a listing of the joint investigators (U.S./U.S.S.R.) and their general responsibilities; 2) a description of the experiment objectives; 3) the protocols for the flight and control experiments; 4) the experiment verification tests; 5) the procedures for specimen collection and labelling; 6) the procedures for animal preparation/tests; 7) the log sheets for experimental data; 8) the requirements/procedures for data transfer and analysis; and 9) an equipment list with specifications and procedures for operation.

In order to coordinate science reporting by both countries, the U.S. investigators agreed to submit postflight science reports to the Soviets prior to submitting manuscripts to science journals for publication. Preliminary Science Reports were submitted to the Soviets six months postflight and Final Science Reports were submitted 13 months postflight and are included in Section III of this report.

G. MISSION OPERATIONS

GENERAL MISSION DESIGN FOR RAT EXPERIMENTS

The overall Soviet design for Cosmos 2044 rat experiments was similar to earlier missions. The rat experiments included basal, synchronous, and vivarium ground control groups. A new feature of the rodent experiments on Cosmos 2044 was a tail-suspension ground control group, in which rats were suspended by their tails in a head-down position for the flight duration (see Morey, E.R.: Spaceflight and bone turnover: Correlation with a new rat model of weightlessness. *Bioscience*. 29, 1979, pp. 168-172). A photo of the system used for the tail-suspension group is shown in Figure 10. Table 5 summarizes pertinent information for flight and control groups. A general description of the primate experiments is provided in Section B, Part I, as well as in the preflight, on-orbit, and postflight sections below.

1. Basal control group

The basal control group provided tissue specimens from which preflight control data could be obtained. This group was sacrificed on the day of launch. Diet, temperature, humidity and lighting for this group were kept consistent with conditions expected inflight.

2. Vivarium control group

The rodents in this group were caged in standard laboratory cages under standard conditions. They were given the same quantity of food per day as the flight group, but the food was provided in a single portion. This group assured that the rats were healthy and well-nourished to allow comparison with animals maintained under flight containment and dietary regimen at Earth's gravity (i.e., synchonous control). Flight conditions (e.g., temperature, humidity, cage size, etc.) were not mimicked for this group.

3. Synchronous control group

The synchronous control group, maintained at a five-day delay from the flight, duplicated the flight experiment except for factors unique to the spacecraft environment, such as weightlessness and radiation. This group experienced conditions of maintenance, feeding, illumination, and temperature that were identical to those of flight. The reentry g-force and postflight transportation conditions of flight animals were not simulated for the synchronous controls.

4. Tail-suspension group

The tail-suspension group was designed to simulate the fluid redistribution and removal of static loading from the hindlimbs that occurs with spaceflight. Decapitation of this control group occurred about one hour after return to a normal postural condition. Reentry g-force and postflight transportation of flight animals were not simulated for this control group.

PREFLIGHT EVENTS

1. Rat Experiments

The ten flight rats were fed on a standard laboratory diet until the twelfth week after birth when they were placed on the flight paste diet. The rats were 15-16 weeks old at the time of flight. Small wounds were surgically created in the bone, muscle and skin of both hindlimbs of five of the ten rats, two days before launch. As mentioned above, rats in the synchronous control group were treated in the same manner as the flight rats in all procedures except those pertaining to the actual flight.

2. Primate Experiments

Two male rhesus monkeys were selected for flight in September 1989. They were housed individually in Bios units. Preflight procedures for the Circadian Rhythm/Temperature Regulation (CR/T) experiment consisted of development and verification of the themistor attachment method, restraint testing of monkeys, skin themistor attachment, conditioning to skin sensor, experiment verification tests and bioengineering tests. For the neuromuscular study, preflight procedures included obtaining muscle biopsies from uninstrumented limbs of flight-candidate monkeys, implantation of EMG electrodes, bioengineering tests and preflight EMG recordings. Preflight procedures conducted for the vestibular studies included: implantation of head restraint rings and brain electrodes; installation of U.S. motor-driven rotators in the Soviet test laboratories; animal training for head restraint and rotation/tilt paradigm testing; bioengineering and verification tests; and recording of vestibular nerve afferents and eye movements. Studies on monkeys, using the rotators, were carried out preflight.

3. Radiation Dosimetry and Spectrometry Experiments

Final assembly of the flight and ground control dosimeter units for the U.S./U.S.S.R. experiment was performed by the U.S. After environmental testing in the U.S., the temperature recorders were transported to the U.S.S.R. where Soviet specialists were trained in the operation of the recorders and their ground-support hardware. The two temperature recorders, using four probes each, were activated by Soviet specialists and attached to radiation dosimetry hardware mounted outside the spacecraft.

LAUNCH, ON-ORBIT AND REENTRY EVENTS

1. Rat Experiments

Soviet data from earlier missions indicate that accelerations are less than 4 G at launch and reentry, with a maximum deceleration of 30 G at landing. Details regarding lighting, internal environmental specifications, and provision for food and water are given in the previous section. Average food consumption was 45 g per day for the flight rats and 50 g for the synchronous group. Water consumption averaged 2-3 ml per rat per day.

2. Primate Experiments

Measurements recorded inflight for the CR/T experiment were skin temperature, axillary temperature, motor activity, heart rate, and Bios ambient temperature at the top and bottom of each capsule. EMG activity during the performance of various tasks was recorded inflight by Soviet specialists. Recordings of nerve activity, and eye and head movements were also made during inflight paradigms.

3. Radiation Dosimetry and Spectrometry Experiment

The clamshell covers for the dosimeter containers were open during launch and closed during reentry. Measurements were made for the total on-orbit duration. These included high energy neutron fluence, LET spectra < 5 keV/μm, low energy neutrons, attenuation of space radiation as a function of shielding, fluxes and energy spectra of heavy, low-energy charged particles outside the spacecraft, and high energy neutron and proton environments inside and outside the spacecraft. In addition, measurements were made on calculated absorbed dose, flux and fluence of protons, galactic cosmic ray nuclei as a function of shielding depth, and the geographical position and phase of the solar cycle. Thermoluminescent detectors were used to measure the total average mission dose of radiation. Measurements were made inside and outside the spacecraft (see Benton, E.V.: Radiation Experiments on Cosmos 2044, below).

POSTFLIGHT EVENTS

1. Rat Experiments

The animals were recovered from the landing site without delay and in good health. Rats were sacrificed at the same time of day for all groups except the tail-suspension. Dates of sacrifice are shown in Table 5. Tissues were collected and preserved as specified in the Experiment Management Plans (EMPs). Flight tissues were maintained at the temperatures specified in the EMPs and returned to Moscow for further processing as required. The US/USSR rat experiments were very successful on Cosmos 2044. A record number of tissues were obtained from this mission. Many tissues were subjected to multiple and more-extensive analyses than on previous missions. Tissues from rats with injured gastrocnemius muscles, broken fibulas and skin wounds were obtained, enabling studies of inflight tissue repair to be carried out for the first time by U.S. scientists. The availability of tissues from the tail-suspension group provided the first opportunity to directly compare data from this model with flight data.

2. Primate Experiments

Recovery of the animals was satisfactory. For the neuromuscular adaptation study, postflight EMG activity of the flight monkeys and two flight-pool monkeys were recorded. Muscle biopsies were taken from 3 leg muscles of the flight animals at 30 hours after recovery. (Biopsy samples were obtained from some of the same muscles that were analyzed in rats.) Postflight measurements of vestibular nerve afferent activity of the flight monkeys and two flight-pool monkeys were also

made. Vestibular Ocular Reflex (VOR), Optokinetic Nystagmus (OKN), and Optokinetic After Nystagamus (OKAN) measurements on the flight monkeys and other flight-pool monkeys were made for the neurovestibular experiments. Postflight procedures for the CR/T experiment consisted of transfer of data from the flight hardware to the ground-support hardware and functional testing/calibration of the flight hardware.

A postflight control study utilizing the flight monkeys was conducted at 45 days post-recovery. This control was a high-fidelity simulation of the flight environment conducted in a mock-up of the flight biosatellite, exclusive of microgravity. (See Experiment K-7-35, Circadian Rhythms and Temperature Regulation, Part II. Metabolism: P.I.: C.A. Fuller.)

3. Radiation Dosimetry and Spectrometry Experiment

Dosimeters were placed in a lead-lined transport box immediately after recovery and delivered to Moscow. The cobalt activation foils were analyzed by the U.S. investigator. Temperature recorder data were read out with ground support hardware in Moscow and the data were sent to the U.S. on a computer disk. A synchronous control experiment was also conducted in which ground control units identical in number and type to the flight unit were shipped to the launch site and back to the U.S. for analysis in order to expose the dosimeters to identical background radiation exclusive of the radiation exposure received by the flight hardware.

TABLE 1

COSMOS BIOSATELLITE MISSIONS WITH U.S. PARTICIPATION.

Mission Parameters	**782**	**936**	**1129**	**1514**	**1667**	**1887**	**2044**
Launch	11/25/75	08/03/77	09/25/79	12/14/83	07/10/85	09/29/87	09/15/89
Recovery	12/15/75	08/22/77	10/14/79	12/19/83	07/17/85	10/12/87	09/29/89
Duration (days)	19.5	18.5	18.5	5.0*	7.0	12.5	14.0
Orbital Period (min.)	90.5	90.7	90.5	89.3	89.4	90.7	89.3
Apogee (km)	405	419	406	288	270	403	294
Perigee (km)	226	224	226	226	211	222	216
Inclination (deg.)	62.8	62.8	62.8	82.3**	82.4**	62.3	82.3**
NASA TM No.***	78525	78526	81299/ 81289	88223	108803	102254	this volume

* Mission duration shortened for the first rhesus monkey flight.

** Higher orbital inclination for radiation experiments.

***NASA Technical Memorandums (TM)- available, by number, through the NASA Ames Research Center, Space Life Sciences Payloads Office (SLSPO).

TABLE 2

EXPERIMENTS FLOWN ON COSMOS 2044

I. Rat Experiments

Cardiovascular Studies

Title of Study	*Investigators**
Lipid Peroxidation of the Heart and Kidneys	A.A. Markin (USSR)
Morphological and Biochemical Examination of Heart Tissue	M. Goldstein, M. Mednieks, D. Philpott, D.Thomason, (USA); I.A. Popova (USSR),
Electron Microscopy of the Heart	W. Baranska (Poland)
Measurement of Heart Atrial Natriuretic Peptide Concentrations	L. Keil (USA); I.A. Popova (USSR)

Bone Studies

Bone Biomechanical Properties	A.V. Bakulin, V.S. Oganov (USSR)
Biochemistry of Intact and Injured Bones	I.A. Popova (USSR)
Morphometric and EM Analyses of Tibial Epiphyseal Plates	P.J. Duke (USA); G.N. Durnova (USSR)
Bone Histomorphology and Histochemistry	G.N. Durnova, A.S. Kaplansky (USSR); C. Nouges (France)
Kinetics of Cellular Activities	C. Alexander , L. Vico (France)
Bone Cartilage	J. Feldes (Hungary)
Osteogenic Cell-Precursors	C. Grinpas (Canada)
Bone Minerals	K. Hecht (GDR)
Bone Biochemistry, Mineral Distribution, and Calcium Regulating Hormones	S. Arnaud (USA); G.N. Durnova, A.S. Kaplansky, I. Popova (USSR)
Gravity and Skeletal Growth	S. Doty, L.P. Garetto, E.R. Holton, T.C. Lorenz (USA); G.N. Durnova, A.S. Kaplansky (USSR)
Mineral Distribution and Balance	C. Cann (USA); V.I. Loginov, L.V. Serova (USSR)
Neutron Activation Analysis of Bone Macro- and Trace Elements	T.E. Burkovskaya (USSR)

*For Principal Investigator (PI), see Section III, Science Reports

TABLE 2

EXPERIMENTS FLOWN ON COSMOS 2044 (CONT.)

I. Rat Experiments (cont.):

Muscle Studies

Title of Study	*Investigators**
Muscle Contractile Properties	L.M. Murashko, V.S. Oganov (USSR)
Muscle Histomorphology, Histochemistry, and Electron Microscopy	E.I. Ilyina-Kakueva, O.M. Pozdnyakov (USSR); D. Desplanches (France)
Muscle Biochemistry	A.A. Markin (USSR)
Biochemistry of the Sarcoplasmic Reticulum and Ca Transport in Membranes	Y. Mounier (France)
Biochemistry of Myofibrillar Proteins	T. Szilagyi (Hungary)
Metabolic and Morphologic Properties of Muscle Fibers	V.R. Edgerton (USA); E.I. Ilyina-Kakueva, V.S. Oganov (USSR)
Morphological, Histochemical, Immunocytochemical, and Biochemical Investigation of Nerve and Muscle Breakdown	S. Ellis, D.A. Riley (USA); E.I. Ilyina-Kakueva, V.S. Oganov (USSR)
Messenger RNA Levels in Skeletal and Smooth Muscles	F.W. Booth, N.W. Weisbrodt (USA); E.I. Ilyina-Kakueva, V.S. Oganov, K.S. Smirnov (USSR)
Effects of Microgravity in the Muscle Adductor Longus of Rats	N.G. Daunton (USA); E.I. Ilyina-Kakueva (USSR)
Skeletal Muscle Atrophy in Response to 14 Days of Weightlessness	X.J. Musacchia (USA); E.I. Ilyina-Kakueva, V.S. Oganov (USSR)
Effect of Microgravity on Myosin Isoform Expression in Rodent Skeletal Muscle	K.M. Baldwin (USA); E.I. Ilyina-Kakueva, V.S. Oganov (USSR)
Insulin Receptors	R. Kvetnansky (Czechoslovakia)
Biomechanical, Biochemical, and Morphological Alterations of Intramuscular and Dense Fibrous Connective Tissues	J. Maynard, A. Pedrini-Mille, A.C. Vailas (USA); G.N. Durnova, A.S. Kaplansky (USSR)
Effect of Spaceflight on Metabolic Enzymes of Type I, II-A, and II-B Muscle Fibers	O.H. Lowry (USA); E.I. Ilyina-Kakueva (USSR)

*For Principal Investigator (PI), see Section III, Science Reports

TABLE 2

EXPERIMENTS FLOWN ON COSMOS 2044 (CONT.)

I. Rat Experiments (cont.):

Blood Studies

Title of Study	*Investigators**
Cytological Studies in Bone Marrow& Peripheral Blood	N.A. Chelnaya, L.V. Serova (USSR)
Erythroid Colony Formation In Vitro and Erythropoietin Determinations	R. Lange (USA); N.G. Khrushcov, T.V. Michurina, L.V. Serova (USSR); A. Vacek (Czechoslovakia)
Stem Cells in Bone Marrow and Spleen	A. Vatsek (Czechoslovakia)
Hormones in Blood	R. Kvetnansky (Czechoslovakia)
Hormones and Enzymes in Blood	I.A. Popova (USSR)
Natriuretic Factor in Blood, Atrium, and Kidneys	C. Gharib (France)
Fatty Acids in Blood	I. Ahlers (Czechoslovakia)
Erythrocyte Metabolism	S.M. Ivanova (USSR)
Nucleic Acids in Lymphocytes, Spleen, and Thymus	E. Misurova (Czechoslovakia)
Electron Microscopy of Erythrocytes	L.A. Sidorenko (USSR)

Neuroendocrine System Studies

Histology of the Pituitary	E.I. Alekseev (USSR)
Pituitary Oxytocin and Vasopressin Content	L. Keil (USA); I.B. Krasnov (USSR)
Pineal Physiology After Space Flight: Relation to Gonadal Function	D.C. Holley (USA); I.B. Krasnov (USSR)
Growth Hormone Regulation, Synthesis, and Secretion	R. Grindeland, P.S. Sawchenko (USA); E.I. Ilyina-Kakueva, I.B. Krasnov, I. Popova, I. Victorov (USSR)
Histology of Epiphyseal Neuroglia	P. Groza (Rumania)
Catecholamines in the Adrenals	R. Kvetnansky (Czechoslovakia)

*For Principal Investigator (PI), see Section III, Science Reports

TABLE 2

EXPERIMENTS FLOWN ON COSMOS 2044 (CONT.)

I. Rat Experiments (cont.):

Brain and Spinal Column Studies

Title of Study	*Investigators**
Histology of the Adrenals and Lymph Organs	A.S. Kaplansky (USSR)
Histology and Electron Microscopy of the Thyroid and Parathyroid Glands	G.I. Plakhuta-Plakutina, V.I. Loginov, N.P. Dmitrieva (USSR)
Electron Microscopy, Histochemistry, and Histology of the Somatosensory Cortex	L.N. Dyachkova, T.A.. Leontovich, L.M. Gerstein (USSR)
Electron Microscopy, Histochemistry, and Histology of the Visual Cortex	L.N. Dyachkova, A.N. Kardenko, T.A. Leontovich (USSR)
Hypothalamus: Histochemistry and GABA Enzymes	I.B. Krasnov (USSR)
Pons Varolii and Medulla Oblongata: Histochemistry, Electron Microscopy, Enzymes, Vestibular Nuclei	I.B. Krasnov, L.N. Dyachkova (USSR)
Dendrite Tree of Gigantic Neurons of the Reticular Nucleus	T.A. Leontovich (USSR)
Cerebellum	I.G. Lyudkovskaya (USSR)
Cortex, Electron Microscopy and Histochemistry of the Nodulus Enzymes, GABA	I.B. Krasnov (USSR)
Morphology and Histochemistry of the Lumbar Enlargement, Cervical Enlargement, and Intervertebral Ganglia	V.I. Drobyshev, I.V. Polyakov (USSR)
Metabolic Enzymes, Neurotransmitter Amino Acids, and Neurotransmitter Associated Enzymes in Selected Regions of the Central Nervous System	O.H. Lowry (USA); I.B. Krasnov (USSR)
Study of Muscarinic and GABA Receptors in the Sensory-Motor Cortex and Spinal Cord	N.G. Daunton, L.-C. Wu (USA); I.B. Krasnov (USSR)
Ventral Horn Responses to Spaceflight	V.R. Edgerton, B. Jiang (USA); I.B. Krasnov (USSR)

*For Principal Investigator (PI), see Section III, Science Reports

TABLE 2

EXPERIMENTS FLOWN ON COSMOS 2044 (CONT.)

I. Rat Experiments (cont.):

Lung Studies

Title of Study	*Investigators**
Lung Histology	A.S. Kaplansky (USSR)
Lung Morphology	J.B. West (USA); A.S. Kaplansky (USSR)

Gastrointestinal System Studies

Biochemistry of the Stomach, Small Intestine, and Pancreas	K.V. Smirnov (USSR)
Histology of the Stomach, Small Intestine, Large Intestine, Salivary Glands, and Pancreas	P. Groza (Rumania)
Effects of Spaceflight on the Proliferation of Jejunal Mucosal Cells	R.W. Phillips (USA); K.L. Smirnov (USSR)
Histochemistry of Small Intestine Protista	Z. Loida (Czechoslovakia)
Electron Microscopy of the Pancreas	Permyakov (USSR)

Liver Studies

Stem Cells	A. Vatsek (Czechoslovakia)
Insulin Receptors in the Liver	L. Makho (Czechoslovakia)
Aminotransferases in the Liver	S. Nemeth (Czechoslovakia)
Proteins, Amino Acids, and Glycolysis in the Liver	I.A. Popova (USSR)
Lipid Metabolism in the Liver	I. Ahlers (Czechoslovakia)
Hepatic Function in Rats After Space Flight	S. Cormier, A. Merrill (USA); I.A. Popova (USSR)

*For Principal Investigator (PI), see Section III, Science Reports

TABLE 2

EXPERIMENTS FLOWN ON COSMOS 2044 (CONT.)

I. Rat Experiments (cont.):

Other Studies

Title of Study	*Investigators**
Fluid-Electrolyte Metabolism in Bones, Heart, Liver, Kidneys, and Skin	Yu.V. Natochin, L.V. Serova (USSR)
Electron Microscopy of the Vestibular Apparatus	I.B. Krasnov (USSR)
Receptors of Catecholamines in the Spleen and Myocardium	R. Kvetnansky (Czechoslovakia)
Immunology Studies	I.V. Konstantinova, A.T. Lesnyak (USSR)
Spermatogenesis	L.V. Serova (USSR)
Effects of Microgravity on Testicular Function	R.P. Amann (USA); L.V. Serova (USSR)
White Fat: Insulin and Lipids	I. Ahlers, L. Makho (Czechoslovakia)
Rodent Tissue Repair	B.W. Festoff, W.T. Stauber, A. Vailas (USA); T.E. Burkovskaya ,E.I. Ilyina-Kakueva, A.S. Kaplansky (USSR)
Trace Elements in the Skin and Hair	K. Hetch (GDR)
Level and Function of Immune Cells	A. Mastro, G. Sonnenfeld (USA); B.B. Fuchs, I.V.Konstantinova, A.T. Lesnyak, A.L. Rakhmilevich (USSR)

*For Principal Investigator (PI), see Section III, Science Reports

TABLE 2

EXPERIMENTS FLOWN ON COSMOS 2044 (CONT.)

I. Rat Experiments (cont.):

Other Studies

Title of Study	*Investigators**
Physiological Effects of Spaceflight	Ye.A. Ilyin (USSR)
Circulatory Homeostasis and the Erythroid Function	V.I. Lobachik (USSR)
Fluid-Electrolyte Metabolism	M.A. Dotsenko (USSR)
Blood Cell (Erythrocytes, Lymphocytes) Metabolism and Erythrocyte Membrane Status	S.M. Ivanova (USSR)
Immunological Research	I.V. Konstantinova (USSR)
Cellular Immunity	A.T. Lesnyak (USSR)
Biological Rhythms and Thermal Regulation	C.A. Fuller (USA); V.Ya. Klimovitsky (USSR)
Biorhythmic Analysis of EEG During Sleep	X.U. Baizer (FRG); G.G. Shlyk (USSR)
Water-Saline Homeostasis	M.A. Dotsenko (USSR)
Autonomic / Eye Movement Interactions	M.G. Sirota (USSR)
Vestibular-Ocular Reflex (VOR)	B. Cohen (USA); I. Kozlovskaya, (USSR)
Vestibular Primary Afferents and Eye Movements	M.J. Correia (USA); I. Kozlovskaya (USSR)
Attentional Changes Monitored Through Electrocortical Recording	A. Rougeul-Buser (France)
Functional Neuromuscular Adaptation	V.R. Edgerton (USA); I. Kozlovskaya (USSR)
Ultrastructure of Skeletal Muscle	V.V. Stepantsov (USSR)

*For Principal Investigator (PI), see Section III, Science Reports

TABLE 2

EXPERIMENTS FLOWN ON COSMOS 2044 (CONT.)

II. Primate Experiments

III. Radiobiological and Dosimetric Studies

Title of Study	*Investigators**
Radiation Measurements	E.V. Benton (USA); V. Dudkin (USSR)
Effects of Single Hits of Heavy Ions of Galactic Cosmic Rays on Air-Dry Seeds	E.N. Maksimova (USSR)
Remote Effects from Heavy Ions of Galactic Cosmic Rays on Objects with Different Rates of Metabolism	V.M. Abramova (USSR)
Radiobiological Experiments with Crepis Capillaris Seeds	L.N. Kostina (USSR)
Experiment with Bubble-Detectors	G. Ing (Canada); E.E. Kovalev(USSR)

IV. Gravitation Biology Studies

Embryogenesis in Drosophila	L.P. Filatova (USSR)
Chlamydomonas Cell Culture	O.V. Gavrilova (USSR)
Beetle-2 Biorhythm Experiment	A.M. Alpatov (USSR)
Bacterial Metabolism Experiment	M. G. Tairbekov (USSR)
Molecular Control of the Immune Response	L. Schaffard (France); I.V. Konstantinova (USSR)
Structural and Functional Organization of Cells Obtained from Protoplasts	E.I. Kordyum (USSR); T.H. Iversen (Norway); O. Rasmussen (Denmark)
"Stick Insect" Experiment	A.M. Alpatov (USSR); J. Mossland (Netherlands)
Worm Regeneration Experiment	A.M. Alpatov(USSR)
Ant-Hill Experiment	A.M. Alpatov (USSR)
Newt Experiment	V.I. Mitashov (USSR)
Chlorella-Bacteria-Guppy Fish System	G.I. Meleshko, V.N. Sychev (USSR)
Amphipod-Chlorella-Microorganism System	G.I. Meleshko, V.N. Sychev (USSR), (Britain)

*For Principal Investigator (PI), see Section III, Science Reports

TABLE 3

ELECTRODES AND SENSORS IMPLANTED IN PRIMATES FOR RECORDING OF PHYSIOLOGICAL PARAMETERS.

Central electrodes	#
Active electrocorticographic electrodes (ECoG)	2
Subcortical monopolar electrodes for four neurographic leads (NG-1, NG-2, NG-3, NG-4)	4
Skull indifferent electrode for two ECoG leads, (ECoGi)	1
Electrodes for two electrooculographic leads, (EOG)	4
Skull common electrode for biopotentials from central and peripheral electrodes, (Ec)	1
Neck electromyographic electrodes, (EMGn)	2
pO_2 electrodes	2
Peripheral electrodes and sensors	
Electrocardiographic electrodes, (EKG)	2
Calf electromyographic electrodes for two leads, (EMGc)	4
Body temperature transducer	1

TABLE 4

PRIMATE CARDIOVASCULAR DATA BEFORE AND AFTER FLIGHT

Parameter	**Zhakonya**		**Zabiyaka**	
	Before	After	Before	After
Age	3.5 years		3.5 years	
Body weight, (g)	3900	3700	3770	3850
Blood Pressure (mm Hg)	105/70	100/80	100/70	90/65
Heart rate, (beats/min, ave)	140	120	135	146
Blood: Hemoglobin (g%)	15.4	16.0	14.2	15.2
Erythrocytes (cu. mm)	8050	7850	6850	7350
Leukocytes (cu. mm)	18100	28600	13800	32100
Hematocrit (%)	50	57	43	51
Erythrocyte Sedimentation Rate (mm/hr)	1	2	3	12

TABLE 5

SUMMARY OF RODENT EXPERIMENT DESIGN

Group	Housing	Surgery	Flight Conditions	Food:Day/ Portions	Water	Sacrificed
Flight	Group	09/12/89	Yes	55g/4 portions	Unlimited	09/29/89
Synchronous Control	Group	09/17/89	Simulated	55g/4 portions	Unlimited	10/04/89
Basal Control	Group	Not done	No	55g/1 portion	Unlimited	09/15/89
Vivarium Control	Group	09/22/89	No	55g/1 portion	Unlimited	10/05/89
Tail-suspension Study	Individual	09/21/89	No	55g/1 portion	Unlimited	10/08/89

Figure 1. Food consumption by Zabiyaka inflight.

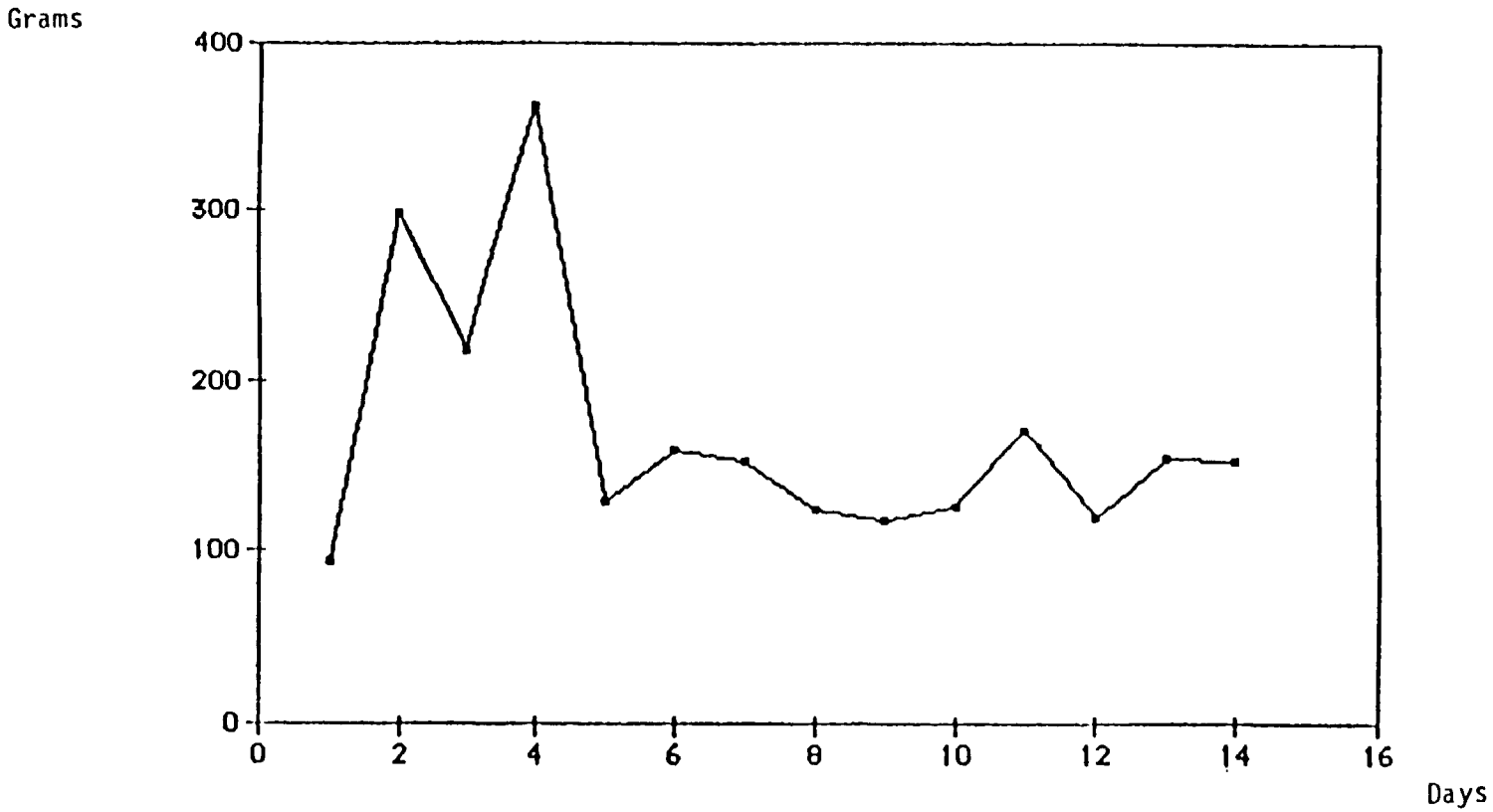

Figure 2. Food consumption by Zhakonya inflight.

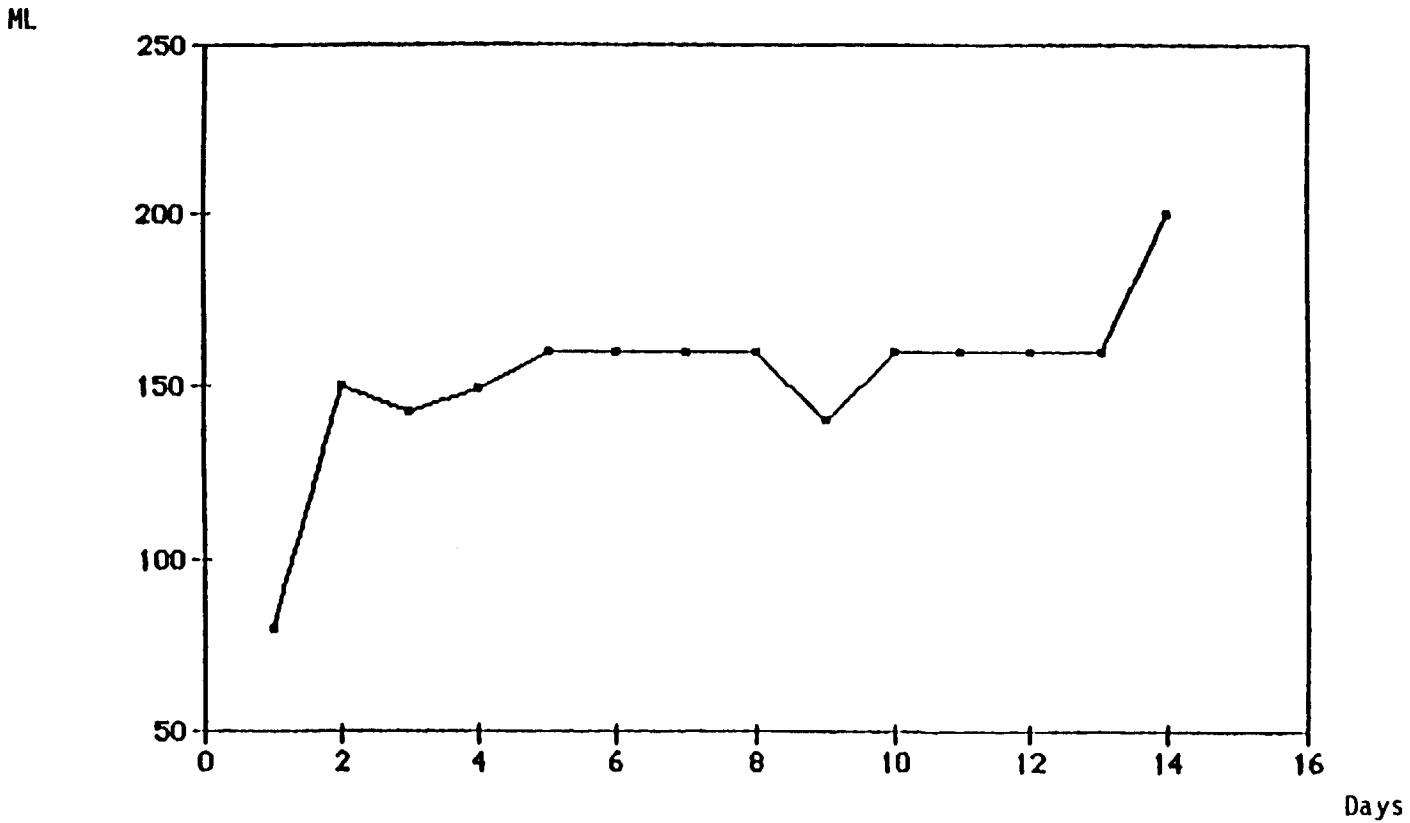

Figure 3. Juice consumption by Zabiyaka inflight.

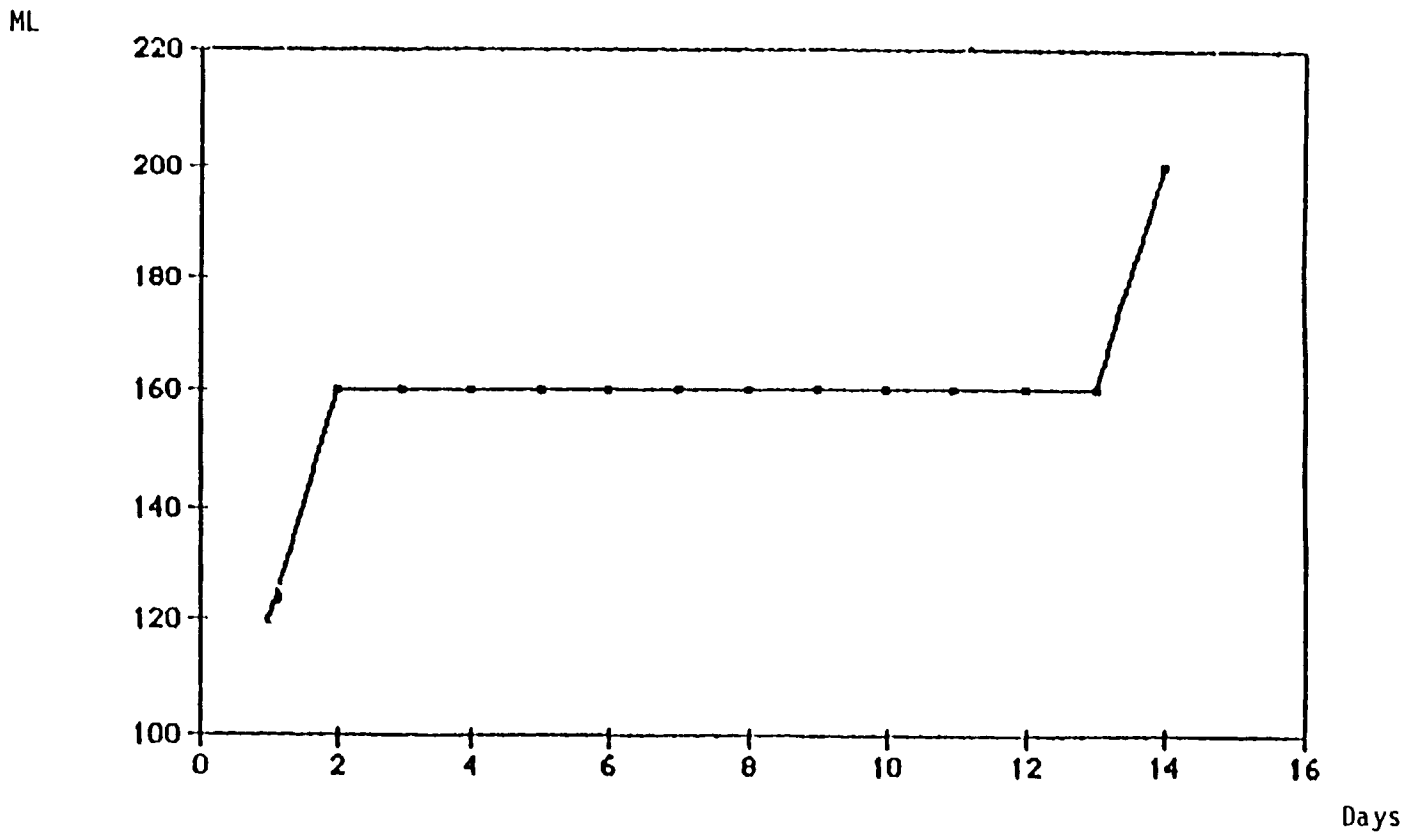

Figure 4. Juice consumption by Zhakonya inflight.

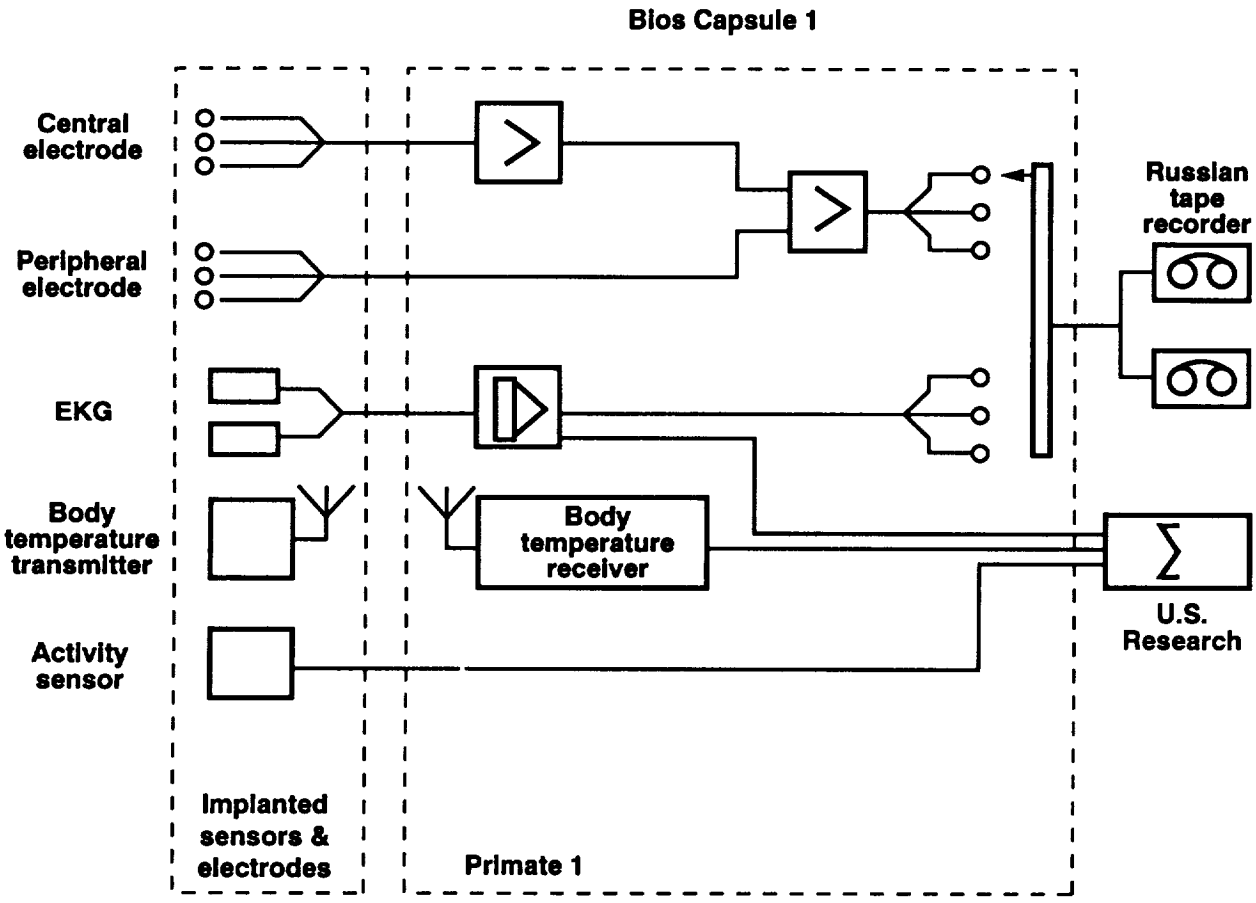

Figure 5. Data flow schematic for Cosmos 2044 spacecraft.

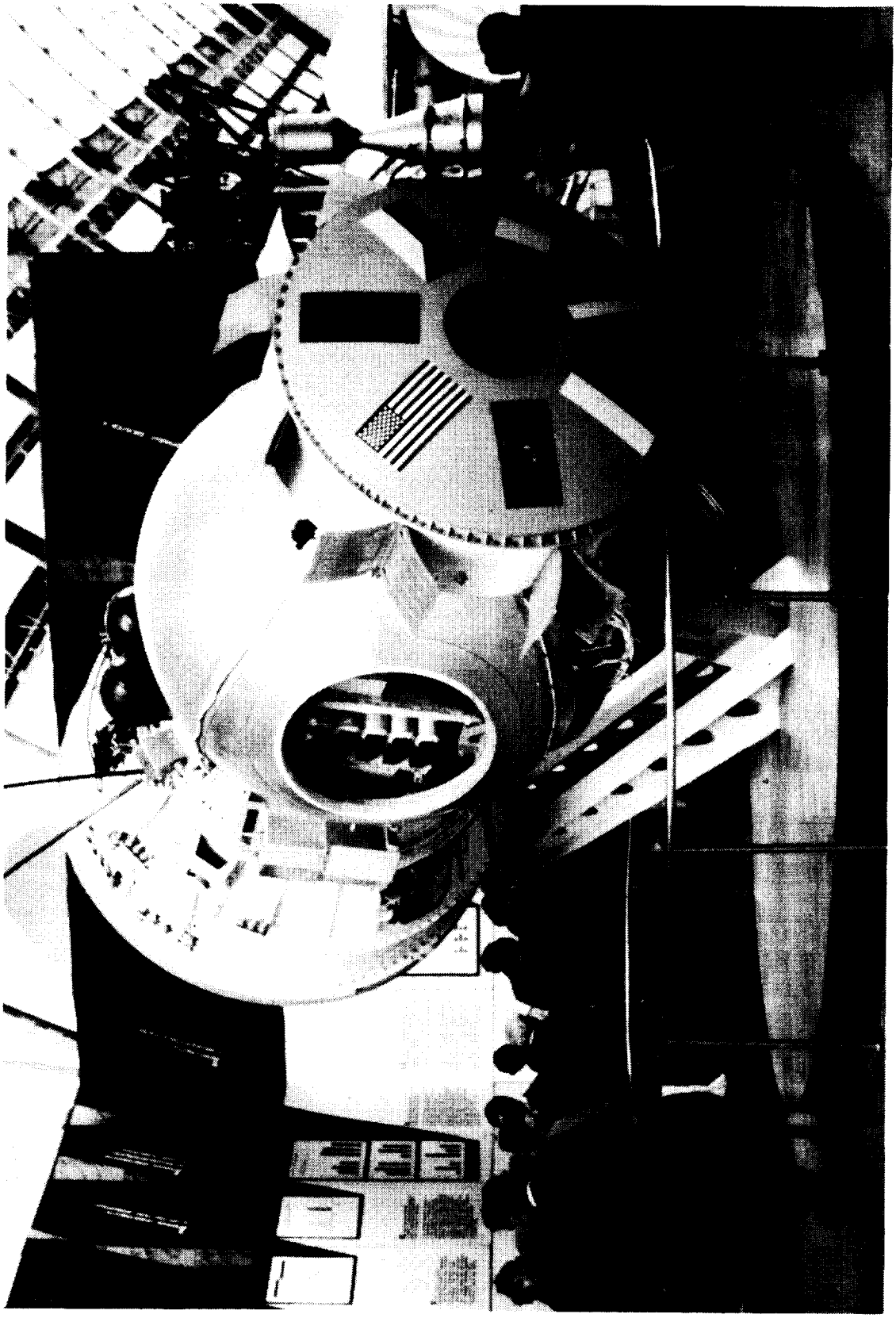

Figure 6. Cosmos spacecraft

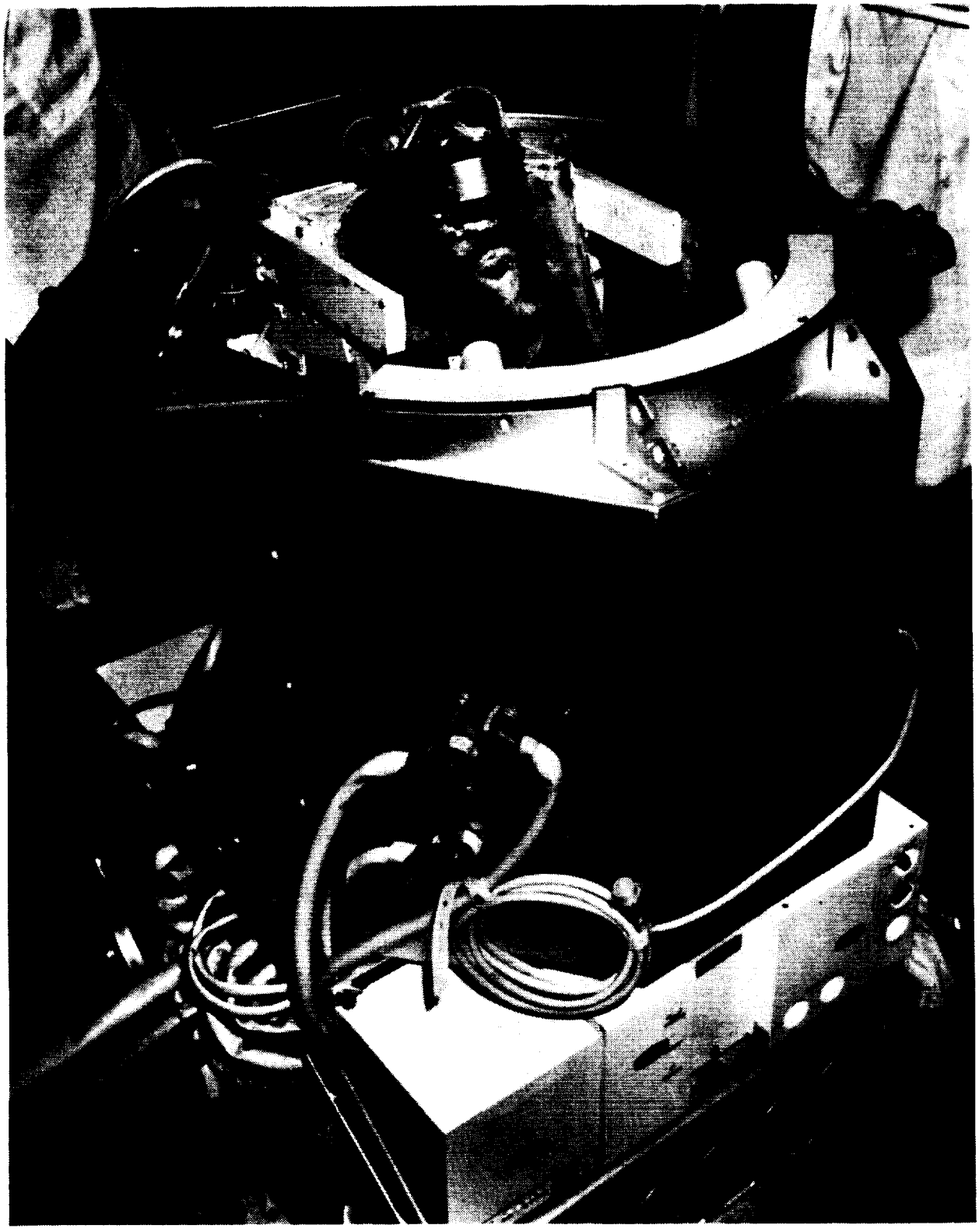

Figure 7. Primate-Bios.

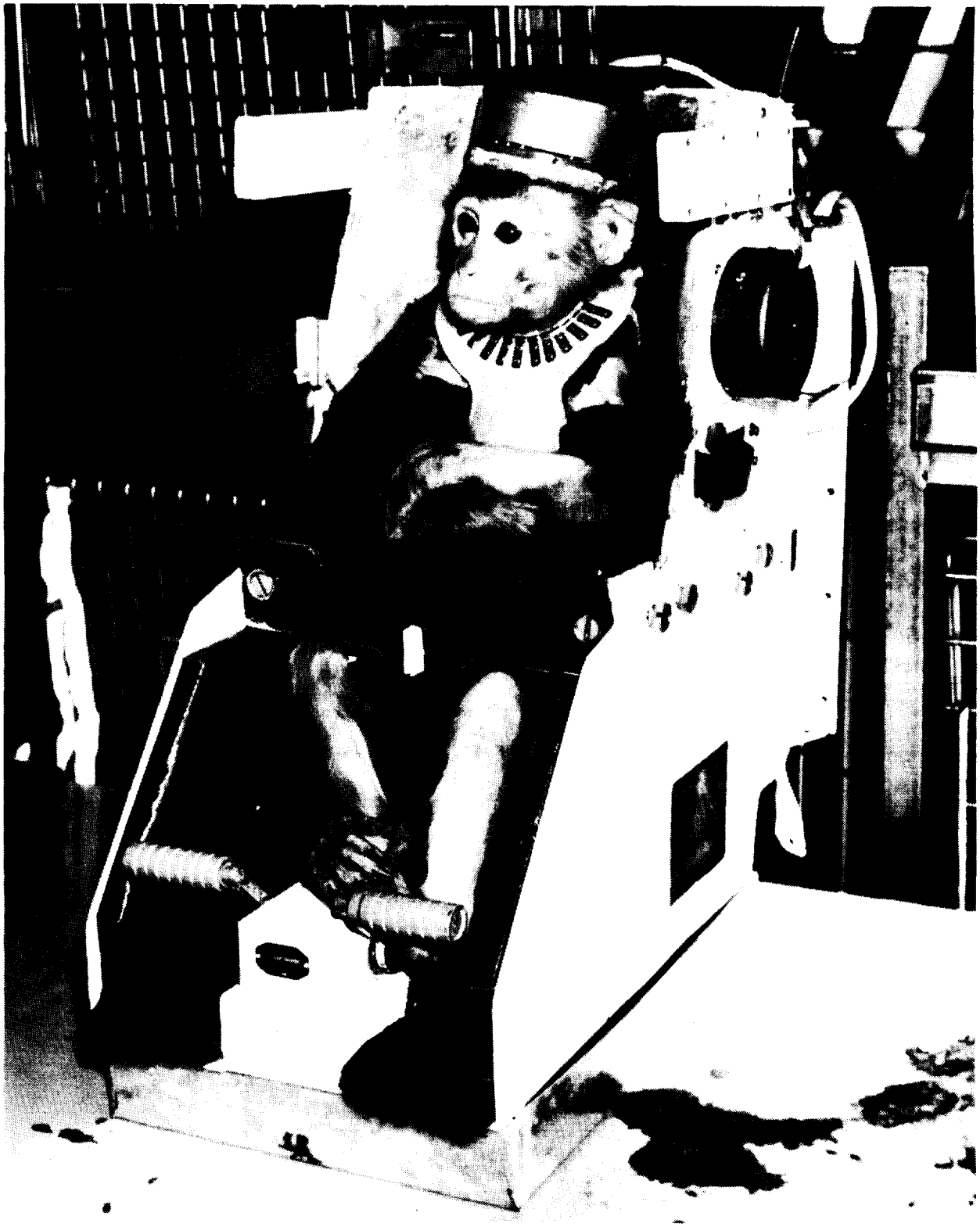

Figure 8. Primate in Bios restraint chair.

Figure 9. Flight monkeys.

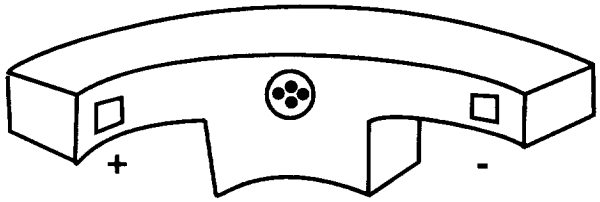

Figure 10. Gaze Fixation Reaction Psychomotor. The monkey gazes at a semi-circular panel. The central target looks like four bright dots. The peripheral "positive" target looks like "E" and the peripheral "negative" target, like "I". This is the arrangement that was used in previous Cosmos and Cosmos 2044 flights and this test procedure was also similar. If the "+" target is presented, the monkey must pull the response lever for which he will be rewarded with 1 gram of juice; if he fails to pull the response lever or if he pulls it when the "-" target is presented he will be punished: the central target will be switched on with a 5 second delay; in other words, the monkey won't get a juice reward. If the monkey performs correctly, he will get 256 grams of juice within a relatively short period.

Figure 11. Tail suspension study equipment.

II. U.S. FLIGHT AND GROUND-SUPPORT HARDWARE

A. HARDWARE OVERVIEW

This chapter contains a description of the U.S. equipment developed to support U.S./U.S.S.R. joint experiments conducted on the Cosmos 2044 mission. Included are descriptions of flight and ground-support hardware, as well as descriptions of test procedures used for verification of hardware performance. A summary list of this hardware by experiment, is included as Table 1.

1. Flight Hardware Description and Test Plan

A high level of cooperation is essential for the success of a joint spaceflight mission. This was especially true of the Cosmos 2044 mission because of extensive hardware integration requirements. The U.S. supplied flight hardware for two inflight experiments on Cosmos 2044. This flight experiment included two 4-channel temperature recorders (forerunners to the Shuttle-qualified ATR-4) and two 8-channel solid state recorders for the Circadian Rhythm/Temperature (CR/T) experiment. Soviet support for this hardware was critical because U.S.S.R. specialists were involved in many of the experimental procedures.

Enhanced radiation data were obtained as a function of varying solar activity for the radiation dosimetry experiment using improved detectors and the temperature recording capability of the portable temperature recorders. The recorders were designed to be used with radiation dosimeters outside the spacecraft, thereby being exposed to a near-vacuum environment and extreme temperatures. Since the temperature recorders were in thermal contact with the spacecraft and they were covered in mylar foil to protect them from radiated energy, it was estimated by Russian physicists that the recorders would experience a temperature range of no more than ±50 C. They were therefore tested in excess of this temperature range. Ninety-G impact tests were conducted for both the temperature recorders and CR/T signal processer (CR/T-SP) to ensure their ability to endure the impact of landing and still retain stored flight data. The 90-G requirement was set by Soviet engineers to simulate a condition where one parachute does not open on reentry.

The CR/T hardware was also extensively tested. Testing with rhesus monkeys was performed for the flight duration to verify all system components. Functional tests were conducted to verify system performance and detect system degradation if it occurred. Thermal cycle tests and random vibration tests were conducted to ensure that the CR/T system met operational requirements at specified temperature and vibration levels. The battery packs were tested to confirm their capability to power the CR/T-SP for the mission duration. See Table 2 for summary of environmental testing performed on the temperature recorders and CR/T flight hardware.

2. Ground-Support Hardware Description and Test Plan

A large amount of ground support equipment was used for the primate experiments for preflight and postflight testing. The quantity of data collected on this mission necessitated the use of ground-based computers and complex supporting software.

The preservation of biospecimens from the Cosmos 2044 mission required the design and development of shipping containers for the transfer of tissue samples postflight between the recovery site and Moscow, and from Moscow to the U.S. These biotransporters were designed to maintain and preserve biospecimens at specific temperature ranges from -70 to +23^{0}C. There was a shift towards the use of passive biotransporters on this mission, as compared with previous missions, because of their higher reliability.

All biotransporters were extensively tested to ensure operation within the appropriate temperature ranges for the required duration. These tests are described in detail in a later section.

3. Hardware/Software Documentation and Data Transfer

Procedures and specifications for all U.S. experiments aboard the biosatellite were provided to the Soviets in the EMPs. Data sheets for the experiments, as required, were provided in the EMPs. Some neurovestibular data and raw EMG data were recorded on analog data recorders for transfer to the U.S. Other neurovestibular data were recorded on computer data storage media.

The CR/T hardware manual included the reference manual for the Vitalog recorder and software. This manual provided specifications and operation procedures for the hardware and software used in the CR/T experiment. Software, custom developed for the flight hardware configuration, was used for testing the system, starting data recording, reading and saving data, providing on-screen graphical displays of data, and creating printed copies.

The temperature recorder's Operation Manual described procedures for the operation and maintenance for the recorder and its components, including the ground computer and system software.

B. EXPERIMENT-SPECIFIC HARDWARE

M. Skidmore, J. Connolly
NASA-Ames Research Center

1. Circadian Rhythm/Temperature Regulation (CR/T) Experiment

Flight Hardware

Eight parameters were measured in this experiment. Motor activity was monitored via a piezoelectric sensor attached to the monkey's restraint jacket. Thermistors attached to the monkey's skin at the ankle, thigh and temple regions measured skin temperature, and thermistors at the top and bottom of the primate chair monitored ambient temperature. Axillary temperature and ECG-derived R-wave signals were provided by the U.S.S.R. All eight parameters were recorded on the Circadian Rhythm / Temperature Regulation Signal Processor (CR/T-SP), provided by the U.S.

The CR/T-SP is a self-contained signal processing and digital data storage device. It consists of circuitry which conditions incoming physiological signals for data processing and a microprocessor-controlled digital data recorder which stores data for later recovery by a ground-based computer. For this flight all parameters were recorded at 5-minute intervals.

Motor Activity was presented to the CR/T-SP as voltage pulses associated with movement of the piezoelectric sensor. These pulses were counted and stored as counts. The U.S.S.R supplied axillary temperature and R-wave signals were presented to the CR/T-SP in the form of voltage pulse trains where each pulse had a duration of 70 μsec. In the case of R-wave pulses, the inter-pulse interval was measured and a running average for heart rate was maintained. The axillary temperature pulsatile signal was in the range of 400 to 1000 Hz. A frequency to voltage conversion was performed and this voltage was stored as a digital value. Pre- and post-flight calibrations of the axillary temperature system and the CR/T-SP allowed conversion of the stored digital values to temperature in degrees C.

The CR/T-SP (Figure 1) was powered by a removable lithium battery power pack (Figure 2). The battery pack contained 16 non-rechargeable lithium batteries. A CR/T-SP interface box (CR/T-IB) provided an interconnection point between the CR/T-SP and the sensors (Figure 3).

Ground Support Hardware

The Ground Readout Unit (GRU) was used to test the operation of the CR/T-SP, to begin data sampling and to recover data stored in the CR/T-SP. A standard IBM PC served successfully as the GRU during tests/experiments in the U.S. and the U.S.S.R. Computer software for use with the CR/T-SP and GRU, and data-listing software were also supplied to the U.S.S.R.by the U.S. A Signal Simulator provided simulated signals for all 8 measurement parameters (Figure 1).

2. Radiation Dosimetry

Flight Hardware

A set of radiation dosimetry and spectrometry measurements were conducted using passive detector systems located inside and outside the spacecraft. Dosimeters located internal and external to the spacecraft included 3,^{59}Co activation foils, 4,^{6}Li(n, a)T foils and 8,^{232}Th fission foils. In addition, about 300 Thermoluminescent Detectors (TLDs) and 20 CR-39 Plastic Nuclear Track Detectors (PNTDs) were mounted external to the spacecraft. This hardware was developed by the U.S. investigator and is described in Science Report K-7-41, included in Section III, Part D of this document.

Two 4-channel temperature recorders were mounted on the outside of the spacecraft within the U.S.S.R. clam shell type enclosures used to house numerous radiation experiments. The temperature recorders were wrapped in a special mylar foil to protect them from radiated thermal energy. These temperature recorders are small, self-contained, battery-operated recorders that measure and record temperature data at preselected sampling rates (Figure 3). The data are stored in solid-state memory and read out using a ground-based computer. The postflight data summaries are shown as Figures 8 and 9 in the Benton (K-7-41) science report. These temperature recorders are capable of measuring temperatures ranging from -50°C to +50°C with a resolution of 0.5°C and an accuracy of ±1°C.

Ground Support Hardware

Initialization of the temperature recorder and read-out of its stored data was accomplished using recorder System Software and an IBM-compatible computer which communicated with the recorder via an AC-powered Computer Interface Unit. This unit translated the parallel-bit data stored in the recorder into serial data for downloading. A Field Tester was used to check the operational status of the temperature recorders. This was a device which could be used to check the temperature measurements of the different temperature probes. A lead-lined box was used to transport the dosimeters in order to eliminate any pre-or post- flight contamination due to background radiation.

3. Neurovestibular Experiments

Ground Support Hardware

Frontal and roll scleral search coils were surgically implanted in the right eye of flight and control monkeys to record eye movements in response to vestibular and optokinetic stimuli pre- and postflight. Vestibular and optokinetic stimuli were provided by a rotator (Figure 4) and a 3-axis planetary optokinetic stimulator (Figure 5). Eye movement recordings were made with animals in an upright position and at various angles of tilt with respect to the gravitational axis of the Earth. Optokinetic stimuli were projected onto a dome-like screen that surrounded the animal's visual field. The optokinetic stimulator consisted of a light surrounded by a moving ball, cut out to project stripes 5 degrees apart. The motor and ball were mounted on a gimbal. The moving ball was driven

by a velocity signal so that the animal could receive steps of surround velocity up to 150 degrees per second. A primate chair with modified head restraint was used for these pre- and postflight studies. Eye movement recordings was performed using a Neurodata Eye Coil System. All data were recorded on computer diskettes with an analog tape back-up.

Eye position and discharges from semicircular canal and otolith afferents in response to complex vestibular stimulation were also measured. Flight and control monkeys were implanted with head restraint devices, eye movement electrodes and afferent recording electrodes. Vestibular stimulation included ground-based studies in normal gravity and microgravity studies during orbital spaceflight. Animals were rotated in a restraint chair mounted on a hand-driven rotator at the launch site in order to verify proper placement of brain electrodes. A computer-controlled, motor-driven rotator was used to perform the preflight and postflight recordings in Moscow. Raw data were copied onto an analog tape recorder. Inflight data on eye movement and neurograms were shared, along with pre- and postflight data.

C. BIOTRANSPORTER DEVELOPMENT

M. Skidmore
NASA-Ames Research Center

+23°C ACTIVE BIOTRANSPORTER

1. Development & Operation.

A biotransporter with a thermoelectric heating/cooling unit was used to transfer specimens by aircraft from the recovery site to Moscow. It was designed to maintain a temperature range of +21°C to +25°C for a minimum of 48 hours, for an ambient temperature range of -28°C to +41°C.

Several issues had to be considered because of the requirement for operation in an aircraft. Previous experience with the Cosmos 1887 mission had demonstrated that while extreme ambient temperatures were unlikely, size and weight were important considerations. Accordingly, it was determined that the optimal configuration was to provide a small power supply connected to the biotransporter via a power cable.

The biotransporter was a Precision Temperature Chamber manufactured by United States ThermoElectric, Chico, CA. The external dimensions were 17.5 x 11.75 x 16.5 inches and the inner sample chamber had a usable volume of approximately 0.45 cubic feet. The selectable options for the internal temperature set-point were 6, 23 and 37°C. The biotransporter power supply (BPS) consisted of a battery pack, power conversion circuit, and special cables all housed in a "ZERO" (Zero Corp., San Diego, CA) carrying case. The biotransporter could be powered from the enclosed battery pack or externally from either 28Vdc or 220Vac power sources. Fuse protection was provided for all options.

The biotransporter power supply battery pack (BPS-BP) contained 8 individual battery packs, each with 16 non-rechargeable lithium batteries similar to those used to power the CR/T-SP (Figure 2). The BPS-BP provided 18 Vdc which was then regulated to the 12 Vdc required to operate the biotransporter. The power conversion circuit also accepted input power at either a 220 Vac (50 or 60 Hz) or 28 Vdc and converted it to 12 Vdc. Three cables were supplied with the BPS but only one could be used at any time. One cable was used when the internal batteries were providing power, another when 28 Vdc external power was available, and the third when 220 Vac external power was available. The weight of the BPS, including cables, was 35.5 lbs.

2. Test Plan

All testing was conducted with the internal temperature set-point at 23°C, unless otherwise mentioned. Tests were performed to baseline the requirements for the power supplies, and to ensure that the biotransporter was capable of maintaining the selected temperature over a range of ambient temperatures for the required time.

3. Test Procedure

Nominal current consumption tests were carried out to determine baseline requirements for batteries and power supplies. The unit was connected to a 12Vdc power supply and instrumented to record current consumption and internal temperature while the ambient temperature was +24 ±1°C. Results showed that the range of current consumption was 0.1 to 2.6 amps. The current demands were not stable, but were sensitive to the difference between the internal and external temperature and whether the unit was heating or cooling. The operation of the biotransporter was tested during temperature cycling in an environmental chamber.

For this test, the unit and a BPS were installed in a test chamber which was programmed to alternate on 12 hour cycles between 10°C and 28°C for a 72 hour period. A small sample vial, filled with water, was placed inside the biotransporter. The water in the sample vial was at approximately 21°C when it was placed in the biotransporter. A temperature sensor was installed in the sample vial and immersed in the water. Results demonstrated that temperature was maintained within the specified limits for nearly 53 hours. The maximum temperature differential that the unit could maintain from the ambient temperature was also determined by testing in the environmental chamber. It was found during this testing that the biotransporter could hold the +23°C set -point within ± 2°C for an ambient temperature as low as -28°C and for ambient temperature as high as +41°C.

A final test was performed to determine the rate at which the temperature of the sample chamber would approach ambient temperature if power was removed. This last test was also used to estimate the rate at which chamber temperature would return to the set point when power was restored. It was found that with power removed the internal temperature of the unit would move toward ambient at a rate of approximately 1°C/hr when the ambient temperature was 10° to 15°C different than the internal temperature. When power is restored under these conditions, the internal temperature returns to the setpoint at a rate of approximately 0.7°C/hr.

+4°C ACTIVE BIOTRANSPORTER

1. Development & Operation

A 4°C biotransporter (with thermoelectric unit) was used to transfer specimens by aircraft from the recovery site to Moscow. It was designed to maintain a temperature range of +2°C to +10°C for a minimum of 48 hours. The biotransporter could maintain its temperature over an ambient temperature range of -34.8°C to +23.4°C. It was similar in design to the +23°C active biotransporter described above, and was also connected to a small separate power supply via a power cable identical to the BPS-BP described above.

The biotransporter was a UST PTC 3100 Precision Temperature Chamber (Figure. 7). Its external dimensions were 21 by 17.75 by 20 inches and its inner sample chamber had a usable volume of approximately 0.72 cubic feet. The set point of the internal temperature was adjustable from 0°C to 49°C.

2. Test Plan

The complete biotransporter was tested to verify that the 4°C biotransporter would hold an internal temperature within the range of +2 to +10°C, for a minimum of 48 hours. All testing was conducted with the biotransporter's set point at +4°C, unless otherwise specified. Tests were performed to baseline the requirements for the power supplies, to verify the battery pack design, and to ensure that the biotransporter unit was capable of maintaining the selected temperature over a range of ambient temperatures, for the required period of time.

3. Test Procedure

Baseline requirements for batteries and power supplies were determined by means of nominal current consumption tests. The biotransporter was connected to a 12Vdc power supply and instrumented to record current consumption and internal temperature while the ambient temperature was +24 ±1°C. The biotransporter drew approximately 0.2 amps while heating, and about 1.6 amps while cooling. The current demands appeared stable. The operation of the biotransporter was tested during tem. It was found during this testing that the biotransporter could hold the +2°C to the + 10°C temperature range for ambient temperatures as low as -34°C and as high as +23°C. A final test was performed to determine the rate at which the temperature of the sample chamber would approach ambient temperature if power was removed. This last test was also used to estimate the rate at which chamber temperature would return to the set point when power was restored. It was found that with power removed the internal temperature of the unit would move toward ambient at a rate of approximately 1.1°C/hr when the ambient temperature was 15° to 20°C different than the internal temperature. When power is restored under these conditions, the internal temperature returns to thperature cycling in an environmental chamber. The temperature was cycled between 10°C and 28°C for a period of 72 hours. Each extreme was held for a period of 12 hours.

For this test, the biotransporter was loaded with simulated biosamples, precooled to +4°C beforehand. Temperature sensors were then installed in the unit. The biotransporter was powered by its lithium battery pack (BSP-BP). Results showed that temperature was maintained within the range of +2°C t o +10°C for nearly 59 hours. The maximum temperature differential that the biotransporter could tolerate and still maintain temperature was determined by testing in the environmental chambere setpoint at a rate of approximately 0.6°C / hr.

+4° C PASSIVE BIOTRANSPORTER

1. Development and Operation

A 4°C passive biotransporter was designed to maintain biospecimens at temperatures between +2°C and +10°C for a minimum of 72 hours. The unit was used for transport of specimens from Moscow to NASA-Ames in the baggage hold of a passenger airliner. The biotransporter consisted of three nested containers. The innermost container, which held the biosamples, was an aluminum can with a close-fitting lid. The second container, which held the aluminum sample container, was a chest formed of polyethylene with Styrofoam insulation. Phase change gel could be inserted in this container, under and around the sample container. The outer container was an 'Anvil' shipping case custom manufactured to hold the second container surrounded on all sides by Styrofoam panels. The phase change gel used to provide passive cooling was a commercial product with a phase change point of 0.1°C. See Figure 8 for the basic configuration of the biotransporter.

2. Test Plan

The complete biotransporter was tested to verify that the 4°C passive biotransporter would hold internal temperature within a range of +1 to 10°C, for a minimum of 72 hours, for ambient temperatures ranging from -20 to +28°C.

3. Test Procedure

Phase change gel (layers 1, 2, and 3 - see Figure 8) was placed in the bottom of the polyethylene insulated container and covered with an aluminum sheet (layer 4). Then, at least 75 lbs. of dry ice was placed on top of the aluminum sheet. The container was closed and left for at least 48 hours, the goal being to bring the bottom three layers of phase change gel to -70°C. After 48 hours, the dry ice was removed and a single layer of phase change gel (at 4°C) was placed on top of the aluminum sheet. On top of this layer of 4°C gel, a 1/4-inch thick piece of closed foam was then placed (layer 6) sized to cover the entire surface.

The aluminum sample chamber was prepared with 15 Teflon sample vials mounted in three custom racks. These racks were filled with water and arranged as shown in Figure 8. In order to monitor simulated sample temperatures, thermocouples were placed inside the vials and submerged in the water positions indicated. The remaining space was filled with phase change gel preconditioned to 4°C. The sample container was then placed on top of the closed cell foam inside the polyethylene container. All containers were then closed and latched, and the entire assembly was placed into an environmental chamber. The chamber was programmed to simulate anticipated worst case ambient temperature conditions. The resulting temperature profile was 18 hours at 23°C, 6 hours at -20°C, 66 hours at 28°C, followed by a constant 23°C until any sample temperature exceeded the target values (ie. +1°C to +10°C). Results showed that the samples remained within the +1°C to +10°C temperature range for 11 days.

-70°C PASSIVE BIOTRANSPORTER (DRY ICE)

1. Development and Operation

The -70°C dry ice biotransporter was used to transport specimens in an airliner cargo hold from Moscow to NASA-Ames. The unit was designed to maintain biospecimens in a frozen state for a minimum of 48 hours. The construction of the biotransporter differed from the +4°C passive biotransporter in that the inner sample/dry ice container could hold five plastic-coated, wire-mesh baskets. The baskets were placed one on top of the other. The bottom three were used for biospecimens. The top two baskets were used for dry ice. Additional dry ice could be added to the insulated container up to a maximum of 160 lbs. In practice, it was possible to use this biotransporter without the wire-mesh baskets to allow the maximum amount of dry ice to be added. The insulated container fit into an exterior insulated case suitable for shipping.

2. Test Plan

Tests were conducted to ensure that the biotransporter was capable of maintaining the required temperature range over a period of at least 48 hours.

3. Test Procedure

Because the ARC environmental chamber could not accommodate the fully-assembled -70°C biotransporter, only the inner insulated container was used. This was considered appropriate since use of the external insulated shipping case would only enhance the biotransporter's performance. Three sample racks were prepared containing five teflon vials each with a thermocouple inserted through the top of the center vial of each rack. The racks were individually wrapped in several layers of bubble packing material and each was placed in a different sample basket. The sample baskets were placed into the insulated container, one on top of the other, and the thermocouple leads were routed to the outside. A wind-up temperature recorder was placed in one of the three sample baskets. The fourth and fifth racks, filled with approximately 80 lbs of dry ice, were added and the cover was closed. The container was then placed in the environmental chamber. A thermocouple was attached to the outside of the container to record the ambient temperature. All four thermocouples were connected to a temperature recorder. After the temperatures of the internal thermocouples (three) dropped below -5°C, the environmental chamber's temperature control was set for 29±2°C and the chamber was started. The test was continued for 48 hours. Temperature print-outs were provided at 20-minute intervals throughout the test. At the 48 hour point the average sample chamber temperature was -50.1°C, with an average rate of change of +1.1°C per hour.

In actual use, with more than 100 lbs. of dry ice in the sample chamber, temperatures well below freezing (as evidenced by the large blocks of dry ice still in place) were maintained for 6 days.

BIOMAILERS

After biosamples were shipped to the U.S. in appropriate biotransporters, they were repackaged and shipped directly to investigators throughout the country using "biomailers". Two biomailer types were developed to ship samples using overnight mail to investigators. One type was an insulated package cooled by a water-ice solution capable of maintaining a temperature range of +1°C to +10°C for 48 hours. Another type was an insulated package cooled by dry ice, capable of maintaining a frozen state for at least 48 hours.

TABLE 1

SUMMARY OF HARDWARE BY EXPERIMENT

Experiment: Country	Flight	Ground
General U.S.S.R. Supplied Equipment:		
	Cosmos Biosatellite and Launch System Flight Primate Chair and Accompanying Hardware (Primate-Bios) Flight Rat Holding Facility and Accompanying Hardware (Bios-Vivaria) Flight Data Recording Systems	Field Laboratory with Generators and Environmental Control Equipment (set up at recovery site) Biosatellite Mock-Up (Synchronous Flight Simulation) Rodent Tail-Suspension Cage Systems
Circadian Rhythm and Temperature Regulation (K-7-35):		
I. U.S. Supplied	Circadian Rhythm / Thermoregulation Signal Processor (CR/T-SP) Interface Box (CR/T-IB) & Interconnecting Cables Sensors and Attachment Supplies	Ground Readout Unit (GRU) GRU / CR/T-SP Computer Software Signal Simulator Data Listing Software (VITAGRAPH)
II. U.S.S.R. Supplied	Temperature Transmitters (for implantation and axillary temperature measurement) R-Wave Signal from EKG Transmitter (for measurement of heart rate)	
Functional Neuromuscular Adaptation to Spaceflight (K-7-33):		
I. U.S. Supplied		Biopsy Sample Containers, Tools, Primate Restraint Chair (for postflight biopsy) TEAC XR-510 Tape Recorder and Tapes (for transfer of raw EMG data) Biotransporters (see Rodent Experiments)
II. U.S.S.R. Supplied	Foot Lever System Muscle EMG implants	Liquid Nitrogen, Freon 12, and Dry Ice (for biotransporters)

TABLE 1 (cont.)

SUMMARY OF HARDWARE BY EXPERIMENT

Experiment: Country	Flight	Ground
Effect of Spaceflight on Vestibular Ocular Reflex (VOR) (K-7-30):		
I. U.S. Supplied		Primate Chair (with modified head restraint) Head-Fixed Coil System Rotator Three-Axis Planetary Optokinetic Stimulator Computer System and Software (for eye position data recording)
II. U.S.S.R. Supplied		Zeiss Operating Microscope
Vestibular Primary Afferents in Normal, Hyper-, and Hypogravity (K-7-31):		
I. U.S. Supplied		Two-Axis motor-driven Rotator and Animal Restraintwith Controlling Computer Two-Axis Hand Driven Rotator and Animal Restraint (for on-site testing) Computer and Software (for template isolation of single action potentials from multiple train unit) Buffer and Physiological Amplifiers Hydraulic Microdrive (for electrodes), 100 Microelectrodes, and 12 Electrode Platforms Surgical Supplies (for head implant surgery)
II. U.S.S.R. Supplied		Active Head Movement Test Apparatus

TABLE 1 (cont.)

SUMMARY OF HARDWARE BY EXPERIMENT

Experiment: Country	**Flight**	**Ground**
Radiation Dosimetry and Spectrometry; Passive Systems (K-7-41):		
I. U.S. Supplied	300 Thermoluminescent Detectors (TLDs) 20 CR-39 Plastic Nuclear Track Detectors (PNTDs) 2, 4-Channel Temperature Recorders and external temperature sensors (8). 3, ^{59}Co Activation Foils (5 x 5 x 0.6 cm), 150g 4, ^{6}Li (n, a) T Foils 8, ^{232}Th Fission Foils	IBM Compatible Computer, Computer Interface Unit, and System Software for Temperature Recorders Dosimeter Transport Box Field Tester for Temperature Recorders
II. U.S.S.R. Supplied	Nuclear Track Emulsions ATR-4 Mounting Devices	
Rodent Biosample Experiments (see section III-A):		
I. U.S. Supplied		+ 23^{0}C Active biotransporter + 4^{0}C Active biotransporter + 4^{0}C Passive biotransporter -70^{0}C Passive biotransporter (dry ice) Cell Culture Equipment Biosample Containers, Tools, and Other Supplies
II. U.S.S.R Supplied		Liquid Nitrogen, Freon 12, and Dry Ice (for biotransporters)

TABLE 2

SUMMARY OF 2044 TEST PARAMETERS

Functional Test

- Verified operation of each function

Thermal Cycle Test

- Storage: -16°C to +62°C, 1 cycle - 1 hour duration at extremes (CR/T)
- Operation: -16°C to +62°C, 5 cycles - 1 hour duration at extremes (CR/T)
- Operations: -35°C to +55°C, 5 cycles (temperature recorders)

Random Vibration Test (3 axis, 60 seconds duration each)

• 20 HZ	• 0.005 G2/HZ
• 20-50 Hz	• +6 db/oct
• 50-1000 Hz	• 0.03 G2/HZ
• 1000-2000 Hz	• -6 db/oct
• Composite	• 6.5 G (rms)

Lot Sample Test

- Verified operational lifetime of nominal battery pack.

Burn-In Test

- Screening test for commercial device, +62°C for 100 hours

Impact Test (3 axis, both directions)

- 90 G Impact with a duration of 10 msec

High Humidity Test

- 98% at 25°C for 96 hours

Pressure Differential Test

- Storage: 1.0 microtor, 4 hours duration (temperature recorder)

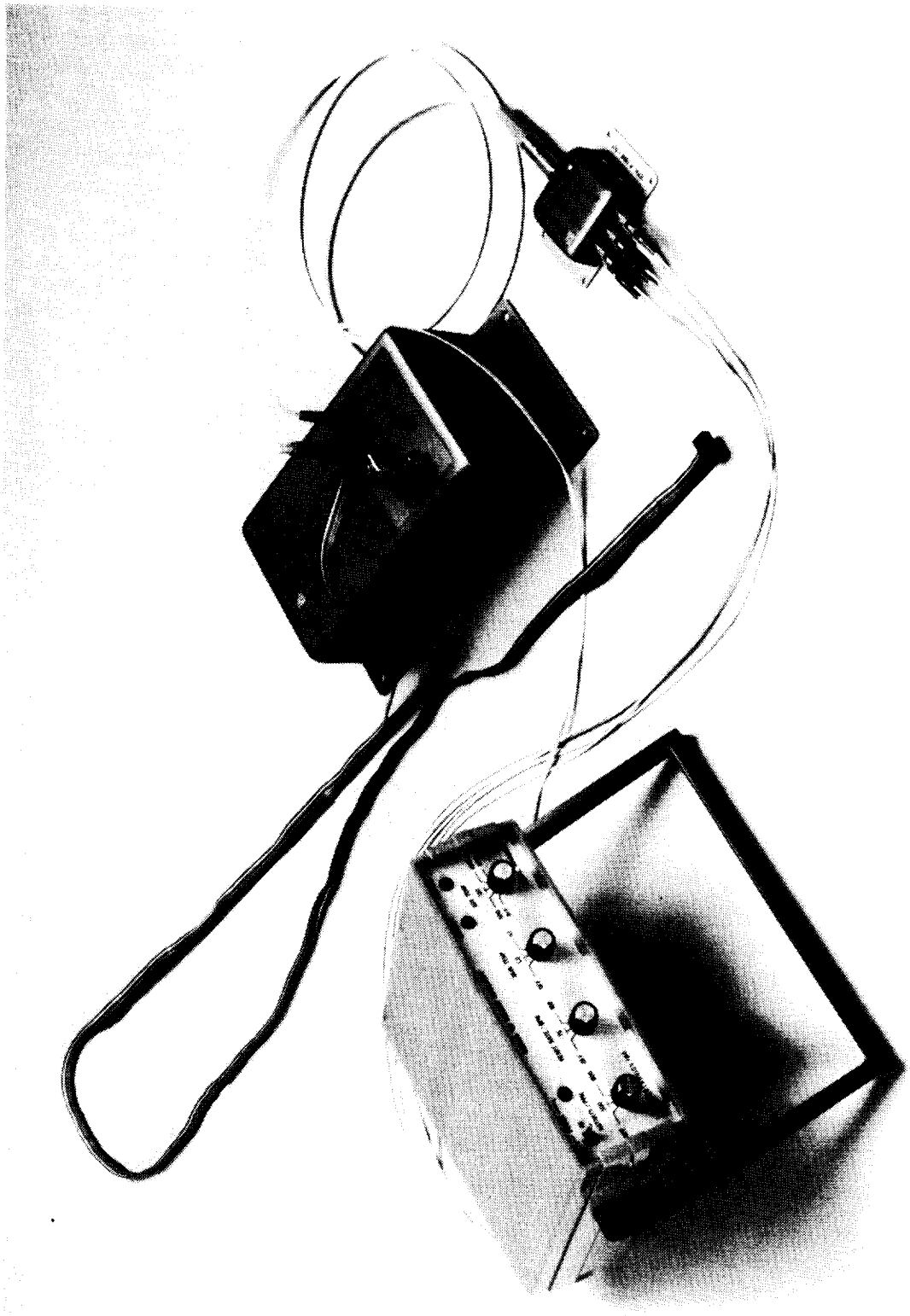

Figure 1. CR/T flight signal processor/recorder with ground-based signal simulator.

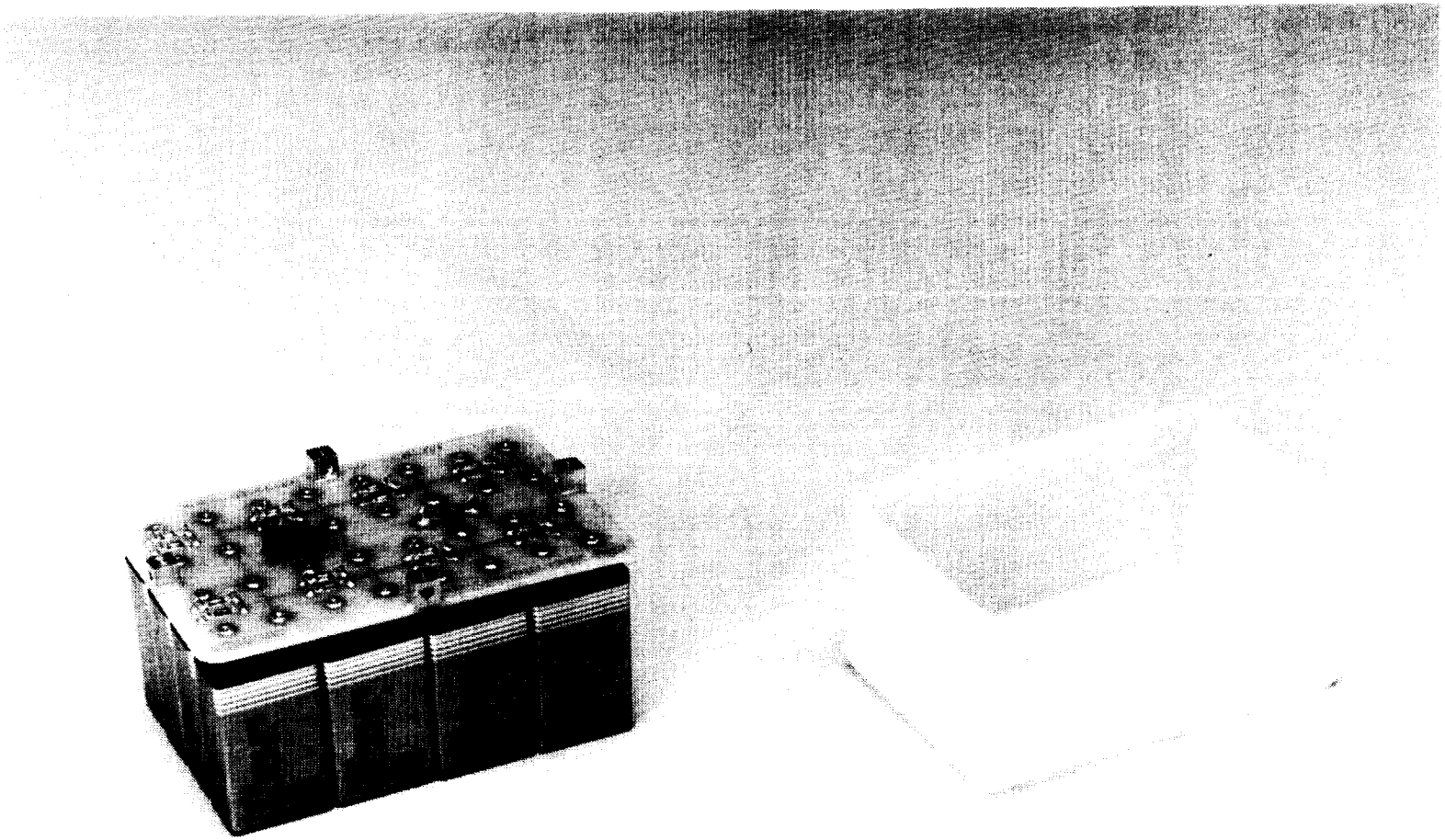

Figure 2. CR/T flight hardware (battery pack. disassembled showing 16 lithium batteries).

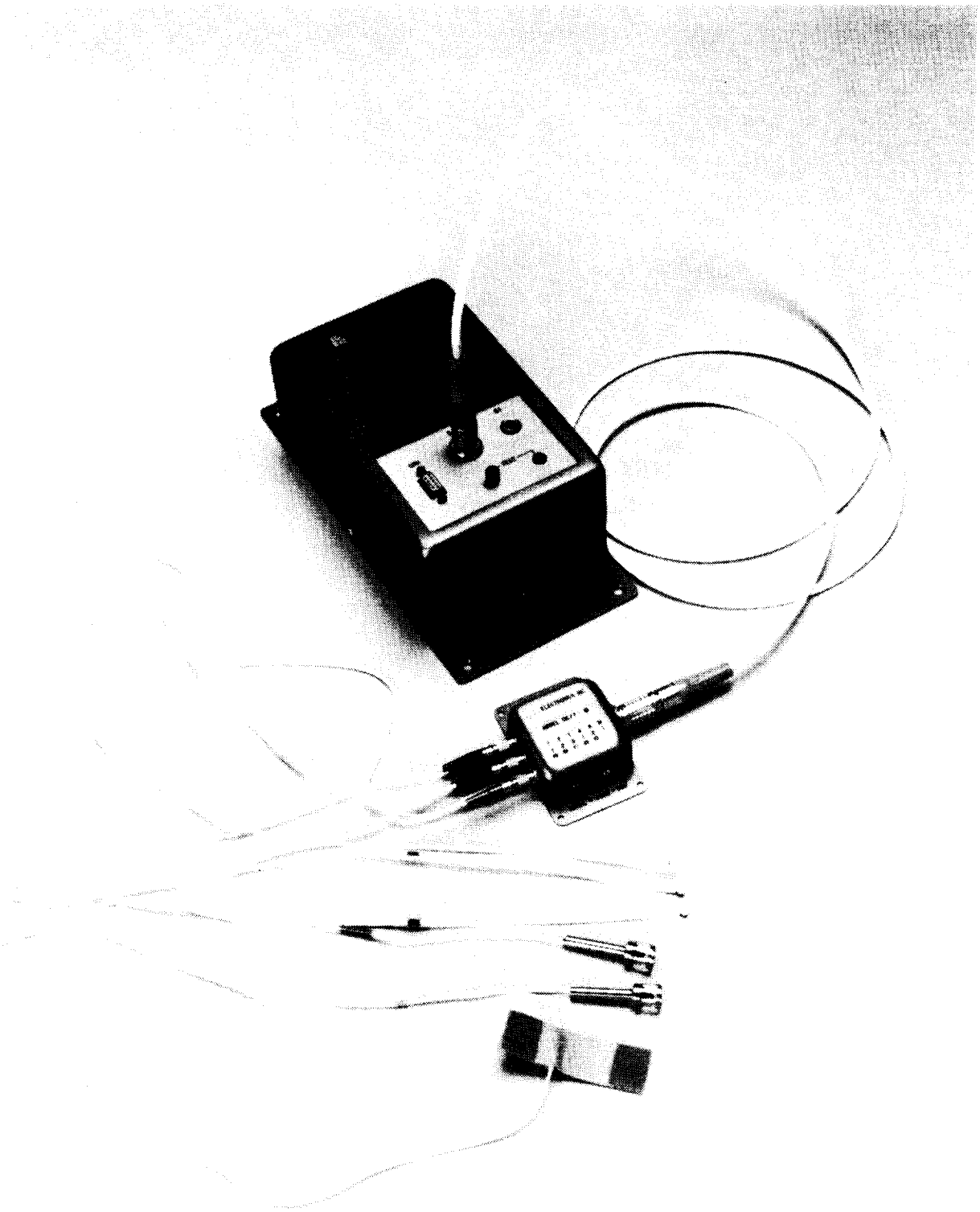

Figure 3. CR/T flight hardware (signal processor, interconnection unit 6 U.S. sensors).

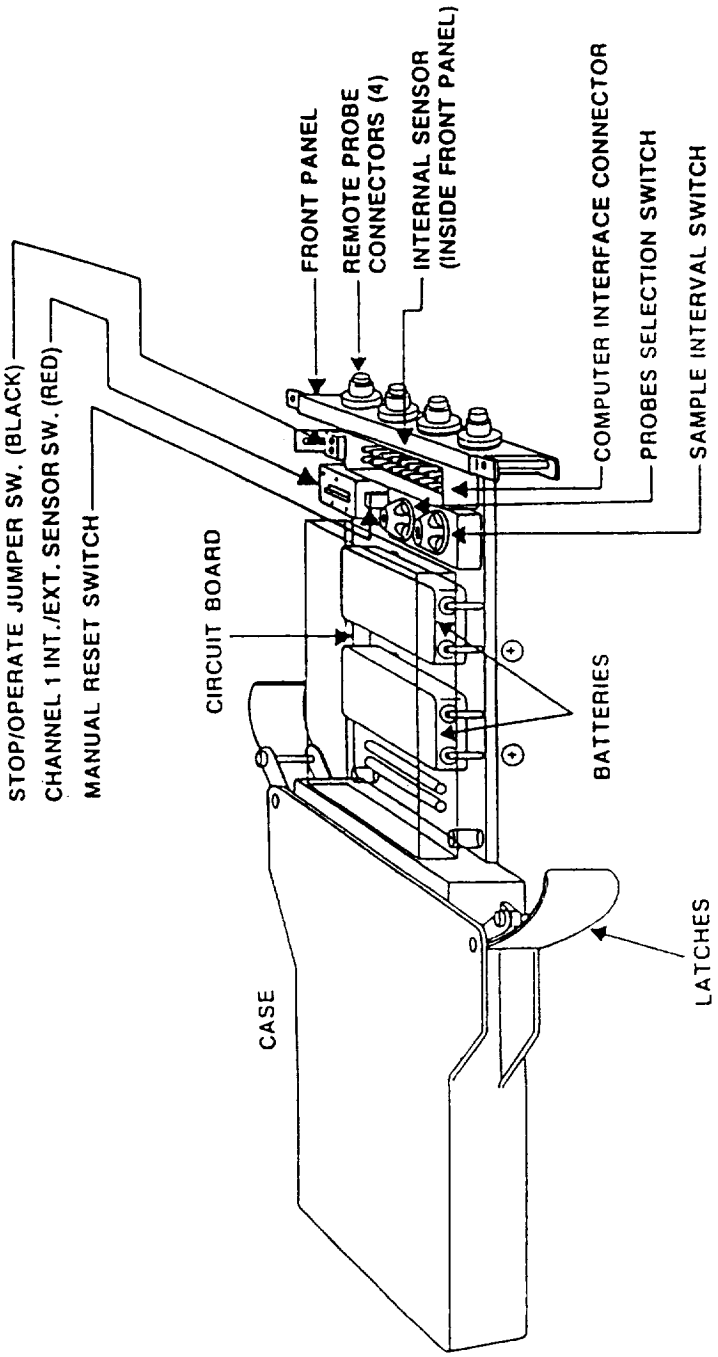

Figure 4. 4-Channel temperature recorder.

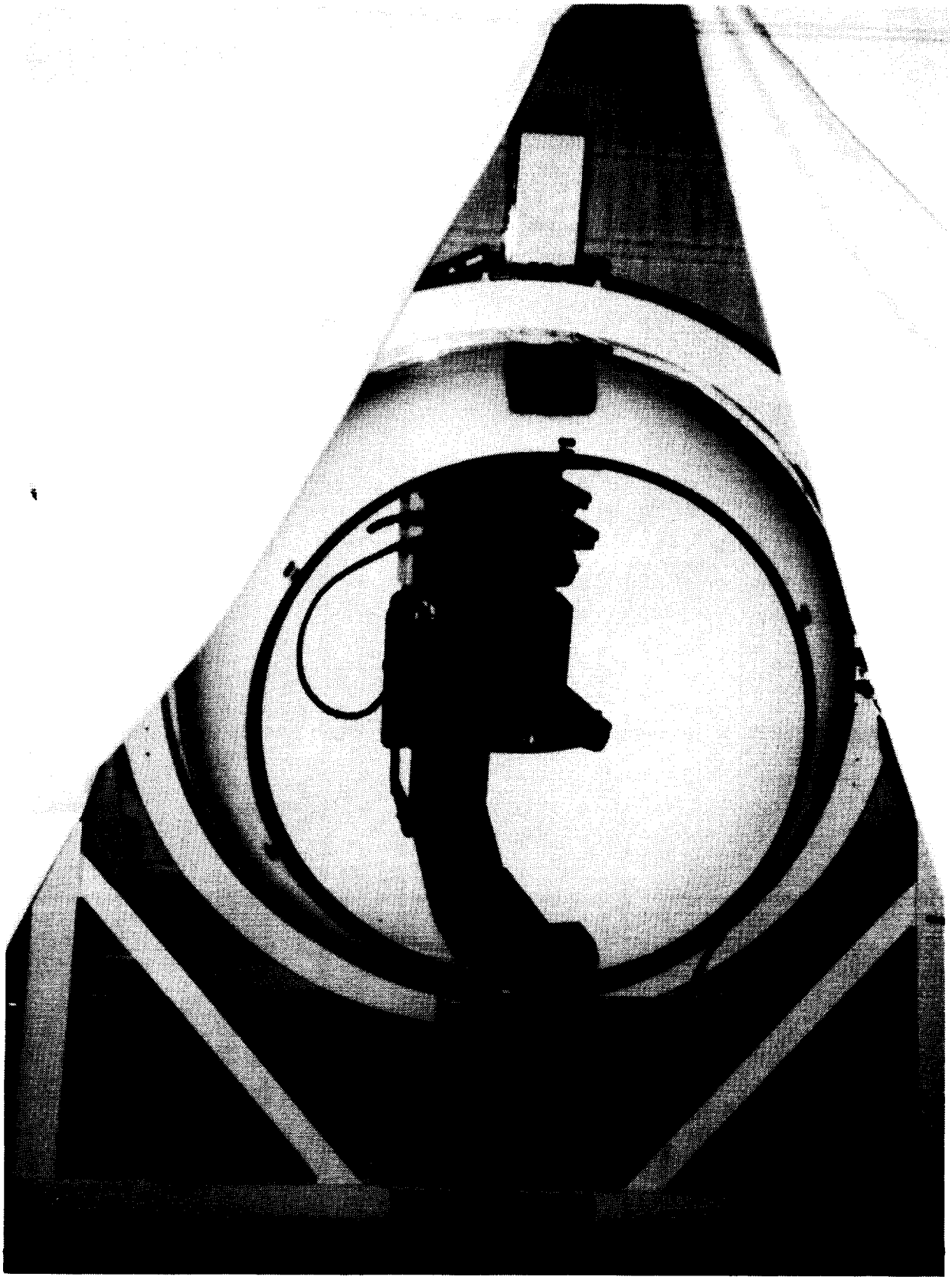

Figure 5. Optokinetic rotator.

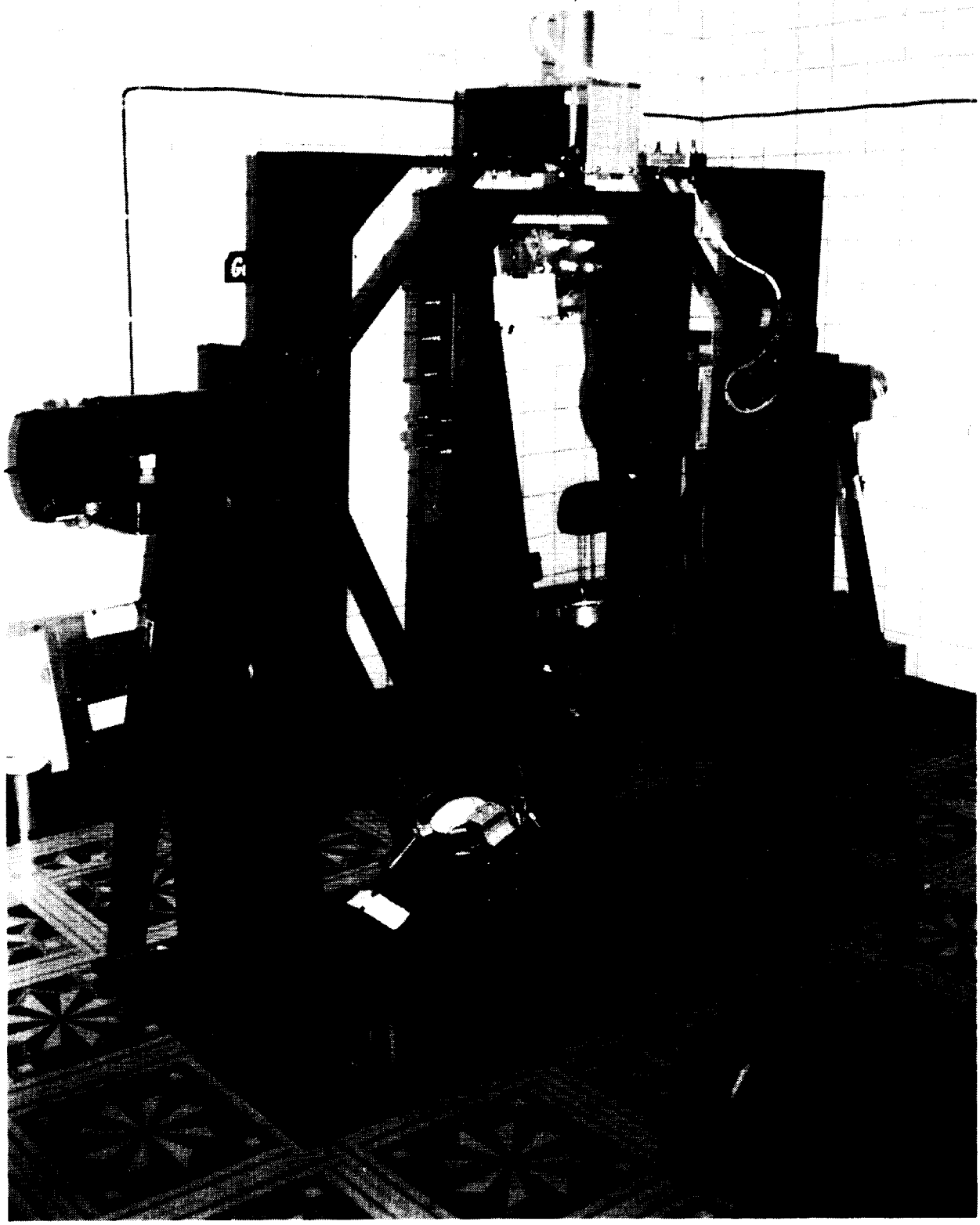

Figure 6. Three-axis stimulator.

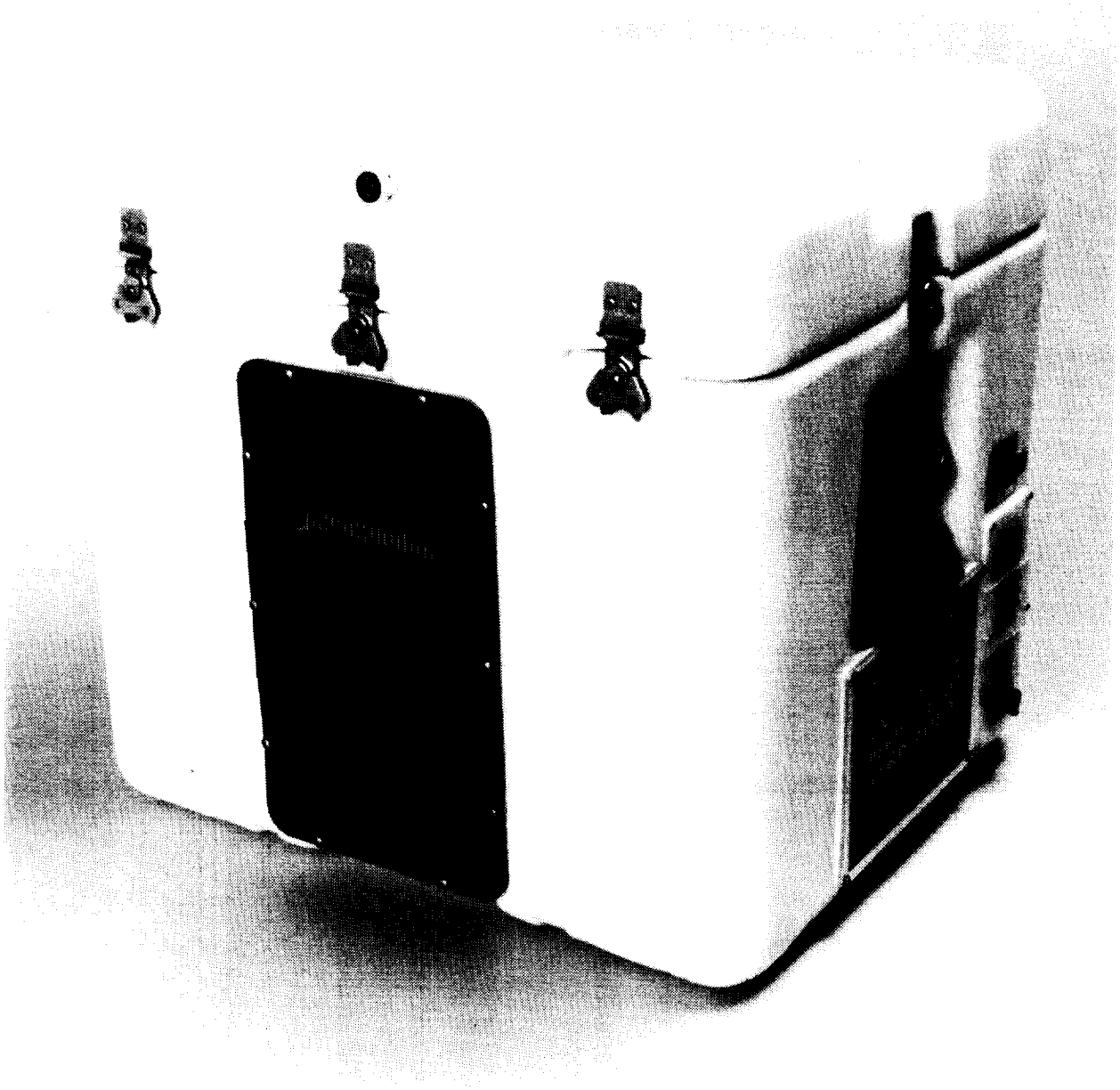

Figure 7. +4°C biotransporter.

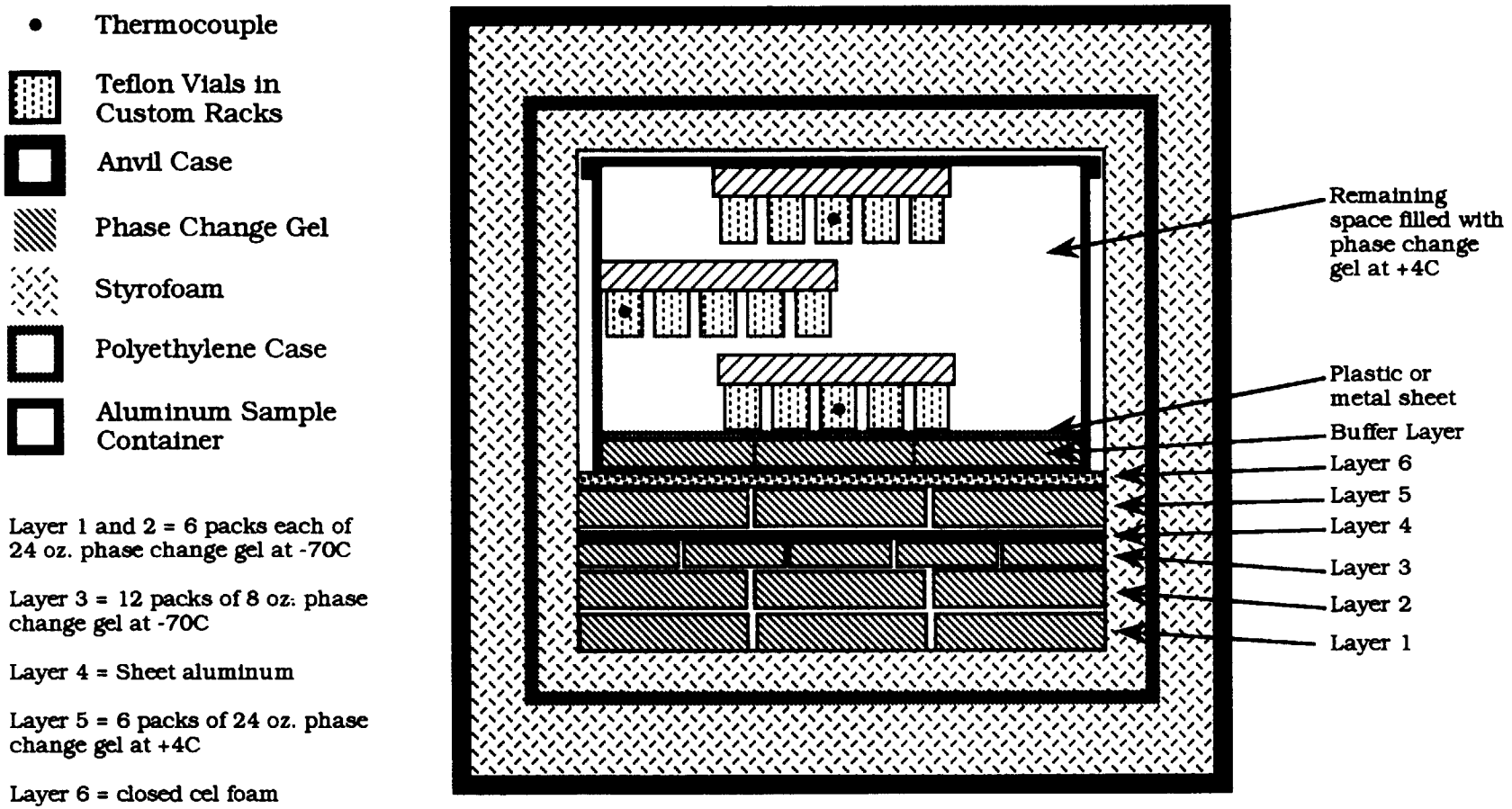

Figure 8. Passive +4° C biotransporter test configuration.

III. SCIENCE REPORTS

A. RAT STUDIES

EXPERIMENT K-7-01

BONE BIOCHEMISTRY, MINERAL DISTRIBUTION AND CALCIUM REGULATING HORMONES IN RATS AFTER THE COSMOS 2044 BIOSATELLITE FLIGHT

PART I: CIRCULATING PARATHYROID HORMONE AND CALCITONIN IN RATS AFTER SPACEFLIGHT

PART II: COLLAGEN, CROSS-LINKS, OSTEOCALCIN AND MINERAL CONCENTRATIONS IN THE DIAPHYSIS OF RAT FEMURS

Principal Investigator:

Sara Arnaud, M.D.
NASA Ames Research Center
Moffett Field, CA

Co-Investigators:

G. Mechanic *
M. Yamauchi
University of North Carolina
Chapel Hill, NC

P. Buckendahl
University of California
Santa Cruz, CA

T. Bromage
Hunter College
New York, NY

P. Fung
R. Grindeland
NASA Ames Research Center
Moffett Field, CA

G.N. Durnova
I.A. Popova
A. Kaplansky
Institute of Biomedical Problems, U.S.S.R.

* Deceased 1/5/91

EXPERIMENT K-7-01

PART I: CIRCULATING PARATHYROID, HORMONE, CALCITONIN AND OSTEOCALCIN IN RATS AFTER SPACEFLIGHT

S. Arnaud, P. Fung, I.A. Popova, E. Morey-Holton and R.E. Grindeland

ABSTRACT

Parathyroid hormone and calcitonin, two major calcium regulating hormones, were measured in the plasma of 5 experimental groups of 5 rats to evaluate post-flight calcium homeostasis after the 14 day Cosmos 2044 flight. Parathyroid hormone values in the flight animals (F) were slightly higher than in the appropriate cage and diet controls (S) (44±21 vs 21±4 pg/ml, $p<0.05$), but the same as the vivarium controls (V) who had different housing and feed schedules. Neither V nor S showed the hyperphosphatemia and hypermagnesemia found in F, features of early renal insufficiency (creatinine in F = 0.9±0.3 vs S = 0.6±0.1 NS). Plasma calcitonin in F was the same as basal (B), and lower than V, but not S controls. This difference in F and V (22±11 vs 49±16 pg/ml, $p<0.05$), proved to be due to failure of circulating calcitonin in F to show the normal age-dependent increase in growing rats that we demonstrated in age-matched controls in a separate experiment. Basal values for parathyroid hormone and calcitonin were unchanged after two weeks tail suspension, a flight simulation model, in either 54 or 130 (T) day old rats. After 4 weeks serum calcium was higher and parathyroid hormone lower than in ambulatory controls used in a time course experiment. Post-flight circulating levels of parathyroid hormone appear to reflect disturbances in calcium homeostasis from impaired renal function of undetermined cause, whereas levels of calcitonin reflect depression of a normal growth process.

INTRODUCTION

The functional status of the parathyroid gland and the calcitonin producing cells of the thyroid is critical to the alterations in calcium and bone metabolism during space flight because of the major role each hormone has in their regulation (3). To date, measurements of parathyroid hormone in the serum of astronauts in space have been unrevealing, showing no change from pre-flight values post-flight (11, 13, 19). Calcitonin values were below the detection limit of the assay after the Skylab missions (11).

Post-flight histologic examinations of parathyroid and thyroid glands in small animals have been inconclusive. Bailey et. al. reported no morphologic changes in either the parathyroid or the thyroid of mice flown on the Apollo 17 flight (4). Plakhuta-Plakutina et. al. found focal hypertrophy of rat parathyrocytes with no generalized hyperplasia (17). The primary source of circulating calcitonin, C cells in the thyroid gland, have shown variable responses to individual space flights. Soviet histologists reported increased numbers of C cells that seemed to persist during recovery from the 3 week Cosmos 605 and 782 biosatellite missions (17). These changes were reversed in Cosmos 936 where animals showed moderate symptoms of thyroid hypofunction. C cell nuclear volume and number were low compared to counts in cells from rats centrifuged during the flight (18). Following the 7 day flight of Cosmos 1667, ultrastructure study of rat thyroid C cells revealed fewer total and active cells than in the controls (19).

The purpose of this experiment was to document the early post-flight levels of two calcium regulating hormones after a two week space flight. We recognized that both parathyroid

hormone and calcitonin have half lives shorter that the 8-11 hours that elapsed between landing and necropsy of the rats in Cosmos 2044 (3). Nevertheless, to our knowledge, circulating parathyroid hormone and calcitonin in rats have not been measured previously in any flight experiment, either in-flight or post-flight. We report post-flight evidence for impaired calcium homeostasis from exposure to space flight as well as the status of both hormones in the immediate post-flight period.

METHODS AND MATERIALS

Three separate experiments are described.

1. Flight Experiment

Experimental animals for the flight experiment were 5 groups of 5 male rats, aged 16-18 weeks. The details of the protocols and general procedures for feeding and necropsy for each control group, basal (B), vivarium (V), synchronous (S) and the 2 experimental groups, flight (F) and tail-suspension (T) are given in other papers (7, 24). Relevant to calcium homeostasis were feeding schedules of paste diet 4 times daily in F and S, and of a paste diet of the same composition, once daily in B, V, and T groups. The protocols were initiated in a staggered fashion so that, although there are slight differences in the ages of the rats at necropsy, the experimental period for all groups was 14 days except F (16 days). Food consumption was 9-10 g/d less in F than S and V controls. Average daily weight gains, g/day, during the experimental period were highest in V controls (4.6) than in any of the other groups, F (1.0), S (2.6), and T (2.6).

2. Flight Simulation Experiment

The time course of changes in hormone concentrations and serum calcium was determined in a flight simulation experiment (tail-suspension) conducted at Ames Research Center. Fifty-four animals, 35 days of age, averaged 155±6 g at the start of the experiment. After 4 weeks, the suspended group weighed 278±11 g and the weighted controls 285±6 g. Six control rats were bled by cardiac puncture after anaesthesia with methoxyflurane and then euthanized for four weeks. The same weekly necropsy schedule was carried out in 6 rats in which the hindquarters were elevated to eliminate weight bearing and to induce a cephalad fluid shift by the technique of Wronski and Morey (25).

3. Age and weight controls for flight experiment

The slower growth rates of Soviet that American experimental rats necessitated weight and age controls to determine the relative influence of weight and age on plasma calcitonin. At Ames Research Center twelve male Simonsen albino rats, aged 84±7 days, weighing 346±20 g, the same weights as the rats used in the flight experiment were bled by cardiac puncture under methoxyflurane anesthesia for weight controls. An additional 18 animals for a total of 30 animals were sacrificed at 110 (n=9), 120 (n=9) and 136 (n=12) days of age to serve as age controls for the flight experiment. At necropsy body weights in the age controls ranged from 358-487 g. Blood was obtained for hormone assay by decapitation, as in the flight experiment.

ANALYTICAL METHODS

Body and adrenal weights were recorded at necropsy, 8-11 hours after landing in F or 1-2 hours after being taken from suspension in T. Blood was collected through a heparinized funnel after decapitation, plasma separated, stored at -20 °C and shipped on dry ice from Moscow, USSR to Ames Research Center, Moffett Field, CA, USA.

Plasma calcium, magnesium, phosphorus, and protein were determined in Dr. Merrill's laboratory (11). Parathyroid hormone and calcitonin were measured by radioimmunoassay kits (Nichols, Inc., San Juan Capistrano, CA.) modified for samples of 50 ul. The parathyroid hormone assay uses an antibody raised to an N-terminal fragment (1-34) of human hormone and human standard. The calcitonin assay uses an antibody raised to synthetic human hormone, human standards and label. Both assays have been biologically validated in the rat by Kalu et al (10). Intra-assay and inter-assay variation for the parathyroid hormone was 5.6 and 10.7% respectively, and for the calcitonin assay, 4.2. and 8.2%. To minimize the effects of assay variation, samples from each experiment group were included in each assay.

STATISTICAL ANALYSIS

Differences in 5 groups in the flight experiment and in the 2 groups of the 4 week suspension controls were evaluated by 1 way analysis of variance (ANOVA) and the Student-Newman-Keuls test for differences in the means (6). The student's *t* test was used to evaluate the means of the flight experiment (results in Table 10, the groups in the age and weight control experiment and in addition to the ANOVA, the control and suspended values at each time point in the 4 week flight simulation experiment. Interrelationships among the parameters measured in the 25 animals in the flight experiment were determined by a regression analysis program from SPSS, Inc. (16). Linear regression programs were used to evaluate the suspension, age and weight control studies done at Ames Research Center (6).

RESULTS

Values for age, body weight, adrenal weight and parameters of calcium homeostasis in the 4 groups of the flight experiment are listed on Table I. The same data for the 5th group, T, is listed on Table 2 to facilitate comparison with F. ANOVA revealed group differences in body weight ($p<0.001$), adrenal weight ($p<0.05$), total protein ($p<0.01$), magnesium ($p<0.005$), phosphorus ($p<0.005$), creatinine ($p<0.05$), parathyroid hormone ($p<0.05$) and calcitonin ($p<0.05$). The Students *t* test showed differences in parameters in different groups as enumerated on Table I, and between F and T as indicated on Table 2. Parathyroid hormone in F was higher than in S, the appropriate cage and diet control (Figure 1a). Calcitonin was the same in all groups except V that was higher than B ($p<0.05$) (Figure 1b).

Table 2 compares the results of determinations in T to F to evaluate tail suspension as a model for space flight. Only serum creatinine ($p<0.01$) and total protein ($p<0.01$) were different in T than F. Results of the 4 week simulation study in rats 12 weeks younger than in the flight experiment are depicted in Figure 2. Parathyroid hormone showed no change from basal as a function of time during the 4 weeks of suspension. However, parathyroid hormone in the 4th week was lower in suspended that the 4th week control animals (34±5 vs 48±10 pg/ml, $p<0.015$). Concurrent 4th week total serum calcium was higher in suspended than controls (10.8±.3 vs 10.3±.3 pg/ml, $p<0.01$). There were no differences in weeks 2 and 3 of suspension. Calcitonin was the same at all time points in both control and suspended rats and ranged from 10.9±2 to 12.6±2 ph/ml in the controls and 11.1±2 to 13.0±3 pg/ml weekly in the suspended rats. The age controls for the flight experiment showed calcitonin in rats aged 110, 120 and 136 days to be 19.2±4.5, 23.5±4.3, and 24.8±6.5, pg/ml, as illustrated in Figure 3, with values in 136 day old rats higher than 110 day old animals, $p<0.05$. The 84 day old weight controls showed average calcitonin levels of 17.6±4, the same as average values in the 110 day old rats in B.

Individual calcitonin values in this group or the older age controls were unrelated to body weight ($r=-0.211$ in 12 or $r=0.289$ in 30 rats).

The interrelationships in the parameters of calcium homeostasis in the flight experiment (B,V,S,F,T) were examined by a correlation matrix of all the variables measured. The r values of variables relating to the hormones measured, adrenal weight and creatinine are listed on Table 3. Noteworthy for influences of adrenal hyperactivity in this flight are higher adrenal weights in rats with lower body weights, lower plasma total protein concentrations, and lower levels of both parathyroid hormone and calcitonin. While creatinine values in F were not different from other groups because of variability, the relationships between creatinine and total protein, phosphorus and magnesium are helpful in identifying dehydration as a factor in the impaired clearances of these two ions. In addition to the r values on Table 3, magnesium correlated with phosphorus ($r=0.474$, $p<0.05$) and calcium with total protein ($r=0.575$, $p<0.005$).

DISCUSSION

Measurable differences in opposite directions for apparently unrelated reasons, were found in plasma concentrations of both parathyroid hormone (PTH) and calcitonin (CT) in rats within 8-11 hours following space flight. Because of the short half-lives of the hormones, the differences are indicative of the function of the calcium endocrine system during the first 8-11 hours post-flight. The values also reflect impaired renal function and delayed development of the C-cells of the thyroid in the flight group that must have occurred during the preceding two weeks in space.

Slightly increased plasma PTH in the flight group, compared to the appropriate diet and cage controls (S), were indicative of mild secondary hyperparathyroidism, most likely related to impaired kidney function. The data that supports this explanation in the flight animals are increases in plasma magnesium, phosphorus and a trend to increased creatinine, findings regularly associated with renal failure and found in no other group (2). The correlation of creatinine with phosphorus and magnesium points toward reduced renal clearance of these ions and impaired renal function as the source of hyperphosphatemia and hypermagnesemia in F. Additional evidence of impaired renal function is found in the increased concentration of blood urea nitrogen in F, enumerated in another paper in this volume (12).

Neither frank hypocalcemia that invariably provokes, nor hypercalcemia that suppresses the secretion of PTH were found in the flight experimental groups (see Table 1). However, individual rats, showed an inverse relationship between total serum calcium and PTH, (see Table 3) evidence of the well known negative feedback system that regulates PTH secretion within the normal range of serum calcium. The highest serum calcium levels of the 5 groups were in S, the group with the same caging and feed schedule as the flight animals, and, therefore, the appropriate control for F. The rat is a species in which serum calcium is sensitive to dietary intake (1).

There is also the possibility that the stress of landing and corticosterone excess may have contributed to the modest increase in PTH in F compared to S. The stimulus for secondary hyperparathyroidism from glucocorticoid excess is thought to be due to reduced intestinal absorption of calcium followed by reduced plasma calcium (5). This explanation seems unlikely since the rats with the largest adrenals were not the flight group, but the synchronous controls whose hormone levels were appropriately low for their level of plasma calcium. If increases in PTH were related to adrenal hyperplasia, one might expect plasma levels to relate positively to adrenal weights; we found the opposite.

Circulating CT was higher in the normal V than B group, but the same in B and F. Age and growth dependent increases in CT are reported in aged rats (1), and normal 6-12 year old children (22), and in growing rats (21). The circulating values for CT in rats in the flight experiment were correlated, in a linear fashion, with the weight of the animal, similar to the observations of Monsour et al who found the number of calcitonin-containing cells in the thyroid glands of male Wistar rats weighing 320-400 g, 100 days of age, related to body weight (13). To evaluate the relative roles of chronologic age or body weight on circulating calcitonin, we conducted an experiment that controlled for ages and body weights in the flight experiment rats. The results of this indicate that the differences in B and V can be attributed to chronologic age. This implies that values in the flight animals, relative to their aged matched controls, V, were due to generalized failure of normal development with age, rather than failure of weight gain per se. The observation of fewer C cells in the thyroid glands of the flight that control animals following the Cosmos 1667 7 day flight is consistent with this notion (19), but we cannot identify the specific developmental abnormality.

The renal status of the flight animals probably did not influence their CT levels significantly since an underfunctioning kidney is more often associated with higher than lower blood levels of hormone (8). The other complication of space flight, stress, for periods up to 14 days has not been observed to alter plasma CT (15).

The adequacy of the tail-suspension model as a simulation for calcium regulating hormone status is an important question to resolve. Differences in the measures of protein metabolism, total protein and creatinine, that were found during flight simulation did not appear to influence calcium regulating hormone values (see Table 2). PTH was not affected by unloading the lower half of the skeleton after 2 weeks. However, after 4 weeks suspension, PTH levels tended to be suppressed, in association with increases in serum calcium, as observed in an immobilization study in humans (23). Plasma CT, on the other hand, in 110 day old rats (see Table 2 and Figure 1b) failed to show the normal increase with age after 2 week suspension, similar to F. Younger rats, whose plasma CT is relatively low, did not show an effect of suspension for as long as four weeks. It appears that the factors responsible for the normal increase in circulating peptide between 110 and 136 days of age in rats are vulnerable to both tail suspension and space flight. This indicates that the tail-suspension model mimics suppressed secretion, synthesis or other aspects of CT metabolism in the C-cells of the thyroid or other sources that is a consequence of space flight, but not the mild hyperparathyroidism that is probably secondary to impaired kidney function in the rats after space flight.

ACKNOWLEDGEMENTS

This work was supported by grants from the Biomedical Research Program 199-26-12-02 and -09, Space Biology 199-40-42-01, and Flight Projects 199-14-12-08.

REFERENCES

1. Armbrecht, H.J., T.V. Zenser, C.J. Gross, and B.B. Davis. Adaptation to dietary calcium and phosphorus restriction changes with age in the rat. Am.J. Physiol., 239:E322-E327, 1980.

2. Arnaud, C.D. Hyperparathyroidism and renal failure. Kidney International 4:89-95, 1973.

3. Aurbach G.D., S.J. Marx, and A.M. Spiegel. Parathyroid hormone, Calcitonin and the Calciferols In: Textbook of Endocrinology, Ed R.H. Williams, W.B. Saunders Co, 1981. pp 922-1031.

4. Bailey O.T., L.M. Kraft , H.R. Brashear, and A.V. Talmage. The effects of cosmic particle radiation on pocket mice aboard Apollo XVII: Appendix III. Thyroid and parathyroids. Aviat. Space Environ. Med. 46:650-652, 1975.

5. Ferretti, J.L., L. Bazan, D. Alloatti, and R.C. Puche. The intestinal handling of calcium by the rat in-vivo as affected by cortisol effect of dietary calcium supplements. Calc. Tiss. Res. 25:1-6, 1978.

6. Glantz S. Primer of Biostatistics. New York: McGraw-Hill, 1987.

7. Grindeland R.E., M.F. Vasques, R.W. Ballard, and J.P. Connolly . Cosmos 2044 Mission Overview. J. Appl Physiol. 73: Suppl.:1S-3S, 1992.

8. Hyenen, G. and P. Francimont. Human calcitonin radioimmunoassay in normal and pathological conditions. Eur. J. Clin. Invest. 4213-22, 1974.

9. Kalu, D.N., R. Lockerham, P. Uy Byung, and B.A. Roos. Lifelong dietary modulation of calcitonin levels in rats. Endocrinology 113:2010-2016, 1983.

10. Kalu D.N., E.J. Masoro, and B.P. Yu, et al. Modulation of age-related hyperparathyroidism and senile bone loss in Fischer rats by soy protein and food restriction. Endocrinology 122:1847-1854, 1988.

11. Leach C.S. and P.C. Rambaut. Biochemical responses of the Skylab crewman: an overview. In: Johnston R.S., L.F. Dietlein, eds. Biomedical results from Skylab. Wash.DC:NASA SP-377, 204-216, 1977.

12. Merrill A.H, R.E. Mullens, R.E. Grindeland, and I.A. Popova. Analysis of plasma from Cosmos 2044 Rats. J. Appl. Physiol. 73:Suppl.:132S-135S, 1992.

13. Monsour P.A., B.J. Kruger, and A. Barnes. Calcitonin cell population and distribution in the thyroid gland of the rat. J. Morph. 186:271-278, 1985.

14. Morey-Holton E.R., H.K. Schnoes, and H.F. DeLuca, et. al. Vitamin D metabolites and bioactive parathyroid hormone levels during Spacelab 2. Aviat. Space & Envir. Med. 59:1038-1041, 1988.

15. Morimoto S., A. Fausto, S.J. Birge, and L.V. Avioli. Effect of short- and long-term restraint stress on plasma calcium and calcitonin in the rat. Horm. Metab. Res. 18:818-820, 1986.

16. Norusis M.J. SPSS/PC+ for the IBM/XT/AT. SPSS, Inc., 1986.

17. Plakhuta-Plakutina G.I. Morphological distinctions of the rat thyroid and parathyroid following long-term space flights. Space Biol. Med. 13:113-118, 1979.

18. Plakhuta-Plakutina G.I. Effect of weightlessness and artificial gravity on the morphology of the thyroid gland (aboard KOSMOS-936). Archiv Anatomii, Gistologii i Embriologii 3:17-22, 1979.

19. Plakhuta-Plakutina G.I., N.P. Dmitriyeva, Ye.A. Amirkhanyan. The thyroid C-cell system in rats after space flight on the COSMOS-1667 biosatellite. Space Biol. Med. 22:26-32, 1988.

20. Pozharskaya, L.G. and V.B. Noskov. Hormonal regulators of calcium metabolism following spaceflights of various durations. Kosm. Biol. Aviakosm. Med. 24:18-20, 1990.

21. Roos, B.A., C.W. Cooper, A.L. Frelinger, and L.J. Deftos. Acute and chronic fluctuations of immunoreactive and biologically acute plasma calcitonin in the rat. Endocrinology 103:2180-2186, 1978.

22. Shainkin-Kerstenbaum R., B. Funkenstein, and A. Conforti, et al. Serum calcitonin and blood mineral interrelationships in normal children aged six to twelve years. Pediat. Res. 11:112-116, 1977.

23. Stewart, A.F., M. Adler, C.M. Byers, G.V. Segre, and A.E. Broadus. Calcium homeostasis in immobilization: an example of resorptive hypercalciuria. N. Eng. J. Med. 306:1136-40, 1982.

24. Vailas, A.C., R. Vanderby Jr., D.A. Martinez, R.B. Ashman, M.J. Ulm, R.E. Grindeland, G.N. Durnova, and A. Kaplansky. Adaptations of young adult rat cortical bone to 14 days spaceflight. J. Appl. Physiol. 73:Suppl.:45-95, 1992.

25. Wronski, T.J. and E.R. Morey-Holton. Skeletal response to simulated weightlessness: a comparison of suspension techniques. Aviat. Space Environ. Med. 58:63-68, 1987.

Table 1. Parameters of calcium homeostasis, and related measurements in rats after the Cosmos 2044 spaceflight and flight controls. (Mean ± SD).

	Basal	Vivarium	Synchronous	Flight
Age, days	109	129	127	123
Body weight, g	320 ± 10	363 ± 5[a,c,d]	343 ± 16[c]	338 ± 5[c]
Adrenal wt, mg/100 g BW	- - -	12.1 ± 1.1	14.6 ± 2.0[b]	13.0 ± 0.7
Plasma				
Total calcium, mg/dl	10.7 ± 0.36	11.0 ± 0.17	11.2 ± 0.09[b,c]	10.9 ± 0.36
Total protein, g/dl	6.5 ± 0.33	6.1 ± 0.33	6.8 ± 0.33[b]	6.7 ± 0.5[b]
Magnesium, mg/dl	1.32 ± 0.11	1.28 ± 0.11	1.24 ± 0.09	1.52 ± 0.11[a,b,c]
Phosphorus, mg/dl	6.1 ± 0.92*	7.2 ± 0.3[c]	6.6 ± 0.65	8.2 ± 1.12[a,c]
Creatinine, mg/dl	0.6 ± 0.09	0.6 ± 0.09	0.6 ± 0.09	0.9 ± 0.31
Parathyroid hormone, pg/ml	38.2 ± 12[a]	41.2 ± 9[a]	20.9 ± 4[b,c]	44.4 ± 21[a]
Calcitonin, pg/ml	27.3 ± 5	49.1 ± 16[c,d]	31.9 ± 17	21.8 ± 11[b]

[a]$p < 0.05$ vs S, [b]$p < 0.05$ vs V, [c]$p < 0.05$ vs B, [d]$p < 0.05$ vs F by the Student's t test.

*n = 4, n = 5 in all other means.

Table 2. Comparison of body weight, adrenal weight, and parameters of calcium homeostasis in the plasma of flight and tail-suspended rats from Cosmos 2044 (mean ± SD).

	Flight	Tail-suspension
Age, days	123	131
Body weight, g	338 ± 5	326 ± 17
Adrenal wt. mg/100 g BW	13 ± 0.7	15 ± 1.0
Total calcium, mg/dl	10.9 ± 0.36	10.7 ± 0.18
Total protein, g/dl	6.7 ± 0.5	5.8 ± 0.26*
Phosphorus, mg/dl	8.2 ± 1.1	7.1 ± 1.1
Magnesium, mg/dl	1.52 ± 0.11	1.32 ± 0.18
Creatinine, mg/dl	0.9 ± 0.31	0.4 ± 0.09*
Parathyroid hormone, pg/ml	44.4 ± 21	36.2 ± 23
Calcitonin, pg/ml	21.8 ± 11	23.4 ± 10

*Denotes difference $p < 0.01$.

Table 3. Correlation coefficients of parameters of calcium homeostasis in plasma, body and adrenal weights in rats from Cosmos 2044 experiment. (n = 25 except for adrenal weight where n = 20).

	Adrenal weight	Creatinine	Parathyroid hormone	Calcitonin
Body weight, g	–0.786**	–0.049	0.128	0.455*
Total calcium, mg/dl	0.002	0.176	–0.434*	0.156
Total protein, g/dl	–0.329*	0.542**	–0.475*	–0.278
Phosphorus, mg/dl	–0.195	0.573**	0.307	–0.105
Magnesium, mg/dl	–0.061	0.460*	0.041	–0.367
Parathyroid hormone, pg/ml	–0.505*	0.002	---	0.369
Calcitonin, pg/ml	–0.504*	–0.275	0.369	---

*Describes significance level <0.05 and ** <0.01.

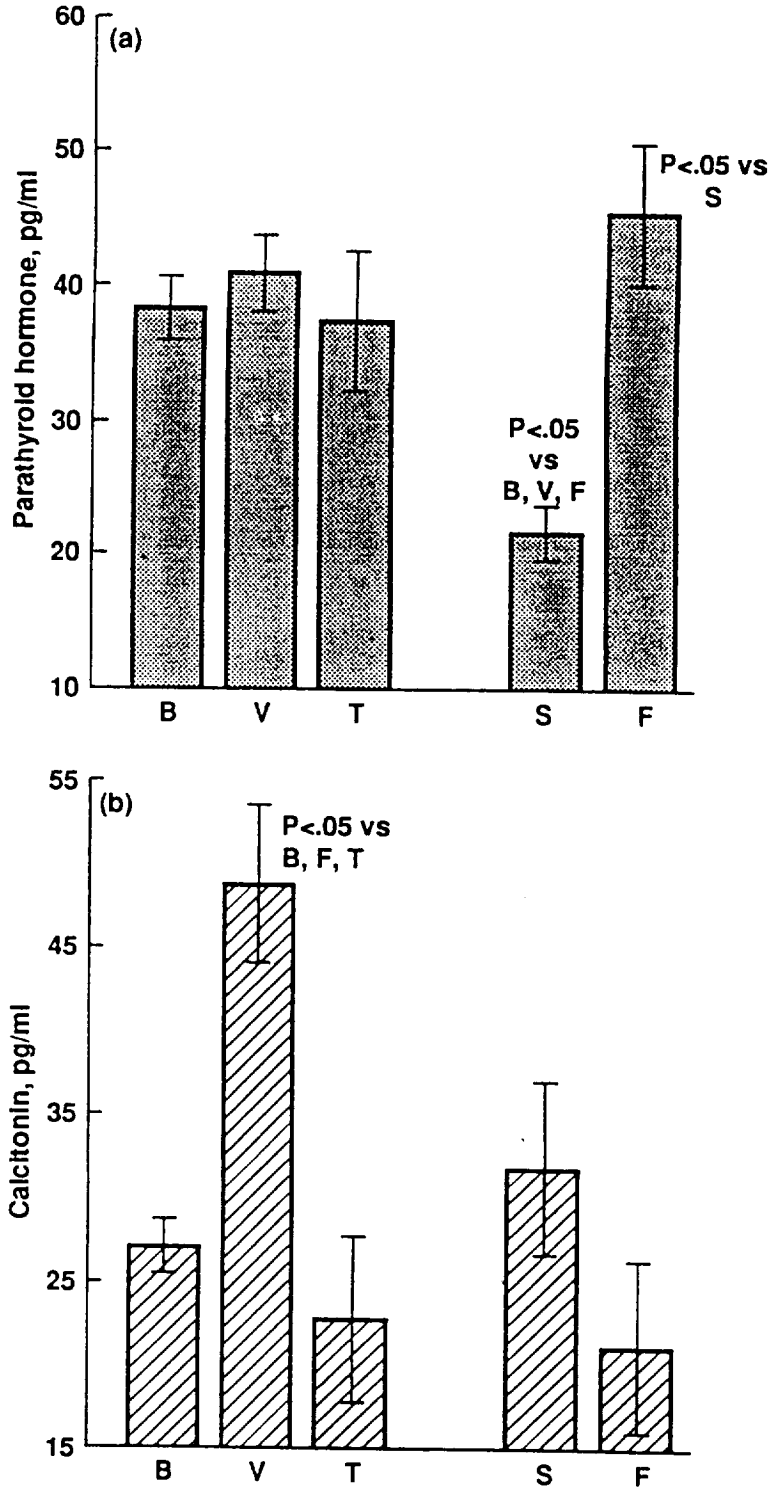

Figure 1. Mean (SD) concentrations of parathyroid hormone (PTH) (1a) and calcitonin (1b) in basal (B), vivarium (V), tail-suspended (T), synchronous (S), and flight (F) rats. The three groups B, V, and T had the same diet schedule and caging, which were different from F, whose appropriate diet and cage control is S.

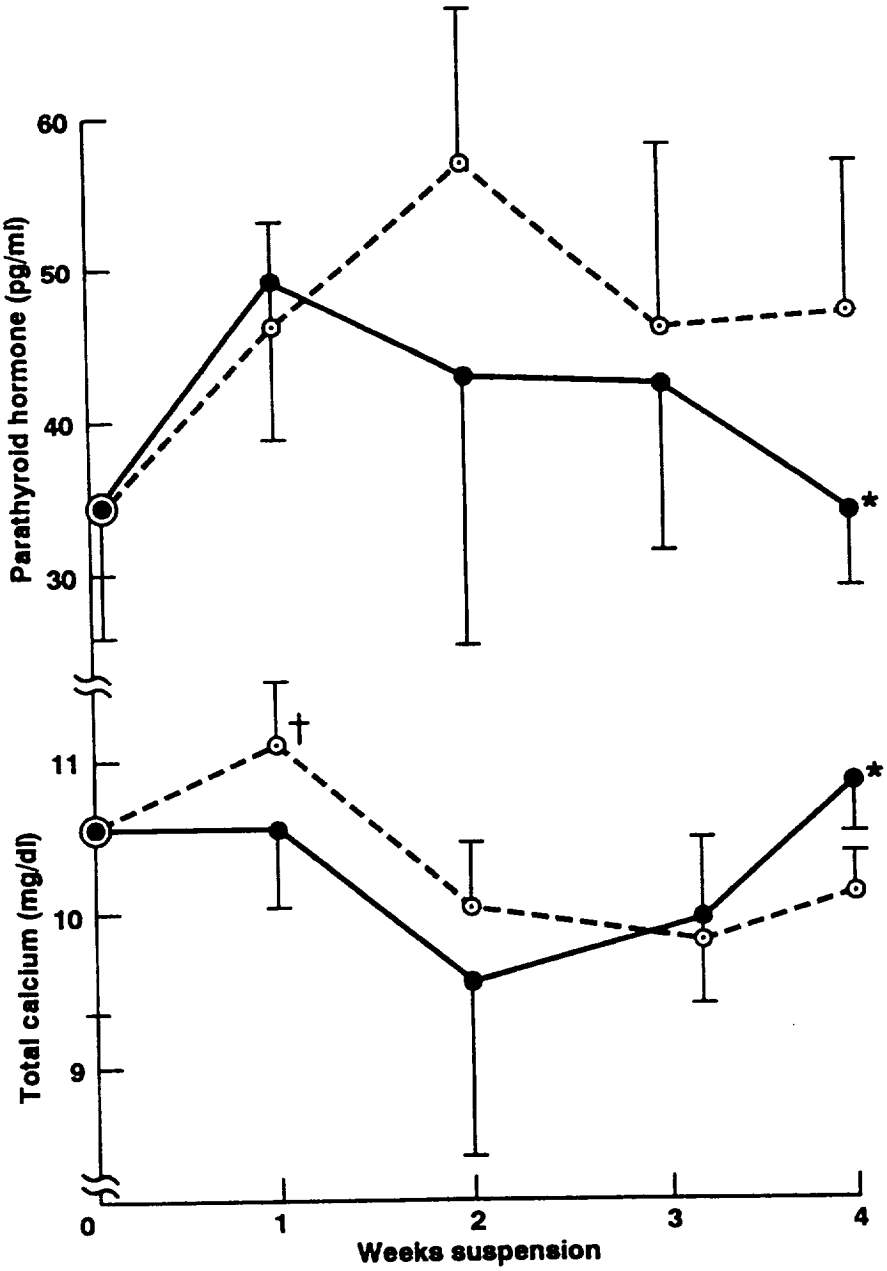

Figure 2. The time course of changes in total serum calcium and parathyroid hormone in 5–9-week-old tail-suspended rats (solid lines) compared with controls (dashed lines). There are no changes in the concentration of parathyroid hormone as a function of time in either group (n = 6/group). At 4 weeks, the hormone concentration is lower in the suspended than in the control group. Total serum calcium is higher during the first week in controls than during the third and fourth weeks, but there are no differences from basal in tail suspension.

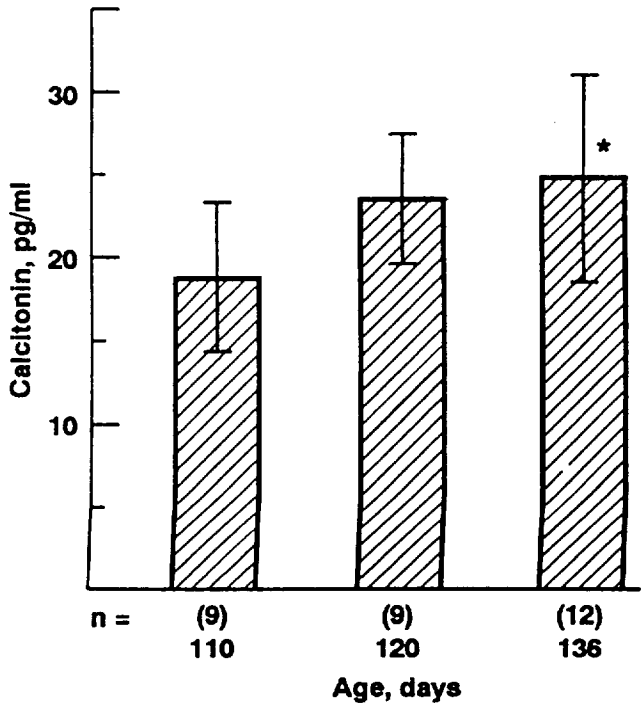

Figure 3. Mean (SD) plasma calcitonin in rats of differing age to match the age of animals in the flight experiment. Values at 136 days are higher than at 110 days, a phenomenon unrelated to their weight gain.

PART II: COLLAGEN, CROSS-LINKS, OSTEOCALCIN AND MINERAL CONCENTRATIONS IN THE DIAPHYSIS OF RAT FEMURS

M. Yamachi, S.B. Arnaud, P. Buckendahl, G. Durnova, T. Bromage, and G. Mechanic

ABSTRACT

The location and nature of the defect in collagen and mineral that occurs during space flight was determined in 4 sections of the femoral diaphyses from 18 week old rats flown aboard the Cosmos 2044 biosatellite (F). The controls were preflight (B), vivarium (V), synchronous or feed, cage and environmental factor controls for flight (S), and a flight simulation model (T). Examination of the microanatomy, tissue types, and alignment of collagen fibers by circularly polarized light revealed no group differences. At the molecular level, in both F and S, biochemical analysis of the most distal section of the diaphysis showed mineral deficits associated with reduced levels of the reducible cross-link, dehydrodihydroxy-lysinonorleucine (DHLNL). The ratio of the nonreducible cross-link, pyridinoline, to its lysl analogue was consistently lower in the distal than proximal sections of the groups tested (V,F,T) with no group differences. The flight simulation model, T, showed changes in cross-links similar to F and S, but no associated mineral deficit. Mean values of elements measured in each section of all groups revealed significant associations ($p<.005$) between the non-collagenous protein, osteocalcin (OC) and calcium ($r=0.774$), phosphorus ($r=-.624$) and DHLNL/HLNL ($r=.833$).

These findings locate mineral deficits in the distal femoral diaphysis of the growing rat femur during space flight. Changes in both OC and reducible cross-links are associated with the mineral deficit. Similar changes in the environmental controls (S) suggest that exposure to microgravity is only one aspect of space flight leading to these changes.

INTRODUCTION

American and Soviet scientists agree that the well documented deficits in bone in the skeletons of young rats after space flight reflect microgravity effects at the interface of mineral and matrix. After missions lasting one (20), two (16) and three weeks (17,24,25), the deposition of mineral is reduced. The ratio of calcium to hydroxyproline that normally increases in growing bone, remains at pre-flight levels (1).

The nature of the biochemical alteration(s) in either mineral or matrix that seems to inhibit mineralization remains unknown. Depressed mineralization of matrix could be due to defective synthesis of matrix (31), failure of maturation of newly synthesized collagen (27), abnormalities in non-collagenous proteins (21,23) or cross-links (38), reduced local supply of mineral from reduced vascularity and perfusion (1) or local physico-chemical phenomenon involving body fluid shifts or the changing biomechanical forces during space flight. This experiment focused on the alterations in the collagen cross-links.

SUMMARY OF PREVIOUS WORK

Our continuing effort has been to identify the location and structure of collagen where mineral deficits occur in microgravity. The most rapidly growing bones (i.e. vertebra rather than humerus in 60 day old rats) (21), and the rapidly growing ends of long bones are the most vulnerable sites (16). Biochemical analysis of the proximal and distal diaphysis of the femur revealed reduced concentrations of calcium, phosphorus, and a non-collagenous protein, osteocalcin (OC) in the *distal* region of flight femurs compared to controls. In the *proximal* diaphysis hydroxyproline concentration was increased and there was no mineral deficit (16). The separate regions in which differences in mineral and collagen concentrations occurred seemed to be related to the rates of normal growth activities in 2 areas of the diaphysis. Accumulation of hydroxyproline

predominates in the proximal, and of mineral, in the distal half in 14 week old animals. Since the flight animals were stressed from landing off course and on the ground for two days before necropsy (13), it was not possible to attribute the changes in bone biochemistry to exposure to micro-gravity.

CURRENT STUDY

This report describes the microanatomy of the femoral diaphysis, the results of the biochemical analyses for mineral, collagen, crosslinks and osteocalcin, in 4 regions of the diaphysis.

MICROANATOMY OF THE FEMORAL DIAPHYSIS

Microanatomy methods

At necropsy, the right femur was removed, the whole bone sterilized by dipping in a solution 70% ethanol. The proximal and distal ends were then cut off aseptically. The marrow cavity was flushed with saline. All three pieces of the bone were then placed in 70 percent ethanol buffered with 1 N ammonium hydroxide (pH 7.4) and stored at 4^{o} C for shipment from Moscow to Ames Research Center. The specimens were subsequently shipped to Hunter College for sectioning and histologic examination.

Two sections, one 500 and one 100 microns thick were cut from the proximal, mid-diaphysis and distal sections of the femoral diaphysis. Sections were cut with a 3" diamond wafering blade on an ISOMET low speed (Bueler) saw lubricated with 70 percent ethanol adjusted to pH 7.4. Anatomical markers were used to locate the area for cutting the 500 micron sections as follows: The *proximal* sections were taken at the maximum width of the linea aspera from the shaft, *mid-diaphysis* within the region most narrowed mediolaterally, normally about 5.5 to 5.8 mm distal to the proximal section, and the *distal* section within a slightly anteroposteriorly (a-p) compressed region just proximal to the a-p metaphyseal flare, but within the mediolateral metaphyseal flare, normally about 7 mm distal from the mid-diaphyseal section. The 100 micron sections were taken just distal to the 500 micron section in the proximal and mid-diaphyseal areas, and just proximal to the distal 500 micron section. All 500 micron sections were embedded in polymethylmethacrylate and prepared for image analysis as previously reported (16).

The shaft was divided into 4 parts as illustrated in Figure 1. Proximal 1 is between the inferior edge of the lesser trochanter to the first proximal 500 micron section. Proximal 2 is from the 100 micron section to the midshaft section. Distal 1 and Distal 2 areas extend midway from the mid-diaphyseal section to just above the level of the epiphyseal cartilage. These bone fragments were air dried and subsequently prepared for biochemical analysis by methods described below. The 100 micron sections, from the 1st, 3rd, and 5th cuts in Figure 1, were examined histologically and by circularly polarized light.

Microanatomy Results

Four tissue types are identified and distributed in the sections as illustrated in Figure 2. All experimental groups showed the same microanatomical distribution of bone tissue types without apparent quantitative differences.

Proximal

Circumferential lamellar deposits of cancellous bone of periosteal origin (#1) characterize the anterior sleeve of the bone and similar deposits of endosteal origin (#2) are seen on the posterior inner sleeve. The bone tissue becomes a mixture of complex tissue types away from the medullary

canal toward the linea aspera crest, laterally. The edge of the rat linea aspera is a rapidly proliferating zone which contains a thick slip of cartilage-like material called "chondroid bone" (8) and fetal bone with numerous spaces. Lamellar periosteal deposits (#3) are seen in all areas that are undergoing formation except for a small area of resorption at the tip of the crest of the linea aspera. There is a thin patina of circumferential lamellar bone (#4) over the entire endosteal surface.

Mid-diaphysis

All periosteal surfaces show deposits of bone, particularly at superstructures related to muscle attachment sites posteriorly and laterally (#3). Endosteal compact coarse cancellous bone deposits throughout (#1) and circumferential lamellar bone (#2) anteriorly, comprise the inner cortical bone of the femoral shaft. A thin layer of lamellar bone (#4) lines most of the endosteal surface of the medullary canal.

Distal

The distal section is composed of bone formed on the inner metaphyseal surface and is coarse cancellous bone of endosteal origin (#1) primarily. Smaller areas of circumferential lamellar bone tissue appear along the endosteal surfaces anteriorly and posteriorly (#2). The entire periosteal surface is resorptive.

Collagen fiber orientation

Collagen fiber orientation was evaluated by the degree of brightness with circularly polarized light revealed no differences in all experimental groups. Collagen fibers that are oriented parallel with the plane of the section are bright and those oriented perpendicular to the plane of the section are dark, as illustrated in Figure 3.

Proximal

The principal orientation of all tissue types (#2,3,4) is parallel to the plane of the section. A small anterior periosteal deposit is dark or perpendicular to the plane of the section (#1).

Mid-diaphysis

Periosteal deposits (#3) are oriented parallel to the plane of the section as is the thin lamellar bone lining the medullary cavity (#4). The coarse cancellous endosteal bone (#1 and #2) is mainly dark.

Distal

Posterior, medial and lateral cortices show brightness (#1 and #2). The anterior cortex is mainly dark with fibers oriented perpendicular to the plane of the sections.

Discussion of Microanatomy

The histology, in terms of bone tissue types at each section level, does not change between experimental groups. Based on the above descriptions, the distal section contains the most new bone formed over the experimental period, the proximal the next most new bone and the midshaft section, the least new bone formed. Our interpretations of the growth dynamics of the rat femur indicate that the most distal region of the femoral shaft is the most active. Endosteal deposits will increase the length of the bone and periosteal resorption will convert the flared metaphysis into the narrower shaft. Thus endosteal coarse cancellous bone deposits prevail here. This is important because cancellous bone, being three-dimensionally complex, contains much more surface area per

unit volume and hence more active bone formation to keep pace with epiphyseal growth. All bone types at each section level contain primary vascular canals. There were no observed secondary Haversian systems.

Although we were not able to quantify linear apposition rates in the femur, others, using calcein label, have shown new bone formation rates of 7.9 microns per day in the midshaft of the femur of 100 day old rats, weighing approximately 300 gms (28). This would represent the accumulation of about 110 microns of new bone over the anterior-endosteal and posterior-periosteal surfaces during the 14 day experimental period. This amount of bone is easily visualized, and in this experiment neither influenced the relative proportions of tissue types nor the collagen fiber orientation.

Circularly polarized light (CPL) examination was undertaken because of recent experimental evidence that shows longitudinally oriented collagen fiber bundles and crystallites are better able to withstand tensile forces and transversely oriented collagen fiber bundles and crystallites are better able to withstand compressive forces (2,22). This relationship has been demonstrated in human long bones (5,7) and the horse radius (5). Cosmos 2044 rat femurs are generally bright or composed of transversely oriented collagen posteriorly and generally dark anteriorly or composed of longitudinally oriented collagen. This would suggest that the femur is bent in the antero-posterior direction, the posterior cortex experiencing compression and the anterior cortex, tension. The narrow seams of collagen laid down over the experimental period (i.e. endosteal lamellae distally, endosteal and periosteal lamellae at the midshaft and proximal levels) showed no gross differences among groups. This suggests that the developmental constraints have the highest priority over the manner in which preferred collagen fiber orientations are established. While future studies with more precise quantitation of light intensity may show alterations in collagen fiber orientation and in bone mineral density as a result of space flight, collagen *alignment* in the femur in this study did not appear to change.

BIOCHEMISTRY OF THE FEMORAL DIAPHYSIS

There is abundant evidence for a close relationship between the collagen fibril and mineralization (12). It appears that the initial mineral deposit occurs at the specific regions (gap regions) within collagen fibrils along the axial period in an orderly fashion (34). At the initial stage of mineralization, the intermolecular cross-linking is stoichiometrically formed between 16c-Hylald in the COOH-terminal nontriple helical portion of a collagen molecule and residue 87-Hyl in the triple helical portion on a neighboring molecule. Thus the connected intermolecular cross-linking in the fibril forms a sheet-like structure which may provide a stable template for an orderly precipitation of mineral (14,40). The recent data indicate that this connectivity is reduced with maturation and mineral growth, a structure favoring mineralization (18).

Collagen cross-linking is initiated by conversion of the e-amino group of specific peptidyl Lys and Hyl to aldehyde (30). There are four major cross-links in mineralized tissue collagen: dehydro-dihydroxylysinonorleucine (deH-DHLNL), dehydro-hydroxylysinonor-leucine (deH-HLNL), pyridinoline and its lysyl analog, deoxypyridinoline (LP) (9,37). The former two are reducible with sodium borohydride and the latter two are nonreducible. Generally, the relative amounts of collagen cross-links are tissue specific (9,37). In addition, within the same tissue the cross-link pattern changes by aging (10), metabolic activity (40), degree of mineralization (26,39), and by external forces such as mineral growth (40).

The Cosmos 2044 flight of two weeks duration offered the opportunity to determine the pattern of collagen cross-links and mineral composition in the proximal, central and distal regions of the diaphysis the growing femur. Although we recognized that unavoidable delays in launch placed the experimental animals in a more advanced stage of normal skeletal growth than the animals in Cosmos 1887, we did not think this would greatly influence the diaphyseal location of any changes

in the chemical composition of bone in relation to the morphology. A major addition in experimental groups for the flight animals was the inclusion of a bone from a flight simulation model, tail suspension. This allowed comparison of segmental bone biochemistry in the shaft of the femur in rats exposed to the model with the same in animals exposed to space flight.

Biochemical Methods

Experimental protocol

The experimental details of the Cosmos 2044 mission are detailed in another paper in this report (33). Information relative to bone growth is repeated here. The experimental animals, 5 in each group, were about 109 days of age, weighing an average of 320 g at the beginning of the flight or tail suspension periods. The ages of each group at necropsy was slightly different to accommodate the necropsy schedule, but the duration of each experimental period was 14 days except in the flight group (16 days). Flight animals (F) were housed in group cages, 10 per cage, the same dimensions as the synchronous controls (S). Slightly larger cages were used to house the basal (B), and vivarium controls (V). The tail suspended animals (T) were housed in individual cages, and the hind limbs unweighted by the technique of Wronski and Morey-Holton (36). B, V, and T were fed the same diet as S and F, but given once a day instead of the 4 evenly divided aliquots given to F and S. The S group, subjected to the same diet schedule, temperature changes, and transportation to the launch site as F is the appropriate control for microgravity effects on bone.

Four bone fragments from each diaphysis were air dried and sent to Dr. Mechanic in North Carolina. The bones were furthur dried by lyophilizing to a constant weight and were then ground to a fine powder in a liquid nitrogen-cooled mill (Spex Industries, Edison, N.J.). Two weighed aliquots of the powders were made: one for determination of minerals and osteocalcin and one for determination of hydroxyproline and cross-links.

Chemical Analyses

Calcium and phosphorus were determined in portions of the powders extracted with 0.5 M ethylenediaminetetraacetic acid (EDTA) for 24 hours. Calcium was measured by atomic absorption spectrometry and phosphorus by a Fiske-Subbarow method modified for UV detection of the phosphomolybdate complex. Osteocalcin was assayed following extraction with 0.5 M EDTA containing protease inhibitors as previously reported (19).

For hydroxyproline and collagen cross-link analyses, the bone powder was demineralized with 0.5 M EDTA for one week at 4°C with 3-4 changes. The residue was then thoroughly washed with cold distilled water and lyophilized. The dried material was reduced with standardized NaB^3H_4 by the method described previously (40). The specific activity of NaB^3H_4 was determined. The reduced samples were hydrolyzed with 6N HCl *in vacuo* in an N_2 atmosphere for 20 hours at 110°C. The hydrolysates were dried by speed vacuum centrifugation (Savant instruments, Inc.) and the residues dissolved in distilled water and filtered. An aliquot of each sample was taken for hydroxyproline assay (35). The hydrolysates with known concentration of hydroxyproline were then subjected to cross-link analyses to determine the reducible and nonreducible cross-links. The reducible cross-links were quantified by integrating the radioactivity of the respective cross-link peaks measured by an on-line FLO-One Beta instrument (Radiomatic Instrument and Chemical Co., Tampa, FL) and converting the numbers into nanomoles based on the specific activity of NaB^3H_4. Pyridinoline (PYR) and its lysyl analogue (LP) were determined by a fluorescence flow monitor (Shimadzu Instrument Co., Japan) calibrated by an apparently pure PYR tryptic peptide isolated from bovine achilles tendon. Each cross-link was quantified in terms of moles of cross-link per mole of collagen based on the hydroxyproline value of 300 residues per collagen molecule.

Statistics

Analysis of variance was used to determine differences between concentrations of compounds measured in the 5 experimental groups and also among the 4 sites (2 proximal and 2 distal) of each group. When group differences were present, the difference of the means was determined by the Student-Neumann-Kuels test. Simple linear regression analysis was used to evaluate the relationships among the chemical components analyzed (11).

Results of Chemical Analysis

The results of the measurements of calcium, phosphorus, hydroxyproline and osteocalcin in the 4 regions of the diaphysis in the 5 experimental groups are listed on Table 1. Values represent the mean and standard deviation of 5 animals except where indicated by the number in the parenthesis.

Group differences

There were differences in calcium only in the distal D-2 section where the means in S and F were similar and lower than in the other groups. Phosphorus values were lower in B than in all other groups in D-1, $p<.002$), and lower in F and S than T in the most distal section, D-2, ($p<.002$). Hydroxyproline was lower in the proximal section, P-1, of V than all other groups. This low value accounted for the higher ratio of calcium to hydroxyproline in V than B.

There were no group differences in the concentration of osteocalcin. As shown in Table 2, the reducible cross-link, DHLNL was lower in the most distal sections, D-2 of S,F and T compared to B, $p<.001$.

Means in T, F, and S were lower than B, and in T lower than V, $p<.05$. HLNL was the same in all groups, so that the low DHLNL in F accounted for the low ratio of DHLNL/HLNL in most distal section of F compared to B, $p<.05$.

Table 3 summarizes the few measurements of the non-reducible cross-link, PYR and L-PYR that could be done on the limited quantity of sample. There are no group differences in the most proximal or the most distal regions of the diaphysis.

Regional differences

Calcium concentration showed regional differences in V,S, and F groups with mid-diaphyseal regions tending to show higher values than either proximal or distal ends. In V, Ca was lower in P-1 than D-1, $p<.05$; in S, Ca was lower in P-1, D-1 and D-2 than P-2, $p<.005$, and in F, Ca was lower in P-1 and D-2 than P-2 and in D-2, lower than D-1, $p<.002$. In T there were no differences in Ca. Pi concentrations showed differences in the same regions as Ca with lower values in P-1 and D-2, significant in V, $p<.002$, S, $p<.02$, and F, $p<.002$. Femurs from B and T did not show regional differences.

Hydroxyproline concentrations tended to be higher in the distal ends of the bones than in the middle sections in B, $p<.01$, S, $p<.05$ and T, $p<.05$ and did not vary significantly in V or F. The Ca/HYP ratios tended to be higher in the mid-diaphysis than at either end in B, $p<.001$, F, $p<.002$ and T, $p<.001$ but not in V or S where the variability and limited number of measures precluded valid statistical analysis. There were no regional differences in the concentration of osteocalcin. However, mean values in each area were related to the concentration of Ca ($r=0.774$, $p<.001$).

HLNL concentration was the same in all regions; however, DHLNL values were lower in the more distal than proximal sections in S, F, and T, relative to B ($p<.001$). Low DHLNL, primarily, accounted for the lower DHLNL/HLNL ratios in the most distal sections of S ($p<.002$), F

($p<.005$) and T ($p=.055$) compared with P-2 sections. Concentrations of PYR were lower and of its isomer, L-PYR, higher in D-2 than P-1 sections of V, F, and T. This resulted in an approximately 40 percent lower ratio of PYR/L-PYR in D-2 than P-1 in the 3 groups where data was available for comparison, V, F, and T.

Relationships among chemical constituents of sections

The relationships of mean values for Ca, Pi, HYP, crosslinks, and OC were examined for all groups (n=20). Ca and Pi were related to one another ($r=0.915$, $p<.001$) and to OC ($r=0.774$, $p<.001$ for Ca and 0.624, $p<.003$ for Pi). Mineral levels were unrelated to the concentration of crosslinks or HYP. However the ratio, DHLNL/HLNL, was related to OC ($r=0.833$, $p<.001$), Ca ($r=0.699$,$p<.001$) and Pi ($r=0.476$, $p<.05$) and not to HYP ($r=-.356$, NS).

Discussion of Biochemistry

Biochemical analysis of four regions of the femoral diaphysis after two weeks in space has revealed evidence of a mineral deficit in the distal diaphysis associated with reduced ratios of the sodium borohydride reducible cross-links, DHLNL/HLNL. Neither the mineral deficit nor the low crosslink ratios were confined to the flight bones. The concentration of DHLNL tended to be lower in all 3 experimental groups than in the vivarium controls. The ratio of DHLNL/HLNL was lowest in F. Curiously, the ground based model, T, showed the lowest values for both DHLNL *and* HLNL with *no* associated mineral deficit. This is the first time that we have observed this abnormality in the composition of matrix, i.e. low ratios of reducible cross-links, associated with reduced concentrations of mineral.

These results differ from and extend those we obtained from less extensive analyses of the femurs from the Cosmos 1887 rat femurs. The pooled powders showed slightly higher values for reducible cross-links in proximal than distal sections, and higher, rather than lower ratios in F and S than V and B. Increased DHLNL in the proximal section (equivalent to P-2 in this study) was not at the site of the mineral deficit (16). In the Cosmos 1887 study, increased DHLNL/HLNL seemed to reflect the exaggerated response of collagen metabolism in an area of bone that was normally actively accumulating matrix to either a systemic (i.e. steroid induced increase in collagen turnover) or effects from local biomechanical stress from the 48 hours on the ground before necropsy. It is of interest and that the cross-link biochemistry in the tibia of chronically immobilized non-human primates was more similar to Cosmos 1887 than 2044, showing evidence of new collagen synthesis 10 weeks after immobilization (38). It is not known if the primate bone was subjected to a brief loading period before necropsy that may have stimulated new matrix production, if endocrine or nutritional factors account for the osteoblastic activity, or if high bone turnover is maintained in the monkey during long periods of disuse.

These apparently discrepant results in the measurements of the reducible cross-links of collagen in disuse and space flight could be due to species differences (rat vs. monkey), the age of the animal, real differences in the temporal response of bone formation to a biomechanical stimulus or significant site specific changes in collagen maturation, undetected in powders from large sections of bone. In view of the short time duration between landing and necropsy, the depressed cross-link concentrations in the most actively growing region of the femur probably represent the response to the changing mechanical stresses on bone associated with the space flight. The presence of the same regional changes in the femurs of synchronous controls as in the flight rats indicates that an element of space flight other than microgravity per se *or* in addition to microgravity may be important in the changes observed.

Tail suspended animals showed the most depressed concentrations of the reducible cross-links and would therefore, appear to be a satisfactory model for future collagen studies. However, the mineral deficit observed in the distal femurs of S and F was not present in T. Unless an artifact

from processing or the shorter time elapsing between necropsy and discontinuing the suspension prevented the mineral deficit, this observation limits the application of the femur in this model to the study of a mineral deficit. It also suggests that cross-link differences are not necessarily causally related to the mineral deficit in the flight bones, assuming the sequence of events in bone formation is the same at 1 g as at 0 g.

Through the analysis of different sections of the femur of the normal earth-based V group, we found differences in concentrations of non-reducible cross-links in the most proximal and most distal areas that have not been observed previously. There was more hydroxylation of cross-links and amino acids in the distal end. These proximal and distal differences were not affected by space flight or suspension. While PYR concentrations were unaffected by space flight, a finding in agreement with a report on the humerus (32), values for pyridinoline tended to be slightly higher in the ground-based model. This finding requires confirmation in larger numbers of animals since the concentrations of pyridinoline are low in the rat, relative to other species.

In general, our results confirm our previous conclusion that the distal end is the site of cortical bone in the femur most likely to show the effects of space flight. The vulnerability of this end is most likely due to its active growth rate in the 18 week old rat. Earlier studies indicate that different bones will show different responses to space flight (24), not only due to their rate of growth at the beginning of the flight, but possibly also because of differences in the endocrine and biomechanical stresses in space flight experiments. There is also a temporal sequence of adaptation to consider. In acute disuse secondary to nerve resection, Landry et al found formation of bone maximally depressed after 12 days, normal after 28 and then again reduced to a subnormal level after 49 days (15). Whether the pattern of adaptation will be the same during space flight awaits analyses of bone at different time points in flight from longer space flights.

Recently, it has been shown that collagen cross-link density varies depending on the sites within the tissue. For example, a nonreducible stable cross-link in skin, histindinohydroxylysinonor-leucine was found to be more abundant in the portion of skin not exposed to sun than in the sun-exposed skin (42). In gingival tissue, a variation of cross-linking also exists among different sites of the tissue (29). The site difference in cross-linking could be related to the amounts of stress, physical forces and metabolic activity in certain sites of tissue. Within the same bone, a regional difference in cross-linking was observed (16). In the present study, we also observed a clear trend toward lower hydroxylation of cross-linking amino acids in the distal end than in other portions of the diaphysis. This resulted in the lower values of DHLNL/HLNL and Pyr/LP in this portion of bone (see Table II and III). The cause of this alteration in a post-translational modification is not clear at this point. More detailed studies such as *in situ* estimates of metabolic activity and the level of mechanical load in different portions of bone are required to understand regional differences in the molecular structure of collagen.

REFERENCES

1. Aratow, M., Hargens, A.R., Meyer, J.-Uve and Arnaud, S.B. Postural Responses of Head and Foot Cutaneous Microvascular Flow and Their Sensitivity to Bed Rest. Aviat. Space Environ. Med. 62:246-251, 1991.

2. Ascenzi, A. Mechanical Hysteresis Loops from Single Osteons: Technical Devices and Preliminary Results. J. Biomech. 18:391-398, 1985.

3. Banes, A. J., M. Yamauchi, and G. L. Mechanic. Nonmineralized and Mineralized Compartments of Bone: the Role of Pyridinoline in Non-mineralized Collagen. Biochem. Biophys. Res. Commun. 113:975-981, 1983.

4. Boyde, A and Riggs, C.M. The Quantitative Study of the Orientation of Collagen in Compact Bone Slices. Bone 11:35-39, 1990.

5. Burnell, J. M., E. J. Teubner, and A. G. Miller. Normal Maturational Changes in Bone Matrix, Mineral, and Crystal Size in the Rat. Calcif..Tissue Int. 31:13-19, 1980.

6. Carando, S., Portigliatti-Barbos, M., Ascenzi, A. and A. Boyde. Orientation of Collagen in Human Tibial and Fibular Shaft and Possible Correlations with Mechanical Properties. Bone 10:139-142, 1989.

7. Enlow, D.H. Principles of Bone Remodeling. Charles C. Thomas, Springfield, Illinois, 1963.

8. Eyre, D.R., Paz, M.A., and Gallop, P.M. Cross-linking in Collagen and Elastin. Ann Rev. Biochem., 53:717-748, 1984.

9. Fujimoto, D., Yamauchi, M., Katz, E.P. and Mechanic, G.L. Aging and Cross-linking of Skin Collagen. Biochem. Biophys. Res. Comm. 152:898-903, 1988.

10. Glantz, Stanton A. Primer of Biostatistics. McGraw-Hill Book Company, 1981. pp 1-352.

11. Glimcher, M.J. Recent Studies of the Mineral Phase in Bone and Its Possible Linkage to the Organic Matrix by Protein-Bound Phosphate Bonds. Philos. Trans. R. Soc. Lond. 304:479-508, 1984.

12. Grindeland, R.E. Cosmos 1887: Science Overview. FASEB 4:10-15, 1990.

13. Katz, E.P., Wachtel, E., Yamauchi, M., and G.L. Mechanic. The Structure of Mineralized Collagen Fibrils. Conn Tiss. Res. 21:149-158, 1989.

14. Landry, M. and H. Fleisch. Rhw Influence of Immobilisation on Bone Formation as Evaluated by Osseous Incorporation of Tetracyclines. The J. of Bone and Joint Surg. 46B:764-771, 1964.

15. Mechanic, G. L., Arnaud, S.B., Boyde, A., Bromage, T.G., Buckendahl, P., Elliott, J.C., Katz, E.P., and Durnova G. Regional Distribution of Mineral and Matrix in the Femurs of Rats Flown on Cosmos 1887 biosatellite. FASEB J. 4:34-40, 1990.

16. Morey, E.R. and Baylink, D. J. Inhibition of Bone Formation During Spaceflight. Science (Washington, DC) 201:1138-1141, 1978.

17. Otsubo, K., Katz, E.P., Mechanic, G.L., and M. Yamauchi. The cross-linking Connectivity in Bone Collagen Fibrils: The COOH-terminal Locus of Free Aldehyde. BIOCHEM 31: 396-402, 1992.

18. Patterson-Allen, P.E., Brautigam, C.E., Grindeland, R.E., Asling, C.W., and Callahan, P.X. A Specific Radioimmunoassay for Osteocalcin with Advantageous Species Cross Reactivity. Anal. Biochem. 120:1-7, 1982.

19. Patterson-Buckendahl, P., S. B. Arnaud, G. L. Mechanic, R. B. Martin, R. E. Grindeland, and C.E. Cann. Fragility and Composition of Growing Rat Bone After One Week in Spaceflight. Am J. Physiol. 252 (Regulatory Integrative Comp. Physiol. 21) R240-R246, 1987.

20. Patterson-Buckendahl, P.E., Grindeland, R.E., Martin, R.B., Cann, C.E., and S.B. Arnaud. Osteocalcin as an Indicator of Bone Metabolism During Spaceflight. The Physiologist 28:S227-229, 1985.

21. Portigliatti-Barbos, M., Bianco, M., Ascenzi A., and A. Boyde. Collagen Orientation in Compact Bone: I. Distribution of Lamellae in the Whole of the Human Femoral Shaft with Reference to its Mechanical Properties. Metab Bone Dis. Relat. Res. 5:309-315, 1984.

22. Price, P.A., Williamson, M.K., Haba, T., Dell, R.B., and W.S.S. Jee. Excessive Mineralization with Growth Plate Closure in Rats on Chronic Warfarin Treatment. Proc. Natl. Acad. Sci. U.S.A. 79:7734-7738, 1982.

23. Prokhonchukov, A.A., Desyatnichenko, K.S., and Tigranyan, R. A. Mineral Phase and Protein Matrix of Rat Osseus Tissue Following Flight Aboard the Cosmos-1129 Biosatellite. Space Biol. Med. 16:87-92, 1982.

24. Rogacheva, I.V., Stupakov, G.P., Volozhin, A.I., Pavlova, M.N, and Polyakov, A.N. Rat Bone Tissue After Flight Aboard Cosmos-1129 biosatellite. Koxm. Biol. Aviakosm. Med. 18:39-44, 1984.

25. Russell, J.E., and Avioli, L.V. The Nature of Collagen Cross-links in Bone in the Chronic Uremic State. Biochem J. 145:119-120, 1975.

26. Simmons, D. J., Russell, J.E., and Grynpas, M.D. Bone Maturation and Quality of Bone Material in Rats Flown on the Space Shuttle 'Space-lab-3 Mission'. Bone Mineral 1:485-493, 1986.

27. Sontag, W. Quantitative Measurements of Periosteal amd Cortical-endosteal Bone Formation and Resorption in the Midshaft of Male Rat Femur. Metab. Bone Dis. Relat. Res. 5:309-315, 1984.

28. Tanner, J., Yamauchi, M and Simpson, D.M. Collagen Cross-Linking in Bovine Gingiva. Arch. Oral Biol. 36:111-115, 1991.

29. Tanzer, M.L., Crosslinking of Collagen, in Biochemistry of Collagen, Ramachandran, G.N. and Reddi, A.H. eds., Plenum Press, New York, 1976, pp 137-162.

30. Turner, R.T., Bell, N.H., Duval, P., Bobyn, J.D., Spector, M., Holton, E.M., and Baylink, J.D. Spaceflight Results in Formation of Defective Bone. Proc. Soc. Exp. Biol. Med. 174:224-228, 1983.

31. Vailas, A.C., Zernicke, R.F., Grindeland, R.E., Kaplansky, A., Durnova, N., Li, K-C, and D.A. Martinez. Effects of Spaceflight on Rat Humerus Geometry, Biomechanics and Biochemistry. FASEB J. 4:47-54, 1990.

32. Vailas, R., Vanderby, Jr., R.B., Martinez, R.B., Ashman M.J., Grindeland, R.E., Durnova, G.N., and A. Kaplansky. Adaptations of Young Adult Rat Cortical Bone to 14 days of Spaceflight. J. Appl. Physiol. 73: 4S-9S, 1992.

33. Weiner, S. and Traub, W. Organization of Hydroxyapatite Crystals Within Collagen Fibrils. FEBS Lett. 206:262-266, 1986.

34. Woessner, J.F., Jr. The Determination of Hydroxyproline in Tissue and Protein Samples Containing Small Proportions of this Imino Acid. Arch. Biochem. Biophys. 93:440-447, 1961.

35. Wronski, T.J. and E.R. Morey-Holton. Skeletal Responses to Simulated Weightlessness: a Comparison of Suspension Techniques. Aviat. Space Envir. Med. 58:63-68, 1987.

36. Yamauchi, M. and Mechanic, G.L. Cross-linking of Collagen in Collagen CRC Press, Inc. Boca Raton, Florida. Nimni, M. editor, 1:157-172, 1988.

37. Yamauchi, M., Young, D.R., Chandler, G.S., and Mechanic, G.L. Cross-linking and New Bone Collagen Synthesis in Immobilized and Recovering Primate Osteoporosis. Bone 9:415-418, 1988.

38. Yamauchi, M., Banes, A.J., Kuboki, Y., and Mechanic, G.L. A Comparative Study of the Distribution of the Stable Cross-link, Pyridinoline, in Bone Collagens from Normal, Osteoblastoma, and Vitamin D-deficient Chicks. Biochem. Biophys. Res Commun. 102:59-65, 1981.

39. Yamauchi, M., Katz, E.P., and Mechanic, G.L. Intermolecular Cross-linking and Stereospecific Molecular Packing in Type I Collagen Fibrils of the Periodontal Ligament. Biochemistry 25:4907-4913, 1986.

40. Yamauchi, M., Katz, E.P., Otsubo, K., Teraoka, K. and G.L. Mechanic. Cross-Linking and Stereospecific Structure of Collagen in Mineralized and Nonmineralized Skeletal Tissues. Conn. Tiss. Res. 21:159-169, 1989.

41. Yamauchi, M., Prisayanh, P., Haque, Z., and Woodley, D.T. Collagen Cross-Linking in Sun-exposed and Unexposed Sites of Aged Human Skin. J. Invest. Dermatol. 97:938-941, 1991.

TABLE 1

Concentration of Calcium, Phosphorus, Hydroxyproline, and Osteocalcin in the femoral diaphaysis, μg//mg dry bone.

	Basal	Vivarium	Synchronous	Flight	Tail
Proximal 1					
Ca *	1.51 ± 22	131 ± 17 (4)	148 ± 11 (4)	148 ± 28	143 ± 30
P	57 ± 12	55 ± 13 (4)	61 ± 13	61 ± 9	64 ± 13
HYP	36.1 ± 04.6	19.4 ± 1.4	-	28.5 ± 3.0	25.7 ± 6.0
OC	1.81 ± .47	1.32 ± 0.27 (4)	1.69 ± .27 (4)	1.46 ± .09	1.42 ± 0.45
Ca/HYP *	3.83 ± .53	6.78 ± 0.44 (3)	-	5.23 ± .91	5.74 ± 1.24
Proximal 2					
Ca	165 ± 35	149 ± 32	191 ± 28(3)	195 ± 29	194 ± 22 (4)
P	69 ± 14	65 ± 9	80 ± 11 (3)	84 ± 16	78 ± 18
HYP	-	21.2 ± 9.8 (3)	24.2 ± 2.4 (2)	22.7 ± 4.1	20.1 ± 4.3
OC	1.64 ± .28	1.68 ± .60 (4)	1.88 ± .42 (3)	1.76 ± .46 (4)	1.99 ± 0.59
Ca/HYP	-	7.9 ± 4.2 (3)	-	8.88 ± 2.2	9.42 ± 1.4 (4)
Distal 1					
Ca	174 ± .30	184 ± 23	140 ± 17 (4)	173 ± 16	158 ± 27
P *	68 ± 9	86 ± 9	61 ± 4 (4)	75 ± 6	72 ± 9
HYP	25.0 ± 2.9	23.5 ± 12.2 (3)	21.6 ± 5.2 (4)	26.1 ± 4.4	18.0 ± .6 (4)
OC	1.57 ± .46	1.87 ± .39 (4)	1.42 ± .29 (4)	1.58 ± .27	1.72 ± .35
Ca/HYP	6.94 ± .64	10.58 ±6.59 (3)	6.85 ± 1.9 (4)	6.83 ± 1.45	8.98 ± 1.47 (4)
Distal 2					
Ca *	147 ± 18	151 ± 20 †	129 ± 10 (4) †	130 ± 9 †	161 ± 21
P *	62 ± 7	69 ± 9 †	52 ± 9 †	58 ± 3 †	74 ± 9
HYP	34.2 ± 6.1 †	31.5 ± 16.2 (3)	35.8 ± 9.5 †	28.5 ± 5.0	23.9 ± 2.1 (4) †
OC	1.42 ± .47	1.25 ± .34	1.33 ± .25	1.29 ± .28	1.40 ± .19
Ca/HYP	4.53 ± 1.56 †	6.48 ± 3.23 (3)	4.16 ± 1.69	4.72 ± .99 †	5.74 ± 1.24 †

The asterisk (*) indicates group differences, $p<.05$ or less and the cross,(†), placed nest to components in the Distal 2 fragments, indicates regional differences in the same group. A dash (-) identifies insufficient sample for analysis. Means ± SD are from the analysis of 5 samples unless followed by parentheses.

TABLE 2

Concentration of Reducible Crosslinks/300nm Hydrxyproline, nmoles, in the femoral diaphysis of rats flown on Cosmos 2044.

	Basal	Vivarium	Synchronous	Flight	Tail
Proximal 1					
DHLNL	1.299 ± .28	1.135 ± .22	1.364 ± .40	0.964 ± .17	1.048 ± .25 (4)
HLNL	0.732 ± .20	0.719 ± .14	0.831 ± .30	0.653 ± .19	0.621 ± .09 (4)
Ratio	1.80 ± .16	1.59 ± .23	1.68 ± .16	1.52 ± .29	1.53 ± .59
Proximal 2					
DHLNL	1.600 ± .19	1.404 ± .16	1.230 ± .36	1.167 ± .16 (4)	1.160 ± .23
HLNL	0.894 ± .23	0.784 ± .07	0.717 ± .22	0.514 ± .11 (3)	0.742 ± .15
Ratio	1.77 ± .15	1.79 ± .13	1.73 ± .09	1.98 ± .44 (3)	2.22 ± .80
Distal 1					
DHLNL	1.477 ± .06 (3)	1.401 ± .26	1.031 ± .04	1.057 ± .26	1.200 ± .37
HLNL	0.864 ± .11 (3)	0.819 ± .13	0.680 ± .10	0.632 ± .12	0.760 ± .13
Ratio	1.73 ± .29	1.74 ± .37	1.54 ± .18	1.66 ± .12	1.54 ± .21
Distal 2					
DHLNL *	1.510 ± .28	1.303 ± .13 (4)	1.010 ± .23 (4)	0.977 ± .19	0.744 ± .19 †
HLNL	0.966 ± .22	0.920 ± .21	0.779 ± .09 (4)	0.816 ± .05 †	0.655 ± .22
Ratio *	1.58 ± .16	1.33 ± .19	1.29 ± .13 †	1.19 ± .17 †	1.24 ± .27 †

The asterisk (*) indicates group differences, $p<.05$ or less and the cross (†), placed next to components in the Distal 2 fragments, indicates regional differences in the same group. Means ± SD are from the anaysis of 5 samples unless followed by a parentheses. A dash (-) indentifies insufficient sample for analysis.

TABLE 3

Consentration of Non-Reducible Crosslinks in regions of the femoral diaphysis of rats flown on Cosmos 2044.

	Basal	Vivarium	Synchronous	Flight	Tail
Proximal 1					
Pyr	-	0.11 ± .02 (3)	-	0.09 ± .01 (3)	0.12 ± .05 (3)
L-Pyr	-	0.03 ± .00 (3)	-	0.02 ± .01 (3)	0.02 ± .01 (3)
Ratio	-	3.66 ± .60 (3)	-	3.78 ± .40 (3)	3.84 ±. 20 (2)
Distal 2					
Pyr	0.05 ± .01 (4)	0.07 ± .02 (4)†	0.06 ± .01 (4)	0.06 ± .01 †	0.09 ± .03 *
L-Pyr	0.04 ± .01 (4)	0.05 ± .01 (4)†	0.05 ± .05 (4)	0.04 ± .01 †	0.06 ± .02
Ratio	1.36 ± .40 (4)	1.57 ± .20 (4)†	1.36 ± .30 (4)	1.42 ± .20 †	1.45 ± .30 †

The asterisk (*) indicates group differences, $p<.05$ or less and the cross (†), placed next to components in the Distal 2 fragments, indicates regional differences in the same group. Means ± SD are from the anaysis of 5 samples unless followed by a parentheses. A dash (-) indentifies insufficient sample for analysis.

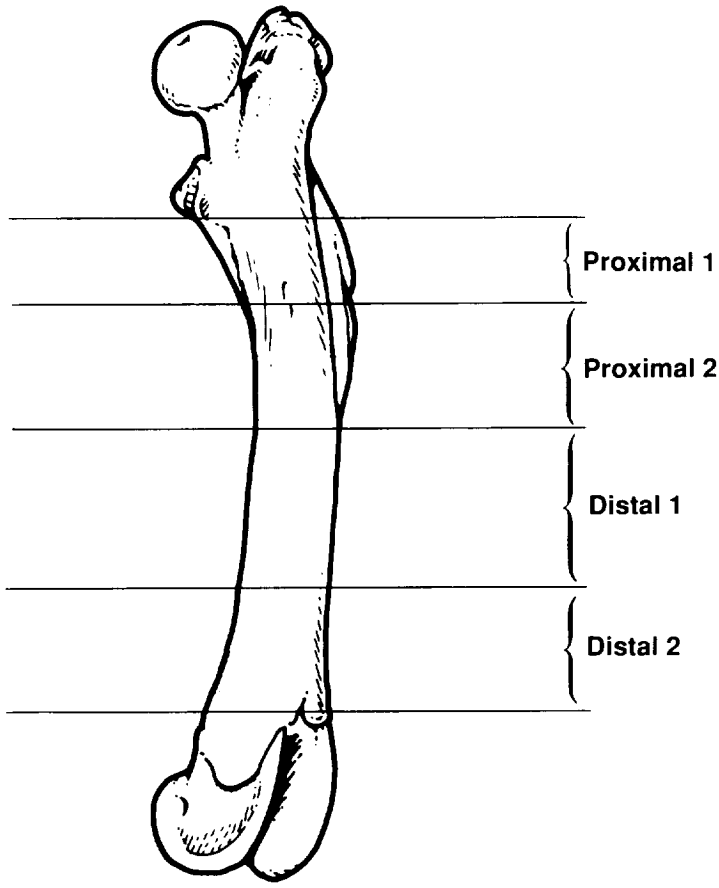

Figure 1. Sections of the rat femur used for histologic and chemical analysis. Experiment K-7-01.

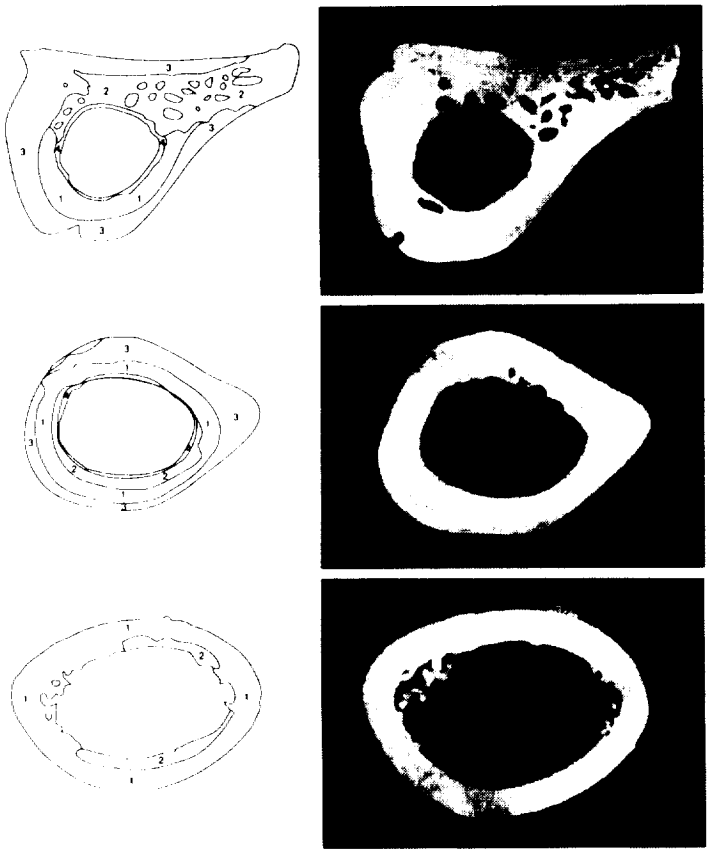

Figure 2. Tissue types (1–4) in the proximal, central, and distal cross sections of the femur from Cosmos 2044 rat femur.

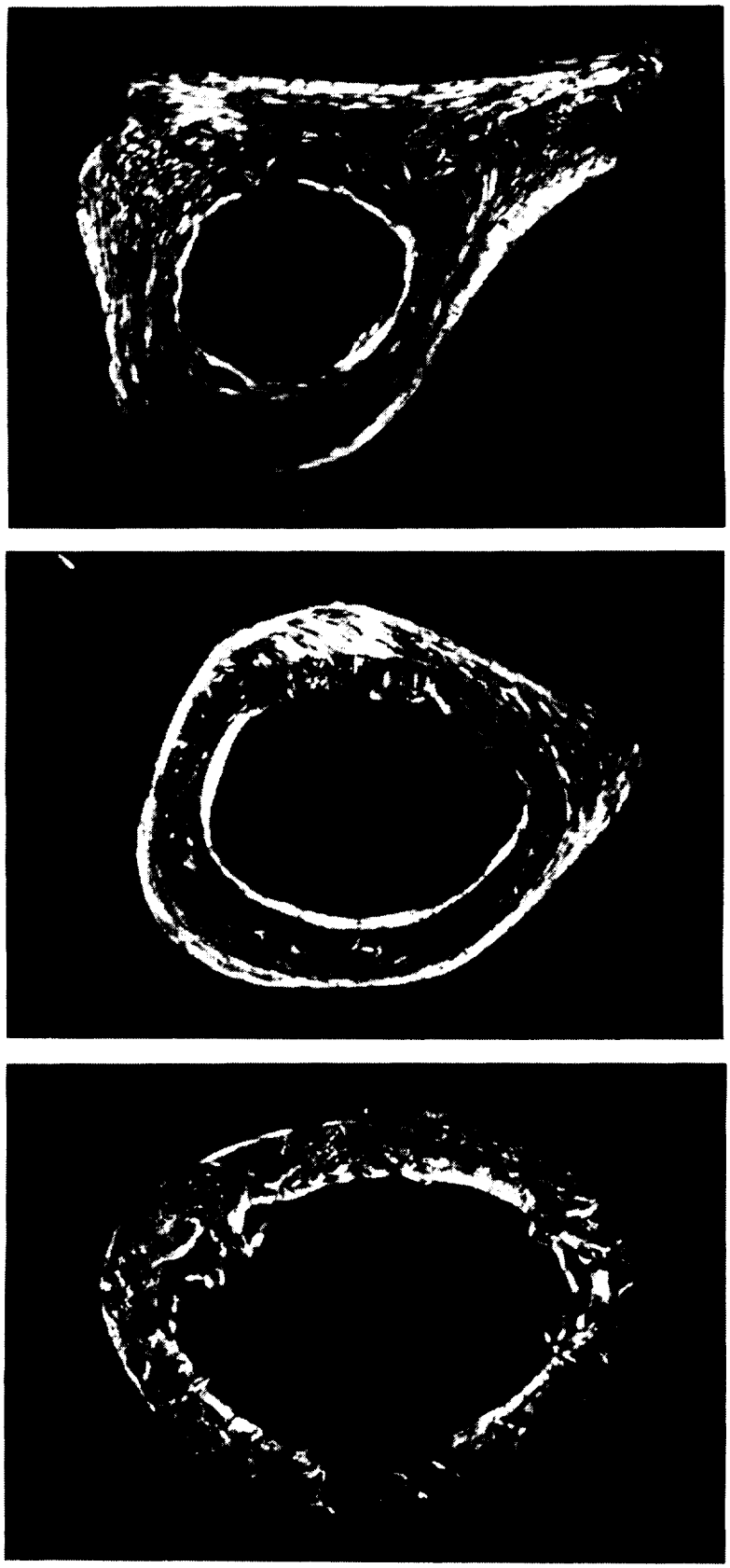

Figure 3. Proximal, central, and distal sections of rat femur viewed by polarized light to show collagen orientation. Experiment K-7-01.

EXPERIMENT K-7-02

BIOMECHANICAL, BIOCHEMICAL AND MORPHOLOGICAL ALTERATIONS OF INTRAMUSCULAR AND DENSE FIBROUS CONNECTIVE TISSUES AFTER 14 DAYS IN SPACEFLIGHT

PART I: CONNECTIVE TISSUE STUDIES

Principal Investigator:

A.C. Vailas
Director of Biodynamic Laboratory
University of Wisconsin
Madison, WI

Co-Investigators:

G.N. Durnova
A. Kaplansky
Institute of Biomedical Problems
Moscow, USSR

R. Vanderby
B. Graf
D. Martinez
R. Thielke
M. Ulm
S. Kolis
P. Griffith
V. Choy
University of Wisconsin

PART II: THE EFFECTS OF MICROGRAVITY ON THE COMPOSITION OF THE INTERVERTEBRAL DISC

Co-Investigators:

J.A. Maynard
J. Fiedler-Toester
Departments of Orthopedic Surgery
and Exercise Science
The University of Iowa

R. Grindeland
NASA-Ames Research Center
Moffett Field, CA

R. Ashman
University of Texas

A. Pedrini-Mille
C.B. Chung
J. Sears
Department of Orthopaedic Surgery
The University of Iowa

V.A. Pedrini
Departments of Orthopaedic
Surgery and Biochemistry
The University of Iowa

I.B. Krasnov
Institute of Biomedical Problems
Moscow, USSR

PART I: CONNECTIVE TISSUE DATA SET
BONE AND TENDON STUDIES

A.C.Vailas, R. Vanderby, B. Graf, J. Sears, R. Ashman, R. Grindeland, D. Martinez, R. Thielke, M. Ulm, S. Kolis, P. Griffith, V. Choy, A. Kaplansky, G. Durnova, I.B. Krasnov

The connective tissue studies were extensive and involved a tremendous collaborative effort from all scientists. We all realize that flight opportunities are few and expensive and everyone is thankful to the Soviet Union and NASA for the chance to continue the research effort in connective tissue.

In many ways, Cosmos 2044 has contributed significantly to an important issue (Does spaceflight of short duration induce significant changes in connective tissue structure and composition that would contribute to alterations of tissue biomechanical properties in a skeletally mature organism?) Our results associated with bone length, bone radial growth, mass and composition confirm that rats in this experiment are mature animals. Furthermore, this entire study demonstrates that spaceflight induced no significant changes in all parameters studied for achilles and patellar tendons, humeri and 5th lumbar vertebral bodies. However, we were surprised about the results regarding the biochemical properties of non lesioned skin which showed a significant increase in DNA/mg collagen ratio. This unique finding may suggest that spaceflight alters the skin's physiology associated with collagen. It seems from previous flight experiments, that young growing animals were most affected by short duration spaceflight and mature rodents are less responsive. However, our results do not rule out the possibility the connective tissues obtained from mature rats would exhibit changes in tissue structure and composition after exposure to spaceflight of greater than 14 days. In some cases, tail suspension induced changes in tissue as compared to control groups which would suggest that the model in some ways does not mimic all aspects of spaceflight as an effector of connective tissue.

Unfortunately, the skin wound healing experiments were problematic, because we could not derive definitive conclusions. Immunocytochemical studies (collagen type III and macrophage physiology) were highly variable and it was difficult for investigators to get consistent binding. Also, skin lesions were not standardized and well marked for subsequent post hoc analysis. However, normal skin samples yielded interesting results that may involve collagen turnover and maturation. Specifically, the data indicated that spaceflight induced an increase in the amount of nuclear material that supports a given quantity of collagen (structural protein). Further investigation is needed to understand this finding. We still have more skin and will continue our efforts to expand on this issue.

It should be noted that a number of unique methods were applied such as (1) ultrasonics for humerus elastic properties, (2) lysylpyrodinoline collagen crosslink analysis in cortcal bond and (3) skin biochemical markers using enzymatic digestion.

STRUCTURAL AND MATERIAL PROPERTIES OF RAT HUMERUS

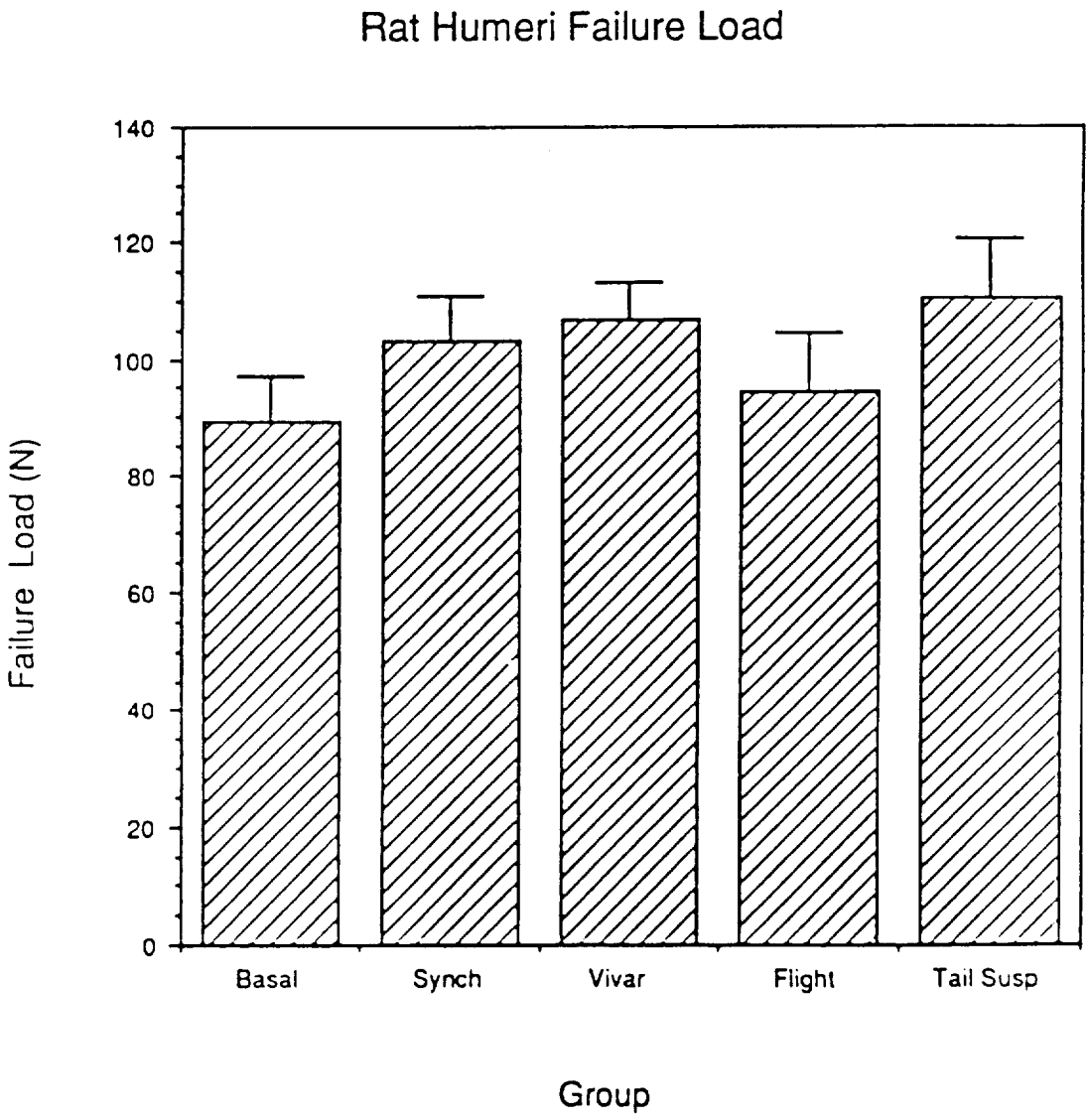

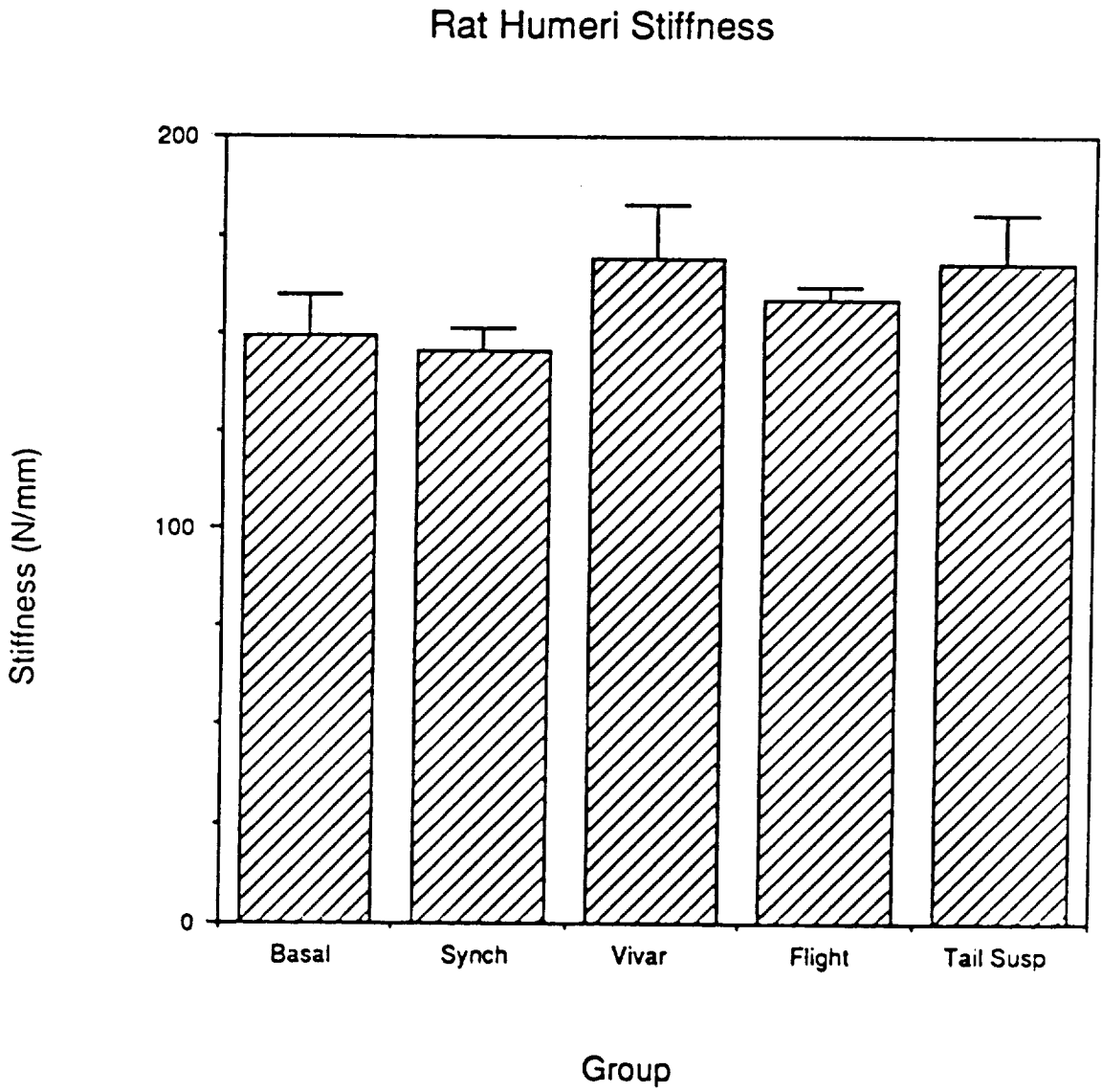
Rat Humeri Stiffness
200
100
0
Stiffness (N/mm)
Basal
Synch
Vivar
Flight
Tail Susp
Group

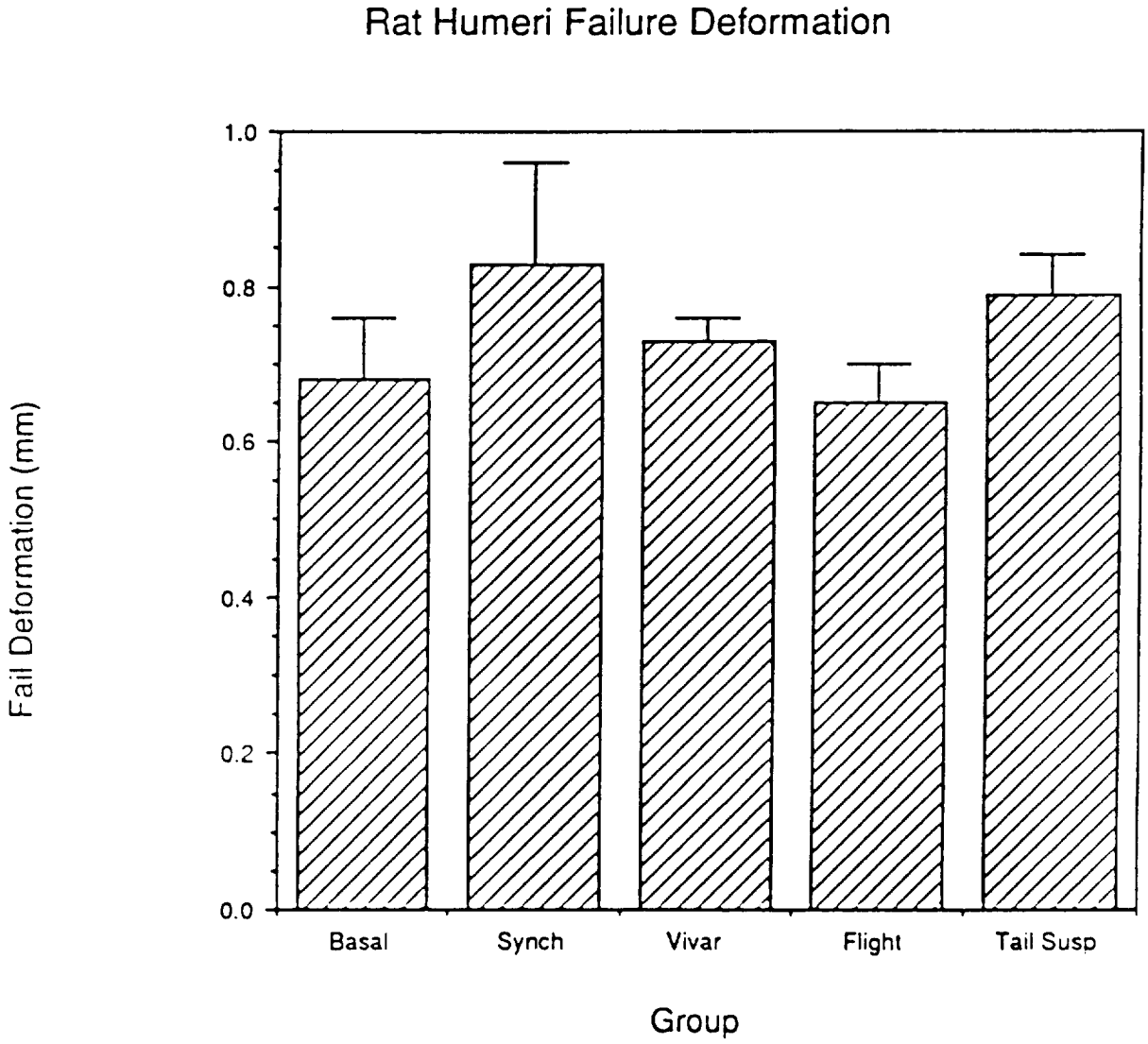
Rat Humeri Failure Deformation
Fail Deformation (mm)
1.0
0.8
0.6
0.4
0.2
0.0
Basal
Synch
Vivar
Flight
Tail Susp
Group

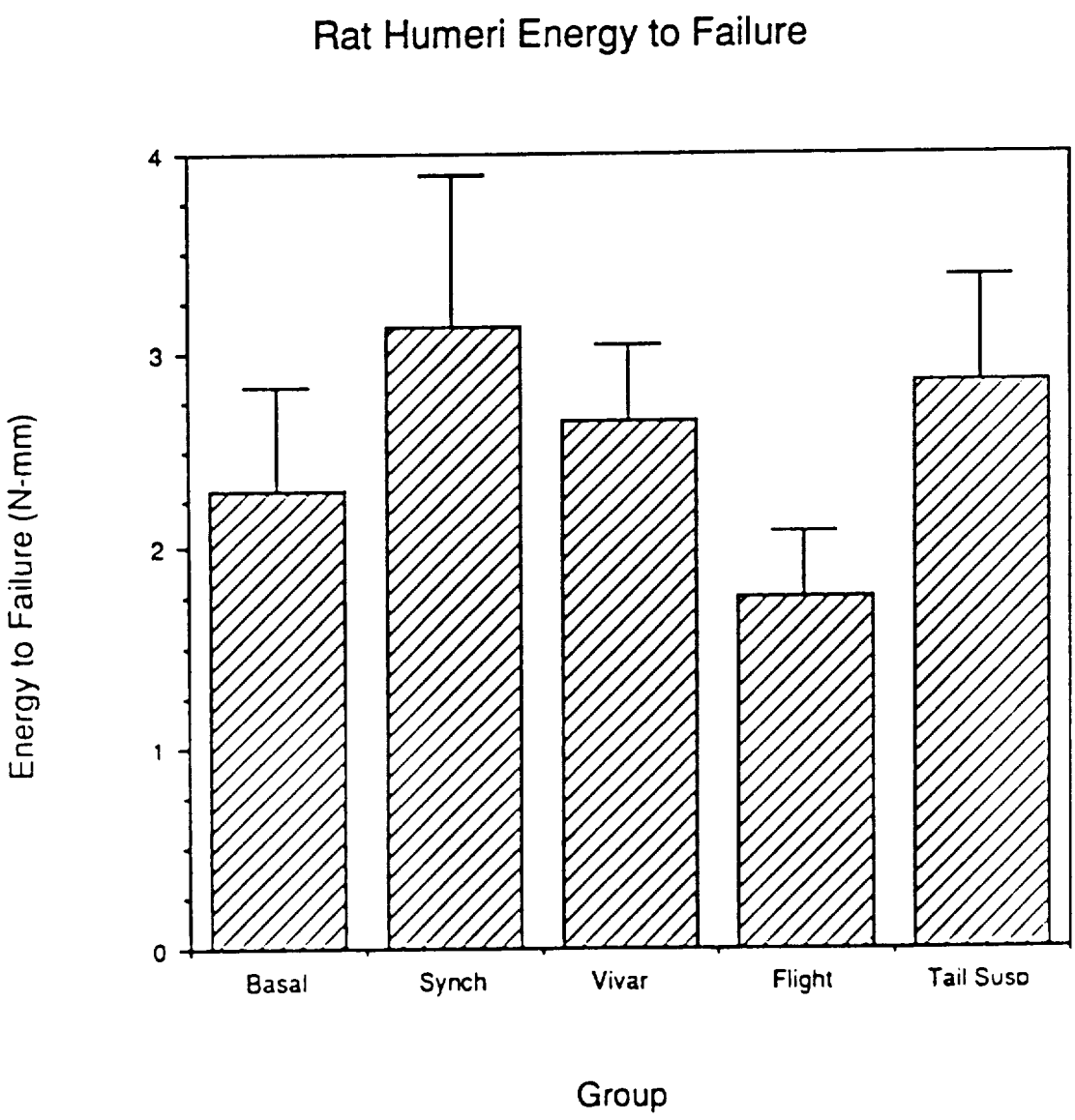
Rat Humeri Energy to Failure
Energy to Failure (N-mm)
4
3
2
1
0
Basal
Synch
Vivar
Flight
Tail Suso
Group

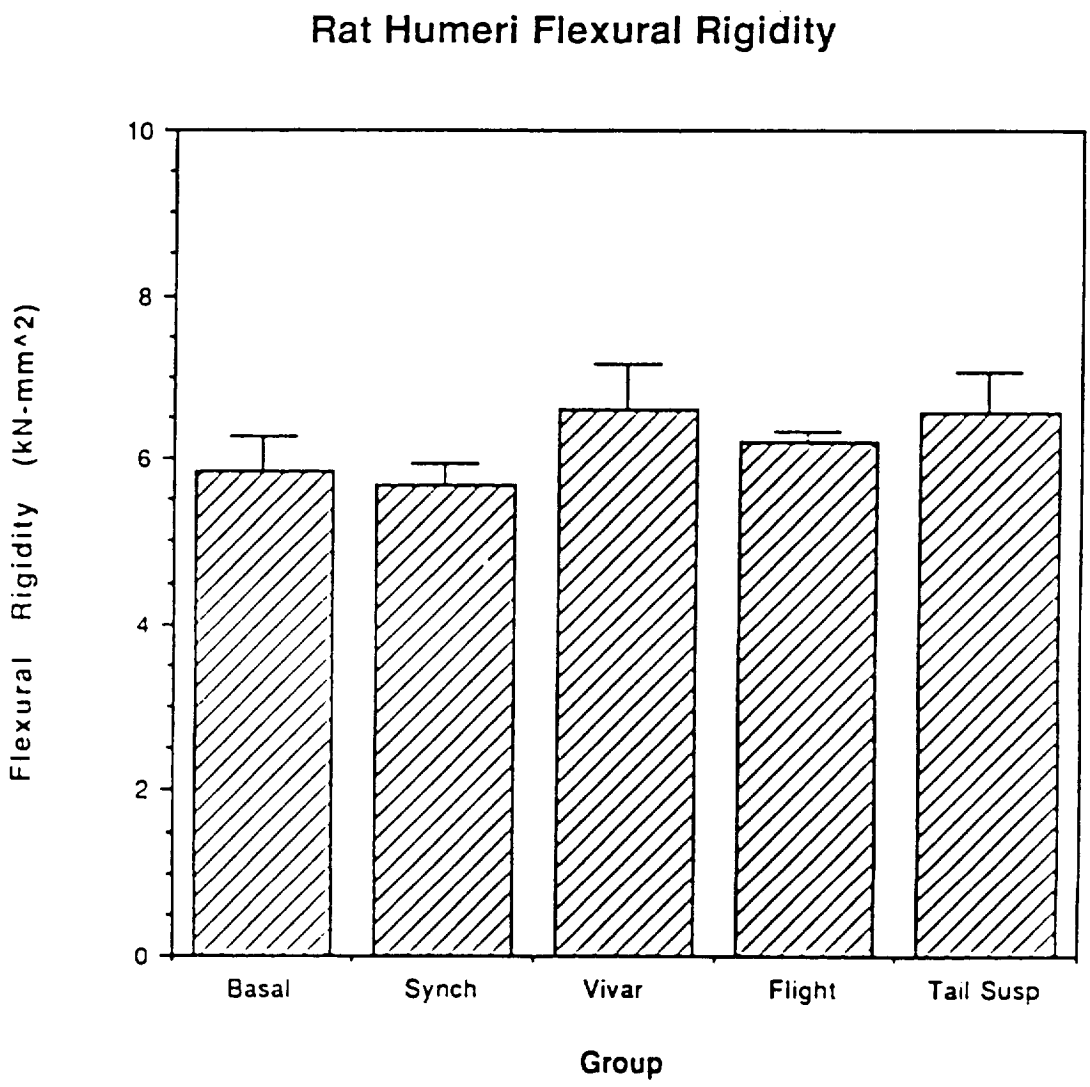
Rat Humeri Flexural Rigidity
Flexural Rigidity (kN-mm^2)
10
8
6
4
2
0
Basal
Synch
Vivar
Flight
Tail Susp
Group

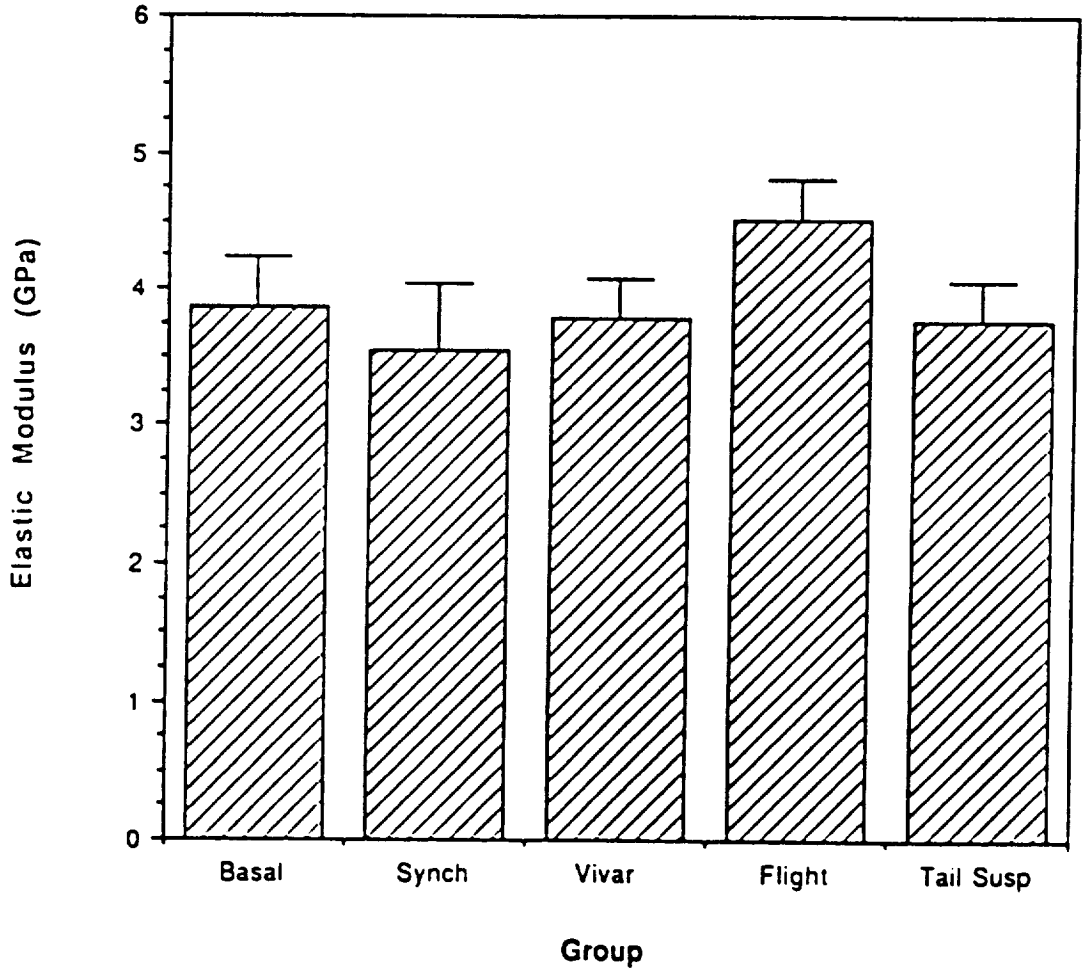
Rat Humeri Elastic Modulus
Elastic Modulus (GPa)
6
5
4
3
2
1
0
Basal
Synch
Vivar
Flight
Tail Susp
Group

Rat Humeri Elastic Modulus (calculated from morphologic data)

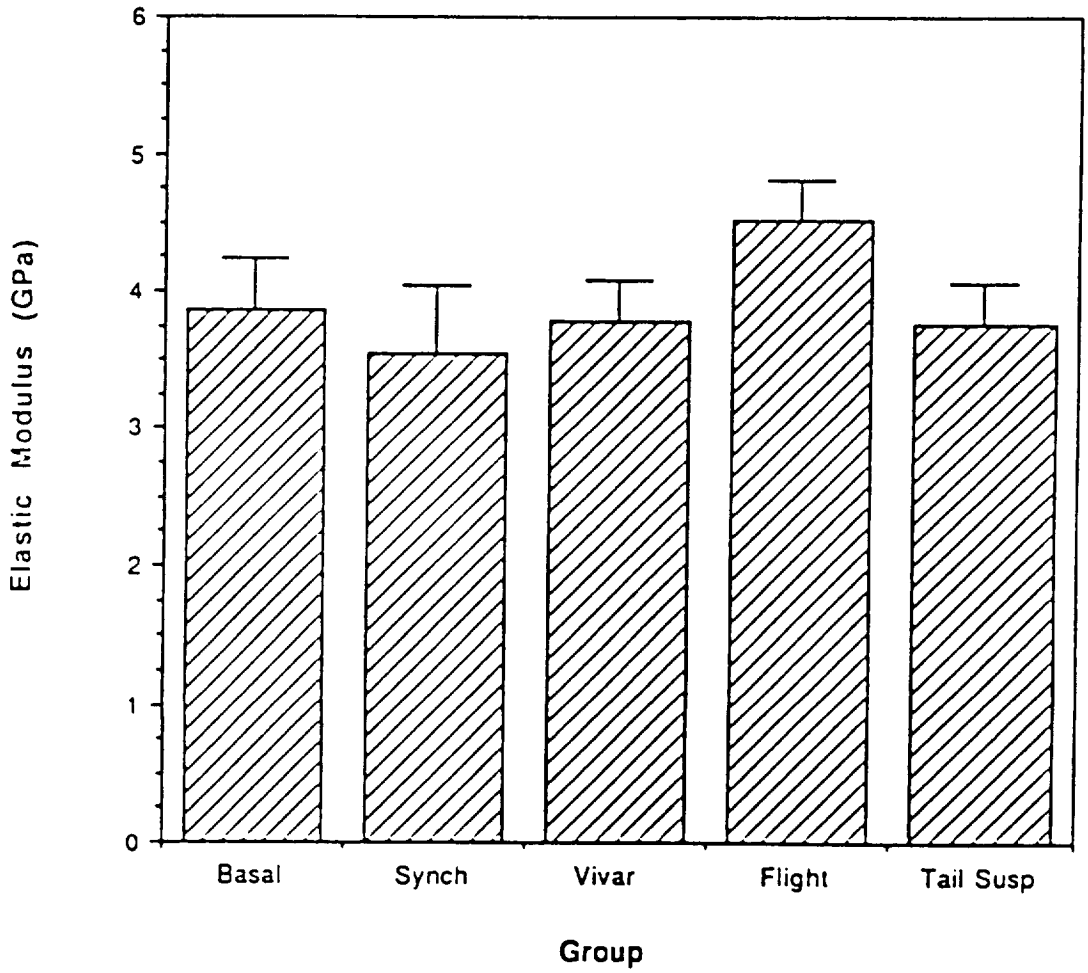

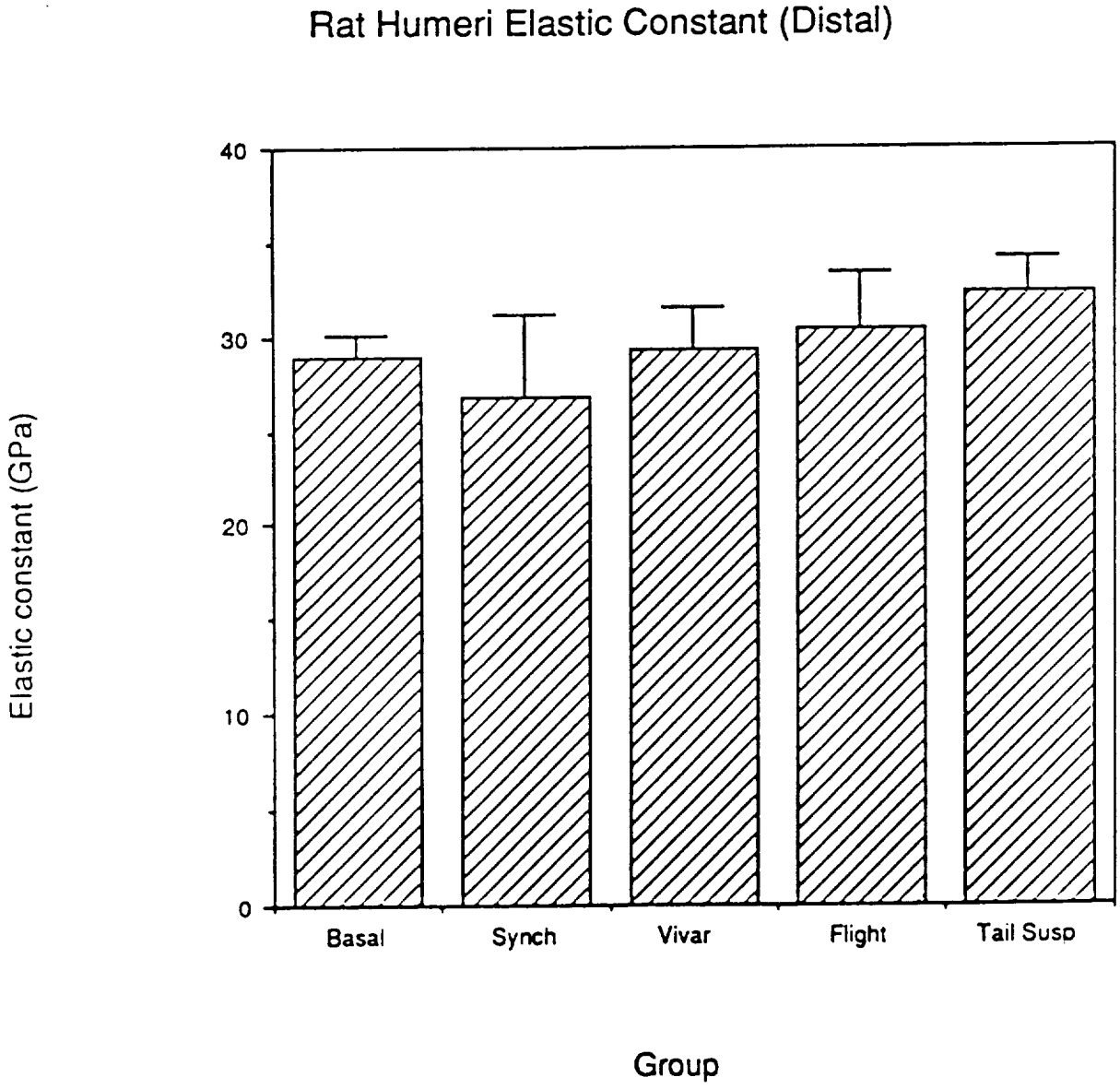
Rat Humeri Elastic Constant (Distal)
Elastic constant (GPa)
40
30
20
10
0
Basal
Synch
Vivar
Flight
Tail Susp
Group

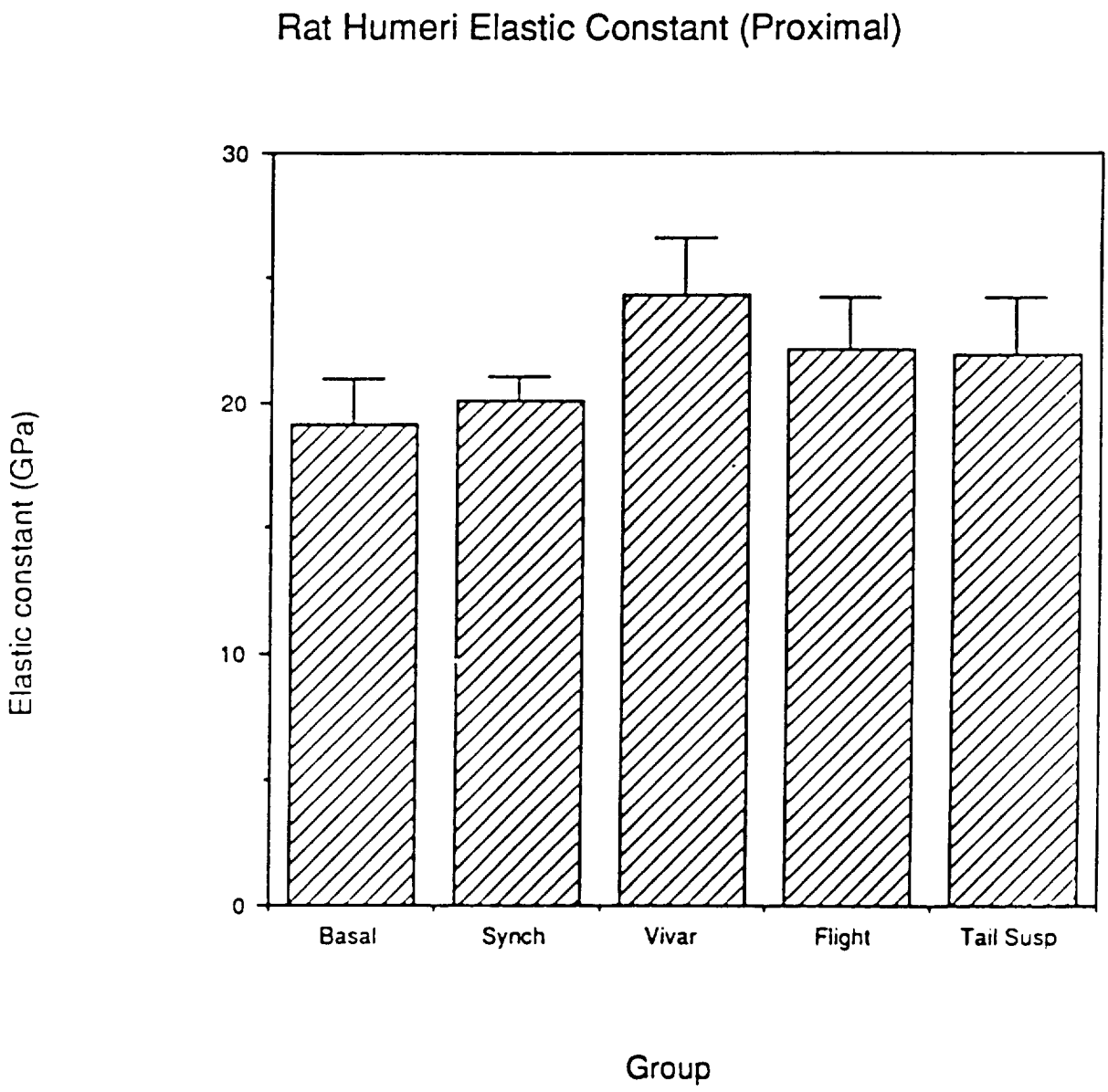
Rat Humeri Elastic Constant (Proximal)
Elastic constant (GPa)
30
20
10
0
Basal
Synch
Vivar
Flight
Tail Susp
Group

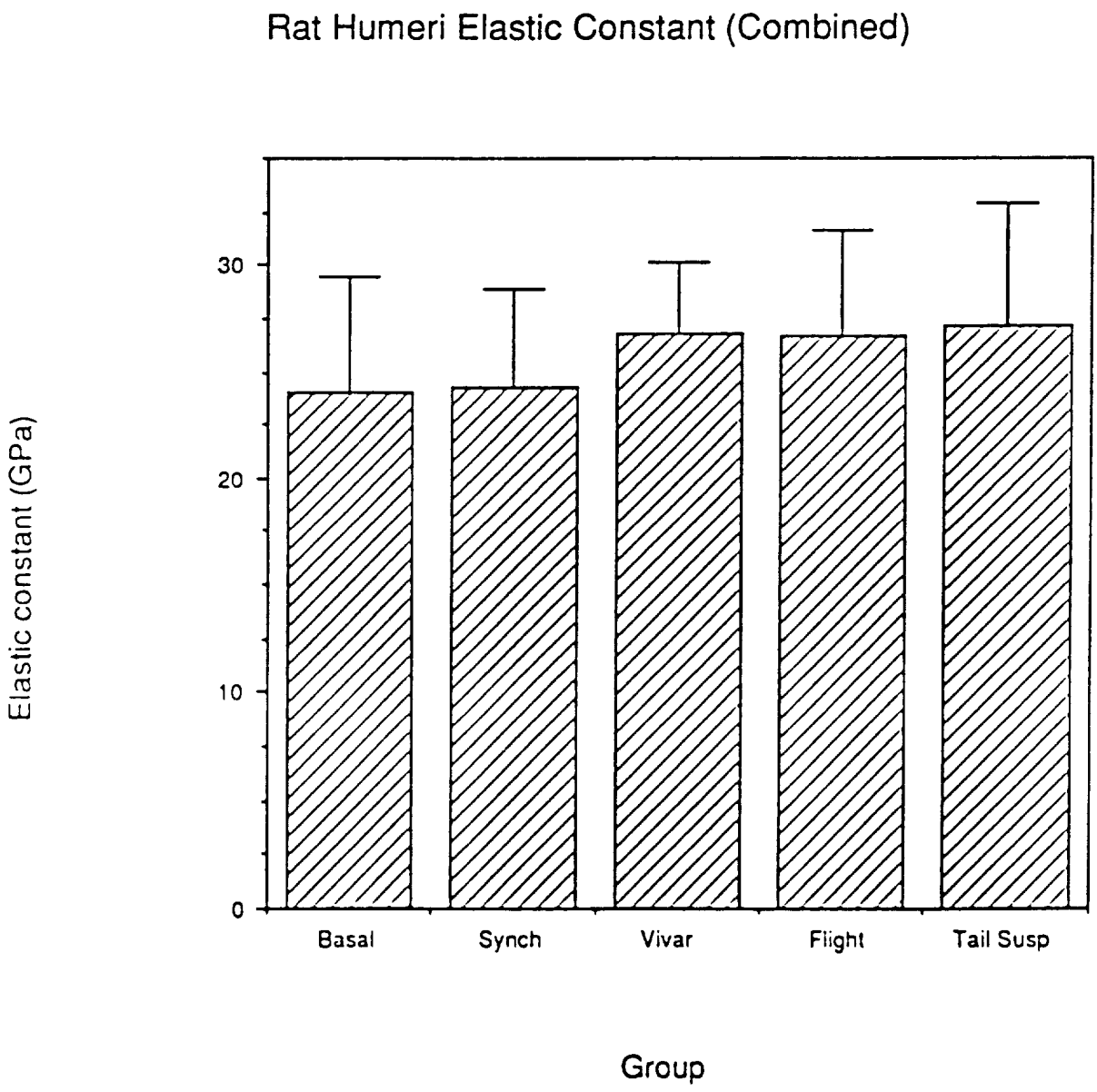
Rat Humeri Elastic Constant (Combined)
Elastic constant (GPa)
30
20
10
0
Basal
Synch
Vivar
Flight
Tail Susp
Group

MID DIAPHYSEAL MORPHOLOGICAL PROPERTIES OF HUMERUS

Cortical Bone Lengths

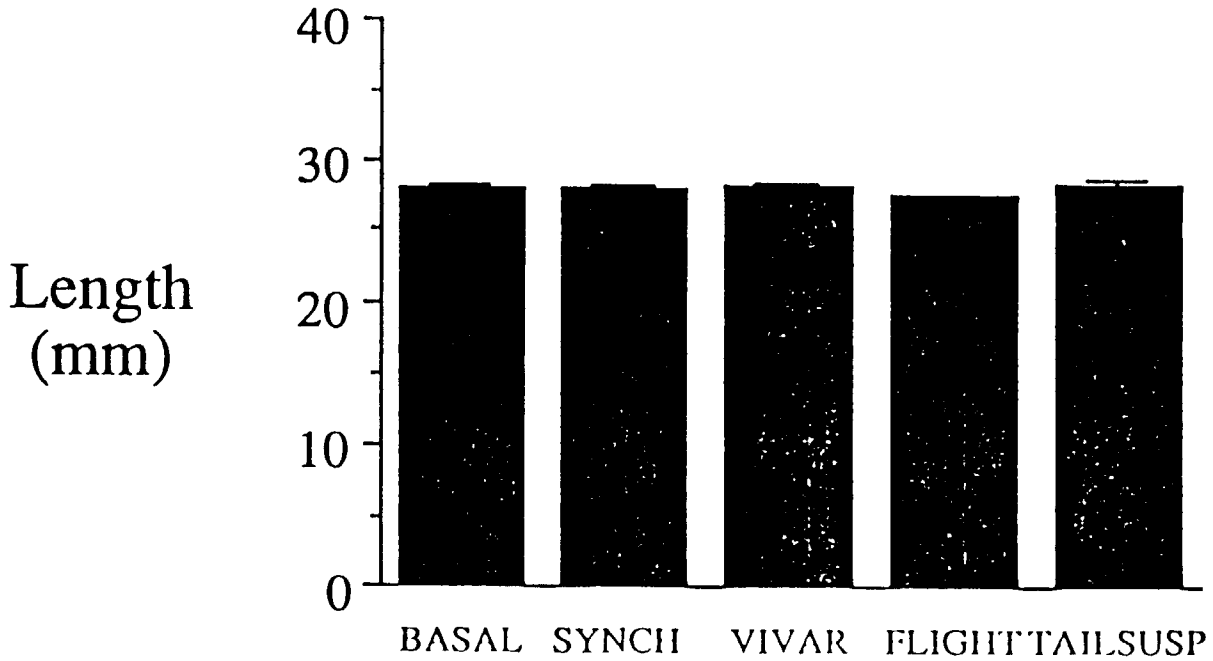

Cortical Bone Density

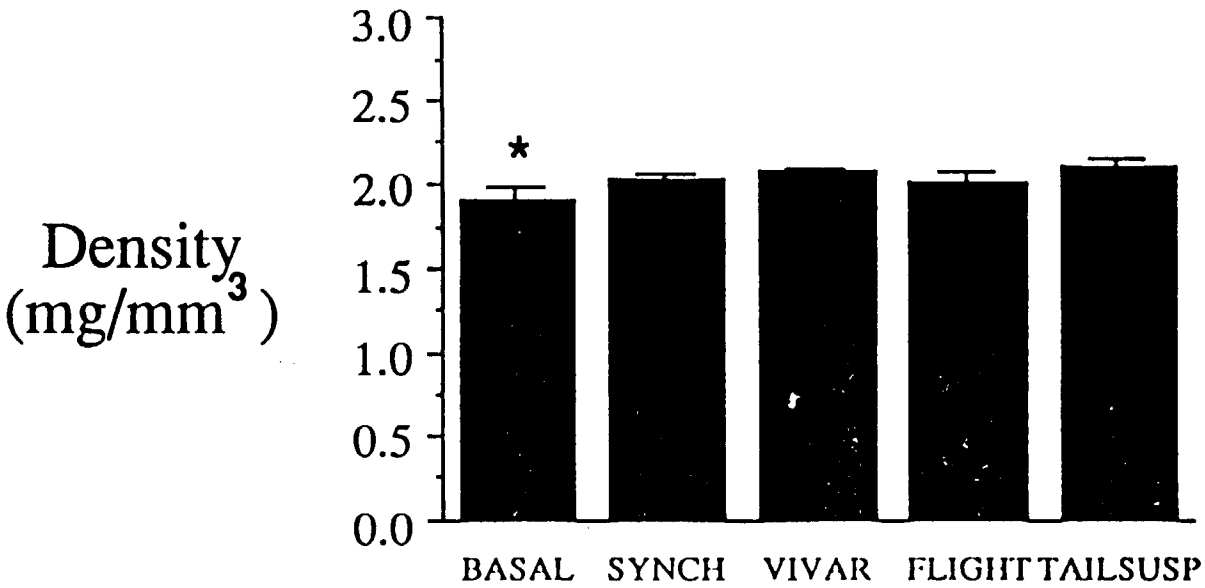

* Basal group is significantly ($p \leq 0.05$) different from the Tailsusp group.

Cortical BoneTotal Cross-sectional Area

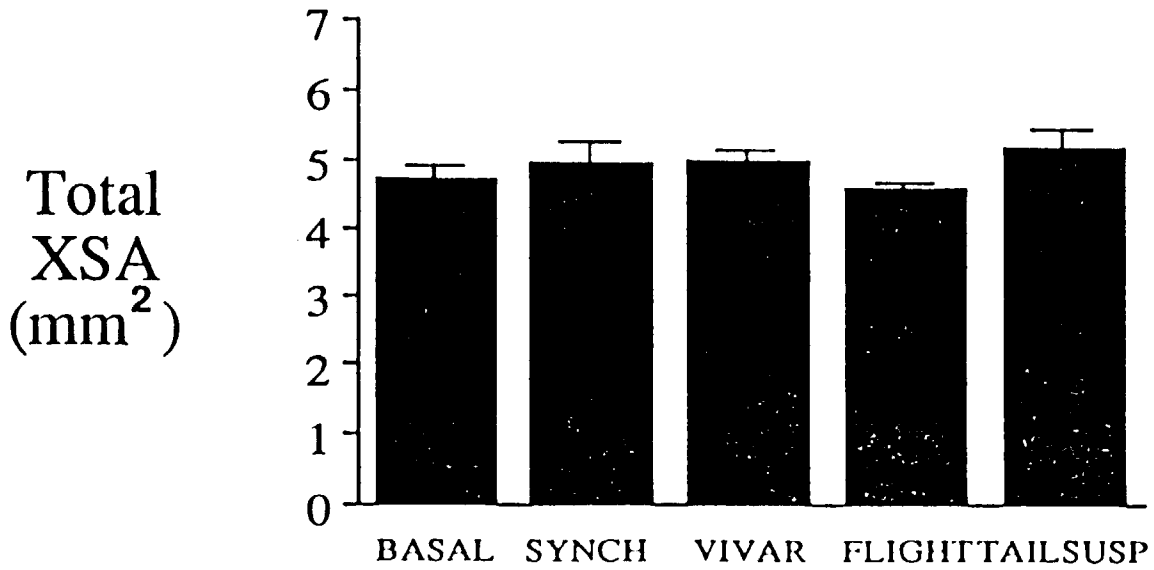

Cortical Bone Cross-sectional Areas

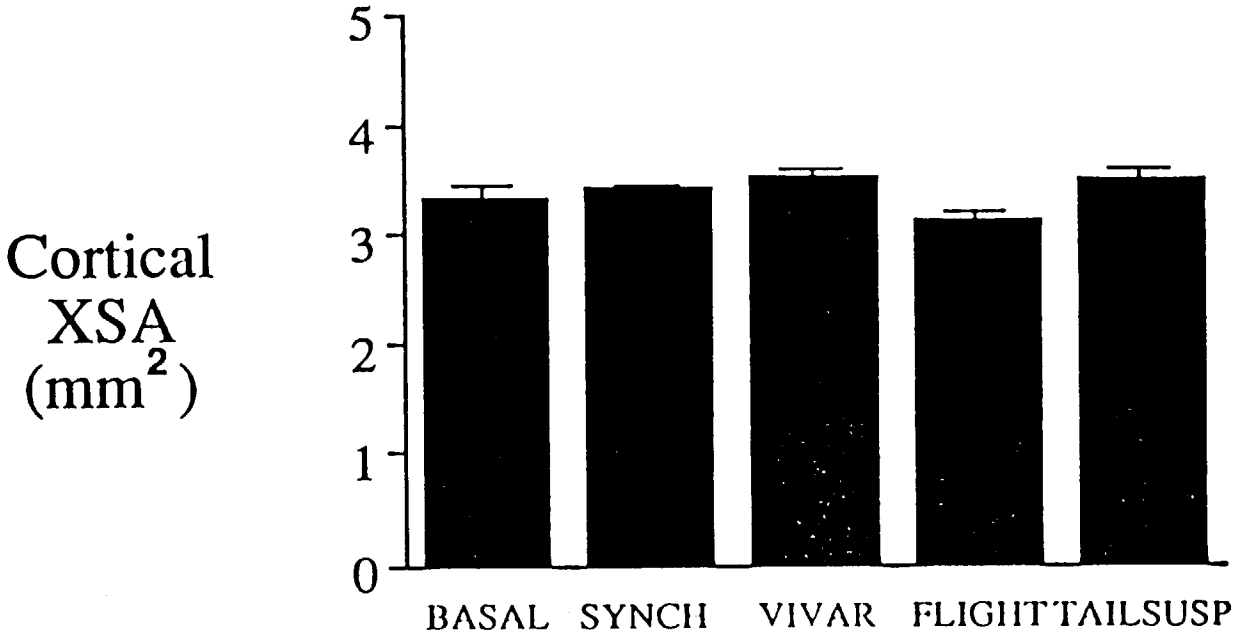

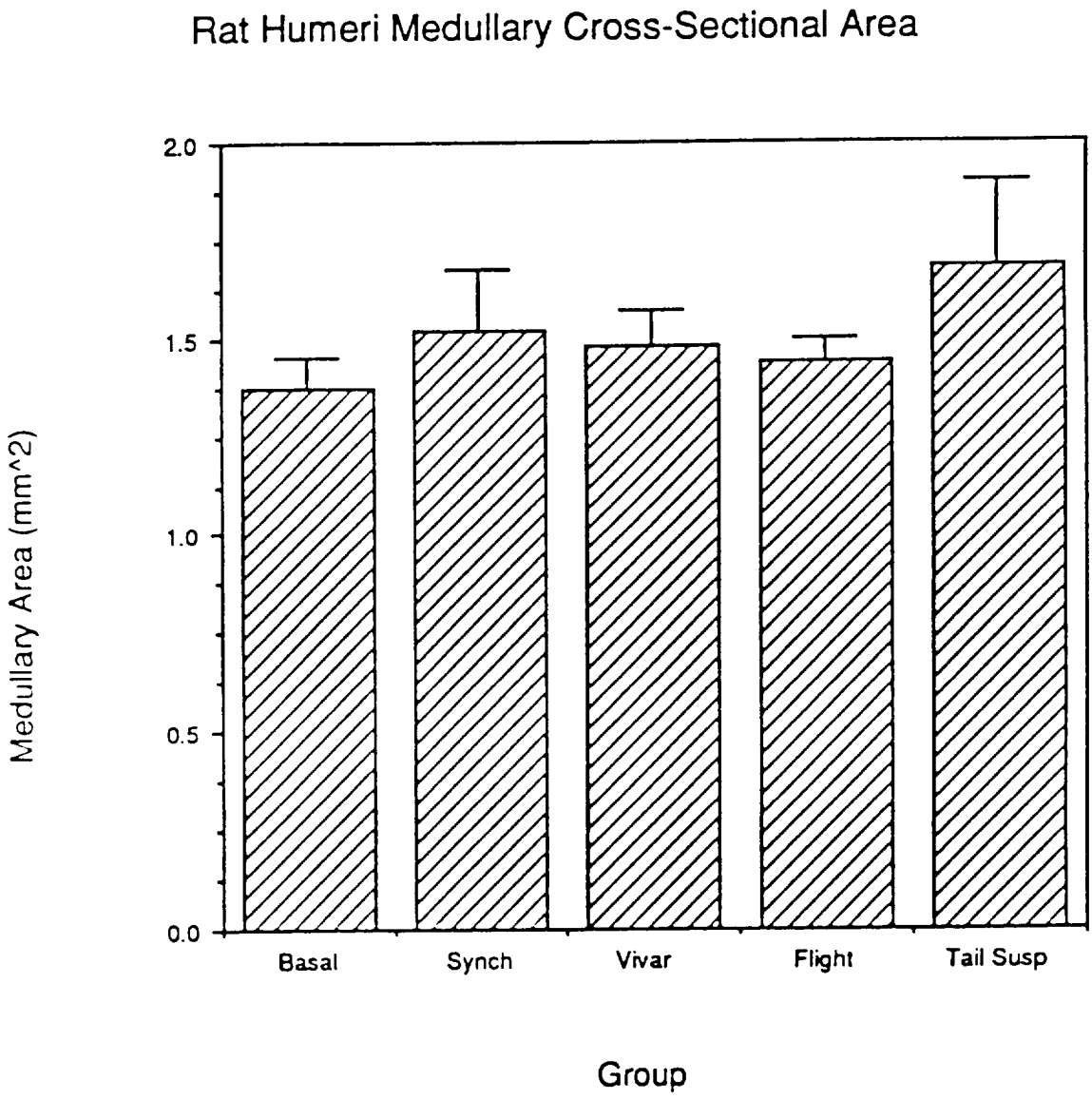
Rat Humeri Medullary Cross-Sectional Area
Medullary Area (mm^2)
2.0
1.5
1.0
0.5
0.0
Basal
Synch
Vivar
Flight
Tail Susp
Group

Rat Humeri Area Moment of Inertia about Cranial-Caudal Line

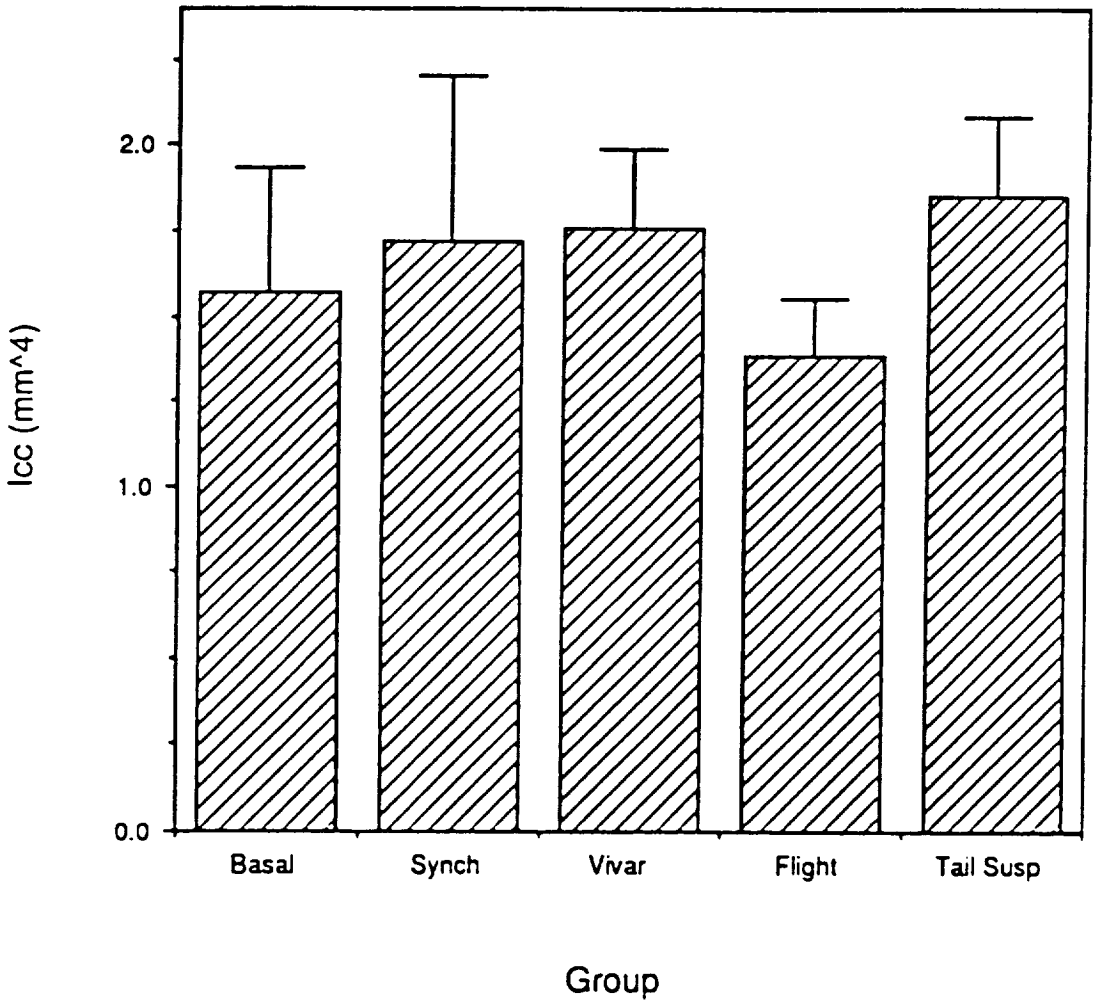

Rat Humeri Area Moment of Inertia about Medial-Lateral Line

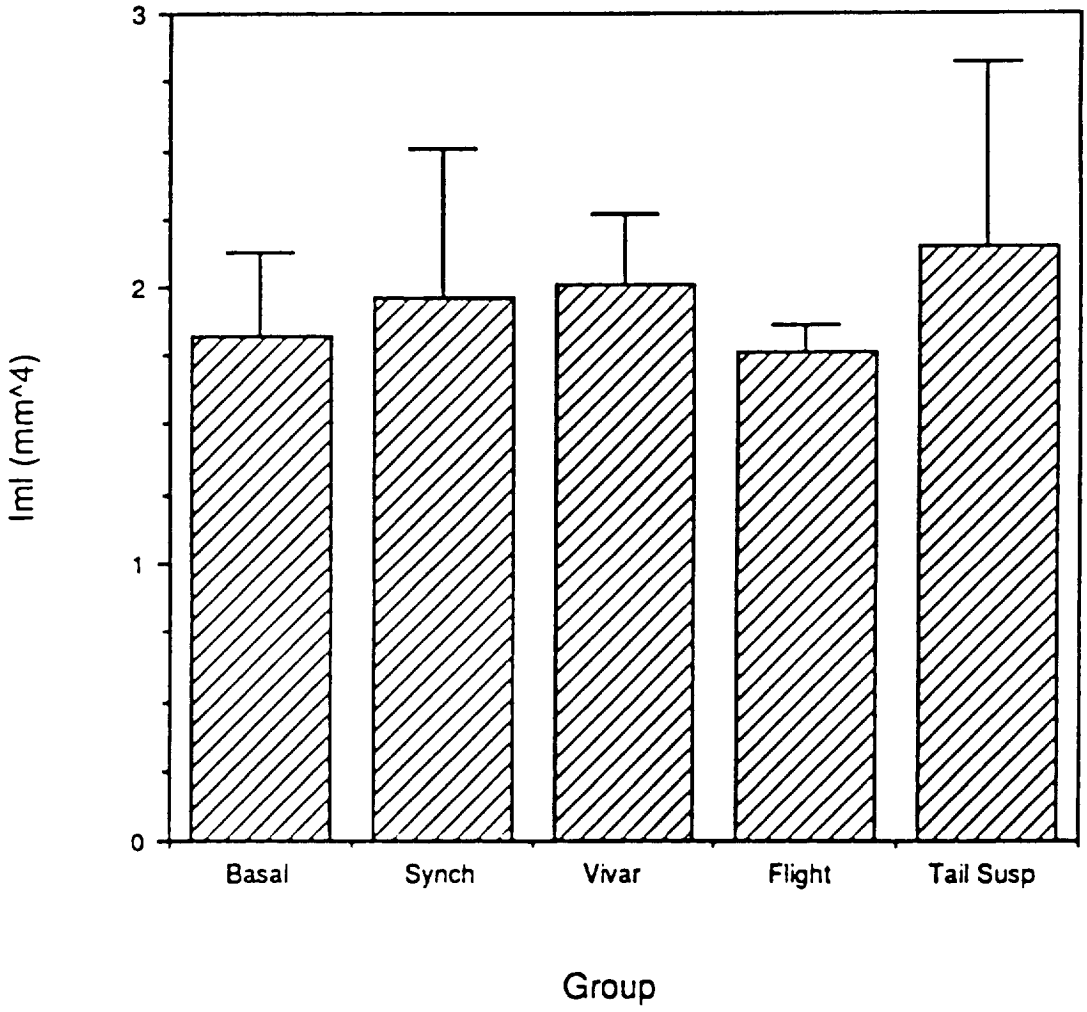

Cortical Bone Regional Thickness

Thickness (mm)	BASAL	SYNCH	VIVARIUM	FLIGHT	TAIL SUSPENSION
Anterior	.663±.059	.622±.024	.685±.037	.681±.031	.695±.052
Posterior	.474±.025	.486±.018	.467±.015	.422±.011	.459±.011
Medial	.526±.023	.504±.016	.489±.011	.459±.025	.497±.059
Lateral	.584±.026	.562±.027	.602±.018	.555±.028	.593±.012

Values are Means±SE.

No significant differences were found between groups ($p > 0.05$).

Cortical Bone Perimeters

Perimeters	BASAL	SYNCH	VIVARIUM	FLIGHT	TAIL SUSPENSION
Periosteal (mm)	8.75±0.16	8.76 ±0.30	8.86±0.15	8.59±0.08	9.07±0.28
Endosteal (mm)	4.67±0.14	4.80±0.25	4.74±0.17	4.74±0.04	5.06±0.39

Values are Means±SE.

No significant differences were found between groups ($p > 0.05$)

Cortical Bone Diameters about the Centroid

Diameters	BASAL	SYNCH	VIVARIUM	FLIGHT	TAIL SUSPENSION
Maximum (mm)	2.75±0.05	2.76±0.07	2.80±0.06	2.77±0.04	2.89±0.13
Minimum (mm)	2.24±0.08	2.34±0.09	2.31±0.03	2.19±0.04	2.33±0.05

Values are Means±SE.

No significant differences were found between groups ($p > 0.05$)

Cortical Bone Area Moments of Inertia

Diameters (mm^4)	BASAL	SYNCH	VIVARIUM	FLIGHT	TAIL SUSPENSION
X Axis	1.43±0.15	1.62±0.24	1.58±0.09	1.28±0.06	1.68±0.12
Y Axis	1.95±0.09	2.06±0.21	2.18±0.14	1.87±0.05	2.32±0.27

Values are Means±SE.

No significant differences were found between groups ($p > 0.05$)

MID DIAPHYSEAL BIOCHEMICAL PROPERTIES OF HUMERUS

TABLE 1. *Humerus middiaphysial matrix concentrations and collagen crosslink molar ratios*

	BASAL	SYNCH	VIVAR	FLIGHT	T-SUSPENDED
Calcium Concentration (μg/mg dry wt.)	292 ± 10.6	286 ± 3.4	267 ± 22.0	292 ± 7.5	288 ± 6.4
Hydroxyproline Concentration (μg/mg dry wt.)	17.2 ± 0.32	16.9 ± 0.24	15.8 ± 1.44	18.3 ± 0.26	18.5 ± 0.08
Hydroxylysyl-pyridinoline Crosslink (M/M)	0.311 ± .01	0.329 ± 0.01	0.329 ± 0.01	0.310 ± 0.00	0.311 ± 0.01
Lysylpyridinoline Crosslink (M/M)	0.298 ± .02	0.303 ± 0.01	0.299 ± 0.01	0.271 ± 0.01	0.268 ± 0.01

Values represent Means ± SE.

TABLE 2. *Parameters of humerus cortical bone composition per unit volume* $(mm)^3$

	BASAL	SYNCH	VIVAR	FLIGHT	T-SUSPENDED
Total Collagen Content ($\mu g/mm^3$)	233 ± 9.1	246 ± 5.4	235 ± 22.6	265 ± 9.2	271 ± 9.5
Total Calcium Content ($\mu g/mm^3$)	552 ± 5.9	581 ± 12.4	556 ± 47.4	591 ± 24.7	590 ± 17.2
Ca^{++}/Collagen Ratio	2.37 ± 0.07	2.37 ± 0.06	2.39 ± 0.10	2.22 ± 0.04	2.18 ± 0.05
Cortical Bone Density (mg/mm^3)	1.90 ± 0.07	2.02 ± 0.03	2.07 ± 0.03	2.02 ± 0.05	2.12 ± 0.03

Values represent Means ± SE.

L-5 LUMBAR VERTEBRAE BIOMECHANICAL AND MORPHOLOGICAL PROPERTIES

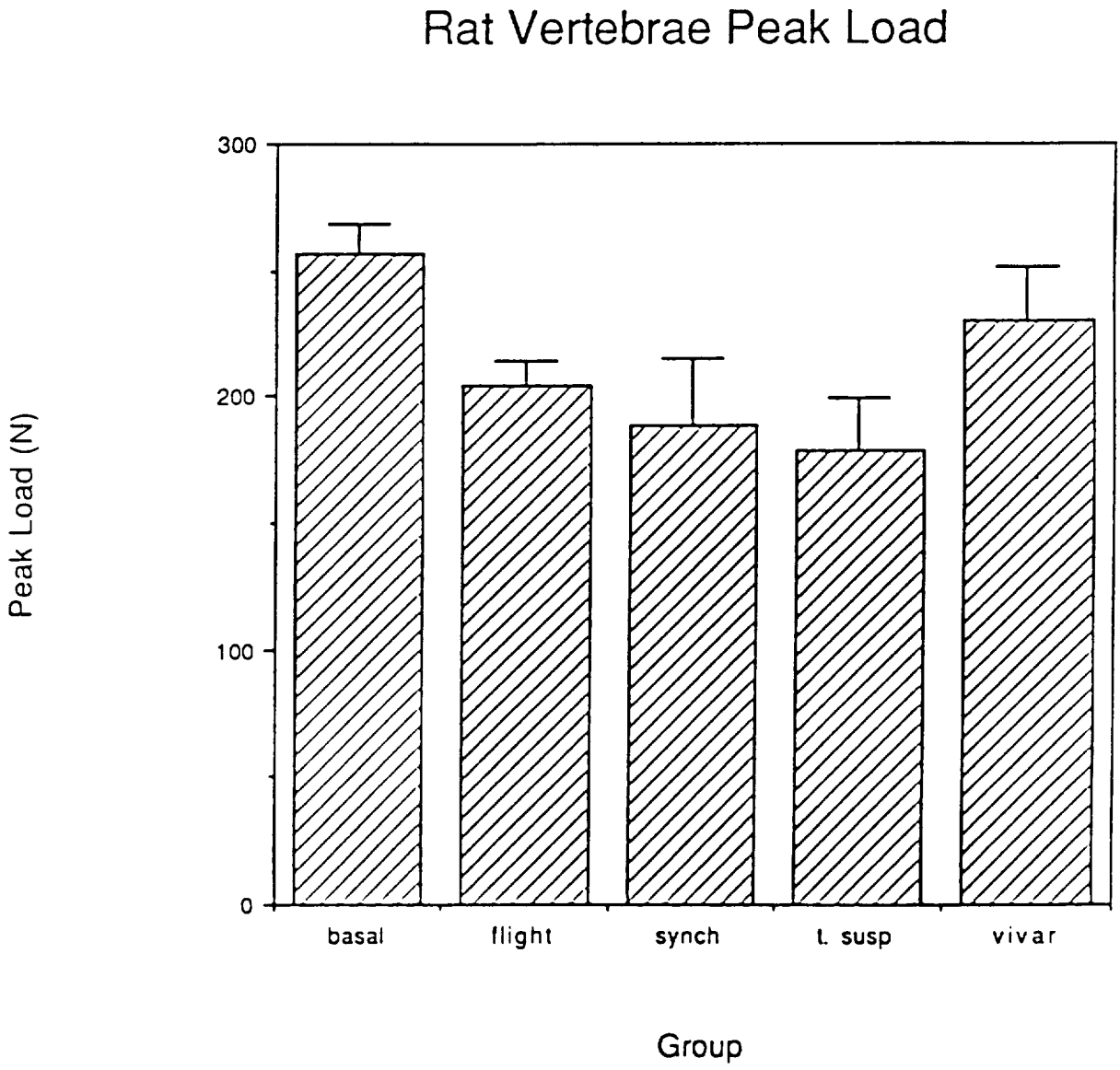

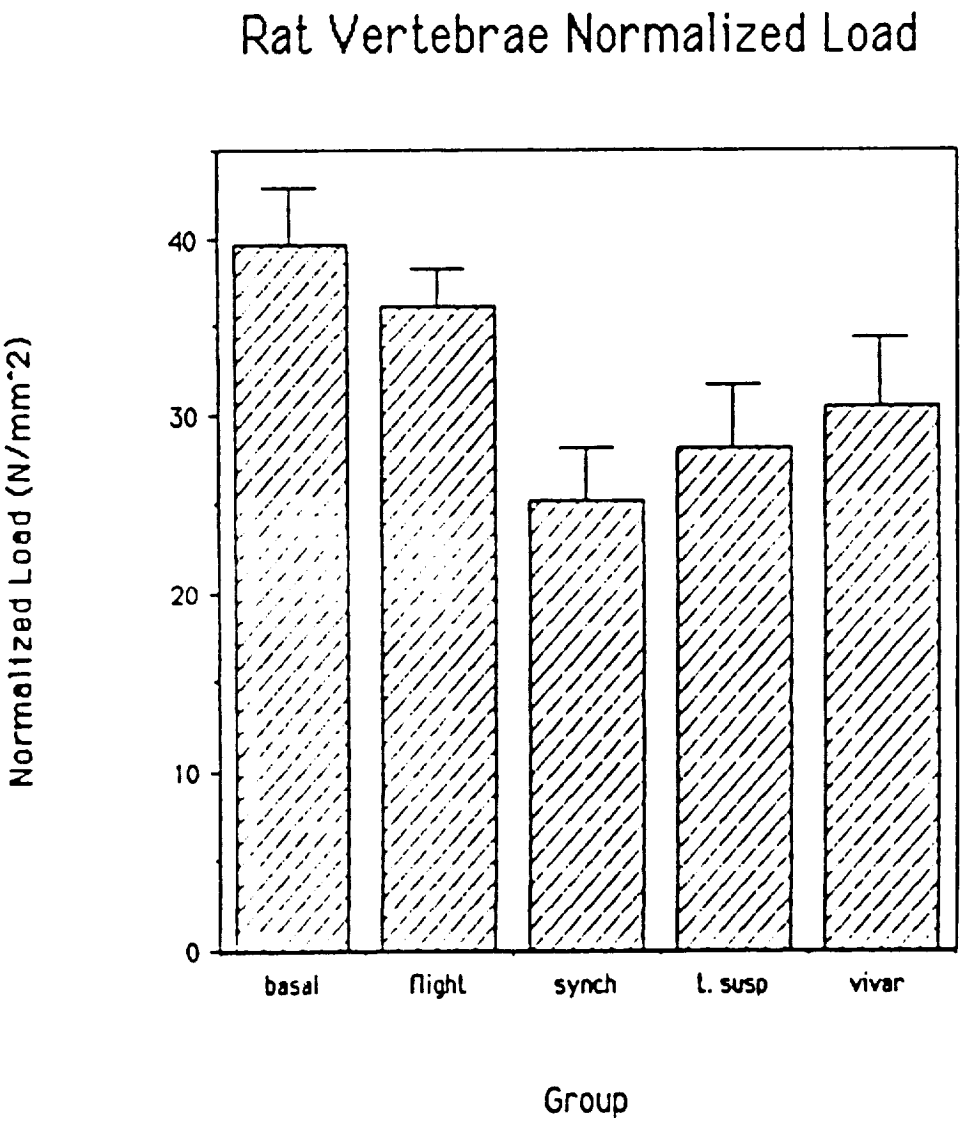
Rat Vertebrae Normalized Load
Normalized Load (N/mm^2)
0
10
20
30
40
basal
flight
synch
t. susp
vivar
Group

Rat Vertebrae Cross-sectional Area

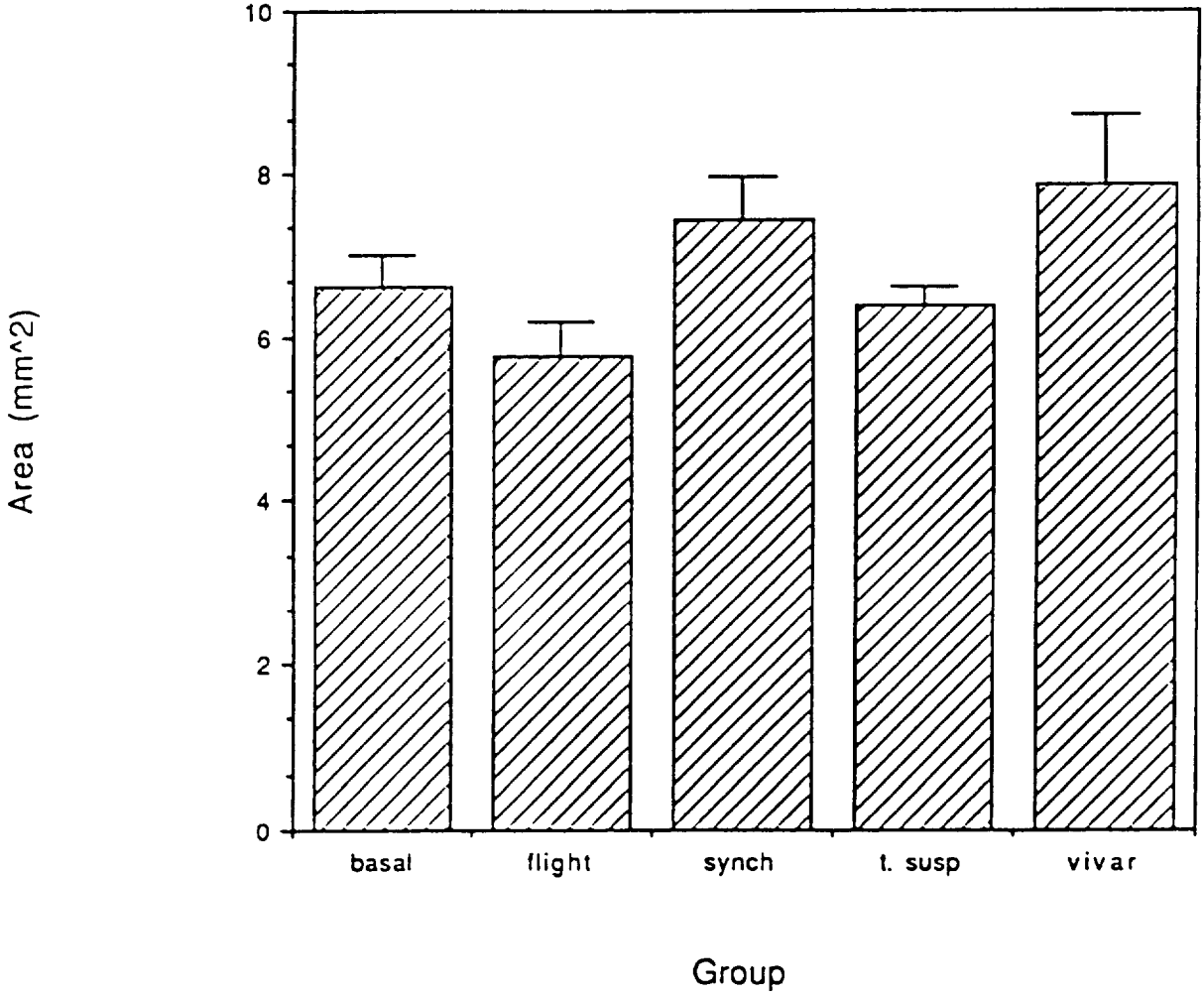

L-5 LUMBAR VERTEBRAE BIOCHEMICAL PROPERTIES

TABLE 3. *Vertebral body mineral composition*

	BASAL	SYNCH	VIVAR	FLIGHT	T-SUSPENDED
Calcium Concentration (μg/mg dry wt.)	226 ± 2.6	225 ± 2.6	221 ± 6.0	225 ± 4.0	225 ± 3.0
Ca^{++}/Collagen Ratio	1.64 ± 0.13	1.71 ± 0.05	1.67 ± 0.03	1.64 ± 0.04	1.44 ± 0.03

Values represent Means ± SE.

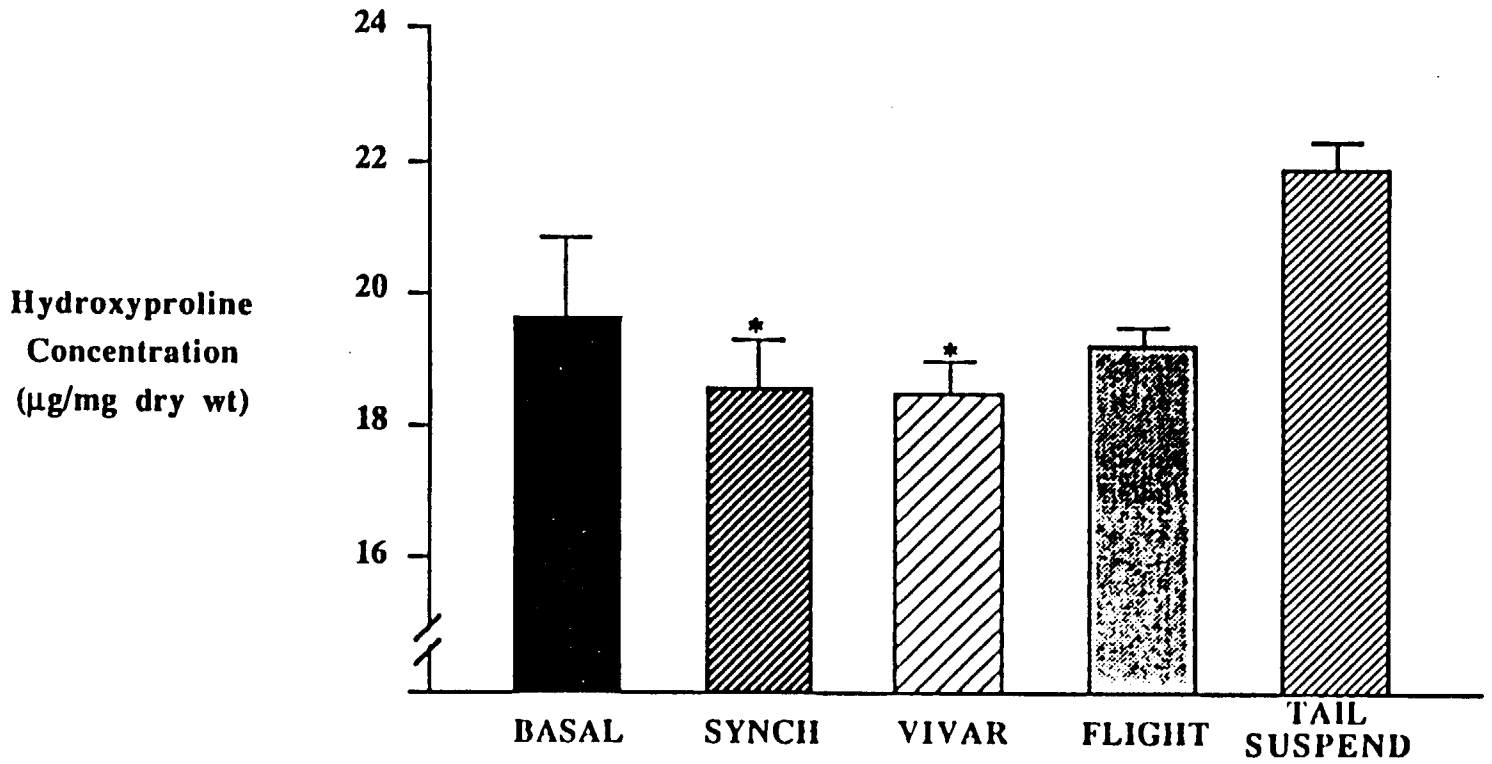

Figure 1. Vertebral body hydroxyproline concentration (µg/mg dry weight). *Synch and Vivar groups are significantly less than the Tail-suspended group ($p \leq 0.05$).
Values represent Means ± SE.

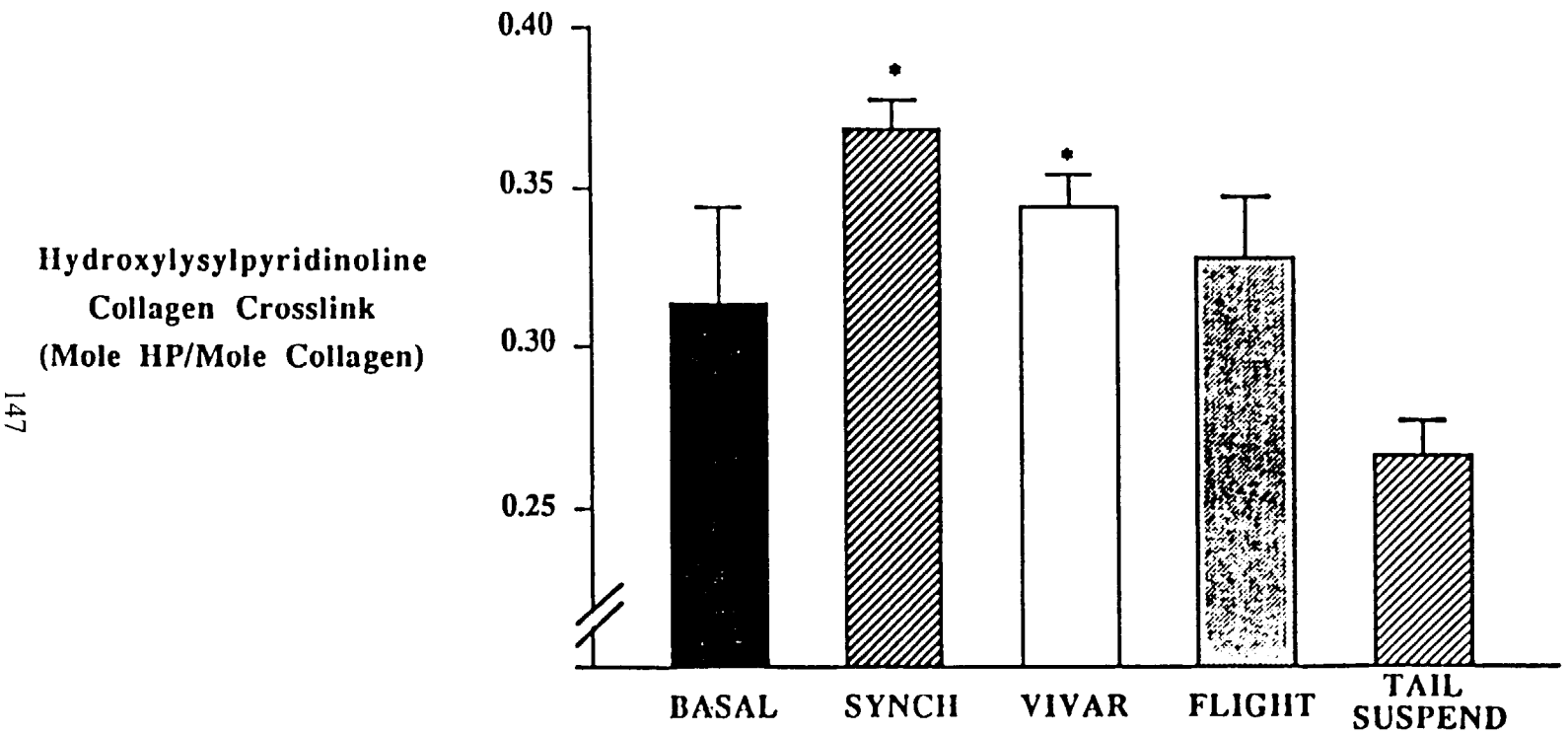

Figure 2. Vertebral body hydroxylysylpyridinoline crosslink content.
*Synch and Vivarium groups are significantly different from the Tail-suspended group ($p \leq 0.05$).
Values represent Means ± SE.

PATELLAR AND ACHILLES TENDON BIOCHEMICAL PROPERTIES

149

TABLE 4. *Patellar tendon DNA, uronic acid and collagen concentration, and crosslink content*

	BASAL	SYNCH	VIVAR	FLIGHT	T-SUSPENDED
DNA (μg/mg dry wt)	8.95 ± 0.39	8.10 ± 0.71	9.12 ± 0.66	9.79 ± 0.81	9.04 ± 0.42
Uronic Acid (μg/mg dry wt)	1.07 ± 0.13	1.16 ± 0.04	1.36 ± 0.10	1.34 ± 0.03	1.35 ± 0.24
Hydroxyproline (μg/mg dry wt)	72.88 ± 4.0	105.47 ± 13.4	92.27 ± 3.7	95.05 ± 6.2	91.88 ± 6.8
Hydroxylysyl-pyridinoline Crosslink (M/M)	0.286 ± 0.01	0.253 ± 0.03	0.313 ± 0.03	0.275 ± 0.01	0.268 ± 0.03

Values represent Means ± SE.

TABLE 5. *Achilles tendon DNA, uronic acid and collagen concentration, and crosslink content*

	BASAL	SYNCH	VIVAR	FLIGHT	T-SUSPENDED
DNA (μg/mg dry wt)	8.41 ± 0.56	8.67 ± 0.60	8.88 ± 0.78	7.69 ± 0.30	8.06 ± 0.62
Uronic Acid (μg/mg dry wt)	1.39 ± 0.03	1.67 ± 0.22	1.64 ± 0.06	1.57 ± 0.07	1.71 ± 0.37
Hydroxyproline (μg/mg dry wt)	95.57 ± 3.3	101.42 ± 6.4	97.40 ± 10.7	99.45 ± 5.0	109.17 ± 3.8
Hydroxylysyl-pyridinoline Crosslink (M/M)	0.308 ± 0.02	0.318 ± 0.04	0.336 ± 0.05	0.309 ± 0.05	0.288 ± 0.03

Values represent Means ± SE.

EXPERIMENT K-7-02

PART II: THE EFFECTS OF MICROGRAVITY ON THE COMPOSITION OF THE INTERVERTEBRAL DISC

A. Pedrini-Mille, J.A. Maynard, G.N. Durnova, I.B. Krasnov,
V. A. Pedrini, C. B.Chung, J. Fedler-Troester

ABSTRACT

The size, water content, and composition of lumbar annuli of rats flown for 14 days on Cosmos Mission 2044 were compared to those of three control groups and a tail suspension experimental model. Our data indicate that as a result of weightlessness 1) there was a significant ($p<0.05$) reduction in the weight of the annuli which was attributed to an actual loss of tissue components and not to water loss; 2) the annular matrix became proportionally more collagenous ($p<0.02$), but without abnormal changes in the relative proportions of Type I and II collagen or in the number of pyridinoline cross-links; 3) the collagen-proteoglycan ratio in the annuli of flight animals was significantly greater ($p<.001$) than that of the three control groups combined; 4) when the annuli were immersed in water or saline solutions for two hours, more proteoglycans ($p<0.001$) leached out of the annuli of flown rats than from the tissue of control animals, suggesting the presence of abnormal or smaller proteoglycans. Safranin-O staining, however, indicated a normal spatial distribution of the proteoglycans within the annulus. Tail suspension did not affect the size of the annuli, but it seemed to affect the annular matrix composition, since more proteoglycans ($p<0.05$) leached out from the tissue of suspended animals than from the normal annuli. The reduction in size of the annulus and the abnormal ratio between the fibrous collagenous network and the proteoglycan gel caused by spaceflight may indeed affect the biomechanical properties of the annulus and problems could occur at the return to normal gravitational field. The observed changes may be temporary and totally reversible *if* injuries are avoided in the interim period.

INTRODUCTION

The intervertebral disc is formed by three structures: the nucleus pulposus (NP), the annulus fibrosus (AF) and the cartilaginous endplates (EP). Each of these structures consist primarily of collagen, proteoglycans (PG) and water. These components are primarily responsible for the functional properties of the disc which involve the ability to withstand compression with axial loads and the rotational and shear forces associated with movement. The NP consists primarily of Type II collagen and nonaggregating PG. Due to the high concentration of PG in the NP, the tissue attracts water and exerts a swelling pressure which enables it to support an applied load. The AF is primarily composed of Types I and II collagens embedded in a PG gel. The fibers are oriented in concentric lamellae with each lamella running at 60^{o} angles to the adjacent band. Such alignment enables the fibrous annulus to sustain the rotational and shear forces associated with movement and the swelling forces exerted in all directions by the NP (12).

The effects of weightlessness on the disc have not been well defined. Tyrrell et al. (28) reported that fluid loss together with disc deformation is primarily responsible for changes of nearly 1% in human height between morning and night. Thorton et al. (27) attributed fluid imbibition as being most likely accountable for the 5 cm increase in height associated with spaceflight. Measurements

Key Words: Intervertebral Disc, Annulus Fibrosus, Spaceflight, Collagen, Proteoglycans, Weightlessness

of the swelling pressures of rat lumbar discs on Cosmos Flight 1887 did not reveal any difference between flight and control rats, but it is not clear whether the swelling pressure of the disc did not change or whether it had returned to normal because of the delay in the recovery of the animals after landing. (11)

Our study was designed to determine the effects of 14 days of weightlessness on the size, water content and composition of the lumbar annuli in rats flown on Cosmos Mission 2044. Changes in the composition of the AF may render it unable to withstand the swelling pressures of the NP and/or the stress and strain associated with movement under load, making the return to normal gravitational fields potentially hazardous. Maintaining the integrity of the disc may be extremely important since Stupakov and Korolev, as cited by Vailas et al. (31), reported the compression stiffness and strength of the vertebra are decreased after spaceflights.

MATERIALS AND METHODS

Ten male Czechoslovakian-Wistar rats were flown on the Cosmos 2044 Flight for 14 days. Flight, housing, feeding, recovery and sacrifice conditions were as described in the Mission Description section of this technical report. Tissues from rats numbered 6-10 were used in our projects.

After sacrifice, the spinal column between lumbar vertebra L3-L6 including the L3-4 and L6-S1 intervertebral discs were isolated intact, hermetically wrapped and frozen in liquid nitrogen and transported to The University of Iowa in transporter vials packed in dry ice.

After receiving the tissues, the intervertebral discs between lumbar vertebra L3-4, L4-5, L5-6 and L6-S1 were isolated while frozen. Discs L4-5 and L5-6 from each of the five animals per group were used for the biochemical studies. Two of the L3-4 and L6-S1 discs from each group were used for electron microscopy studies, one L3-4 and L6-S1 disc from each group was used for light microscopy, and the remaining two L3-4 and L6-S1 discs from each group were stored as back-up tissue for either biochemical or microscopy studies if needed. The nucleus pulposus was removed from each disc with the aid of a 16-gauge syringe needle. After the intervertebral disc annuli were isolated, the lumbar vertebrae L4 and L5 were transported to the University of Wisconsin for bone studies.

Light Microscopy

The discs for light microscopy were isolated and thawed while being fixed in 1.5% glutaraldehyde in 0.05M cacodylate buffer, 1.0% buffered formalin and 0.5% ruthenium red for 24-48 hours. Each disc was then cut into two halves along the anterior-posterior axis, dehydrated in ethanol, cleared in xylene and embedded in paraffin. One of the halves from each disc was flat embedded and the other half turned 90 degrees so as to obtain both horizontal and sagittal sections of the disc. All sections were stained using the Safranin-O technique for proteoglycans.

Electron Microscopy

The two L3-4 and L6-S1 annuli for electron microscopy were isolated while frozen and thawed in 5 ml of cold (2-4^{o}C) 2.5% glutaraldehyde in 0.1M cacodylate buffer (pH 7.4) for 15-30 minutes. Each disc was then further trimmed while immersed in glutaraldehyde so as to divide each disc into anterior, transitional and posterior components. The transitional area represented a small segment on the anterior one-half of the annulus fibrosus immediately adjacent to the nucleus pulposus. Small pieces consisting of several laminae from each of the three areas were then stripped from each large component and placed in 2.5% glutaraldehyde in 0.1M cacodylate buffer (pH 7.4) and ruthenium red (2:1) for four hours, after which they were washed in 0.1M cacodylate buffer

(3 ten-minute baths) and post-fixed in 1% osmium tetroxide in 0.1 M cacodylate buffer and ruthenium red (1:1) for two hours. They were then washed in cacodylate buffer, dehydrated *in* ethanol and acetone and embedded in Spurr embedding media. Following polymerization (60oC., 24 hours) thin sections were cut, stained with uranyl acetate and lead citrate and examined in a Hitachi H-7000 electron microscope at 75 kilovolts. Cross-section electron micrographs were taken at 20,000 magnification to determine collagen fibril size in each of the three locations, collagen fibril size frequency distributions in each location and subjective analysis of collagen-proteoglycan relationships as revealed by ruthenium red staining. Longitudinal sections were photographed at 20,000 and 60,000 magnifications to determine collagen fibril-proteoglycan relationships relative to the collagen fibril banding characteristics.

Biochemistry

The lyophilized L4-L5 annuli of each animal were finely minced, weighed and digested with papain at 60oC for 24 hours (20). All papain digests were taken to the same volume (2ml) and then centrifuged to eliminate any undigested material. Aliquots of each digest containing between 150-600 µg of dry tissue were used for hexuronate determination as described by Blumenkrantz et al. (4). Other aliquots of the papain digest, also containing between 150-600 µg of tissue, were hydrolyzed in 6N HCl at 130oC for four hours. After drying under vacuum, the hydrolyzates were dissolved in 1 ml of water, microfuged and then filtered through 45 µm filters. 0.1 ml of the filtered hydrolyzates were used to determine hydroxyproline using 1 ml sample volume (33). To determine the collagen pyridinoline cross-links 600 µl aliquots of each hydrolyzate were applied to a SepPak cartridge previously activated with 5 ml of acetonitrile and washed with 10 ml of water. The sample was then washed down from the cartridge with 2 ml of water, collected directly into a cryotube and lyophilized. The lyophilized eluate was then dissolved in 150 µl of pre-filtered pyridoxamine in 0.2% HFBA (1-nmole/ml). A small aliquot of each sample was used to redetermine hydroxyproline to establish whether a loss of sample had occurred during the purification steps. Under the conditions used no loss of sample was found. Twenty µl aliquots of each sample were then applied to an HPLC Beckman Ultrasphere C18 column (4.6 x 250 mm) protected by a precolumn containing the same stationary phase (e.g. 4.6 x 50 mm Beckman C18 precolumn or Pierce C18 cartridge). The column was eluted isocratically with 0.01M HFBA in 15% acetonitrile at a flow rate of 1 ml/min (20). The cross-links were quantitated with a Shimadzu RF-530 fluorescence monitor with excitation set at 295 nm and emission at 395 nm. The amount of pyridinoline cross-links in the tissue was calculated as residues per mole of collagen, assigning to pyridoxamine a fluorescence equal to 3.1 times that of the cross-links (9) and to collagen a weight equal to 7.14 times the measured amount of hydroxyproline and a molecular weight of 300,000.

To determine the relative proportion of Type I and II collagens in the tissue, the annuli from L5-L6 were cut in relatively large pieces and extracted with 5M guanidinium chloride (pH 6.7) for 24 hours at 5oC with stirring. Guanidine was then removed by suction and the tissue washed at least three times with water, one of the washes lasting about 15 hours at 5oC. The water was then suctioned off and the tissue minced and lyophilized. The lyophilized samples were weighed, suspended in 70% formic acid just previously bubbled with nitrogen for 10 minutes (1 mg of tissue/ml formic acid) and stirred for 10-15 minutes at room temperature. CnBr was dissolved in acetonitrile to obtain a concentration of 20% and an aliquot of this solution added to the tissue suspension to give a concentration of CnBr equal to tenfold the weight of the tissue. The samples were covered and stirred at 37oC for four hours. Each sample was then diluted at least fourfold with water, lyophilized, redissolved in 1 ml of water, microfuged and the clear supernatant lyophilized. The CnBr peptides were weighed, dissolved in treatment buffer (0.125 M tris-Cl pH 6.8, 4%SDS, 20% glycerol, 10% 2-mercaptoethanol) to obtain a concentration of 3 mg/ml, incubated at 37oC for one hour and separated by slab gel electrophoresis by the Laemmli method (15) using a 10% separating gel and a 5% stacking gel. Each well was loaded with 20 µl of sample equal to 60 µg of peptides. The gels were stained with 0.125% Coomassie Blue R-250 in

50% methanol in 10% acetic acid and destained for one hour with 50% methanol and 10% acetic acid, followed by a second destaining solution containing 7% acetic acid and 5% methanol. The gels were read with a densitometer (E.C. Apparatus Corp.) and a a2CB3-5 used to quantitate Type I collagen and a1CB10 for Type II collagen. CnBr peptides from purified Type I collagen from rat tail tendon and Type II collagen from human nucleus pulposus were used as standards. Type I and II collagen peptides were separately dissolved to obtain concentrations of 4 mg of peptides per ml. The two solutions were then mixed to obtain Type I-Type II peptide concentration ratios of 0.11, 0.25, 0.43, 0.67, 1.0, 1.5, 2.3, 4.0 and 9.0. For each concentration ratio, separate wells containing 20, 30, 40, 50, 60, 70, 80 and 90 µg of the peptides were filled. The intensity of the stain of the peptides from each sample was read with a densitometer and the ratio between a2CB3-5 and a1CB10 calculated and related to the known proportions of the two types of collagen placed in the well. In our experience the absolute intensity of the stain relates very poorly to the concentration of the peptide probably because of significant differences in the staining and destaining procedures from gel to gel. To the contrary, the ratio of the intensity of stain of the two peptides from the same well correlates very well with the ratio between Type I and Type II collagen (r=0.997). Visibly significant difference in staining between gels does not affect the results since both peptides are equally affected and the ratio between the two remains unchanged.

RESULTS

Body weights

A statistically significant increase in body weight is observed when the animals in the basal group, sacrificed at the time of the launch, are compared to those in the vivarium group, kept in colony cages until the end of the flight (Table 1). The significant increase in body weight (Basal 320 ± 5; Vivarium 363 ± 5) most probably reflects normal growth occurring between 109 and 129 days. Assuming a linear growth between 109 and 129 days (Fig. 1), the mean body weight of the 127-day-old animals in the synchronous group should be 358 g. At 343 g the animals therefore are 4.3% lighter than predicted by the normal curve. The actual weight of the animals in the flight group is 3.5% less than predicted by the curve and the weight of the suspended group 7.7% less (Fig.1). Compared by Student's t-test of unrelated samples, the body weights of the animals in the synchronous group are not significantly different from those of animals in the flight and suspended group ($p>0.05$). We can therefore conclude that, when the age differences are accounted for, the experimental conditions to which the synchronous, flight and suspended groups were submitted to, have little effect on the body weight of the animals.

Weight of Annuli

The first weight of the annulus was determined at the time of dissection (Time 0), the second weight after the sample was immersed in water for one-two hours, i.e., until two consecutive readings taken 30 minutes apart indicated that a stable weight had been reached (Stable Time). Each sample was then lyophilized and the dry weights determined. The time of hydration necessary to reach constant weight varied somewhat between samples, possibly because of differences in thickness. A stable weight was always reached within two hours. Allowing the sample to stay in the hydrating medium (water or saline) for up to three hours did not significantly change its weight.

For each animal we determined the weights of the L4-L5 and L5-L6 annuli. The weights of the two annuli were not significantly different, therefore their mean values (L4-L6, Table 1) were used to compare groups.

The wet and dry weights of the annuli from the three control groups (basal, vivarium, synchronous) were not significantly different from each other, although the annuli from the

youngest group (basal) were consistently the heaviest (Table 1). The flight conditions at 1 g, as experienced by the synchronous group, did not affect the wet or dry weight of the annuli that were practically identical to those of the vivarium group (Table 1). To the contrary, weightlessness for 14 days did affect the wet and dry weights of the annuli from the flight group as they were significantly smaller (20%-25%) than the annuli from the synchronous or vivarium groups (Table 1). The weights of the annuli of the suspended animals were within normal limits and significantly different only from those of animals in the flight group
(Table 1).

Water Content

The water contents of the annuli from L4-L5 and L5-L6 of the same animal were very similar in all cases; therefore, their mean values (L4-L6) were used in comparing groups (Table 2).

At the time of dissection (Time 0), water represented 52%-57% of the weight of the annuli. This amount was consistent from animal to animal and from group to group (Table 2). When the annuli were allowed to sit in water or saline solution, they imbibed water to a constant level which represented 70%-77% of the weight of the annulus (Table 2). No significant differences were noted between control and experimental groups. We can therefore conclude that weightlessness negatively affects the size of the annulus but it does not impair the ability of the tissue, expressed per unit weight, to imbibe water and therefore to swell.

Light Microscopy

There was no discernible difference in the light microscopic features of the intervertebral discs as revealed by the Safranin-O reaction among the five different groups. In all specimens there was an intense Safranin-O reaction in the nucleus pulposus and in the transitional zones of the annulus fibrosus adjacent to the nucleus pulposus. Closer to the periphery, the Safranin-O reaction decreased in intensity with the stain remaining in the pericellular area along the rows of cells between collagen bands, and finally totally disappearing at the outer edge of the disc. The cells in the transitional area appeared rounded and were housed in large lacunae. These were typical fibrocartilage cells, whereas the cells at the periphery were smaller and elongated, characteristic of fibroblasts (Fig. 2).

Electron Microscopy

Collagen Fibril Diameters

The mean collagen fibril diameter in the anterior, posterior and transitional areas was determined from the cross-section electron micrographs. Separate mean fibril diameters at the anterior and posterior locations in the L3-L4 and L6-S1 discs were determined for each of the two animals in each group, with the exception of the L6 vivarium group where only one specimen was available. In the transition areas, time and tissue constraints limited the measurements to only one animal per group. The number of fibrils measured per specimen ranged from 152 in the transitional area of the synchronous group to 491 in the anterior area of the vivarium group. The largest fibrils were found in the anterior locations and the smallest in the transitional areas; however, as indicated by the standard deviations there was a wide range in fibril sizes within each location (Fig. 3).

Differences in collagen fibril size between the three locations within a single specimen were determined by the Student's t-test (Tables 3 and 4). The difference between mean collagen fibril diameter in the anterior versus posterior location was significant at the 0.001 level in all groups, with the anterior fibrils mean being the larger in all cases except for the basal group L6-S1 disc. The anterior fibrils were also larger than transitional fibrils ($p<.001$) in all cases except for the vivarium group L3-L4 disc and the basal group L6-S1 disc. There were also significant

differences in the transitional versus posterior locations in the basal L3-L4 disc ($p<.05$), vivarium L3-L4 disc ($p<.001$), synchronous L3-L4 disc ($p<.001$), tail suspension L3-L4 disc ($p<.001$) and in the basal L6-S1 disc ($p<.001$). However, in the tail suspension L3-L4 disc and the basal L6-S1 disc, the posterior mean diameter was greater than the transitional mean diameter whereas the opposite was true in the basal L3-L4, vivarium L3-L4 and synchronous L3-L4 discs. In summary, the largest fibrils are located in the anterior region of the rat annulus and the smallest fibrils in the transition area in most specimens.

Because of the large standard deviations associated with the mean collagen fibril diameters, frequency distributions of collagen fibrils size in the anterior, posterior and transitional areas for both the L3-L4 and L6-S1 discs were determined for each group using 20 nanometer increments ranging from 30 to 270 nanometers (Figs. 4-9). One hundred fibrils in each location were measured from each animal studied. In the anterior locations the greatest percentage of fibrils were in the 70-90 nm category in all groups except in the L6-S1 tail suspension group where there appeared to be a uniformity of fibrils ranging from 50 to 130 nm and in the L3-L4 vivarium group where nearly equal percentages of fibrils were found in the 70-90 and 90-110 nm ranges. In the posterior locations, the greatest fibril percentage was found in the 50-70 nm class in all groups except for the L3-L4 vivarium, L6-S1 tail suspension and L6-S1 flight groups where the peak(s) fibril percentages were found in the 90-110, 50-70 and 90-110, and 50-70 and 70-90 nm categories respectively.

In the transition area the greatest percent of fibrils were found in the 70-90 nm range except for the L3-L4 vivarium (90-110), L3-L4 tail suspension (50-70) and L6-S1 vivarium (90-110) groups. Hence, in contrast to the mean collagen fibril diameters which were markedly different, the greatest percent of total fibrils tended to be in the 70-90 nm range in both the anterior and transitional locations and in the 50-70 nm class in posterior locations. Further, anterior locations exhibited the greatest overall range in fibril diameters, whereas the transitional areas tended to have the smallest overall range in fibril diameters. If the frequency distributions are divided into small (<110 nm) and large (>110 nm) components, in general the anterior regions contain between 50%-70% small fibrils, the posterior region 70%-90% small fibrils and the transitional area 90%-100% small fibrils (Table 5).

Collagen-Proteoglycan Relations

Ruthenium red staining delineated electron dense particles in regular periodic array along the collagen fibrils in all groups. Such particles were previously identified as proteoglycans (PG) by Laros and Cooper (16) and by Luft (17). Due to the small sample size it was impossible to determine if there were significant differences in the concentration of these particles among the various groups since they were readily apparent in some sections from all groups. The anterior locations tended to exhibit larger fibrils and fewer PG particles overall than the posterior or transitional areas. In the anterior region the basal group appeared to have the greatest concentration of PG granules and the flight group the poorest concentration. The PG granules were difficult to discern in some cross sections; however, in others they were readily apparent and nearly always found in regular periodicity near the D-bands of longitudinal sections (Figs. 10-13). In the transitional and posterior regions there appeared to be an increased density of granules, accompanied by a decrease in collagen fibril size (Figs. 12-13). These areas also revealed the most intense Safranin-O staining (Fig. 2).

Biochemistry

Proteoglycans

It has been reported that PG leach from the swollen disc and "disc slices" in vitro can double their volume and lose more than 50% of their PG (2, 22, 29). To determine the degree of "leaching

out" of the annular PG during two hours of imbibition, the hydrating medium of each sample was lyophilized, redissolved in a small volume of water and the amount of hexuronate determined by the Blumenkrantz method. The amount of hexuronate remaining in the annulus was determined by the same method after papain digestion of the tissue. The total amount of hexuronate originally present in the annulus was calculated from the amount of hexuronate in the imbibition medium plus the amount remaining in the tissue (Table 6).

The annuli of the basal and vivarium groups contain nearly identical amounts of PG, while the annuli of the synchronous group contain nearly 20% more hexuronate than the tissue from the other two control groups (Table 6). The difference between the three control groups, however, is statistically nonsignificant due to the small sample size and the large standard deviation associated with each group. The Student's t-test of unrelated samples also indicate that there are not significant differences between the total amount of hexuronate in the annuli of each control group and either the flight or the suspended groups (Table 6). The same conclusion is reached when the three control groups are combined (Group B-V-S, Table 6) and compared to the two experimental groups.

The amounts of hexuronate leaching out from the annuli of the three control groups varies from 5% of the total in the synchronous group to 10% of the total in the basal and vivarium groups (Table 6). The annuli of the flight group release nearly 20% of their hexuronate in their hydrating media. The amount is significantly greater ($p<.001$) than the amount released by the 15 animals in the control groups (Table 6 groups B-V-S).

The amount of PG released by the annuli of the suspended group is also significantly greater ($p.<.05$) than the amount of hexuronate leaching out from the tissues of controls (Table 6).

Collagen

The mean hydroxyproline content of the annuli of the three control groups is $5.91 \pm 0.80\%$ of the dry weight (Group B-V-S, Table 7) with no significant differences between groups. The annuli of flight animals otherwise are significantly more collagenous than the controls and hydroxyproline represents $6.93 \pm 0.59\%$ of the dry weight of the tissue ($p<.02$). The amount of hydroxyproline in the annuli of suspended animals is very similar to the amount formed in control tissue (Table 7).

The fibrous framework of the annulus is found by Type I and II collagens. The ratio between the two fibrillar collagens changes in a gradient-like fashion within the annulus, Type II predominating in the inner portion and Type I in the outer region (8). Type I represents between 40% and 43% of the fibrillar collagen of the annuli of the three control groups. Weightlessness or tail suspension do not significantly affect the proportion of Type I and Type II in the annuli (Table 7). It should be noted that we are finding in the rat annuli nearly three times more Type II collagen than found in the pig annulus (8). The discrepancy is to a large extent attributable to the presence of the endplates on the annular sample, although the animal species and the methodology are contributing factors.

Hydroxylysylpyridinoline (HP) represents the prevalent intermolecular cross-link in the mature collagen fibrils of the annulus, replacing the borohydride-reducible cross-links. The basic mechanism of cross-linking appears to be the same in Type I and Type II collagen, although Type I generally contains about half the number of HP residues found in Type II (7, 10). The annular collagen of the three control groups contain between 0.61 and 0.69 HP residues per mole of collagen and the differences between groups were not statistically significant. The annular collagen of the flight group contain 0.71 HP residues per mole of collagen, the collagen from the suspended group 0.62 residues per mole. Neither of the two experimental groups is significantly different from the controls (Table 7).

Collagen-Proteoglycan Ratio

Based upon the assumption that hydroxyproline represents 14% of the collagen molecule and hexuronate 20% of the weight of the proteoglycans, mean collagen-proteoglycan ratios were calculated for each group and for the three control groups (basal, vivarium, synchronous) combined (Table 8). The mean collagen-PG ratios of the flight group (7.71) was significantly greater than determined in the three control groups either individually ($p<.04$) or combined ($p<.001$). The tail suspension group mean collagen-PG ratio (6.28) was significantly greater than the synchronous controls ($p<.05$) and the combined control groups ($p<.04$). There were no significant differences between any of the control groups nor between the flight and tail suspension group (Table 8).

DISCUSSION

The 14-day spaceflight adversely affected the size of the annulus fibrosus. The wet and dry weights of the annuli from flight animals were 20%-37% smaller than found in the three control groups and 35% smaller than those of the tail suspension animals. Our data indicate no relationship between body weight and size of the annuli as the youngest and lightest animals (basal) demonstrated the largest annuli.

In spite of the difference in the size of the annuli, there was no difference among the five groups in the water content of the tissue expressed as percent of tissue weight at dissection nor was there any difference in its ability to imbibe water when exposed to water or saline. At dissection the water content was approximately 55% of the weight in all annuli and rose to approximately 75% after two hours of imbibition, at which point no further increase in water content and, hence, swelling occurred. From these data it appears that the reduction in size of the annuli from the flight animals represents a true loss of tissue constituents and not merely a fluid loss. In previous studies of bone exposed to weightlessness, the reduction in bone has been related to a suppressed growth rate more so than to an increase in resorption (6, 13, 14, 25, 31, 32, 34). The mechanisms causing the reduction in size of the annulus fibrosus remain to be identified and certainly warrant further investigation.

The physiological function of the annuli is related to its size and its composition. The total PG content, as indicated by the hexuronate analyses, was not altered by flight or tail suspension. In addition, the experimental conditions did not affect the spatial distribution of the PG within the annulus as indicated by Safranin-O staining. In all groups the Safranin-O reaction was intense near the nucleus pulposus and weak at the periphery, indicating a decreasing gradient in PG concentration from center to periphery. While the PG of the nucleus pulposus are readily extracted by low salt concentration media, the PG of the annulus usually require a dissociative medium, i.e. 4M guanidine, and indeed only 5%-10% of the PG were found to escape from the annuli of controls immersed in water or saline within a two-hour period. Significantly more hexuronate, however, leached out in the same time period from the two experimental groups strongly suggesting a change in the nature of the PG population.

The annulus contains seven types of collagen (I, II, III, V, VI, IX, XI), although Types I and II represent more than 80% of the collagen and form the fibrous framework of the annulus (8). Collagen represents 42% of the dry weight of the annuli of the three control groups. The smaller annuli of the flight group contain 49.5% collagen and therefore are significantly ($p<.02$) more collagenous than their normal counterparts, although weightlessness does not significantly affect either the relative proportions of Type I and Type II collagens nor the number of intermolecular nonreducible cross-links. The slightly reduced PG content and the increased collagen content

result in a mean collagen-PG ratio in the flight group significantly greater than each of the control groups individually ($p<.04$) and all control groups combined ($p<.001$). The collagen-PG ratio of the tail suspension model is also significantly greater than the ratio found in the controls ($p=.04$, Table 8).

If we consider the weight as well as the composition of the annuli, the biomechanical demands placed upon the annulus by nearly identical body weights (340 g) are sustained in the control groups by 455 µg PG and 2110 µg collagen and in the flight group by only 300 µg PG and 1781 µg collagen. This represents 34% less PG and 15% less collagen to sustain identical body weights upon return to 1 g. Therefore, not only did weightlessness produce a significant change in the collagen-PG ratio, which may alter the mechanical properties of the disc, but the flight animals also have markedly smaller discs and therefore less total collagen and PG. This may be very important in governing the tensile stress associated with the fibrous component of the annulus and/or the compression strength regulated by the ground substance. The suspended animals contain 418 µg PG and 2267 µg collagen, representing 8% less PG but 7% more collagen compared to the controls.

If the collagen fibrils are to have high tensile strength, they need to be large in order to maximize the possibility of intermolecular cross-links, but if the collagen network is to return to its original form after compression, the network must have sufficient collagen-ground substance interactions to inhibit non-recoverable creep. This latter property can best be met with small fibrils (18, 19). Hence, tissues like the disc are comprised of a wide variety of collagen fibril sizes to meet both requirements. Our data indicate that within any single disc the largest fibrils are in the anterior region and a greater proportion of small fibrils in the transitional and posterior regions. This suggests that, in the rat, the anterior area might be submitted to higher tensile forces, whereas the transition and posterior regions sustain greater compressive forces. Interestingly, at the L3-L4 disc only the tail suspension model demonstrated a larger mean fibril diameter in the posterior region compared to the transitional region. This raises the question as to whether altered spinal forces resulting from tail suspension contributed to an increase in posterior region collagen fibril size. There appears to be a tenfold difference in the mean collagen fibril diameters reported by Postacchini et al. (21) compared to our findings as they reported fibril diameters ranging from 180 nm to 2900 nm in the annuli of Wistar rats. We believe they may have made their measurements in angstrom units and erroneously reported the results in nanometers which would account for the tenfold difference in the two studies. Both studies, however, found the fibrils in the transition zone to be smaller and more uniform in size than at the periphery. Eyre (8) has also demonstrated that there is a decrease in Type II collagen extending from the central regions to the periphery in the annulus fibrosus. Therefore, the smaller fibrils near the nucleus pulposus most likely are representative primarily of Type II collagen whereas the large fibrils at the periphery represent Type I collagen.

Previous investigations have indicated that age, mechanical requirements, degree of glycosylation and ground substance quantity and composition are the major factors determining collagen fibril size (1, 3, 5, 18, 19, 23, 24, 26). Of these the mechanical requirements certainly would be altered in both the flight and suspension groups, and we have shown a marked increase in the collagen-PG ratio and an increased leaching out of PG in both experimental groups. Therefore, it seems reasonable to expect that prolonged weightlessness would alter collagen fibril size particularly in the anterior region where 40% of the fibrils have a diameter greater than 100nm. Further, tail suspension may alter spinal forces enough to affect the collagenous network of the annulus. In order to delineate the effects of weightlessness on the collagenous framework of the annulus fibrous, additional studies using similar methods but with increased sample size will be required.

SUMMARY AND CONCLUSIONS

The present study of the size, water content and composition of the lumbar annuli in rats flown on Cosmos Mission 2044 indicate that:

1. The wet and dry weights of the annuli of the flight group are significantly less than found in the three control groups ($p<.05$).

2. Tail suspension does not significantly affect the weight of the annuli.

3. The amount of water retained by the annuli or absorbed by the annuli during a two-hour imbibition time, expressed as percent of tissue weight, is not affected by either weightlessness or tail suspension.

4. PG represent an average of 8.5% of the dry weight of the rats' annuli. Age differences between the basal and vivarium groups do not significantly affect the amount of PG of the annulus. No significant differences were found between the PG content of the annuli of control groups and the annuli of the two experimental groups (flight and suspended). The presence of similar amounts of PG in all groups studied is consistent with the ability of the annuli of flight animals to retain, on the basis of unit weight, as much water as the control tissue, since the water content of the tissue largely depend on the PG concentration.

5. No discernible differences were observed in the distribution of PG within the discs of control or experimental animals. In all cases an intense Safranin-O staining was noted in the nucleus pulposus and in the transitional zone between nucleus and annulus. The intensity of the stain decreased from the center to the periphery of the disc and was totally absent at the outer edge of the disc.

6. Upon sitting in water at room temperature for two hours, the annuli of the three control groups lost an average of 8.5% their hexuronate to the hydration media. Significantly more hexuronate leached out of the annuli of the two experimental groups: 19.2% from the annuli of the flight group ($p<.001$), 12.2% from the annuli of the suspended group ($p<.05$).

7. The mean hydroxyproline content of the annuli of the three control groups is $5.91 \pm 0.80\%$ of the dry tissue weight, very similar to the amount found in the suspended animals ($5.88 \pm 0.71\%$). The annuli of the flight group otherwise are significantly more collagenous than the controls ($p<.02$) and hydroxyproline represents $6.93 \pm 0.59\%$ of the dry weight of the tissue.

8. The collagen-PG ratio in the flight group was significantly greater than that of each control group ($p<.04$) and all control groups combined ($p<.001$), indicating a structural change in the composition of the annulus fibrosus exposed to 14 days weightlessness.

9. When the weight and composition of the annuli are taken in consideration it can be calculated that the discs of the flight animals are required to support body weights nearly identical to those of the control groups with 34% less PG and 15% less collagen.

10. Weightlessness or tail suspension do not significantly affect either the ratio between Type I and II collagens forming the annular network nor the number of intermolecular pyridinoline collagen cross-links.

11. Significant differences in collagen fibrils sizes were observed between the anterior, transitional, and posterior regions of the annulus. The anterior region contained the largest percentage of fibrils larger than 110 nm (40% of the total), the transitional the smallest percentage (15% or less of the total).

The methodology used in our study is capable of delineating the fundamental chemical and structural changes caused by weightlessness on the annulus fibrosus. Our findings indicate that after 14 days weightlessness the annulus fibrosus is undergoing alterations in the composition of its matrix components as indicated by the collagen-proteoglycan ratio, the amount of proteoglycan leaching out of the tissue and the increased collagen content. The tail suspension model does not produce changes identical to those caused by weightlessness, e.g. the reduction in the size of the annulus. The changes in the matrix, however, observed in the tail suspension model may indicate a similar but slower ongoing process that may eventually produce findings similar to those of the flight animals. Future research involving the annulus fibrosus should focus on whether prolonged weightlessness may predispose the disc to injury, whether the observed changes in the annulus are reversible and, if so, the time period required to restore the disc to its normal status.

ACKNOWLEDGEMENTS

The authors wish to thank Dr. A.S. Kaplansky and the Soviet Cosmos recovery and dissection teams. Without their skills and cooperation these studies could not have been carried out. In addition we wish to thank Dr. Richard Grindeland and his colleagues at the NASA Ames Research Center for providing us with the opportunity to participate in the Joint NASA-Cosmos Life Science Research Program. We would also like to thank Mr. Thomas Moniger for his help in the preparation of the electron microscopy specimens and Ms. Betty Dye for her excellent secretarial and editorial skills in the preparation of this final report.

REFERENCES

1. Anderson J.C., R.I. Labedz, M.A. Kewley. The Effect of Bovine Tendon Glycoprotein on the Formation of Fibrils from Collagen Solutions. Biochem. J. 168:345-351, 1977.

2. Bayliss, M.T., J.P.G. Urban, B. Johnstone, S. Holm. In Vitro Method for Measuring Synthesis Rates in the Intervertebral disc. J. Orthop. Res. 4:10-17, 1986.

3. Birk, D.E., M.A. Lande. Corneal and Scleral Collagen Fiber Formation In Vitro. Biochem. Biophys. Acta. 670:362-369, 1981.

4. Blumenkrantz, N., G. Asboe-Hansen. New Method for Quantitative Determination of Uronic Acids. Anal. Biochem. 54:484-489, 1973.

5. Borcherding, M.S., L.J. Blacik, J.W. Sittig, M.B. Bizzeu, H.G. Weinstein. Proteoglycans and Collagen Fibre Organization in Human Corneoscleral Tissue. Exp. Eye Res. 21:59-70, 1975.

6. Doty, S.B., E.R. Morey-Holton, G.N. Durnova, A.S. Kaplansky. Cosmos 1887: Morphology, Histochemistry, and Vasculature of the Growing Rat Tibia. FASEB J. 4:16-23, 1990.

7. Eyre, D.R. Collagen Cross-Linking Aminoacids. Methods Enzymol. Vol. 143, 1986.

8. Eyre, D.R. Collagens of the Disc in The Biology of the Intervertebral Disc. Edited by P. Ghosh, CRC Press, Vol. I, pp 171-188, 1988.

9. Eyre, D.R., T.J. Koob, K.P. Van Hess. Quantitation of Hydroxyphridinium Cross-Links in Collagen by High-Performance Liquid Chromatography. Anal. Biochem. 137:380-388, 1984.

10. Eyre, D.R., M.A. Paz, and P.M. Gallop. Cross-Linking in Collagen and Elastin. Annual Rev. Biochem. 53: 717, 1984.

11. Grindeland, R.E., Cosmos 1887: Science Overview. FASEB J. 4:10-15, 1990.

12. Hukins, D.W.L., Disc Structure and Function in The Biology of the Intervertebral Disc. Edited by P. Ghosh, C.R.C. Press Vol. I, pp. 1-37, 1988.

13. Jee, W.S.S., T.J. Wronski, E.R. Morey, D.B. Kimmel. Effects of Spaceflight on Trabeculer Bone in Rats. Am. J. Physiol. 244:R310-R314, 1983.

14. Kaplansky, A.S., G.N. Durnova, Z.F. Sakharova, Y.I. Ilyina-Kakuyeva. Automorphometric Analysis of Rat Bones After Spaceflight Aboard Cosmos 1667 Biosatellite. Space Biol. Med. 21: (5), 33-40, 1987.

15. Laemmli, U.K. Cleavage of Structural Proteins During the Assembly of the Head of Bacteriophage T4. Nature 227:680-685, 1970.

16. Laros, G.S., R.R. Cooper. Electron microscopic visualization of protein polysaccharides. Clin. Orthop. 84:179-192, 1972.

17. Luft, J.H. Electron Microscopy of Cell Extraneous Coats as Revealed by Ruthenium Red Staining. J. Cell Biol. 23:54A, 1966.

18. Parry, D.A.D., G.R.C. Barnes, A.J. Craig. A Comparison of the Size of Collagen Fibrils in Connective Tissues as a Function of Age and a Possible Relation Between Fibril Size Distribution and Mechanical Properties. Proc. Roy Soc. Lond. (Biol) 203:305-321, 1978.

19. Parry, D.A.D., A.J. Craig, G.R.C. Barnes. Tendon and Ligament from the Horse: an Ultrastructure Study of Collagen Fibrils and Elastic Fibers as a Function of Age. Proc. Roy, Soc. Lond (Biol) 203:293-303, 1978.

20. Pedrini-Mille A., V.A. Pedrini, J.A. Maynard, A.C. Vailas. Response of Immature Chicken Meniscus to Strenuous Exercise: Biochemical Studies of Proteoglycan and Collagen. J. Orthop. Res. 6:196-204, 1988.

21. Postacchini, F., M. Bellocci, M. Massobrio. Morphologic Changes in Annulus Fibrosus During Aging an Ultrastructure Study in Rats. Spine 9:596-603, 1984.

22. Pousty, I., M.A. Bari-Kham, W.F. Butler. Histology of the Disc. Histochem. J. 7:361-365, 1975.

23. Schofield, J.P., I.L. Freeman, D.S. Jackson. The Isolation and Amino Acid and Carbohydrate Composition of Polyomeric Collagens Prepared from Various Human Tissues. Biochem J. 124:467-473, 1971.

24. Scott, J.W., C.R. Orford, E.W. Hughes. Proteoglycan-Collagen Arrangements in Developing Rat Tail Tendon. An Electron Microscopical and Biochemical Investigation. Biochem J. 195:573-581, 1981.

25. Simmon, D.J., M.D. Grynpas, G.D. Rosenberg. Maturation of Bone and Dentin Matrices in Rats Flown on the Soviet Biosatellite Cosmos 1887. FASEB J. 4:29-33, 1990.

26. Svoboda, E.L.A., T.P. Howley, D.A. Deporter. Collagen Fibril Diameter and Its Relation to Collagen Turnover in Three Soft Connective Tissues in the Rat. Connect. Tissue Res. 12: 43-48, 1983.

27. Thorton, W., W. Hoffler, J. Rummel. Anthropometric Change and Fluid Shifts on Skylab. Skylab Symposium, August 28, 1974.

28. Tyrrell, A.R., T. Reilly, J.D.G. Troup. Circadian Variation in Stature and the Effects of Spinal Loading. Spine 10: 161-164, 1985.

29.Urban, J.P.G., A. Maroudas. Swelling of the Intervertebral Disc In Vitro. Connect. Tissue Res. 9:1-10, 1981.

30. Urban, J.P.G., J.F. McMullin. Swelling Pressure of the Lumbar Intervertebral Discs: Influence of Age, Spinal Level, Composition, and Degeneration. Spine 13:179-187, 1988.

31. Vailas, A.C., R.F. Zernicke, R.E. Grindeland, A. Kaplansky, G.N. Durnova, K-C Li, D.A. Martinez. Effects of Spaceflight on Rat Humerus Geometry, Biomechanics, and Biochemistry. FASEB J. 4:47-54, 1990.

32. Vico, L. D. Chappard, S. Palle, A.V. Bakulin, V.E. Novikov, C. Alexandre. Trabecular Bone Remodeling After Seven Days Weightlessness Exposure (Biocosmos 1667). Am. J. Physiol. 255:R243-R247, 1988.

33. Woessner, J.F. Jr. The Determination of Hydroxyproline in Tissue and Protein Samples Containing Small Proportions of This Iminoacid. Arch. Biochem. Biophys. 93:440-447, 1961.

34. Wronski, T.J., E.R. Morey-Holton, S.B. Doty, A.C. Maese, C.C. Walsh. Histomorphometric Analysis of Rat Skeleton Following Spaceflight. Am. J. Physiol. 252:R252-R255, 1987.

TABLE 1

WET AND DRY WEIGHTS OF ANNULI OF COSMOS 2044 RATS

GROUPS		BASAL	VIVARIUM	SYNCHRON	FLIGHT	SUSPENDED
Age of Animals (days)		109	129	127	123	131
Weight of Animals (g)		320±5	363±5	343±17	338±5	339±21
Wet Weight of Annuli (mg)						
Time O	L4-L5	12.2±0.5	10.3±2.1	10.3±3.1	7.7±1.110	3±1.7
	L5-L6	12.8±3.8	9.8±3.7	10.6±1.3	8.2±2.0	136±3.1
	L4-L6	12.5±2.7	0.1±2.9	10.5±2.2	7.9±1.6	12.0±2.9
Stable Time	L4-L5	21.1±2.4	18.7±4.4	16.5±2.9	15.0±1.5	15.1±1.8
	L4-L6	22.0±4.5	18.2±7.8	19.5±3.4	16.5±3.7	20.5±4.4,
	L4-L6	21.5±3.4	18.4±6.0	18.0±3.4	15.8±2.8	17.8±4.5,
Dry Weight of Annuli (mg)						
	L4-L5	6.0±1.5	5.0±1.0	4.7±1.3	3.6±0.5	4.5±0
	L5-L6	5.5±1.7	4.5±1.7	4.4 ±0.3	3.6±0.9	6.3±1.5,
	L4-L6	5.8±1.5	4.8±1.3	4.5±0.9	3.6±0.7	5.4±1.5,

All Data = mean ± standard deviation

TABLE 2

WATER CONTENT OF ANNULI OF COSMOS 2044 RATS

	GROUPS	BASAL	VIVARIUM	SYNCHRON	FLIGHT	SUSPENDED
Time O	L4-L5	56.4±6.5	51.2±1.3	52.2±4.0	53.7±4.2	56.3±3.6
	L5-L6	56.8±2.9	53.6±0.8	58.6±4.8	56.4±3.6	53.9±1.4
	L4-L6	6.6±4.7	52.4±1.6	55.4±5.4	55.0±4.0	55.1±2.9
Stable Time	L4-L5	71.0±7.8	73.0±2.6	71.8±4.5	76.3±3.2	70.2±3.6
	L5-L6	75.3±4.2	74.3±2.3	77.0±4.2	78.4±2.5	69.4±1.8
	L4-L6	73.2±6.3	73.6±2.4	74.4±5.0	77.4±2.9	69.8±2.7

All Data = mean ± standard deviation

TABLE 3

t-TEST-p-VALUES COMPARING MEAN COLLAGEN FIBRIL DIAMETERS IN THREE LOCATIONS WITHIN L3-4 DISC

GROUP	MEAN ± S.D.	ANTERIOR	TRANSITIONAL
Basal			
Anterior	139 ± 52		
Transitional	84 ± 16	p<.001	
Posterior	80 ± 33	p<.001	p<.05
Vivarium			
Anterior	108 ± 40		
Transitional	109 ± 26	NS	
Posterior	82 ± 22	p<.001	p<.001
Synchronous			
Anterior	126 ± 44		
Transitional	80 ± 16	p<.001	
Posterior	63 ± 15	p<.001	p<.001
Flight			
Anterior	92 ± 51		
Transitional	72 ± 15	p<.001	
Posterior	74 ± 17	p<.001	NS
Tail Suspension			
Anterior	108 ± 35		
Transitional	64 ± 16	p<.001	
Posterior	84 ± 21	p<.001	p<.001

NS = nonsignificant

TABLE 4

t-TEST-p-VALUES COMPARING MEAN COLLAGEN FIBRIL

DIAMETERS IN THREE LOCATIONS WITHIN L6-S1 DISC

GROUP	MEAN ± S.D.	ANTERIOR	TRANSITIONAL
Basal			
Anterior	81 ± 20		
Transitional	83 ± 19	NS	
Posterior	122 ± 47	p<.001	p<.001
Vivarium			
Anterior	129 ± 70		
Transitional	No Specimen		
Posterior	85 ± 33	p<.001	No Specimen
Synchronous			
Anterior	132 ± 45		
Transitional	78 ± 16	p<.001	
Posterior	75 ± 18	p<.001	NS
Flight			
Anterior	110 ± 41		
Transitional	85 ± 27	p<.001	
Posterior	85 ± 28	p<.001	NS
Tail Suspension			
Anterior	107 ± 28		
Transitional	80 ± 17	p<.001	
Posterior	79 ± 26	p<.001	NS

NS = nonsignificant

TABLE 5

PERCENT COLLAGEN FIBRILS SMALLER THAN 110 NM IN

ANTERIOR, TRANSITIONAL AND POSTERIOR REGIONS OF LUMBAR DISCS L3-4 AND L6-S1

	ANTERIOR		TRANSITIONAL		POSTERIOR	
	L3-4	L6-S1	L3-4	L6-S1	L3-4	76-S1
Basal(B)	57	68	93	91	86	72
Vivarium(V)	68	63	65	68	82	65
Synchronous(S)	51	45	98	97	83	94
Flight (F)	67	63	99	95	75	71
Tail Suspension(T)	59	70	100	81	89	75

TABLE 6

HEXURONATE IN THE ANNULI OF COSMOS 2044

GROUP	TISSUE	MEDIUM	TOTAL	TISSUE	MEDIUM
	(% Dry Tissue)			(% of Total)	
Basal (B	1.53±0.17	0.15±0.07	1.68±0.23	91.0±2.7	9.0±2.7
Vivarium (V)	1.53±0.29	0.19±0.03	1.72±0.29	88.9±2.4	11.1±2.4
Synchronous(S)	1.94±0.32	0.11±0.05	2.05±0.32	94.6±2.7	5.4±2.7
Controls (B-V-S)	1.67±0.32	0.15±0.06	1.82±0.32	91.5±3.4	8.5±3.4
Flight (F)	1.35±0.33	0.32±0.14	1.67±0.35	80.8±8.2	19.2±8.2
Suspended (T)	1.35±0.26	0.20±0.10	1.55±0.35	87.8±3.3	12.2±3.3

All Data = mean ± standard deviations

TABLE 7

HYDROXYPROLINE, PYRIDINOLINE CROSS-LINKS AND TYPE I AND II COLLAGENS IN THE ANNULI OF COSMOS 2044 RATS

GROUP	HYDROXYPROLINE (% Dry Tissue Wt)	PYRIDINOLINE (Residues/MCollagn)	TYPEI/II COLLAGEN (Ratio)
Basal (B)	5.71±0.35	0.61±0.06	
Vivarium (V)	5.36±0.45	0.63±0.03	0.7
Synchronous (S)	6.64±0.91	0.69±0.12	0.7
Controls (B±V±S)	5.91±0.80	0.65±0.08	0.7
Flight (F)	6.93±0.59	0.71±0.07	0.6
Suspended (T)	5.88±0.71	0.62±0.05	0.7

All Data = mean ± standard deviations

TABLE 8

T-TEST-P-VALUES COMPARING MEAN COLLAGEN-PG RATIO BETWEEN GROUPS

GROUP	MEAN ± S.D.	B	V	S	F	T
Basal	(5.40 ± 0.47)		p=.69	p=.39	p=.02	p=.07
Vivarium	(5.20 ± 1.44)			p=.69	p=.04	p=.19
Synchronous	(4.97 ± 0.91)				p=.02	p=.05
BSV	(5.19 ± 0.96)				p=.001	p=.04
Flight	(7.71 ± 1.77)					p=.14
Tail Suspension	(6.28 ± 0.84)					

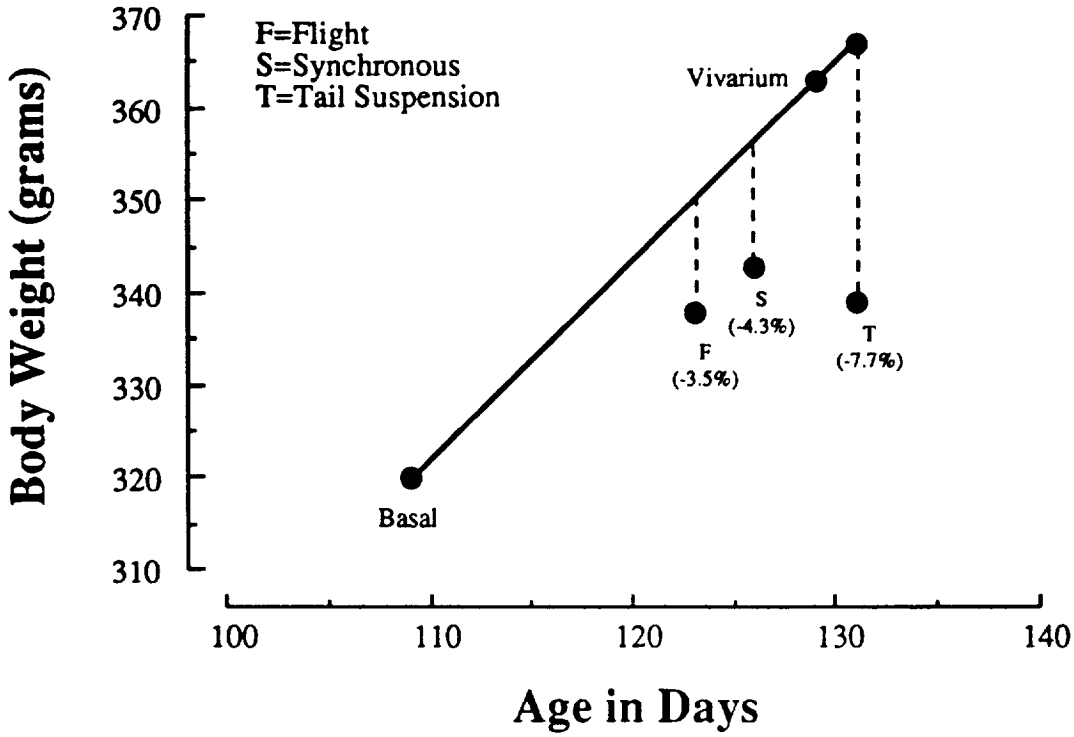

Figure 1. Body weight-age comparisons of five groups involved in Cosmos 2044 Mission. If linear growth rate is assumed from age of basal group to vivarium group, at sacrifice flight animals (F) are only 3.5% below expected values, synchronous controls (S) 4.3% and tail suspension (T) animals 7.7%.

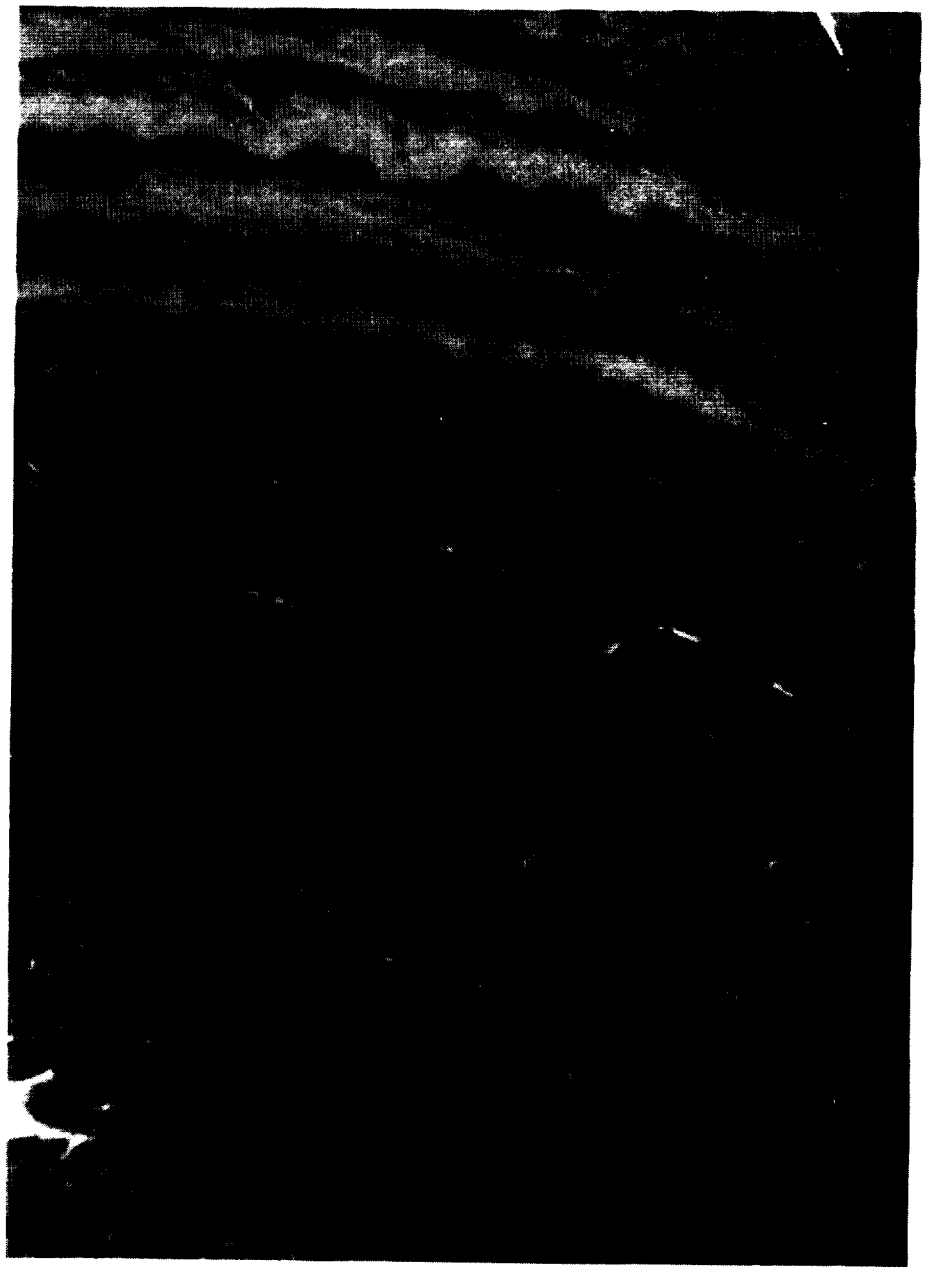

Figure 2. Light microscopy Safranin-O stain demonstrating intense reaction (red) near nucleus pulposis with decreasing intensity (green) toward periphery indicating a decreasing PG gradient from the nucleus pulposus to the periphery. X180.

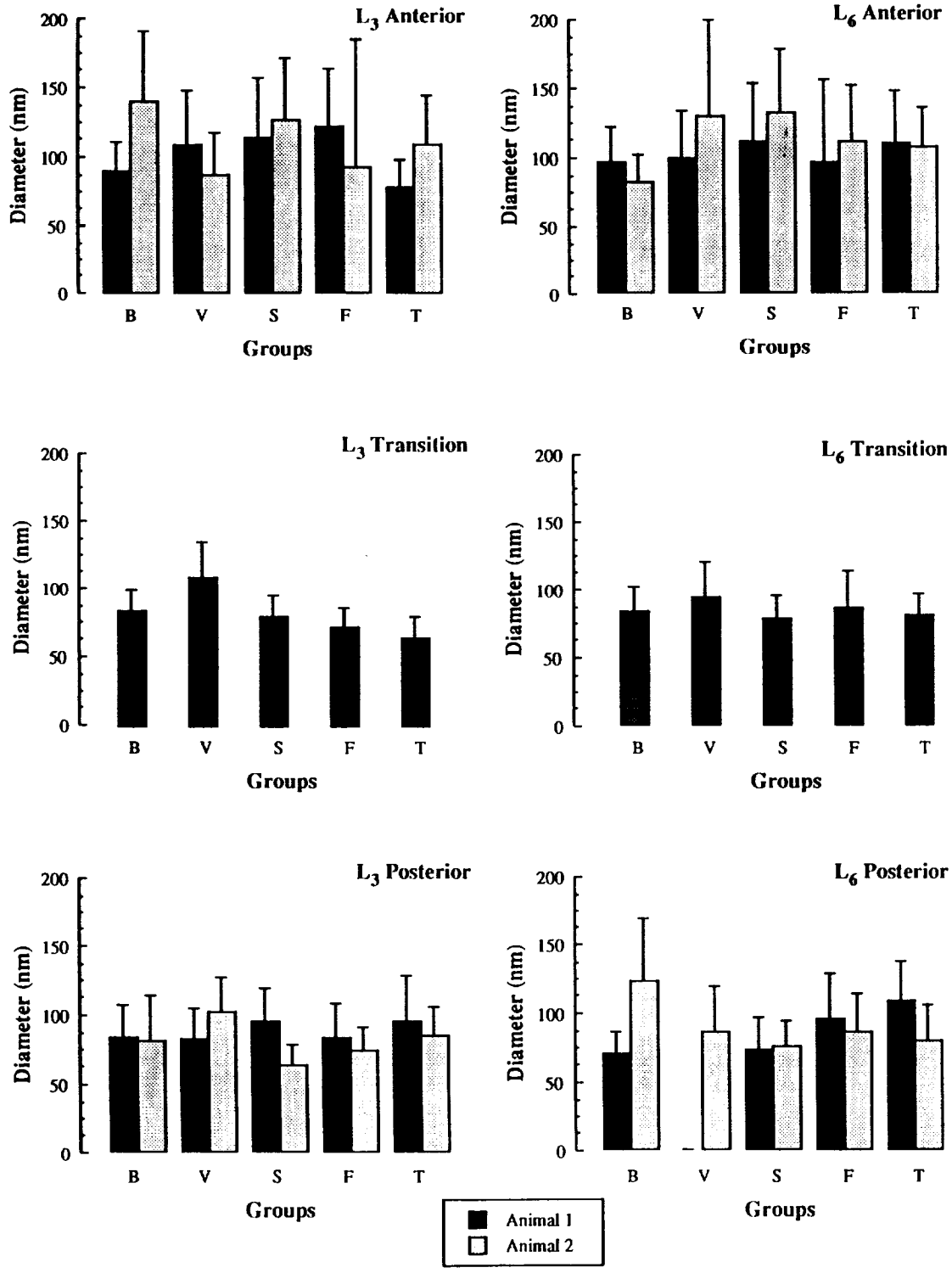

Figure 3. Mean collagen fibril diameters in anterior; transitional and posterior regions of L3-4 and L6-S1 annulus fibrosus for basal (B), vivarium (V), synchronous (S), flight (F) and tail suspension (T) animals. Separate means were calculated for each of the two animals studied in the anterior and posterior regions. Only one animal/group studied in transition area. Bars represent standard deviation.

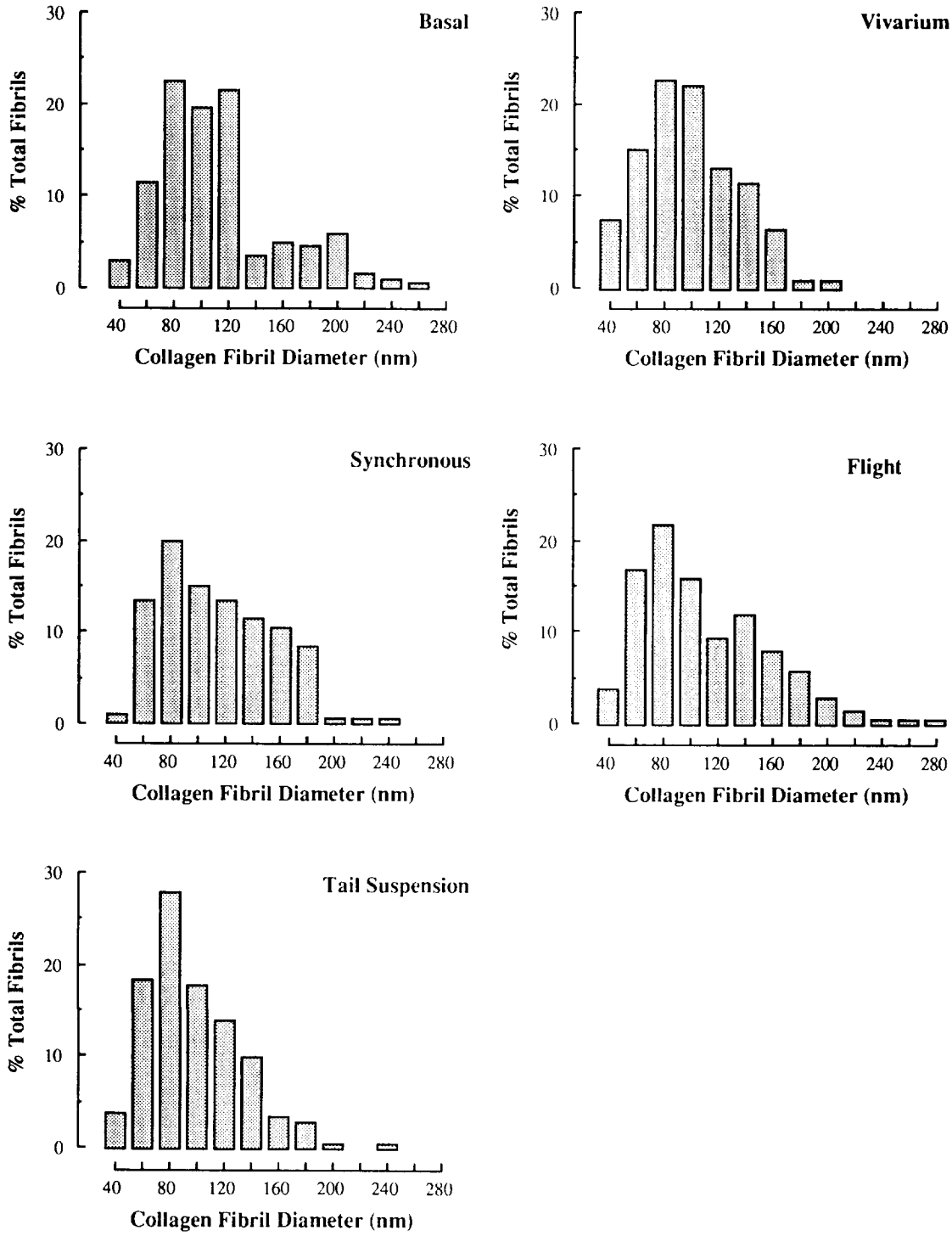

Figure 4. Collagen fibril diameter frequency distributions in anterior region of L3-L4 annulus fibrosus. One hundred fibrils measured from each of the two animals per group.

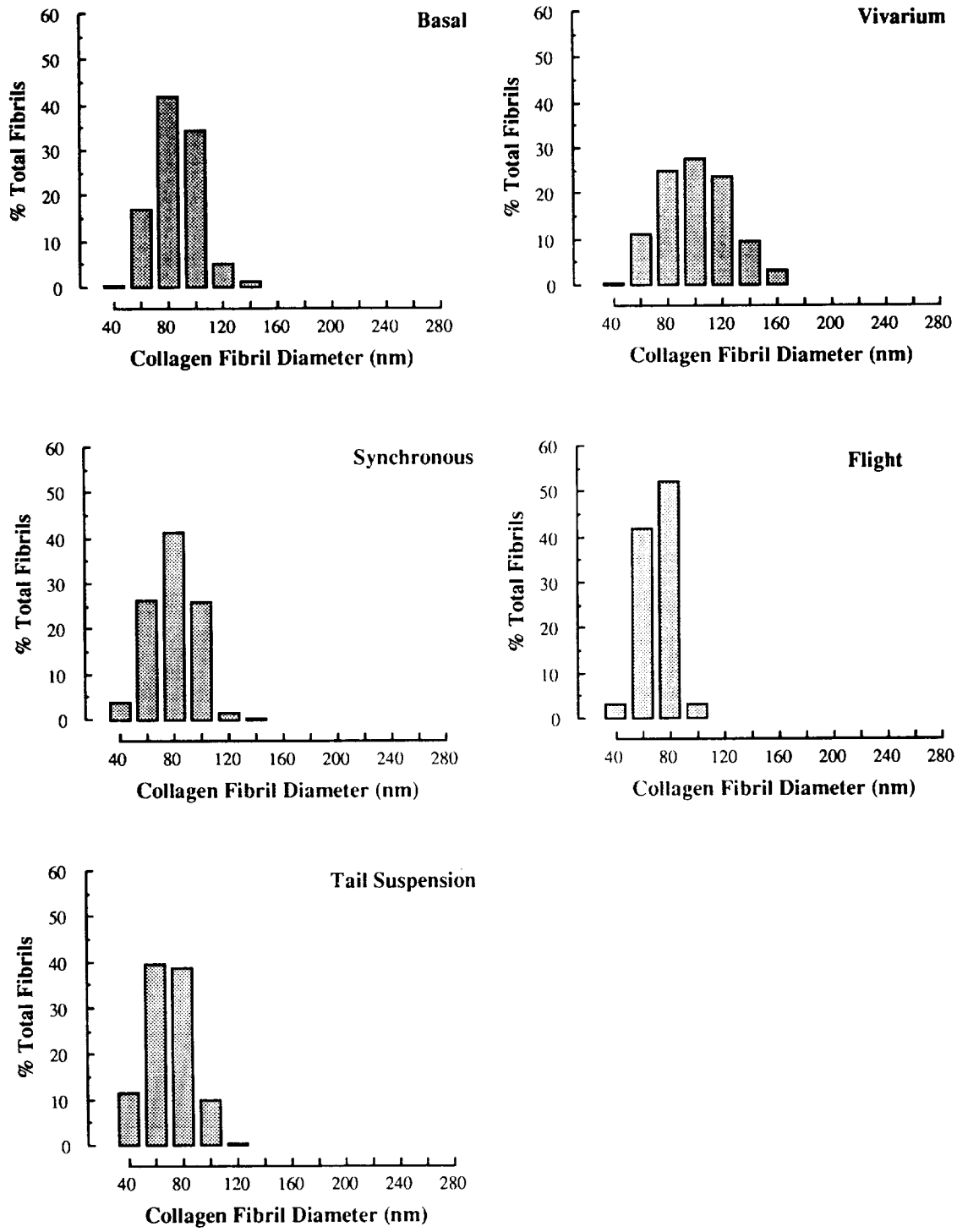

Figure 5. Collagen fibril diameter frequency distributions in transition area of L3-L4 annulus fibrosus. Frequency distributions based on a minimum of 209 fibrils measured in vivarium group to 360 in flight group from one animal in the transition zone.

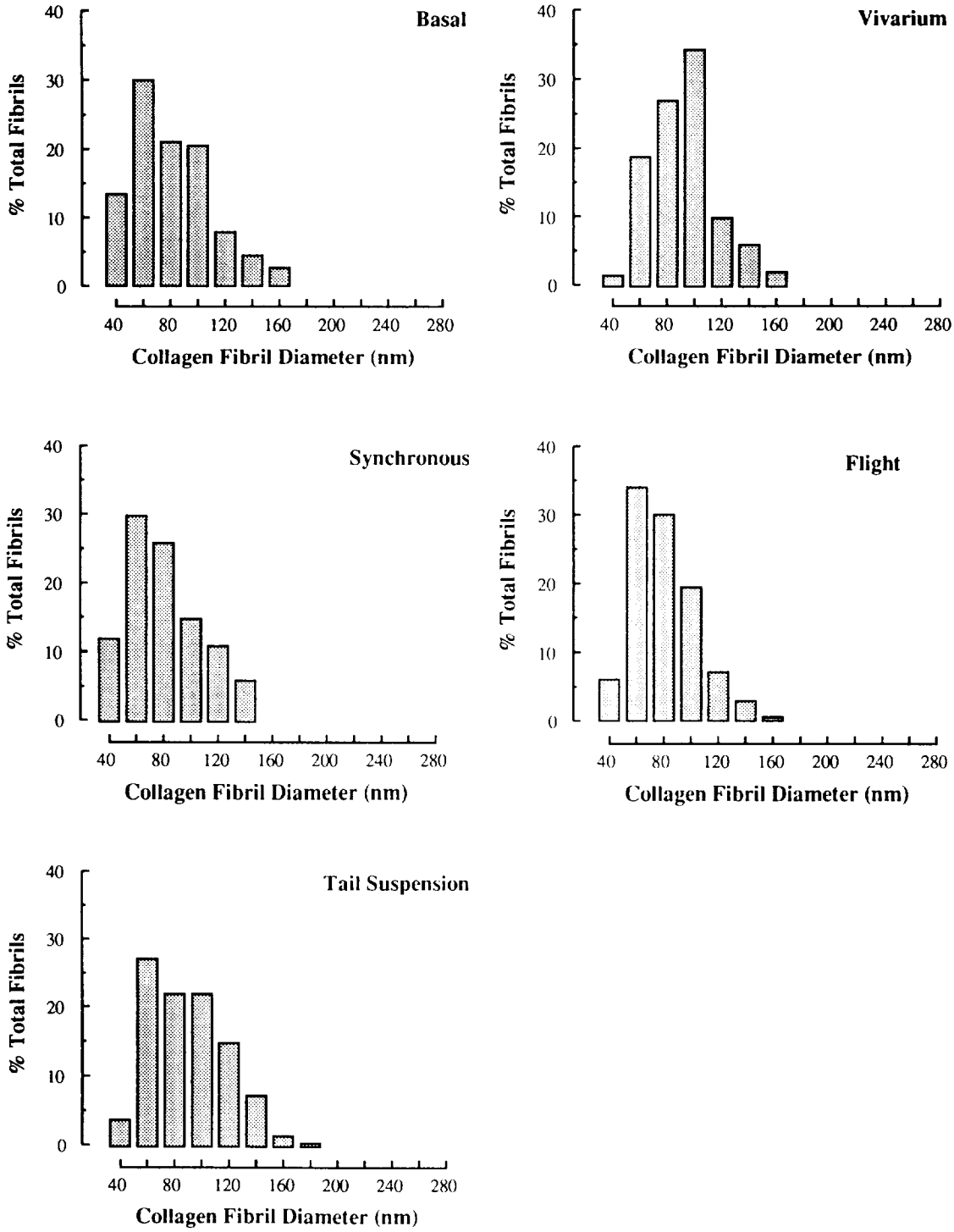

Figure 6. Collagen fibril diameter frequency distributions in posterior area of L3-L4 annulus fibrosus. One hundred fibrils measured from each of the two animals per group.

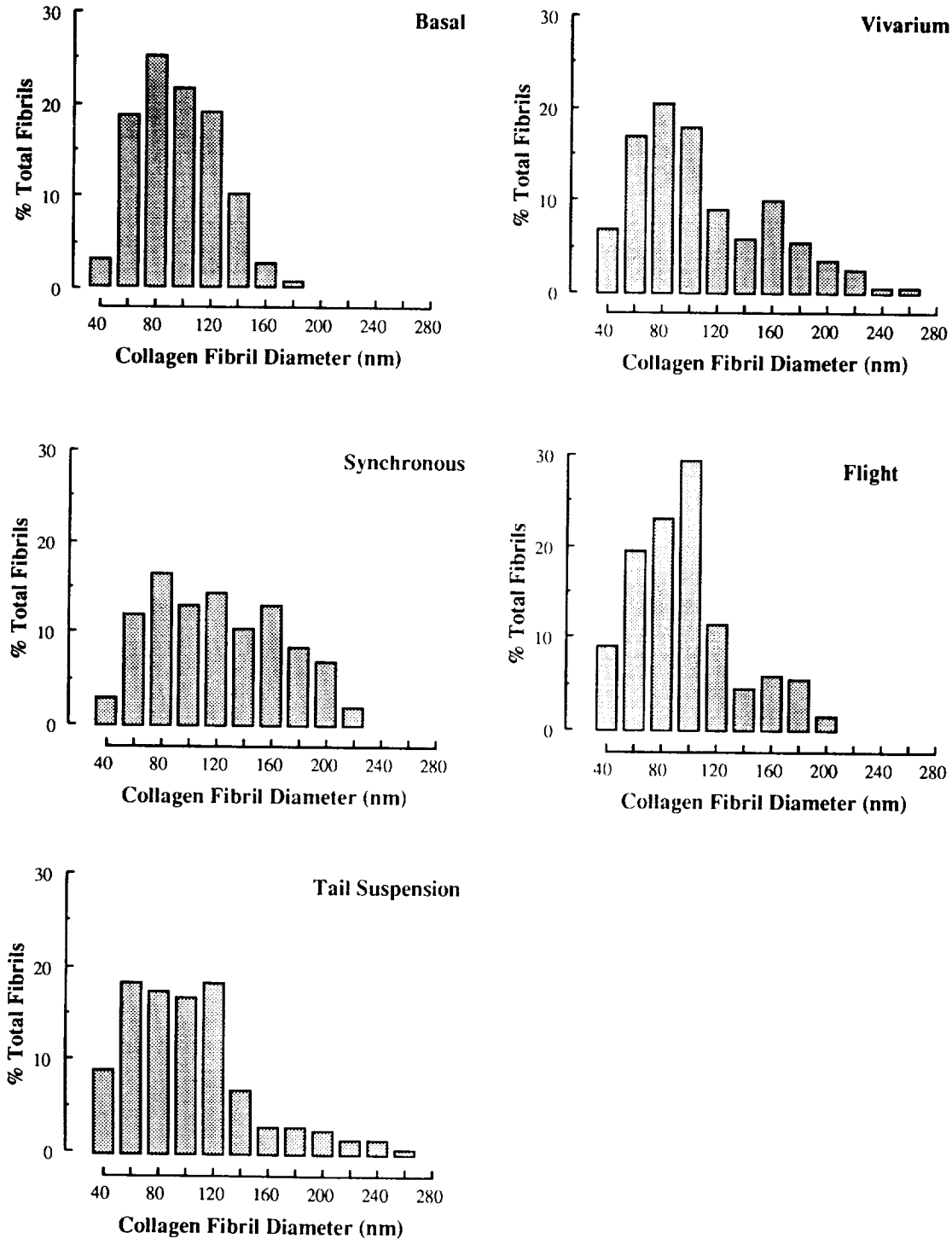

Figure 7. Collagen fibril diameter frequency distributions in anterior region of L6-S1 annulus fibrosus. One hundred fibrosus measured from each of the two animals per group.

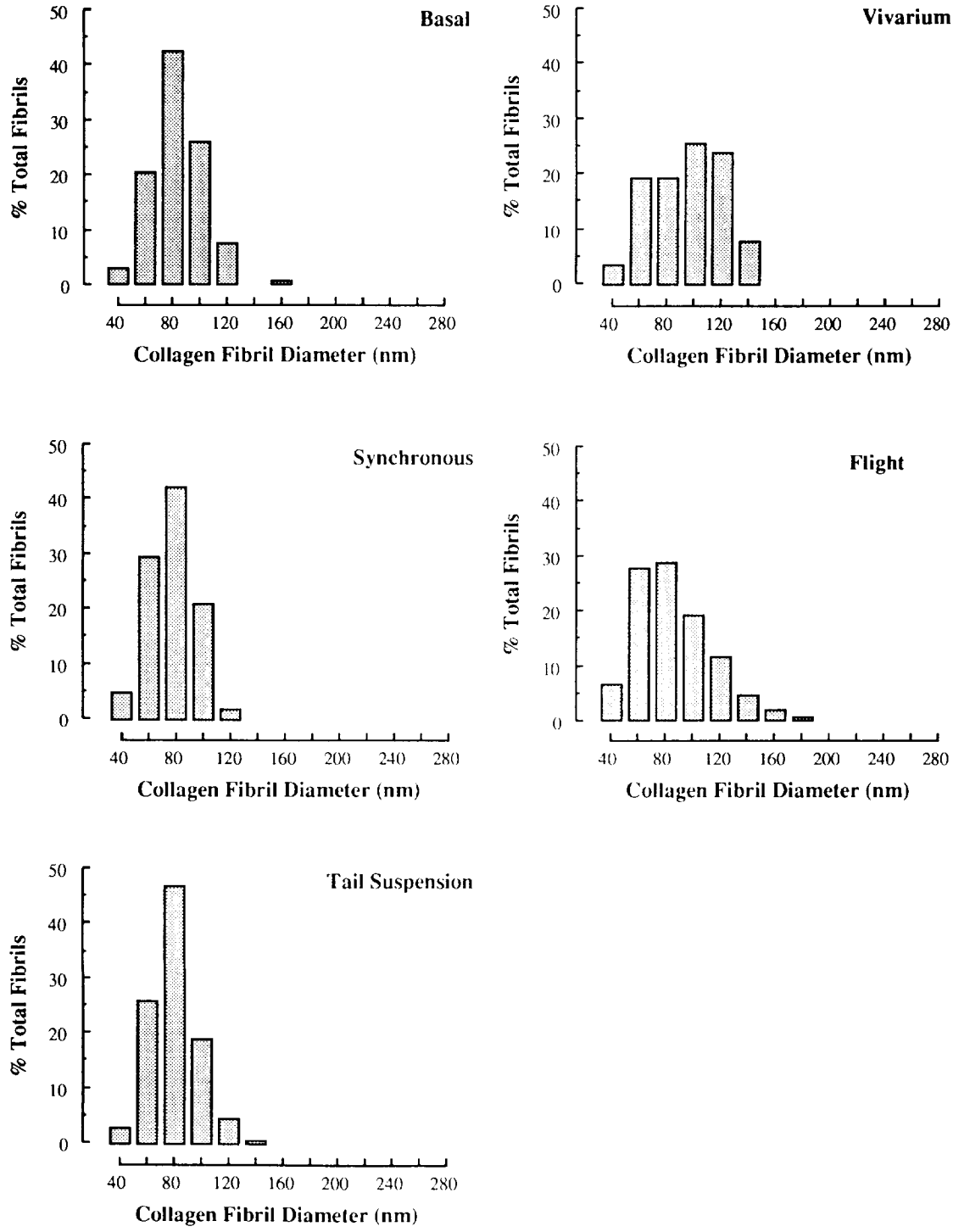

Figure 8. Collagen fibril diameter frequency distributions in transition area of L6-S1 annulus fibrosus. Frequently distributions based on a minimum of 152 fibrils measured in synchronous group to 258 in basal group from one animal in the transition zone.

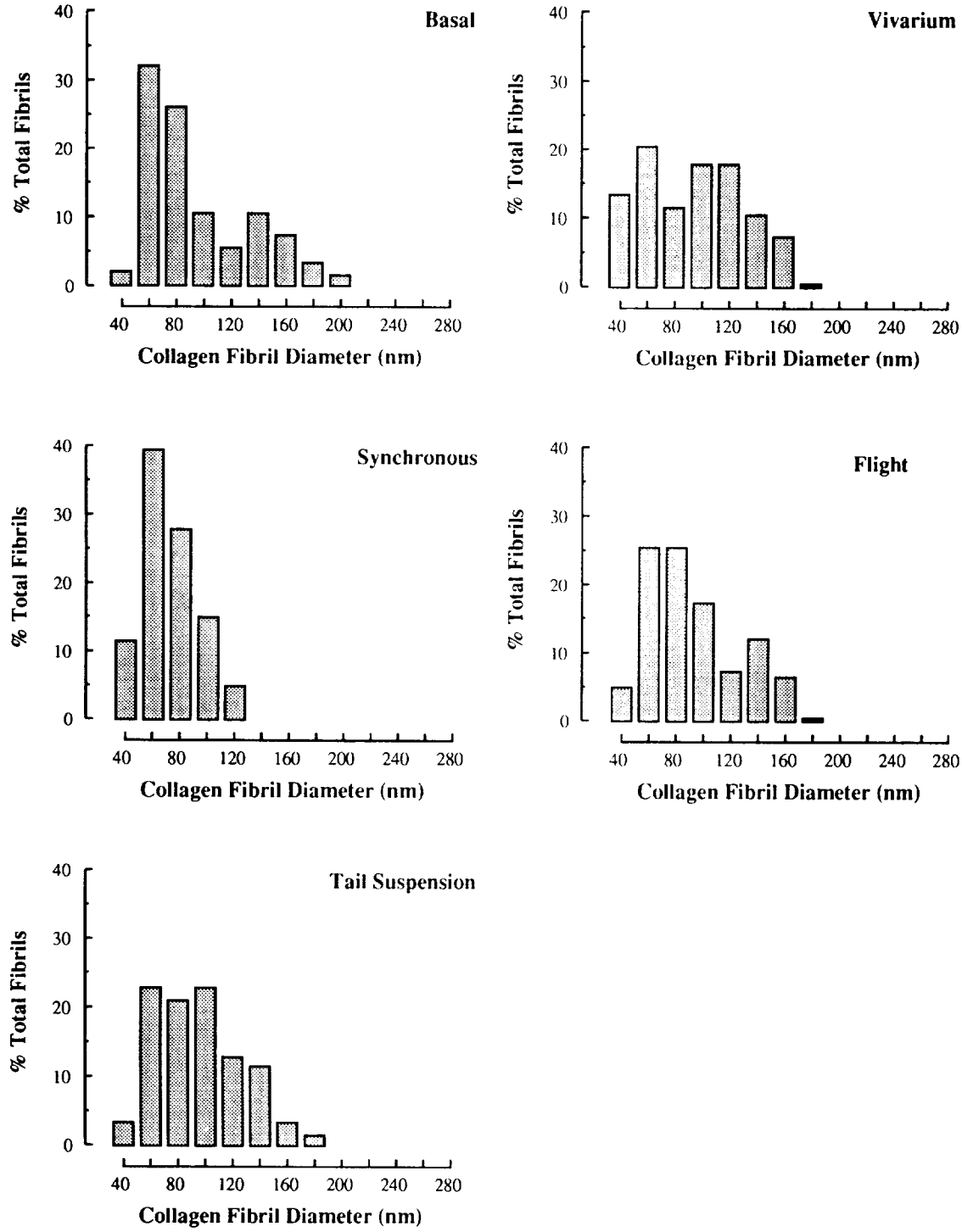

Figure 9. Collagen fibril diameter frequency distributions in posterior area of L6-S1 annulus fibrosus. One hundred fibrils measured from each of the two animals per group.

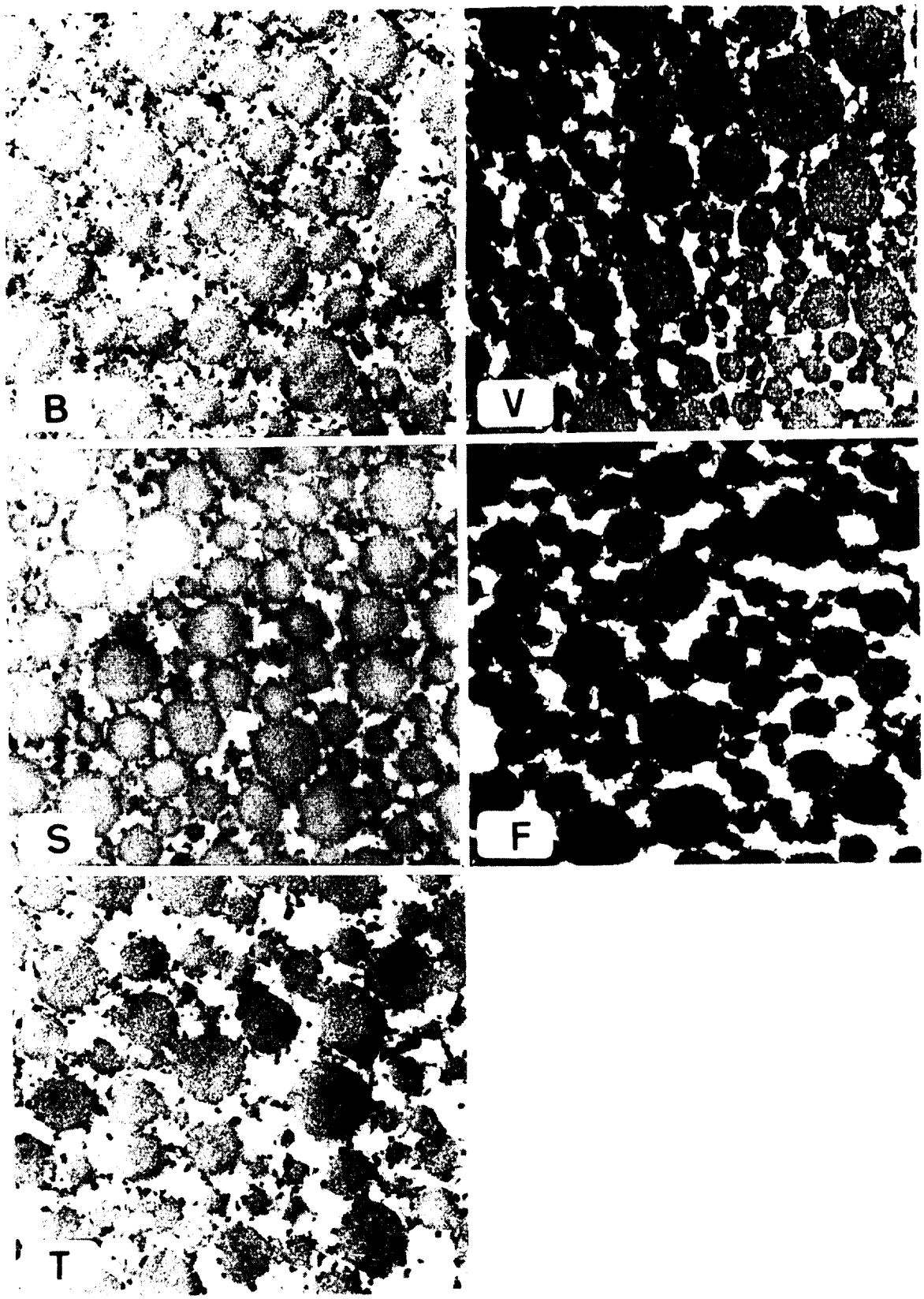

Figure 10.Electron micrographs of collagen fibril cross-sections from anterior region of annulus fibrosus. B = basal, V = vivarium, S = synchronous, F = flight, T = tail suspension. Note PG granules surronding fibrils in B,S, T. X56,000.

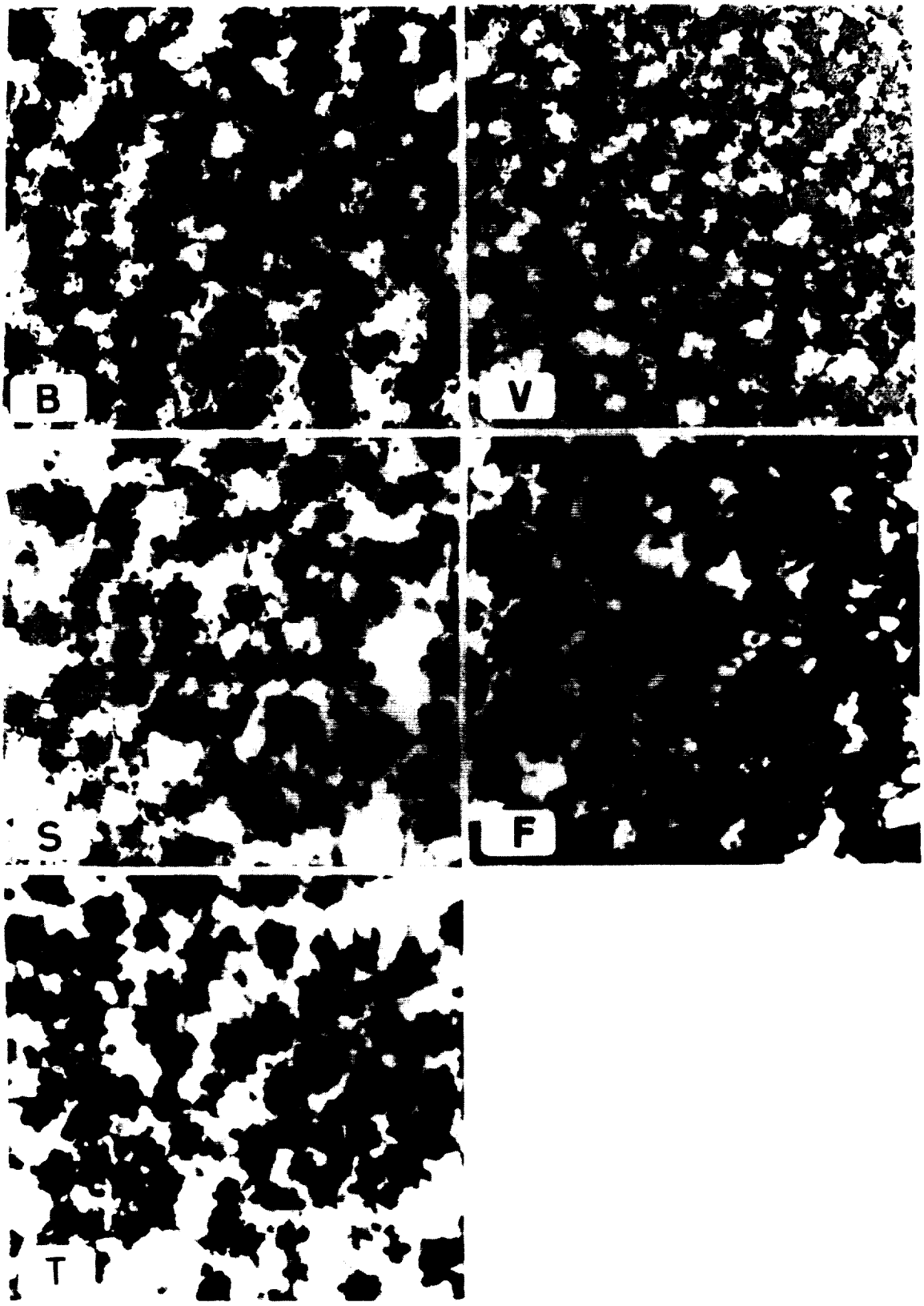

Figure 11. Electron micrographs of collagen fibril cross-sections from transition zone of annulus fibrosus. Compare size and PG granule content to Figure 10. B = basal, V = vivarium, S = synchronous, F = flight, T = tail suspension. X56,000.

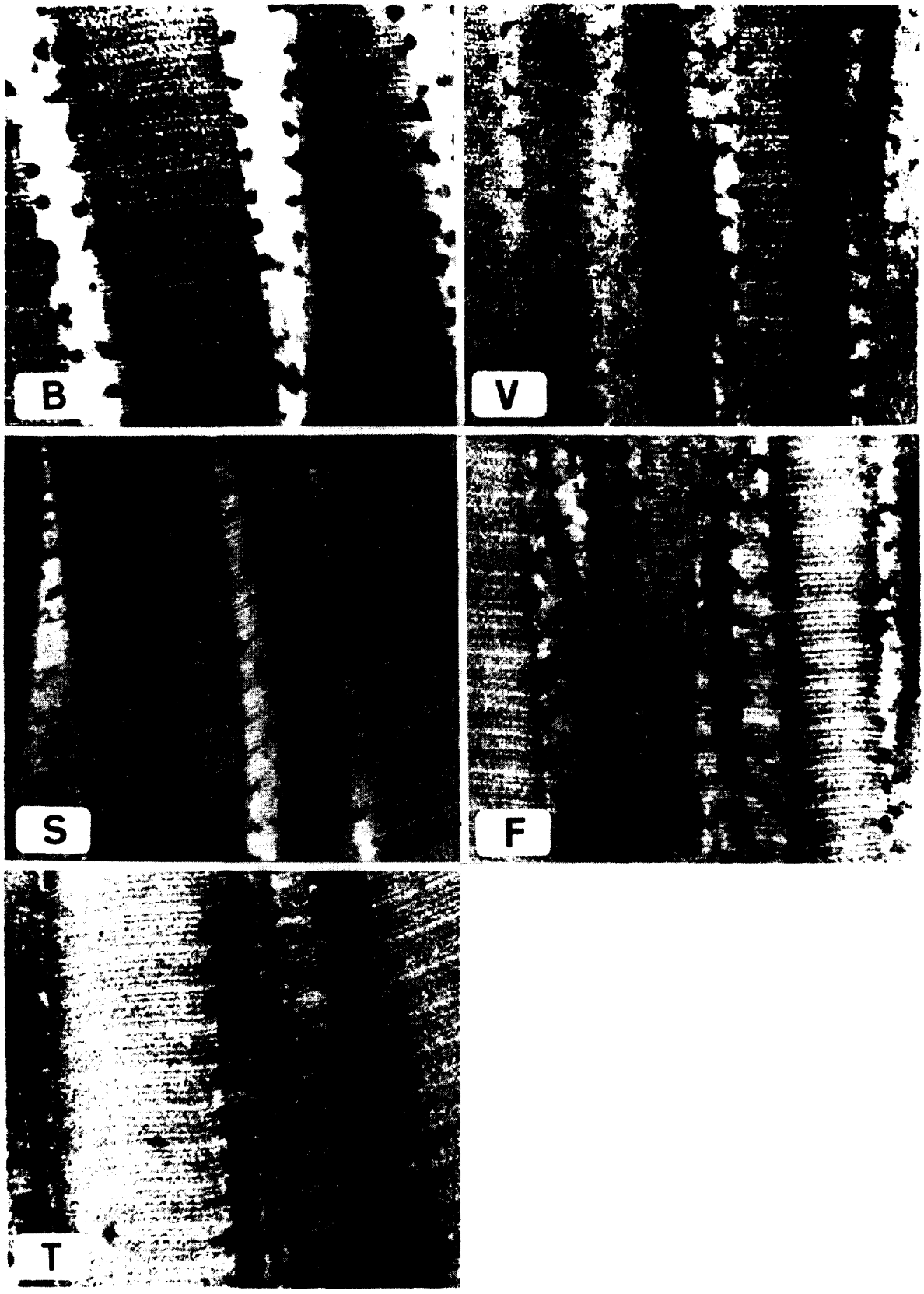

Figure 12. Electron micrographs illustrating longitudinal sections of collagen fibrils from anterior region of annulus fibrosus with PG granules in periodic array along the fibrils. B = basal, V = vivarium, S = synchronous, F = flight, T = tail suspension. X120,000.

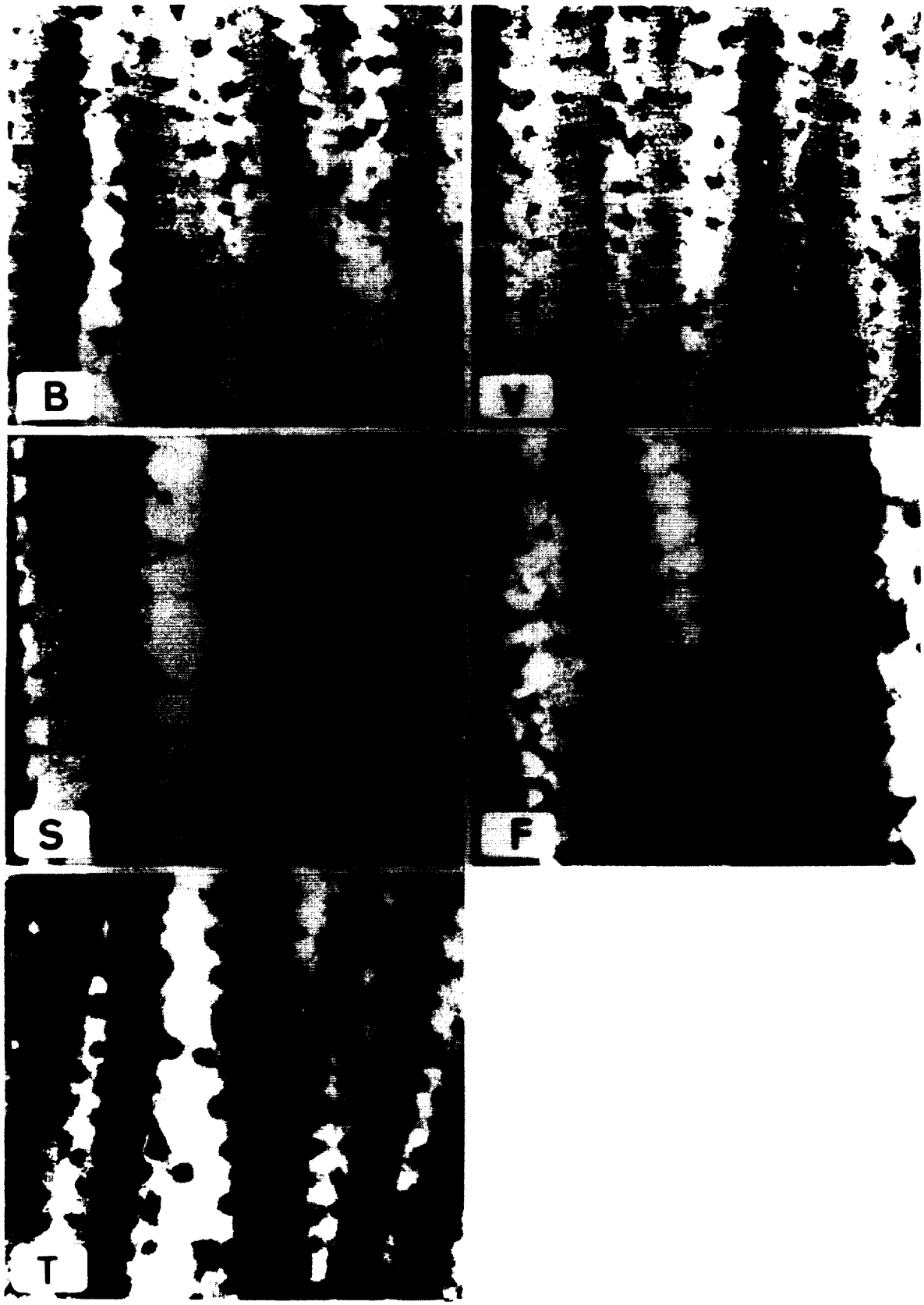

Figure 13. Electron micrographs illustrating longitudinal sections of collagen fibrils from transition zone of annulus fibrosus. Note smaller collagen fibril size and increased size and density of PG granules compared to anterior region (Figure 12). B = basal, V = vivarium, S = synchronous, F = flight, T = tail suspension. X120,000.

EXPERIMENT K-7-03

GRAVITY AND SKELETAL GROWTH

PART I: GRAVITY AND SKELETAL GROWTH

PART II: MORPHOLOGICAL STUDIES OF BONE AND TENDON

PART III: PREOSTEOBLAST PRODUCTION IN COSMOS 2044 RATS: SHORT TERM RECOVERY OF OSTEOBLAST POTENTIAL

PART IV: IMMUNOHISTOCHEMISTRY OF COLLAGENASE IN CALVARIA OF RATS FLOWN ON COSMOS 2044

PART V: BIOMECHANICAL PROPERTIES OF RAT TARSUS BONES (Not Available at Time of Publication))

Principal Investigator:

E.R. Morey-Holton
NASA-Ames Research Center
Moffett Field, CA

Co-Investigators:

S.B. Doty
Hospital for Special Surgery
New York City, NY

R.T. Whalen
NASA-Ames Research Center
Moffett Field, CA

J. J. Jeffrey
Division of Hematology
Dept. of Medicine
Albany Medical College
Albany, NY

W. E. Roberts
L.P. Garetto
Indiana University School of Dentistry
Indianapolis, IN

N.C. Partridge
C.O. Quinn
L. A. Gershan
T. C. Lorenz
St. Louis University School of Medicine
St. Louis, MO

G. Durnova
A. Kaplansky
Institute of Biomedical Problems
Moscow, USSR

EXPERIMENT K-7-03:

PART I: GRAVITY AND SKELETAL GROWTH

E.R. Morey-Holton

SUMMARY

Bone area and perimeter were measured at the tibiofibular junction of rats associated with Cosmos 2044. No major differences were noted between any of the groups. The only significant difference was the larger marrow parimeter in the basal rats as compared to all other groups. The rats were about 25d older than the Cosmos 1887 animals. The data suggest that few bone changes occur in rats launched into space at 107d of age for 14 days.

INTRODUCTION

Experiments flown on the Soviet Cosmos biosatellite 1887 were complicated by the unexpected postflight processing time which was in excess of two days after landing of the satellite. To differentiate between flight response with minimal recovery time and flight response with extended recovery superimposed, Cosmos 2044 was launched and the experiments previously flown on Cosmos 1887 were repeated. However, due to unanticipated flight delays, the rats on Cosmos 2044 were almost one month older than the animals on Cosmos 1887 at launch. Cosmos 2044 was also the first flight experiment to include the ground-based flight-simulation rat model (tail-suspended animals) as a control group.

MATERIALS AND METHODS

Specific pathogen-free, male, Wistar rats from the Institute for Experimental Endocrinology of the Slovakian Academy of Sciences were divided into 4 groups of 10 animals/group and a baseline control group of 5 rats. The flight and synchronous groups were each housed in a single cage which had 10 nozzles for paste diet and 10 lixits for water. Fourteen gram boluses of food (55g/day/nozzle) were delivered every 6 hours beginning at 0200 each day. Water was provided ad libitum. The vivarium animals were housed similarly but were fed in a single bolus each day. The flight rats were launched on September 15, 1989, at 1030 hours and landed at 0600 hours on September 29, 1989. Rats #6-10 were used in this experiment. The flight rats were 14 days older than the basals while the vivarium rats were 6 days older than the flight and the synchronous group was 2 days younger than the vivarium group at the end of the experiment. At the end of each test period, rats were guillotined. One-half of the proximal tibial metaphysis, the tibial shaft, and one skinned foot were place in vials of 2% parformaldehyde in 0.1M cacodylate buffer, plus 0.5% glutaraldehyde, pH 7.4 at 4C for 48hr then rinsed 3 times with 0.1M cacodlylate buffer, pH 7.4 and shipped immersed in the buffer. The maxillae, with teeth, were fixed in phosphate buffered formalin, pH 7.0, stored and shipped at 4C. The calvaria were processed as requested by Dr. Partridge. One foot was skinned and then frozen and shipped frozen. All samples arrived at this laboratory in excellent condition. The proximal tibia and part of the shaft were shipped at 4C by overnight mail to Dr. Doty for processing. Dr. Roberts' samples were similarly shipped by overnight mail. The calvaria were shipped by overnight mail to Dr. Partridge for analysis. All tissue arrived at their destination without incident.

The tibial shafts were dehydrated in ethyl ether and embedded undecalcified in polyester casting resin (Chemco, San Leandro, CA). The portion of the tibial shaft immediately proximal to the tibiofibular junction was sawed into 50 micron-thick cross sections with a Gillings-Hamco thin sectioning machine. Sections were mounted on slides and exposed to incident and polarized light. Area and perimeter measurements were determined using a computerized histomorphometry system as previously described.

Techniques used by Dr. Doty in processing his tissues and the data are discussed in detail in Part II, "Morphological Studies of Bone and Tendon". The techniques and data from Dr. Roberts and his colleagues are discussed in detail in Part III, "Preosteoblast Production in Cosmos 2044 Rats: Short Term Recovery of Osteogenic Potential": Techniques and data from Dr. Partridge are discussed in detail in Part IV: "Immunohistochemisty of Collagenase in Calvaria of Rats Flown on Cosmos 2044". Techniques and data from Dr. Whelan will be discussed in detail in Part V, "Biomechanical Properties of Rat Tarsus Bones", (Report Pending). Part VI, "Intervertebral Disc Swelling and Pressure Associated with Microgravity," could not be completed by Dr. Hargens because frozen thoracic, rather than lumbar, vertebra were received and the disks were not large enough for measurement of disk swelling properties.

RESULTS

The body weight of the basal group on Cosmos 2044 was 320±10g (±S.D.) in comparison to the 316±10g of the same group in Cosmos 1887 (Table 1). The flight group from Cosmos 2044 weighed 35g more and were 18d older than the Cosmos 1887 flight rats. The Cosmos 2044 vivarium group weighed 21g more and were 21d older than the Cosmos 1887 vivarium rats. The Cosmos 2044 synchronous group weighed 6g less and were 16d older than the Cosmos 1887 synchronous group.

Visual observations of tibial cross sections under brightfield or polarized light did not show any obvious differences. Area and periosteal perimeter measurements (Table 1) showed no significant changes between any of the flight period experimental groups. The only differences noted were between the basal group and other groups. The basal group had a significantly larger marrow area than the tail-suspended group, a larger periosteal perimeter than the flight group, and a significantly larger marrow perimeter than all other groups.

DISCUSSION

Data from Cosmos 2044 are difficult to compare with Cosmos 1887 due to the age difference. In spite of the age difference, the basal rats on Cosmos 2044 only weighed 4g more than Cosmos 1887 basals, Cosmos 2044 flight rats gained 16 gms during the flight period vs 9 gained by the Cosmos 1887 rats, the synchronous group on both missions gained essentially the same weight, and the vivarium group on Cosmos 2044 gained 65g vs 25g gained by this group during Cosmos 1887

The larger bones in the basal group of Cosmos 2044 are an unexplained finding and have not been seen before on any Cosmos mission (Table 1). On Cosmos 1887, area and perimeter measurements at the tibiofibular junction only showed differences between the synchronous and basal groups with the synchronous bones being larger (Table 1). With the exception of the marrow perimeter in the synchronous and vivarium group, the area and perimeter measurements in the Cosmos 2044 rats were larger than those found in Cosmos 1887. The larger bones on Cosmos 2044 agree with the older age of the rats and the lack of any increase in bone mass during the flight period indicates that the animals were adults and that bone mass was not accumulating rapidly in any group during the 14d flight period, unlike some of the

animals in Cosmos 1887. Larger, adult rats may require a longer flight period to demonstrate bone changes particularly in cortical bone since the skeleton is turning over more slowly.

ACKNOWLEDGEMENTS

The authors thank the many Soviet scientists who assisted with the experiment by dissecting tissues, preparing samples, and expediting the shipment of biological specimens to this country. We also thank the NASA personnel who made this experiment possible. We are grateful for the technical assistance provided by Charlotte Cone in shipping the bone specimens from our laboratory and analysing the tibial shaft specimens.

TABLE 1

COSMOS 1887

GROUP MEASUREMENT	BASAL	FLIGHT	SYNCHRONOUS	VIVARIUM
Age, d (initial/final)	-/85	86/105	92/111	89/108
Body mass, g				
loading		294 ± 7	313 ± 12	317 ± 12
final	316 ± 18	303 ± 4.5	349 ± 13	342 ± 18
Δ		9 ± 5.8	37 ± 3.6	25 ± 6.1
Bone area, mm^2	3.43 ± 0.23	3.60 ± 0.27	3.94 ± 0.37*	3.75 ± 0.34
Marrow area, mm^2	0.79 ± 0.06	0.77 ± 0.16	0.84 ± 0.17	0.79 ± 0.17
Periosteal perimeter,mm	7.93 ± 0.20	7.97 ± 0.29	8.38 ± 0.29	8.11 ± 0.41
Marrow perimeter, mm	3.37 ± 0.13	3.32 ± 0.31	3.45 ± 0.34*	3.36 ± 0.37

TABLE 2

COSMOS 2044

GROUP MEASUREMENT	BASAL	FLIGHT	SYNCHRONOUS	VIVARIUM	TAIL-SUSPENDED
Age, d (initial/final)	-/109	107/123	114/127	116/129	118/131
Body mass, g					
loading		321 ± 5.2	307 ± 6.8	303 ± 21	303 ± 21
final	320 ± 10	338 ± 4.6	343 ± 15.7	363 ± 4.5	339 ± 21
Δ		16 ± 4.3	36 ± 5.8	65 ± 1.6	37 ± 4.6
Bone area, mm^2	4.79 ± 0.38	4.33 ± 0.19	4.59 ± 0.34	4.61 ± 0.30	4.75 ± 0.51
Marrow area, mm^2	0.99 ± 0.14	0.87 ± 0.07	0.91 ± 0.06	0.89 ± 0.12	0.82 ± 0.10*
Periosteal perimeter, mm	8.93 ± 0.26	8.36 ± 0.25*	8.60 ± 0.28	8.60 ± 0.21	8.73 ± 0.55
Marrow perimeter, mm	3.76 ± 0.28	3.45 ± 0.17*	3.46 ± 0.09*	3.30 ± 0.21*	3.43 ± 0.25*

Data are expressed as mean ± S.D.; n= 5 rats/group
* = significantly different from basal ($p<0.05$)

EXPERIMENT K-7-03

PART II: MORPHOLOGICAL STUDIES OF BONE AND TENDON

S.B. Doty, Ph.D.

SUMMARY

Electron and light microscopy, histochemistry and morphometric techniques were combined in this study to determine the effects of microgravity on bone cells and the vasculature within the diaphysis of the rat tibia. Previous studies indicated that the mid-diaphyseal region of the long bones was responsive to non-weight bearing and space flight. In the present study, vasculature changes at the periosteal and sub-periosteal region were not apparent by light microscopy. Electron microscopy showed that vascular inclusions were present in the flight animals however the blood vessels themselves appeared undamaged. Electron microscopy of the tendons of the foot showed some collagen fibril disorganization but this was not noticeable by light microscopy. Investigations of the osteoblasts lining the endosteal surface indicated a reduction in activity, but morphometric measurements suggested that these alterations were not significantly different from control values.

INTRODUCTION

A previous report (Doty, et al, 1990) described results from Cosmos 1887 in which drastic changes occurred to the vascular system within the diaphyseal bone, evidently in response to the microgravity experience. Also, there was a reduction in alkaline phosphatase activity associated with the endothelial cells of these same blood vessels suggesting a reduction in transport activity. Many of the vessels in the periosteal region were occluded with lipid-like substances. This led to the suggestion that an ischemia may have developed in the periosteum which would explain the reduction in new bone formation in this region as an effect of the space flight (Morey and Baylink, 1978; Wronski and Morey, 1983).

The endosteal and trabecular bone of the metaphysis, which is the most actively growing region in the long bones, has also been shown to have reduced bone formation during space flight (Vico, et al, 1987). The endosteal area of the mid-diaphysis in the growing rat is lined by osteoblasts which are not as active or as numerous as in the metaphyseal region (Jee, et al, 1983). Therefore it has been difficult to determine their response to hypogravity. We have developed a technique which combines morphology and histochemistry in order to evaluate the activity of these cells.

In addition to the study of the vascular supply to the periosteal region and the determination of the endosteal osteoblastic activity, we have also investigated the structural integrity of the tendons attached to the metatarsals of the rat foot. This tissue is sensitive to changes in mechanical stress (Amiel, et al, 1983) and it was thought that the reduced activity imposed by space flight might cause structural changes in these tendons.

METHODS

All tissues were prepared for electron and light microscopy by chemical fixation in 2% paraformaldehyde and 0.5% glutaraldehyde in 0.05 M cacodylate buffer,

pH 7.4. Fixation of tissues occurred over 18-24 hours at 4C. For histochemical purposes, many tissues were decalcified in 10% EDTA in 0.05M Tris buffer, pH 7.2, at 4C. Decalcified tissues were cut into 50μm thick sections with a vibratome for incubation in various histochemical media. Methods for acid and alkaline phosphatase activity, demonstrated by light and electron microscopy, have been described (Doty and Schofield, 1984). All tissues were embedded in Spurr's resin. The silver staining method for collagen has been described by Matthiessen, et al (1985) and can be applied to sections embedded in the plastic resin.

For morphometric measurements of the endosteal osteoblasts, cross sections of mid-diaphyseal bone were embedded in JB-4 resin and polymerized at -20C. The cold polymerization prevented excessive protein denaturation due to the high heat released during polymerization of this methacrylate resin. Section were cut at 3-5 micron thickness and dried onto clean glass slides. Silver staining of these sections was carried out for one hour to visualize the collagen fibers. Those fibers most recently synthesized, such as immediately beneath the osteoblast layer, were the most darkly stained by this method. The osteoblasts were stained for acid phosphatase activity to outline the Golgi complex which is filled with this enzyme activity. Alternately, if we stained the cytoplasmic RNA with pyronine, the Golgi complex which is free of RNA is visualized by negative contrast. To obtain valid morphometric data, the cross sections had to be complete (ie, the entire endosteal surface had to be present in the section), and the osteoblast lining of the endosteum had to cover 100% of the bone surface. The measurements were made at 320X magnification so that the Golgi presence could be easily determined.

RESULTS

Vasculature of Bone

The blood vessels within the diaphyseal bone did not appear to be significantly altered as viewed by light microscopy. In the electron microscope, some dense bodies and lipid-like material was found within the periosteal vessels of the flight group (Figures 1&2). However, there was no apparent vascular degeneration, lipid occlusions, or cell death as we described in the previous Cosmos flight. In addition, the alkaline phosphatase activity of the vascular endothelium was similar in intensity in all groups studied.

In one of the flight animals, the periosteal vessels contained large quantities of a crystalline-like material (Figure 3). With electron microscopy we determined that there was a lattice structure to this material (Figure 4) with a repeat period every 4.35 nm. We have not yet identified this material but it is interesting that many of the high molecular weight fatty acids also have similar periodicities by x-ray diffraction.

Tendon Structure

Tendons connected to the metatarsals were sectioned in a longitudinal plane parallel to their original orientation. The collagen fibrils did not show any variation in their periodicity irrespective of the group studied. However, in the flight group we found fibroblasts which were surrounded by disorganized fibrils (ie, these fibrils were not organized with respect to any of the collagen lamellae already present). In many cases, the space around the fibroblasts was quite large

compared to similar preparations from the control group, and the disorganized fibrils filled this space in a very haphazard manner (Figures 5&6). This finding was not evident in every fibroblast from the flight group and we are still trying to evaluate the extent of this observation, however we did not observe any of this in the control groups.

Activity of Endosteal Osteoblasts

Using the silver and Golgi stained sections, we evaluated the percentage of endosteal osteoblasts which contained a well recognized Golgi complex. Using the Zeiss Videoplan, we measured the osteoid surface along the endosteum and then determined what percentage of overlying osteoblasts contained well formed Golgi systems, and the percentage which had no observable Golgi complex. Osteoblasts covered 100% of the endosteal surface in this mid-diaphyseal region of the tibia. Sections were not evaluated if the cross section was not complete or if the osteoblast layer was mechanically damaged and separated from the bone surface.

The data indicated that for the vivarium and synchronous controls, osteoblasts with active Golgi systems covered 76.9 ± 2.85 (SD) and 79.4 ± 4.2% (SD) of the endosteal surface. In the flight group, the same measurement produced a value of 52.2 ± 20.7% (SD), a lower value than the controls but with a substantially larger measurement error. Thus there is a tendency for the endosteal osteoblasts from the flight group to be less well differentiated and less "active" in bone formation, but the variation between animals was considerable. Its interesting that this variation did not exist among the control groups.

DISCUSSION

The reduction in bone formation due to spaceflight is thought to be caused by a significant reduction in osteoblastic activity (Morey and Baylink, 1978; Wronski and Morey, 1983; Wronski, et al, 1987). Initially this reduction was measured by tetracycline uptake along the periosteal surfaces of long bones (Morey and Baylink, 1978; Wronski and Morey, 1983). As morphometric techniques improved, studies were made of trabecular bone and the bone formation in the metaphyseal region of long bones and vertebrae (Wronski, et al, 1987; Jee, et al, 1983). These latter studies often did not produce the same degree of reductions in formation but these measurements are also more difficult to make. Then in 1990 we found (Doty et al, 1990) that the periosteal and sub-periosteal blood vessels in the mid-diaphyseal region of the rat tibia were altered by spaceflight. These alterations included degeneration of the vascular endothelium, reduction in alkaline phosphatase activity of the endothelium, lipid inclusions within the blood vessels and nearby osteocytes and occasionally cell death within the bone. Thus such changes, which resemble an ischemic condition in bone (Chryssanthou, 1978; Jones, 1985) could explain the reduced bone formation at the periosteal surface.

The blood flow in rat bone occurs in a centrifugal pattern, with the periosteal vessels receiving blood after it has first passed through the marrow space and then bathed the cells of the diaphyseal bone. Thus the endosteal osteoblasts may be less affected by altered blood flow or an ischemic condition, than the periosteal osteoblasts. One purpose in developing a method to evaluate osteoblast function, as we did for this study, is to determine osteoblast function in various areas of bone when labels for determining formation rates are not available. The active

Golgi complex directly relates to the osteoblast's level of differentiation and we were encouraged to find that both control groups contained similar percentages of endosteum which was covered with active osteoblasts. However the range of measurements found for the flight group was unexpected and prevented a definite conclusion regarding osteoblastic activity following space flight. Although the trend was for these endosteal osteoblasts to show a reduced percentage of active cells compared to controls, the data was not highly significant.

The periosteal and sub-periosteal vessels in the long bones from these flight animals did not contain the alterations which were described for Cosmos 1887 (Doty, et al, 1990). By light microscopy, there were no obvious structural changes, lipid inclusions or any apparent cell death. By electron microscopy, we did find small vascular inclusions and lipid droplets within the sub-periosteal vessels. In one flight animal we found large deposits of crystalloid material within the vessels of the periosteum. The chemistry of this material is unknown but the 4.35 nm lattice repeat is similar to that found in fatty acids. The general absence of vascular changes in this study is interesting since the flight was similar in many respects to Cosmos 1887. One difference between these two flights was a delay of almost 55 hours before the animals could be sacrificed following Cosmos 1887 but in the present study the sacrifice was almost immediate. This raises the possibility that the vascular changes could have occurred when the animals became weight bearing following their flight in space. This suggests that following a non-weight bearing period, the resumption of full weight bearing may be detrimental to the vascular system, especially at the periosteal surface of bone. There is no proof for this suggestion but it does indicate that future studies should include the study of "recovery" following space flight.

The effects of microgravity and non-weight bearing may have a more direct effect on tendons and ligaments since they are naturally involved in the transmission of mechanical forces. From our electron microscopic studies, we see that the most recently secreted collagen fibrils (ie, those nearest the fibroblast cell membrane) demonstrate a disorganization which was not seen in the control tendons. The forming fibrils, which are normally secreted in a controlled manner via cytoplasmic channels in the fibroblast (Birk and Trelsted, 1986) appear to be polymerizing in a haphazard fashion. The newly secreted fibrils show no relationship to the previously synthesized fibrils which are arranged in organized lamellae. This loss of control may be mediated through the absence of mechanical forces (Amiel, et al, 1983) due to the non-weight bearing in the space environment, or may be due to some metabolic change within the fibroblast itself (Goldberg, 1979). Evaluation of these effects on the tendon need to be made more quantitative but it will probably have to be done at the electron microscopic level of investigation. It appears worthwhile to compare microgravity effects on tendon and bone since the fibroblast and osteoblast are both synthesizing type I collagen. However these cells probably experience quite different stimuli during weight bearing and might be expected to respond differently to reduced mechanical stresses as experienced during space flight.

REFERENCES

1. Amiel, D., W.H. Akeson, F.L. Harwood, and C.B. Frank. Stress Deprivation Effect on Metabolic Turnover of the Medial Collateral Ligament Collagen. Clin. Orthop. Rel. Res. 172: 265-270, 1983.

2. Birk, D.E. and R.L. Trelstad. Extracellular Compartments in Tendon Morphogenesis: Collagen Fibril, Bundle and Macroaggregate Formation. J. Cell Biol. 103: 231-240, 1986.

3. Chryssanthou, C.P. Dysbaric Osteonecrosis. Clin. Orthop. Rel. Res. 130: 94-106, 1978.

4. Doty, S.B., E.R. Morey-Holton, G.N. Durnova and A.S. Kaplansky. Cosmos 1887: Morphology, Histochemistry and Vasculature of the Growing Rat Tibia. FASEB J. 4: 16-23, 1990.

5. Doty, S.B. and B.H. Schofield. Ultrahistochemistry of Calcified Tissues. In: Methods of Calcified Tissue Preparation. (G.R. Dickson, editor) Elsevier/North Holland Biomedical Press. pp.149-198, 1984.

6. Goldberg, B. Binding of Soluble Type I Collagen Molecules to the Fibroblast Plasma Membrane. Cell 16: 265-275, 1979.

7. Jee, W.S.S., T.J. Wronski, E.R. Morey, and D.B. Kimmel. Effects of Spaceflight on Trabecular Bone in Rats. Am. J. Physiol. 244: R310-314, 1983.

8. Jones, J.P. Rat Embolism and Osteonecrosis. Orthop. Clinics N. Am. 16: 515-633, 1985.

9. Matthiessen, M.E., B. Sogaard-Pedersen and P. Romert. Electron Microscopic Demonstration of Non-mineralized and Hypomineralized Areas in Dentin and Cementum by Silver Methenamine Staining of Collagen. Scand. J. Dent. Res. 93: 385-395, 1985.

10. Morey, E.R. and D.J. Baylink. Inhibition of Bone Formation During Spaceflight. Science 201: 1138-1141, 1978.

11. Vico, L., D. Chappard, A.V. Bakulin, V.E. Novikov and C. Alexandre. Effects of 7-Day Space Flight on Weight Bearing and Non-Weight Bearing Bones in Rats (Cosmos 1667). Physiologist. 30: S45-S46, 1987.

12. Wronski, T.J. and E.R. Morey. Effect of Spaceflight on Periosteal Bone Formation in Rats. Am. J. Physiol. 224: R305-R309, 1983.

13. Wronski, T.J., E.R. Morey-Holton, S.B. Doty, A.C. Maese and C.C. Walsh. Histomorphometric Analysis of Rat Skeleton Following Spaceflight. Am. J. Physiol. 252: R252-R255, 1987.

Figure 1. An electron micrograph of a blood vessel within diaphyseal bone matrix (BM) of a flight animal. The endothelial cell lining (arrows) is intact. A red blood cell (asterisk) and numerous small dense inclusions are contained within the lumen of this vessel. Magnification: 12,000X

Figure 2. This electron micrograph shows a blood vessel from bone of a flight animal. Small lipid-like accumulations (dense black deposits) are present within cells associated with the vascular endothelium. Magnification: 9,000X

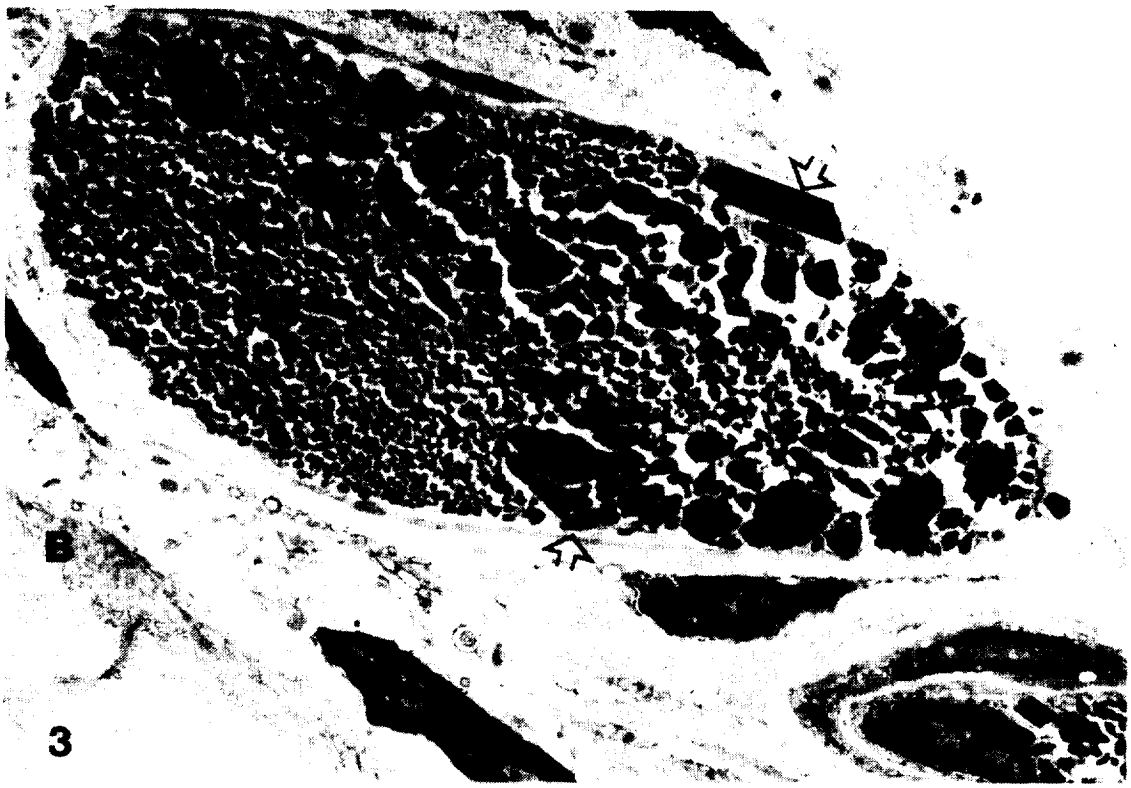

Figure 3. This electron micrograph demonstrates two blood vessels contained within the collagenous layer of the periosteum adjacent to diaphyseal bone (B). Crystalloids (arrows) of various size and shape are packed into these vessels. Magnification: 9,000X

Figure 4.This electron micrograph illustrates one large crystalloid found within the vessel shown in Figure 2. The irregular shape and multiple cracks in the structure suggest that it consists of an organic material rather than being inorganic. The lattice repeats every 4.35 nm. Magnification: 120,000X

Figure 5. shows the collagen lamellae and two fibroblasts from a control tendon. The collagen being released from the cell (arrows) shows early organization and parallel fibril orientation. Magnification: 14,000X

Figure 6. illustrates the tendon fibrils found in flight animals. The newly forming fibrils show a pattern of disorganization and are not arranged in parallel to the lamellae already formed. The disorganized fibrils do show a normal periodicity within each fiber. Magnification: 14,000X.

Figures 5 and 6. These electron micrographs illustrate fibroblasts from tendon and the collagen fibrils associated with these cells. The photos are identically produced for comparison purposes.

EXPERIMENT K-7-03

PART III: PREOSTEOBLAST PRODUCTION IN COSMOS 2044 RATS: SHORT TERM RECOVERY OF OSTEOGENIC POTENTIAL

L.P. Garetto, E.R. Morey, G.N. Durnova, A.S. Kaplansky, and W.E. Roberts

ABSTRACT

The influence of 13.8 day spaceflight and ~8.5-11 h recovery period at 1 g on fibroblast-like osteoblast precursor cells was assessed in the periodontal ligament (PDL) of rat maxillary first molars. Preosteoblasts (C+D cells) and less differentiated progenitor cells (A+A' cells) were identified by nuclear volume analysis (i.e. A+A' = 40-79 μm^3; C+D $\geq$ 120 μm^3). No differences were observed between flight (F) and synchronous (SC), vivarium or basal control groups in either the A+A' (F: 28.0 ± 3.7 vs SC: 27.4 ± 2.2), B (F: 33.1 ± 1.4 vs SC: 32.4 ± 2.4) or C+D (F: 38.4 ± 4.5 vs SC: 39.2 ± 1.6) cell compartments within the PDL (mean ± SEM, n = 5). Compared to previous spaceflight experiments, the present flight data are consistent with a post-flight response to replenish preosteoblasts and restore PDL osteogenic potential. The present data emphasize the need to: 1) unequivocally determine the flight effect by in-flight euthanasia and 2) further assess the post-flight recovery phenomenon.

INTRODUCTION

Studies performed in rats flown on both Soviet and American missions have suggested that osteoblast histogenesis is suppressed following spaceflight (8,18). These reports are consistent with data showing decreased numbers of osteoblasts in the tibial metaphysis (8,22) and a diminished growth in rat tibial diameter after spaceflight (23,24). The data suggest a flight-related decrease in bone formation that occurs as a generalized, systemic phenomenon in both the weightbearing axial skeleton (10,22) as well as in nonweightbearing bones (19,20).

Inhibition of osteoblast differentiation following spaceflight has been evaluated in the rat maxillary molar periodontal ligament (PDL) model (8,18). The PDL is a well-defined cell kinetic model for assessing the proliferation and differentiation of the cells associated with osteoblast histogenesis (12,17). Roberts and Morey (16) have identified distinct cell kinetic compartments of fibroblast-like cells within the PDL that comprise a family of osteoblast precursor cells. In ascending order of differentiation, these compartments are classified according to nuclear volume as: 1) A cells, less-differentiated, self-perpetuating precursor cells; 2) A' cells, committed osteoprogenitors that are derived from A cells and are the source of preosteoblasts; 3) C cells, G_1 stage preosteoblasts; and 4) D cells, G_2 stage preosteoblasts. Each G_2 stage preosteoblast undergoes mitosis and forms two mature osteoblasts (Fig. 1).

In previous experiments, spaceflight induced inhibition of osteoblast histogenesis is indicated by an increased number of early progenitor (A+A') cells (15,18) and a decrease in the number of immediate preosteoblast (C+D) cells (18). This response was strongest in animals from the Cosmos 1129 mission (15) that were euthanized about 6 h following reexposure to a 1g environment. The first evidence of short-term recovery was a partial effect (i.e. elevated numbers of A+A' cells *without* a depressed C+D cell compartment) in ~12 week old rats euthanized 12 h following reentry in the Space Lab-3 mission (15). Younger rats flown on this mission appeared to have fully recovered their osteoblast precursor potential. However, rats flown on Cosmos 1887 and not euthanized until ~55 h following reexposure to 1 g showed an effect opposite to that seen

Index Terms:
Bone; Osteogenesis; cell differentiation; spaceflight; recovery; microgravity.

immediately (6 h) after flight. PDL from the Cosmos 1887 animals exhibited a remarkably strong pattern of preosteoblast (C+D cells) formation and a diminished population of A+A' (early progenitor) cells indicative of a marked osteogenic recovery response (3). This physiological overshoot is similar to a mechanical osteogenic stimulus of a quiescent PDL (17). Taken together, the data from the different spaceflight missions suggests an initial inhibition of osteoblast histogenesis followed by a post-flight recovery response.

The present study of rat PDL from the Cosmos 2044 flight allows further investigation of the osteoblast histogenesis recovery pattern following an 8.5 - 11 h post-flight exposure to 1 g. The data are consistent with a recovery response that was predicted from analysis of previous flights and provide important further evidence for the physiological kinetics of the process.

METHODS

Ten male (specific pathogen free) Czechoslovakian-Wistar rats (Institute of Endocrinology, Bratislava, Czechoslovakia) were flown aboard the Cosmos 2044 satellite for ~13 days, 19 h. A paste diet was provided in 14 gm boluses at 0200, 0800, 1400, 2000 h each day through nozzles in the cage. Water was provided *ad libitum*. The rats were group-caged and maintained on a 16 h photoperiod with the lights on from 0800-2400 h. The flight group was ~17 week old when euthanized. Data for flight animals reported in this paper were derived from rats (animal #F6-#F10) euthanized between ~8.5 - 11 h after landing (final weight 338 ± 2 gm). A complete report of the Cosmos 2044 mission is provided by Grindeland et al. (4) in this issue. A brief description of the mission is provided here.

Three groups of rats were used as controls for the flight animals. Ten basal control rats (final weight for animals #B6-#B10: 320 ± 4 gm) were housed similar to flight animals and euthanized on the launch date (i.e. ~13.8 days prior to flight animal euthanasia). These animals were ~15 weeks old when euthanized. A synchronous control group (10 rats) was maintained in flight-type cages and subjected to a flight-like environment: similar launch forces, vibration, reentry g force, lighting regimen and ambient temperature. Synchronous controls (final weight for animals #S6-#S10: 343 ± 7 gm) were euthanized 5 days after flight animals at an age of ~18 weeks. Finally, an equal number of animals served as vivarium controls. These rats were kept on a lighting and temperature regimen similar to in-flight conditions, but were fed all of their food at a single feeding. The vivarium control animals were euthanized seven days following flight animals at an age of ~18 weeks (final weight for animals #V6-#V10: 363 ± 2 gm).

Following euthanasia, the maxillae from five animals in each group (animals #6-#10) were removed and immersed in neutral buffered formalin for 48 h at 4°C. Fresh fixative was added and the specimens were maintained at about 4°C during shipment to the NASA-Ames Research Center at Moffett Field, CA. After receipt in our laboratory, the samples were demineralized, embedded in plastic, sectioned at 4 μm in the midsagittal plane of the mesial root of the first molar and stained with hematoxylin and eosin. Details of the histological methods are published (15). Only PDL samples with a resorbing (scalloped with occasional osteoclasts) or resting (no morphological evidence of active resorption or formation) alveolar bone margin were selected for analysis.

An ocular micrometer was used to measure the major and minor nuclear dimensions of 100 cells in each PDL under oil immersion at x1,000. Nuclear volume for each cell sampled was calculated according to the formula for a prolate spheroid: Volume = $4/3\pi ab^2$ where a and b are the radii of the major and minor nuclear dimensions, respectively (3,13,14). Only cells oriented in the plane of section and projecting a maximum nuclear dimension were sampled. In 4 μm sections, these criteria were met by cells containing an oval nucleus with a distinct outline and relatively uniform density (17). Each cell was classified as type A+A', B, C, or D according to the following nuclear volume categories: 40-79, 80-119, 120-169 and ≥170 μm^3, respectively (16). The fractional

distribution of each cell type was expressed as a group mean percent ± SEM. PDL width was also measured at three levels within the mid-root region of the mesial root of the first molar.

Nuclear volume and PDL width data from the flight group and the three control groups were analyzed using one-way analysis of variance (ANOVA) with $p \leq 0.05$ considered as statistically significant. An arcsine (angular) transformation of the percent data from the nuclear volume measurements was performed to satisfy the distributional assumptions that underlie the ANOVA (21). Sections from five animals were analyzed from the flight, synchronous control and basal control groups. Due to histological sectioning difficulties, only four animals in the vivarium control group could be analyzed.

RESULTS

A comparison of the PDL cell populations from the three control groups showed no significant differences (Fig. 2). However, there was a tendency for the PDL from the basal control rats to have fewer A+A' cells and more D cells than either the synchronous or vivarium controls. This pattern was also seen in the earlier Cosmos 1887 mission results (3), and may be related to the younger age (by 2-3 weeks) of the basal control animals. Similar cell compartment sizes were seen in both synchronous and vivarium control animals when results from the present experiment were compared to those of the Cosmos 1887 data (3). Because the environment and handling of the synchronous control group most closely simulated that of the flight group, all further comparisons were made between these two groups.

No significant differences between flight and synchronous control animals were seen in any of the nuclear volume compartments (Fig. 3). Similarly, no differences were observed when the width of the PDL from the various groups were compared (Table 1). The present flight data was then compared to that of previous flights with regard to the post-flight recovery time at 1 g. Cosmos 2044 results, when plotted on a graph comparing the temporal recovery response of osteoblast histogenesis from previous spaceflights, fit along the curve describing the best estimate of the short-term recovery pattern (Fig. 4). The lack of difference at the sampling time of the present experiment coincides with the "crossover point"[1] in the osteoblast precursor recovery response.

DISCUSSION

Important emphasis must be placed in distinguishing short-term recovery from the actual effects of microgravity. It is inappropriate to assume that the responses seen following flight are not complicated by return to a 1 g environment. Since animals have not been euthanized while actually in microgravity, the direct effect of spaceflight has not been unequivocally established. These are, however, the only available data. In many ways, understanding the recovery process from spaceflight is more interesting and potentially more significant than the flight effect itself. The ability of an animal's skeleton to *recover* normal mass, strength and osteogenic potential is probably directly related to survival following spaceflight.

The length of time needed to restore osteoblast histogenesis following spaceflight is not known. All flights to date, however, are exceptional opportunities to look at recovery from the microgravity effect associated with spaceflight. The temporal response of osteoblast histogenesis following spaceflight is shown in Fig. 4. In plotting these data, we have made the assumption (which is supported by data from the Cosmos 1129 flight (18) where rats were euthanized ~6 h following reentry) that spaceflight inhibits osteoblast histogenesis. Furthermore, we have assumed that this flight response is similar in all of the flights analyzed. Whether or not these are correct

[1]"Crossover" is defined as that point where cell kinetic compartment size passes through the normal range on its way from a suppressed value to a supercompensated level.

assumptions will be proven only when in-flight euthanasia and dissection are carried out (or at the very least, euthanasia within a very brief period following flight). Nevertheless, prior to analysis of the Cosmos 2044 data, the pattern of recovery from spaceflight showed a "crossover" point at approximately 12 h following reentry (Fig. 4). PDL from animals euthanized prior to this time demonstrated a block in osteogenesis at the A'Æ C cell differentiation step (Cosmos 1129). Euthanasia after a longer recovery period resulted first, in a stimulated ("supercompensatory") osteogenic response (Cosmos 1887), followed by return to control levels within 6 days post-flight (Cosmos 1129). The Cosmos 2044 data fits with the previously existing data and lies within the temporal window (at the crossover point), suggested by the recovery analysis depicted in Fig. 4, where no difference would be expected between the flight and control groups. These results suggest a timecourse of successful recovery of osteogenic potential.

Interestingly, supercompensatory responses following suppression or depletion in physiological systems is noted in other tissues as well. During the recovery period following exercise (11), following reweighting of rats after hindlimb suspension (5,6) and following exposure to microgravity (6,9), muscle glycogen (5,6,11) and liver glycogen (9) levels also show a phase in which they are significantly elevated above control untreated levels. It is possible that this pattern of response may simply be a normal physiological oscillation following a suppressive or depletive signal. Nevertheless, comprehending the physiology of musculoskeletal recovery and establishing muscle and bone interrelationships is an important objective for understanding the physiology of post-flight recovery.

The width of the PDL appears to be an important signal in its osteogenic response (12). In orthodontic treatment, widening of the PDL by orthodontically-derived mechanical force, acts to locally initiate bone formation. The lack of significant difference in width of the PDL in animals flown aboard Cosmos 2044 also suggests a rapid osteogenic recovery response. PDL width in rats euthanized 6 h after the Cosmos 1129 flight were significantly reduced from both synchronous and vivarium control animals, but without a concomitant decrease in cell density near the bone surface (18). These data indicate that the preferential decrease in preosteoblasts (C+D cells) seen in the Cosmos 1129 flight animals involved both a block in differentiation and a block in cell proliferation. In contrast, PDL cell density adjacent to the bone surface in the flight rats from Cosmos 1887 was significantly *increased* ~55 h after return to a 1 g environment compared to synchronous control levels (3). Roberts and Chase (12) reported similar kinetics of cell migration toward the bone surface during osteogenic induction following orthodontic force. The increase in cell density at the bone surface, in addition to the overall kinetic pattern of a decrease in A + A' cells and an increase in C + D cells in the Cosmos 1887 flight animals, indicated a strong osteogenic response in PDL post-flight. Thus, the PDL width data from the Cosmos 2044 rats also fits within the pattern of recovery response suggested by previous flights.

The strong post-flight increase in preosteoblast differentiation seen at 55 h following reentry (Fig. 4) is similar to the osteogenic response seen when PDL is subjected to mechanical stress by orthodontic force (12,17). Placement of a 0.5 mm latex elastic between the maxillary first and second molars induces a transient burst in DNA synthesis by fibroblast-like PDL cells (13,17). Cell kinetic analysis using the nuclear volume method indicates that orthodontic activation induces preosteoblast formation by stimulating an A'Æ C cell conversion. This is shown by an increase in C+D cells (arising from committed (A') osteoblast progenitor cells) within 8-10 h after insertion of the latex elastic (12). A second wave of preosteoblast formation occurs about 40 h later, at approximately 50 h post orthodontic stimulus (17). Assuming a similar kinetic pattern, the increase in the C+D cells seen ~55 h after spaceflight in the Cosmos 1887 rat PDL could be the second wave of preosteoblast differentiation stimulated by return to a 1g environment. Alternatively, the C+D cell response at this time could be the primary wave of differentiation since osteogenesis in these animals is presumably suppressed by the spaceflight. The physiological

significance of this response may be in maintaining an "inventory" of preosteoblasts (C+D cells) that have the capacity of rapidly differentiating into osteoblasts when needed.

It appears that the osteoblast histogenesis pathway, first described in the PDL, is applicable to other sites. Responses similar to the PDL have been seen in the tibial metaphyseal primary spongiosa of rats subjected to head-down tilt, simulating weightlessness (1,2). In addition, Jackson *et al.* (7) reported a shift in the fractional distribution of osteogenic cells in the mandibular condyles of rats flown aboard SL-3 that was similar to that seen in their PDL (15). Since osteogenic surfaces from both weightbearing and nonweightbearing tissues respond in a like fashion, these data suggest a *systemic* effect of microgravity. The mechanism behind such a systemic effect is unknown, but could be the result of microgravity induced fluid shifts or changes in the hormonal environment. Alternatively, multiple local acting factors cannot be ruled out.

The nuclear volume assay used in these studies is a reliable means for assessing the differentiation of osteogenic cells under a variety of experimental conditions (1,16,17). To date, this assay remains the only cell kinetic method for tracking osteogenic cells through their differentiation pathway. Direct determination of the steps in the differentiation pathway requires verification by distinctive biochemical, immunocytochemical or molecular markers for osteoblast precursors.

In conclusion, osteoblast histogenesis data from rats flown aboard Cosmos 2044 were not significantly different from control values. However, analysis of previous flights for post-flight recovery suggest that the animals in the present experiment were sampled at a time when osteogenic cell kinetic compartments were rapidly recovering as a result of the reinstitution of a gravitational field. The rapid recovery response suggested by the present data and that obtained from previous flights, indicates that recovery of osteogenic potential is an important physiological priority following return to a 1 g environment.

ACKNOWLEDGEMENTS

Supported by NASA-Ames Cooperative Agreement NCC 2-594 and NIDR Grant DE 09237-01. The authors wish to express their appreciation the Dr. A.S. Kaplansky and the Soviet dissection team. In addition we also would like to thank Ms. Patsy Dunn, Cheryl Roberts, Caroline Jennermann and Laurie Chen for their expert technical and editorial assistance.

REFERENCES

1. Fielder, P.J., E. R. Morey and W. E. Roberts. Osteoblast Histogenesis in Periodontal Ligament and Tibial Metaphysis During Simulated Weightlessness. Aviat.Space Environ.Med. 57:1125-1130, 1986.

2. Garetto, L.P., G.D. Barkett, E.R. Morey and W.E. Roberts. Nuclear Volume Analysis of Osteoblast Histogenesis in the Rat Tibial Metaphysis During Simulated Weightlessness. In: Fundamentals of Bone Growth, edited by Dixon, A.D. and B. Sarnat, Boca Raton, FL: CRC Press, 1991, p. In Press.

3. Garetto, L.P., M. R. Gonsalves, E. R. Morey, G. Durnova and W. E. Roberts. Preosteoblast Production 55 hours after a 12.5 day Spaceflight (Cosmos 1887). *FASEB J.* 4:24-28, 1990.

4. Grindeland, R.E., R. W. Vasques, R. W. Ballard and J. P. Connolly. Cosmos 2044 Mission Overview. J.Appl.Physiol. 1990.(In Press)

5. Henriksen, E.J., C. R. Kirby and M. E. Tischler. Glycogen Supercompensation in Rat Soleus Muscle During Recovery from Nonweight Bearing. J.Appl.Physiol. 66:2782-2787, 1989.

6. Henriksen, E.J., M. E. Tischler, S. Jacob and P. Cook. Muscle Protein and Glycogen Responses to Recovery from Hypogravity and Unloading by Tail-cast Suspension. Physiologist 28, Suppl.:S193-S194, 1985.

7. Jackson, C.B., W. E. Roberts and E. R. Morey. Growth Alterations of the Mandibular Condyle in Spacelab-3 rats. ASGSB Bul. 1:33, 1988.

8. Jee, W.S.S., T. J. Wronski, E. R. Morey and D. B. Kimmel. Effects of Spaceflight on Trabecular Bone in rats. Am.J.Physiol. 244:R310-R314, 1983.

9. Merrill, A.H., M. Hoel, E. Wang, et al. Altered Carbohydrate, Lipid, and Xenobiotic Metabolism by Liver from Rats Flown on Cosmos 1887. FASEB J. 4:95-100, 1990.

10. Morey, E.R. and D. J. Baylink. Inhibition of Bone Formation during Spaceflight. Science 201:1138-1141, 1978.

11. Richter, E.A., L. P. Garetto, M. N. Goodman and N. B. Ruderman. Muscle Glucose Metabolism Following Exercise in the Rat. J.Clin.Invest. 69:785-793, 1982.

12. Roberts, W.E. and D. C. Chase. Kinetics of Cell Proliferation and Migration Associated with Orthodontically-induced Osteogenesis. J.Dent.Res. 60(2):174-181, 1981.

13. Roberts, W.E., D. C. Chase and W. S. S. Jee. Counts of Labelled Mitoses in the Orthodontically-Stimulated Periodontal Ligament in the Rat. Arch.Oral Biol. 19:665-670, 1974.

14. Roberts, W.E. and W.B. Cox. Morphometric Quantitation of Nuclear Volume Changes During Osteoblast Histogenesis. In: Bone Histomorphometry, edited by Meunier, P.J. Paris: Armour Montagu, 1977, p. 267-273.

15. Roberts, W.E., P. J. Fielder, L. M. L. Rosenoer, A. C. Maese, M. R. Gonsalves and E. R. Morey. Nuclear Morphometric Analysis of Osteoblast Precursor Cells in Periodontal Ligament, SL-3 rats. Am.J.Physiol. 252:R247-R251, 1987.

16. Roberts, W.E. and E. R. Morey. Proliferation and Differentiation Sequence of Osteoblast Histogenesis Under Physiological Conditions in Rat Periodontal Ligament. Am.J.Anat. 174:105-118, 1985.

17. Roberts, W.E., P. G. Mozsary and E. Klingler. Nuclear size as a Cell-Kinetic Marker for Osteoblast Differentiation. Am.J.Anat. 165:373-384, 1982.

18. Roberts, W.E., P. G. Mozsary and E. R. Morey. Suppression of Osteoblast Differentiation During Weightlessness. Physiologist 24(6) Suppl.:S75-S76, 1981.

19. Simmons, D.J., M. D. Grynpas and G. D. Rosenberg. Maturation of Bone and Dentin Matrices in Rats Flown on the Soviet Biosatellite Cosmos 1887. *FASEB J.* 4:29-33, 1990.

20. Simmons, D.J., J. E. Russell, F. Winter, et al. Effect of Spaceflight on the Non-weight Bearing Bones of Rat Skeleton. Am.J.Physiol. 244:319-326, 1983.

21. Sokal, R.R. and F. J. Rohlf. Biometry, New York: W.H. Freeman and Company, 1981. Ed. 2nd pp. 242-262.

22. Vico, L., D. Chappard, S. Palle, A. V. Bakulin, V. E. Novikov and C. Alexandre. Trabecular Bone Remodeling after Seven Days of Weightlessness Exposure (BIOCOSMOS 1667). Am.J.Physiol. 255:R243-R247, 1988.

23. Wronski, T.J. and E. R. Morey. Effect of Spaceflight on Periosteal Bone Formation in Rats. Am.J.Physiol. 244:R305-R309, 1983.

24. Wronski, T.J., E. R. Morey-Holton, S. B. Doty, A. C. Maese and C. C. Walsh. Histomorphometric Analysis of Rat Skeleton Following Spaceflight. Am.J.Physiol. 252:R252-R255, 1987.

TABLE 1

MID-ROOT PERIODONTAL LIGAMENT WIDTH

Group	PDL Width	n
Flight	146.2 ± 15.1	5
Controls		
Synchronous	139.6 ± 7.9	5
Vivarium	163.0 ± 17.9	4
Basal	149.0 ± 11.9	5

See METHODS for details. Values are expressed as mean ± SEM in μm. n represents the number of animals studied in each group.

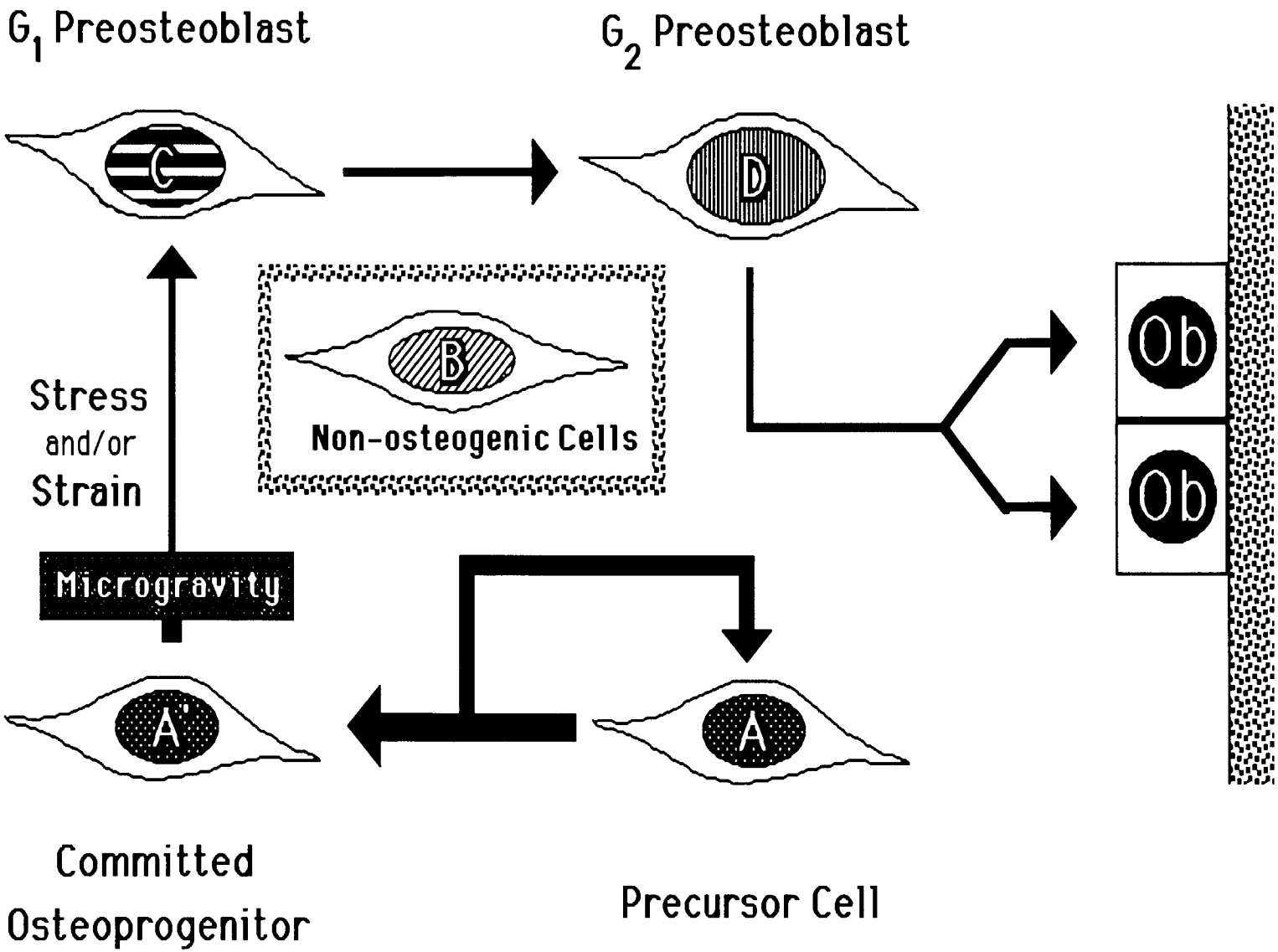

Figure 1. Schematic of cell kinetic model describing the proliferation and differentiation of cells associated with osteoblast histogenesis. Cellular compartments are classified as A+A', B, C or D, according to the following nuclear volume categories: 40–79, 80–119, 120–169, and >170 μm^3, respectively. Microgravity blocks the induction of osteogenesis (i.e., A'→C shift).

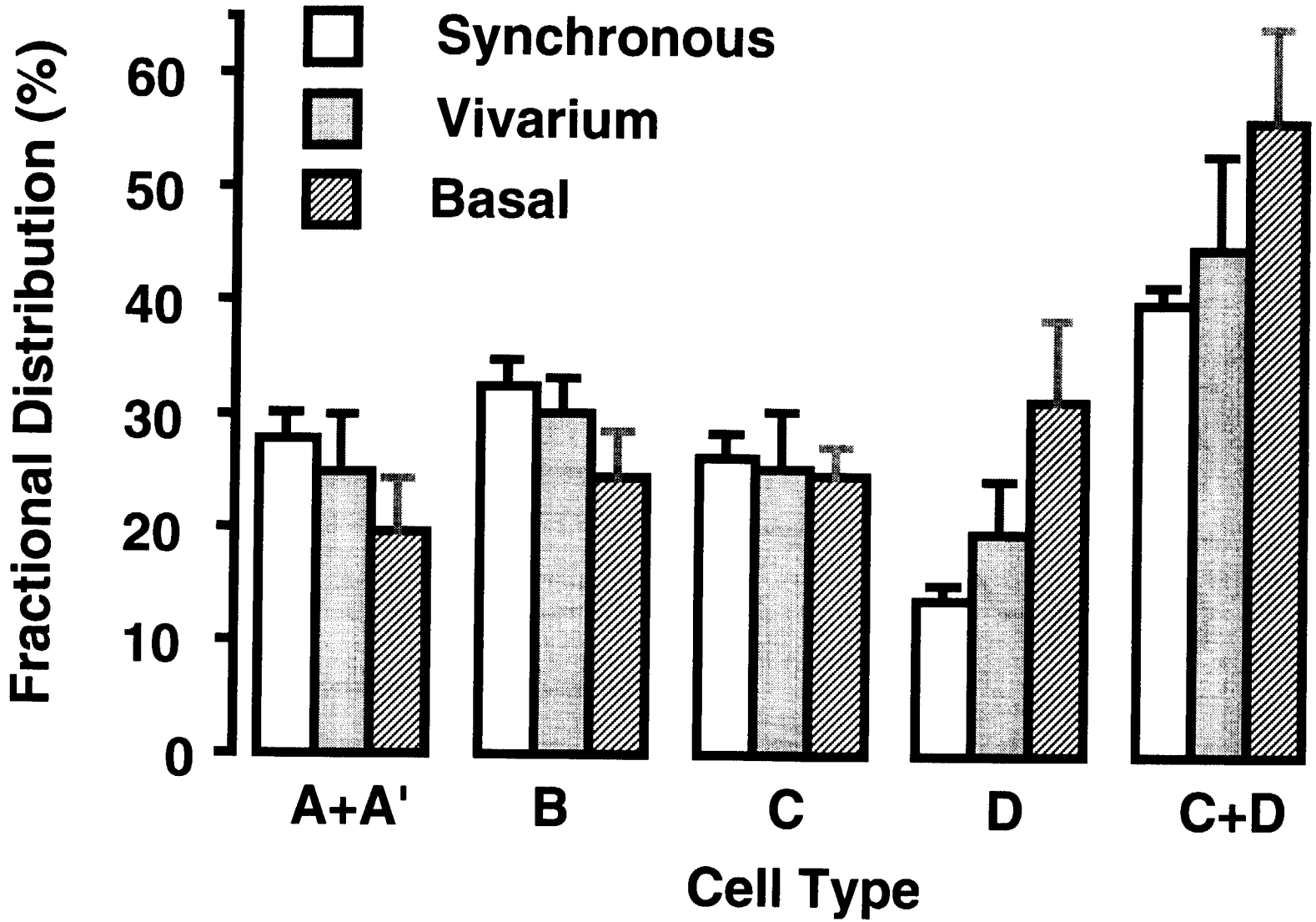

Figure 2. Comparison of the kinetic cell compartments in the control groups. Data is expressed as mean ± SEM with n=5 animals in synchronous and basal groups and n=4 animals in the vivarium group.

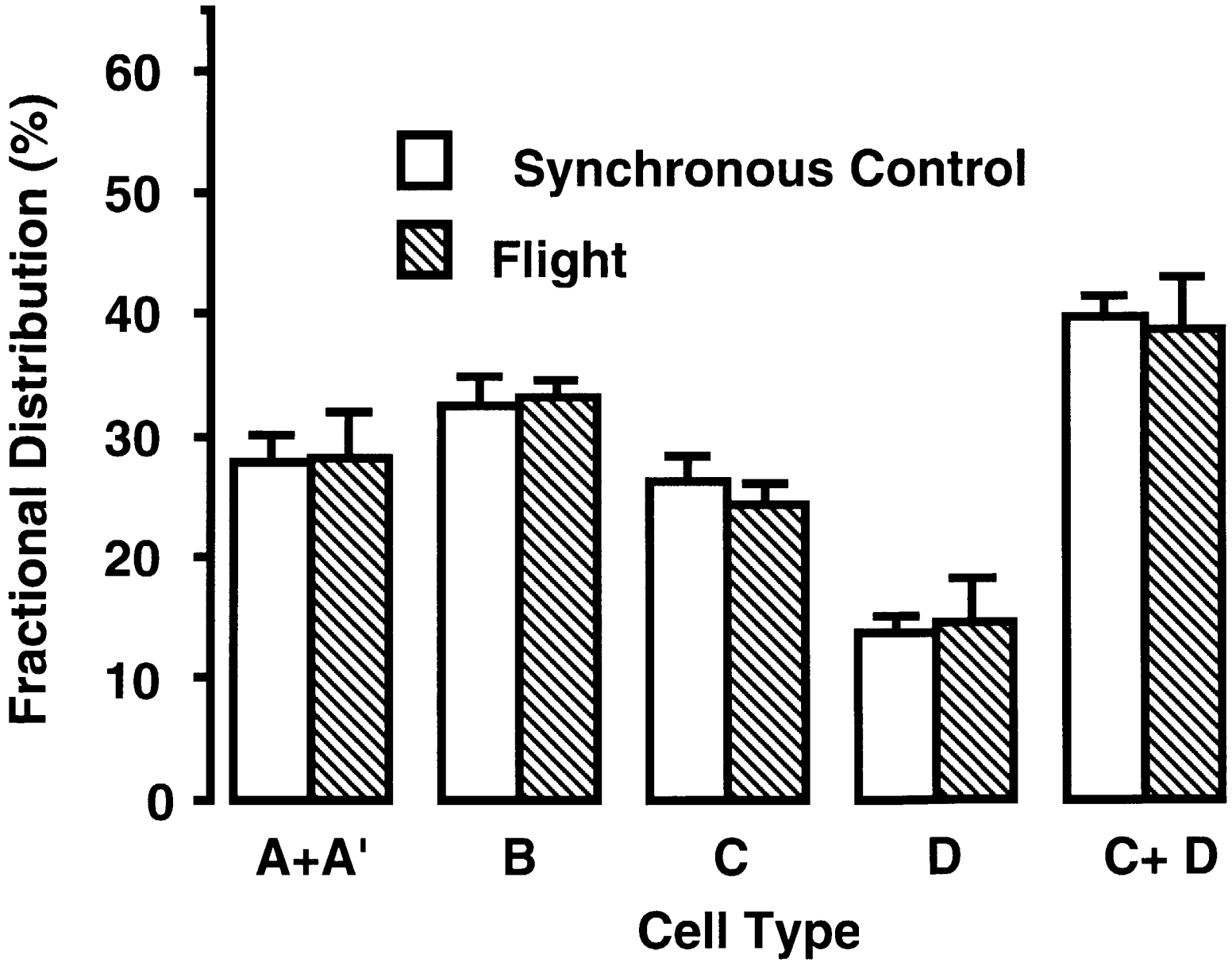

Figure 3. Comparison of kinetic cell compartments in synchronous control and flight groups. Data is expressed as mean ± SEM with n=5 animals/group.

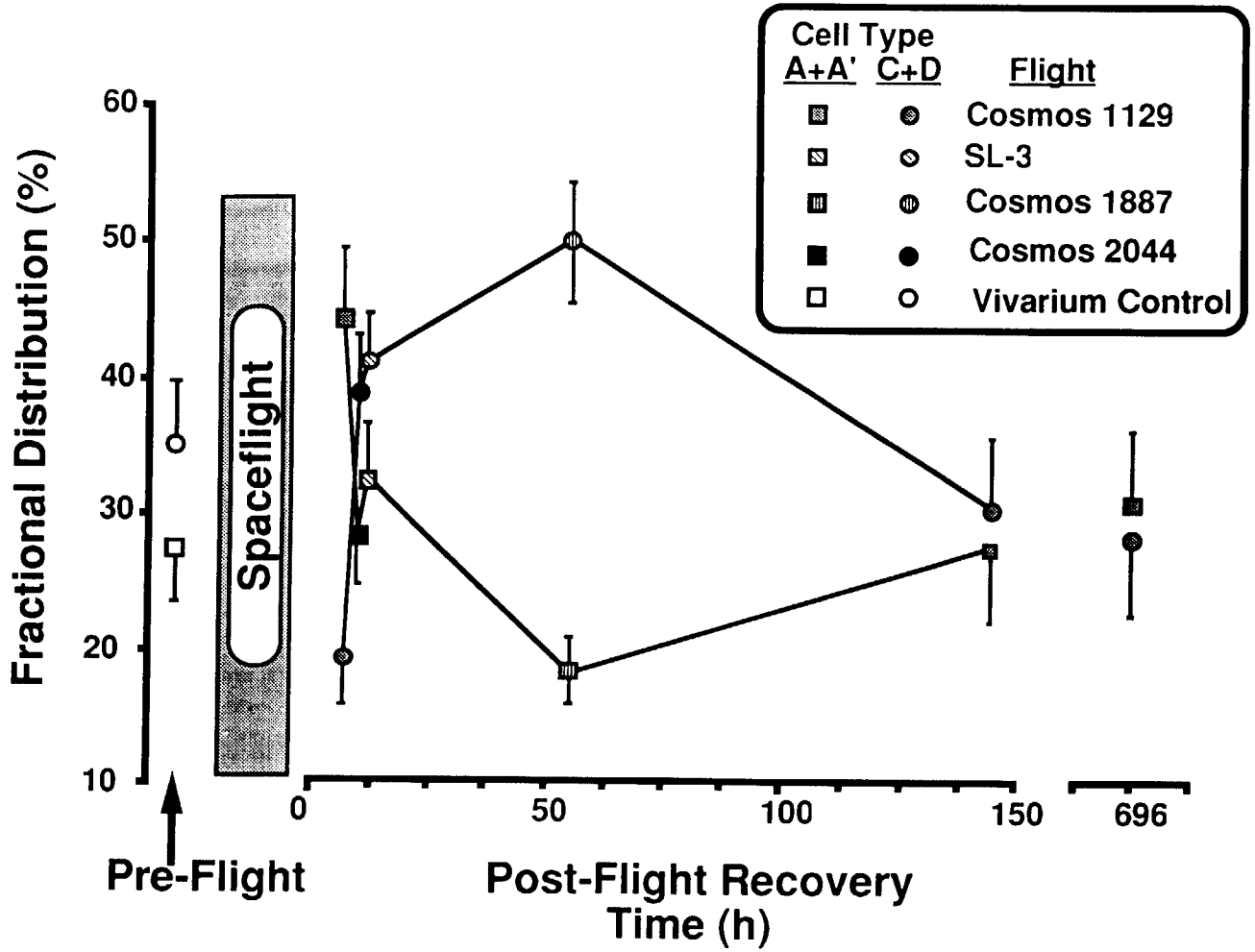

Figure 4. A comparison of all recent spaceflight experiments showing the rapid time-dependent recovery of osteoblast histogenesis. Data are expressed as mean ± SEM for n=4-5 animals per data point.

Experiment	*Flight Duration (days)*
Cosmos 1129	*18.5*
SL-3	*7.0*
Cosmos 1887	*12.5*
Cosmos 2044	*13.8*

EXPERIMENT K-7-03

PART IV: IMMUNOHISTOCHEMISTRY OF COLLAGENASE IN CALVARIAE OF RATS FLOWN ON COSMOS-2044

N.C. Partridge, T.C. Lorenz, E.R. Morey-Holton, G. Durnova, L.A. Gershan, J.J.Jeffrey, A.S.Kaplansky, and C.O. Quinn.

SUMMARY

Investigation of the amount and distribution of the metalloproteinase, collagenase, was determined in calvariae of rats flown on Cosmos 2044 and respective ground controls. The enzyme was detected in frozen sections by an immunohistochemical technique and cellular architecture was assessed by counterstaining with Mayer's hematoxylin. No difference was observed in the quantity or distribution of the enzyme which was seen to be associated with cells lining the marrow spaces, osteocytic canaliculi and deposited in the matrix. This concurred with previous observations that collagenase is a product of osteoblastic cells. Morphologically, there appeared to be a difference in the calvariae of flight animals and tail-suspended rats; in the first group the matrix seemed wider than in controls; in the second group, the marrow space appeared enlarged. It is possible that the shift in blood flow and the change in loading affects the morphology of the calvaria.

INTRODUCTION

A major effect of microgravity is the loss of skeletal mass with attendant hypercalciuria. This effect, observed in both man and experimental animals, results from disruption in the steady state balance between bone formation by osteoblasts and bone resorption by osteoclasts. In man, the decline in skeletal mass under weightlessness correlates with a decrease in bone formation as well as an increase in bone resorption (Whedon, 1982). In growing rats, bone formation is clearly reduced but resorption seems little affected (Morey and Baylink, 1978). Similarly, in the tail-suspended rat model, there is a decrease in the number of osteoblasts and no change in osteoclasts (Halloran et al., 1986) suggesting the defect is mediated through the osteoblast. The osteoblast has been shown to be the target cell for most resorption-promoting agents (Partridge et al., 1980, 1981a,b; Ng et al., 1983; Beresford et al., 1984) and appears to be the vehicle for controlling recruitment and activation of osteoclasts (Rodan and Martin, 1981; Kahn and Partridge, 1987; McSheehy and Chambers, 1986; Takahashi et al., 1988). In addition, this cell has been shown to be directly responsive to mechanical stress (Hasegawa et al., 1985) and to possess stretch receptors (? putative mechanostat; Duncan and Misler, 1989). Thus, the osteoblast seems likely to serve as the gravity-responsive cell whose functions are central to the loss of bone seen in weightlessness. One of the functions of the osteoblast is production of neutral proteases such as collagenase (Heath et al., 1984; Partridge et al., 1987), the only enzyme presently known to degrade fibrillar Type I collagen under physiological conditions of pH (i.e., pH 7.3/7.4).

The present studies were undertaken to investigate whether space flight would change the amount of collagenase detectable in the calvaria of adult rats. In this non-weightbearing bone, collagenase has usually been shown to be associated with bone-lining cells on the endocranial surfaces, surfaces surrounding the marrow cavity, cement lines and osteocytic lacunae (Gershan et al., manuscript in preparation; Bolander et al., manuscript in preparation). We postulated that the change in blood flow and load bearing connected with

the weightlessness of space would change the amount and distribution of collagenase in calvariae. Thus, immunohistochemical staining for collagenase was performed on sections of each calvaria in the five different groups as well as assessment of morphological differences between the test groups.

MATERIALS AND METHODS

Five groups of five specific pathogen-free male Czechoslovakian Wistar rats ranging in age from 107-131 days were used to determine any changes in collagenase staining during weightlessness. The five different groups of rats were the flight animals themselves (14 days flight, F group) and the following ground controls, a basal group (109 days old, B group) killed 2 days after the beginning of the flight, a tail-suspended group (T group) to mimic some of the effects of weightlessness, a synchronous group (S group) which were held under the same restricted conditions as the rats in the flight group and exposed to the simulated environmental parameters of the flight, and a vivarium group (V group) which were also housed in similar cages to the synchronous and flight animals and killed after the end of the flight. The flight, animal conditions and tissue harvest details are described in Grindeland et al. (1991). Calvarial tissue from rats numbered 6-10 were used in our project and were collected from the flight animals (F group) 8-11 h after landing.

Following decapitation, the calvariae were dissected out and a square of calvarial tissue approximately 0.5 cm x 0.5 cm near the suture lines and including some parietal bone was fixed in 4% paraformaldehyde in phosphate-buffered saline (PBS), pH 7.4, at 4°C until the tissues were shipped to Moscow. Once there, the tissues were then demineralized, at 4°C, in 300 mM Na^2EDTA, 100 mM Tris-HCl, pH 7.4 with 3 changes over 4 days. The quarter pieces of calvariae were then embedded in O.C.T. embedding compound (Miles Scientific, Naperville IL) and frozen in Freon-12 cooled in liquid nitrogen for frozen sections. The blocks were stored frozen at
-70°C and shipped to St. Louis on dry ice. Calvariae from 14 day old rats, collected by our standard techniques (notable difference from Cosmos rats, fixation for 30 min) were used as a positive control since animals of this age demonstrate the greatest abundance of immunohistochemical staining for collagenase.

After arrival in St. Louis, 10 μm frozen sections were cut from each block. At first, sections were placed on slides coated with 0.15 M poly-L-lysine and cut from the number 6 animals from the basal, flight and vivarium groups. Sections from these groups were stained either with hematoxylin and eosin or using immunohistochemistry for collagenase. The morphology of the vivarium sections was extremely good and outstanding for frozen sections of demineralized bone. We had some problems with the tissue remaining on the slides with the other groups and had to try alternative techniques to attach the sections. We tried using Chrome-Gel coated slides and Superfrost (Fisher Scientific) polarized slides to retain the sections through the immunohistochemistry procedure. However, neither of these slide preparations were successful in keeping the sections on the slides during immunohistochemical staining. Finally, it was found that Superfrost slides treated with 0.5% gelatin were the most successful slide preparation for preserving sections intact and all sections were placed on this type of slide. Following sectioning, immunohistochemical staining was performed.

For staining, frozen sections of bone from each group as well as from 14 day old rat calvariae were warmed for 2 h at 37°C and then washed with PBS twice for 5 min with gentle mixing. Following this, the sections were fixed in 4% paraformaldehyde in PBS, pH 7.4 for 15 min. The fixative was removed by rinsing in PBS/BSA and the sections were then placed in methanol containing 0.3% hydrogen peroxide for 5 min. This was done to

permeabilize the tissue and destroy any endogenous peroxidase which can interfere with the avidin-biotin-peroxidase complex technique. The methanol/peroxide was removed by washing in PBS/BSA for 10 min twice and the sections were then incubated for 30 min in blocking serum (normal goat serum diluted 1/75 in PBS/BSA). The latter was removed and primary antibody or normal rabbit serum at a dilution of 1/200 in PBS/BSA added. The primary antiserum used was a monospecific polyclonal rabbit anti-rat uterine collagenase (Blair et al., 1986). After incubating for 1 h, the slides were washed overnight in PBS/BSA at 4°C with gentle mixing. The following day, the sections were treated for 30 min with diluted biotinylated second antibody (goat anti-rabbit IgG diluted 1/220 in PBS/BSA according to the manufacturer's recommendations; Vector Laboratories, Burlingame, CA), washed in PBS/BSA for 10 min and subsequently incubated for 40 min with avidin/horseradish peroxidase reagent from the Vector A-B-C kit. The slides were then rewashed for 10 min with PBS/BSA, and incubated with the peroxidase substrate, 275 mM 3-amino-9-ethylcarbazole plus 0.01% hydrogen peroxide for 3-4 min. Some of the sections were counter stained with Mayer's hematoxylin for 1 min. At the end of this time, the slides were mounted in glycerol/PBS (1:1).

RESULTS

Frozen blocks from all five animals in each of the five test groups were sectioned and stained immunohistochemically for the presence of collagenase. The sections were compared to one another and to our positive controls, frozen sections from 14 day-old rats prepared under our standard laboratory conditions. Collagenase staining was detected in all the animals of all five treatment groups. No difference in collagenase staining was observed in any of the groups of test animals. Enzyme was observed associated with cells lining the marrow cavities, embedded in the matrix and appeared to be present in low amounts in the canaliculi of osteocytes. However, the color of the reaction product was slightly different (yellowish orange) from that of our laboratory controls (red) indicating some difference in the preparation or pH of the Cosmos tissues. As well, there was considerably less reaction product in the Cosmos materials compared with the sections from the 14 day-old animals; this was likely a consequence of the older age of the mission animals. We have previously documented the decrease in collagenase with age (Gershan et al., manuscript in preparation).

Morphologically, only two observations were conclusively noted. First, the cranium of the rats in the flight group appeared larger than the cranium of the other test groups. Secondly, the marrow cavity of the tail-suspended rats appeared larger than the marrow cavity of all the other groups. Judging morphological differences between the test groups was difficult since the tissues did not all appear to have been collected from identical sites of the skull. In fact, several of the groups contained substantial amounts of muscle attached to bone which suggested that the skeletal material was obtained close to the neck musculature.

DISCUSSION

No differences were observed in the amount or distribution of collagenase staining in any of the treatment groups of Cosmos rats. This could be due to the fact that these animals were 30 days older than those used for Cosmos 1887 and perhaps less responsive to microgravity. Alternatively, the recovery time may have been too great (8-11 h) and any differences in the flight animals negated by this length of time. We know from work *in vitro*, both with cells and calvarial organ cultures that collagenase production can change dramatically within 8 -12 h of a stimulus (Partridge et al., 1987; Strege et al., 1990; Gershan et al., in preparation). On the other hand, the observations may be a true reflection of the situation and indicate that simulated weightlessness and microgravity have no effect on collagenase production in calvariae. Instead, it may be more worthwhile to examine a load-bearing bone such as the tibia or femur where collagenase has been observed in hypertrophic chondrocytes of the

growth plate (Blair et al., 1989). Nevertheless, the problems of field collection of the tissues and the long period of fixation appears to have affected the quality of the frozen materials making them brittle and difficult to adhere to slides. This could also have affected the antigenicity of collagenase. Alternative techniques of fixation and de-mineralization should be assessed if this study is to be repeated.

There do appear to be morphological differences in the calvariae of the rats exposed to simulated weightlessness (i.e., tail-suspended rats) and microgravity (i.e., flight rats). In both cases, the sections of bone seem thicker, in the first group because of an enhanced marrow cavity and in the second by an increase in the amount of matrix. This was noted in most of the five animals of the two groups. However, we cannot conclusively rule out the possibility that this appearance is due to the bone being selected from a different site compared to the other groups or the sections not being in the exact same orientation. If there is an increase in the amount of matrix in the calvariae, this would correlate with the shift in blood volume towards the head encountered in the weightless environment (Pace, 1977).

REFERENCES

1. Beresford, J.N., J.A.Gallagher, , M. Gowen, M. Couch, J. Poser, D.D. Wood and R.G.G Russell . Biochim. Biophys. Acta 801, 58-65, 1984.

2. Blair, H.C., D.D. Dean, D.S. Howell, S.L. Teitelbaum and J.J. Jeffrey. Connective Tiss. Res. 23, 65-75,1989.

3. Blair, H.C., S.L. Teitelbaum, L.S. Ehlich and J.J. Jeffrey. J. Cell. Physiol. 129, 111-123, 1986.

4. Duncan, R. and S. Misler. FEB S Lett. 251, 17-21, 1989.

5. Grindeland, R.E., M.F. Vasques, R.W. Ballard and J.P. Connolly . J. Appl. Physio., in press, 1991.

6. Halloran, B.P., D.D. Bikle, T.J. Wronski, R.K. Globus, M.J. Levens and E. Morey-Holton . Endocrinology 118, 948-954, 1986.

7. Hasegawa, S., S. Sato, S. Saito, Y. Suzuki and D.M. Brunette. Calcif. Tissue Int. 37, 431-436, 1985.

8. Heath, J.K., S.J. Atkinson, M.C. Meikle and J.J. Reynolds. Biochim. Biophys. Acta 802, 151-154, 1984.

9. Kahn, A.J. and N.C. Partridge. Am. J. Otolaryngology 8, 258-264, 1987.

10. McSheehy, P.M.J. and T.J. Chambers. Endocrinology 119, 1654-1659, 1986.

11. Morey, E.R. and D.J. Baylink. Science 201, 1138-1141, 1978.

12. Ng, K.W., N.C. Partridge, M. Niall, and T.J. Martin. Calcif. Tissue Int. 35, 298-303,1983.

13. Pace, N.. N. Engl. J. Med. 297, 32-37, 1977.

14. Partridge, N.C., R.J. Frampton, J.A. Eisman, V.P. Michelangeli, E. Elms, T.R. Bradley and T.J. Martin. FEBS Lett. 115, 139-142, 1980.

15. Partridge, N.C., D. Alcorn, V.P. Michelangeli, B.E. Kemp, G.B. Ryan, and T.J. Martin. Endocrinology 108, 213-219, 1981a.

16. Partridge, N.C., B.E. Kemp, M.C. Veroni, and T.J. Martin . Endocrinology 108, 220-225, 1981b.

17. Partridge, N.C., J.J. Jeffrey, L.S. Ehlich, S.L. Teitelbaum, C. Fliszar, H.G. Welgus and A.J. Kahn. Endocrinology 120, 1956-1962., 1987

18. Rodan, G.A. and T.J. Martin. Calcif. Tissue Int. 33, 349-351, 1981.

19. Strege, D.W., A.J. Kahn, J.J.Jeffrey and N.C. Partridge. J. Bone Min. Res., 5, 963-971, 1990.

20. Takahashi, N., T. Akatsu, N. Udagawa, T. Sasaki, A. Yamaguchi, J.M. Moseley, T.J. Martin and T. Suda . Endocrinology 123, 2600-2602, 1988.

21. Whedon, G.D. The Physiologist 25, Suppl., S41-S44, 1982.

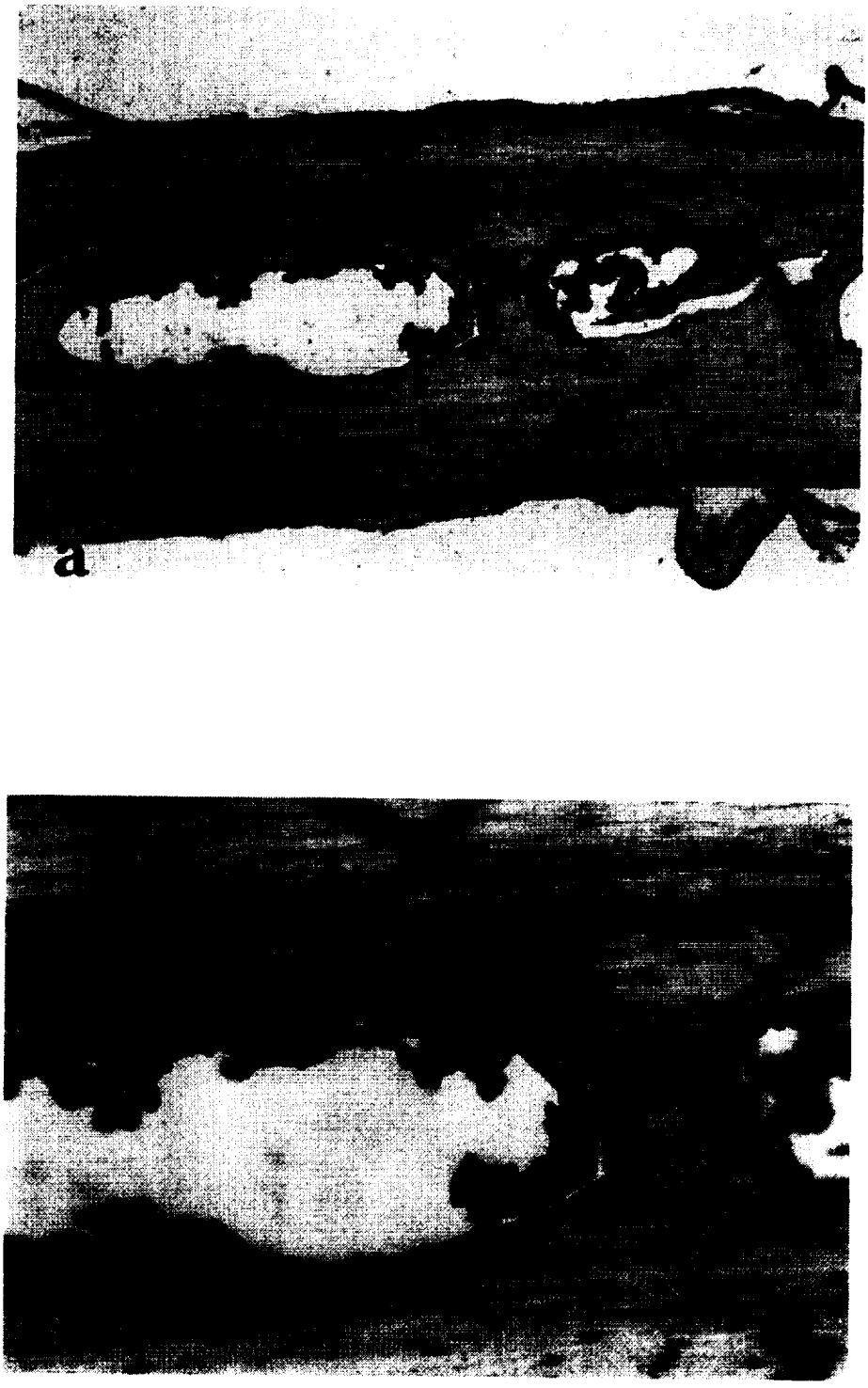

Figure 1. Section of calvaria from basal animal 9. Frozen sections were cut and the tissue stained with Mayer's hematoxylin as described. a). × 100. b). same section and area × 200.

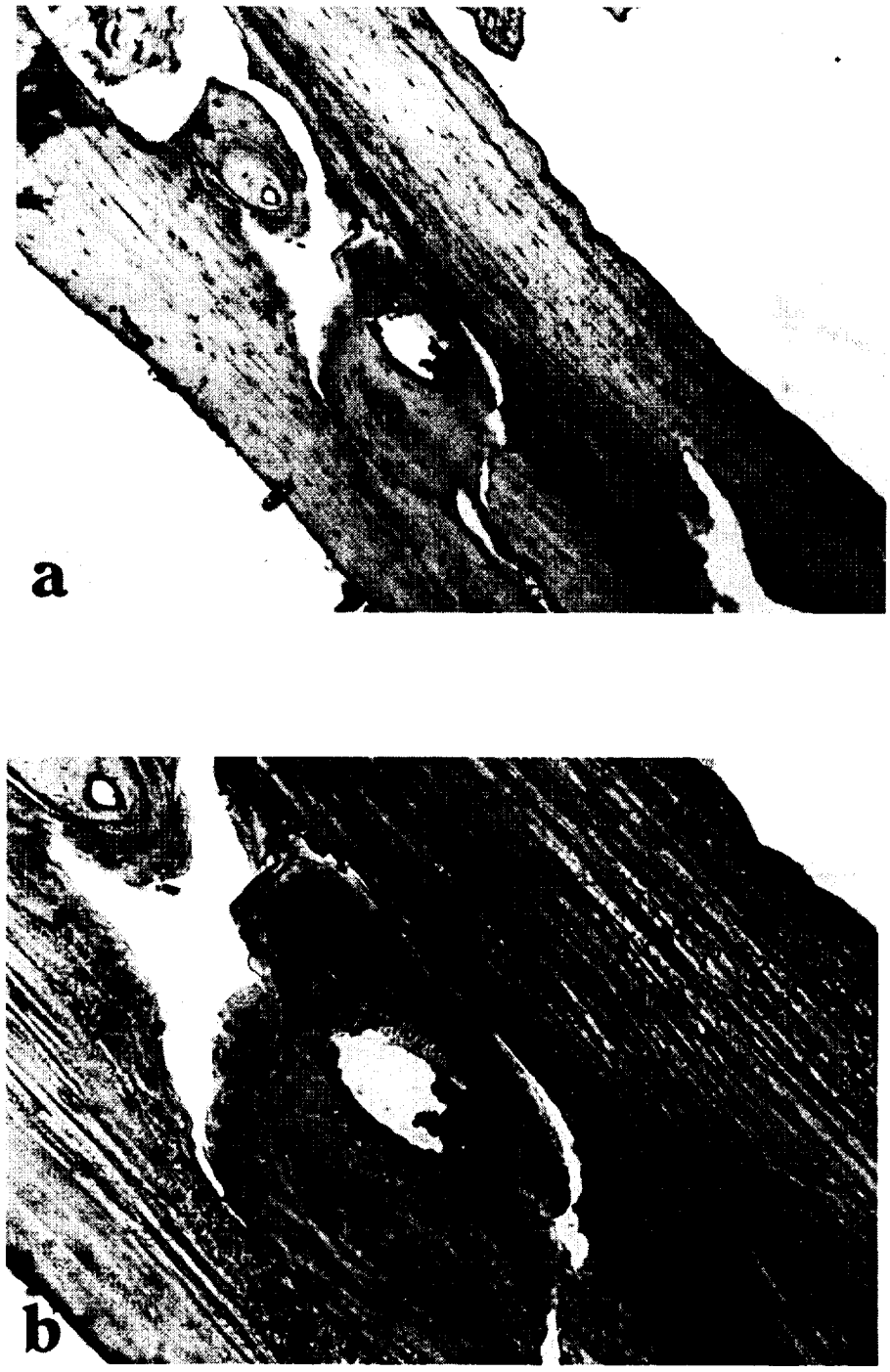

Figure 2. Section of calvaria from flight animal 9 stained as for figure 1. a). × 100. b). × 200.

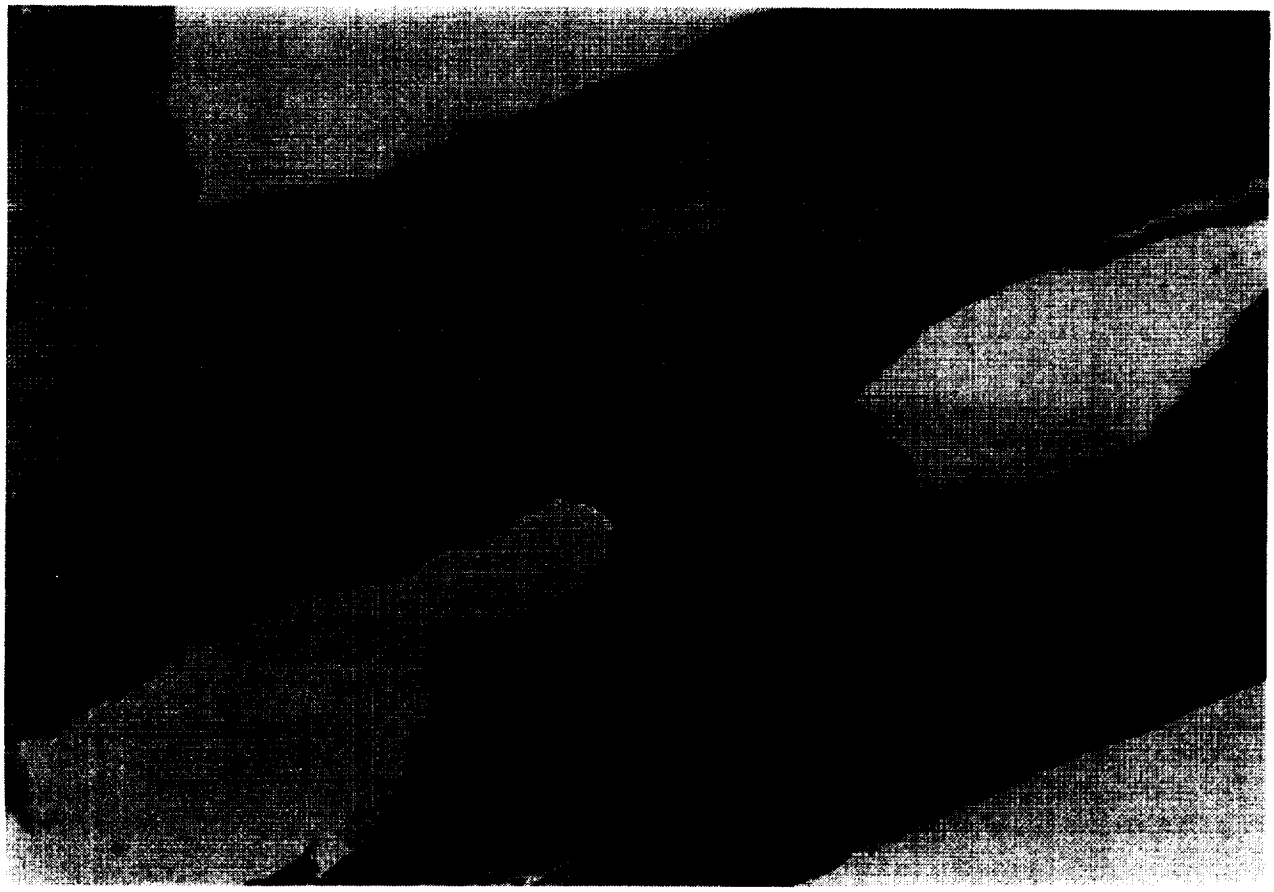

Figure 3. Section of calvaria from synchronous animal 9 stained as for figure 1 × 100.

Figure 4. Section of calvaria from vivarium animal 8 stained as for figure 1 × 100.

Figure 5. Section of calvaria from tail-suspended animal 9 stained as for figure 1. a). × 100. b). × 200.

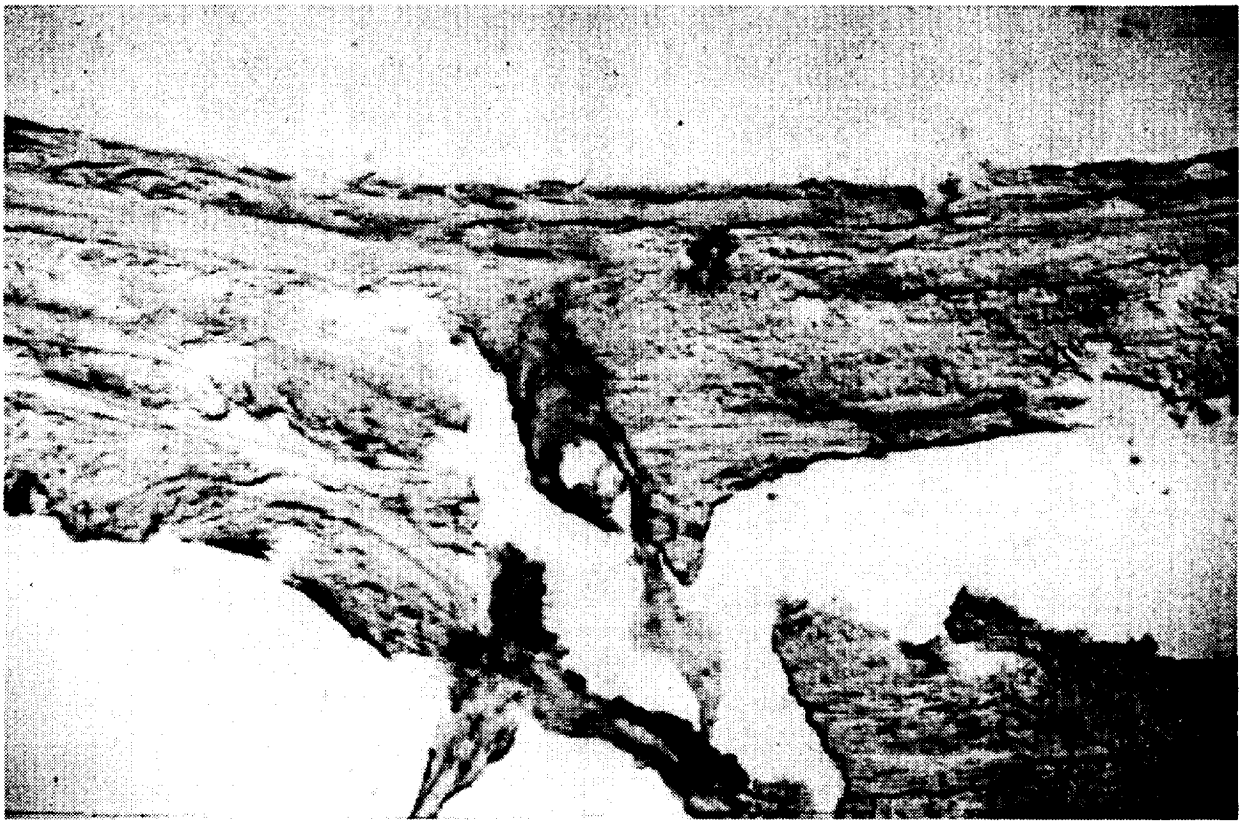

Figure 6. Section of calvaria from tail-suspended animal 10 showing immunohistochemical staining for collagenase. Frozen sections were cut and the tissue processed for collagenase immunostaining then counterstained with Mayer's hematoxylin as described. The red precipitate indicates the localization of collagenase × 100.

EXPERIMENT K-07-04

MINERAL DISTRIBUTION AND BALANCE IN RATS DURING SPACEFLIGHT

Principal Investigator

C. E. Cann
Department of Radiology
University of California
San Francisco, CA 94143

Co-Investigators:

P. A. Patterson-Buckendahl
Department of Radiology
University of California
San Francisco, CA 94143

G. Durnova
A. Kaplansky
Institute for Biomedical Problems
Moscow, Russia

K-07-04

MINERAL DISTRIBUTION AND BALANCE IN RATS DURING SPACEFLIGHT

INTRODUCTION

Previous studies of mineral distribution and homeostasis have shown significant effects of spaceflight on the mineral composition of bones and the handling of major and trace minerals by the intestine. On Cosmos 1129, 2-day timed collections from individual rats showed a significant increase in fecal ash content starting early in flight, when compared to synchronous control rats, predominantly due to progressive increases of excreted sodium and potassium and to a lesser extent calcium (1). Zinc excretion also rose during flight but was back to baseline by the end of the flight. The lack of timed intake data during this flight precluded any calculation of daily balances, but suggested that the alterations were significant enough that they might be evidenced in the bones given a long enough flight. For Cosmos 1887, both excreta and vertebrae were received for analysis of major and trace minerals, as well as other components. However, where bones for individual animals could be analyzed separately, the excreta were obtained as single pools from all animals in the cage and for the whole flight period. The results from Cosmos 1887 (2) confirmed the Cosmos 1129 findings. In addition, analyses of the vertebrae suggested that the bones in the flight rats were more highly mineralized, consistent with data from other investigators obtained from the long bones such as the humerus.

This experiment on Cosmos 2044 was designed primarily to add supplementary and supporting data to that obtained on Cosmos 1887 under similar conditions. This was necessary especially for the excreta analyses where only "single" measurements were made on the pooled samples. The data in this report are given as the new data obtained from this set of specimens, and then as compared to results from Cosmos 1887.

METHODS

Plasma

Plasma osteocalcin was measured using a rat-specific radioimmunoassay for comparison to bone osteocalcin results.

Vertebrae

Vertebral specimens (fifth lumbar vertebral bodies) were received frozen, wrapped in cloth. Five vertebral bodies from each group (basal, vivarium, synchronous controls and flight rats) were included. In addition, a group of bones from tail-suspended rats was received for comparison. All manipulations of the bones were done using titanium tools and non-metallic containers (crucibles, etc) and ultrapure water and other reagents to minimize the possibility of trace metal contamination. In contrast to the samples from Cosmos 1887, only the isolated vertebral bodies were received; therefore the regional analysis of the vertebral bodies vs. the posterior elements could not be done. For analysis purposes, each vertebral body was split into two segments. Samples were not weighed "wet" because of variable hydration status of the cloth (some samples were partially dehydrated). The separate segments were lyophilized and weighed, then analyzed as separate duplicate samples. Analyses were done for calcium (atomic absorption spectrophotometry) and osteocalcin (rat-specific radioimmunoassay). The small size of the samples and the analytical procedures used did not allow for the analysis of magnesium and zinc as had been planned.

Excreta

A single sample of pooled excreta, representing one half of the total pool, was received frozen in plastic bags for each of the four flight groups and the tail-suspended group as defined above. The pools were significantly contaminated with residual food, rat hair, wood shavings (for the ground control groups) and some small metallic shavings. The pool for the tail-suspended group was heavily contaminated with food affixed to the excreta, such that a separation of the excreta could not be done without substantial residual contamination, even though this was attempted. Therefore, these analyses are omitted from this report.

Each of the other samples was carefully cleaned by hand, using titanium forceps to pick out and clean the fecal specimens from the other material. The cleaned samples were then mixed well and weighed, and two random samples (approximately 5 grams each) were taken for analysis. No attempt was made to determine water content or to prevent drying during the cleaning because the flight and synchronous samples were already partially dried by the airflow in the cages. The aliquots were weighed, dried, and then reweighed to determine an average wet:dry weight ratio for the whole sample. Known aliquots of the samples were homogenized in ultrapure water and weighed into nitric acid-cleaned quartz crucibles for ashing at 500°C for 48 hours. Following ashing, the residue for each sample was weighed and dissolved in 2 ml of 1 N ultrapure nitric acid for elemental analysis. Calcium, magnesium, zinc, manganese, and copper were analyzed by atomic absorption spectrophotometry, and phosphorus by the ammonium molybdate procedure. All analyses were done in duplicate and the results averaged. As a further check on the consistency of results, a sample from Cosmos 1887 (basal) was included in the analysis and the results compared to those obtained in the prior analysis.

Diet

Random aliquots of the diet were received along with the excreta samples for the flight, synchronous, and vivarium (including basal and suspended) groups. Following drying, the samples were ashed and analyzed according to the procedures given above for the excreta specimens.

Statistical Analysis

All results where multiple specimens were obtained (plasma, bone) were averaged, and are expressed as means and standard deviations to show the variability. Standard errors can be calculated from SD using N=5 for each group. Comparisons between groups were done using two-sided t tests, with a difference considered significant if the p value was less than 0.05. Results from the duplicate analyses of excreta samples were averaged, and no statistical analyses was done for these results.

RESULTS

Plasma osteocalcin values (mean ± SD) for the flight, synchronous, vivarium, basal and suspended groups were 40.3 ± 11.1, 76.6 ± 9.6, 116.5 ± 11.6, 175.9 ± 36.2, and 78.7 ± 7.6 ng/ml, respectively. The values for the flight, synchronous and suspended were all significantly lower than for vivarium controls. Basal values were higher, as expected, because of the younger age of the basal controls. Values for flight animals were significantly lower than for the synchronous and vivarium controls.

Table 1 gives the results of the analyses of the vertebral bodies. The bones from the flight animals were smaller than those of both the vivarium and synchronous controls, but only significantly so for the vivarium controls because of the variance in the synchronous rats. Bones from suspended rats were smaller than vivarium and synchronous controls, and were not different from flight rats. Some of the variance in the mass measurements may be attributed to the fact that the whole vertebrae were not received, and thus inconsistent separation of the posterior elements from the vertebral bodies may have occurred. There were no significant differences in calcium or osteocalcin concentrations in the bones of flight vs synchronous rats; again, the wide variance just prevented significant results. Calcium in the bones of vivarium rats was higher than flight, synchronous, and suspended groups.

Data for food consumption and blood chemistries pertinent to this report were received from the project office. Food consumption was given as 45 g/day for the flight rats and 53.9 g/day for the synchronous controls. No data were given for the other control groups, so the assumption has been made for this report that they were offered the same 55 g/day/rat and ate the food completely.

The results of the analysis of the fecal specimens is given in Table 2, with the Cosmos 1887 results given for comparison in Table 3. All analyses are given on a dry weight basis after freeze drying. There were no major consistent differences between flight and control groups, except that the concentrations of calcium, phosphorus, and magnesium (major elemental constituents) were lower in the basal group, and this is also reflected in the lower ash content. There were also some inconsistent differences in trace element

concentrations, but these results also can be attributed to significant variation among the diets fed the different groups. Food analyses are given in Table 4 on a dry weight basis following freeze drying, with the expected concentrations also given based on the diet composition data provided to the project by the Russians. There are some significant discrepancies in these results, as well as differences from the data obtained for Cosmos 1887 (Table 5). In particular, the calcium level was significantly higher for Cosmos 2044 than for 1887, and the magnesium and zinc levels were much lower. These dietary differences are reflected in the excreta analyses to some extent, preventing pooling of the data as was planned.

Table 6 gives the calculated total intake and output for each group based on the measurements and the reported intake data for Cosmos 2044, and Table 7 gives similar data for Cosmos 1887 for comparison.

Table 1. Analyses of Vertebral Bodies
(mean ± SD)

	Mass mg	Calcium mg/gm	Osteocalcin ng/mg
Flight	48.4 ± 4.3	173 ± 11	3.12 ± 0.28
Synchronous	56.7 ± 8.2	162 ± 3	3.22 ± 0.64
Vivarium	58.9 ± 5.0	187 ± 5	3.29 ± 0.23
Basal	53.2 ± 6.0	181 ± 4	3.43 ± 0.26
Suspended	46.0 ± 6.2	175 ± 6	2.90 ± 0.44

DISCUSSION

One objective of the analyses done for this experiment was to try to add to the data set obtained for Cosmos 1887 to obtain a more powerful statistical analysis. In theory, this could have been done because the slight differences in flight length (13 days on 1887 vs 14 days on 2044) and in rat body weight (within 20-30 gms) probably would not cause significant differences. The difference in age might have an effect, but because weights were similar this would be expected to be a minimal effect. Several observations can be made when looking at the overall data sets for Cosmos 1887 and Cosmos 2044. There are no gross differences in the major constituents of the vertebrae or the vertebral bodies among the groups following a 2 week spaceflight. The only difference noted was an increase in osteocalcin in the posterior elements of the vertebrae in flight animals on Cosmos 1887, a finding which could not be verified because only the vertebral bodies were delivered for analysis for K-7-04. For Cosmos 1887 the delivery of intact vertebrae made it possible to do a very careful and reproducible dissection of the vertebral bodies from the posterior elements, substantially reducing the variability in weight of the vertebral bodies, whereas for Cosmos 2044, because only the vertebral bodies were delivered, and the dissection was done in another laboratory under uncontrolled conditions, the variability was much higher. This increased variability did not allow differences between groups to reach statistical significance.

It was expected that the diet of Cosmos 2044 would be the same as that of 1887, so that comparisons could be made for mineral content of bones and excreta and balance measurements of major and trace minerals. This was not the case. Calcium, magnesium, zinc and copper intake levels varied dramatically between the flights, from a factor of 2-5 higher (Ca, Cu) to a factor of 5 lower (Mg, Zn). This variation could have come from either inadequate mixing of the diet before sampling for analysis or from a change in the amounts and composition of the materials used to make up the diet. Prior descriptions of the diet have noted its composition of casein, sugar, yeast, sunflower oil, and salt and vitamin mixtures, but it has not been noted if the casein was acid-washed to remove bound calcium or if the mineral concentrations in the yeast were controlled (yeast can have widely variable trace mineral concentrations). In any case, this variation in dietary composition between the flights precludes pooling the data as was planned.

Even though the data cannot be pooled, there are some conclusions that can be drawn, especially when the data from Cosmos 1129 are also considered. First, in all cases the flight rats produced a larger total dry mass of excreta than controls, as well as an increased total ash (i.e. mineral components). Because all samples were carefully cleaned to exclude dietary particulates and other non-fecal material such as hair,

this finding can be stated conclusively. This appears to be a consistent finding which could be explained if there was a generalized decrease in the efficiency of the intestine in absorbing nutrients, both minerals and organic dietary components. This aspect of metabolism in spaceflight has not been studied systematically, and should be an area of investigation in future flights.

Overall mineral balance in these older animals appeared similar between flight and control groups, with some apparent negative balance for a number of elements. However, because these were not strict metabolic balance studies it is difficult to interpret these findings. It does appear, however, that even in the face of the great increase in fecal output the flight animals maintained a reasonable mineral balance relative to controls, indicating that active mineral transport processes in the intestine were not markedly impaired.

SUMMARY

Exposure of older (300 gram) rats to 14 days of microgravity does not alter significantly the composition of the vertebral bodies, either in major minerals or in bone-specific non-collagenous protein. Overall mineral balance appears to be slightly negative in flight, but is not consistently different from controls. However, total excreted mass (dry weight basis) is higher in flight animals, suggesting that the intestine is much less efficient in metabolizing the organic components of the diet, even while maintaining reasonable efficiency for the mineral components. This finding should be investigated to determine if such an inefficiency could lead to malnutrition in spaceflight.

REFERENCES

1. Cann CE, Adachi RR: Bone resorption and mineral excretion in rats during spaceflight. Am. J. Physiol. 244 (Reg. Comp. Integ.): R327-331, 1983.

2. Cann CE, Patterson-Buckendahl PA, Durnova G, Kaplansky A: Trace element balance in rats during spaceflight. Final Report for Experiment K-6-04, Cosmos 1887.

Table 2. Analyses of Cosmos 2044 Pooled Fecal Samples

	ash % dry wt	Ca mg/gm	P mg/gm	Mg mg/gm	Zn µg/gm	Cu µg/gm	Mn µg/gm
Flight	24.9	68.0	39.8	5.62	948	314	186
Synchronous	25.4	73.6	40.1	4.11	975	549	1028
Vivarium	23.5	69.9	38.4	4.06	276	206	1370
Basal	15.9	46.9	21.8	3.32	260	116	198

Table 3. Analyses of Cosmos 1887 Pooled Fecal Samples

	ash % dry wt	Ca mg/gm	P mg/gm	Mg mg/gm	Zn µg/gm	Cu µg/gm	Mn µg/gm
Flight	23.5	61.0	29.0	8.3	248	144	1055
Synchronous	42.2	119.3	42.7	13.4	460	220	1518
Basal	35.3	96.2	37.9	10.1	597	180	1295
Basal-reanal	32.4	91.6	48.3	8.2	603	191	1370

Table 4. Analyses of Cosmos 2044 Food Samples

	ash % dry wt	Ca mg/gm	P mg/gm	Mg mg/gm	Zn µg/gm	Cu µg/gm	Mn µg/gm
Flight	4.57	14.0	5.69	0.13	4.90	35.8	58.6
Synchronous	4.15	12.7	5.68	0.11	5.51	48.1	42.7
Vivarium	3.71	11.0	4.97	0.14	1.44	14.0	104
Expected	n/a	5.27	5.39	0.435	5	5	56.3

Table 5. Analyses of Cosmos 1887 Food Samples

		Ca mg/gm	P mg/gm	Mg mg/gm	Zn µg/gm	Cu µg/gm	Mn µg/gm
Flight		6.95	5.39	0.74	23.2	8.2	65.4
Synchronous		6.75	5.93	0.82	21.8	6.9	62.2
Basal		6.64	4.60	0.70	11.4	8.2	63.2
Expected		5.27	5.39	0.435	5	5	56.3

Table 6. Calculated Total Intake and Output, Cosmos 2044

Intake	mass (gm)	Ca (gm)	P (gm)	Mg (gm)	Zn (mg)	Cu (mg)	Mn (mg)
Flight	1238	17.4	7.04	0.16	6.07	44.3	72
Synchronous	1482	18.8	8.42	0.16	8.16	71.3	63
Vivarium	1540	16.9	7.65	0.22	2.22	21.6	160
Basal	1540	16.9	7.65	0.22	2.22	21.6	160
Output							
Flight	275	18.7	10.9	1.54	260	86	51
Synchronous							
Vivarium	110	7.69	4.22	0.45	30.4	22.7	151
Basal	131	6.13	2.85	0.43	34.0	15.1	26

Table 7. Calculated Total Intake and Output, Cosmos 1887

Intake	mass (dry)	Ca (gm)	P (gm)	Mg (gm)	Zn (mg)	Cu (mg)	Mn (mg)
Flight	1172	8.14	6.32	0.87	27.2	9.6	77
Synchronous	1172	7.91	6.95	0.96	25.6	8.1	73
Basal	1232	8.18	5.67	0.86	14.0	10.1	78
Output							
Flight	164.7	10.05	4.78	1.37	40.9	23.6	174
Synchronous	103.7	12.37	4.43	1.39	47.6	22.9	157
Basal	132.0	12.70	5.00	1.33	78.8	23.8	171

EXPERIMENT K-7-06

MORPHOMETRIC AND EM ANALYSES OF TIBIAL EPIPHYSEAL PLATES FROM COSMOS 2044 RATS

Principal Investigator:

P.J. Duke
University of Texas Health Science Center
Dental Science Institute/Orthodontics
Dental Branch
Houston, Texas

Co-Investigators:

D. Montufar-Solis
University of Texas Health Science Center
Dental Branch/Orthodontics
Houston, Texas

G. Durnova
Institute of Biomedical Problems
Moscow, USSR

EXPERIMENT K-7-06

MORPHOMETRIC AND EM ANALYSES OF TIBIAL EPIPHYSEAL PLATES FROM COSMOS 2044 RATS

P.J. Duke, D. Montufar-Solis, G. Durnova

SUMMARY

Previous studies have shown that spaceflight has significant effects on cartilage differentiation within the growth plate, changes which could lead to the observed decreases in linear bone growth and trabecular bone mass. In this study, growth plates of rats flown aboard the Cosmos 2044 biosatellite mission (14 d flight plus 10 h recovery at 1g) were analyzed by the same histomorphometric and electron microscopic methods used for other flights and compared to basal, vivarium, and synchronous controls, and tail-suspended animals. Flight rats had an increase in height of the proliferative zone (PZ) that was significantly greater than vivarium controls, and a decrease in the hypertrophic/calcification zone (HCZ) that differed significantly from all controls. Cell number in the PZ was significantly greater than synchronous controls, and a decrease in cell number in the HCZ which was significantly different from vivarium controls. Computerized planimetry studies showed no differences between any of the groups with regard to plate area, perimeter, or shape factor. Electron microscopy studies found no difference in collagen fibril length and width, or PGG density, perhaps due to alteration of fibrils with age. The lack of response in tail-suspended animals was also attributed to age.

INTRODUCTION

Rapid longitudinal growth of the appendicular skeleton is made possible by cartilaginous growth plates at the ends of the bones. Decreased longitudinal bone growth in growing rats exposed to microgravity (Wronski, et al., 1981) as well as decreased trabecular bone mass (Jee, et al., 1983) result at least in part from changes in cartilage differentiation occurring within the growth plate as a result of spaceflight (Duke, et al., 1990).

The plate also serves as a record of change, since it takes 2 to 3 days for a cell to move from the reserve (RZ) of the growth plate to the calcified zone (CZ) (Sissons, 1971). This means that even in spaceflights with long recovery times, the growth plate still shows signs of the activity decline experienced in space (Duke, J. and Montufar-Solis, D., 1989).

The following summarizes growth plate studies to date:

Cosmos 1129. The first study of growth plates of spaceflown rats was carried out with plates from growing rats flown aboard Cosmos 1129 (an 18.5d flight, 6h recovery at 1g). In these animals, matrix vesicle production and mineralization in the plate was delayed, and collagen fibrils in trabecular bone did not mature (Matthews, 1981).

Spacelab 3. Growth plates of Spacelab 3 (SL3) rats (7d flight, 12h recovery) were subjected to a more detailed morphometric study, which found cartilage differentiation to be greatly affected. Heights of plates and of zones of flight animals were less than controls, with fewer cells per column (Duke, et al.,1985). The decreased height resulted in a reduced area in flight animals, and the shape factors (4 π area/perimeter^2) were also different. Flight animals had shorter, thinner

collagen fibrils, more proteoglycan granules (PGG) per unit area, and a different pattern of zonal distribution of PGG size (Duke, and Montufar-Solis, 1989) and matrix vesicle number (Duke and Montufar-Solis, unpublished observations).

SL3-simulation. To examine whether the 12h of re-exposure to Earth's gravity after landing might have affected SL3 results, Ames Research Center carried out a simulation using the Morey-Holton tail suspension model (Morey, 1979). Animals were suspended for 7 days and sacrificed either at R+Ø (to simulate shuttle touchdown) or R+12 (time after touchdown when SL3 animals were sacrificed). All suspended animals had decreased plate height and cell number/column. The effect of the 12h of reloading was an additional significant decrease in the R+12 group, resulting in percent changes strikingly similar to those seen in SL3 (Montufar-Solis and Duke, 1988).

Cosmos 1887. Proximal tibial growth plates of rats flown aboard the 12.5d Cosmos 1887 mission (recovery time 53.5h at 1g) were also analyzed using histomorphometric techniques (Duke, et al., 1990). Due to the long antemortem exposure to 1g, not only were effects of spaceflight on cartilage differentiation seen, but also the beginnings of recovery from that exposure. The proliferative zone of flight animals was found to be significantly ($p \leq 0.01$) larger than that of controls, while the reserve and hypertrophic/calcification zones were significantly reduced. Flight animals also had more cells per column in the proliferative zone than did controls and less in the hypertrophic/calcification region. The total number of cells, however, was significantly greater in flight animals, which was interpreted as the beginning of the rebound effect. This effect was seen on previous Cosmos missions where tibial length of rats sacrificed 25d postflight was the same as or greater than controls (Yagodovsky et al., 1976; Holton and Baylink, 1978; Holton, et al., 1978). No difference was found in perimeter or in shape factor, but area was significantly less in flight animals. Electron microscopy showed that collagen fibrils in flight animals were wider than in controls, an effect which is probably part of the rebound phenomenon.

The present study reports results of histomorphometric and electron microscopy studies of growth plates from rats flown aboard the Cosmos Biosatellite 2044 (a 14d mission; 10 h recovery).

METHODS

Details of the flight are found in Grindeland, et al.,(1990). In brief, twenty-five Czech Wistar rats, after acclimation to housing and diet, were assigned to one of five groups: flight, synchronous controls, vivarium controls, basal controls, or tail suspension. Synchronous controls were housed aboard a mockup of the spaceflight capsule and subjected to noise and vibration, and vivarium controls were housed in the vivarium. For tail suspension, rats were suspended by tail harnesses in a manner similar to the Morey-Holton suspension model (Morey, 1979), but did not have full rotational movement. Basal controls were sacrificed at the beginning of the mission to provide baseline data.

Tissue Preparation

Rats in the basal group were decapitated at the beginning of the flight (at 109 days of age); flight rats after 14 days of spaceflight and 10 hours of recovery (123d old); and synchronous, vivarium and tail suspension groups at 127, 129 and 131 days of age respectively.

In order to provide tissue for various studies, the tibia was divided by a series of cuts (Fig.1). First, epiphyses of right tibias were cut from the shaft just above the tibial crest and then split in half in the sagittal plane. One of these halves was fixed in cold (4°C) 2% paraformaldehyde in 0.1 M cacodylate buffer with 0.5% glutaraldehyde, pH 7.4. The tissue was maintained at 4°C for the 48 hour fixation period. Samples were rinsed three times with 0.1 M cacodylate buffer and split in 2 pieces longitudinally. One piece was decalcified in cold (4°C) 10% EDTA in 0.1 M Tris-HCl

buffer, pH 7.4, for 6 wk. After decalcification, epiphyses were split twice more in the sagittal plane; outer portions were embedded in Spurr for electron microscope studies, and the middle portions were embedded in Paraplast for light microscopy. The undecalcified portion was embedded in Spurr for differential staining of calcified cartilage.

The other half was split at the dissection site in the coronal plane, and the two quarters frozen individually in liquid nitrogen. One quarter remained at -70°C with a water crystal to prevent drying during transport and upon arrival at the DSI was returned to liquid nitrogen. The other, after 48 hours, was transferred to cold (-70°C) anhydrous methanol with 2.5% glutaraldehyde plus 0.5% uranyl acetate for 38 days, and then infiltrated with Spurr. These samples will be used for immunohistochemistry and microprobe studies respectively.

Computerized Planimetry

Area, perimeter, and shape factor were determined by computerized planimetry using a Bioquant System IV. Video images of coronal sections (5μ) from the central region of the plate, stained with hematoxylin or toluidine blue, were traced in outline and digitized. Nine serial sections were traced for each animal.

Light Microscopy

The definition of zones for light microscopy was according to Reinholt et al., 1984. The portion of the plate from the upper border to the top of the first cell column was defined as the reserve zone (RZ, see Fig. 2). The portion of the cell column where the ratio of cell width to cell height was greater than 2 was defined as the proliferative zone (PZ), and the remainder of the column, i.e. that portion with a ratio of cell width to height less than 2, was termed the hypertrophic/calcification zone (HCZ). (Because of decalcification, these zones were combined.) An ocular micrometer was used to make height measurements. Three measurements per section (left, middle, right) were made for both height and cell number per column and combined to obtain a mean value per animal. Means of nine sections were averaged to obtain a mean per animal.

Electron Microscopy

Statistical Analyses

After orientation of the blocks by thick sections, thin vertical sections were stained with uranyl acetate and lead citrate and examined in a Jeol 100 CXII electron microscope. A series of micrographs were taken in the longitudinal septa of PZ, HZ, and CZ (Calcification Zone) and measurements of collagen fibril length and width and PGG density on these micrographs were made using a ZIDAS digitizing tablet. (HZ is distinguished from CZ at the ultrastructural level by a lack of degeneration.) Means per section were averaged to obtain means per animal.

One-way analysis of variance was used to compare group means. The statistical package used was SYSTAT version 4.1 (Systat Inc., Evanston, Ill.) with significant values having $p \leq 0.01$.

RESULTS

Light Microscopy

Representative sections of growth plates are shown in Fig. 2. Mean heights of zones and of total growth plates are shown in Figures 3 and 4. The only significant differences seen were in the flight animals: an increase in the PZ relative to vivarium and tail suspended groups; and a decrease

in the HCZ relative to all other groups. There were no significant differences between groups in either the RZ or the total plate.

Mean cell number shows an increase in the flight animals in the PZ, which differs significantly from the PZ of Basal, Synchronous and Tail suspension groups. Cell number in the HCZ was significantly decreased relative to the basal, vivarium and tail suspension groups. Total cell number/column was increased significantly in flight animals over synchronous controls.

Computerized Planimetry

No differences were seen in plate area, perimeter, or shape factor (Table 1).

Electron Microscopy

At the ultrastructural level, in decalcified tissue, the calcification zone is distinguished by cellular degeneration. In all groups in this study the calcification zone was greatly reduced. Much effort was required to find columns in which the CZ could be measured, and in many cases no CZ could be recognized. Flight, Tail, and Vivarium groups had at least one region in which pictures were taken for fibril size studies, but in basal and synchronous animals, no CZ has yet been found. HZ was also reduced in all groups, with most of the cells present being typical of early hypertrophy. These changes in the zones are probably age-related, since these animals were at least 3 weeks older than animals used in previous studies. Other observations concern the appearance of the collagen fibrils. Within the same animal, there were some septa with well-defined fibrils, some septa where fibrils were present though not easily discernible, and some septa where no fibrils could be seen. In the second case, the fibrils appear to be "unraveling". In several animals, this unraveling occurs in HZ but not in PZ (Fig. 5). Its appearance in the HZ may be due to the action of collagenases which have been identified in this zone (Dean, et al., 1985) and could be related to the decline of plate activity with age. Electron microscopy studies found no difference in collagen fibril length and width, or PGG density (Figs. 6,7,8).

DISCUSSION

Results from spaceflight studies are difficult to interpret because of numerous variables, any of which can affect the growth plate (Table 2). With Cosmos 2044, a new variable has been added--age. Nonetheless, our 2044 results can be interpreted within the framework of our previously proposed model (Duke, et al., 1990). In this model, which is based on the comparisons shown in Fig. 9, cells accumulate in the reserve zone during unloading, as was seen in the SL3-sim+Ø animals. (Our assumption is that a similar buildup in the reserve zone occurs also in space, although there is as yet no data to support that speculation.)

This buildup of cells is due to a lack of their differentiation into proliferating chondrocytes mediated, at least in part, by a decline in growth hormone in both suspended and spaceflown animals (Hymer, et al., 1985; Motter, et al., 1987; Grindeland, et al.,1990). The lack of differentiation results in a decline in the PZ and the HCZ as seen in Spacelab 3 rats. A decrease in height and number of cells in the PZ was not seen in SL3 - sim+Ø animals, perhaps because they are still subject to gravitational effects, or possibly because of a difference in mechanisms of decreased bone growth in suspended vs. spaceflown animals (Vico, et al., 1987).

Upon reloading, cells are stimulated rather rapidly (within 12 hours) to move from the reserve zone into the proliferative zone. In SL3 and Cosmos 1887, this rapid differentiation left the reserve zone significantly depleted with respect to controls, and in 1887, with its very long recovery time, resulted in a huge increase in PZ height and especially cell number. The PZ of SL3 animals, with only 12 hours of recovery time, was still significantly depressed from control values.

In these previous studies, (SL3, SL3-sim, and Cosmos 1887) the HCZ was in all cases significantly reduced.

Cosmos 2044 animals, with about a 10 hour recovery time, had RZs that did not differ from controls, and a PZ with an insignificant increase in height and a significant increase in cell number. As with other flights, the HCZ was greatly reduced in both height and cell number. In the case of Cosmos 1887 and 2044, the total plate height was not significantly different from controls, but the cell number per column was significantly greater. The closely packed cells in the columns of these animals, can be seen in Figure 2, indicating that proliferation is going on, but that matrix production has not yet returned to normal.

Because of the recovery seen in the PZ, and the very large decrease in the HCZ, 2044 animals resemble 1887 animals (comparable g exposure) more than they do SL3 animals (comparable recovery time). 2044 and 1887 animals are also more similar in age. Because of flight delays, the 2044 animals at the beginning of the flight were about the same age as the 1887 animals at the end of that flight. Comparisons of 2044 groups showed no difference from basal controls, whereas in 1887 animals, there was a striking decline in plate size during the course of the experiment (Duke et al., 1990). Based on the tail suspension studies, the aging growth plate appears to be less responsive to unloading. Previous suspension studies using younger animals found decreases in height and number of cells per column of the growth plate when compared to synchronous controls (Montufar-Solis, D. and Duke, J. 1988; Duke J., et al., unpublished observations).

The recovery of the PZ within the 12 hour period may simply be due to less supression during flight, as is seen here in the tail suspension animals, and, again, may be age related. In contrast to previous studies, collagen length and width of spaceflown rats did not differ significantly from controls. This is probably due to the postulated removal of the fibrils which made measurement difficult or impossible. Figure 5 shows a portion of the PZ and HZ of a flight rat.(Other animals show these structures also). The fibers in the PZ appear to be loosely structured, and in the HZ, only a dense material remains. At higher magnifications, no fibrillar structure is present.

In conclusion, this study shows again that cartilage differentiation within the growth plate is altered by spaceflight; that recovery appears to be underway after only 12 hours of 1g exposure; and that older animals with less active growth plates are not good candidates for this type of study.

REFERENCES

1. Dean, D., Muniz, O., Berman, I., Pita, J.C., Carreno, M., Woessner, J.F. and Howell, D. S. 1985. High Collagenase Content of Rachitic rat Growth Plates. Trans. Orthop. Res. Soc., 10: 203.

2. Duke, J., Janer, L., Morrow, J. and Campbell, M. 1985. Microprobe Analyses of Epiphyseal Plates from Spacelab 3 Rats. Physiologist 28(Suppl.): S217-S218.

3. Duke, J. and D. Montufar-Solis. 1989. Analyses of Epiphyseal Plates from Cosmos 1887 Rats: a Preliminary Report (Abstract). ASGSB Bulletin 2:51.

4. Duke, J. and Montufar-Solis, D., 1989. Proteoglycan Granules in Growth Plates of Spacelab 3 Rats. In Proceedings of the Third International Conference on the Chemistry and Biology of Mineralized Tissues (Glimcher, M.J., ed), Chatham, MA Oct 16-21, 1988, p 836, New York, NY.

5. Duke, J., Durnova, G. and Montufar-Solis, D. 1990. Histomorphometric and Electron Microscopic Analyses of Tibial Epiphyseal Plates from Cosmos 1887 rats. FASEB J. 4:41-46.

6. Grindeland, R.E., Vasques, M.F., Ballard, R.W., and Connolly, J.P. 1990. Cosmos 2044 Mission Overview. J. Appl. Physio. Vol. XXX

7. Holton, E.M. and Baylink, D.J. 1978. K005: Quantitative Analysis of Selected Bone Parameters. In Final Reports of US Experiments Flown on the Soviet Satellite Cosmos 782 (Rosenzweig, S.N. and Souza, K.A. eds), NASA TM-78525, pp. 321-351, Moffett Field, Calif.

8. Holton, E.M., Turner, R.T., and Baylink, D.J. 1978. K205: Quantitative Analysis of Selected Bone Parameters. In Final Reports of US Experiments Flown on the Soviet Satellite Cosmos 936 (Rosenzweig, S.N. and Souza, K.A., eds), NASA TM-78526, pp.135-178, Moffett Field, Calif.

9. Hymer, W.C., Grindeland, R., Farrington, M., Fast, T., Hayes, C., Motter, K., and Patil, L. 1985. Microgravity Associated Changes in Pituitary Growth Hormone (GH) Cells Prepared from Rats Flown on Spacelab 3. Physiologist 28(Suppl.): S197-S198.

10. Grindeland, R.E., Vale, W., Hymer, W.C., Sawchenko, P., Vasques, M.F., Krasnov, I. and Victorov,I. 1990. Growth Hormone Regulation, Synthesis, and Secretion in Microgravity. In Final Reports of the US Experiments Flown on the Soviet Biosatellite Cosmos 1887 (Connolly, J.P., Grindeland, R.E., and Ballard, R.W., eds) NASA TM-102254: pp. 419-470. Moffett Field, CA.

11. Jee, W.S.S., Wronski, T.J., Morey, E.R., and Kimmel, D.B. 1983. Effects of Spaceflight on Trabecular Bone in Rats. Am. J. Physiol. 244: R310-R314.

12. Matthews, J.L., 1981. Mineralization in the Long Bones. In Final Reports of US Rat Experiments Flown on the Soviet Satellite Cosmos 1129 (Heinrich, M.R., and Souza, K.A., eds), NASA TM-81289, pp. 199-228, Moffett Field, CA.

13. Montufar-Solis, D. and Duke, J. 1988. Effect of Simulated Spaceflight on Tibial Epiphyseal Plates (Abstract). ASGSB Bulletin 1:34.

14. Morey, E.R., 1979. Spaceflight and Bone Turnover: Correlation with a New Rat Model of Weightlessness. Bioscience 29:168-172.

15. Motter, K., Vasques, M., Hayer, C., Kendal, M., Tietjen, G., Hymer, W.C., and Grindeland, R. 1987. Effects of Microgravity on Rat Pituitary Growth Hormone (GH) Cell Function: Comparison of Results of the SL-3 Mission withRat "Unloading" on Earth. In Space Life Sciences Symposium: Three Decades of Life Science Research in Space, pp. 52-53, Washington, D.C., June 21-26, 1987.

16. Reinholt, F.P. Hjerpe, A., Jansson, K. and Engfeldt, B. 1984. Stereological Studies on the Epiphyseal Growth Plate in Low Phosphate, Vitamin D-Deficiency Rickets with Special Reference to the Distribution of Matrix Vesicles. Calcif. Tissue Int. 36:95-101.

17. Sissons, H.A. 1971. The Growth of Bone. In The Biochemistry and Physiology of Bone (G.H. Bourne, ed), pp 145-180, Academic Press, New York, NY.

18. Vico, L., Bakulin, A.V. and Alexandre, C. 1987. Does 7-day Hindquarters Unloading Simulate 7-day of Weightlessness Exposure in Rat Trabecular Bone? In Third European Symposium on Life Sciences Research in Space (Hunt, J., ed), ESA/ESTEC SP-271, pp. 179-182, Noordwijk, Netherlands.

19. Wronski, T.J. Morey-Holton, E., Cann, C.E., Arnaud, C.D., Baylink, D.J., Turner, R.T., and Jee, W.S.S. 1981. K305: Quantitative Analysis of Selected Bone Parameters. In Final Reports of US Rat Experiments Flown on the Soviet Satellite Cosmos 1129 (Heinrich, M.R., and Souza, K.A., eds.), NASA TM-81289, pp. 101-125, Moffett Field, Calif.

20. Yagodovsky, V.S., L.A. Triftanidi, and G.P. Gorokhova. 1976. Space Fight Effects on Skeletal Bones of Rats (Light and Electron Microscopic Examination). Aviation Space Environ. Med. 47:734-738.

TABLE 1

RESULTS OF COMPUTERIZED PLANIMETRY OF TIBIAL EPIPHYSEAL PLATES FROM COSMOS 2044 RATS

	AREA, mm2	PERIMETER,mm	SHAPE FACTOR
Basal	1.38 ± .14	12.016 ± .703	0.106 ± .009
Flight	1.232 ± .085	13.370 ± .678	0.110 ± .008
Synchronous	1.152 ± .041	11.588 ± .598	0.098 ± .004
Vivarium	1.134 ± .187	11.944 ± .401	0.166 ± .036
Tail	1.192 ± .061	10.218 ± 1.559	0.098 ± .004

*Values are means ±SEM.

TABLE 2

COMPARISON OF SL3 AND COSMOS 1887 AND 2044 FLIGHTS

Parameter	SL3	Cosmos 1887	Cosmos 2044
	7d flight; 12h recovery	12.5d ; 53.5h	14d ; 10h
Strain	Taconic Farm	Czech Wistar	Czech Wistar
Weight	198 g	325 g	320 g
Age	7 weeks	12 weeks	15 weeks[1]
Diet	Teklad L-356	Soviet Paste	Soviet Paste
	Food bars	(70% water)	(70% water)
Water	Ad libitum	Ad libitum	Ad libitum
Housing	1 rat / cage	10 rats / cage	10 rats / cage
Light/Dark	12:12	16:8	16:8

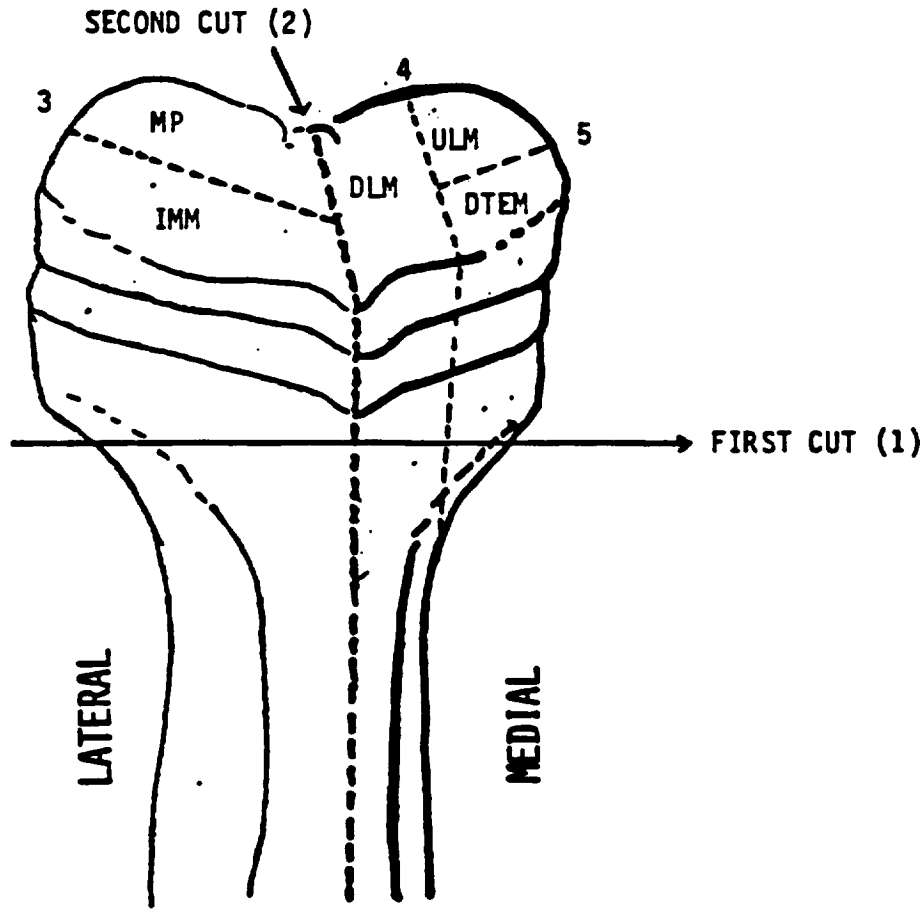

Figure 1. Dissection of growth plate for experiment. Numbers indicate sequence of cuts. Abbreviations refer to tissue usage. MP = microprobe; IMM = immunochemistry; DLM = decalcified light microscopy; DTEM = decalcified transmission electron microscopy; ULM = undecalcified light microscopy.

Figure 2. Representative sections of growth plates from each group (bar = 100μm). B, basal; F, flight; S, synchronous; V, vivarium; T, tail suspended. RZ, reserve zone; PZ, proliferative zone; HCZ, hypertrophy/calcification zone. (Cosmos 2044).

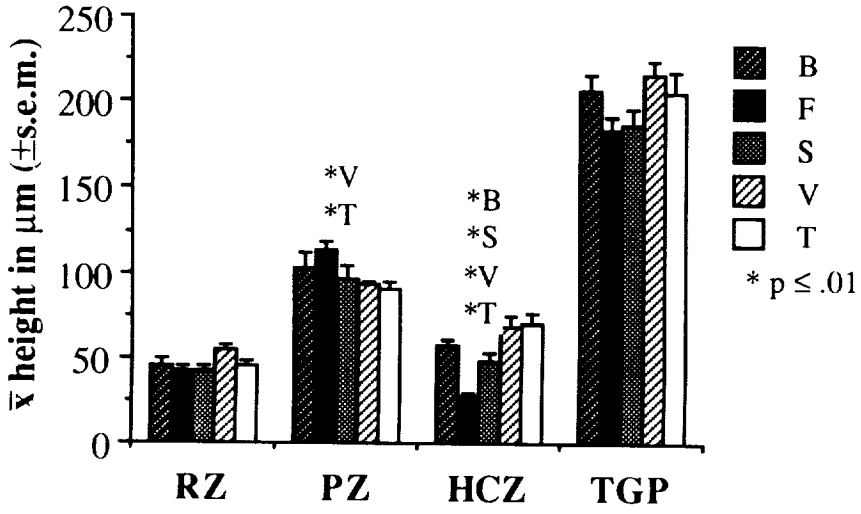

*Figure 3. Mean height per zone and total growth plate. All groups were compared by ANOVA; significantly different groups are indicated by letter atop bar and level of significance by * (p≤ 0.01). Values are means plus standard errors. B, basal; F, flight; S, synchronous; V, vivarium; T, tail suspended.*

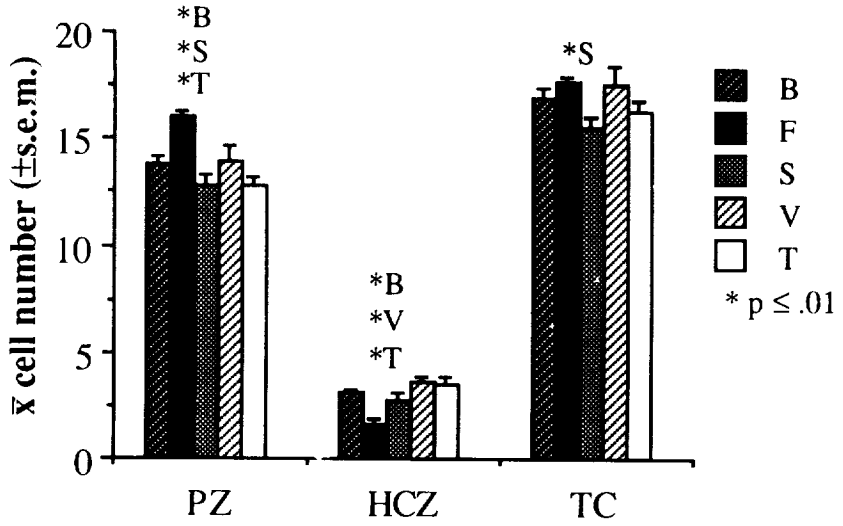

*Figure 4. Mean cell number per zone and total growth plate. All groups were compared by ANOVA; significantly different groups are indicated by letter atop bar and level of significance by * (P ≤ 0.01). Values are means plus standard errors. B, basal; F, flight; S, synchronous; V, vivarium; T, tail suspended.*

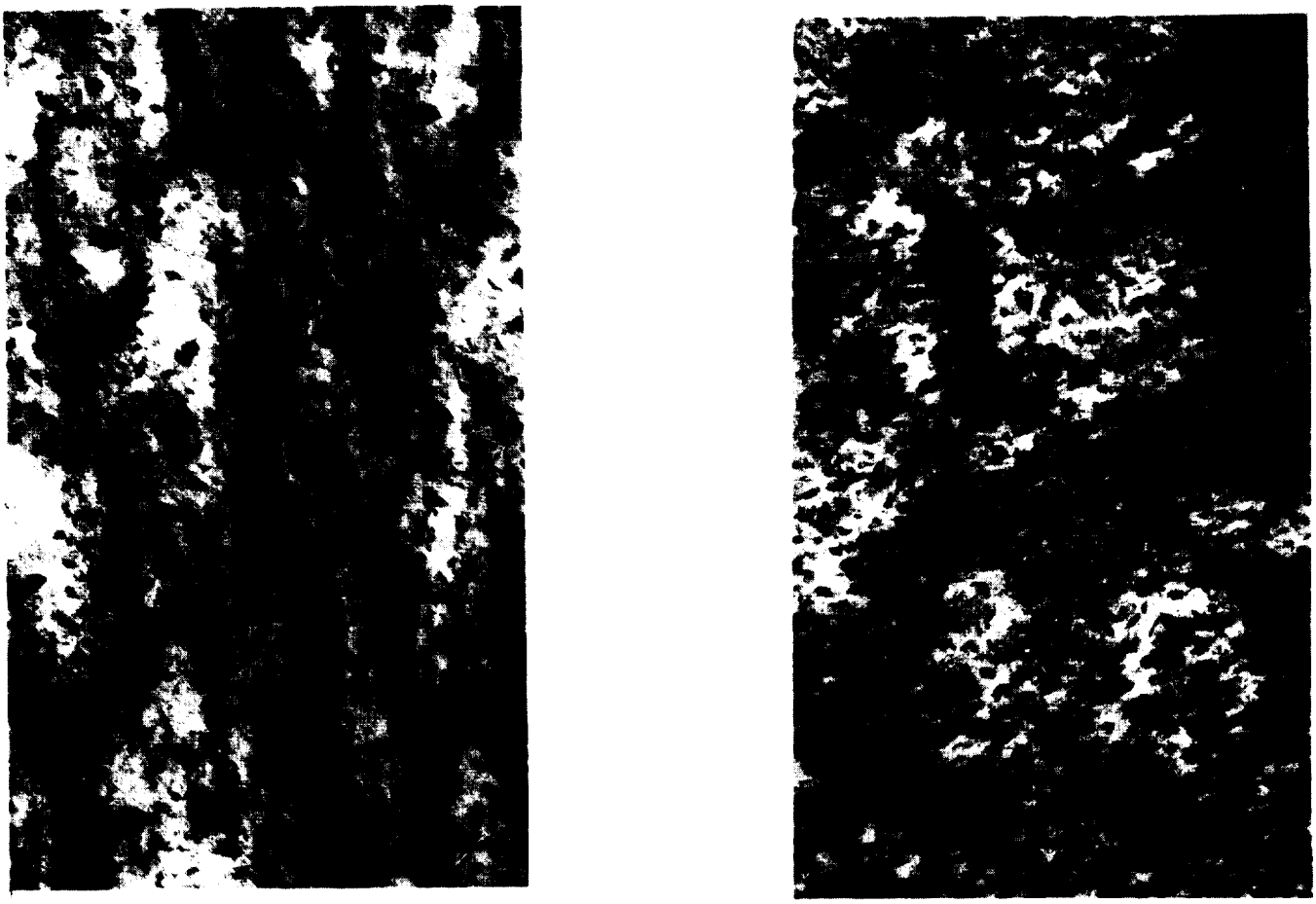

Figure 5. Collagen fibrils in PZ (left) and HZ (right). (Bar = 100nm).

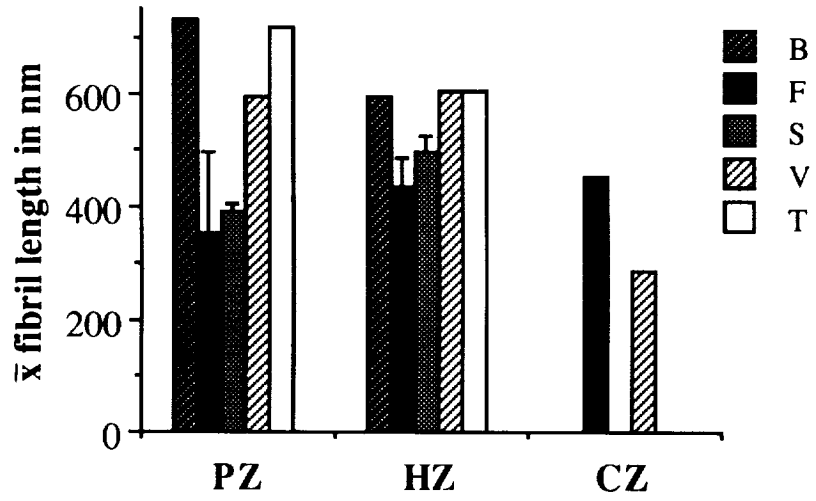

Figure 6. Mean collagen fibril length per zone of growth plate. B, basal; F, flight; S, synchronous; V, vivarium; T, tail suspended.

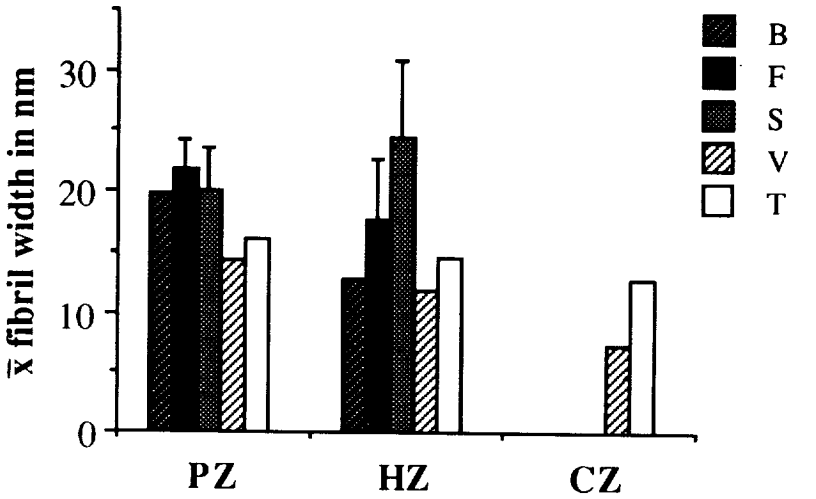

Figure 7. Mean collagen fibril width per zone of growth plate. B, basal; F, flight; S, synchronous; V, vivarium; T, tail suspended.

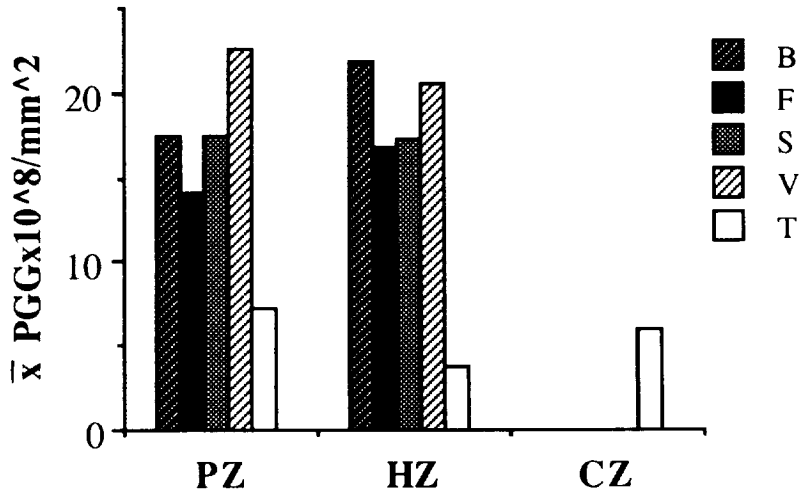

Figure 8. Mean proteoglycan granules per mm^2 per zone of growth plate. B, basal; F, flight; S, synchronous; V, vivarium; T, tail suspended.

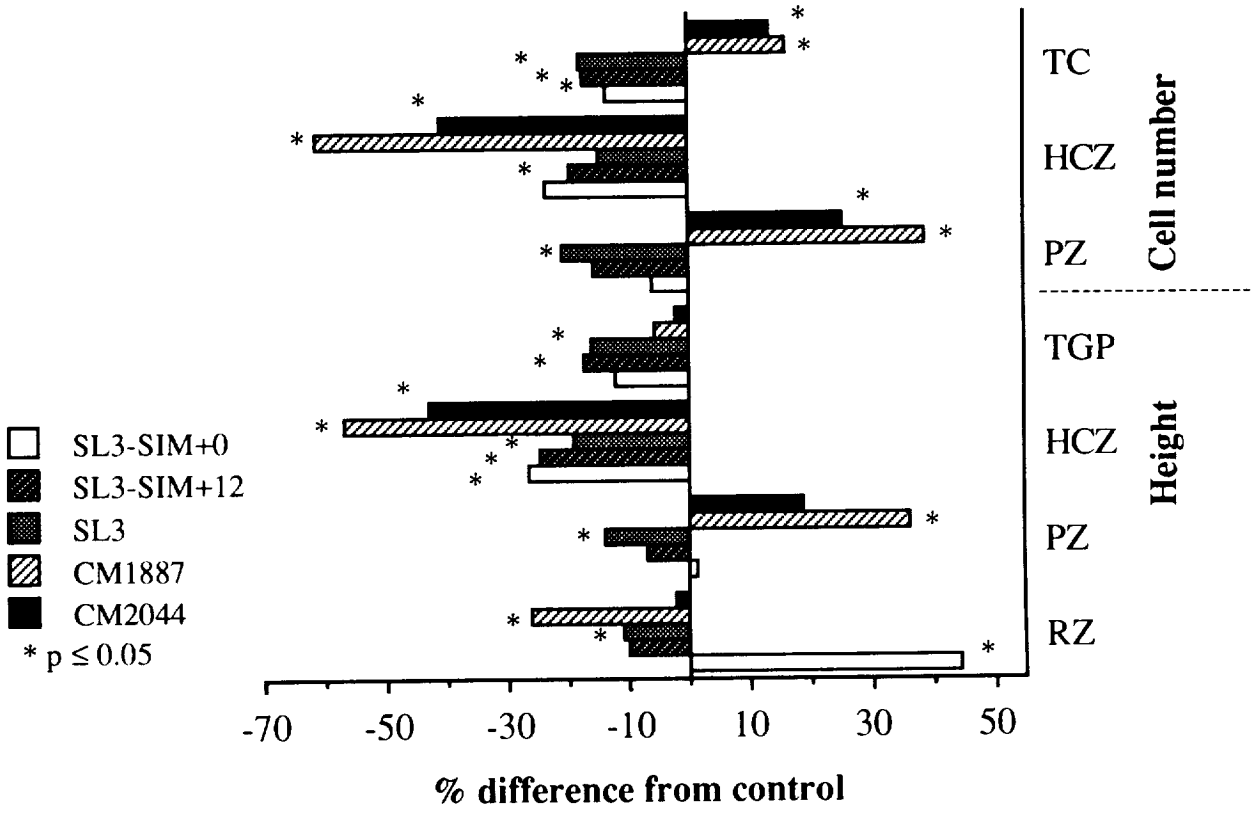

Figure 9. Changes in growth plate parameters.in Cosmos 2044, Cosmos 1887, Spacelab 3 and the Spacelab 3 simulation. Data expressed as 100 x (experimental - control)/control. For Cosmos 1887, the synchronous control was used. For SL3 and SL3-sim, there was only one control. (*) P≤0.05.

EXPERIMENT K-7-07

PART I: METABOLIC AND MORPHOLOGIC PROPERTIES OF MUSCLE FIBERS AND MOTOR NEURONS AFTER SPACEFLIGHT, COSMOS 2044

PART II: VENTRAL HORN CELL RESPONSES TO SPACEFLIGHT AND HINDLIMB SUSPENSION

Principal Investigator:

V. Reggie Edgerton
Department of Kinesiology
2859 Slichter Hall
Brain Research Institute
University of California
Los Angeles, CA

Co-Investigators:

Yoshi Ohira
Department of Kinesiology
2859 Slichter Hall
University of California
Los Angeles, CA

Bian Jiang
Roland Roy
Brain Research Institute
University of California
Los Angeles, CA

J.J. Leger
J.F. Marini
Reseau de Recherches Neuromusculaires
INSERM U6
Marseille, France

E. I. Ilyina-Kakueva
V. Oganov
Institute of Biomedical Problems
Moscow, USSR

PART I: METABOLIC AND MORPHOLOGIC PROPERTIES OF MUSCLE FIBERS AFTER SPACEFLIGHT, COSMOS 2044

V. Reggie Edgerton, Bian Jiang,
J.J. Leger, J.F. Marini, Yoshi Ohira, and Roland Roy

INTRODUCTION

The present data from Cosmos 2044 rats allows us to address several issues that were raised by the results of Cosmos 1887, but have remained unresolved. For example, the wet muscle weight of the soleus from Cosmos 1887 suggested only slight muscle atrophy although the fiber size data showed about 40% atrophy. Since the 1887 rats remained at 1 G for about 48 hrs. after landing, it was hypothesized that muscle edema was significant. In fact, data from other investigators of 1887 rats (e.g., Baldwin and colleagues) found a lower protein concentration in the flight than control vastus intermedius muscle. The fiber atrophy, as reflected by fiber cross sectional area, was similar in the 2044 and 1887 rats, while wet muscle weight was reduced markedly in 2044 rats. Therefore, it appears that when the atrophied muscle become edematous post flight (due presumably to the sudden enhanced activity of a severely atrophied muscle) that the fibers do not enlarge but the interfiber space becomes expanded. It also suggests that this edematous effect probably occurs as a result of sudden elevated activity of the soleus as would be expected based on the fact that this muscle is highly active just in quiet standing, and this activity, perhaps, induces exercise hyperemia.

A second issue that is addressed in the present work is the adaptability of selected metabolic enzymes to spaceflight. Previous data have shown that the soleus muscle maintains its oxidative potential remarkably well, even during severe atrophy after spaceflight or hindlimb suspension. Further, previous data suggest that alpha-glycerophosphate dehydrogenase activity is elevated in at least some fibers after spaceflight and after hindlimb suspension.

Finally, a question not addressed in any previous studies of suspension or spaceflight is whether the myosin ATPase activities of single fibers changes in parallel with the changes in expression of fast myosin. By combining myosin ATPase activity and monoclonal antibody staining for slow and fast heavy chains this question can be addressed.

METHODS

Serial sections, 10 mm thick, were cut at -20°C in a cryostat. Qualitative staining of myofibrillar adenosine triphosphatase (ATPase) was performed with preincubation at pH 8.7. Quantitative staining for myofibrillar ATPase activity was performed pH 8.6. Triplicate sections were stained at 37°C with ATP in the substrate medium and two sections were stained without ATP. The difference in optical density between the with and without substrate was used to calculate activity (OD/min).

Both succinate dehydrogenase (SDH) and a-glycerophosphate dehydrogenase (aPD) activities were also stained both with and without substrate (succinic acid and a-glycerophosphate, respectively) as was described by Martin et al. (1). The matched areas from these sections were digitized by using a computer-assisted image analyzing system. The cross-sectional area and optical density (OD) of each fiber matched for all of the sections were analyzed. Additional serial sections were stained with monoclonal antibody against fast or slow myosin heavy chain. Fibers were identified as having reacted positively for the slow, fast or both antibodies.

RESULTS

Significant atrophy was found in both dark and light myosin ATPase fibers following spaceflight and tail suspension (Table 1). In the suspended rats, the dark and light ATPase fibers ("Type II" and "I") were 40 and 38% smaller than control rats. The dark and light ATPase fibers of the flight rats were 28 and 38% smaller. Since most fibers were dark ATPase stained, the overall effect of suspension and flight were approximately the same.

In response to spaceflight and tail suspension, the % distribution of dark ATPase fibers was significantly increased (Table 2). This increase seemed to be due to some light-staining fibers staining intermediately (Table 2, Fig. 1). Similar results were obtained by immunocytochemical analysis (Table 2). The % distribution of fibers which were positive to a monoclonal antibody for fast myosin heavy chain increased from 9.6 (control) to 24.1% after spaceflight. However, the % fibers responding positively to slow myosin antibody did not change (Table 1). At this time, similar data on suspended rats have not been obtained. Approximately 16% of fibers responded positively to both slow and fast myosin antibodies after spaceflight. Fibers that expressed both fast and slow myosin did not exist in the control soleus. The % distribution of fast fibers detected by monoclonal antibody were approximately 10% less than that detected by alkaline ATPase staining in both control and flight muscles. The former values were obtained from approximately 1700 fibers and the latter ones were from approximately 95 fibers per animal. It is not certain at this time whether the 10% difference between dark myosin ATPase staining and the antibody identification of fast fibers was due to sampling error or whether it represents a true difference between the two assays.

The ATPase activity in light ATPase fibers was less in flight than control muscle (Table 2). The activity of SDH also was less than control in dark ATPase fibers following spaceflight and tail suspension. To date, the significance of these differences are uncertain in that a simple t-test was run rather than an analysis of variance with a nested design, as is more appropriate. No significant change was observed in GPD activity in any type of fibers. However, there is some suggestion that the GPD activity was higher in the suspended than synchronous control rats, particularly among the dark ATPase staining fibers. Those fibers that stained intermediately with ATPase had intermediate quantitative ATPase, SDH and GPD activities suggesting that these fibers were in a transitional state.

TABLE 1

SIZE AND ENZYME ACTIVITIES OF SOLEUS MUSCLE FIBERS

		CSA (μm^2)	ATPase (Δ OD/min x 10^3)	SDH (Δ OD/min x 10^4)	GPD (Δ OD/min x 10^4)
S. Control	Dark	2711 ± 236	166 ± 9	812 ± 87	16.1 ± 5.2
	Int. med.	—	—	—	—
	Light	3586 ± 207	89 ± 5	494 ± 50	6.5 ± 2.6
Tail-suspended	Dark	1611** ± 180 (41%)	157 ± 16	543*± 40	28.2 ± 5.4
	Int. med.	—	98 ± 9	468 ± 30	18.7 ± 5.4
	Light	1951*** ± 174 (38%)	76 ± 8	372 ± 18	8.4 ± 2.2
Flight	Dark	1941* ± 141 (28%)	135 ± 16	538*± 67	12.8 ± 5.1
	Int. Med.	—	75 ± 8	402 ± 35	8.5 ± 3.5
	Light	2223*** ± 103 (38%)	64*± 8	352 ± 35	5.5 ± 3.4

Mean ± SEM. *: $P < 0.05$, **: $P < 0.01$, and ***: $P < 0.001$ by unpaired t test. CSA: cross-sectional area. Intermediately and dark staining fibers were combined in the tail-suspended and flight muscles in calculating CSA.

(%): % atrophy relative to control rats

TABLE 2

PERCENTAGE OF FIBERS EXPRESSING SLOW AND FAST MYOSIN IN THE SOLEUS MUSCLE

	% Dark Fiber (n)	% Int. Med. Fiber	SmAB % + (n)	FmAB % + (n)	S + FmAB % +
S. Control	20.8 ± 2.8 (93)	0 ± 0	90.4 ± 0.9 (1739)	9.6 ± 0.9 (1739)	0
Tail-suspended	30.4* ± 2.2 (96)	7.4**±3.2	—	—	
Flight	33.6* ± 4.7 (94)	14.2**±3.5	91.4 ± 0.8 (1689)	24.1*** ± 1.0 (1687)	15.5*** ± 0.6

Mean ± SEM *: $P < 0.05$, **: $P < 0.01$, and ***: $P < 0.001$ by unpaired t test. SMAB % +: slow myosin antibody, % positive, F: fast.

(n) = mean number of fibers analyed per rat

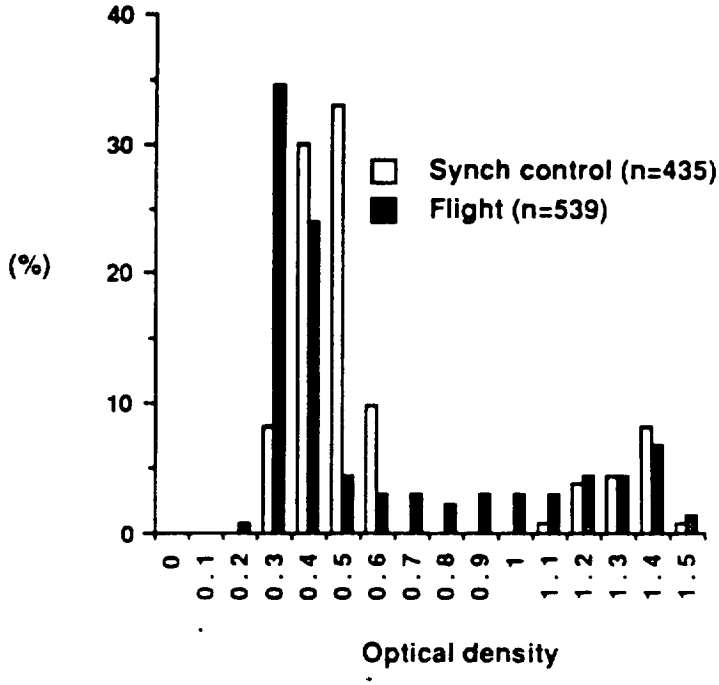

Figure 1. Base-preincubation ATPase.

EXPERIMENT K-7-07

PART II: VENTRAL HORN CELL RESPONSES TO SPACEFLIGHT AND HINDLIMB SUSPENSION

B. Jiang, R.R. Roy, E.I. Ilyina-Kakueva, I.B. Krasnov, V. Oganov, AND V. R. Edgerton

ABSTRACT

Spaceflight or hindlimb suspension result in a loss of mass and in alterations of the metabolic and contractile protein profiles of skeletal muscles towards that resembling faster muscles. Given the influence of motoneurons on muscle properties, ventral horn cells of the lumbosacral enlargement of the spinal cord were studied to determine whether similar adaptations were present in these cells. Three groups of rats (n = 5/group) were studied: control, 14-day spaceflight and 14-day hindlimb suspension. Spinal cords were quick-frozen and the succinate dehydrogenase (SDH) activity and cross-sectional area (CSA) of the soma of ventral horn cells were measured using a computer enhanced image processing system. Briefly, the optical density (OD) for SDH activity was determined after 8 min of incubation in a reaction medium which gave a steady-state enzymatic reaction. Soma sizes were determined in cells having a visible nucleus. Although, there were no significant differences among the three groups in mean CSA and SDH activity, the population distributions of both variables shifted significantly. In the flight rats, there was a shift toward smaller cells. Compared to control, the population distribution of SDH activities in the flight rats shifted toward higher activities, while the distribution shifted toward lower activities in the suspended rats. When considering the interactive effects within individual cells, there was a higher percentage of small cells having high SDH activities in the flight compared to control or suspended rats. These contrasting effects of spaceflight and hindlimb suspension suggest that the changes observed in ventral horn cells were due to factors other than simply the absence of weight support.

Key Words: succinate dehydrogenase activity; soma cross-sectional area; hypogravity; weightlessness.

INTRODUCTION

The effects of spaceflight on rat hindlimb muscles have been investigated extensively. An atrophic response has been reported at both the muscle and the single fiber level in rats flown aboard the Cosmos series of biosatellites (4,9,12,14,15). Immunohistochemical analyses indicate also that there is an increase in the percentage of muscle fibers expressing fast myosin heavy chains in the soleus of flight rats (15,19). Given the influence of motoneurons on muscle properties and the synchrony of changes in motoneurons and muscle fibers in response to spinalization (6,8), one might expect changes in those neurons associated with the control of the muscles affected by spaceflight.

Presently there have been little data describing the effects of unloading the hindlimbs on motor or sensory neurons or interneurons. Polyakov et al. (20) reported no change in lower lumbar motoneuron soma and nuclei volume from the same flight rats as reported in the present paper (Cosmos 2044). These data are in contrast to the increase in motoneuron size reported for an earlier flight (Cosmos 1887), although the differential effects could be related to the time elapsed between landing and tissue sampling, i.e., 6-8 and ~48 hours for Cosmos 2044 and 1887, respectively. It also has been reported that the turnover of water-soluble proteins in lumbar motoneurons was reduced in biosatellite rats (18). In addition, the absolute and relative levels of

RNA and proteins in the rat motoneurons decreased during a 120-day "hypokinesia" experiment (18). These protein adaptations were associated with a lower excitability of the extensor pool, whereas the flexor pool was unaffected. Both soma size and succinate dehydrogenase (SDH) activity, an oxidative marker enzyme, have been associated with the level of excitability of neurons (10). Thus, the specific purposes of the present study were to study 1) the activity of SDH and the soma size and 2) the interrelationships between the soma size and SDH activities of lumbar ventral horn cells after 14 days of spaceflight (Cosmos 2044) or of hindlimb suspension.

MATERIALS AND METHODS

Experimental animals

Three experimental groups of male rats (n = 5/group) were studied. Ground-based rats maintained under conditions similar to spaceflight, i.e., cage size, temperature, lighting, and food and water availability for the duration of the mission, served as synchronous controls (see 9 for details). A second group was exposed to a 14-day spaceflight (Cosmos 2044). A third group of rats had their hindlimbs suspended for 14 days. The flight rats were killed within 12 hours after returning to 1G. The control and suspended rats were killed on a similar time schedule. The control, flight and suspended rats were 127, 123 and 131 days of age and had a mean body weights of 343, 338 and 339 g, respectively, when sacrificed.

Histochemical procedures

From each rat, the lumbar enlargement of the spinal cord was removed rapidly, cut into blocks ~1 cm long and quick-frozen in freon cooled with liquid nitrogen. The data in the present study represent samples from the upper portion of the lumbar enlargement (see 20 for similar data from the lower region). Serial cross-sections (10 μm thick) were cut in a cryostat at -20^0C. To avoid repeated sampling of the same cells, every fifth section was kept for analysis.

The SDH activity, an oxidative marker enzyme, was determined using a modification of the procedures described by Martin et al. (14) and Chalmers et al. (2). Briefly, the SDH activity reaction medium contained 100 mM phosphate buffer (pH, 7.8), 0.9 mM sodium azide, 0.9 mM 1-methoxyphenazine methylsulfate, 1.5 mM nitro blue tetrazolium, 5.6 mM EDTA-disodium salt and 48 mM succinate disodium salt. Under these conditions, SDH activities were shown to be linear from 2 to 12 min. Therefore, in the present study, the SDH assay was run at room temperature for 8 minutes at which time the sections were rinsed in distilled water and mounted on slides.

Tissue analysis

Tissue sections were digitized at a 25x magnification as grey level pictures on a computer enhanced image processing system and were stored on magnetic tapes as described in detail elsewhere (14). Briefly, an array of picture elements (pixels) was quantified to be one of 256 grey levels that is then converted automatically to an optical density (OD). The somas of ventral horn cells, excluding any first order dendritic processes, were outlined and the number of the pixels in each enclosed object was summed to determine the area and OD. A population of 60-100 ventral horn cells from each rat was analysed. In cells containing a nucleus, the nuclear area was omitted from the OD calculation and SDH activities were determined as $OD \cdot min^{-1}$. The cross-sectional area (CSA) of the soma and the relationship between SDH activity and CSA were determined only for those cells with a visible nucleus.

Statistical analyses.

When testing for differences in mean CSA and SDH activity, a one-way nested analysis of variance was used for overall group comparisons with the degrees of freedom represented by the number of rats in each group. Statistical significance was determined at $P \leq 0.05$ and the Bonferroni adjustment was used to determine any differences among the three groups using an adjusted significance level of $P \leq 0.017$ (.05/3). To determine differences in the population distributions in CSA and SDH activity among the three groups, the Kolmogorov-Smirnov test was used with the degrees of freedom represented by the number of ventral horn cells in each group. The level of significance was set at $P \leq 0.05$.

RESULTS

Soma size.

The mean soma CSA of the ventral horn cells was unaffected by 14 days of spaceflight or hindlimb suspension (Fig. 1). There was a significant shift, however, in the frequency distribution of CSA toward smaller somas in flight rats compared to either control or suspended rats. For example, 70% of the cells in the flight group had soma sizes <390 μm^2 compared to 55 and 53% in the control and suspended groups. There was no significant difference in the distribution of soma size between the control and suspended groups.

SDH activity.

The mean SDH activity was similar among the three groups (Fig. 2). The frequency distributions of SDH activity in the three groups, however, were significantly different from each other. There was a significant shift toward higher SDH activities in the flight, whereas in the suspension group, the population distribution of SDH was shifted toward lower activities compared to the control group.

Interrelationships between SDH activity and soma size.

To illustrate the relationship between SDH activity and soma size for ventral horn cells with a visible nucleus, a scatterplot was constructed for each group (Fig. 3, left). In all three groups, the relatively small cells showed a wider range of SDH activities than the relatively large cells. The scatterplots then were divided into quadrants based on the means of SDH and CSA of the control group (Fig. 3, right). The large, high SDH cells comprised the smallest percentage in each group. Spaceflight resulted in a high percentage of small, high SDH cells, whereas hindlimb suspension had a high percentage of low SDH cells.

DISCUSSION

Studies from previous Cosmos biosatellite and space shuttle flights showed that a variety of metabolic, contractile, physiological and morphological properties of rat skeletal muscle were altered after brief exposures (5-21 days) to spaceflight (see 18 and 22 for reviews). The greatest loss in muscle mass has been noted in the predominantly slow extensors, e.g., the soleus and the adductor longus (11,13,16,18,19,21), a moderate amount in predominantly fast extensors, e.g., the medial gastrocnemius and plantaris (13,16,21) and the least in flexors, e.g., the extensor digitorum longus and tibialis anterior muscles (5,12,13,18,21). This differential atrophy is evident also at the muscle fiber level, e.g., the fibers in the soleus of flight rats atrophy twice as much as those in the medial gastrocnemius (11,13,16,19). Although the concentration of SDH in soleus muscle fibers was not significantly different from controls, there was a reduction in the total amount of SDH activity (i.e., SDH x CSA) and an increase in the activity of a glycolytic enzyme,

i.e., a-glycerophosphate dehydrogenase, following spaceflight (4,12,13,16,19). Baldwin et al. (1) has reported an increase in myosin ATPase activity and a preferential degradation of slow myosin in homogenates of the vastus intermedius, a predominantly slow knee extensor, following the Cosmos 1887 spaceflight. These data suggest that there are significant changes in the turnover rate and kind of proteins in some muscles after unloading. Consequently, if the muscle fibers and the associated neurons are to remain coordinated, some adaptation would be expected in the ventral horn cells of flight or suspended rats.

The results of the present study indicate that 14 days of either spaceflight or hindlimb suspension has no significant effect on the mean CSA and SDH activity of a mixed population of neurons located in the lumbar ventral horn. An absence of an effect of spaceflight or hindlimb suspension on 8 different enzymes, including 6 metabolic enzymes, also was found in single neurons isolated from 11 different regions of the hippocampus of rats from the same flight as the present study (15). The frequency distributions of CSA and SDH activity, however, showed a high percentage of small, high SDH activity cells in the flight rats and a high percentage of low SDH activity cells in the suspended rats. These data suggest that there are selected neuron populations that are affected by spaceflight and suspension. Further, the contrasting effects found in these two experimental treatments suggest that spaceflight is more than simply the absence of weight bearing.

In other experimental models in which neuromuscular activity is reduced, motoneurons have shown an ability to maintain many of their normal properties. For example, Chalmers et al. (3) have reported no change in mean SDH activity or soma size in adult cats 6 months after spinal transection or spinal isolation, i.e., spinal transection plus bilateral dorsal rhizotomy. Electrophysiologically, no alteration in resting membrane potential (7) or action potential amplitude (17) was observed in either soleus or medial gastrocnemius motoneurons of cats up to 7 months after low thoracic spinalization. Further, the duration of afterhyperpolarization of gastrocnemius motoneurons was unchanged after spinalization (8). It has been shown, however, that muscle and motoneuron properties can be altered in concert. For example, Cope et al. (6) showed a decrease in afterhyperpolarization duration and an increase of voltage threshold in soleus motoneurons of chronic spinalized cats. In addition, a coordination between motoneuron and muscle unit properties was demonstrated as follows: 1) the normal correlation between motoneuron afterhyperpolarization duration and muscle contraction time was nearly as strong 4 months after spinalization, and 2) the motoneuron electrical properties were strongly correlated with a combination of muscle unit mechanical properties in both normal and spinal cats. In a similar study in which the motoneurons were studied 2-4 months after spinalization in kittens or in adult cats, the change in muscle twitch contraction time was accompanied by a decrease in the duration of afterhyperpolarization in the motoneuron (8). Czeh et al. (7) demonstrated that the changes in afterhyperpolarization of soleus motoneurons was reduced by chronically stimulating the nerve distal to a tetrodotoxin cuff, i.e., blocking neuromuscular transmission, suggesting that afterhyperpolarization was at least partially dependent upon some factor related to the presence or absence of muscle activation.

The present data are consistent with the interpretation that some neurons in the ventral horn were affected by spaceflight and suspension. These data do not permit us to define which population of neurons were affected. Indeed, the changes reported could reflect changes in gamma motoneurons or even interneurons as well as alpha motoneurons. The marked differential responses of individual skeletal muscles are consistent with the suggestion that only selected populations of motoneurons were affected. For example, only the motoneurons of the predominantly slow muscles might be expected to have changed dramatically. Further, based on the ~15% increase in the proportion of fibers expressing fast myosin in the soleus of the flight rats (19), few motoneurons, relative to all lumbar flexor and extensor motoneurons, may have been affected by this flight. Further, these data raise the issue of a possible differential sensory modulation of proprioceptive and/or vestibular input given the differences in the response of some neurons to

spaceflight compared to hindlimb suspension. It seems obvious that to address these issues it will be essential to utilize techniques which permit the identification of specific neuronal populations.

ACKNOWLEDGEMENTS

This study was supported, in part, by NASA Grant NCC 2-535. We gratefully thank Dr. Richard E. Grindeland for his efforts in facilitating the interactions between the American and Soviet investigators in the Cosmos Biosatellite Program.

REFERENCES

1. Baldwin, K.M., R.E. Herrick, E. Ilyina-Kakueva and V.S. Oganov. Effects of Zero Gravity on Myofibril Content and Isomyosin Distribution in Rodent Skeletal Muscle. FASEB J. 4:79-83, 1990.

2. Chalmers, G.R., and V.R. Edgerton. Single Motoneuron Succinate Dehydrogenase Activity. J. Histochem. Cytochem. 37:1107-1114, 1989.

3. Chalmers, G.R., R.R. Roy, and V.R. Edgerton. Effect of Quantity of Action Potentials on Motoneuron Oxidative Capacity. Soc. Neurosci. Abstr. 15:919, 1989.

4. Chi, M.M. Y., R. Choksi, P. Nemeth, I. Krasnov, E. Ilyina-Kakueva, J.K. Manchester, and O. H. Lowry. Effects of Microgravity and Tail Suspension on Metabolic Enzymes of Individual Soleus and Tibialis Anterior Fibers. J. Appl. Physiol. (Submitted, this volume).

5. Chui, L.A., and K.R. Castleman. Morphometric Analysis of Rat Muscle Fibers Following Spaceflight and Hypogravity. Physiologist 23, Suppl.: S76-S78, 1980.

6. Cope, T. C., M. Fournier, S. C. Bodine, and V. R. Edgerton. Soleus Motor Units in Chronic Spinal Transected Cats: Physiological and Morphological Alterations. J. Neurophysiol. 55:1202-1220, 1986.

7. Czeh, G., R. Gallego, N. Kudo, and M. Kuno. Evidence for the Maintenance of Motoneuron Properties by Muscle Activity. J. Physiol. Lond. 281:239-252, 1978.

8. Gallego, R., P. Huizar, N. Kudo, and M. Kuno. Disparity of Motoneuron and Muscle Differentiation Following Spinal Transection in the Kitten. J. Physiol. 281:253-265, 1978.

9. Grindeland, R.E., M.R. Vasquez, R.W. Ballard, and J.P. Connolly. Cosmos 2044 Mission Reviews. J. Appl. Physiol. (Submitted, this volume).

10. Ishihara, A., H. Naitoh, H. Araki and Y. Nishihara. Soma Size and Oxidative Enzyme Activity of Motoneurones Supplying the Fast Twitch and Slow Twitch Muscles in the Rat. Brain Res. 446:195-198, 1988.

11. Jiang, B., Y. Ohira, R.R. Roy, Q. Nguyen, E. I. Ilyina-Kakueva, V. Oganov, and V.R. Edgerton. Adaptation of Fibers in Fast Muscles of Rats to Spaceflight (Cosmos 2044) and Hindlimb Suspension. J. Appl. Physiol. (Submitted, this volume).

12. Manchester, J. K., M. M.- Y. Chi, B. Norris, B. Ferrier, I. Krasnov, P. M. Nemeth, D. B. McDougal, J.R., and O. H. Lowry. Effect of Microgavity on Metabolic Enzymes on Individual Muscle Fibers. FASEB J. 4:55-63, 1990.

13. Martin, T.P., V.R. Edgerton, and R.E. Grindeland. Influence of Spaceflight on Rat Skeletal Muscle. J. Appl. Physiol. 65:2318-2325, 1988.

14. Martin T. P., A.C. Vailas, J.B. Durivage, V.R. Edgerton, and K.R. Castleman. Quantitative Histochemical Determination of Muscle Enzymes: Biochemical Verification. J. Histochem. Cytochem. 33:1053-1059, 1985.

15. McDougal, D.B.Jr., M.E. PusateriI, J.G. Carter, I. Krasnov, E. Ilyina-Kakueva, J. Manchester and O.H. Lowry. The Effect of Microgravity and Tail Suspension on Selected Enzymes and Amino Acids of the Hippocampus. J. Appl. Physiol. (Submitted, this volume).

16. Miu, B., T.P. Martin, R.R. Roy, V. Oganov, E. Ilyina-Kakueva, J.F. Marini, J.J. Leger, S.C. Bodine-Fowler, and V.R. Edgerton. Metabolic and Morphologic Properties of Single Muscle Fibers in the Rat after Spaceflight, Cosmos 1887. FASEB J. 4:64-72, 1990.

17. Munson, J. B. R. C. Foehring, S. A. Lofton, J. E. Zengel, and G. W. Sypert. Plasticity of Medial Gastrocnemius Motor Units Following Cordotomy in the Cat. J. Neurophysiol. 55:619-633, 1986.

18. Oganov, V.S. Neurotrophic Influences in the Adaptation of Skeletal Muscles and Motor Functions in Weightlessness. In: G. A. Nasledov (editor). Mekhnizmy Neyronal'noy Regulyatsii Myshechnoy Funktsii [Mechanisms of Neural Regulation of Muscle Function]. Leningrad: Nauka, 1988: pp. 107-136.

19. Ohira, Y., B. Jiang, R.R. Roy, V. Oganov, E. Ilyina-Kaueva, J.RR. Marini and V.R. Edgerton. Rat Soleus Muscle Fibers Responses to 14 days of Spaceflight (Cosmos 2044) and Hindlimb Suspension. J. Appl. Physiol. (Submitted, this volume).

20. Polyakov, I.V., V.I. Drobyshev and I.B. Krasnov. Morphological Changes in the Spinal Cord and Intervertebral Ganglia of Rats Exposed to Different Gravity Levels. Physiologist 34:S187-S188, 1991.

21. Riley, D. A., S. Ellis, G. R. Slocum, T. Satyanarayana, J. L. W. Bain, and F. R. Sedlak. Hypogravity-Induced Atrophy of Rat Soleus and Extensor Digitorum Longus Muscles. Muscle Nerve 10:560-568, 1987

22. Roy, R.R., K.M. Baldwin, and V.R. Edgerton. The Plasticity of Skeletal Muscle: Effects of Neuromuscular Activity. In: Exerc. Sports Sci. Rev. 19: 269-312, 1991.

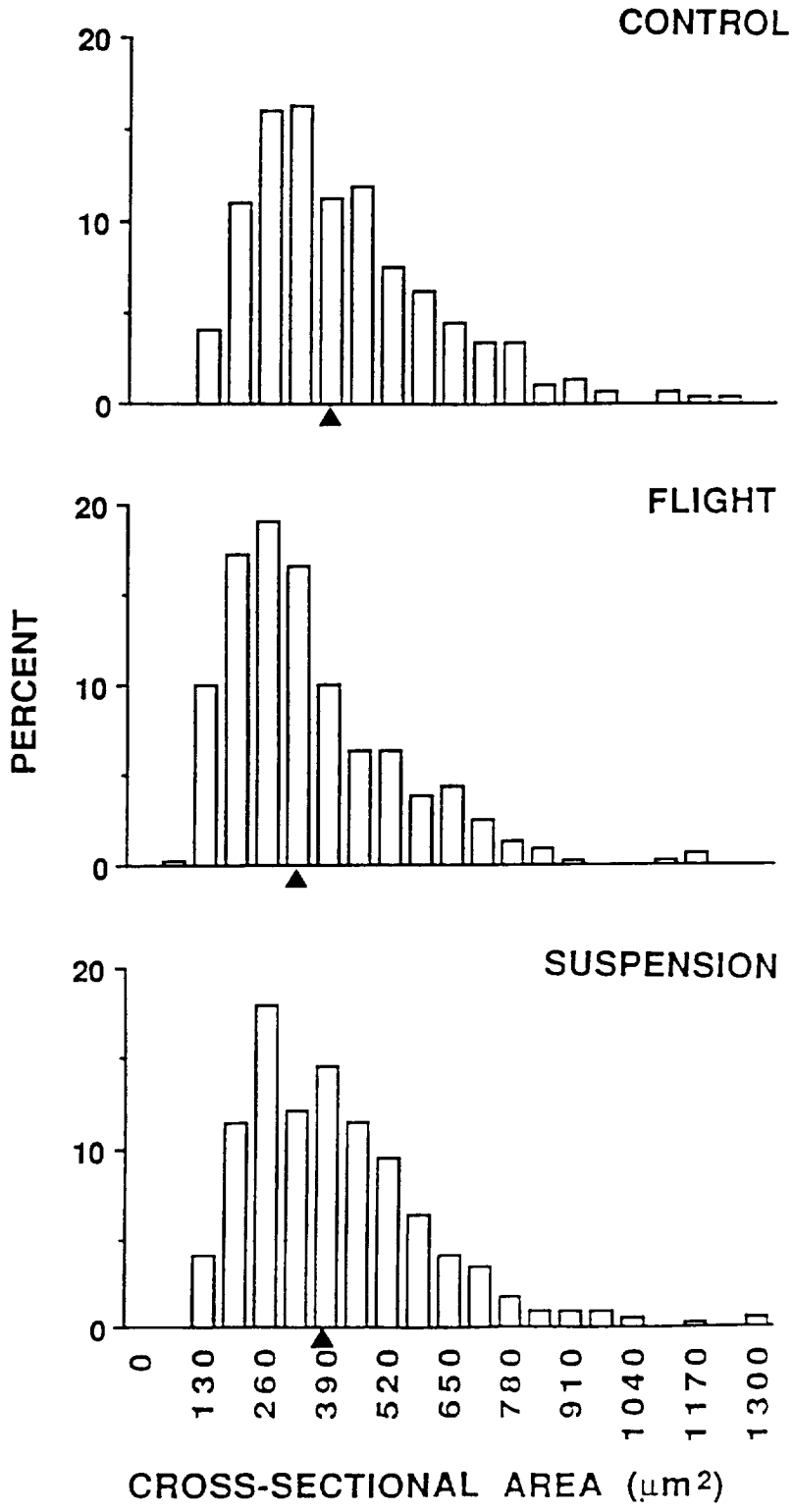

Figure 1. Percent frequency distribution of the soma cross-sectional area of lumbar ventral horn cells from each group. There was a shift toward smaller-sized cells in flight compared to control and suspended rats ($P<0.05$). The distribution of sizes in the control and suspended rats were similar. The arrowhead at the bottom of each scale represents the mean for each distribution, i.e., 417±91 (n = 293), 350±82 (n =319) and 409±89 (n = 351) mm^2 for the control, flight and suspended groups, respectively.

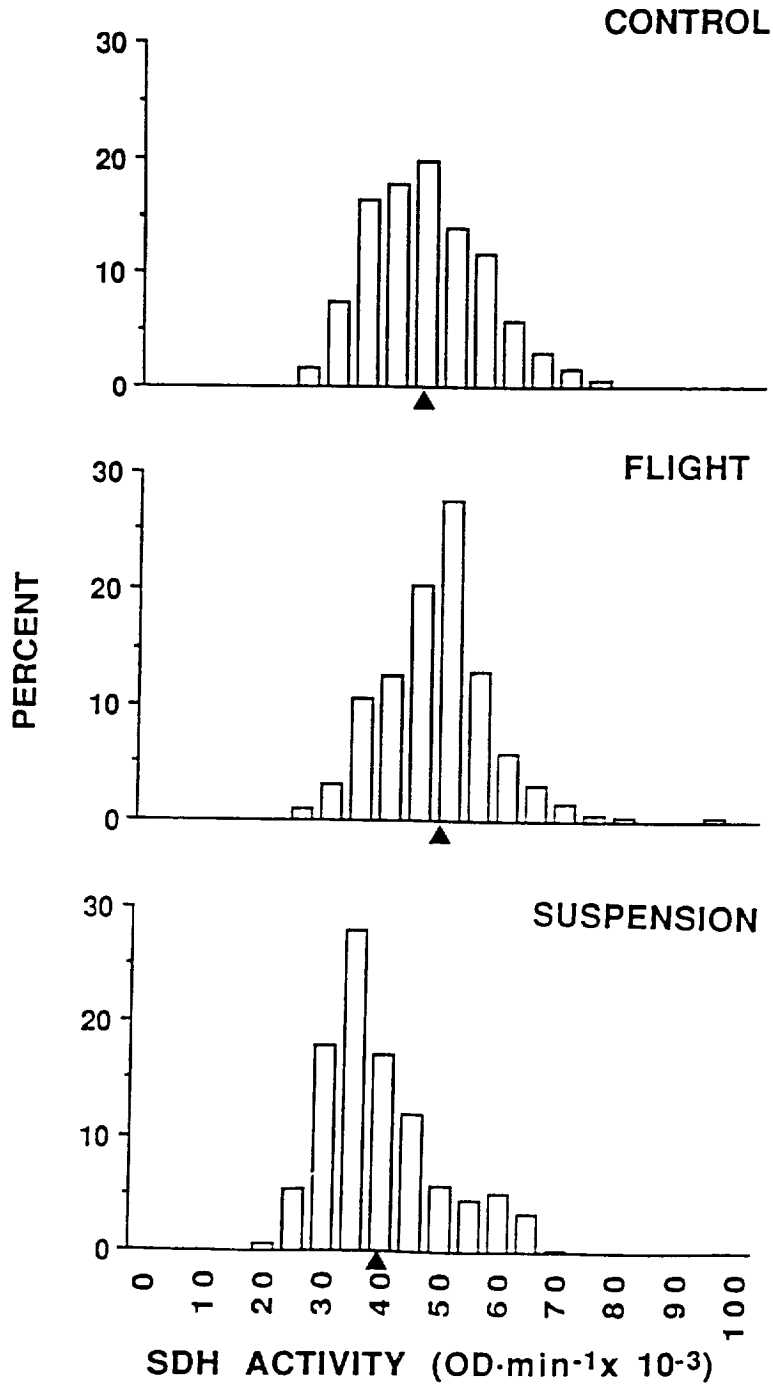

Figure 2. Percent frequency distribution of succinate dehydrogenase (SDH) activity of lumbar ventral horn cells from each group. All distributions were significantly different from each another ($P<0.05$). There was a shift toward higher SDH activities in the flight and lower activities in the suspended rats. The arrowhead at the bottom of each scale represents the mean for each distribution, i.e., 45.4±4.6 (n = 323), 48.1±4.1 (n = 360) and 40.2±4.5 (n = 389) OD·min^{-1} x 10^{-3} for the control, flight and suspended groups, respectively.

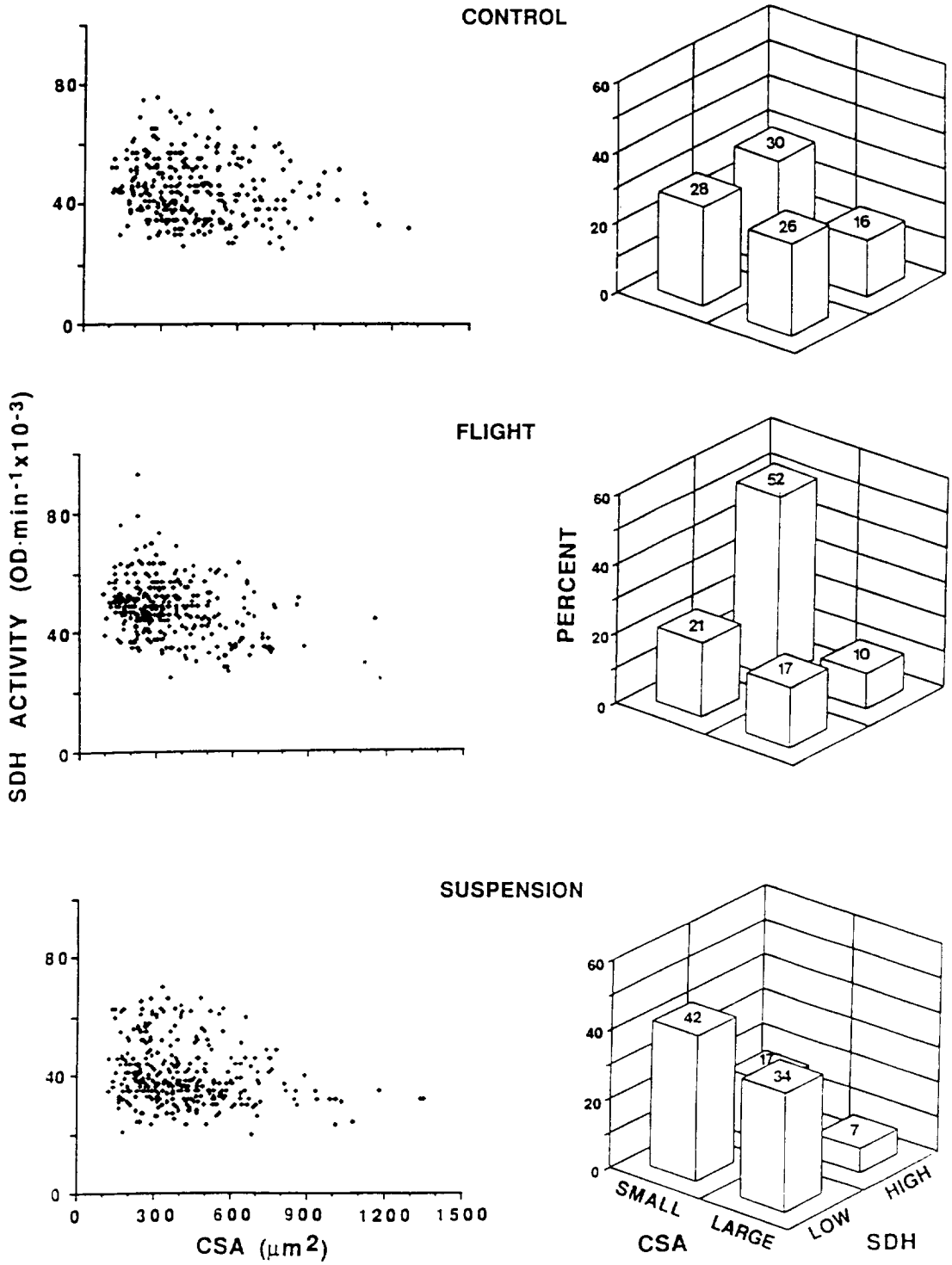

Figure 3. Relationship between succinate dehydrogenase (SDH) activity and soma cross-sectional area (CSA) of lumbar ventral horn cells from each group. In the scatterplots on the left, each symbol represents a single cell. The total number of ventral horn cells was 293, 319 and 351 in control, flight and suspension groups, respectively. On the right, the scatterplots are divided into quadrants based on the mean values of SDH and CSA of the control. Those values below and above the mean SDH are classified as having low and high activities and those values below and above the mean CSA are classified as small or large cells. The percentages of cells located in the quadrant representing small cells with a high SDH activity were 30, 52 and 17% for the control, flight and suspended groups.

EXPERIMENT K-7-08

SKELETAL MUSCLE ATROPHY IN RESPONSE TO 14 DAYS OF WEIGHTLESSNESS

Principal Investigator:

X.J. Musacchia
Department of Physiology and Biophysics
University of Louisville, KY

Co-Investigators:

J.M. Steffen
Department of Biology
University of Louisville, KY

R.D. Fell
Exercise Physiology Laboratory
University of Louisville, KY

E.I. Ilyina-Kakueva
V.S. Oganov
Institute of Biomedical Problems
Moscow, USSR

EXPERIMENT K-7-08

SKELETAL MUSCLE ATROPHY IN RESPONSE TO 14 DAYS OF WEIGHTLESSNESS:VASTUS MEDALIS

X.J. Musacchia, J.M. Steffen, R.D. Fell, V.W. Oganov and E.I. Ilyina-Kakueva

INTRODUCTION

Muscles of the hindlimb in the rat have been used to demonstrate the effects of unloading in weightlessness and in models developed to mimic the response seen during exposure to microgravity. In the complex of hindlimb muscles the greatest atrophic effects have been seen in chiefly slow twitch fiber muscles, e.g. soleus (SOL) (Musacchia et al., 1980; Martin et al., 1988; Ilyina-Kakueva et al., 1986; Riley et al., 1987). In contrast, chiefly fast twitch muscle, e.g. extensor digitorum longus (EDL), has been reported to show the least effects (Musacchia et al., 1980; Martin et al., 1988; Ilyina-Kakueva et al., 1976; Musacchia et al., 1987; Steffen and Musacchia, 1986; Riley et al., 1987).

This report deals with the vastus medialis (VM), a muscle composed chiefly of fast twitch fibers. These are divided between oxidative glycolytic and glycolytic fibers (Ariano et al., 1973) at a ratio of about one to four, respectively. Armstrong and Phelps (1984) reported a three percent population of slow oxidative fibers. The VM is comparable in fiber composition to the EDL, which is composed chiefly of fast twitch oxidative glycolytic (42-59%) and glycolytic (38%-56) fibers and a few slow twitch (2-3%) fibers (Ariano et al., 1973; Armstrong and Phelps, 1984). Although there are some differing views about the fast twitch fiber content, presumably due to variation in the portion of the muscle from which the stained preparations were taken, it is clear that the greatest portion of the muscle is made up of fast twitch fibers.

The VM is not a load bearing muscle, and thus provides the opportunity to study physiological effects of lengthy exposures to microgravity separate from the additional effects of unloading. Each muscle contributes to the overall structural and functional integrity required to resist long term effects of disuse pathology and the necessary requirement of recovery.

On September 15, 1989 at 10:30 a.m. the Soviets launched a biosatellite aboard COSMOS 2044 and 14 days later, September 12229 at 6:00 a.m. the orbiter landed. Rats were exposed to conditions of weightlessness in a manner that was comparable to an earlier flight of approximately 12 days, COSMOS 1887. We obtained the VM from these flight rats and compared the flight adaptation response to our previous VM study (Musacchia et al., 1988). In addition the VM provided an opportunity to make comparisons with another fast twitch muscle, the EDL, from rats that had been flown in both USSR and NASA biosatellites. The EDL has been used in both microgravity flights (Ilyina-Kakueva et al., 1976; Oganov and Potapov, 1976; Castleman and Chui, 1978; Steffen and Musacchia, 1986) and in earthside hindlimb unloading experiments (Musacchia et al., 1980; Fitts et al., 1986).

In the present study several control approaches were used. Tail suspended (T) animals were used because hindlimb unloading is known to produce muscle disuse atrophy (Riley et al.,, 1987; Musacchia et al., 1990). Further continued verification of earthside models is critical to the

planning of space flight experiments. The synchronous controls (S) are useful in estimating the effects of physical insults, in addition to weightlessness, that are seen in all launches and landings. The vivarium (V) an basal (B) controls provide subjects that are comparable to the vast majority of controls for which there are data in the literature. Although no control may be perfect, there are features about each of the above that served a practical purpose.

The principal objectives of the present study were to ascertain how the VM responded to 14 days of microgravity exposure and to determine if hindlimb unloading under earthside condition was comparable. Three experimental approaches were used: a histochemical evaluation of microscopic morphology, including fibers and capillaries, an assessment of biochemical composition, including protein, DNA and RNA concentrations and an estimation of metabolic capacity.

MATERIALS AND METHODS

VM muscles were obtained from each of the five rats exposed to 14 days of: flight (F) under conditions of of weightlessness, tail suspended (T) with hindlimbs unloaded, synchronous controls (S) treated comparably with weightless flight rats, vivarium controls (V) with environmental conditions comparable to synchronous subjects with vibration stress, and basal controls (B) which are sedentary subjects maintained under routine laboratory conditions. With the exception of the T rats, descriptions for each type of treatment will be provided (Grindeland et al., personal communication). Tail suspension for unloading the hindlimbs was initially described by Ilyin and Novikov (1980).

Muscles from five rats in each group were frozen in liquid nitrogen and shipped on dry ice. From each muscle a piece was taken from the belly for histochemical analysis. Muscle cross sections were stained for myosin ATPase under different pH conditions and used for distinguishing fiber types and capillaries as described in an earlier report (Musacchia et al., 1987). Fiber cross-sectional area (μm^2) and cell density (cells/μm^2) measurements were made and capillary density (cap/mm^2) was assessed using an automated image analysis system. Statistical differences between experimental groups were assessed by Student's t test.

A second portion of each muscle was utilized for protein, RNA and DNA determinations. Both contents (mg) and concentrations (mg/mg net weight) were determined. Procedures were previously described (Steffen and Musacchia, 1986). The remainder of each muscle was lyophilized and powdered with a Wiley Mill. Lactate dehydrogenase (LDH) and citrate synthase (CS) activities (μmol/min/gm) and triglyceride concentrations (mg/g) were measured on lyophilized samples (Pesce et al., 1964; Srere, 1969; Entenmann, 1957). For comparisons between various groups, analysis of variance was used to assess statistical significance.

RESULTS

During the course of two weeks all the rats gained weight (Table 1). The flight rats gained only 5% while the control groups gained between 10 and 18%. There were significant differences between body weights of rats in the V and B groups at the time of euthanasia. VM muscle weights are presented in Table 2. Wet weight of VM muscles of V controls were significantly larger than those of F rats.

The VM is composed chiefly of Type II fibers; however, there is a distinct portion that contains a mixture of Type I and II fibers. Cross-sectional areas were measured from locations of mixed fiber populations (Type I and Type II) and from areas where only the fast twitch fibers (Type II) were found. These data are presented in Figures 1 and 2. In these figures each column represents 250 measurements, 50 each from the muscles taken from the five animals in each group. In the mixed fiber portion (Fig. 1), the Type 1 fiber areas were significantly smaller in the F animals when compared to V, S, and B animals, and the Type II fibers were smaller in F animals compared

with all other groups. Type I fibers were comparably reduced in F and T subjects; however, the Type II fibers in T rats were not significantly different from those in the control groups. Thus, in the mixed fiber portion, the slow twitch fibers showed similar responses in the F and T subjects, while the fast twitch fibers were smaller only in F rats (Fig. 1). In that portion of the muscle chiefly composed of fast twitch fibers (Fig. 2), the F rats showed some reduction in areas when compared to V, T, and B groups, but not in S animals.

Fiber densities (number of fibers per mm^2) were assessed in the mixed portion (without differentiating between Types I and II) and in the predominantly Type II portion (Fig. 3). Each column represents 750 fibers, with 150 fibers measured for each animal in both unmixed portions. The fiber densities in both portions were larger in the F rats when compared to V, T, S, and B groups. In general, these data show an inverse relationship to the cross-sectional area measurements, particularly in the mixed portions from the VM in F animals.

The capillary densities presented in Figure 4 were assessed by counting 200 capillaries per animal in both mixed and unmixed portions; thus each column represents 1000 capillaries. These measurements are rather comparable to the fiber density measurements. The F animals have significantly greater numbers of capillaries in the mixed portion when compared with V, T, S, and B groups. In the Type II portion, with the exception of the reduction in capillaries in the V rats, others remained at comparable levels. The parallel relationship between fiber and capillary changes are seen in Figure 5. There were no significant differences between any of the five groups of rats.

Muscle protein content (mg) was similar in all groups with the exception of the vivarium controls, which had significantly greater protein contents (Fig. 6). In contrast, protein concentrations (mg/mg wet weight) ranged from 19-22% and did not differ statistically between any of the experimental groups. Muscle RNA content (μg) followed the pattern described for protein content, with the vivarium group exhibiting a significantly ($P<0.05$) greater content compared with all other groups (Fig. 7). RNA concentration (μg/mg wet weight) was also significantly greater in the vivarium animals compared with all other experimental groups. There were no significant differences in RNA content or concentration between the other experimental groups. DNA content (μg) and concentration (mg/g wet weight) exhibited a pattern comparable to that of muscle RNA. DNA content and concentration (Fig. 8) were both significantly greater in the vivarium animals compared with all the other groups. There were, however, no statistical differences in DNA content or concentration between any of the other experimental animal groups.

Anaerobic capacity of the VM was greater in the F compared to the S controls (Table 3). Similarly, V muscle anaerobic capacity was greater than T rat muscles. No significant differences existed between F or T muscles. On the other hand, no significant differences were observed in the oxidative capacity between any groups as estimated by citrate synthase activity (Table 4). Triglyceride stores of VM were greater in F compared to T, but neither were significantly different from any of the control groups (Table 5).

DISCUSSION

The vastus medialis presents a complex picture of responses to unloading. Our data show that the Type II fibers, in both the mixed portion and the unmixed portion, were affected by 14 days of weightlessness. This was particularly evident in those reduced cross-sectional areas in Type I fibers measured in the mixed portion of the muscle, which averaged between 20-30%. It is notable that there was a similar atrophy in F and T slow twitch fibers in the mixed portion of the VM, suggesting a good correlation between ground-based and flight protocols. Although non-load bearing muscles chiefly composed of Type II fibers are generally considered to be much less responsive to unloading, it was notable that there were significant losses in cross-sectional areas (10-15%) in these fibers from the mixed portion F animals. The view that significant changes can

occur even in predominantly Type II muscles was evidenced by the increase in fiber densities in F animals. This occurred in both the mixed portion and in the unmixed portion of VM. Responses of the VM in tail suspended rats were similar to that of F rats in Type I fiber area changes. Type II fiber responses in T rats were not significantly different from those observed in the control groups.

Analysis of biochemical parameters consistently indicated greater content of protein, RNA, and DNA in vastus medialis muscles from the vivarium animals compared with the other experimental groups. This is not surprising in light of the direct relationship between protein content and muscle weight. Vastus medialis weights (Table 2) averaged from 13-23% greater in the vivarium animals than in other groups. The explanation for greater RNA and DNA concentrations in the vivarium group as well is unknown. There is no *a priori* rationale for anticipating significant increments in these parameters in this group. It is of interest that the vivarium control group also exhibited an increased protein concentration in the vastus medialis from rats on the previous COSMOS 1887 biosatellite mission (Musacchia et al., 1988).

Due to the protocol followed in this study, less dry tissue was available for analysis. Results were similar to those found in COSMOS 1887, in that the VM showed only small alterations in metabolic capacity as a result of flight. However, part of this lack of significant differences could be due to a great deal of variability in control group body weights, as well as differences in muscle weights between the time of sacrifice and the time they were analyzed in our lab.

Similar results were noted on COSMOS 1887, in that the F rats' VM contained the greatest concentration of triglyceride stores and the B and V rats' the least. This may pertain to the feeding regimens used rather than any effect specific to flight conditions.

From these VM studies several conclusions can be made. There are some significant changes in the VM in rats exposed to weightlessness for 14 days. There is a loss in weight when compared to the vivarium controls but not in comparison to the other controls. While there were minimal muscle weight differences between groups, muscle weights may be a less sensitive measure of change or atrophy than fiber area measurements. Losses in fiber area and increases in fiber density of F animals were qualitatively similar to those seen in soleus and EDL taken from rats after 7 days of weightless flight in SL3 (Musacchia et al., 1990). These results suggest that even non-load bearing muscles, such as the VM, show measurable responses to weightless flight. Biochemical responses, most evident in the V group, were clearly related to muscle weight. Metabolic studies indicate small reductions in this fast twitch muscle, with a tendency for increased anaerobic capacity.

ACKNOWLEDGEMENTS

The investigators would like to acknowledge the help of the Soviet dissection team headed by Dr. A.S. Kaplansky and the excellent technical assistance of M.J. Dombrowski in the histochemical studies.

REFERENCES

1. Ariano, M.A., R.B. Armstrong, and V.R. Edgerton. Hindlimb Muscle Fiber Populations of Five Animals. J. Histochem. Cytochem. 21:51-55, 1973

2. Armstrong and Phelps. Muscle Fiber Type Composition of the Rat Hindlimb. Am. J. Anat. 171:259-272, 1984.

3. Entenmann, C. General Procedures for Separating Lipid Components of Tissue. Methods in Enzymol. 3:301-302, 1957.

4. Ilyin, E.I. and V.Y. Novikov. A Stand for Simulation of Physiological Effects of Weightlessness in Laboratory Experiments on Rats. Kosm. Biol. Aviakosmich. Med. 3:79-80, 1980.

5. Ilyina-Kakueva, E.I., V.V. Portugalov, and N.P. Krivenkova. Space Flight Effect on Skeletal Muscles of Rats. Aviat. Space Environ. Med. 4(7):700-703, 1976.

6. Martin, T.P., V.R. Edgerton, and R.E. Grindeland. Influence of Spaceflight on Rat Skeletal Muscle. J.Appl. Physiol. 65(5):2318-2325, 1988.

7. Musacchia, X.J., J.M. Steffen, R.D. Fell, and J. Dombrowski. Skeletal Muscle Response to Spaceflight, Whole Body Suspension, and Recovery in Rat. J. Appl. Physiol. 69(6):2248-2253, 1990.

8. Musacchia, X.J., J.M. Steffen, R.D. Fell, and J. Dombrowski. Comparative Morphology of Fibers and Capillaries in Soleus Following Weightlessness and Suspension. The Physiologist. 31:A32, 1988.

9. Musacchia, X.J., J.M. Steffen, R.D. Fell, and J. Dombrowski. Physiological Comparison of Rat Muscle in Body Suspension and Weightlessness. The Physiologist. 30 .(No.1 Suppl.):S102-S105, 1987.

10. Musacchia, X.J., D.R. Deavers, G.A. Meininger, and T.P. Davis. A Model for Hypokinesia: Effects on Muscle Atrophy in the Rat. J. Appl. Physiol. 48:479-486, 1980.

11. Pesce, A., R.H. McKay, F. Stolzenback, R.D. Cahn, and N.O. Kaplan. Comparative Enzymology of LDH. J. Biol. Chem. 239:1753-1761, 1964.

12. Riley, D.A., S. Ellis, G.R. Slocum, T. Satyanarayana, L.W. Bain, and F.R. Sedlak. Hypogravity-Induced Atrophy of Rat Soleus and Extensor Digitorum Longus Muscles. Muscle and Nerve. 10:560-568, 1987.

13. Srere, P.A. Citrate Synthase. Methods in Enzyml. 13:3-5, 1969.

14. Steffen, J.M. and X.J. Musacchia. Effect of Hypokinesia and Hypodynamia on Protein, RNA, and DNA in Rat Hindlimb Muscles. Am. J. Physiol. 247(16):R728-R732, 1986.

TABLE 1

BODY WEIGHTS (grams) AT TIME OF LOADING AND EUTHANASIA

	Loading	Euthanasia
Flight	321 ± 2	338 ± 2
Vivarium	298 ± 1	363 ± 2
Tail Suspended	298 ± 1	339 ± 10
Synchronous	307 ± 3	343 ± 7
Basal		320 ± 4

TABLE 2

WET WEIGHTS OF VASTUS MEDIALIS MUSCLES

	mg Wet	mg/B.W.	mg Frozen**
Flight	294.6 ± 10.6+	0.87 ± 0.03	280.2 ± 9.4
Vivarium	356.8 ± 18.2*	0.98 ± 0.05	355.4 ± 15.9
Tail Suspended	302.8 ± 25.2	0.89 ± 0.06	286.4 ± 23.4
Synchronous	290.8 ± 32.2	0.89 ± 0.10	280.2 ± 31.1
Basal	317.0 ± 25.3	0.99 ± 0.07	301.2 ± 21.4

+ Mean ± S.E.
* Significantly different from Flight ($P<0.05$)
** There was apparently a small freeze drying artifact produced through preparation and storage of muscles. At the time of use, most muscle weights were lower than those obtained for fresh tissue.

TABLE 3

ANAEROBIC CAPACITY IN VM

Treatment	Lactate Dehydrogenase Activity (μmol / min / g)
Flight	1307 ± 92*
Vivarium	1364 ± 84
Tail Suspended	996 ± 46**
Synchronous	860 ± 41
Basal	1341 ± 82

* significantly different from S
** significantly different from V

TABLE 4

OXIDATIVE CAPACITY IN VM

Treatment	Citrate Synthase Activity (μmol / min / g)
Flight	85 ± 0.9
Vivarium	107 ± 3.8
Tail Suspended	78 ± 9.1
Synchronous	98 ± 10.6
Basal	80 ± 3.3

TABLE 5

TRIGLYCERIDE STORES IN VM

Treatment	Triglyceride (mg / g dry weight)
Flight	45 ± 5.6*
Vivarium	18 ± 3.3
Tail Suspended	12 ± 4.3
Synchronous	24 ± 7.1
Basal	36 ± 11.0

* significantly different from T

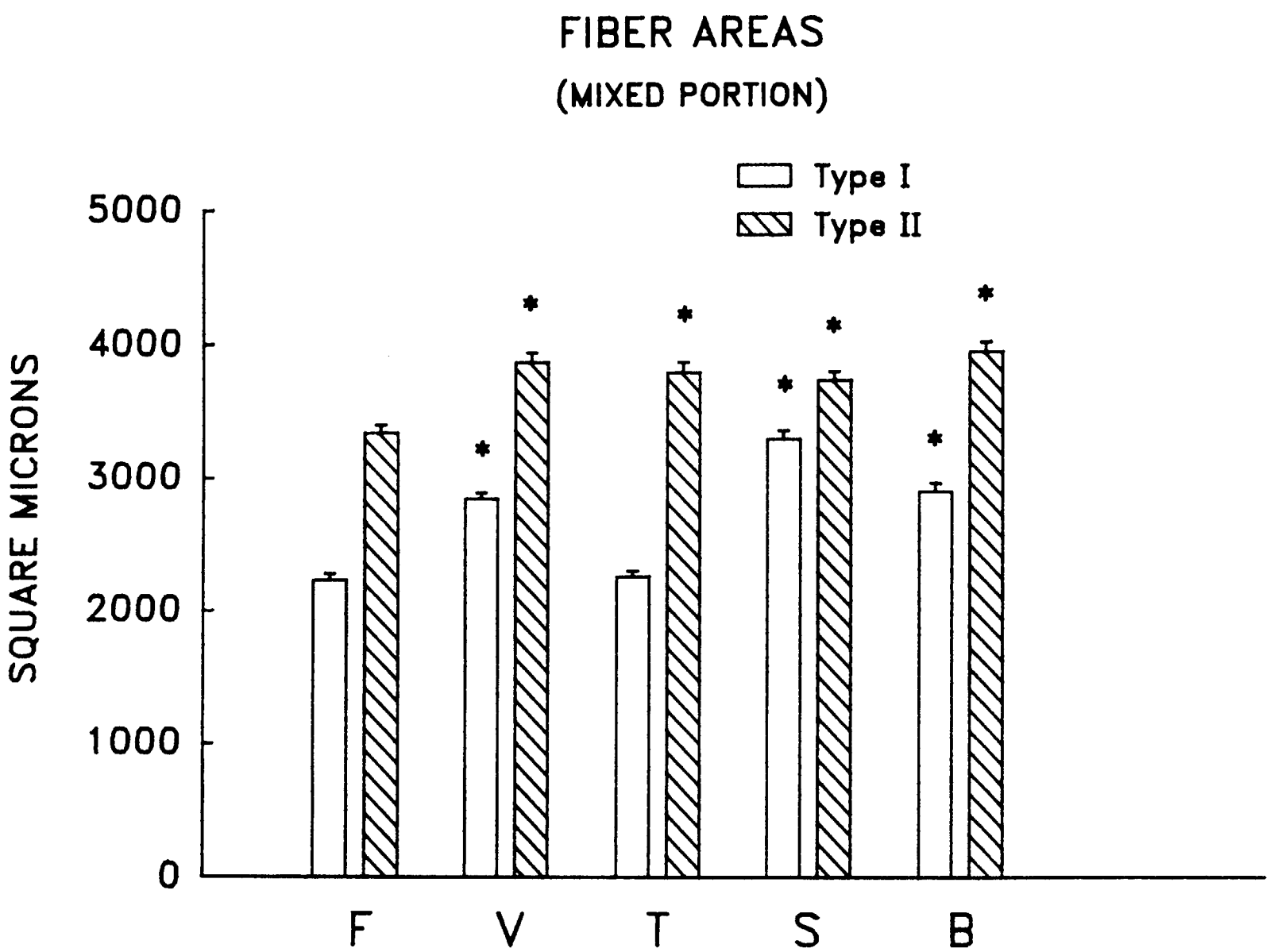

*Figure 1. Cross-sectional areas of Type I and Type II fibers in the portion of muscle with mixed fiber population. Means and S.E. are given. * indicate significant differences ($p<0.05$) from flight (F) rats.*

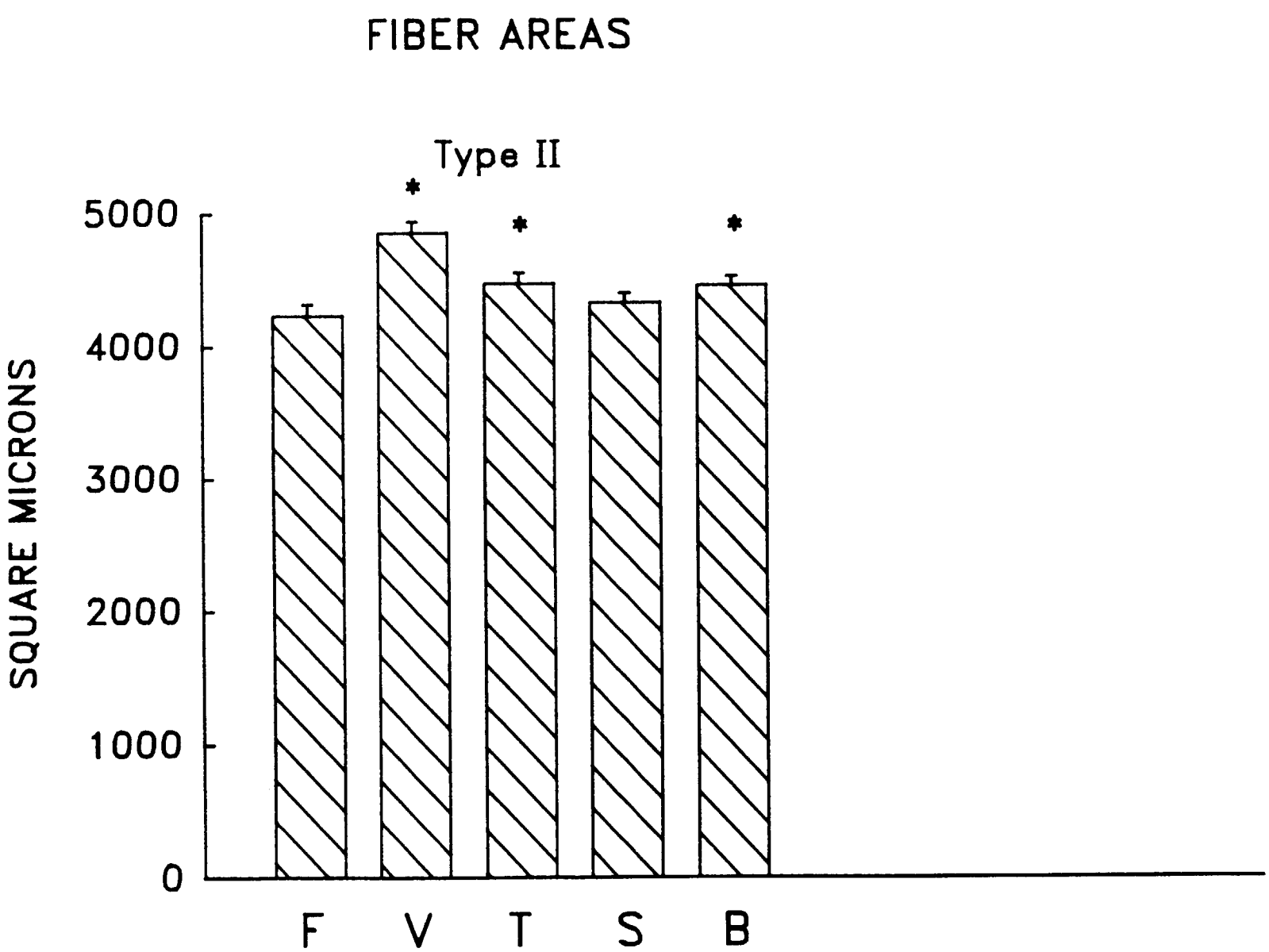

*Figure 2. Cross-sectional areas of Type II fibers in the portion of muscle with predominant population of twitch fibers. Means and S.E. are given. * indicate significant differences from flight (F) rats.*

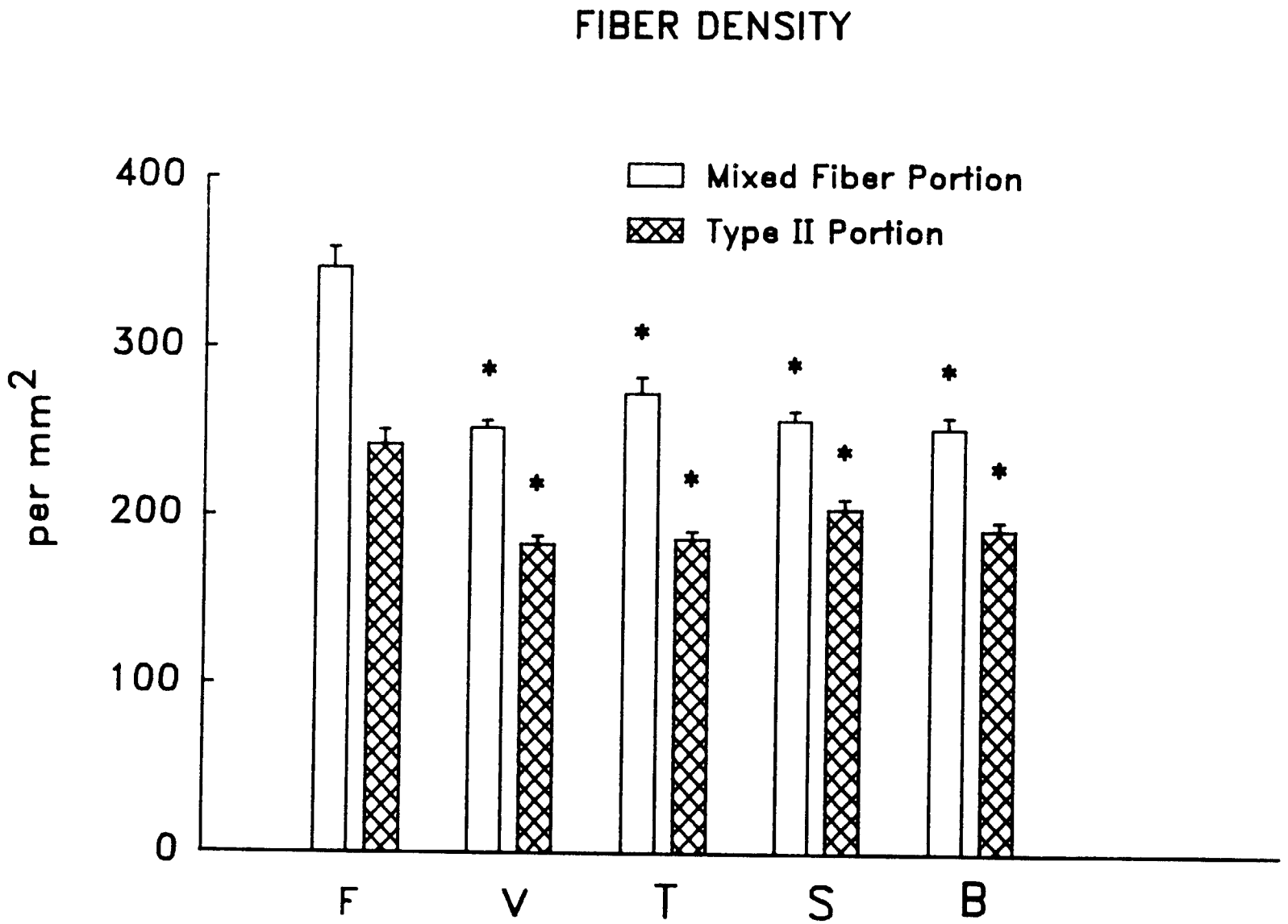

*Figure 3. Fiber densities, both Type I and Type II fibers in the portion of muscle with mixed fiber population (open columns), and Type II fibers only in the portion of muscle with predominant population of fast twitch fibers (cross hatched columns). Means and S.E. are given. * indicate significant differences (P<0.05) from flight (F) rats.*

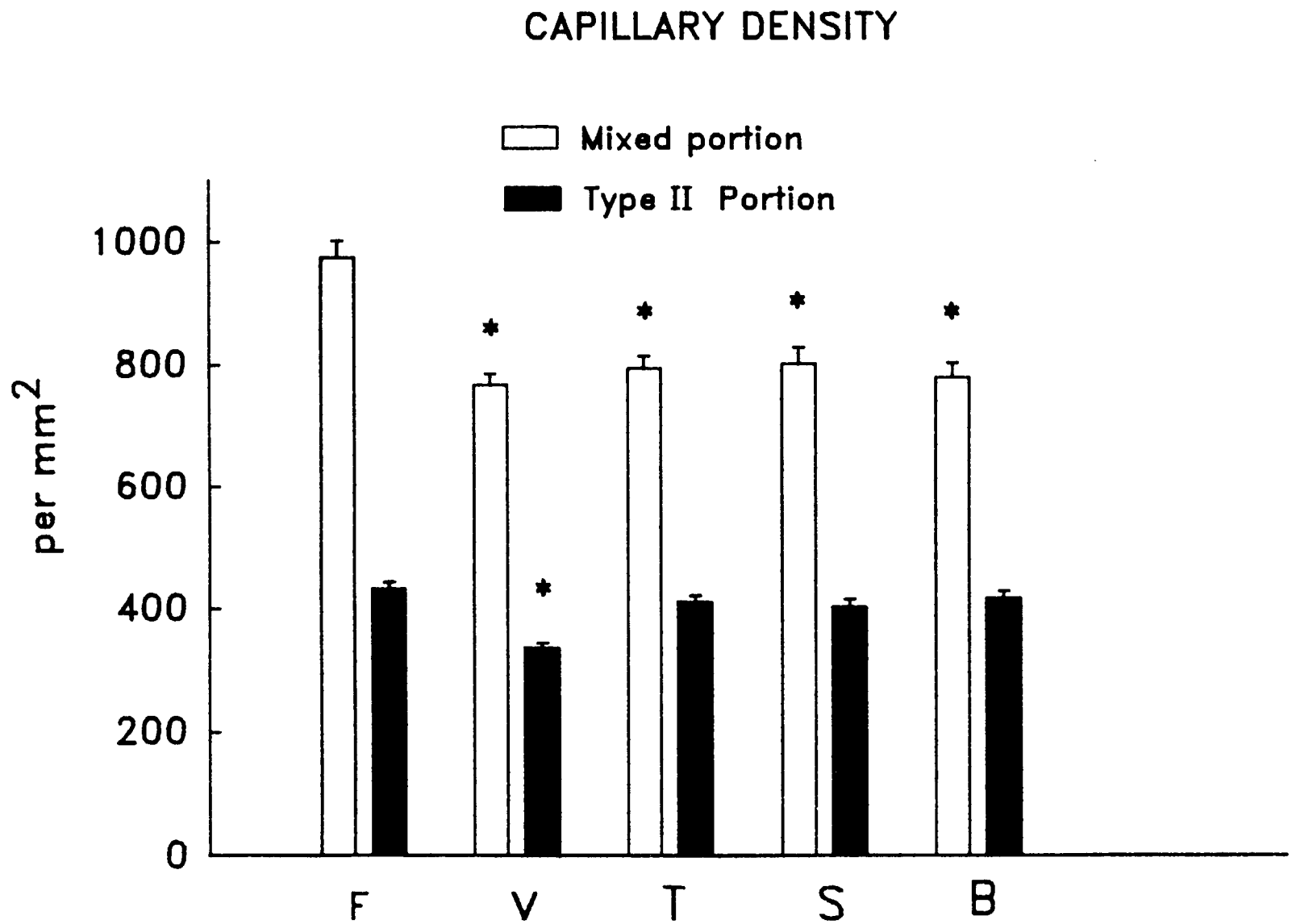

*Figure 4. Capillary densities in the portion of muscle with mixed fiber population (open columns) and in the portion of muscle with predominant populations of fast twitch fibers (solid block columns). Means and S.E. are given. * indicate significant differences (P<0.05) from flight (F) rats.*

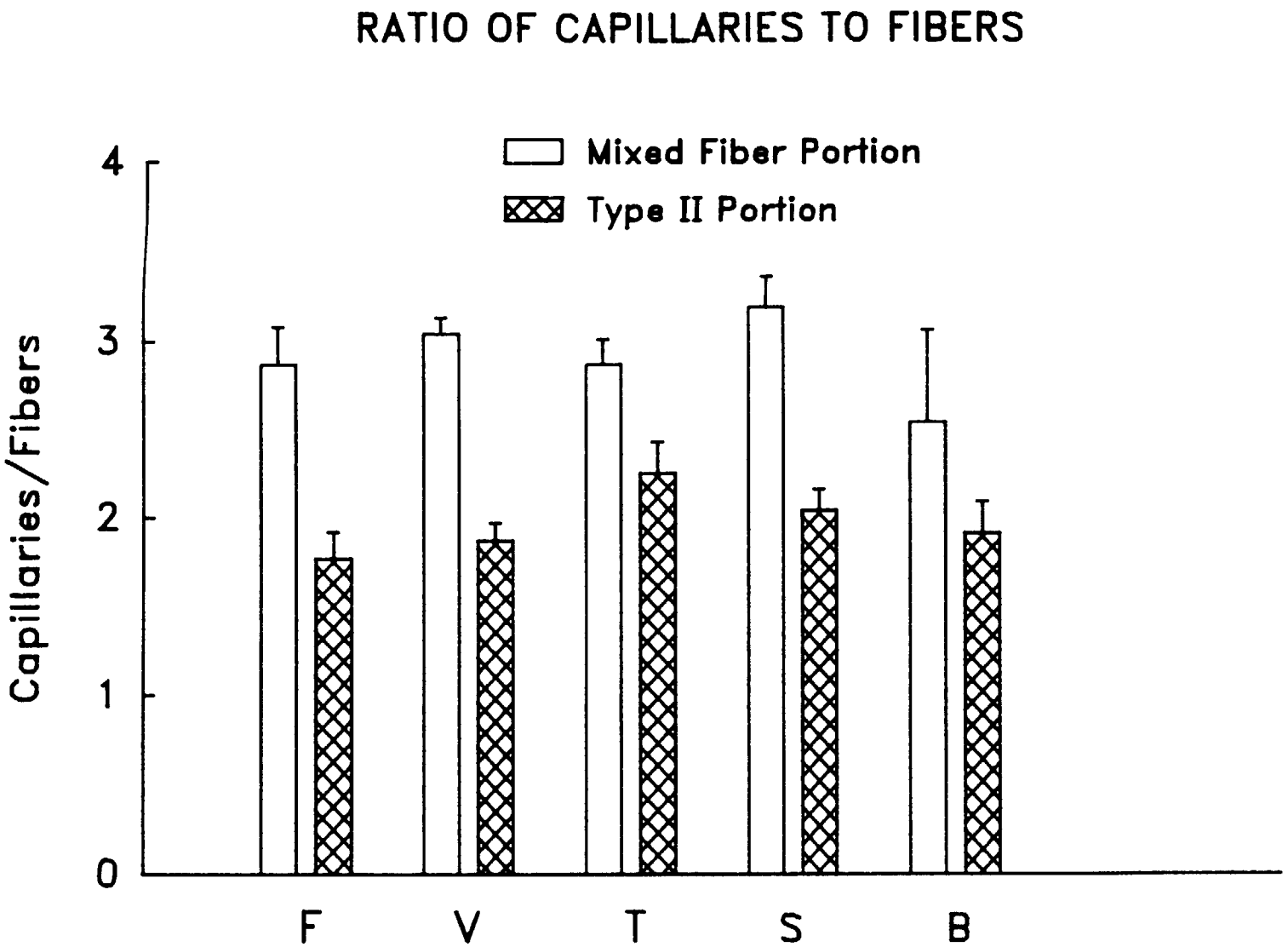

Figure 5. Ratio of capillaries to fibers in the portion of muscle with mixed fiber population (open columns) and in the portion of muscle with predominantly fast twitch fibers (cross hatched columns). Means and S.E. are given.

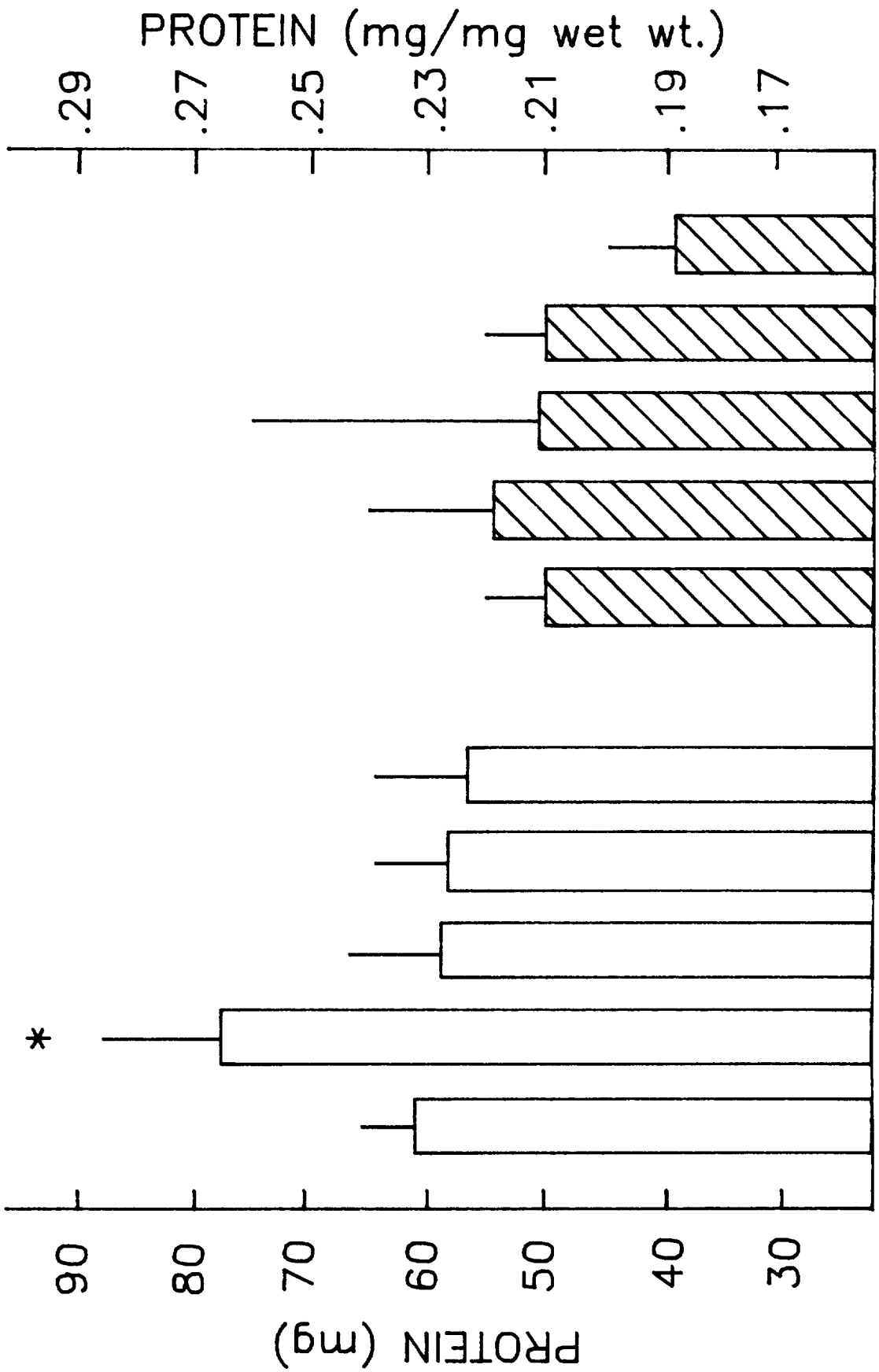

*Figure 6. Protein content (open columns) and concentration (cross hatched columns) in vastus medialis muscles. Mean and S.E. are given. * indicates significantly different (P<0.05) from all other groups.*

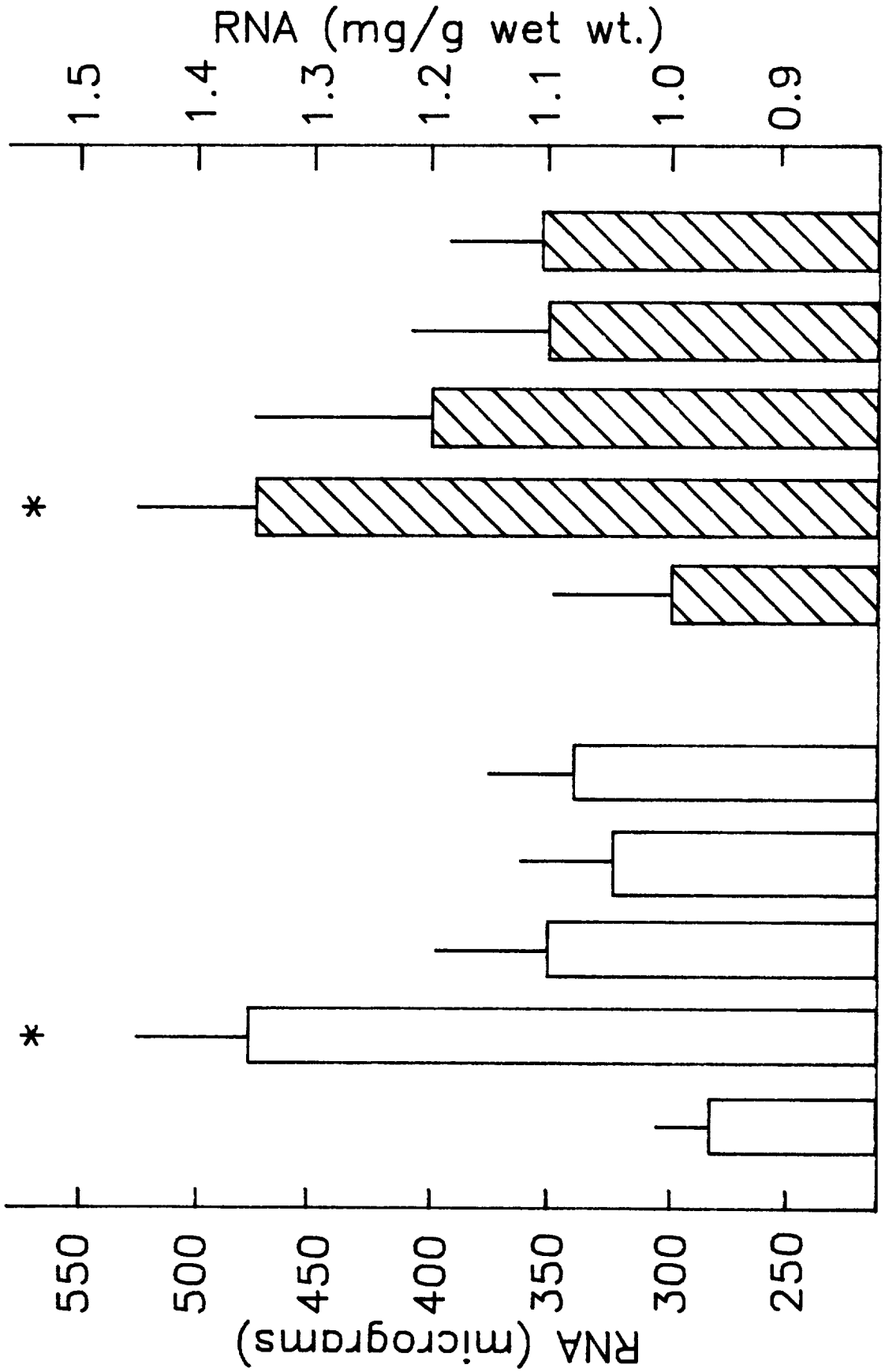

*Figure 7. RNA content (open columns) and concentration (cross hatched columns) in vastus medialis muscles. Mean and S.E. are given. * indicates significantly different ($P<0.05$) from all other groups for RNA content and from all other groups except T for RNA concentration.*

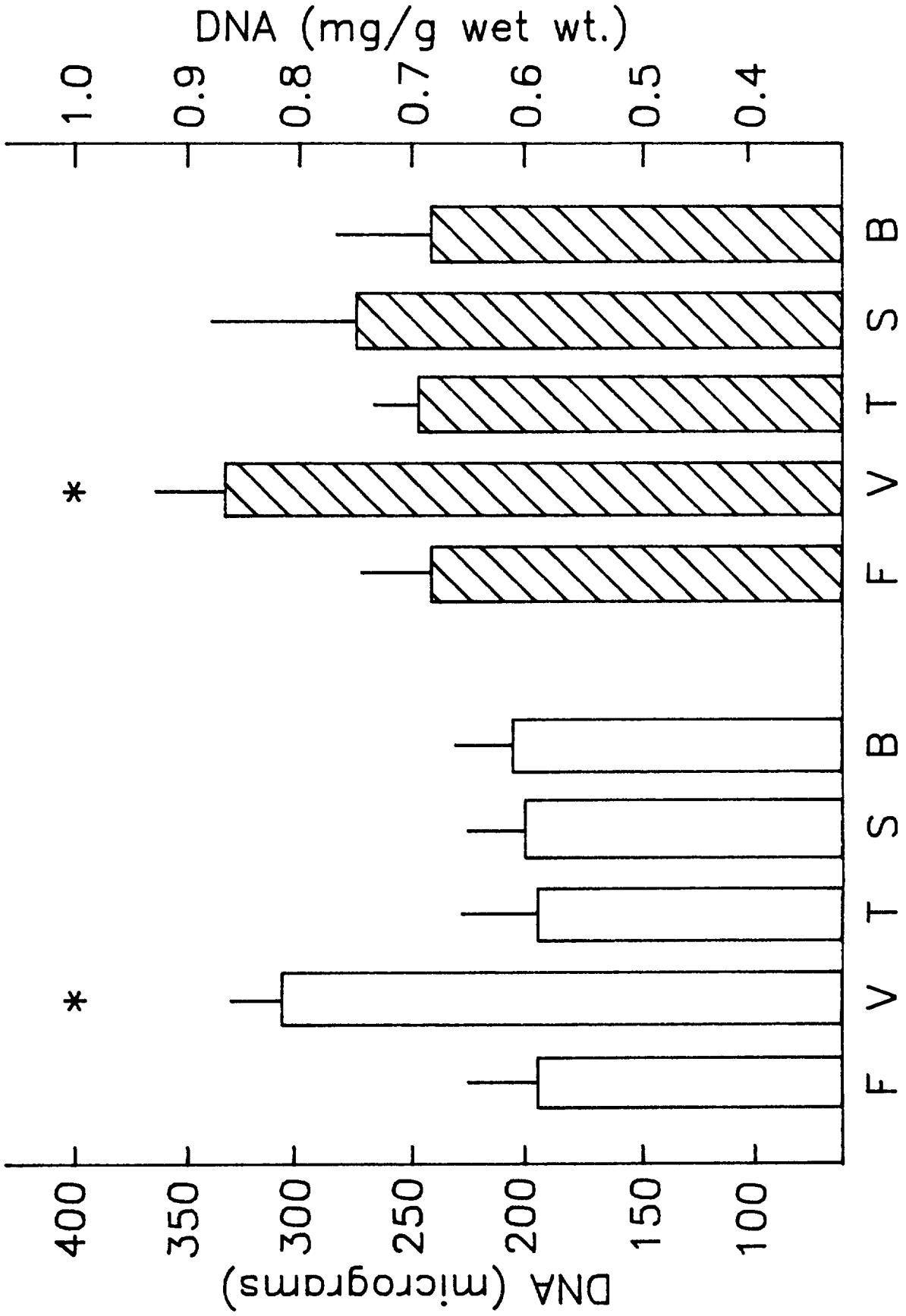

*Figure 8. DNA content (open columns) and concentrations (cross hatched columns) in vastus medialis muscles. Mean and S.E. are given. * indicates significantly different ($P<0.05$) from all other groups for DNA content and for all groups except S for DNA concentration.*

EXPERIMENT K-7-09

MORPHOLOGICAL, HISTOCHEMICAL, IMMUNOCYTOCHEMICAL, AND BIOCHEMICAL INVESTIGATION OF MICROGRAVITY-INDUCED NERVE AND MUSCLE BREAKDOWN

PART I: MUSCLE BIOCHEMISTRY

PART II MUSCLE STUDIES

Principal Investigator:

D A. Riley
Medical College of Wisconsin
Milwaukee, WI

Co-investigators:

S. Ellis
San Jose State University
San Jose, CA

A. L. Haas
G. R. Slocum
J. L. W. Bain
Frank R. Sedlak
Medical College of Wisconsin
Milwaukee, WI

J. F.Y. Hoh
University of Sydney
Sydney, Australia

C.S. Giometti
Argonne National Laboratory
Argonne, IL

E. I. Ilyina-Kakueva
V. S. Oganov
Institute of Biomedical Problems
Moscow, USSR

EXPERIMENT K-7-09

MORPHOLOGICAL, HISTOCHEMICAL, IMMUNOCYTOCHEMICAL, AND BIOCHEMICAL INVESTIGATION OF MICROGRAVITY-INDUCED NERVE AND MUSCLE BREAKDOWN

PART I: MUSCLE BIOCHEMISTRY

D.A. Riley, S. Ellis, A.L. Haas, G. R. Slocum, J. L. W. Bain, F.R. Sedlak, J.F.Y. Hoh, E.I. Ilyina-Kakueva, and V.S. Oganov.

SUMMARY

The present work reconfirms that adductor longus (AL) muscle fibers atrophy during spaceflight and tail suspension (hindlimb unloading). However, the mean wet weight of flight AL muscles was near normal whereas that of the suspended AL muscles was significantly decreased. Interstitial edema, not present in the suspended AL, largely accounts for this finding. SO fibers are more atrophied than FOG and FG fibers, and SO fibers synthesize fast myosin, producing hybrid fibers containing both slow and fast myosin isoforms. In the flight AL, absolute mitochondrial content decreases but the relatively greater breakdown of myofibrillar proteins maintains mitochondrial concentration near normal in the central regions of fibers. Subsarcolemmal mitochondria are preferentially lost and decrease below normal. Upon return to weightbearing, the weakened muscles exhibit eccentric contraction-like lesions, disruption of the sarcomeres and the supporting connective tissue, and the thrombosis of the microcirculation. Segmental necrosis of muscle fibers, denervation of neuromuscular junctions, and extravasation of rbc's was minimal. The lymphocyte antibody markers did not indicate a significant immune reaction. The flight AL exhibited more eccentric lesions than the suspended AL; the high reentry G forces experienced by the flight animals, but not the suspended group, appear to explain this difference. Muscle atrophy appears to increase the tendency to form eccentric contraction-like lesions following reloading; this may reflect weakening of the muscle fiber cytoskeleton and extracellular matrix. Microcirculation is also compromised by spaceflight such that there is increased formation of thrombi in the postcapillary venules and capillaries. The blockage leads to edema within a few hours of resuming weightbearing and 2 days later, extensive tissue necrosis and microhemorrhages as

observed in Cosmos 1887. The possibility exists that muscle-derived emboli will travel to the lungs, producing a more serious health problem. Countermeasures designed to maintain the health of the muscle and the organism during spaceflight and upon return to Earth's gravity will have to deal effectively with the multifaceted nature of the problem which clearly goes beyond simple muscle fiber atrophy.

INTRODUCTION

Extended exposure of humans to spaceflight produces a progressive loss of muscle strength. The mechanism of this process must be defined in order to construct rational countermeasures. Our previous flight investigation of rats flown 1 week aboard Spacelab 3 revealed that the majority of the soleus fibers exhibited simple atrophy, but up to 1% showed segmental necrosis [32]. Rats orbited for 2-3 weeks during previous Cosmos Biosatellites missions manifested more severe atrophy and greater tissue necrosis, suggesting that the degenerative processes were progressive [2,11,17-20,33,37]. Another contributing factor to consider is that the amount of tissue necrosis appears to increase with longer exposure of the flight rats to terrestrial gravity [18,33]. The purpose of the present investigation was to examine hindlimb muscle from flight rats killed as close to landing as possible so that changes induced by spaceflight and early readaptation to weightbearing can be defined and compared with those present after the longer exposure of Cosmos 1887.

METHODS

Tissue Acquisition and Processing

The adductor longus (AL), extensor digitorum longus (EDL) and plantaris (Plt) muscles were excised immediately from 5 flight rats killed by decapitation 9-12 hours after landing. The same muscles were obtained from the basal, vivarium, and synchronous ground-based controls as well as tail suspended (hindlimb unloaded) rats (n=5/group). No investigations were made on the soleus muscles from this mission because, unlike Cosmos 1887, Dr. Edgerton was unable to supply tissue sections. The synchronous group alone was subjected to simulated launch vibration (50-70 Hz, 0.4 mm amplitude, for 10 min) and acceleration (4G for 10 min, constant 7 min) and reentry deceleration (6G for 5 min, constant 3 min) and impact (50G for 10 msec); these values are generic for Soviet biosatellite missions. The suspended animals were returned to weightbearing before decapitation on a schedule matching that of the flight rats. One third each of the AL and EDL muscles were pinned on a mild stretch to plastic sticks and immersion fixed for electron microscopy in 4% glutaraldehyde, 2% paraformaldehyde, 0.1 M cacodylate buffer (pH 7.2), and 5 mM $CaCl_2$. After buffer rinses, specimens were postfixed with 1.3% OsO_4 and stored in cacodylate buffer at 2-10°C for 3-6 weeks until processed into epoxy resin. Semithin sections (0.5 µm) were cut and stained with toluidine blue and used to determine the characteristics of focal, eccentric contraction-like lesions and to identify regions of interest for ultrastructural examination. Ultrathin sections were cut and poststained with uranyl acetate and lead citrate and examined in a JEOL 100 CXII electron

microscope. The data described in this report were derived from tissues sampled in regions not distorted by dissection or other artifacts.

Whole Plt muscles and the remaining portions of AL and EDL muscles were both quick frozen and stored in liquid nitrogen until utilized. Cryostat sections (6-10 μm) were cut for biochemical, histochemical and immunohistochemical studies. Following completion of serial sectioning for histological staining, ten to fourteen 10 μm frozen sections were collected on the knife and dissolved *en masse* in 100 μl of a solution (62.5 mM Tris-HCl, pH 6.8, 10% glycerol, 5% 2-mercaptoethanol and 2.3% sodium dodecyl sulfate) that had been heated for 5 minutes in boiling water. After cooling to room temperature, the solution vial was capped tightly and frozen at -80°C. These frozen samples, along with portions of the EDL and Plt muscles were shipped on dry ice to Dr. Ellis who performed 2-D gel electrophoresis and enzyme assays; the biochemical results are reported separately.

Tissue Staining and Analysis

The serial sections were collected on plain glass or 0.05% chrome alum-0.5% gelatin-coated slides and histochemically reacted for endplate acetylcholinesterase counterstained with hematoxylin and eosin, alkaline and acid myofibrillar ATPase colored conventionally with ammonium sulfide or toluidine blue to reveal mast cells, and mitochondrial a-glycerophosphate and succinic dehydrogenases as performed previously [31-34]. Indirect immunofluorescence or immunoperoxidase was utilized to localize antibodies against ubiquitin conjugates, tripeptidyl aminopeptidase, C3 component of complement, IgG, fibrinogen, fixed tissue macrophages (ED-2), blood monocytes (ED-1), Ia antigen (OX-6), cytotoxic and suppressor T cells (OX-8), Rt-Ia antigen (OX-18), all peripheral T cells (P4/16), granulocytes (MOM), pan T cells and neutrophils (W3/13), platelet IIb IIIa fibronectin receptor, red blood cell (rbc)/endothelial cell antigen, fast myosin, and slow myosin [12,14,15,30]. In all cases, control sections were treated with second antibody alone and the primary antibody solution was replaced with an appropriate serum or PBS. Sections exposed solely to PBS were examined to ascertain the levels of endogenous autofluorescence. All of the positive immunostaining described in Results was eliminated when the primary antibodies were omitted. The sources for the antibodies used were Organon Teknika Corporation-Cappel (C3, IgG, fibrinogen, rbc), Serotec Bioproducts for Science (ED-2,ED-1,OX-8,P4/16,MOM,W3/13,W3/25), Seralab Accurate Chemical & Scientific Corporation (OX-6,OX-18), Dr. A.L. Haas (ubiquitin conjugates), Dr. J.F.Y. Hoh (fast and slow myosins), Dr. S. Ellis (tripeptidyl aminopeptidase) and Dr. T. Kunicki (platelet IIb IIIa) [12,14,15,30].

Because of the marked regional fiber type differences in the AL and the variability of which region remained for light microscopy after removal of the electron microscopy portion, the central third of the AL muscle section, common to all light microscopic specimens, was studied to determine the percentages of fibers showing segmental necrosis, fiber type areas, fiber type percentages, and mast cell number (Fig. 1). The percentages of fibers with segmental necrotic lesions in acetylcholinesterase/hematoxylin & eosin-stained sections we

determined for all groups, except the synchronous group which was inexplicably destroyed by ice crystal artifact before arrival at our laboratory. Fast-twitch glycolytic (FG), fast-twit oxidative glycolytic (FOG), and slow-twitch oxidative (SO) fiber types were classified as defined previously [32]. In alkaline ATPase-reacted sections of AL muscles, moderately staining fibers were designated intermediates (I). The alkaline ATPase sections were used for measurement of fiber cross sectional areas in all groups. Areas of at least 30 fibers of each type were determined by computerized planimetry (Bioquant System IV). Mast cells were counted in the toluidine blue-stained alkaline ATPase sections.

In the flight, synchronous, tail suspended and vivarium groups, estimates of interstitial edema for the AL and EDL muscles of were made by quantifying the percentage area of muscle fibers and non-muscle fiber connective tissue within longitudinal, toluidine blue-stained plastic sections (0.5 μm). The measurements were conducted utilizing the Video Counting & Microdensitometry and MEG X programs of the R&M Bioquant System IV. These sections from the midbelly endplate region and distal ends of the muscle were also used to document the occurrence, length, and areas of eccentric contraction-like lesions (2 or more disrupted sarcomeres) on otherwise normal-appearing fibers. Overall, 3-22% of the fibers were rejected from sampling because they appeared distorted from tissue processing artifacts. Qualitative atrophic changes in muscle fibers, nerves, neuromuscular junctions, microcirculatory vessels, interstitial tissue and the myotendinous junctions were assessed by surveying thin sections of AL and EDL muscles from the vivarium, synchronous, tail suspended and flight groups. Ultrastructural quantitation of mitochondrial changes were performed for flight and vivarium AL's as described previously [32]; the vivarium control muscles were from Cosmos 1887 because the side of the AL taken for electron microscopy matched that of the Cosmos 2044 samples. This comparison is valid because the vivarium controls from the two missions are the identical strain of rats obtained from the same source, and they are closely matched for body weight and age. Statistical treatment of data employed appropriate parametric or nonparametric tests as indicated.

RESULTS

Muscle Atrophy and Fiber Type Changes

When compared to the synchronous, flight, basal, and vivarium animals, the mean wet weight or average AL muscle-weight to body-weight ratio of suspended rats was significantly ($p<0.05$) decreased (T Tukey LSD after Box-Cox trans-formation). There were no differences between groups for the EDL muscle wet weights. At the muscle fiber type level, the areas of SO fibers of the flight and suspended AL muscles were not equal to the vivarium control ($p<0.05$, Tukey HSD); the flight AL muscles were decreased 32% in area, and those of the suspension rats were down by 36%. The intermediate and FOG fiber types were not significantly different. As in the AL, the SO fibers of the Plt exhibited significant atrophy (around 20%) whereas changes in the other fiber types were not different when flight was compared to synchronous and

suspension was compared to vivarium ($p<0.01$, Student t test). For the EDL, the SO fibers of the flight rats showed a 17% increase ($p<0.05$, Student t test) when compared to the synchronous controls; no significant differences were present between the other groups and other fiber types.

When the percentages of SO and intermediate fibers in the AL muscles of flight, synchronous, and vivarium groups were compared by a Kruskall-Wallis test, there was a significant ($p<0.05$) decrease of 26% in SO fibers. The intermediate fibers increased by 14-18%, and the FOG fibers were up by 8-11%, but these changes did not test significant. The increase in fibers staining darkly for alkaline myofibrillar ATPase implied elevated expression of fast myosin in SO fibers during atrophy induced by spaceflight and hindlimb unloading. This isozyme expression was demonstrated directly by the observation of increased numbers of fibers staining for both slow and fast myosin antibodies (Figs. 2-5).

At the ultrastructural level, a 53% decrease in subsarcolemmal mitochondria concentration was detected in the AL muscle fibers in the flight group compared to vivarium ($p<0.01$, Student t test, Box Cox transformation). This was consistent with the marked reductions of histochemical succinic and a-glycerophosphate dehydrogenases activities at the periphery of muscle fibers. The concentration of total intermyofibrillar mitochondria in the central regions of muscle fibers was down by 16% from controls, but this change did not test significant. Mitochondrial profiles in the A bands increased by 89% while I band mitochondrial concentration was down significantly by 22% ($p<0.05$, Student t test). Previous studies of the soleus muscle of 7-day-suspended rats revealed an increase in the ratio of cell surface membrane to muscle fiber area during atrophy [34]; in the present study, the ratio of surface membrane area to fiber area of the flight AL fibers was not different from that of vivarium control fibers.

Eccentric Contraction-like Lesions

Eccentric (lengthening) contraction-like lesions were defined as foci in which the A bands of at least 2 contiguous sarcomeres had an extracted depolymerized appearance, and the Z bands were widely separated as if excessively pulled apart (Fig. 6). This phenomenon frequently involved neighboring muscle fibers at the same level (Fig. 6). The stretch-like lesions were only detected in the AL muscle fibers of the flight and tail suspended groups. In the flight AL, 47% of the fibers had at least one lesion whereas 15% of the fibers were affected in suspended muscles. The average lesion area% was 2.3% for flight and 0.3% for suspension. In the flight AL, lesions were generally longer (median length, 18 μm) and wider, involving more sarcomeres, than the lesions (median length, 11 μm) in the suspended animals (Fig. 7). In the flight AL, the occurrences of lesions were similar in the midbelly and distal regions.

Ultrastructurally, these lesions showed a disrupted tangle of broken thick and thin filaments markedly diminished in numbers, and the Z bands were smeared in appearance and less dense than adjacent intact Z bands (Fig. 8). Amazingly, helical polyribosomes characteristic of translation of myosin mRNA [35] were common

within the lesions, indicating synthesis of contractile proteins to repair the damage (Fig. 9). Mitochondria and the T and SR membranes, though displaced, appeared largely intact, consistent with a shearing lesion of the myofibrils, limiting damage to within the muscle fiber leaving the cell membrane intact. The endomysium next to indented regions of fibers with peripheral eccentric-like lesions sometimes appeared physically separated, as if torn at the time that the fiber was stretched (Fig. 10). Similar indented regions in control fibers did not show damaged endomysium (Fig. 11).

The myotendinous junctions of flight AL muscle fibers were compared with those of synchronous control fibers. In the controls, the finger-like extensions of the fibers that interdigitated with the connective tissue matrix and cells of the tendon were solidly packed with myofibrils (Fig. 12). In contrast, the muscle fiber projections were sparsely filled with thin myofibrils in the flight AL, and the junction between the muscle fiber and the matrix of the tendon was indistinct (Fig. 13).

Microcirculatory Changes and Interstitial Edema

Marked regional thrombosis was detected immunohistochemically by the platelet, rbc, and fibrinogen antibodies in the AL muscles of the flight rats (Figs. 14-16). Ultrastructural examination of these regions demonstrated that most of the thrombi were in the postcapillary venules and, to some extent, capillaries (Figs. 17,18). A low level of rbc extravasation was present (Fig. 17,28). Activated platelets showed degranulation (Figs. 18,19). The rbc's in thrombi lost their discoid shape whereas those trapped by post-mortem pooling retained their biconcave discoid shape (Figs. 18-20). Electron dense, coarse fibrin-like deposits [26] were common in the connective tissue and within clogged microvessels (Figs. 18,21); this distribution agreed with the interstitial and intravascular immunostaining observed for fibrinogen antibodies (not illustrated). Discontinuity of the endothelium was prevalent in the thrombotic vessels of the flight AL but very rarely encountered in the AL muscles of the controls (Figs. 19,22).

Within the thrombotic region, the fixed-tissue macrophages, resolved by ED-2 antibodies and electron microscopy, were mildly hypertrophied in the flight AL compared to the basal, vivarium, synchronous, and suspension groups (Fig. 23). The MOM antibodies revealed an increase in granulocytes compared to the controls (Figs. 24,25); at the electron microscopic level, it appeared that neutrophils were the predominate granulocyte type present. The level of OX-6 staining was somewhat increased, indicating elevated expression of Ia antigen by fixed tissue macrophages. The ED-1 antibodies for monocytes did not show increased staining. None of the markers for cytotoxic and suppressor T cells (OX-8), RT-Ia on mature T cells, lymphocytes (OX-18), all peripheral T cells (P4/16), and monocytes and helper T cells markers (W3/25) were noticeably different from the AL muscles of the control rats; this suggested a lack of a significant immune reponse at the time point examined.

The non-muscle fiber area of the vivarium control AL was about 6.5%. The atrophic AL of the suspended group was similar (7.0%), indicating no change in interstitial

tissue area. In the flight AL, the non-muscle fiber interstitial area increased to 15%, suggestive of edema. The EDL and Plt non-muscle fiber areas of experimental and control animals were not different . High levels of mast cell degranulation did not appear in any of the muscles because no differences in mast cell number/muscle fiber number were found in the experiment and control groups for the AL, EDL, and Plt muscles; however, small amounts of mast cell secretion would not be detected by the toluidine blue stain [36]. In sections of vivarium, basal, tail suspended, and synchronous AL muscles, C3 and IgG showed low levels of immunostaining in the perimysium and endomysium. A slight elevation of this immunoreactivity was noted in the muscles of the flight rats. The widened interstitial region in the flight AL fibers was filled with C3 and IgG immunoreactivity, at somewhat higher than normal levels. Some necrotic fibers were surrounded and possibly infiltrated by these two proteins.

Tissue Damage

Within the sampled middle third of the AL, the percentage of muscle fibers with segmental, necrotic-like lesions (invasion by mononuclei cells, cell membrane fragmentation, and contraction clot formation) was about 2.3% for the flight muscles compared to none in the suspended and vivarium control animals (Fig. 23). Some of the necrotic fibers were intensely immunoreactive for slow myosin, indicating clumping of myofibrillar proteins (Fig. 4). They were also highly immunoreactive for ubiquitin conjugates, consistent with regions of high protein turnover (Fig. 26). Other fibers, which did not appear fragmented, exhibited a mottled appearance for ubiquitin conjugate staining (Fig. 26). The capillaries and venules in the thrombotic regions of the flight AL showed intense immunostaining for ubiquitin conjugates; non-thrombotic regions and control muscles had very little ubiquitin immunostaining in the microvessels (Fig. 26). Ultrastructural examination of cross sections of flight AL muscles in the thrombotic regions indicated that the mottled ubiquitin staining was associated with the eccentric sarcomere lesions within fibers with intact cell membranes, and the vascular staining reflected ubiquitin conjugates in the platelets aggregated in greater density than normal (Fig. 27). Tripeptidyl aminopeptidase immunoreactivity was generally higher in FOG and FG fibers of control and experimental rats; this protease was not elevated in lesioned fibers. The rare damaged neuromuscular junctions with fragmented terminals only occurred in the region of thrombi and heaviest muscle fiber damage (Fig. 28). Most neuromuscular junctions were intact, except for vacated postjunctional membrane seen in control and experimental muscles indicative of aging [4] (Fig. 29).

DISCUSSION

Many of the changes observed in this Cosmos 2044 biosatellite mission were expected from the results of previous rodent spaceflight investigations [2,11,17-20,23,32,33,37]. The slow antigravity AL muscle was the most atrophic, and at the fiber type level, SO fibers were the most decreased in area. Interestingly, in the EDL, the SO fibers were significantly hypertrophied. This may have been a consequence of the "foot drop" plantarflexion posture assumed by rats in microgravity which caused chronic stretching of the EDL and stimulation of fiber growth [34]. The plantarflexion

posture is apparently only assumed when rats are housed in the gang type cage used for this mission and the Space Shuttle middeck experiments because an earlier Biosatellite 936 study reported shortening of the EDL muscle length postflight [5]. The single animal tube type cages utilized on the 936 mission were much shorter vertically. The close contact of the rat with the ceiling and the floor of the tube cage would have inhibited constant plantarflexion; indeed, the cage may have caused dorsiflexion accounting for the shortening of the EDL. The overall decrease in muscle fiber area for the flight AL was 23% compared to 30% for the suspended AL. In apparent contradiction, the mean wet weight of the flight AL was not different from the vivarium control whereas the average wet weight of the suspended AL was diminished by 40%. A partial explanation is that the flight AL muscles were edematous which increased the muscle wet weight. The immunohistochemical staining of the interstitium shows that serum proteins accumulate during edema so the ratio of water to mg protein in the muscle is likely to remain near normal. These results indicate that wet weight measurements can seriously underestimate the amount of muscle atrophy. Consistent with previous studies of hindlimb suspension, as well as spaceflight, was the observed increased expression of fast myosin in the slow AL muscle fibers of both groups [8,23,37]. This increased the occurrence of hybrid fibers containing both myosin isoforms and suggested that hindlimb unloading promoted expression of fast myosin. Subsarcolemmal mitochondria concentrations were significantly decreased in flight AL muscle fibers, but the central intermyofibrillar mitochondrial content remained near normal. Mitochondrial profiles were more common in the A bands and diminished in the I bands. While absolute mitochondrial content decreases during fiber atrophy, the greater loss of contractile proteins selectively preserves mitochondrial concentration centrally [21]. This conservation helps maintain fatigue-resistance as fibers atrophy [7,13]; however, in spite of this process, recent unpublished data from studies, utilizing more strenuous fatigue tests than have been used previously, demonstrate that the soleus muscles of suspended rats are more readily fatigued (Dr. R. Fitts, personal communication). A decrease in absolute mitochondrial content implies that some mitochondria are degenerating and accounting for the decrease in subsarcolemmal profiles. Another possibility for subsarcolemmal loss is that, according to the reticulum theory of mitochondrial distribution at the periphery, some of the subsarcolemmal loss may be due to retraction of the mitochondrial reticulum (processes) into the A bands [22].

The most prominent lesions detected in flight and suspended AL muscle fibers were eccentric (lengthening) contraction-like lesions of the sarcomeres. Nearly half of the flight fibers were affected whereas only 15% were lesioned in the suspended AL. The pulling apart of sarcomeres with disruption of the A and Z bands has been reported for numerous investigations of human and non-human animal models of eccentric exercise [1,14,24,25,28,29,36]. The common finding is that immediately or within a few hours of performing lengthening contractions sarcomeres undergo disruption [28,29]. Two days later, the muscles are painful, serum levels of leaked muscle proteins are increased, and histologically there is extensive muscle fiber necrosis and interstitial edema [3,9]. The results of Cosmos 1887 and 2044 fit this scenario very well. For the Cosmos 1887 12.5-day-flight, rats were killed two days after landing; extensive muscle tissue necrosis, microhemorrhages and edema occurred in the AL and soleus

muscles [33]. The present findings for the Cosmos 2044 14-day-flight show that rats killed 9-12 hours after landing exhibit extensive sarcomere disruption and significant edema, but minimal tissue necrosis and rbc extravasation. The elegant quantitative studies of McCully and Faulkner which electrically stimulated mouse EDL muscles while lengthening by a servomotor in precisely controlled increments demonstrated that as few as 15 lengthening contractions with a force of at least 85% of maximum muscle tension were sufficient to produce immediate diminished tension output, probably reflecting sarcomere disruption, and a delayed degeneration and subsequent regeneration of damaged muscle fibers [24,25]. Their data supports a direct correlation of muscle injury with peak force development during lengthening contractions. The present results raise a number of questions. Were the flight and suspended AL muscles exposed to forceful lengthening contractions? If yes, what accounts for the higher incidence of sarcomere disruption in the flight compared to the suspended muscle? The complete absence of detectable lesions in the synchronous control muscles argues against their formation being due to dissection trauma. The flight and suspended AL muscles atrophied 23% and 30%, respectively, but the body weight remained near normal. This meant that the workload on the AL muscle following return to weightbearing was increased over normal. Assuming that the atrophic muscle fibers were more fatigable, it was likely that during weightbearing, the least fatigable still active fibers, were heavily loaded and eccentrically stretched causing damage. The flight and suspended rats were returned to weightbearing and killed on similar schedules, but the postflight peak force loads were likely much greater for the flight animals. The flight rats experienced deceleration forces of 6 and 50 G's (see Methods). The suspended rats were simply let down and not exposed to the reentry G force profile. The synchronous rats were subjected to the reentry G forces, but they did not manifest sarcomere lesions. Thus, it seems that the peak force applied to the muscles postflight determines the amount of eccentric lesions. Furthermore, because the synchronous AL muscles did not atrophy or show lesions, it appears that atrophy, induced by spaceflight or suspension, renders the AL muscle more vulnerable to lengthening contraction damage. The present results indicate that the susceptibility to injury may involve diminution of the myofibril cytoskeleton during degradation of contractile proteins and weakening of the connective tissue harnessing the contractile force of the muscle [10,27,38]. These properties will be investigated further in future flight experiments.

Previous investigators examining lengthening contraction injury have concluded that the sarcomere lesions seen within the first few hours of completing the exercise are precursors to the destruction of the muscle fiber cell membrane and segmental fiber necrosis [28]. Our findings indicate that eccentric-like lesions and delayed tissue necrosis may not be causally related. In Cosmos 2044, the flight AL muscles of the rats killed 9-12 hours after landing had extensive regional areas of thrombosis within the postcapillary venules and capillaries. Blockage of the microcirculation by platelets, rbc's and fibrin most likely caused the interstitial edema which led to ischemia and anoxia-induced tissue necrosis, especially in muscles resuming a high level of contractile activity following return to weightbearing. We observed abundant polyribosomes within the disrupted sarcomeres suggesting that synthesis of contractile proteins and rapid repair of the eccentric lesions was underway. These fibers had

intact cell membranes. There was no evidence of calpain (calcium activated protease) digestion of Z bands that would indicate breakdown of the cell membrane and the in rush of calcium [discussed in 29]. Thus, fibers with eccentric lesions should have recovered if it was not for the accompanying compromised microcirculation, the probable culprit causing the tissue necrosis. Since thrombosis and interstitial edema were not significant in the suspended AL, it appears that atrophy and return to low level weightbearing do not result is microcirculatory problems. However, stressing the atrophic flight muscle with a large workload postflight does appear to bring on microcirculatory deficits. Ilyina-Kakeuva has blamed the compromised microcirculation on faulty vascular tone [18-20]. The reason for increased platelet activation (clumping) is unknown. During atrophy, muscle fibers are reduced in size more rapidly than the microvascular network which becomes relatively more abundant [6]. This results in a tortuous microvascular network. The high rate of blood flow demanded by the reloaded working flight AL muscles is likely to cause turbulence in the tortuous vessels. This would damage endothelial cells, expose platelets to collagen and stimulate coagulation events. Physical trauma may directly activate platelets. We conclude that the tissue necrosis and microhemorrhages result from compromised microcirculation and not from sarcomere lesions. The sarcomere lesions may contribute indirectly because these lesions decrease the amount force generated by a fiber [24,25]; this would increase the workload on intact active fibers which, in turn, would require more energy and be more susceptible to reduced blood flow. Future flight experiments are necessary to define the primary sites of change within the atrophic muscles that lead to eccentric contraction-like lesions, thrombus formation, and interstitial edema, and to assess whether anticoagulation drug therapy can reduce postflight deterioration of skeletal muscle tissue.

ACKNOWLEDGMENTS

The authors gratefully acknowledge the superb efforts of the NASA and Soviet teams who collaborated to obtain the excellent specimens used in this study. Special thanks and recognition go to Dr. E.I. Ilyina-Kakueva, Dr. V.S. Oganov, Dr. R. Ballard, Mr. J. Connolly, Dr. R.E. Grindeland, Dr. M. Vasques and Dr. A.S. Kaplansky who headed the Soviet dissection team.

REFERENCES

1. Armstrong, RB, R.W.Ogilvie, and J.A. Schwane. Eccentric Exercise-Induced Injury to Rat Skeletal Muscle. J. Appl. Physiol. 54:80-93, 1983.

2. Baranski, S, W. Baranska, M. Marciniak, and E.I.Ilyina-Kakueva. . 1979. Ultrasonic ("Ultrastructural") Investigations of the Soleus Muscle After Spaceflight on the Biosputnik 936. Aviat. Space Environ. Med. 50:930-934.

3. Byrnes, W.C., P.M. Clarkson, J.S. White, S.S. Hsieh, P.N. Frykman, and R.J. Maughan, 1985. Delayed Onset Muscle Soreness Following Repeated Bouts of Downhill Running. J. Appl. Physiol. 59:710-715.

4. Cardasis, C.A.and D.M. LaFontaine, 1987. Aging Rat Neuromuscular Junctions: a Morphometric Study of Cholinesterase-Stained Whole Mounts and Ultrastructure. Muscle Nerve 10:200-213.

5. Castleman, K.R., L.A. Chui, and J.P Van Der Meulen, 1978. Spaceflight Effects on Muscle Fibers: Final Reports of U.S. Experiments Flown on Soviet Satellite Cosmos 936. Rosenzweig, SN, Souza, KA. Eds. NASA Technical Memorandum 78526 pp. 274-289.

6. Desplanches, D, M.H. Mayet, B. Sempore, and R.Flandrois, 1987. Structural and Functional Responses to Prolonged Hindlimb Suspension in Rat Muscle. J. Appl. Physiol. 63:558-563.

7. Fell, R.D., L.B. Gladden, J.M. Steffen, and X.J. Musacchia, 1985. Fatigue and Contraction of Slow and Fast Muscles in Hypokinetic/Hypodynamic Rats. J. Appl. Physiol. 58:65-69.

8. Fitts, R.H., J.M. Metzger, and D.A. Riley, 1986. Models of Skeletal Muscle Disuse: A Comparison of Suspension Hypokinesia and Hindlimb Immobilization. J. Appl. Physiol. 60:1946-1953.

9. Friden, J, P.N. Sfakianos, and A.R. Hargens, 1986. Muscle Soreness and Intramuscular Fluid Pressure: Comparison Between Eccentric and Concentric Load. J. Appl. Physiol. 61:2175-2179.

10. Funatsu, T, H. Higuchi, S. Ishiwata, 1990. Elastic Filaments in Skeletal Muscle Revealed by Selective Removal of Thin Filaments with Plasma Gelsolin. J. Cell Biol. 110:53-62.

11. Gazenko, O.G., A.M. Genin, Y.A. Il'in, V.V. Portugalov, L.V. Serova, and R.A. Tigranyan, 1978. Principal Results of Experiment with Mammals Onboard the Kosmos-782 Biosatellite. Kosmich. Biol. Aviakosmisch. Med. 6:43-49.

12. Haas, A.L. 1988. .Immunochemical Probes of Ubiquitin Pool Dynamics. Ubiquitin. Rechsteiner, M. Ed. Plenum Publ. pp. 173-206.

13. Herbert, M.E., R.R. Roy, V.R Edgerton, 1988. Influence of One-Week Hindlimb Suspension and Intermittent High Load Exercise on Rat Muscles. Exp. Neurol. 102:190-198.

14. Hikida, R.S., P.D. Gollnick, G.A. Dudley, V.A. Convertino, and P. Buchanan, 1988. Structural and Metabolic Characteristics of Human Skeletal Muscle Following 30 days of Simulated Microgravity. Aviat. Space Environ. Med. 60:664-670.

15. Hoh, J.F.Y., and S. Hughes, 1988. Myogenic and Neurogenic Regulation of Myosin Gene Expression in Cat Jaw-Closing Muscles Regenerating in Fast and Slow Limb Muscle Beds. J. Muscle Res. Cell Motil. 9:59-72.

16. Hoh, J.F.Y., S. Hughes, P.T. Hale, and R.B.Fitzsimons, 1988. Immunocytochemical and Electrophoretic Analyses of Changes in Myosin Gene Expression in Cat Lmb Fast and Slow Muscles During Postnatal Development. J. Muscle Res. Cell Motil 9:30-47.

17. Ilyin, E.A., 1983. Investigations on Biosatellites of the Cosmos Series. Aviat. Space Environ. Med. Suppl. I 54:S9-S15.

18. Ilyina-Kakueva, E.I., and V.Y. Portugalov, 1977. Combined Effect of Spaceflight and Radiation on Skeletal Muscles of Rats. Aviat. Space Environ. Med. 48:115-119.

19. Ilyina-Kakueva, E.I., and V.V. Portugalov,. 1981. Structural Changes in the Soleus Muscle of Rats Flown Aboard the Cosmos Series of Biosatellites and Submitted to Hypokinesia. Kosmich. Biol. Aviaksomich. Med. 15:37-40.

20. Ilyina-Kakueva, E.I., V.V. Portugalov, N.P. Kirvenkova, 1976. Spaceflight Effects on the Skeletal Muscle of Rats. Aviat. Space Environ. Med. 47:700-703.

21. Jaspers, S.R., J.M. Fagan, S. Satarug, P.H. Cook, and M.E. Tischler,1988. Effects of Immobilization on Rat Hindlimb Muscles Under Non-Weight-Bearing Conditions. Muscle Nerve 11:458-466.

22. S.P. Krikwood, E.A. Munn, and G.A. Brooks, 1986. Mitochondrial Reticulum in Limb Skeletal Muscle. Am. J. Physiol. 251:395-402.

23. Martin, T.P., V.R. Edgerton, and R.E. Grindeland, 1988. Influence of Spaceflight on Rat Skeletal Muscle. J. Appl. Physiol. 65:2318-2325.

24. McCully, K.K., and J.A. Faulkner, 1985. Injury to Skeletal Muscle Fibers of Mice Following Lengthening Contractions. J. Appl. Physiol. 59:119-126.

25. McCully, K.K., and J.A. Faulkner, 1986. Characteristics of Lengthening Contraction Associated With Injury to Skeletal Muscle Fibers. J. Appl. Physiol. 61:293-299.

26. Muller, M.F., H. Ris, and J.D. Ferry, 1984. Electron Microscopy of Fine Fibrin Clots and Fine and Coarse Fibrin Films. J. Mol. Biol. 174:369-384.

27. Nakagawa, Y., M. Totsuka, T. Sato, Y. Fukuda, and K. Hirota, 1989. Effect of Disuse on the Ultrastructure of the Achilles Tendon in Rats. Eur. J. Appl. Physiol. 59:239-242.

28. Newham, D.J., G. McPhail, K.R. Mills, and R.H.T. Edwards, 1983. Ultrastructural Changes After Concentric and Eccentric Contractions of Human Muscle. J. Neurol. Sci. 61:109-122.

29. Ogilvie, R.W., R.B. Armstrong, K.E. Baird, and C.L. Bottoms, 1988. Lesions in the Rat Soleus Muscle Following Eccentrically Biased Exercise. Amer. J. Anat. 182:335-346.

30. Piotrowicz, R.S., R.P.Orchekowski, D.J. Nugent, K.Y. Yamada, and T.J. Kunicki, 1988. Glycoprotein Ic-IIa Functions as an Activation-Independent Fibronectin Receptor on Human Platelets. J. Cell Biol. 106:1359-1364.

31. Riley, D.A., J.L.W. Bain, S. Ellis, and A.L. Haas, 1988. Quantification and Immunocytochemical Localization of Ubiquitin Conjugates Within Rat Red and White Skeletal Muscles. J. Histochem. Cytochem. 36:621-632.

32. Riley, DA, S. Ellis, G.R. Slocum, T. Satyanarayana, J.L.W. Bain, and F.R. Sedlak, 1987. Hypogravity-Induced Atrophy of Rat Soleus and Extensor Digitorum Longus Muscles. Muscle Nerve 10:560-568.

33. Riley, D.A., E.I. Ilyina-Kakueva, S. Ellis, J.L.W. Bain, G.R. Slocum,and F.R. Sedlak, 1990. Skeletal Muscle Fiber, Nerve and BloodVessel Breakdown in Space-flown Rats. FASEB J. 4:84-91.

34. Riley, D.A., G.R. Slocum, J.L.W. Bain, F.R. Sedlak, T.E. Sowa, and J.W. Mellender, 1990. Rat Hindlimb Unloading: Soleus Histochemistry, Ultrastructure, and Electromyography. J. Appl. Physiol. 69:58-66.

35. Shimada, Y, D.A. Fischman, and A.A. Moscona, 1967. The Fine Structure of Embryonic Chick Skeletal Muscle Cells Differentiated In Vitro. J. Cell Biol. 35:445-453.

36. Stauber, W.T., V.K. Fritz, D.W. Vogelbach, and B. Dahlmann, 1988. Characterization of Muscles Injured by Forced Lengthening. I. Cellular infiltrates. Med. Sci. Sports Exerc. 20:345-353.

37. Takacs, O, M. Rapcsak, A. Szoor, V.S. Oganov, T. Szilagyi, S.S. Oganesyan, and F. Guba, 1983. Effect of Weightlessness on Myofibrillar Proteins of Rat Skeletal Muscles with Different Functions in Experiment of Biosatellite Cosmos-1129. Acta Physiol. Hung. 62:228-233.

38. Vailas, A.C., D.M. Deluna, L.L. Lewis,S.L. Curwin, R.R. Roy, and D.K. Alford, 1988. Adaptation of Bone and Tendon to Prolonged Hindlimb Suspension in Rats. J. Appl. Physiol. 65:373-376.

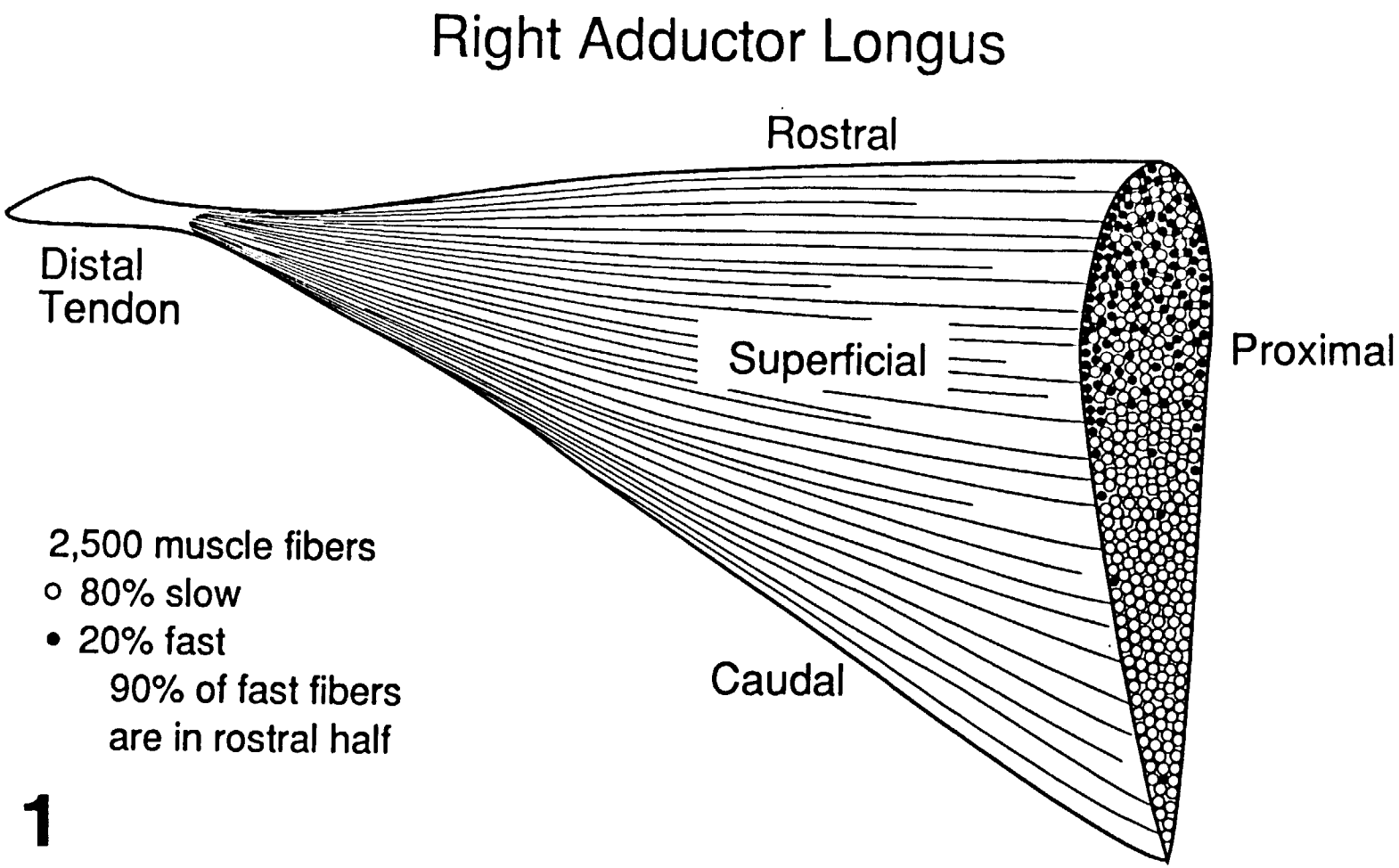

Figure 1. The adductor longus (AL) muscle is fan-shaped with a proximal short aponeurotic attachment to the pubic ramus and a distal fusiform tendon attaching to the femur. The rostral half of the muscle contains a mixture of FOG and SO fibers whereas the caudal half is nearly all SO fibers. Either the rostral or caudal third of the muscle was removed for electron microscopy fixation, and the remaining protion was quick frozen for light microscopy. To achieve uniform sampling, quantitation of fiber type properties at the light microscopic level were conducted on the regions of the tissue sections corresponding to the middle third of the muscle.

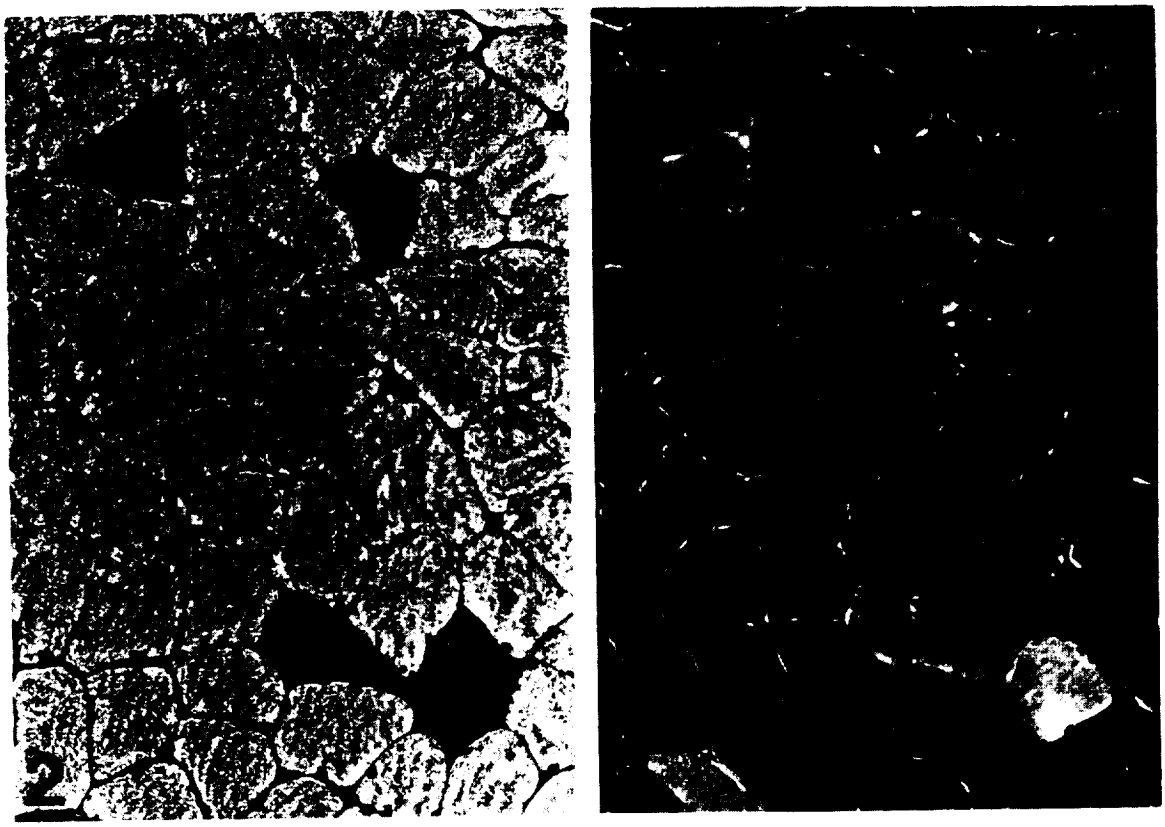

Figure 2. (left) AL muscle of a basal control animal. The cross section is stained for anti-slow myosin by indirect immunofluorescence. The majority of the fibers are immunoreactive SO fibers which contain slow myosin. The four non-immunostained fibers are type FOG. X185.

Figure 3. (right) A section serial to Fig. 2 stained with anti-fast myosin. The FOG fibers are immunoreactive whereas the SO fibers lack staining above background. X185.

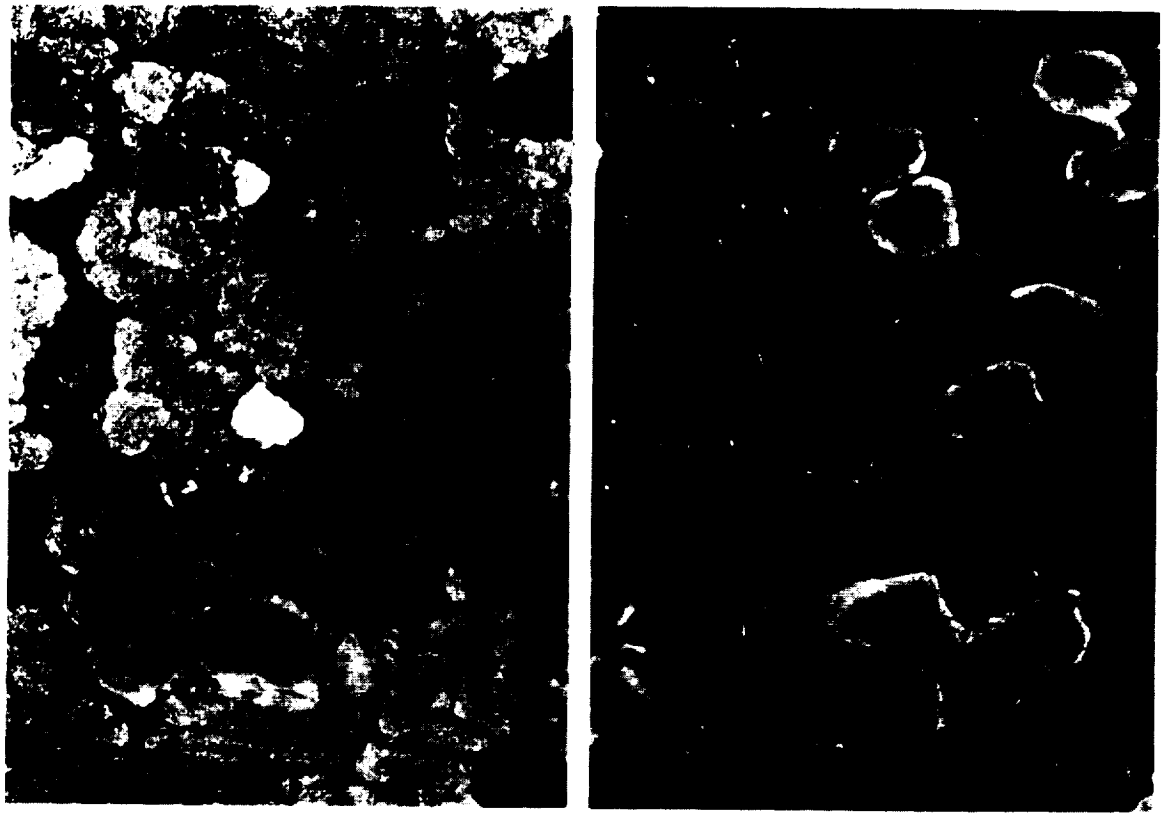

Figure 4. (left) Cross section of a flight AL muscle immunostained for slow myosin. The SO fibers are immunoreactive and display greater atrophy than FOG fibers. Fragmented necrotic fibers stain very intensely. The fiber labeled "X" contains slow and fast myosin (see Fig. 5). X185.

Figure 5. (right) A section serial to figure 4 stained with anti-fast myosin. As in the control, the SO fibers are mostly negative, although there is an increase in hybrid fibers expressing both myosins (X). The necrotic fibers are not highly reactive for fast myosin. X185.

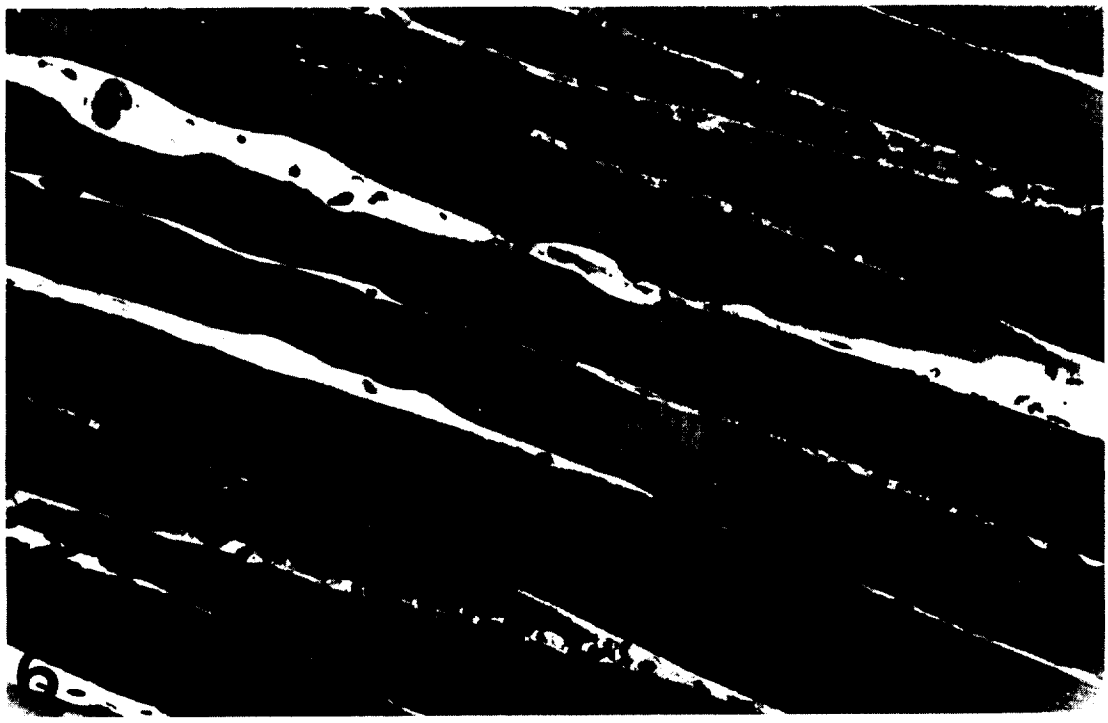

Figure 6. Toluidine blue-stained, longitudinal semithin section of AL fibers in a flight muscle. The normal cross stiations are easily seen. Nearly all fibers exhibit pale foci of widened cross striations. These foci represent eccentric contraction-like lesions. The lesions frequently affect adjacent fibers at the same level suggesting a transverse band of stretch damage. X375.

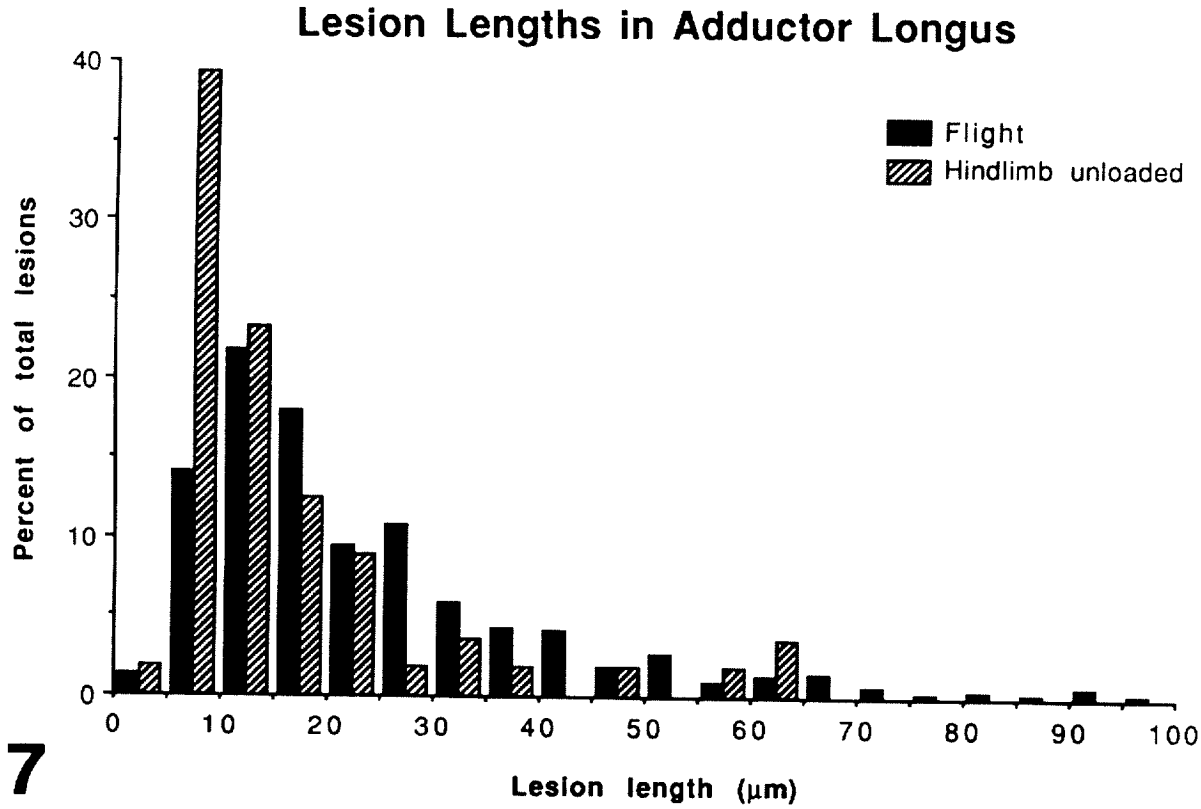

Figure 7. Eccentric contraction-like lesions are present in 47% of the fibers of flight AL muscles and 15% of the fibers in tail suspended rats. The histogram demonstrates that in both conditions, the majority of the lesions range from 5 to 30 microns long. Most of the lesions in the tail suspended animals are short. The flight animals contain the longest lesions.

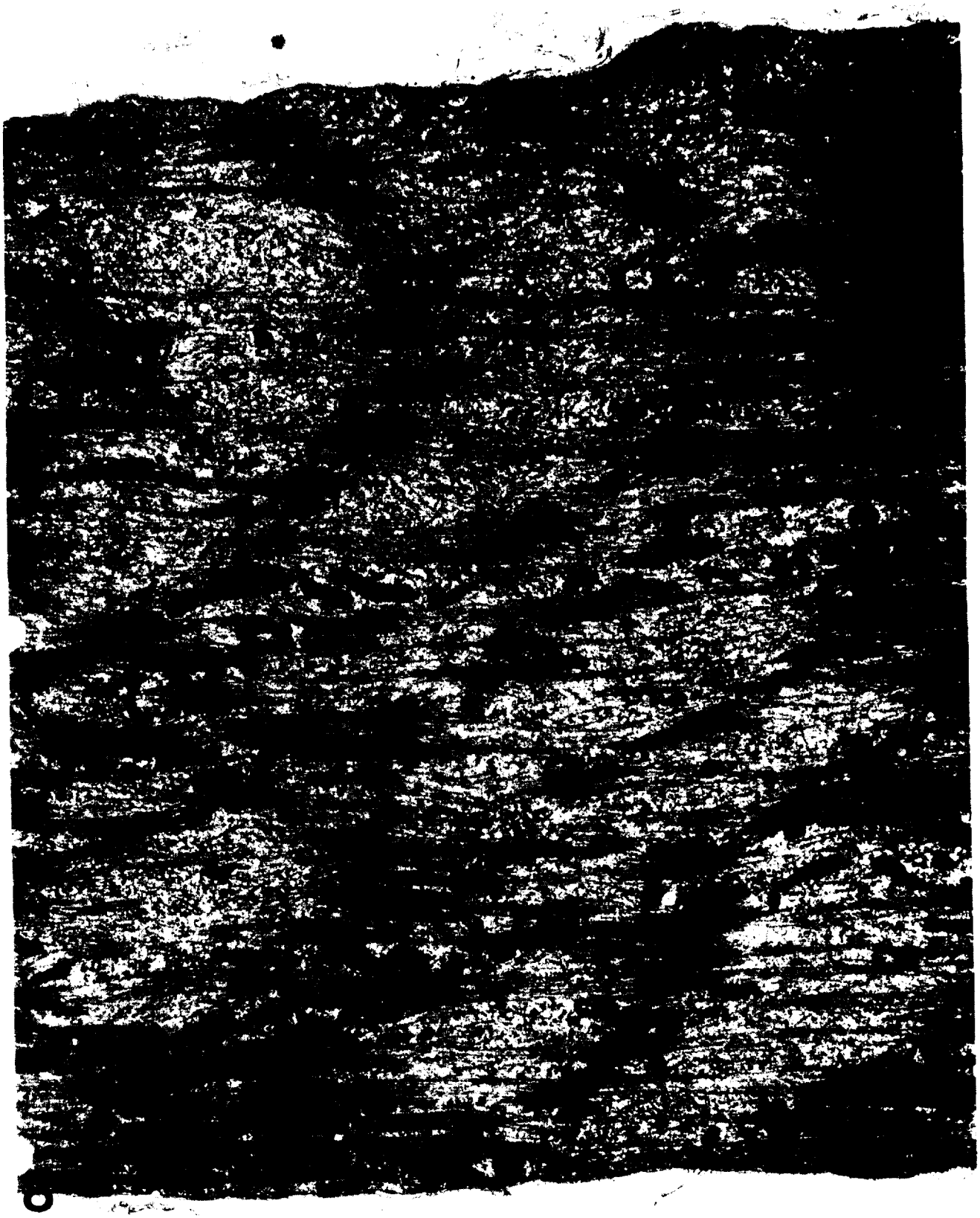

Figure 8. A longitudinal section of a flight AL muscle fiber with an eccentric contraction-like lesion involving the full width of the fiber. The few intact sarcomeres are highly contracted. The disrupted sarcomeres appear to have been pulled apart. Broken thick filaments form tangled, disoriented masses in place of A bands. The Z bands are wavy and have a streaming appearance. Some bundles of thick filaments appear clumped to the thin filaments and Z bands. X13,200.

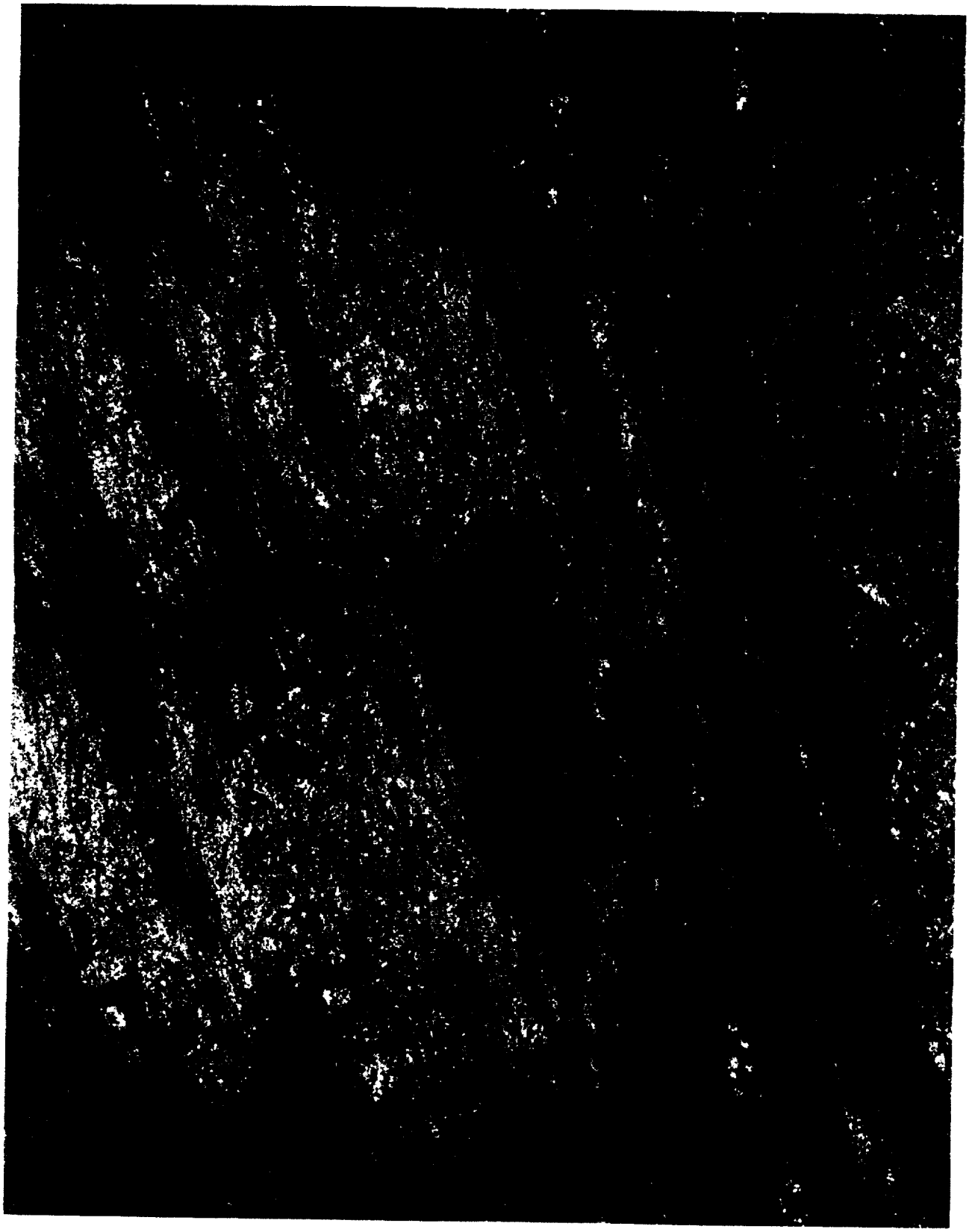

Figure 9. A high magnification view of an eccentric contraction-like lesion. Within the disrupted sarcomeres, there are many dark granular ribosomes. The helical polyribosomes (arrows) are indicative of translation of myosin mRNA. X22,800.

Figure 10. An eccentric contraction-like lesion at the periphery of a flight AL muscle fiber. Some mitochondria are swollen with extracted matrix; this may represent degeneration but more likely reflects immersion fixation artifact. The endomysium adjacent to the fiber lesion appears to have been torn by the same force that damaged the myofibrils. X11,600.

Figure 11. Longitudinal section of an AL muscle in a synchronous control. A quiescent fixed-tissue macrophage lies next to the intermuscular nerve bundle. The surrounding extracellular matrix is fairly dense. The very short sarcomeres and infolding of the muscle cell membrane are indications of a contracted fiber. X11,600.

Figure 12. A longitudinal section of the myotendinous junction of a synchronous control AL muscle fiber. Myofibrils completely fill the finger-like extensions of the muscle fiber that interdigitate with the connective tissue of the tendon. X10,800.

Figure 13. A longitudinal section of the myotendinous junction region of a flight AL muscle fiber. The finger-like projections of the muscle fiber are only partially filled with myofibrils. The boundary between the muscle fiber and the connective tissue of the tendon is less distinct than normal. X10,800.

Figures 14-16 show serial cross sections of an AL muscle of a flight rat. The muscle shows regional thrombosis. All figures are X86.

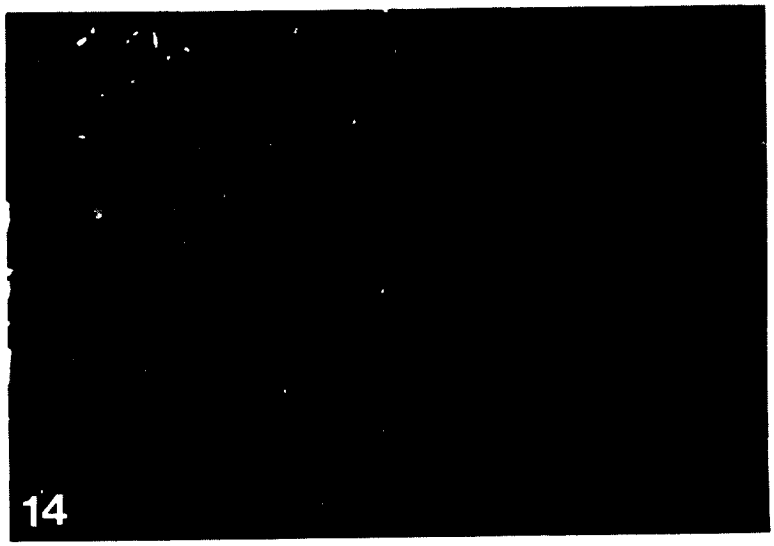

Figure 14. Immunostaining for anti-platelet IIb IIIa receptor reveals focal accumulation of platelets in the microcirculatory vessels at the left side of the section.

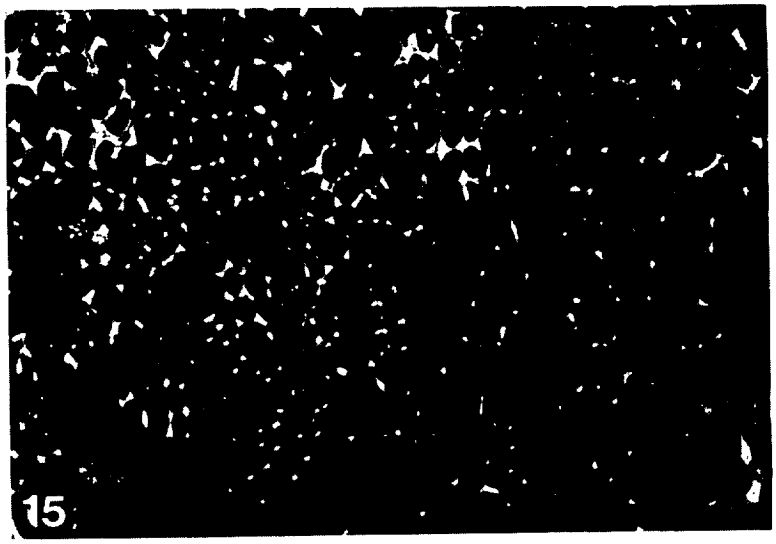

Figure 15. A serial section stained with an anti-rbc marker demonstrates increased accumulation of rbc's in the region of thrombosis. Staining of the endomysium occurs in both control and experimental muscles, suggesting a common epitope with the rbc.

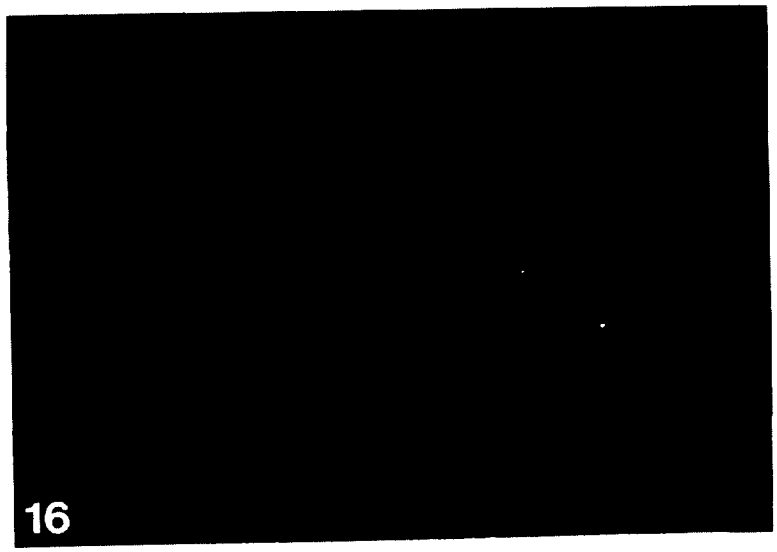

Figure 16. Omission of the primary antibody and treatment with fluorescent second antibody eliminates staining and confirms specificity of the immunostaining.

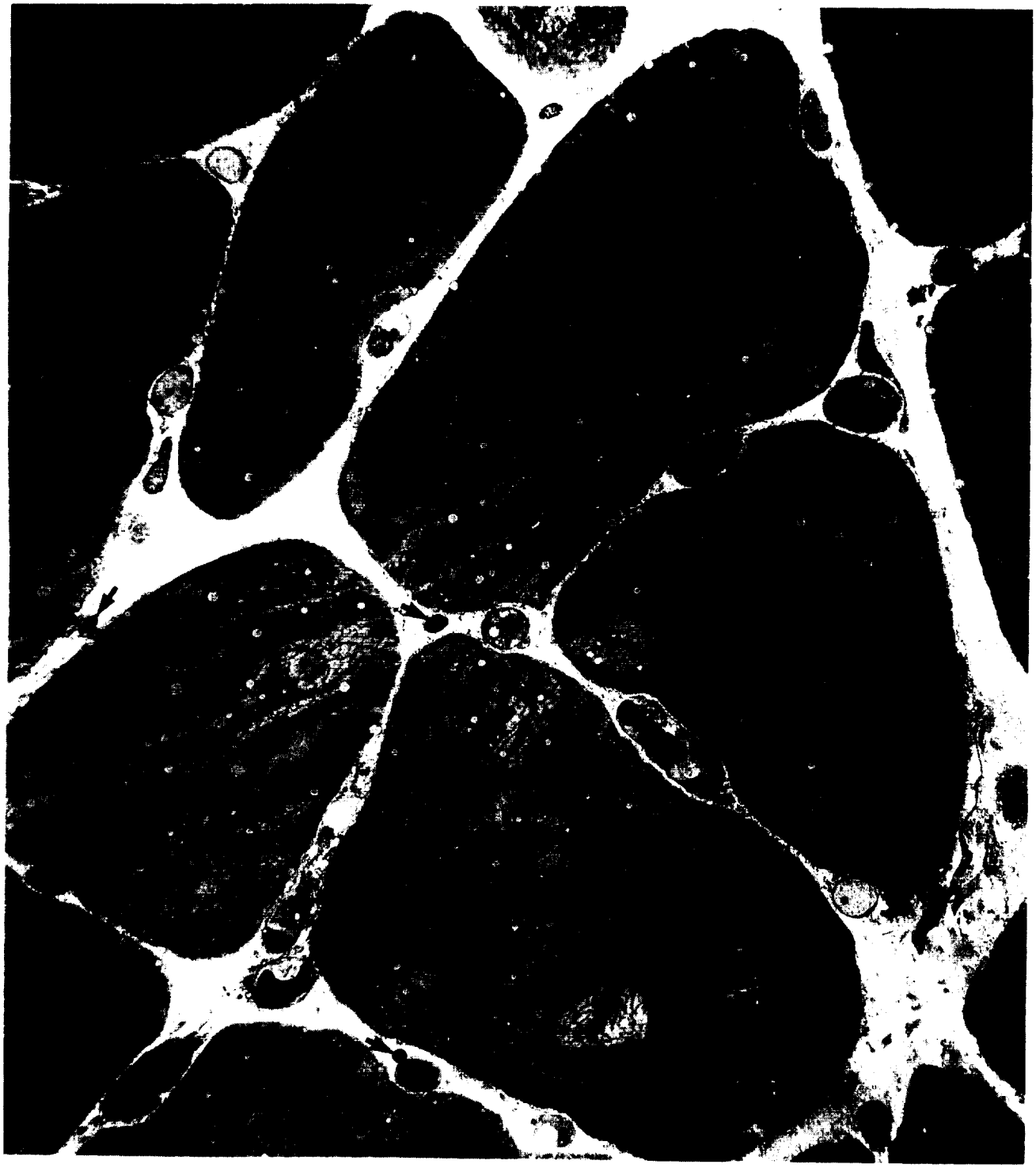

Figure 17. Cross section of a flight AL possessing atrophic muscle fibers surrounded by capillaries and postcapillary venules occluded by platelets and red blood cells. Some capillaries are patent. A few extravasated rbc's (arrows) lie free in the interstitium. X1,980.

Figure 18. Cross section of an AL muscle in a flight animal. The postcapillary venule is packed with activated platelets devoid of secretory vesicles and dense rbc's closely opposed to one another having lost their discoid shape. Tufts of electron dense coarse fibrin-like protein are distributed in the extracellular matrix (lower right). X16,500.

Figure 19. A capillary packed with platelets and rbc's in a flight AL muscle. The endothelium of the capillary is discontinuous; this permits contact of platelets with fibronectin which is a potent activator. X11,200.

Figure 20. Capillary in a synchronous AL. These normal rbc's, which are not involved in a thrombus, have retained their discoid shape. They are surrounded by amorphous serum. X11,200.

Figure 21. Longitudinal section of a flight AL. The capillary is filled with fibrin-like dense material. The neighboring muscle fibers show disruption of myofibrils and swelling of mitochondria. X10,000.

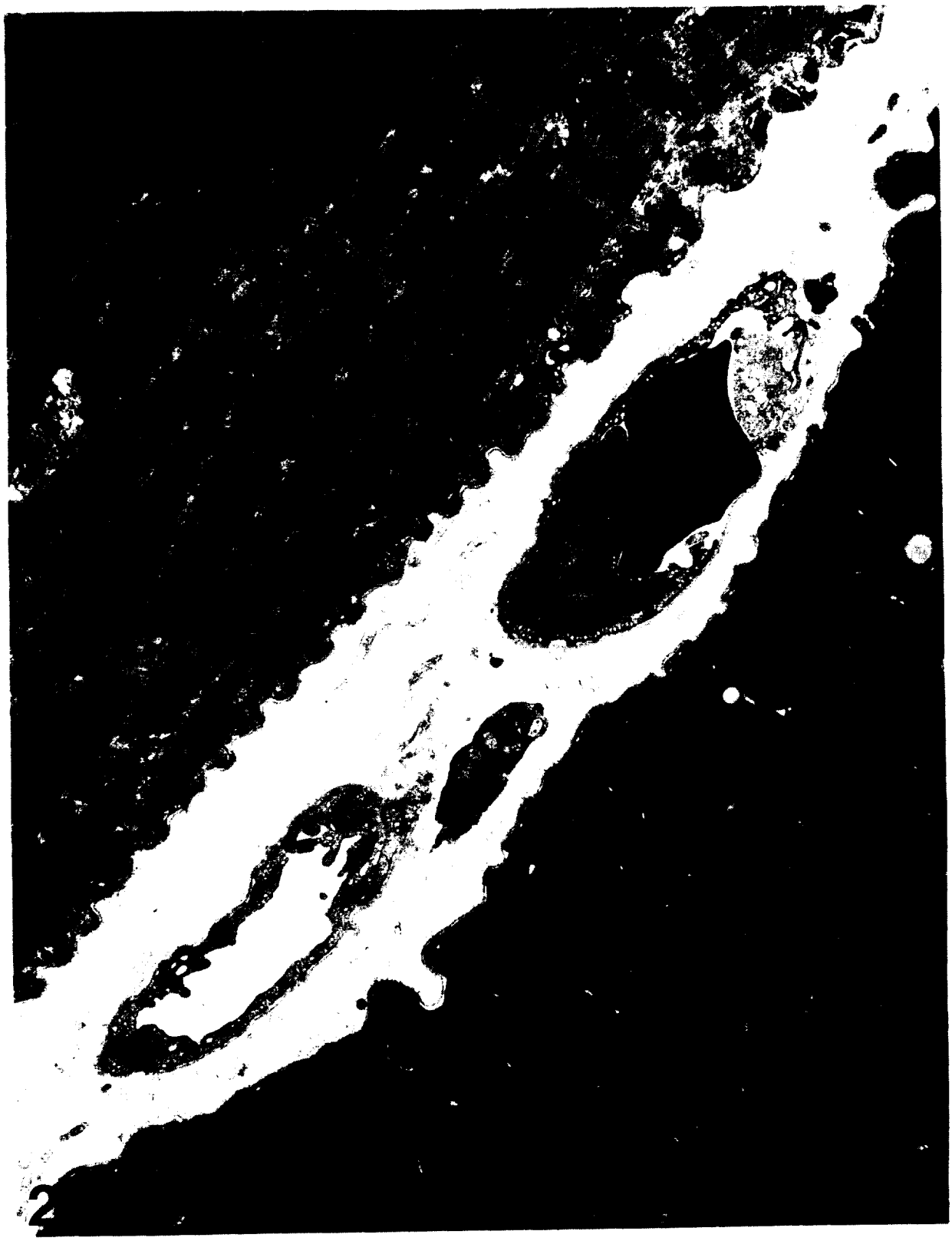

Figure 22. Longitudinal section of an AL muscle in a synchronous control animal. This micrograph illustrates a very rare event in normal muscle; the capillary endothelial lining is discontinuous allowing contact of the platelet and rbc with the basal lamina. X14,000.

Figure 23. Cross section of a flight AL. Figures 14-16 show serial cross sections of an AL muscle of a flight rat. The muscle shows regional thrombosis. All figures are X86. The muscle fiber appears acutely necrotic. The contractile proteins are extracted in the center of the fiber and supercontracted at the periphery. The myonucleus is abnormally flattened. In the upper right, there is membranous cellular debris in the interstitium near an activated fixed tissue macrophage containing numerous phagocytic vacuoles and lysosomes. X8,100.

Figure 24. An AL muscle section from a flight animal. The left side of the section is in a region of microcirculatory blockage by platelets and rbc's. The microvessels are immunoreactive for MOM antibody which primarily identifies neutrophils associated with thrombi. Neutrophils are more numerous in the capillaries than normal. X170.

Figure 25. A section of a normal AL muscle from a basal control rat. Most of the section is nonreactive for MOM antibody, except for immunostaining in the larger blood vessels. X170.

Figure 26. A region of microcirculatory occlusion and interstitial edema in a flight AL muscle. Disrupted fibers are common, and they are intensely reactive for ubiquitin conjugate antibody, suggesting enhanced turnover of contractile proteins. The microcirculatory vessels show elevated immunostaining, consistent with accumulation of platelets and other non-mature rbc's which contain ubiquitin conjugates. X86.

Figure 27. Cross section of flight AL. The muscle fibers surrounding the occluded capillaries exhibit disorganization and hypercontraction of myofibrils, indicative eccentric contraction-like lesions. The endomysium is filled with membranous cellular debris and wisps of dense coarse fibrin-like material. X7,800.

Figure 28. In this region of a flight AL, the capillaries are blocked by platelets and rbc's. Two extravasated rbc's are present. The myelinated nerve fiber shows vacuolization of the axoplasm and abnormal infolding of the myelin sheath. The neuromuscular junction, near the myonucleus of the lower muscle fiber, appears to be degenerating because the nerve terminal is fragmenting and exposed postjunctional membrane is present. X7,800.

Figure 29. A neuromuscular junction on an AL muscle fiber of a synchronous rat. The junction is normal appearing except for the portion of postjunctional membrane (upper right) not contacted by nerve terminals or schwann cell processes. This feature is commonly observed in aging animals. X18,800.

EXPERIMENT K-7-09

MORPHOLOGICAL, HISTOCHEMICAL, IMMUNOCYTOCHEMICAL, AND BIOCHEMICAL INVESTIGATION OF MICROGRAVITY-INDUCED NERVE AND MUSCLE BREAKDOWN

PART II: MUSCLE STUDIES

S. Ellis , D.A. Riley, and C.S. Giometti

SUMMARY

Two types of analyses were performed on the muscle samples received from rats flown on Cosmos 2044. The first was a two-dimensional gel electrophoretic resolution of the proteins extracted with 9 M urea from sections of the adductor longus muscles. The second was an analyses of the plantaris and extensor digitorum longus for three protease activities using synthetic peptide derivatives: lysosomal tripeptidyl peptide hydrolase, cytosolic multicatalytic protease and cytosolic activity for free calpain protease activity.

The electrophoretic analyses of the adductor longus muscle showed a strong similarity in the pattern of specific protein changes between the atrophying flight and the tail - suspension muscle, except that the degree of change was more intense in the flight muscle. The flight muscle showed a reduction in the phosphorylated light chains 1 and 2 and the appearance of fast muscle light chains 1, 2 and 3, suggesting that a conversion of fiber types was initiated by hypogravity. Moreover, the muscle light chain $LC1_{sa}$ in the adductor longus had a markedly reduced concentration in the flight muscle. Both of these changes occurred in the adductor longus muscle of the tail - suspension model, but to a notably lesser degree. This suggests that tail suspension does not entirely mimic the muscle atrophy induced by microgravity.

The lysosomal tripeptide peptidyl hydrolase activities of the plantaris and EDL muscles showed a 12% and 28% increase ($p \leq 0.02$) in the tail suspension group, respectively. These increases are indicative of a rather modest increase in lysosomal activity. The flight EDL showed a 19% increase of tripeptidyl peptide hydrolase activity, whereas the flight plantaris remained unchanged.

The free calpain activities of the plantaris and EDL muscles showed a significant increase ($p \leq 0.02$) in the flight and tail suspension muscles as compared to the vivarium, synchronous and basal control groups. This indicates that the free calpain proteolytic activity (difference between total calpain and calpastatin activity) is elevated in the cytosol to a similar degree by microgravity as compared to tail suspension.

The multicatalytic protease activity did not change because of microgravity or its simulation and, therefore, appears not to be involved in the relatively minor atrophy that is sustained by the plantaris and EDL.

INTRODUCTION

Earlier studies on the effects of microgravity simulation by means of hindlimb unloading showed marked changes in the relative concentrations of several proteins in rat soleus and EDL muscles as revealed by 2 - dimensional gel electrophoresis (1). One among several proteins which incurred a major change in relative concentration was MSN #33 which we have recently identified by sequence as resembling muscle myosin light chain LC1sa.[1] The Cosmos 2044 offered an opportunity to determine if qualitatively similar changes in protein pattern occured in skeletal muscle after exposure to the microgravity of space flight as occurred in the unloaded hindlimb model. It should be noted that this protein has been found only in rat slow muscles (soleus and adductor longus), and corresponds to the myosin LC1sa in the two dimensional electrophoretic patterns described in a recent review of different types of myosin chains (3).

The atrophy induced in soleus hindlimb unloading displayed increased lysosomal tripeptidyl peptide hydrolase activity (2). This protease is bound to lysosomal membranes and, in addition to having a role in the successive stages of protein breakdown, it may also be involved in the activation of peptide hormones, as for example, insulin - like growth factor I by truncation to the des - (1 - 3) - IGF - I (4), and also possibly in alteration the half - lives of intracellular proteins (5). From Cosmos 2044, only plantaris and EDL muscle sections were available for estimation of the concentration of this protease in the different experimental groups.

Two other protease activities were estimated in the plantaris and EDL. They were the free calpain activity (e.g., that portion of the calpain not inhibited by the endogenous calpastatin) and the multicatalytic protease complex. Calpain is a calcium - activated cysteine protease, generally associated with a peptide inhibitor called capastatin. In order to measure the total calpain the inhibitor must be removed. However, the net uninhibited activity is also a useful index of proteolytic potential. The multicatalytic protease complex hydrolyzes synthetic substrates containing hydrophobic, basic and acidic residues in the P_1 position. It constitutes a major extralysosomal proteolytic system that contains at least three distinct proteolytic activities attributable to a different component of the complex which is composed of 15 - 20 polypeptides of 22 - 33,000 molecular weight having isoelectric points that range from 3 to 10 (6,7). The complex can be isolated from muscle in a latent form that can be activated by ATP in the presence of Mg^{++}, but not by ADP or AMP (8). Its role in protein breakdown is not clear but it may be involved in development - specific processing (9) and in the tissue remodeling that occurs in muscle atrophy (10).

METHODS

Extract Preparation:

Frozen sections of muscle were crushed by a Bessman micropulverizer at -80°C, and suspended in cold water in the ratio of 10 micrograms of tissue (wet weight) per microliter of water. The suspension was further dispersed by a microhomogenizer in 1.5 ml microcentrifuge tubes. The suspension was centrifuged for 5 minutes at 10,000xg at 5° and the supernatant solutions were stored frozen at -80° for subsequent analysis.

Enzyme Assays:

The supernatant solutions were analyzed for the multicatalytic protease in a 1 ml of 100 mM Tris - HCl buffer, pH 8.0, with 0.5 mM succinyl - Leu -Val- Tyr - AMC[2] as substrate. Specific activity estimates were based on initial reaction rates since the kinetics of hydrolysis were non - linear. Calpain was assayed in 0.1M Tris - HCl pH 7.0 in the presence of 1mM $CaCl_2$ with 1mM succinyl - Leu - Tyr - AMC as substrate. Tripeptidyl peptide hydrolase activity remaining in the pellet after decantation of the supernatant solutions was solubilized with 1% Brij-35 in 0.09M acetic acid in the same volume as for the aqueous extraction.

Tripeptidyl peptide hydrolase activity was measured by the hydrolysis of Ala-Ala-Phe-AMC in 50 mM sodium acetate buffer pH 4.0. Substrate hydrolyses were monitored fluorometrically at 37^{o} by continuous recording of the formation of 7 - amino - 4 - methyl coumarin. A Turner fluormeter Model 111 equipped with 7-60 excitation and 2A-12 emission filters and a recorder served to monitor generation of AMC fluoresence.

Gel Electrophoresis:

Two dimensional gel electrophoresis was performed according to the ISO-DALT procedures described by Giometti (1, 11) on cryostat sections of the adductor longus muscle. The tissues were dissolved in 9M urea, 1% dithiothreitol, 4% Nonidet P40 and 2% ampholytes (LKB pH 3.5-10) at a concentration of 20 microliters per mg. wet muscle. The second dimension was performed on a 9 to 18% linear polyacrylamide gradient.

RESULTS

Two - dimensional gel electrophoresis revealed several notable changes in the protein pattern of the AL muscles from flight and tail suspension rats when compared to the synchronous group. The presumptive myosin LC1sa (MSN #33) was distinctly decreased in the tail suspension rats (Fig. 1) compared to synchronous group (Fig. 2), thus confirming previous findings (1). The flight ADL muscle appears to have been reduced even more extensively than tail suspension AL muscles, e.g., to barely perceptible amounts (Fig. 3). No difference in the myosin LC1sa or other spots was apparent between the synchronous, vivarium and basal groups.

An additional significant change was evident in the satellite spots around the MLC1s and 2s. The synchronous control as well as the basal and vivarium controls (not shown) displayed weakly stained proteins corresponding to the myosin LC1f, LC2f and LC3f typically present in fast - twitch muscle fibers. In both the flight and tail suspension AL muscles there was a distinct intensification of the fast myosin light chains LC1f and LC2f which did not occur in the basal, synchronous and vivarium groups. This change suggests that the AL has sustained an increased formation of fast myosin.

Two weakly stained satellite spots anodically adjacent to the myosin LC1s and LC2s showed reduced intensities in the flight and suspension groups compared to the three control groups. These protein spots are displaced from LC1s and LC2s to positions that correspond to more negatively charged moieties, e.g., phosphorylated LC1s and LC2s. If this interpretation can be verified by the use of ^{32}P, it would suggest that the phosphorylated light chains in the flight and the suspension groups are reduced in relative concentrations.

Proteolytic assays performed on the fast twitch plantaris and EDL muscle are summarized in Table 1. The tripeptidyl peptide hydrolase of the EDL was significantly elevated in both the flight and the tail suspension groups, whereas the plantaris showed no change. Free calpain was elevated only in muscles from the flight and the tail suspension groups. In both the plantaris and the EDL muscles of the tail suspension group the multicatalytic protease was unchanged under our assay conditions, i.e., extraction with water in the absence of activators such a sodium dodecyl sulfate or adenosine triphosphate. No differences were found between the three control groups.

DISCUSSION

Two - dimensional gel electrophoresis of urea extracts of the AL muscle from flight and tail suspension rats revealed several principal changes in the satellite region of the myosin light chains. First, the concentration of the slow myosin LC1sa isoform was preferentially reduced in both groups, more markedly in the AL muscle of the flight rats. Second, the intensity of the fast myosin LC1f and LC2f chains increased substantially in the two experimental groups but little change was apparent in LC3f. Thus it appears that there is a differential expression of the three fast muscle light chains of the atrophying AL muscle. Third, the more anodically located protein spots, presumed to be phosphorylated and more acidic forms of the myosin LC1s and LC2s, were reduced in relative concentration in the AL of the two experimental groups in comparison to the three control groups. These results are interpreted as indicating the initiation of slow to fast muscle myosin conversion. It should be noted that the myosin LC1sa isoform exists in very low amounts in rat fast muscle EDL.[3] This interpretation accords with the findings of Riley et al. (Cosmos 2044, Final Science Report) who observed in the AL muscle of the flight suspension groups an increase fast fiber type population detected by histochemical staining for ATPase. Moreover, anti -myosin immunochemistry showed the formation of fast / slow myosin hybrids in slow fibers of the AL.

The changes in protease activities of the plantaris and EDL were modest but anticipated. These muscles are predominantly of the fast twitch type and therefore atrophied substantially less than the slow twitch AL and soleus muscles. The elevated TPH may be taken to indicate an increase number of lysosomes of endogenous origin or from infiltrating macrophages. However, other interpretations are possible in view of preliminary evidence for the presence of TPH immunoreactivity in the sarcoplasmic reticulum [4] of skeletal muscle as well as in lysosomal membranes.

The increased net calpain activity suggests that this proteolytic system is activated during the minor atrophy sustained by the plantaris and EDL. The soleus muscle sustains considerably greater increases in the net calpain activity in parallel with its marked atrophy after hindlimb unloading for five days (11). It has been proposed that the target proteins of calpain (a calcium activated cysteine protease) are the troponin C superfamily of calmodulin binding proteins among which is included the myosin light chain kinase (12) which phosphorylates the myosin light chain LC2f (13). If the elevated net calpain activity does indeed inactivate myosin light chain kinase, it may account for the reduced levels of the phosphorylated light chains in the two experimental groups. Continuing studies will examine the phosphorylated chains and evaluate the kinase and protein phosphatase activities in the atrophying muscles in order to explain the changes in the concentrations of the phosphorylated light chains.

The multicatalytic protease was unchanged under our assay conditions, i.e., extraction with water in the absence of activators such as sodium dodecyl sulfate (13), ATP (8), and long chain fatty acids (13). Continuing studies are underway to evaluate the effects of these

activators as well as the recently reported dual protease activity found at pH 4 (14) in addition to the alkaline pH optimum. These analyses may reveal a role for the multicatalytic protease in contractile protein degradation during muscle atrophy. However, MCP assays of skeletal muscle from starving rats (15) showed a drop of activity in the gastrocnemius muscle, but no change in the immunoreactive MCP protein. This finding suggests that the reduced activity was presumably due to other alkaline proteases.

The original research plan submitted for Cosmos 2044 proposed assays for muscle parvalbumin and the carbonic anhydrase III isozyme. The limited quantity of muscle tissue available to us prohibited performing these analyses.

ACKNOWLEDGEMENTS

We wish to express our gratitude to Dr. E. I. Ilyina-Kakueva of the Institute of Biomedical Problems, USSR Ministry of Health, Moscow, USSR, and to Dr. R.E. Grindeland of Ames Research Center, NASA, Mountain View, California for providing the muscle samples analyzed in this study. Our especial thanks to Dr. L. Yengoyan, Department of Chemistry, San Jose State University, San Jose, California for putting at our disposal his laboratory facilities and offering generous cooperation in expediting this research.

REFERENCES

1. Ellis, S., C.S. Giometti and D.A. Riley. Changes in Muscle Protein Composition Induced by Disuse Atrophy: Analysis by Two-Dimensional Electrophoresis. The Physiologist Suppl., 159-160, 1985.

2. Riley, Danny A., S. Ellis, G.R. Slocum, T. Satyanarayana, J.L.W. Bain and F. Sedlak. Hypogravity Induced Atrophy of Rat Soleus and Extensor Digitorum Longus Muscles. Muscle and Nerve 10: 560-568, 1987.

3. Barton, P.J.R., and Buckingham, M.E. The Myosin Alkali Light Chain Protein and Their Genes. Biochem. J. 231: 249-261, 1985.

4. Ballard, F. John, G.L. Francis, C.J. Bagley, L.Szabo, and J.C. Wallace. Effects of Insulin-Like Growth Factors on Protein Metabolism: Why Are Some Molecular Variants More Potent?. Biochem. Soc. Symposium No. 55, 91-104, 1989.

5. Bachmair, A.., D. Finley, and A. Varshavsky. In Vivo Half-Life of a Protein as a Function of Its Amino-Terminal Residue. Science 234:179-186, 1986.

6. Tanaka, K., T. Yoshimura, A. Kumatori, A. Ichidara, A. Ikai, M. Nishigai, K. Kameyama, and T. Takagi. Proteosomes (Multi-protease Complexes) as 20 S Ring-Shaped Particles in a Variety of Eukaryotic Cells. J. Biol. Chem. 263: 16209-16217, 1988.

7. Dahlmann, B., L. Kuehn, M. Rutschmann and H. Reinauer. Purification and Characterization of Multicatalytic High-Molecular-Mass Proteinase from Rat Muscle. Biochem. J. 228: 161-170, 1985.

8. Driscoll, J. and A.L. Goldberg. Skeletal Muscle Proteosome Can Degrade Proteins in an ATP-Dependent Process That Does Not Require Ubiquitin. Proc. Natl. Acad. Sci. USA 86: 787-791, 1989.

9. Falkenburg, P., C. Haass, P.M. Kloetzel, B. Niedel, F. Kopp, L. Kuen and B. Dahlmann. Drosophila Small Cytoplasmic 19S Ribonucleo-Protein is Homologous to the Rat Multicatatlytic Protease. Nature 331: 190-192, 1988.

10. Darr, K.C. and E. Schultz. Hindlimb Suspension Suppresses Muscle Growth and Satellite Cell Proliferation. J. Appl. Physiol. 67: 1827-1834, 1989.

11. Giometti, C.S. Muscle Protein Analysis by Two-Dimensional Gel Electrophoresis. CRC Reviews in Clinical Laboratory Sciences 18: 79-109, 1982.

12. Wang, K.K.K., A. Villalobo, B.D. Roufogalis. Calmodulin-Binding Proteins as Calpain Substrates. Biochem. J. 262: 693-706, 1989.

13. Dahlmann, B., M. Rutschmann, L., Kuehn and H. Reinauer. Activation of the Multicatalytic Proteinase from Rat Skeletal Muscle by Fatty Acids or Sodium Dodecyl Sulfate. Biochem. J. 228: 171-177, 1985.

14. Mason, R.W. Characterization of the Active Site of Human Multicatalytic Proteinase. Biochem. J. 265: 479-484, 1990.

15. Dahlmann, B., L. Kuehn, H. Reinauer and John Kay. Multicatalytic protease activity in skeletal muscle from starving rats. Biochem. Soc. Trans. 15: 963-964, 1987.

FOOTNOTES

[1] S. Ellis, W. Henzel, D.A. Riley, in preparation.

[2] Abbreviations: AMC, 7-amino-4-methyl coumarin; EDL, extensor digitorum longus; AL, adductor longus; MLC s and f, myosin light chains slow and fast, respectively ; TPH, tripeptidyl peptide hydrolase; LC1sa, rat myosin isoform of LC1s; MCP, multi-catalytic protease.

[3] S. Ellis, D.A. Riley, C.S. Giometti, unpublished data.

[4] D.A. Riley, unpublished data.

TABLE 1

SUMMARY OF PROTEASE ASSAYS ON RAT PLANTARIS AND EDL

Muscle/	TPH		Free Calpain		Multicatalytic Protease	
	Mean F.U. min^{-1} ml. ± S.D.					
PLANTARIS						
Flight	1855	125	63*	5	1525	98
Tail	1800	120	58*	7	1460	160
Syn	1690	162	45	4	1365	103
Basal	1665	105	40	5	1320	112
Vivar.	1680	175	42	5	1475	90
EDL						
Flight	1365*	105	86*	6	1355	130
Tail	1460*	92	81*	4	1610	188
Syn	1190	80	65	10	1480	100
Basal	1140	77	54	8	1530	96
Vivar.	1100	82	68	9	1425	101

* $p \leq 0.02$ (t test) vs.pooled Syn, Basal, Vivar.; 5 muscles per group; F.U. = Fluorescence Units

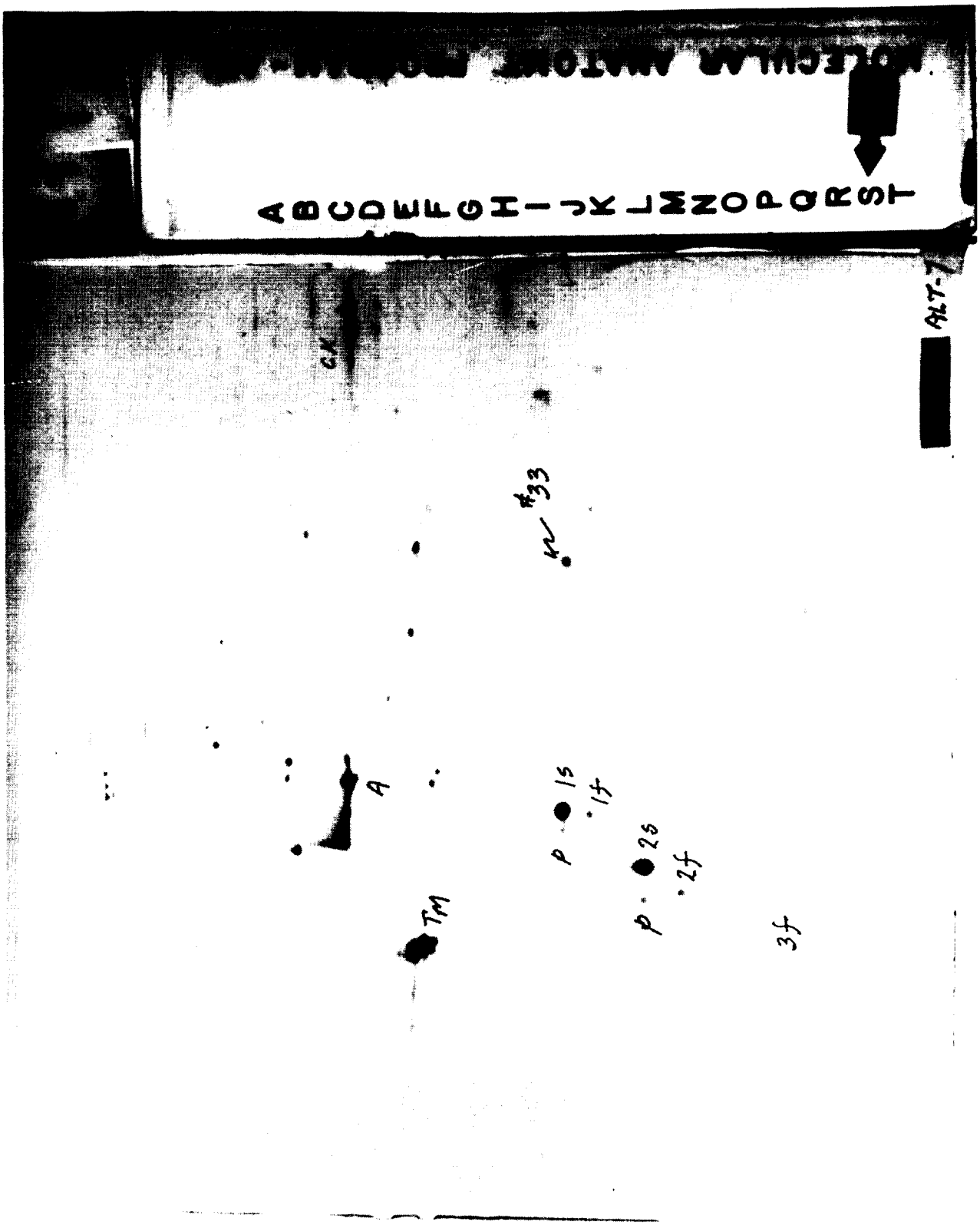

Figure. 1. Two-dimensional gel electrophoretic patterm of a urea extract of an adductor Longus muscle obtained from a tail suspension rat. Abbreviations: Tm, tropomyosin; A, actin; CK, creatine kinase; myosin slow light chains, 1s, 1sa, 2s; myosin fast light chains, 1f, 2f, 3f. Visualization by Coomassie R-250 stain.

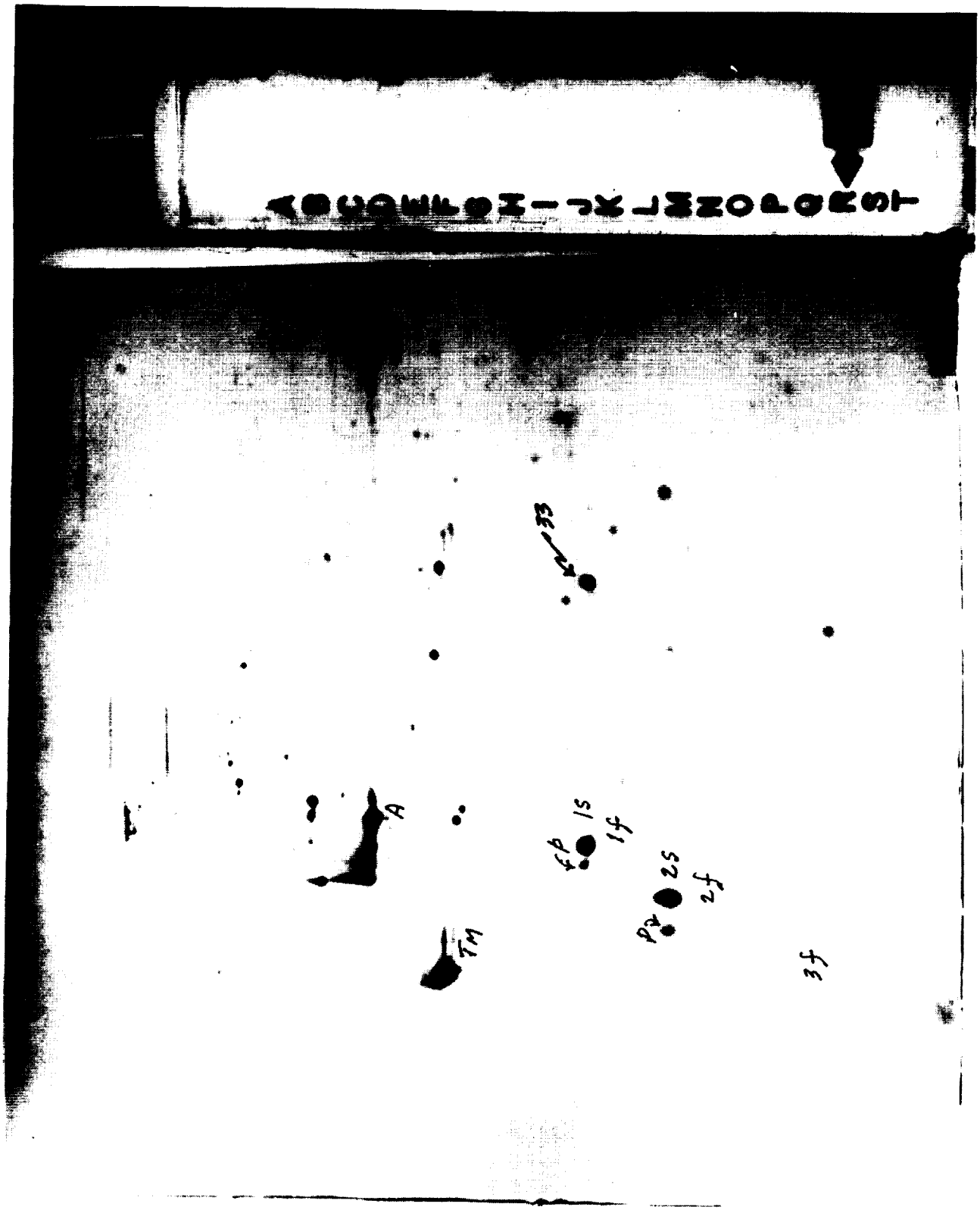

Figure 2. Two-dimensional gel electrophoretic pattern of a urea extract of an adductor longus muscle obtained from a synchronous rat. See legend for figure 1 for abbreviations.

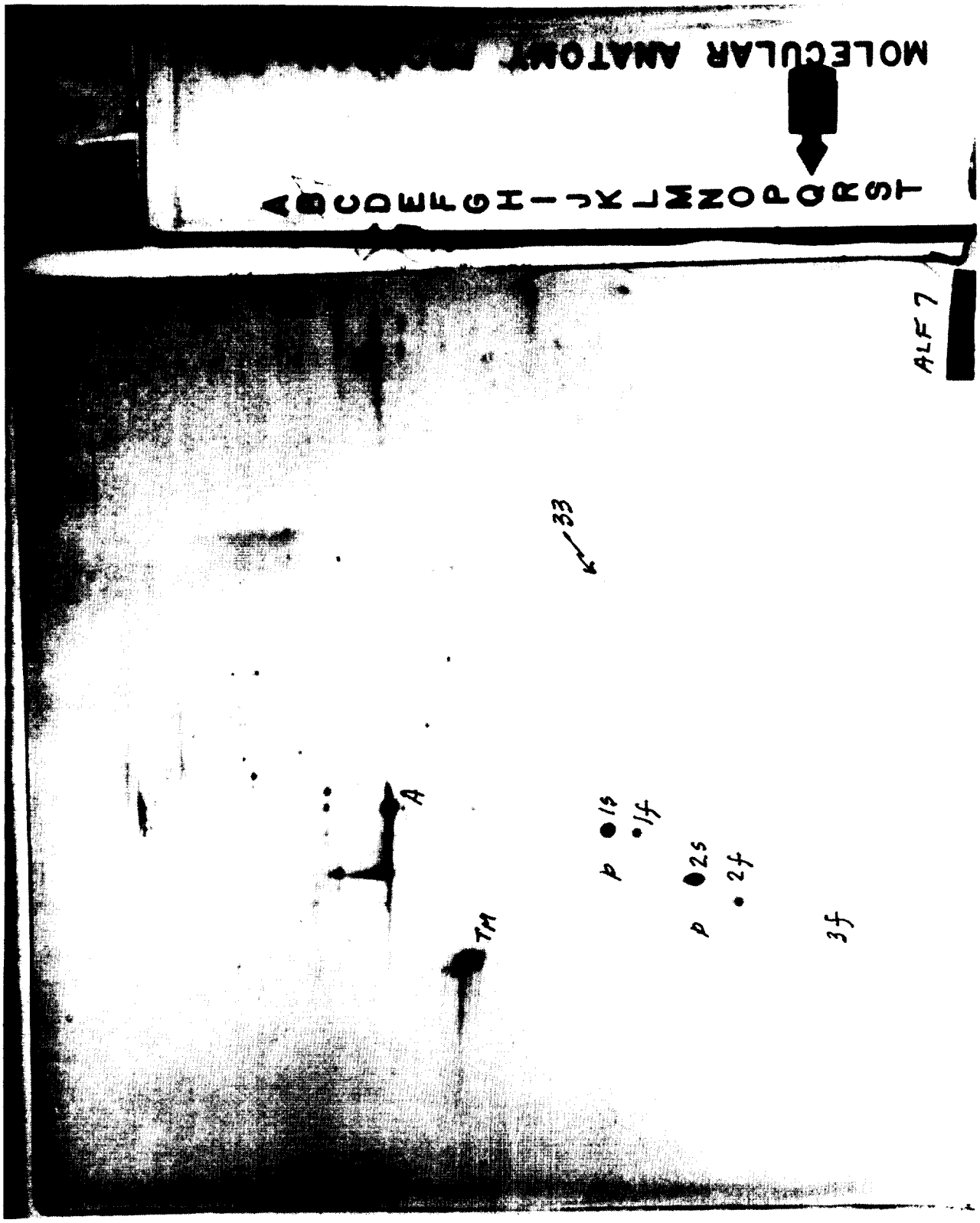

Figure 3. Two-dimensional gel electrophoretic pattern of a urea extract obtained from flight rat. See legend for figure 1 for abbreviations.

EXPERIMENT K-7-10

EFFECTS OF ZERO GRAVITY ON CONTRACTILE PROTEIN CONTENT AND ISOMYOSIN DISTRIBUTIONS IN FAST AND SLOW QUADRICEPS MUSCLES OF RODENTS FLOWN ON COSMOS 2044

Principal Investigator:

Kenneth M. Baldwin
University of California
Irvine, CA

Co-Investigators:

Robert E. Herrick
University of California
Irvine, CA

E. I. Ilyina-Kakueva
V. S. Oganov
Institue of Biomedical Problems
USSR Ministry of Health
Moscow, USSR

EXPERIMENT K-7-10

EFFECT OF ZERO GRAVITY ON CONTRACTILE PROTEIN CONTENT AND ISOMYSOSIN DISTRIBUTION IN FAST AND SLOW QUADRICEPS MUSCLES OF RODENTS FLOWN ON COSMOS 2044

K.M. Baldwin, Robert E. Herrick, E.I. Ilyina-Kakueva and V. S. Oganov

SUMMARY

The purpose of the present study was to extend previous findings on the effects of 14 days of spaceflight on the biochemical properties of rodent fast-twitch and slow-twitch knee extensor muscles. A primary focus was to ascertain the effect of zero gravity on whole homogenate protein, myofibril protein yields, myofibril ATPase, isomyosin distribution patterns and alpha glycerophosphate dehydrogenase activity in vastus intermedius (VI), vastus lateralis (VL), and vastus medialis (VM) muscles of Control (C), Flight (F), and Suspended (S) animal groups, N =5 each. Surprisingly, the muscle mass of the VI muscle, which consists predominantly of slow-twitch fibers, did not undergo atrophy in either the F or S groups, relative to C groups. However, there was evidence that myofibril yields in the VI were reduced as a result of both flight and suspension. This suggests that degradation of the myofibril machinery in slow-twitch muscle is an early event in the adaptation to zero gravity. Other parameters were not altered in the VI or the other muscles in response to either zero gravity or suspension, with the exception that suspension did induce isomyosin shifts in the VI muscle. Overall, the findings in the present study, with regard to the VI, are not fully consistent with observations reported previously on the Cosmos 1887 mission. The findings, in part, suggest that there may have been some technical difficulties in cleanly removing the VI from the quadriceps complex. This may account for the differences in mass noted in the present vs previous study concerning VI flight muscles. Also, the isomyosin patterns noted for the VI muscle in the various groups of rats suggest that a greater relative proportion of fast isoforms were present in the samples than what is normally expected, further suggesting that the muscle may not have been cleanly dissected.

INTRODUCTION

Previous findings on animals exposed to zero gravity clearly show that hindlimb muscles involved chiefly in antigravity function and comprised largely of slow-twitch fibers undergo greater degrees of atrophy as compared to synergists comprised predominantly of fast-twitch fibers (1,5,7). In the recent Cosmos 1887 Biosputnik mission, we also reported that zero gravity induced a selective degradation of the myofibril pool relative to other protein fractions in the vastus intermedius muscle, which consists largely of slow-twitch fibers (1). No such preferential loss of myofibril protein was observed in the vastus lateralis, which contains very little slow-myosin (1). This finding, although surprising, was in agreement with observations obtained on the ground-based rodent hindlimb suspension model (7). Furthermore, there was evidence that the relative proportion of slow/fast isomyosins was decreased providing evidence that the bias of contractile protein expression in the vastus intermedius was shifted in the direction of more fast types in animals exposed to space flight (1,5). The purpose of the present study was to build on these findings by performing analyses consisting of myofibril protein content, isomyosin distribution, and alpha glycerophosphate dehydrogenase activity on an expanded portion of the quadriceps muscle complex (vastus intermedius, vastus medialis, vastus lateralis) in rodents flown on the Cosmos 2044 Biosputnik 14 day mission, which occurred in September, 1989. The central hypothesis being tested in this project was that unloading conditions of zero gravity induce transformations in protein expression such that glycolytic

enzyme markers and fast isomyosin are up regulated in predominantly slow muscles with little or no change occurring in muscles already expressing fast isomyosins and high glycolytic enzyme activity.

METHOD

Experimental design and rodent groups

The muscles used for analysis in this study were obtained from animals selected for the Cosmos 2044 Biosputnik flight. Adult male Wistar rats (n = 5 in each group) were obtained from the Institute of Experimental Endocrinology, Bratislava, Czechoslovakia. The rats were initially assigned to one of five groups designated as basal controls (BS); Flight (FG); synchronous control (SC); vivarium control (VC); and suspended (S). In the present study, to simplify the reporting of the data and the interpretation of the findings, data from both the SC and VC groups were combined into a single group designated as control (C), because the biochemical results were similar in these two groups. Due to limited resources, analyses were not performed on the basal controls.

Flight animals were housed in a single cage and provided with a paste diet given in 16 gram boluses spaced 6 hrs apart for a total of 55 grams per day. The other groups, with the exception of the suspension group, were also grouped housed in similar cages; however, they were given the same caloric equivalent except it was administered in a single bolus. The light /dark cycle was such that the lights were on from 8:00 AM to 12:00 PM each day. Synchronous controls were treated like the flight rats as closely as possible with regard to launch g-forces, vibration, reentry g forces, and ambient temperatures.

Animal groups were killed according to the following schedule. Flight animals were sacrificed immediately upon their return from 14 days of space flight; whereas, the SC, VC, and S groups were killed 2, 6, and 8 days later, respectively. All tissue harvesting was at the same time each day for the various groups. Animals subjected to suspension were suspended by the tail traction technique for 14 days (7).

Tissue sampling

At the time of sacrifice, the animals were weighed and specific organ components were removed, including the muscles of the anterior thigh. The vastus intermedius (VI), vastus lateralis (VL), and vastus medialis (VM) muscles were removed, cleaned of visible fat and connective tissue, weighed and placed in vials containing 100% glycerol. The vials were stored at liquid nitrogen temperature and were eventually shipped by NASA to Irvine, California on dry ice in late October, 1989, at which time biochemical analyses were begun.

Tissue homogenation, myofibril extraction and myofibril ATPase, and alpha glycerophosphate dehydrogenase activity

The muscles were first washed free of glycerol and homogenized in a buffer containing 250 mM sucrose containing 2mM EDTA and 10 mM Tris buffer, pH 7.0. Aliquotes of this homogenate were taken and processed for total protein analysis (Figure 3) according to the biuret method (4). An additional aliquot was removed and frozen for later analysis of alpha glycerophosphate dehydrogenase activity as described previously (2). Next, the myofibril fraction was collected by spinning the sample at 1000 x g for 15 minutes and the resulting crude myofibril fraction was subjected to purification by the detergent treatment technique of Solaro et al (6), as described in detail previously (1). After the final washing step, the myofibrils were suspended in 150 mM KCl-20 mM imidazole (pH 7.0) and the

concentration was adjusted to 6 mg/ml by use of the biuret protein assay (4). Myofibril yields are reported as mg/g (Figure 4) and mg/muscle (mg/g x muscle weight)(Figure 5). Aliquots of the myofibril suspension were used immediately for determination of myofibril ATPase activity (see below), and the remainder of the myofibril suspension was prepared for storage (-20 oC) by suspending 1 volume of myofibril suspension with 2 volumes of a buffer consisting of 75% glycerol, 25 mM sodium pyrophosphate, 1 mM EGTA, and 0.5 mM 2-mercaptoethanol (pH 8.8).

Myofibril ATPase specific activity was determined at a free calcium concentration of 10^{-4} by use of an EGTA buffer system as described in detail previously (7). Activity was expressed as nanomoles of inorganic phosphate released per milligram of myofibril protein per minute (Figure 6).

Electrophoresis of myofibrils

Aliquots of mofibrils suspended in the glycerol buffer were subjected to polyacrylamide electrophoresis to separate the native myosins according to the method of Hoh et al (3). Briefly, native polyacrylamide gel electrophoresis was performed on 6-cm-long gels that were 4% total acrylamide, 2.5% bis(acrylamide) (expressed as a percentage of the total acrylamide), 10% glycerol and 20 mM tetrasodium pyrophosphate (pH 8.8 at 4 oC). Gels were prerun at 90 V (15 V/cm) maintained constant for 30 min prior to sample application. Approximately 5 micrograms of protein was electrophoresed for 20 hr at 90 V maintained constant. Gels were stained at the end of electrophoresis for 2 hr with a solution that was 0.1% Coomassie Blue R-250, 30% isopropyl alcohol, and 10% glacial acetic acid. The gels were destained by diffusion in a solution that was 20% methanol and 10% glacial acetic acid.

Quantitation of myosin isoforms

Gel bands of the native myosins separated by pyrophosphate electrophoresis were analyzed densitometrically by directly scanning the gels at 630 nm using a Zeineh Soft Laser Scanning Densitometer (Biomed Instruments, Inc., Fullerton, Ca.) connected to an IBM PC equipped with the appropriate program for integration of peak areas. The relative proportions of myosin isoforms were obtained from the gel scan and corresponded to the percent area under the peaks of absorption of the isoform bands. Previously, we identified five isomyosins in mixed fibered rodent skeletal muscle in order of their decreasing ability to migrate as follows: fast-myosins 1-3 (Fm1, Fm2, and Fm3), intermediate myosin (Im), and slow myosin (Sm) (8). These isomyosins have been fully characterized in terms of their heavy-chain and light chain composition (8). In figures 7-9, we present the distributions of isomyosin in the three muscles examined.

Statistical analysis

All values are expressed as the mean and standard error. Intergroup comparisons were made by using one-way analysis of varience. The significance of differences between two groups was tested using Student's t test. Differences were considered significant at the 0.05 level of confidence.

RESULTS AND DISCUSSION

Body weight, muscle weight, body weight/muscle weight

In this paper the data obtained from Cosmos 2044 have been organized so that comparisons can be made across three groups; controls (consisting of the combination of synchrony and vivarium controls), flight, and suspended animals. When possible, data were compared to Cosmos 1887, because the experiments were similar in duration and group comparisons for the two flights were available. Body weight of the Control group averaged 348 $\pm$ 9 grams as compared to 338 $\pm$ 2 and 339 $\pm$ 11 for the Flight and Suspended groups, respectively. Body weights of the control animals in 2044 are in the same range as for 1887, but the Flight group body weights of 1887 (303 $\pm$ 3) were significantly lower than the flight animals of the present study. Similarly, the muscle weights reported in Figure 1 indicate that there was little evidence of significant atrophy in any of the vastus muscles of the flight animals. The same conclusion applies to suspension although there were slight reductions in the VL and VM muscle weights (Figure 1). Normalizing the muscle weight data by correcting for body weight does not alter the interpretation of findings (Figure 2). The muscle weight data concerning the VI, in particular, are most surprising, because a consistent finding in the suspension model has been a significant loss in VI (and soleus) muscle mass in response to two or more weeks of suspension of adult female rats (7). We speculate that since the VI is a very difficult muscle to cleanly dissect, if any additional tissue is carried along with the bulk of the muscle, precise measurements in muscle weight may be difficult to obtain on this tissue. As discussed below, there appears also to be more fast myosin protein in the VI muscles analyzed from Cosmos 2044 than what we routinely see on female rats studied in the laboratory at Irvine. This could be the result of gender/animal variation as well as differences in investigator dissection technique.

Muscle protein and myofibril yields

As presented in Figure 3, neither flight nor suspension had an impact on altering the total protein content of any of the quadriceps muscles. However, both the VI and VM of the flight group had significantly lower myofibril content as compared to the control group (Figure 4). This observation is consistent with previous reports suggesting that unloading of muscles comprised heavily of slow myosin results in selective degradation of the myofibril system relative to other protein pools. This alteration appears to occur even when there is no evidence of atrophy. This is seen when the mass of the muscle is taken into consideration. As shown in Figure 5, the yield of myofibrils in the VI of flight animals, expressed on a per muscle basis, is not different from controls.

Myofibril ATPase

Myofibril ATPase activity was elevated only in the VI muscle of the suspended group (Figure 6). Myofibril ATPase was not altered in either the VL or VM in either flight or suspended groups. The increase in activity in the VI of the suspended but not the flight group is somewhat surprising, because the enzyme was elevated in the Cosmos 1887 flight (1). However, in that flight the overall composition of the myosin isozyme pool appeared to be shifted from the standpoint that there were greater amounts of both slow and intermediate myosin lost in that study as compared to the present study (see below).

Myosin isoform distribution

Figures 7-9 present the isomysoin distribution for the three muscles across the experimental groups. In control animals Sm and Im myosin are expressed to a greater relative degree in the VI relative to the VL and VM muscles. This distribution of the slower isoforms most

likely accounts for the lower myofibril ATPase activity in the VI muscle relative to the other two muscles. It is also worthy of note that the expression of the relative expression of fast/slow is much greater in the VI of the Cosmos rats as compared to animals routinely studied in the laboratory at Irvine (8). As indicated above, this could be due in part to tissue sampling or to variation in isomyosin expression across different strains and genders of rats. The only significant shift in isoform pattern of physiological significance is the decrease in Sm and increase in Fm3 among the VI of the suspension group (Figure 7). This shift in isoform expression is consistent with the myofibril ATPase data presented in Figure 6. Why such a shift did not occur in the flight animals is difficult to resolve at the present time.

Alpha glycerophosphate dehydrogenase activity (GPD)

Consistent with the myofibril ATPase and isomyosin data summarized for the various muscles, GPD activity was lowest among control groups in the VI (Figure 10). This is consistent with the long standing notion that muscles expressing an abundance of the slow myosin isoform also express relatively low levels of glycolytic related enzymes and vice versa. Although the VI of the suspended group showed a tendency for increasing GPD activity, this difference was not statistically significant. Therefore, it was surprising that the VM of the suspended group had a significant elevation in GPD activity. In view of the lack of alterations in isomyosin expression in this muscle this response is most puzzling.

Summary and conclusions

In conclusion, the most significant observation in the present study was the lack of any evidence of atrophy of the VI muscle in either the flight or suspension groups. This observation is in contrast to previous experiments involving both flight and suspended rodents (1,5.7). In spite of this lack of atrophy there was some evidence that suspension, in particular, affected the VI muscle based on myofibril yields and isoform distributions. Nevertheless, the overall degree of impact is dramatically reduced as compared to that seen with the previous studies on these same parameters. Future experiments need to carefully consider the technical difficulty in removing the VI muscle from the vastus complex for morphological and biochemical analysis. Beyond these considerations, it is not apparent why 14 days of space flight had such a little impact on the VI muscle, which in normally quite sensitive alterations in weight bearing activity.

This research was support by a special grant for Cosmos 2044.

REFERENCES

1. Baldwin, K. M., R. E. Herrick, E. Ilyina-Kakueva, and V. S. Organov. Effects of zero gravity on myofibril content and isomyosin distribution in rodent skeletal muscle. FASEB J. 4: 79-83, 1990.

2. Baldwin, K. M., W. W. Winder, R. L. Terjung, and J. O. Holloszy. Glycolytic enzymes in diferent types of skeletal muscle: adaptation to exercise. Am. J. Physiol. 225: 962-966, 1973.

3. Hoh, J. F. Y., P. A. McGrath, and R. I. White. Electrophoretic analysis of multiple forms of myosin in fast-twitch and slow-twitch muscles of the chick. Biochem. J. 157: 87-95, 1976.

4. Gornall, A. J., C. J. Bardawill, and M. M. David. Determination of serum proteins by means of the biuret method. J. Biol. Chem. 177: 751-756, 1949.

5. Miu, B., T. P. Martin, R. R. Roy, V. Organov, E. Ilyina-Kakueva, E. Marini, J. F. Leger, S. C. Bodine-Fowler, and V. R. Edgerton. Metabolic and morphologic properties of single muscle fibers in the rat after spaceflight, Cosmos 1887. FASEB J. 4: 64-72. 1990.

6. Solaro, R. J., D. C. Pang, and F. N. Briggs. The purification of cardiac myofibrils with triton X-100. Biochim. Biophysics Acta. 245: 259-262, 1971.

7. Thomason, D. B., R. E. Herrick, D. Surdyka, and K. M. Baldwin. Time course of soleus muscle myosin expression during hindlimb suspension and recovery. J. Appl. Physiol. 63:130-137, 1987.

8. Tsika, R. W., R. E. Herrick, and K. M. Baldwin. Subunit composition of rodent isomyosins and their distribution in hindlimb skeletal muscle. J. Appl. Physiol. 63: 2101-2110, 1987.

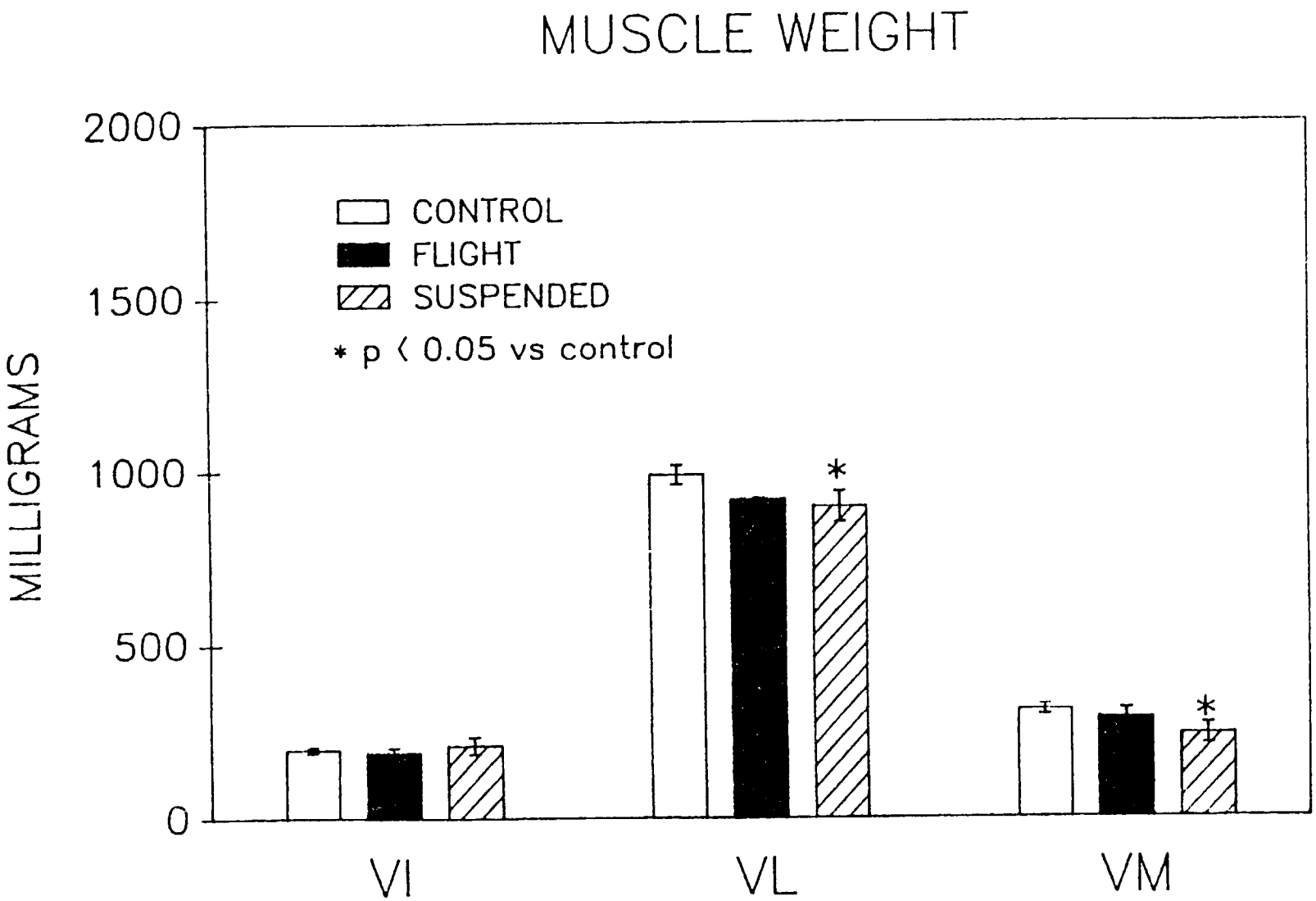

Figure 1. Muscle weights of the quadriceps muscles of control, flight, and suspended animals.

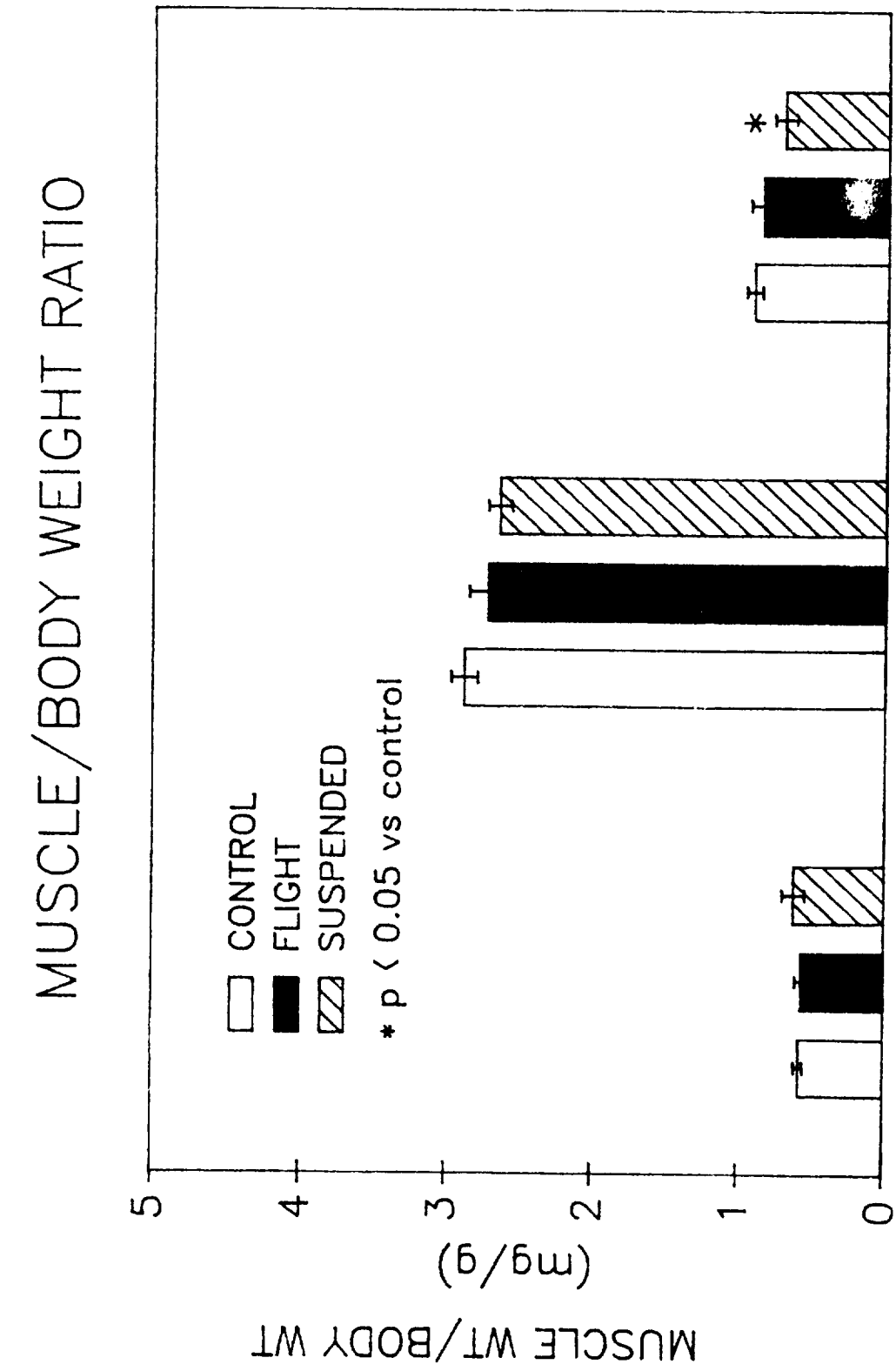

Figure 2. Muscle weight/body weight of the quadriceps muscles among control, flight, and suspended groups.

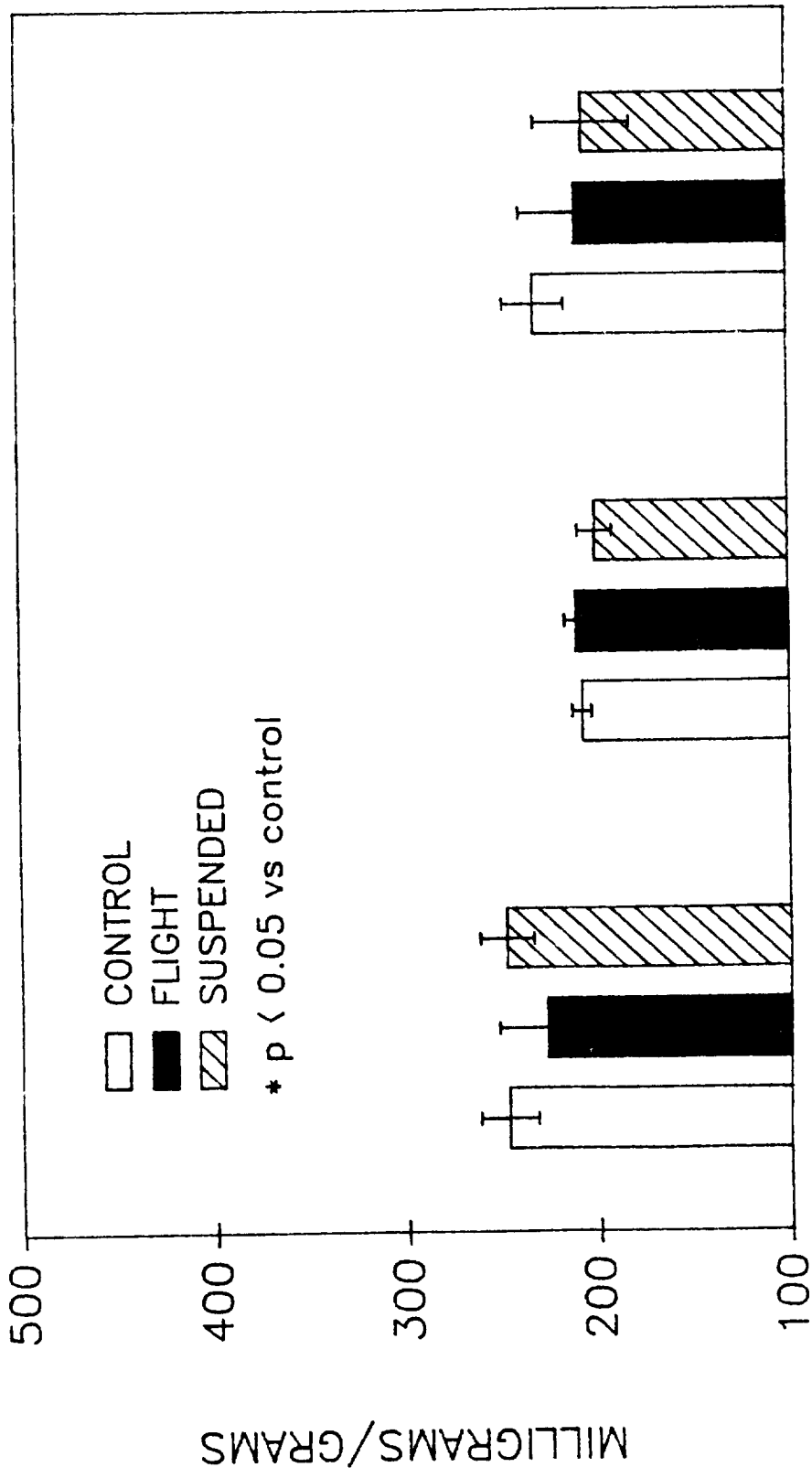

Figure 3. Total muscle protein among muscles of experimental groups.

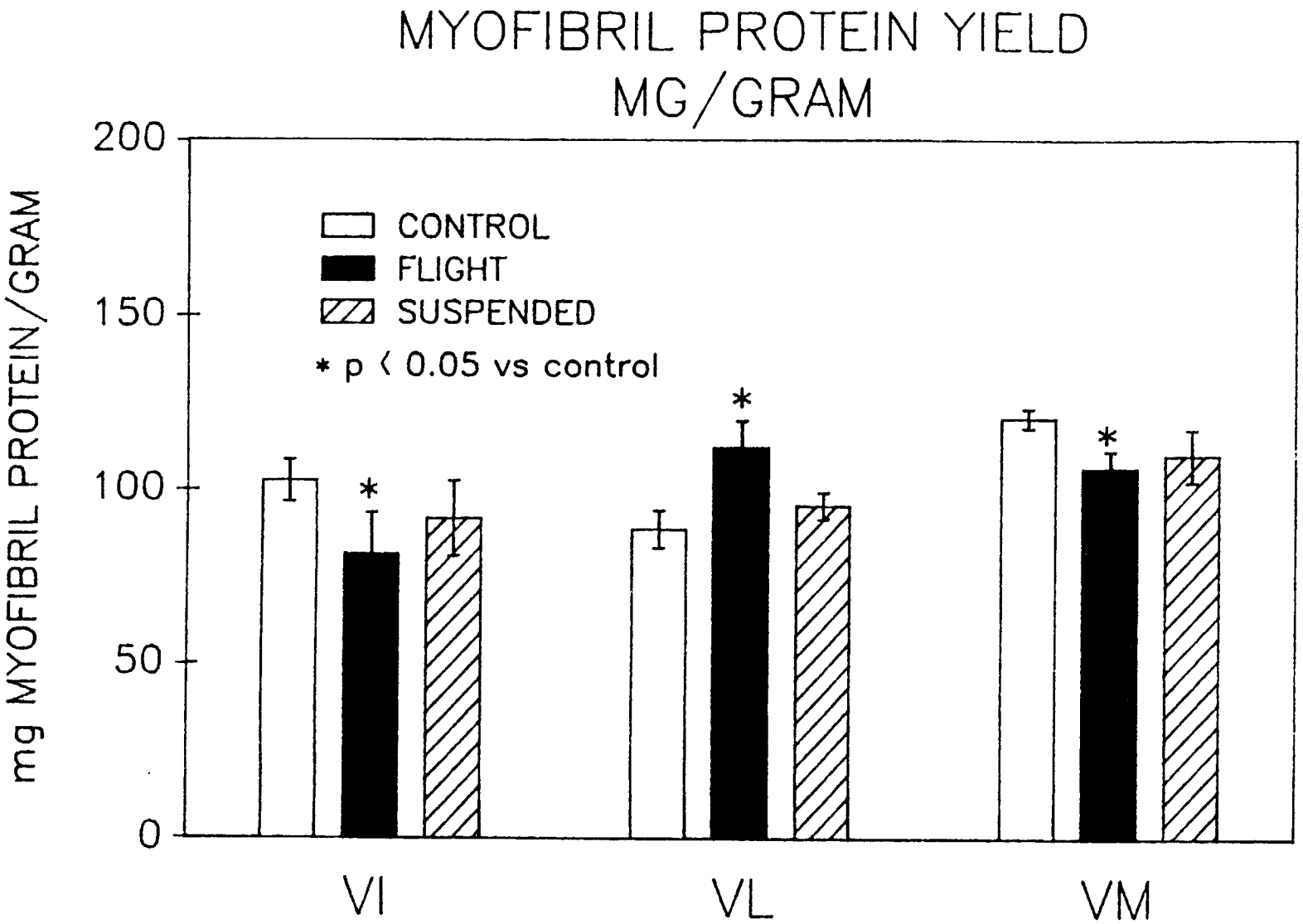

Figure 4. Myofibril protein yields (mg/gram of muscle) among muscles of the experimental groups.

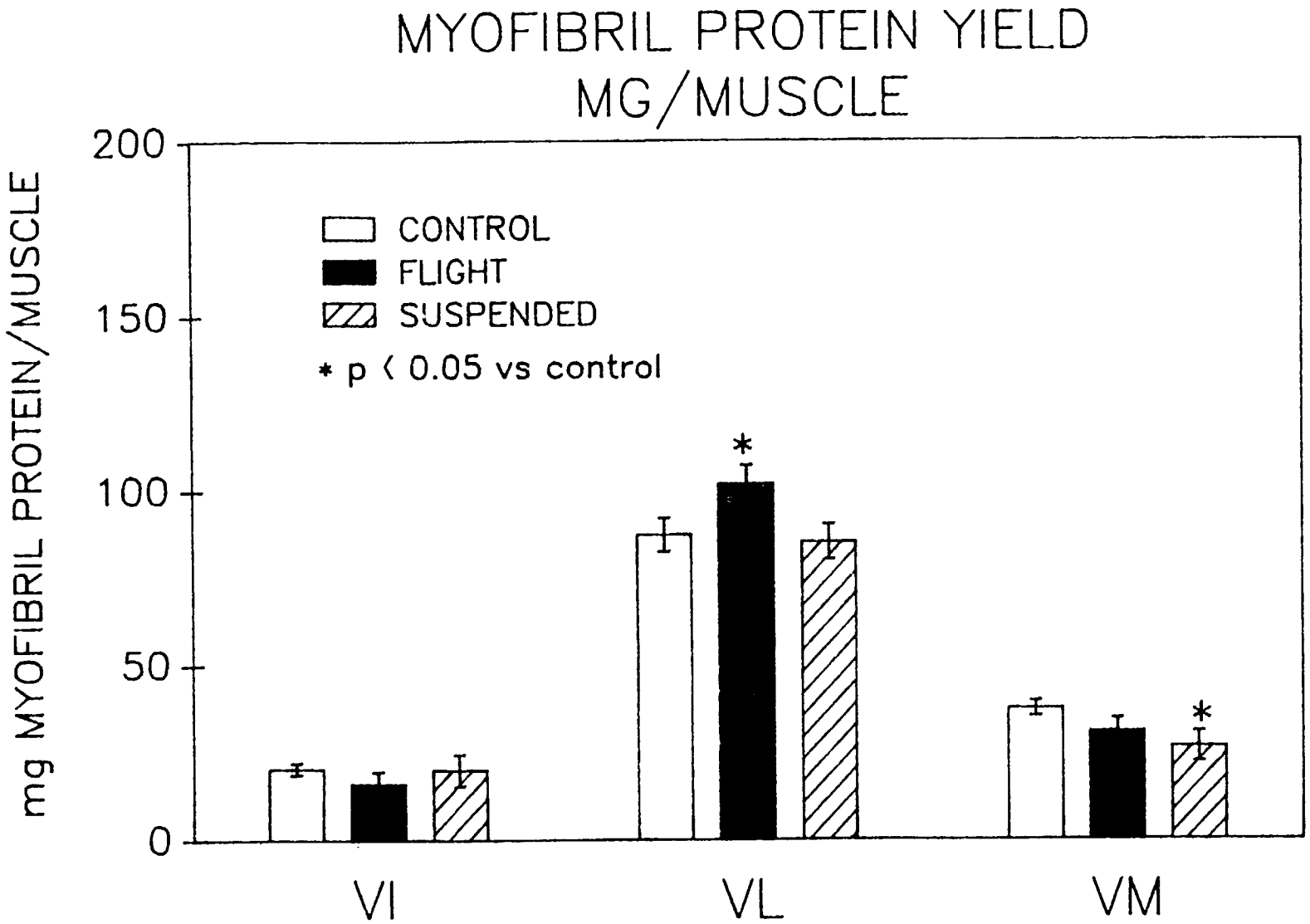

Figure 5. Myofibril yields normalized per muscle among muscles for the experimental groups.

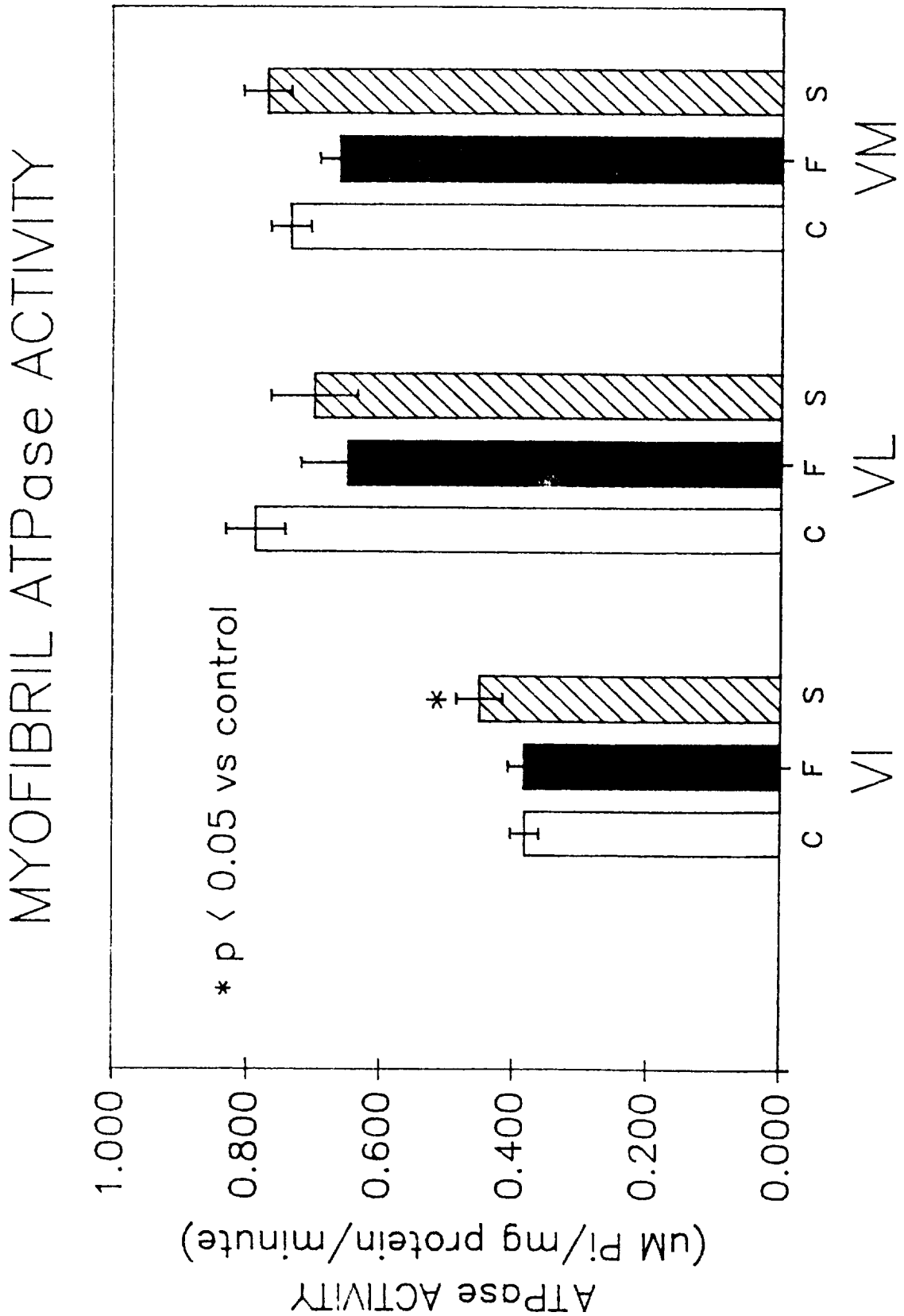

Figure 6. Myofibril ATPase among muscles for the experimental groups.

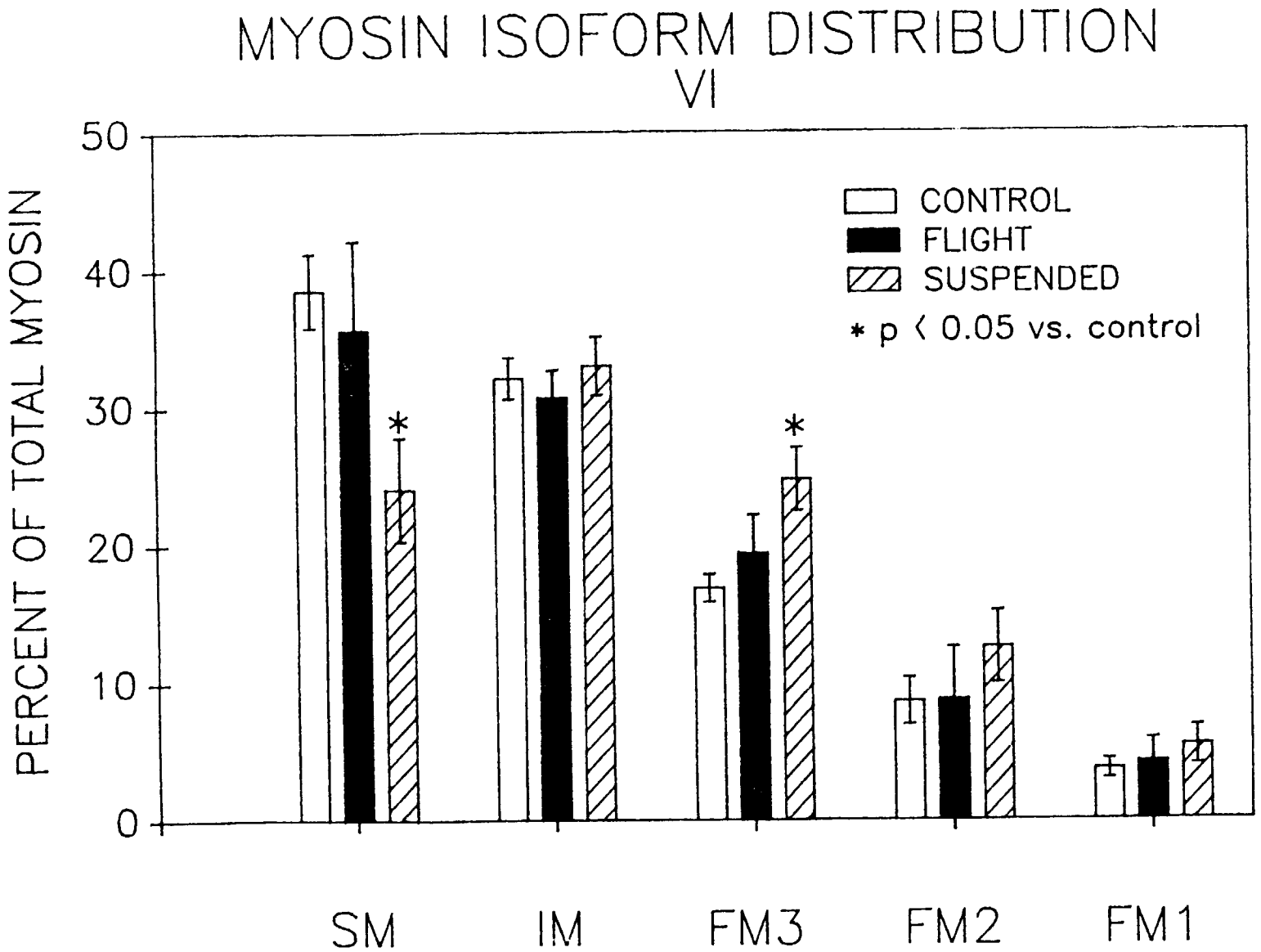

Figure 7. Myosin isoform distributions in the vastus intermedius muscle of the experimental groups.

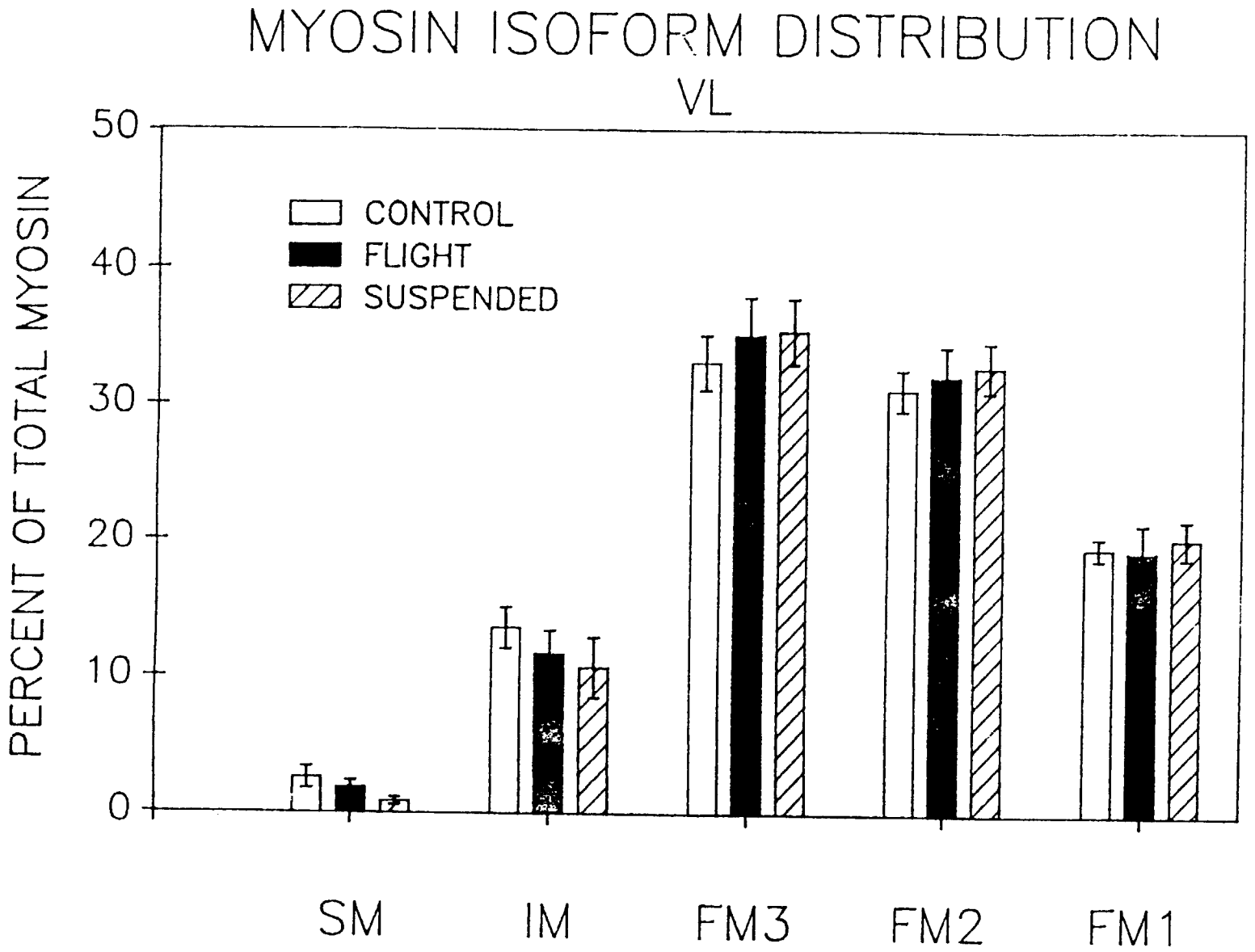

Figure 8. Myosin isoform distributions in the vastus lateralis muscle of the experimental groups.

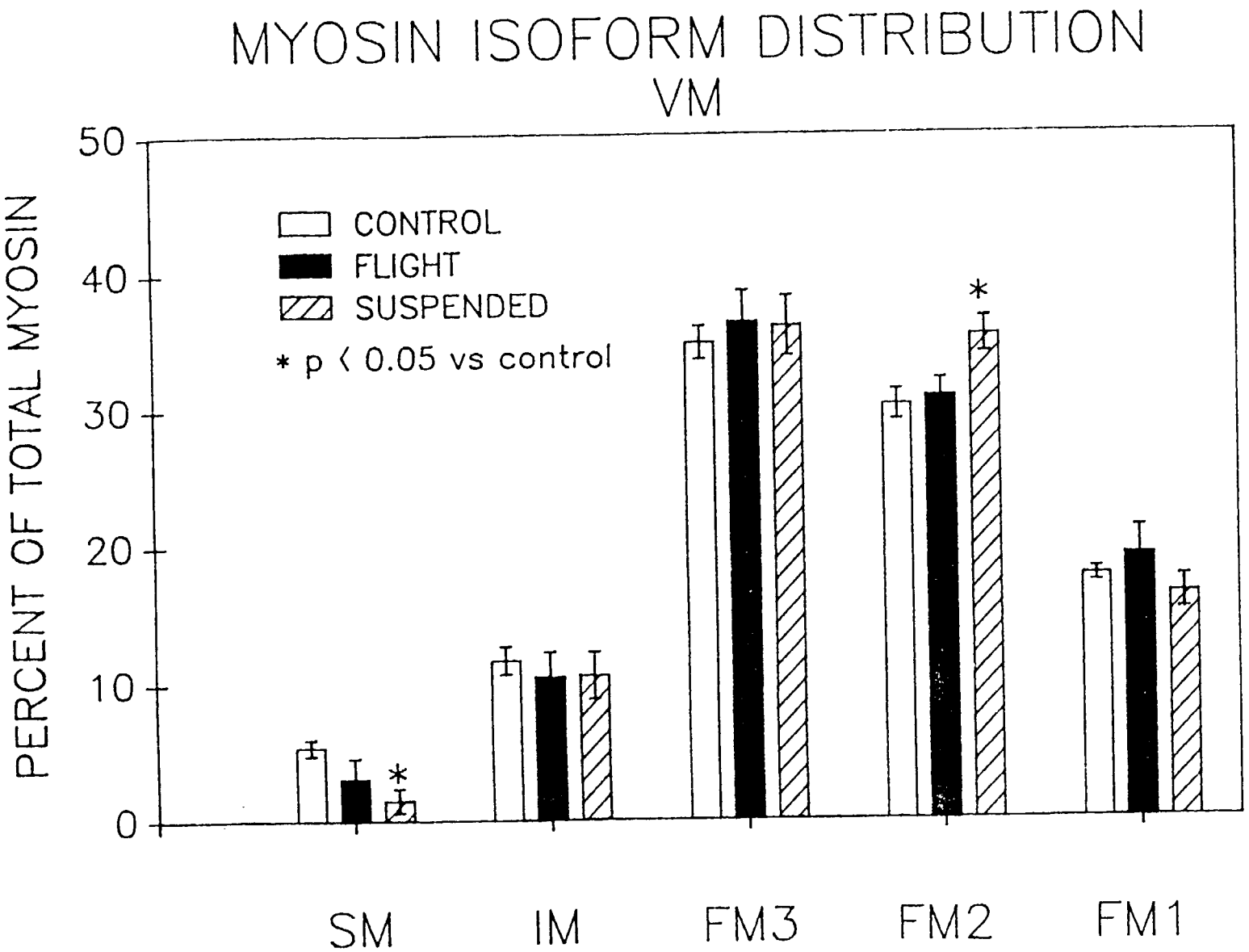

Figure 9. Myosin isoform distributions in the vastus medialis muscle of the experimental groups.

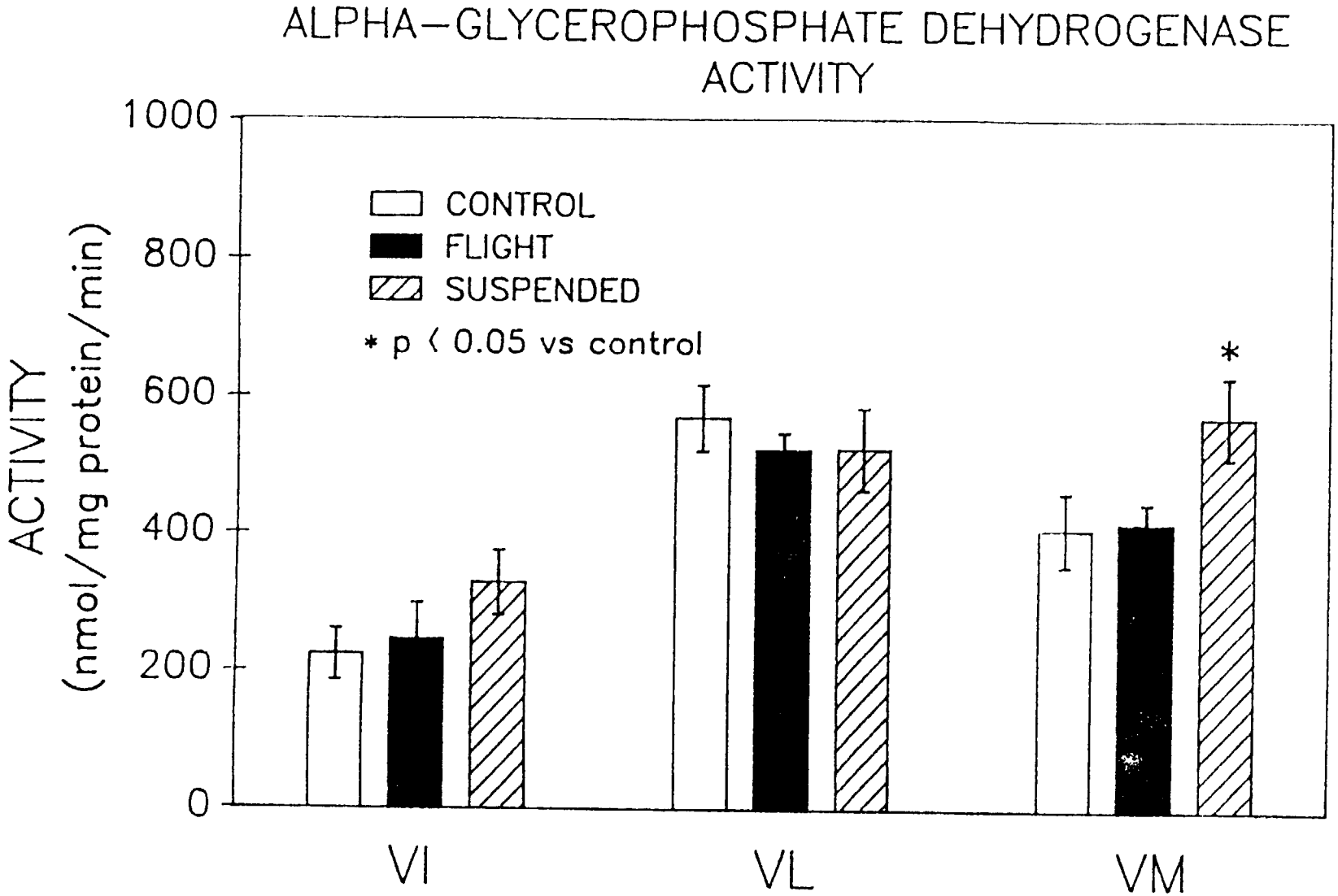

Figure 10. Alpha glycerophosphate dehydrogenase activity in the various muscle of the experimental groups.

EXPERIMENT K-7-11

mRNA LEVELS IN SKELETAL AND SMOOTH MUSCLE

PART I: SOME mRNA'S DECREASE IN SKELETAL MUSCLE DURING SPACEFLIGHT

Principal Investigator:

Frank W. Booth
Dept. of Physiology and Cell Biology
University of Texas Medical School
Houston, TX

Co-Investigators:

V.S. Oganov
E.I. Ilyina-Kakueva
K.V. Smirnov
Institute of Biomedical Problems
Moscow, USSR

P.R. Morrison
Donald B. Thomason
Dept. of Physiology and Cell Biology
University of Texas Medical School
Houston, TX

PART II. mRNA LEVELS IN SMOOTH MUSCLE

Co-Investigators:

Norman Weisbrodt
Dept. of Physiology and Cell Biology
University of Texas Medical School
Houston, TX

Mildred Lai
Donald B. Thomason
Dept. of Physiology and Cell Biology
University of Texas Medical School
Houston, TX

EXPERIMENT K-7-11

PART I: SOME mRNA'S DECREASE IN SKELETAL MUSCLE DURING SPACEFLIGHT

F.W. Booth, D.B. Thomason, P.R. Morrison,
V.S.Oganov , E.I. Ilyina-Kakueva, and K.V. Smirnov

Skeletal muscle of humans (see Buchanan for refs) and animals (see Martin for ref) atrophy in spaceflight. It is believed that the removal of weightbearing by a skeletal muscle induces its atrophy (Alford). The sequence of chemical steps linking the non-weightbearing to the loss of muscle protein remains unknown. Using a model of non-weightbearing at 1 g to mimic the effect of microgravity on skeletal muscle, decreases in the mRNAs for skeletal "alpha" actin and cytochrome c have been observed in skeletal muscle (Babij). The purpose of this study was to determine if similar events occur in skeletal muscle of rats during spaceflight.

METHODS.

Muscles were received on dry ice from Dr. Richard E. Grindeland of NASA. Experimental groups were described in an earlier manuscript (Grindeland). RNA was extracted from skeletal muscle by the LiCl-urea method (Auffray). Hybridizations were performed with a ^{32}P-labelled rat skeletal "alpha" actin probe consisting of 560 bases of the coding region (Nedel) and with a ^{32}P-labelled 960-base fragment of the rat somatic cytochrome c gene (Scarpulla). Hybridization conditions were as described previously (Babij). RNA denaturing gels indicated that RNA was undegraded and that hybridization stringency was strict enough for specific binding to the designated mRNA. The concentration (amount of probe bound per g total RNA) of the mRNA were determined by RNA dot blots. Following autoradiography, laser beam densitometry (Cosmos 1887) and scintillation counting (Cosmos 2044) were done to estimate ^{32}P bound to the mRNA. Analysis of covariance was used to determine significance among slopes for intensity and for counts per RNA quantity.

RESULTS AND DISCUSSION.

Directional changes in skeletal "alpha" actin mRNA in skeletal muscle during spaceflight were in the same pattern as those previously reported in the non-weightbearing model at 1 g. After 14 days in Cosmos 2044, decreases of 25% and 36% in skeletal "alpha" actin mRNA of the vastus intermediate and lateral gastrocnemius muscles, respectively, were observed (Table 1). In 5 previous experiments for these muscles, as well as the soleus muscle, decreases ranging from 21% - 35% for skeletal "alpha" actin mRNA were noted after 7 or 14 days of non-weightbearing at 1 g. Thus a decrease in pre-translational control for skeletal "alpha" actin mRNA occurs in two non-weightbearing models, tail suspension at 1 g and spaceflight. It seems feasible to pursue the mechanism of the decrease in the ground-based model because of its close correlation to microgravity.

In contrast to the decrease in skeletal "alpha" actin mRNA in calf muscles, no change occurred in the triceps brachii muscle in either Cosmos 1887 or 2044 and in a single measurement in the tail-suspension model at 1 g. It is possible that the differential responses of calf and forelimb muscles to non-weightbearing could be related to recruitment pattern variations between fore- and hindlimbs. Since the gastrocnemius muscle atrophied in non-weightbearing (Cosmos 2044 and tail suspension), while the triceps brachii did not atrophy, a difference in usage is suggested. A future study should measure EMG in the calf and triceps brachii muscles to test this speculation.

Results for directional changes in cytochrome c mRNA in non-weightbearing tend to be similar to directional changes in skeletal "alpha" actin mRNA with certain exceptions (Table 2). No decrease in cytochrome c mRNA was found in the lateral gastrocnemius muscle in Cosmos 2044 and in 1 of 2 tail suspension studies and in the vastus intermediate muscle during the tail suspension study (Table 2). In the vastus intermediate muscle of Cosmos 2044, cytochrome c mRNA was decreased, but it was increased in non-weightbearing.. Thus as opposed to the responses of skeletal "alpha" actin mRNA to non-weightbearing, cytochrome c mRNA changes were not consistent in directionality.

ACKNOWLEDGEMENTS.

We thank the Soviet dissection, headed by Dr. A.S. Kaplansky, and the American team, consisting of Dr. R.E. Grindeland and Ms. Marilyn Vasques, for their contributions to providing us with tissues.

REFERENCES

1. Alford, E.K., R.R.Roy, J.A. Hodgson and V.R. Edgerton. Electromyography of rat soleus, medial gastrocnemius and tibialis anterior during hindlimb suspension. Exp Neurol, 9b: 635-649, 1987

2. Auffray, C, and F. Rouyeon. Purification of mouse immunoglobin heavy-chain mRNAs from myeloma tumor - RNA. Eur. J. Biochem. 107: 303-314, 1979.

3. Babij, P. and F.W. Booth. Actin and cytochrome c mRNAs in atrophied adult rat skeletal muscle. Am. J. Physiol. 254: C651-C656, 1988.

4. Buchanan, P. and V.A. Convertino. A study of the effects of prolonged simulated microgravity on the musculature of the lower extremities in man: an introduction. Aviat. Space Environ. Med. 60: 649-652, 1989.

5. Grindeland, R.E., M.F. Vasques, R.W. Ballard and J.P. Connolly, Cosmos 2044 Mission OVerview, J.Appl. Physiol., In review.

6. Martin, T.P., V.E. Edgerton and R.E. Grindeland. Influence of spaceflight on rat skeletal muscle. J. Appl. Physiol. 65: 2318-2325, 1988.

7. Nedel,U, D. Katcoff, R. Zakut, M.Shan, Y. Carmon, M.Finer, H. Czosnek, I. Ginsberg and D. Yaffe, Isolation and Characterization of Rat Skeletal Muscle and Cytoplasmic Actingenes. Proc. Natl. Acad. Sci., USA 79: 2763-2767, 1982.

8. Thomason, D.B., R.B. Biggs and F.W. Booth. Protein metabolism and -myosin heavy-chain mRNA in unweighted soleus muscle. Am. J. Physiol. 257: R300-R305, 1989.

9. Scarpulla, R.C., K.M. Agne, and R.Wu, Isolation and Structure of a Rat Cytochrome c gene, J. Appl. Physiol., 256: 6480-6486, 1981.

TABLE 1.

PERCENTAGE CHANGE IN SKELETAL
"alpha" ACTIN mRNA PER UNIT OF EXTRACTABLE RNA AFTER NON-WEIGHTBEARING

		MUSCLE		
Study	Soleus	VASTUS Intermediate	LATERAL Gastrocnemius	TRICEPS Brachii
14 days in Cosmos 2044	N.D.	↓25%+	↓36% *	N.S.
14 days tail-suspension	N.D.	↓27% *	↓35% *	N.S.
7 days in Cosmos 1877	N.D.	N.D.	N.D.	N.S.
7 days tail-suspension	↓29%*x ↓21%*x	N.D.	↓33%*x ↓33%*x	N.D.

Values are percentage decrease from appropriate control group. *, P<0.05. +, P=0.06.x , data from Babij et al and Thomason et al ( ). N.S. = non-significant from control. N.D. = not determined.

TABLE 2.

PERCENTAGE CHANGE IN SOMATIC CYTOCHROME c mRNA PER UNIT OF EXTRACTABLE RNA AFTER NON-WEIGHTBEARING

Study	Soleus	MUSCLE		
		VASTUS Intermediate	LATERAL Gastrocnemius	TRICEPS Brachii
14 days in Cosmos 2044	N.D.	↓36%*	N.S.	N.S.
14 days tail-suspension	N.D.	↑42% *	N.S.	N.S.
7 days in Cosmos 1877	N.D.	N.D.	N.D.	N.S.
7 days tail-suspension	↓17%*	N.D.	↓20%*	N.D.

Values are percentage change from appropriate control groups. *, P<0.05. +, data from Babij et al ( ). N.S. = non-significant from control. N.D. = not determined.

EXPERIMENT K-7-11

PART II: mRNA LEVELS IN SMOOTH MUSCLE

Norman W. Weisbrodt, Frank W. Booth, Mildred Lai, Donald B. Thomason

SUMMARY

Intestinal smooth muscle samples from rats flown on Cosmos 2044 were analyzed for changes in weight, protein content, RNA, and mRNA levels for actin. Segments of mid small intestine were removed from the animals, opened lengthwise, rinsed, frozen in liquid nitrogen, and shipped to Houston on dry ice. They were stored at -80C until they were thawed at 4C and their lengths measured. The longitudinal layer of smooth muscle was removed, weighed, and then processed for determinations. Wet weight and protein content were less in tissue taken from flight animals compared to vivarium controls. However, there were no differences among tissues taken from flight animals, synchronous and tail-suspended animals. The differences detected might be explained on the basis of food consumption and/or weight gain. Total RNA, as determined by a method that is not quantitative, differed among tissues from all groups with vivarium > tail-suspended > synchronous > flight. Size fractionation of the RNA demonstrated significant degradation. Analysis of northern blots failed to show any hybridization to a riboprobe for smooth muscle actin. More than likely this was due to the degradation. Although not conclusive, the RNA data suggest that there may be an influence of spaceflight on intestinal smooth muscle gene expression.

INTRODUCTION

The effects of external forces such as gravity on structure and function of the gastrointestinal tract have received little study. A few investigations have been conducted on the effects of positional changes on such gross functions as swallowing (1) and gastric emptying (2). In general, results of these studies have been interpreted as showing no, or minimal effects of gravity. Indeed, the argument is made that since the gut is essentially floating in an enclosed chamber, the abdomen, the influence of gravity would be dissipated. This notion of a lack of effect of gravity on overall function of the gut seems to be supported by the observations that digestion and absorption of food are not markedly impaired during space flights, and that no changes were seen in the proliferation of jejunal mucosal cells in rats that were flown on Cosmos 1887. Although these studies and observations suggest that the net function of the gut is unaltered by gravitational changes, more detailed investigations are warranted. The gut is known to adapt rapidly to many factors so that overall digestion and absorption appear normal (3,4). Such adaptation involves changes in function and structure of many of the cells that comprise the gut. It is only due to their adaptation that no changes in overall gastrointestinal function are seen. Thus, changes in gravitational forces may induce changes in gut cell gene expression even though no altered function occurs.

We have shown that in one model in which gut function is perturbed, intestinal bypass in the rat, both the function and structure of intestinal smooth muscle undergo changes (4-6). Functionally, intestinal motility is altered so that transit through the shortened segment slows down, presumably allowing more time for complete digestion and absorption of foodstuffs. Structurally, there is a muscular hypertrophy accompanied by an increase in contractile proteins. Although the structural changes are not marked until ten or so days after operation, total RNA and mRNA's that code for various actin isoforms are increased by 4 to 5 days after operation (7).

The data from the bypass model suggest that if there are any changes in gut structure associated with space flight, they may be expressed as early changes in gene expression in intestinal smooth muscle. Thus, the purpose of the current experiments was to define the effects of space flight on the weight and protein content, and on the abundance of actin mRNA in intestinal smooth muscle taken from animals flown on Cosmos 2044.

MATERIALS AND METHODS

Four groups of animals, five rats in each group, were treated as described in the Mission Description section of this report. Frozen segments of intestine, one segment from each animal and labeled F6-F10 (Flight), S6-S10 (Synchronous), T6-T10 (Tail Suspended) and V6-V10 (Vivarium) were received. Segments were kept at -60C until assays were performed.

Each segment was placed in 4C saline and allowed to assume its resting length while thawing. Approximately 10 minutes after thawing was judged to be complete, tissue length was measured. Each segment, which had been opened lengthwise and rinsed prior to freezing, was then pinned mucosal side down and any remaining mesentery was removed. A shallow cut, in the transverse axis, was made at one end of the segment. With fine forceps the serosa and the longitudinal muscle (referred to henceforth as longitudinal muscle) were peeled away from the remaining circular muscle and mucosa. The longitudinal muscle was gently blotted on tissue paper and weighed. It then was placed in 5 ml of 4 M guanidinium isothiocyanate, 5 mM Na citrate, 0.1 M mercaptoethanol, 0.5% sarkosyl (pH 7.0) at 20C and homogenized for approximately 1 min using a VirTis homogenizer. A 200 ml aliquot was removed and the remainder of the homogenate was centrifuged at 1,000 g for 10 min, and the supernatant was placed on a 4-ml cushion of 5.7 M CsCl and centrifuged at 100,000 g for 20 h at 20C to pellet the RNA.

A riboprobe was made and used to assess levels of actin mRNA. The plasmid clone pGEM10C was obtained from Drs. Jenny Hsu and Fred R. Frankel, Department of Microbiology, University of Pennsylvania School of Medicine (8). This plasmid contains a cDNA insert that codes for a portion of the 3' untranslated region, all of the coding region, and a portion of the 5' untranslated region of the mRNA that in turn codes for the synthesis of smooth muscle actin. The cDNA insert is flanked on each side by a RNA polymerase promoter, SP6 on one side and T7 on the other. There are restriction sites within the double stranded DNA that can be cleaved with specific restriction endonucleases such that the riboprobes generated using the SP6 promoter are complementary to either the full coding region or just the 3' untranslated region. The clone was treated with the enzyme PvuII to linearize the entire cDNA insert and the adjacent SP6 promoter. Then, 1 mg of digested DNA was added to 20 ml polymerase reaction mixture containing 60 mCi [32P] CTP, 12 mM CTP, 500 mM each of GTP, UTP, and ATP, 10 mM dithiothreitol, 20U RNasin, 15U SP6 polymerase, and 1X SP6 reaction buffer. The reaction was carried out at 37C for 1 h. The reaction was terminated by addition of 10U DNase I for 10 min followed by 1 ml of 100 mM EDTA. The RNA riboprobe transcript then was extracted with phenol/chloroform and precipitated with ammonium acetate and ethanol at -20C. overnight. Typical specific activities were $2x10^8$ DPM/mg DNA.

To check for purity of RNA isolation, to determine the specificity of the probes, and to determine acceptable conditions for hybridization, RNA samples were size fractionated by denaturing gel electrophoresis and transferred to nylon membranes for probe hybridization. Briefly, 1% agarose gels containing 20 mM morpholinopropane sulfonic acid, 0.5 mM ethylenediaminetetraacetic acid, 5 mM Na acetate (pH 7.0), and 2.2 M formaldehyde were run at 80 V for 3-4 h. The gels were stained in 0.5 mg/ml ethidium bromide and

photographed. The RNA then was electrophoretically transferred to nylon membranes in 25 mM Na phosphate (pH 7.0) at 200 mA (1.5 V/cm) for 2 h and 1 A (7 V/cm) for 1 h.

After transfer, all membranes were baked in vacuo at 80C for 1 h. They were prehybridized in 10 ml of a mixture of 5X Denhardt's solution, 750 mM NaCl, 75 mM Na citrate, 50 mM Na phosphate, 0.1 % SDS, 50 % formamide, 200 mg/ml yeast-tRNA, 100 mg/ml boiled sheared herring sperm DNA, pH 7.0, at 55C for 20 h.

The probe was first boiled for 5 min with 1 mg sheared herring sperm DNA and then added to 10 ml of a mixture of 1X Denhardt's solution, 750 mM NaCl, 75 mM Na citrate, 50 mM Na phosphate, 0.1% SDS, 50% formamide, pH 7.0. Hybridization to the membranes was then conducted at 55C for 20 h. Each membrane was then washed under the following conditions: three 45 min washes in 75 mM NaCl, 7.5 mM Na citrate pH 7.0 at 60C followed by two 45 min washes in 15 mM NaCl, 1.5 mM Na citrate, pH 7.0, at 65C. These washes were followed by a five minute wash in 10 mg RNase A in 150 mM NaCl, 15 mM Na citrate, pH 7.0. After hybridization with the riboprobes and washing, the membranes were exposed to X-OMAT AR X-ray film (Kodak) at -80C with two tungstate intensifying screens. A typical exposure time was 24 h. RNA integrity on the gel blots was judged by visual inspection. The Bio-Rad Protein Assay (Bio-Rad, Richmond, CA) was used to determine the protein concentration in the 200 ml aliquots. Prior to making these determinations, bovine serum albumin standards were prepared in the homogenization mixture and in distilled water. Curves relating optical density to albumin concentration in the two solvents were linear and superimposable. Thus, the homogeniz–ation mixture did not appear to interfere with the assay.

The method we used to isolate total RNA yields a product that is relatively pure; however, the recovery is incomplete and variable. With these limitation in mind, we determined the amount of RNA recovered spectrophotometrically and present it as a comparative estimate of the total RNA contained in each segment of longitudinal muscle.

Wet weight, total protein, and total RNA for the longitudinal muscle from each segment were normalized to the length of each segment. These values are expressed as mean ±SEM. Statistical comparisons were made using a one-way analysis of variance with a Duncan's New Multiple Range Procedure. $p < 0.05$ was considered to be statistically significant.

RESULTS

Segment lengths were similar among the four groups - Flight, Synchronous, Tail Suspended, and Vivarium - averaging 5.4, 5.8, 6.2, and 5.7 cm respectively. Longitudinal muscle wet weights, normalized to segment lengths, were similar among the flight, synchronous, and tail-suspended groups. However wet weight of muscle from the vivarium group was greater (Table 1). Total protein of the longitudinal muscle was greatest in the vivarium group, intermediate in the tail-suspended and synchronous groups, and least in the flight group. However, the only statistically significant difference was between the flight and the vivarium groups (Table 1). Total RNA of the longitudinal muscle showed the same trend of vivarium > tail-suspended > synchronous > flight. However, in this instance, there were significant differences among all four groups (Table 1).

As stated above, RNA was isolated from all tissues. However, when analyzed for purity by gel electrophoresis, all samples showed signs of degradation (Figure 1). When this was noticed, samples of RNA previously isolated from muscle that had been taken from either fresh or frozen intestinal segments were run simultaneously with several of the Cosmos

samples. As shown in Figure 2 , only those samples from the Cosmos study showed evidence of degradation.

Although degradation was obvious, we did attempt to assess the presence of mRNA for actin isoforms. None of the Cosmos samples hybridized with the riboprobe. In order to determine if conditions for hybridization were adequate, samples of RNA from intestinal muscle obtained from previous experiments were electrophoresed, blotted, and hybridized along with representative Cosmos samples. As figure 3 indicates, smaller amounts of RNA isolated from non-Cosmos samples fractionated such that a distinct size hybridized with the riboprobe. However, none of the Cosmos samples hybridized with the probe.

DISCUSSION

Comparative studies on intestinal muscle are made difficult due to the lack of a reference point. Due to its great length and to differences in structure along this length, it is not practical to dissect all of the muscle from the entire intestine. Thus, a sample length is taken. To obtain reproducible estimates of length, measurements must be taken under identical conditions. This is the reason for the rigid criteria for tissue handling just prior to length measurement. Once obtained, other determinations then can be expressed as a function of tissue length.

The results of this study further indicate that smooth muscle from the intestine does respond structurally to perturbations imposed on the whole animal. This is in keeping with results obtained from animals that have undergone intestinal bypass and animals that have been infected with various parasites (4-7,9,10). In all cases, changes in wet weight and protein content can be detected. Also, in the case of intestinal bypass, changes in mRNA levels for actin were observed (7). To date, however, the exact mechanisms responsible for the changes are not known.

Changes in wet weight and protein content were observed among the four groups of animals. Of the two, protein probably is the more accurate since wet weight determinations are influenced by the amount of water present both in and on the tissue during weighing. For both parameters values were lower in tissue from flight animals than from animals maintained in the vivarium. There were no significant differences among the flight, synchronous, and tail-suspended groups. However, there was a trend in total protein with lowest values seen in tissue taken from flight animals. These data are difficult to interpret. Since muscle mass may vary in relation to dietary intake, the higher values in the vivarium animals may be related to their higher food intake (4,11). On the other hand, the trend to a decrease in protein in the flight animals may be a result of spaceflight that with longer flights could reach statistical significance. This possibility is somewhat supported by the data on total RNA (see below).

Although interesting, the data on total RNA must be viewed with caution. The method used to isolate RNA from the tissues is designed to yield relatively pure RNA, but it does not completely or reproducibly extract the RNA. However, there is no reason to believe that extraction would be more complete in any one set of tissues. Thus, relative comparisons may be useful. The finding of significant decreases in total RNA that parallel the trends seen in wet weight and protein may be due to earlier changes in RNA induced by the various perturbations. This would be expected since changes in RNA frequently precede changes in protein. The RNA changes may further indicate that diet can influence intestinal smooth muscle since the highest levels were found in tissue from the animal group with the greatest food intake, the vivarium group. Finally, the fact that the lowest levels were found in those animals subjected to spaceflight may indicate an influence of

gravity. However, since hormonal and other changes also occur during flight, the effect, if any, could be secondary.

Changes in muscle gene expression as indicated by changes in mRNA levels for specific proteins could not be evaluated. This is unfortunate since if changes in muscle do occur, they probably would be expressed as early changes in mRNA levels for specific proteins. We already have shown that bypass results in elevations of mRNA levels coding for actin as early as four days after operation, a time at which changes in wet weight and protein are not seen (7). Specific mRNA determinations also are critical since it is possible that non-muscle proteins in the muscle layer could be changing even though the muscle is not. Since wet weight and total protein determinations do not distinguish between muscle and non muscle cells and cell products, a specific marker such as actin mRNA levels would be valuable.

The reasons for the failure to detect mRNA levels are not known. Visualization of size fractionated samples suggests RNA degradation somewhere in the isolation process. All reagents used were checked by extracting both freshly isolated and frozen intestinal muscle harvested from animals at our institution. Since only the samples from the Cosmos study showed degradation and failed to hybridize to the probe, it may be that degradation took place during the preparation, shipment, or storage of the intestinal segments. We have noted that intestinal tissue is sensitive to handling, perhaps due to the number of lytic enzymes contained in the gut.

REFERENCES

1. Bowers, R.L., G.A. Castro, and N.W. Weisbrodt. Alterations in Intestinal Smooth Muscle of the Rat Induced by *Trichinella spiralis*. Gastroenterology 90:1353, 1986.

2. Bowers, R.L., C. Eeckhout, and N.W. Weisbrodt,. Actomyosin, Collagen, and Cell Hypertrophy in Intestinal Muscle after Jejunoileal Bypass. Am. J. Physiol. 250:G70-G75, 1986.

3. Hsu, C-Y.J. and F.R. Frankel. Effect of Estrogen on the Expression of mRNAs of Different Actin Isoforms in Immature Rat Uterus. J. Biol. Chem. 262:9594-9600, 1987.

4. Hunt, J.N., M.T. Knox, and A. Oginski. The Effect of Gravity on Gastric Emptying with Various Test Meals. J. Physiol. 154:270-275, 1965.

5. Ingelfinger, F.J. Esophageal Motility. Physiol. Rev. 38:533-584, 1958

6. Johnson, L.R. Regulation of Gastrointestinal Growth. In: Johnson, L.R., ed. Physiology of the Gastrointestinal Tract. New York.: Raven Press. 1987:301-334.

7. Lai, M., D.B. Thomason,, and N.W. Weisbrodt. Effect of Intestinal Bypass on the Expression of Actin mRNA in Ileal Smooth Muscle. Am. J. Physiol. 258:R39-R43, 1990.

8. Lai, M., D.B. Thomason, Y.F. Li, and N.W. Weisbrodt,. Actin mRNA Expression in Intestinal Smooth Muscle. J. Gastrointestinal Motility. 1:61, 1989 (abstract).

9. Vermillion, D.L., and Collins, S.M.: Increased Responsiveness of Jejunal Longitudinal Muscle in *Trichinella* -InfectedRats. Am.J. Physiol.254:G124-G129, 1988.

10. Weisbrodt, N.W. Response of Intestinal Muscle to Resection and Bypass. In: Seidel, C.L. and N.W. Weisbrodt, eds. Hypertrophic Response in Smooth Muscle. Boca Raton.: CRC Press. 1987:77-84.

11. Weisbrodt, N.W., P.R. Nemeth, R.L. Bowers, and W.A. Weems. Functional and Structural Changes in Intestinal Smooth Muscle after Jejunoileal Bypass in Rats. Gastroenterology 88:958-963, 1985.

TABLE 1.

WET WEIGHT, TOTAL PROTEIN, AND TOTAL RNA IN INTESTINAL MUSCLE

	Flight	Synchronous	Tail-Suspended	Vivarium
Wet weight (mg/cm)	6.26 ± 0.48	5.46 ± 0.46	6.23 ± 0.30	9.02 ± 1.47
Total protein (mg/cm)	0.38 ± 0.017	0.43 ± 0.025	0.42 ± 0.037	0.47 ± 0.026
Total RNA (mg/cm)	0.84 ± 0.21	1.33 ± 0.28	2.66 ± 0.50	3.87 ± 0.54

Values are means ±SEM
Any values not underlined by the same line differ statistically at a p value < 0.05.

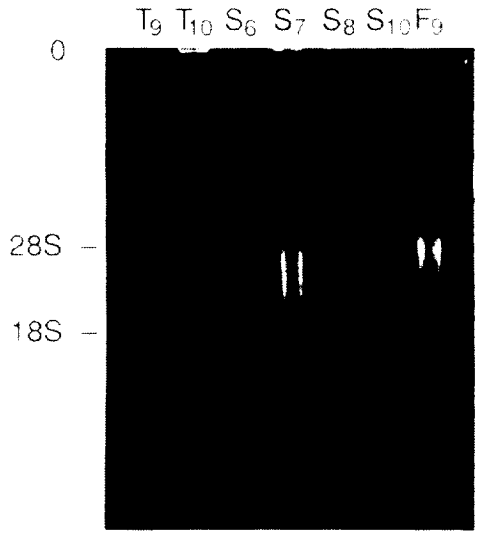

Figure 1. RNA gel blots (Northern blots) of RNA isolated from Tail-suspended (T_{9-10}), Synchronous ($S_{6-8, 10}$), and Flight (F_9) rat intestinal longitudinal muscle. The blots were stained with ethidium bromide. In some samples, hints of 18S and 28S ribosomal subunits are visible. However, in all samples, smearing of the RNA is seen. This represents possible degradation.

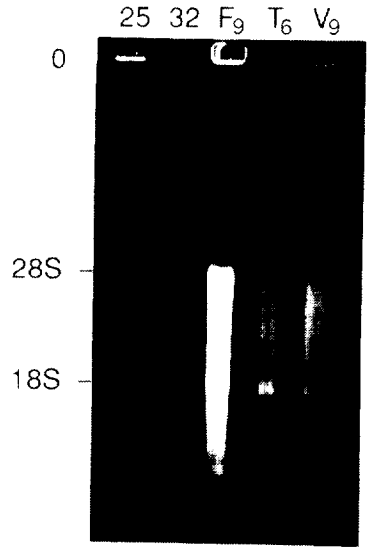

Figure 2. RNA gel blots (Northern blots) of RNA isolated from Flight (F_9), Tail-suspended (T_6), Vivarium (V_9), and non-Cosmos (25,32) rat intestinal longitudinal muscle. The blots were stained with ethidium bromide to show location of 28S and 18S ribosomal RNA subunits in the non-Cosmos samples. Note that these subunits are not readily apparent in the Cosmos samples even though 2.5 times as much total RNA were loaded in these lanes as compared to the non-Cosmos samples. Also note the smearing present in the Cosmos samples.

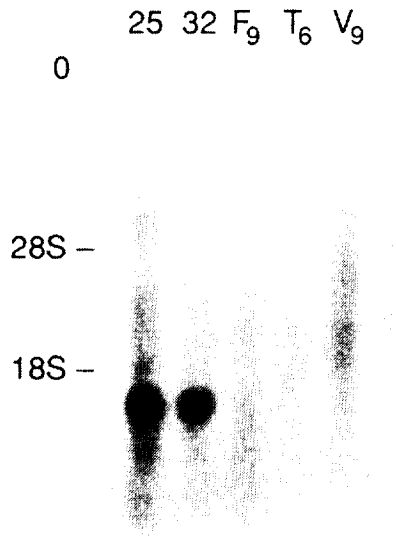

Figure 3. RNA gel blot (Northern blot) that was hybridized to a ribo–probe that hybridizes with actin mRNA. Note that in the non-Cosmos samples (25,32) a major band in the 16S region hybridized with the probe. None of the Cosmos samples (other lanes) showed such hybridization even though 2.5 times as much total RNA was size fractionated.

EXPERIMENT K-7-12

NATRIURETIC PEPTIDE CONTENT OF ATRIA FROM RATS EXPOSED TO 14 DAYS OF SPACEFLIGHT

Principal Investigator:

L. Keil
NASA Ames Research Center
Moffett Field, CA

J. Evans
R. Grindeland
NASA Ames Research Center
Moffett Field, CA

I. Popova
Institute of Medical-Biological Problems
Moscow, USSR

EXPERIMENT K-7-12

NATRIURETIC PEPTIDE CONTENT OF ATRIA FROM RATS EXPOSED TO 14 DAYS OF SPACEFLIGHT

L. Keil, J. Evans, R. Grindeland and I. Popova

SUMMARY

The purpose of this experiment was to determine if spaceflight exposure had an effect on the concentration of natriuretic peptide in heart atria. Acid extracts of atria from flight, synchronous, vivarium and tail suspended control groups were radioimmunoassayed for 1-28 rat atrial natriuretic peptide (ANP). Flight animals, when compared to the other control groups, had lower atrial concentrations of the hormone. The reduced level of ANP in the flight rats may represent one of the changes in hormonal regulation of fluid/electrolyte metabolism that occur during microgravity exposure.

INTRODUCTION

Humans exposed to spaceflight show a reduction in blood volume and alterations in fluid/electrolyte balance (9). These changes lead to orthostatic hypotension upon return to earth and increased hormone secretion necessary to restore blood volume. Although fluid-electrolyte balance in rats has not been determined during flight, post-flight hormone measurements and salt-water loading experiments indicate that rats also respond to microgravity by readjustment of their fluid-electrolyte requirements (4). Atrial natriuretic peptide is a recently discovered hormone, and its secretion is regulated primarily by atrial pressure (5). In humans, head-down bed rest and water immersion increase circulating levels of this hormone, and it is thought to be responsible for the observed natriuresis in these two primary methods for simulating the physiological effects of spaceflight (2,8). The purpose of this experiment was to determine if microgravity exposure had an effect on atrial content of natriuretic hormone.

METHODS

Rats used in this study were four groups of 5 each: Flight (FLT), Synchronous (SYN), and Vivarium (VIV) controls. A fourth group of Tail Suspended (SUS) were included to make a direct comparison of data from this model to that acquired from the FLT animals. Details concerning the treatment, housing and source of the animals are described elsewhere (7).

Atria were collected from each of the above groups within a few minutes after sacrifice. They were placed in individual cryovials and frozen in liquid nitrogen. After freezing, the tissues were maintained in either a -70^{o} C freezer or on dry-ice during shipment.

To prepare the atria for radioimmunoassay (RIA) each atria was thawed, and the extraneous tissue removed. The trimmed atria were blotted, weighed and immediately placed in a 12 x 75 mm polypropylene tube containing 2 ml of 0.1 N HCl and 0.001% PMSF. The tissue was homogenized, and protein content was determined on an aliquot of the acid homogenate (Pierce, Rockford, IL). Another aliquot was placed in a boiling water bath for 5 minutes and then centrifuged at 4600g for 30 minutes. Supernatant from this boiled

aliquot was diluted with assay buffer prior to RIA for the 1-28 bioactive segment of rat atrial natriuretic peptide (rANP)

Antibodies to ANP were developed in male, New Zealand rabbits after multiple injections of 1-28 ANP (BaChem, Torrance, CA) coupled to bovine serum albumin (6) and mixed with Freund's adjuvant. Specificity of the antiserum is shown in Table 1. The amount of standard ANP (BaChem 1-28 ANP) needed to displace 50% of the labeled hormone (ED_{50}) was 30.5 ± 0.8 picograms for a typical standard curve. Inter and intraassay coefficient of variation was 7.4 and 7.1%, respectively.

RESULTS

Atria from the FLT group contained less (3.13 ± 0.13 μg/mg protein, $p < 0.05$) ANP than either the VIV (3.48 ± 0.05), SYN (4.32 ± 0.35) or SUS (3.93 ± 0.30) groups (Fig. 1). Interestingly, atrial ANP concentrations in VIV group was lower ($p<0.05$) than the SYN group maintained in flight type cages. No other significant differences between the groups were noted.

DISCUSSION

Reduction of atrial ANP may reflect an increase in hormone secretion during flight. Flight animals may have experienced a rise in atrial pressure that provoked an increase in ANP secretion, or other factors such as elevated levels of glucocorticoids, epinephrine or vasopressin could have enhanced secretion (1). If increased ANP secretion and a subsequent decrease in atrial ANP content resulted from a headward fluid shift during flight, then a similar reduction in ANP might have been expected in the head-down SUS group; however, no reduction in ANP was noted in this group.

Increases in plasma and atrial ANP has been reported in rats after 2 hr of suspension (3), however no increases were detected after either 6 or 24 hr of suspension. ANP in the antiorthostatic rat model appears to produce only transient changes in atrial ANP in contrast to an apparent prolonged reduction in rats exposed to 2 weeks of spaceflight. Interestingly, rats flown on Cosmos 936 showed dramatic increase in sodium excretion in response to a water load compared to synchronous controls (4). This suggests that flight animals may either secrete additional amounts of ANP in response to volume expansion or the kidneys of these animals are more sensitive to the hormone.

Synthesis of the hormone in the FLT group may have been reduced by a fall in atrial pressure or blood volume. Hematocrit values for the FLT animals were increased, and this may indicate a reduction in plasma volume during flight (7). Lower levels of atrial ANP may simply represent one aspect of adaptation to a microgravity environment. To determine the role of ANP in the regulation of sodium excretion and fluid balance further studies will be required in rats exposed to spaceflight. Unfortunately, the tail suspension does not seem to be an appropriate ground-based model for simulating the effects of microgravity on ANP metabolism.

REFERENCES

1. Brenner, B.M., B.J. Ballermann, M.E. Gunning, and M.L. Zeidel. Diverse Biological Actions of Atrial Natriuretic Peptide. Physiol. Rev. 70(3):655-699, 1990.

2. Epstein, Loutzenhiser, M.R., E. Friedland, R.M. Aceto, M.J. Camargo, and S.A. Atlas. Relationship of Increased Plasma Atrial Natriuretic Factor and Renal Sodium Handling During Immersion-Induced Central Hypervolemia in Normal Humans. J. Clin. Invest. 79:738-745, 1987.

3. Gauquelin, G., C.Kazek, A. Allevard, R.Garcin, J. Bonnod, J.Gutkowska, M.Cantin, and C. Gharib. Early (1 to 24h) Plasma Atrial Natriuretic Factor Changes in the Rat During Antiorthostatic Hypokinetic Suspension. Biochem. Bioph. Res. Comm. 148(2): 582-588, 1987.

4. Gazenko, O.G., Y.V. Natochin, Y.A. Illyin, N.A. Illyushko, Y.I. Kondratiev, Y.A. Lavrova, and Y.I. Shakhmatova. Fluid-Electrolyte Metabolism and Renal Function of the White Rats Aboard Cosmos Biosatellites. Aviat. Space Eviron. Med. 55:695-691, 1984.

5. Goetz, K.L. Physiology and Pathophysiology of Atrial Peptides. Am J. Physiol. 254:E1-E15, 1988.

6. Goodfriend, T., L. Levine, and C.D. Fasman. Antibodies to Bradykinin and Angiotensin: A Use of Carbodiimides in Immunology. Science. 144:1344-1346, 1964.

7. Grindeland, R.E., M.F. Vasques, R.W. Ballard, and J.P. Connolly. Cosmos 2044 Mission Overview. J. Appl. Physiol, 1990.

8. Hodsman, G.P., K. Tsunoda, K. Ogawa, and C.I. Johnston. Effects of Posture on Circulating Atrial Natriuretic Peptide. Lancet. 2: 1427-1429, 1985.

9. Leach, C.S., and P.C. Rambaut. Biochemical Responses of the Skylab Crewmen: An Overview, In: Biomedical Results from Skylab, Washington D.C. NASA SP-377:204-216, 1977.

10. Savina, E.A., A.S.Pankova, E.I.Alekseyev, and V.K. Podymov. Morphological Manifestations of Functional Changes in the Hypothalamic-pituitary Neurosecretory System and Kidneys of Rats after Spaceflight. Aviat. Space and Eviron. Med.47(8):853-855, 1976.

TABLE 1

PERCENT CROSS REACTIVITY OF rANP ANTISERUM #41.

Rat 1-28 ANP	100
Rat Auriculin B	100
Rat Atriopeptin II	20
Rat Atriopeptin I	17
Rat Atriopeptin III	14
Human 1-28 ANP	3
Angiotensin I	<0.01
Angiotensin II	<0.01
Arg-vasopressin	<0.01
Oxytocin	<0.01

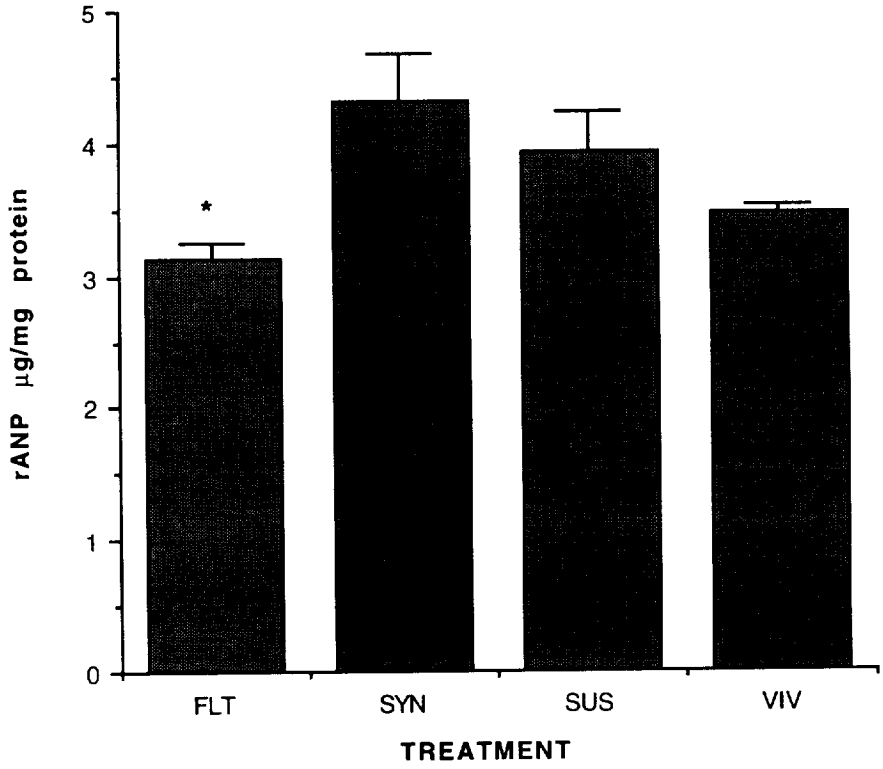

*Figure 1. Atrial ANP content after spaceflight, mean values ± SEM, *p<0.05 when compared to other groups.*

EXPERIMENT K-7-13

MORPHOLOGICAL AND BIOCHEMICAL EXAMINATION OF HEART TISSUE

PART I: ULTRASTRUCTURAL ALTERATIONS IN RAT HEARTS AFTER COSMOS 2044 COMPARED TO COSMOS 1887

PART II: CARDIAC MORPHOLOGY AFTER MICROGRAVITY CONDITIONS

PART III: CYCLIC AMP RECEPTOR PROTEIN DISTRIBUTION IN HEART MUSCLE OF RATS FLOWN ON COSMOS 2044

PART IV: ALTERED MYOSIN EXPRESSION IN RAT VENTRICULAR MUSCLE DURING EXPOSURE TO MICROGRAVITY

Principal Investigator:

D. Philpott
NASA Ames Research Center
Moffett Field, CA

Co-Investigators:

K. Baldwin
University of California
Irvine, CA

F. Booth
University of Texas,
Houston, TX

M. Goldstein
J.P. Schroeter
R.J. Edwards
Baylor College of Medicine
Houston, TX

R. Grindeland
K. Kato
J. Stevenson
NASA Ames Research Center
Moffett Field, CA

M.I. Mednieks
University of Chicago
Chicago, IL

J. Miguel
Linus Pauling Instit. of Science and Medicine
Palo Alto, CA

W. Sapp
Tuskegee University, AB
Tuskegee, AB

D.B. Thomason
University of Tennessee
Memphis, TN

E. I. Ilyina-Kakueva
V. Oganov
I. Popova
Institute of Biomedical Problems
Moscow, USSR

EXPERIMENT K-7-13
PART I: ULTRASTRUCTURAL ALTERATIONS IN RAT HEARTS AFTER COSMOS 2044 COMPARED TO COSMOS 1887

D. E. Philpott, K. Kato, J. Miquel, W. Sapp, and J. Stevenson

SUMMARY

The Russian satellite Cosmos 2044 blasted off in Oct. 1989 and spent 14 days in orbit repeating the 1987 flight of Cosmos 1887. The delayed recovery of the animals on 1887 resulted in extended recovery periods of about 54 hours. It is considered that this long recovery time could have modified the effects of weightlessness, casting doubts on the results. Recovery of Cosmos 2044 went smoothly and animal recovery was reduced to about 12 hours. Flight, synchronous controls and vivarium controls were repeated as in Cosmos 1887 and a fourth set, tail suspension was added to flight 2044. Results in the left ventricles of the rat heart were comparable to those in Cosmos 1887. Statistical analysis showed a significant reduction in flight mitochondria and an increase in glycogen compared to the vivarium controls. The mitochondria and lipid levels in the synchronous control changed in the same direction as the flight but the magnitude was less. Lipid accumulation in the flight left ventricles was significant compared to synchronous and vivarium controls. There was also a significant increase in dense bodies in the flight tissues. During both Cosmos flights (1887 and 2044) there was an indication of slight collagen increase. The 2044 flight confirmed ultrastructure alterations observed after Cosmos 1887.

INTRODUCTION

During a number of space flights and hypokinetic ground studies the cardiovascular system has been a major area of study. The bipedal support of the human being results in a head to toe hemodynamic system very sensitive to gravity changes. The heart can be considered a major player in this balance and, as such any changes, e.g., structural, in this organ, become important. Hypokinetic studies ahave been done on rats (head down tilt), on rabbits (exercise restricted), and on monkeys (body casted). Rat hearts have been studied after space flights from Cosmos 605, 936, 1887 and Shuttle SL3. Baranski, et al., (1980, 1983) found ultrastructural alterations in heart muscle of rats flown on Cosmos 936. The volume density of mitochondria decreased significantly compared to the synchronous and vivarium controls as did the volume density of smooth endoplasmic reticulum. The average number of mitochondria decreased and the volume density of glycogen increased. Damaged mitochondria and myofilament atrophy were observed. These changes were also observed in heart muscle of rats on a one G centrifuge during space flight. Centrifuging the animals during space flight did not prevent the structural changes. Oganessyan and Eloyan (1981) studied cathepsin activity in the heart of rats after Cosmos 605 and found a significant increase of cathepsin in the flight animals as compared to the synchronous controls. The changes were partially normalized by day 25 and 26 after recovery from the flight. Oganessyan and Eloyan (1981) suggested that this indicated reversibility of the proteolytic activity. Kovalenko, et al. (1970, 1972) found a decrease in the number of mitochondria after 120 days of restraint and mitochondrial alterations consisting of nonuniform swelling and changes in the cristae pattern orientation. Heart mass also decreased 4.5 per cent and was accompanied by a decrease in oxygen consumption from 62 to 38 mm/100mg/hr. Rats restrained for 120 days showed a decrease in mitochondrial size and an increase in number of mitochondria by day 14 (Romanov, 1976). The mitochondria appeared structurally normal on days 45 and 60 but by day 120 the size and number had increased. The adaptive mechanisms are still poorly understood.

While tail suspension has yielded a great deal of data, some investigations indicate weightlessness as the necessary criteria for understanding microgravity. In fact, Meerson et al. (1983) studied rat

papillary muscle under isotonic conditions after two months of hypokinesia. The rate of contraction and relaxation was increased 1.5 times. The negative isotropic effect value was unchanged in acidosis but increased 1.5 to 2 times with a calcium deficiency or excess. However, the volume and surface of the longitudinal canaliculi of the sarcoplasmic reticulum were reduced by 57% and the T-system was reduced by 60%. Meerson, et al. concluded that hypokinesia was not a good model for studying contractile function of the heart of man under conditions of long-term rest or weightlessness. Overton and Tipton (1990) studied hindlimb suspension to see if it was associated with development of cardiovascular deconditioning. Their collective results indicated that 9 days of head down tilt in rats does not elicit hemodynamic response patterns generally associated with cardiovascular deconditioning induced by hypogravic conditions.

Nepomnyashchikh and Kolesnikova (1985) severely confined 48 male rats in cages for one month and examined the skeletal and heart muscle. There was connective tissue proliferation, edema and the microcirculatory bed was altered, leading to a degradation of metabolic processes. Myocardial atrophy was evident. They pointed out that when synthetic processes are degraded, albuminolysis occurs and slowing of basic organelle reproduction in the cardiac muscle cells is a strong indication that only the structures of greatest importance are retained.

Philpott, et al. (1985, 1987) found ultrastructural alterations in rat hearts fixed 12 hours after 7 days in space on SL-3. Also, in rat hearts fixed two days after 12.5 days on Cosmos 1887 there were alterations. (Philpott, et al, 1990) The following changes were seen in the left ventricles of the rats from these two flights: a decrease in the volume density of the glycogen and lipid, a decrease in microtubules, and generalized edema in the tissue. Filaments were missing in some of the myofibrils. Supercontraction was observed in some of the affected myofibrils but not as much as in Cosmos 1887.

Our observations (Philpott, et al. 1982) on upright body casted monkeys, following two weeks of immobilization, revealed mitochondrial breakdown with autophagic transformation into multilamellar bodies and increases in lipid and glycogen. The adenylate cyclase activity was lowered, suggesting that during immobilization a decline in metabolic rate results in a surplus of chemicals normally used for energy production.

Rohlenko and Mul'diyarov (1981) considered the mitochondrial changes seen in space flown animals to be similar to those encountered in the presence of diverse forms of myocardial hypoxia. They conclude that when the rats change from the weightless environment of space to earth's gravity, the heart experiences a drastic increase in load compared to weightlessness. Since exposure to microgravity results in changes in the microvasculature, compatible with impaired tissue oxygenation, the increased metabolism associated with readaptation to earth gravity may lead to tissue anoxia and concomitant mitochondrial disorganization. Excessive exercise has also been shown to result in structural degeneration of the myocarium (Sohal, et al. 1968). Kato, et al. (1979) demonstrated supergravity increasing lipid and glycogen concentrations as in microgravity. Shtykhno and Udovichenko (1978) reported a decrease in the number of true capillaries and the appearance of nonfunctioning empty vessels and an opening of arteriovenular shunts. Mailyan et al. (1970), using exercise restriction reported reduced heart function which was accompanied by a decrease in mass and changes in the ultrastructural elements on which biological oxidation processes are dependent. Kovalenko et al., (1972) reported the endothelium of the capillaries exhibited swelling and impairment of the cell membrane structure after exercise restriction.

The reasons for the above changes are still unknown and further research is needed to understand the adaptive mechanisms involved in the response of the heart tissue to microgravity.

METHODS

Five male rats of the Czechoslovakian Wistar strain were used in each of the four categories in Cosmos 2044: Flight (FL), synchronous control (SYN), vivarium control (VIV) and tail suspension (TS). Cosmos 2044 lasted 14 days and tissue preparation took place 12 hours after recovery. None of the delayed recovery problems of Cosmos 1887 was encountered in Cosmos 2044.

The rat hearts were harvested by the Russians and immediately plunged into ice cold saline to reduce metabolic activity. The hearts were then placed on cold dental wax while dissection of the left ventricle progressed (Kato et al., 1987). The dissected samples were immediately placed in teflon screw top vials containing cold Triple Fix (Philpott, 1980), labelled and shipped to Ames Research Center. Upon arrival at Ames Research Center the tissue was immersed in 1% osmic acid plus 1% K3Fe(CN)6 for 1 hour (McDonald, 1984), dehydrated with ascending concentrations of acetone, infiltrated with Epon-Araldite, embedded, sectioned and stained for electron microscopy. Electron micrographs of the samples were taken with a Philips 300 electron microscope. Volume density (VDen) was determined by point counting as described by Weibel (1969), using 240 micrographs (8 x 10) at a magnification of 27,500X. ANOVA was conducted on the data using an Epistat software program. Capillary counts, using randomly selected open grid squares in the electron microscope, were converted to counts per 600 sq u's. Procedures were kept as close as possible to those used for Cosmos 1887.

RESULTS AND DISCUSSION

Cosmos 2044 was flown to compare results from flights of Cosmos 2044 and Cosmos 1887 and to gain additional insight into the effects of microgravity. Recovery from Cosmos 2044 went smoothly and the tissues were obtained 12 hours after the flight; a significant reduction in time compared to the two days before sacrifice of their Cosmos 1887 rats. This was important because there was general concern that the longer recovery period of 1887 would allow some tissue recovery, thus decreasing the observable changes. Results from 2044 on the heart left ventricle do not indicate differences in results during the extended retrieval period of 1887. A tail suspension experiment was added to Cosmos 2044 to see if this technique would yield comparable information.

Reference to Figure 1 shows the post-flight comparison of mitochondria and glycogen in flight (FL), synchronous (SYN), vivarium (VIV) and tail suspension (TS) from Cosmos 2044. Volume density of the glycogen decreased progressively from FL to VIV with the TS located in between the VIV and the SYN. Mitochondrial VDen is highest in the VIV controls, reduced in the SYN and TS and lowest in the FL. Figure 2 shows the excellent preservation obtained in the vivarium controls. An increase in glycogen can be seen in Figure 3 which simulated the condition of flight except for the microgravity. An increase in glycogen can be seen in flight tissue (Figure 4) and the edematous nature is also apparent. It is possible that the edema may be linked to tissue breakdown, with a concomitant increase in osmotic pressure and fluid entry into the cells. An increase in glycogen is often visible around the nucleus including lipid and residual/dense bodies (Figure 5). Tail suspension results appear similar and can be seen in Figure 6 where an increase in glycogen, loose appearance of the tissue and residual bodies are present. Affected myofibrils may exhibit super contraction, filament disorganization, increased glycogen, and lipid (figure 7). Cross section of the altered myofibrils exhibit myofilament loss (figure 8) which can be compared to a cross section area of an unaffected myofibril in Figure 9.

Some lighter staining mitochondria appear among the darker mitochondria (Fig.10). The normal appearing myofibrils generally contained the darker mitochondria suggesting that the decrease in VDen of the mitochondria may be preceded by some morphological alteration. DeGasperis, et al. (1970), Delatglesia and Lumb (1972), Ferrans and Roberts (1971), Rouslin, et al. (1980) and

Taylor and Shaikh (1984), point out that changes in the supply of oxygen and nutrients to the organelles result in fine structural and biochemical changes in the mitochondria of ischemic or anoxic myocardium. A decline in sympathetic nervous activity may also influence mitochondria through an effect on blood perfusion (Popovic, 1981). Hence, both sympathetic and oxygen-mediated mechanisms may underlie the changes. Joseph and Engel (1980), point out that the sympathetic nervous system exerts a trophic influence on the biosynthesis of myofibrils and mitochondria. Therefore, a decreased sympathetic activity during microgravity or immobilization could play a role in their degeneration. Alterations in the capillaries were observed in Cosmos 1887. (Philpott, et al. 1990). Fedorov and Shurova (1973) found capillary alteration in immobilized rabbits which they indicated might impair delivery of oxygen and nutrients to the cells. Tzagoloff (1982) reported that a decrease in blood supply would decrease ATP synthesis which is needed for mitochondrial maintenance and repair. The present data support the view that an optimum work load imposed on the heart, at normal Earth gravity, is essential to preserve mitochondrial function and structure (Miquel, et al. 1980, Miquel, 1982.)

A twoway ANOVA was run on mitochondrial data comparing the FL, SYN, VIV and TS. Comparison of the mean data for numbers across all samples showed statistically significant differences (FL mean = 36.5, SYN mean = 42.2, VIV mean = 44.8 and TS mean = 41.7; F =17.9; df 3/165, P < 10 (-6) indicating that the VDen of the mitochondria was reduced in the flight animals. The row effect was not significant. Comparison of the SYN and TS did not show a significant difference. The glycogen data were also subjected to two way ANOVA (FL mean = 21.2, SYN mean = 13.6, VIV mean = 6.8, TS mean = 8.2; F = 195; df 3/165, P<10 (-6)) indicating a significant difference between columns but not between rows. ANOVA analysis of the lipid and residual/dense bodies resulted in a significant difference between columns but not between rows. The lipid results were FL mean = 1.18, SYN mean = 0.44, VIV mean = 0.48 and TS mean = 0.86. SYN and VIV lipid were about equal while the TS and FL were elevated. Residual/dense body counts were FL mean = 1.17, SYN mean = .59, VIV mean = .55 and TS mean = .87. These organelles are indicative of lysosomal activity, another indication of tissue loss.

The lipid increase is generally observed in TS and exercise restriction in previous flights when microgravity data was collected. Shidlovskaya (1985) suggests that in the early stages of hypokinesia lipid peroxidation can be blocked. The increase in dense bodies is an indication of increased lysosomal activity which is expected in muscle atrophy.

Since an ultrastructural change was seen in the capillaries of Cosmos 1887 (Philpott, et al. 1990) it was decided to make a count per unit area of the capillary bed in the Cosmos 2044 left ventricle. Capillary counts per 600 sq. u's resulted in FL = 18.7, SYN = 11.1, VIV = 9.4 and TS = 16.5. The results of the count indicate that there is a requirement for an increase in the number of capillaries in the flight and tail suspension animals. Atrophy may play a role in bringing capillaries closer together. It was not possible to determine if all the capillaries were functional. However, there was a visual increase in the number of platelets in the FL and TS tissue and none in the SYN and VIV. The flight tissue in Cosmos 2044 appeared to have a small increase in collagen comparable to the observation in Cosmos 1887. The increase was not considered significant, but it may indicate a progressive change during long term flights. If so, a gradual increase could be a problem for sustained flights and collagen accumulation should be monitored in any prolonged flight experiments. Nepomnyashchikh and Kolesnikova (1985) found connective tissue proliferation in rats during one month of exercise restriction. Bourne, et al., (1977) studying horizontal body casted monkeys for 2 to 6 months found a collagen increase, as measured by hydroxyproline, elevated lipid levels and some muscle thinning. There was also an increase in total free lysosomal enzyme activities in the ventricles, indicating the occurrence of active degradation.

The role of reentry and readaptation to one G may be an important factor in the observed tissue changes. When pocket mice were returned from the Apollo 17 moon flight the mice had trouble standing in their cages and moved about generally dragging their bodies (Philpott, personal observation). Rohlenko and Mul'dyarov (1981) observed that, return to one G produces a drastic increase in cardiac load, and data showing excessive exercise to cause myocardial degeneration. Sohal et al. (1968) suggests post flight events, re-entry and re-adaptation, may be responsible for some of the changes. This may help explain why the longer recovery period of 1887 appeared not to have a significant effect on the myocardium.

CONCLUSION

Results from Cosmos 2044 indicate observational and statistically significant changes taking place in the left ventricle of the rat hearts. The longer recovery period in Cosmos 1887 does not appear to have produced any significant recovery. The events which prevented a shorter recovery period, the difficult rescue and transportation problems may have produced its own stress. It is also important to point out that longer periods needed for recovery have been reported. Oganessyan and Eloyan (1981) found partial recovery of the cathepsin activity after 25 to 26 days. At present, our understanding of the basic mechanisms of cardiovascular deconditioning and recovery are poorly understood. The previous data, reviewed and presented here, suggest that microgravity is necessary to obtain the complete picture of heart changes during flight. Indeed, until the tissues can be fixed during flight the role of re-entry and recovery before sacrifice will be difficult to determine.

ACKNOWLEDGEMENTS

This work was supported in part by NASA/Ames Research Center cooperative agreement in NCC2-12 and NCC2-*455* (to W. J. Sapp, Tuskegee University). Tuskegee Ultrastructure Facility support was provided by NIH/DRR/RCMI grant GI2RR03059-01A1.

REFERENCES

1. Baranski, S., M. Kujawa and A. Kaplanski. Ultrastructural Qualitative and Quantitative Evaluation of Cytoplasmatic Structures of Heart Muscle of Rats Living Aboard Biosputnik Kosmos 936. The Physiologist. 23:S38-S39, 1980.

2. Baranski S., Subcellular Investigation of theInfluence of Real and Modulated Weightlessness upon Performance and Regeneration Processes in Nuscular Tissues. The Physiologist 26:41, 1983.

3. Bourne, G. H., M. N. Golarz and H. M. McClure. The Orbiting Primate Experiment (OPE). In: The Use of Nonhuman Primates in Space, (R. C. Simmonds and G.H. Bourne Eds.) NASA CP-005, Washington, D.C., 1977.

4. DeGasperis, C., A. Miani, and R. Donatelli. Ultrastructural Changes in Human Myocardium Associated with Ischemic Arrest. J. Mol. Cell. Cardiol. 1:169, 1970.

5. Delatglesia, F. A.and G. Lumb. Ultrastructural and Circulatory Alterations of Myocardium in Experimental Coronary Artery Narrowing. Lab. Invest. 27:17, 1972.

6. Fedorov, I. V.and I. F. Shurova. Content of Protein and Nucleic Acids in the Tissue of Animals During Hypokinesia. Kosmicheskaya Biologiya I Meditsina. 7:17, 1973.

7. Ferrans, V. J. and W.C. Roberts. Myocardial Ultrastructure in Acute and Chronic Hypoxia. Cardiol. 56:144:1971.

8. Joseph, J.J. and B.T. Engel. Nervous Control of the Heart and Cardiovascular System. Aging 12:101 1980.

9. Kato, K., A Baloun and D.E. Philpott. Effect of Supergravity on the Areas of Lipid Droplets and Mitochondria in the Heart Left Ventricle. J. Ultrastruc. Res. 69:350, 1979.

10. Kato, K., D. Philpott and J. Stevenson. A Simple Method to Improve Heart Fixation with Ice Water. J. Elect. Micros. Tech. 7: (2), 133, 1987.

11. Kovalenko, Ye. A., V. L. Popkov and I. Yu. Kondrat'yev. Pathological Physiology. 6: 3-8, 1970.

12. Kovalenko, Ye. A., V.L. Popkov and E.S. Mailyan. Kosmicheskaya Biologiya I Meditsina. 4: 3-8, 1971.

13. Kovalenko, Ye. A., Yu. S. Galushko and I.A. Nitochkina. Space Biol. and Aerospace Med. 1: 125-129, 1972.

14. Mailyan, E.S., L.I. Grinberg and Ye. A. Kovalenko. Adaptatsiva K. Myshechnoy Deyatel'nosti I Gipokinezil. Novosibirsk, 111-113, 1970.

15. McDonald, K. OsFeCN-uranium Staining Improves Microfilament Preservation and Membrane Visulaization in a Variety of Cell Types. J. Ultrastructural Res. 86: 107-118, 1984.

16. Meerson, F.Z., A. I. Saulya, G. Guski, G.Vasilef, L.M. Belkina, G.I. Markovskaya, M.V. Shimkovich, L.M. Saltykova and V.V. Mayshev. Heart Contractile Function and Cardiomyocyte Ultrastucture in Protracted Hypokinesia in Growing Animals. Pathol. Fiziol. Eksp. Ter. 0: (1) 27-33, 1983.

17. Miquel, J. A.C. Economos, J. Fleming and J.E. Johnson, Jr. Mitochondrial Role in Cell Aging. Exp. Gerontol. 15: 575, 1980.

18. Miquel, J. Comparison between the Weightlessness Syndrome and Aging. In: Space Gerontology (J. Miquel and A.C. Economos, Eds.), NASA, Washington, D.C., 1982.

19. Nepomnyashchikh, L.M., L.V. Kolesnikova, G.I. Nepomnyashchikh. Myocardial Tissue Organization in Rats Under Hypokinesia (a Stereological Investigation), Arhiv Anatomii, Gistologii I Embrologii. 88: (1) 57-62, 1985.

20. Oganessyan, S.S., and M.A. Eloyan. Cathepsin Activity of Skeletal Muscle and Myocardial Myofibrils after Exposure to Weightlessness and Accelerations. Kosmicheskaya Biologiya I Aviakosmicheskaya Meditsina. 15: 38-42, 1981.

21. Overton, J.M. and C.M. Tipton. Effect of Hind Limb Suspension on Cardiovascular Responses to Sympathomimetics and Lower Body Negative Pressure. J. Appl. Physiol. 63: (1) 355-362, 1990.

22. Philpott, D.E., R. Corbett, C. Turnbill, S. Black, D. Dayhoff, J.,McGourty, R. Lee, G. Harrison and L. Sovick. Retinal changes in Rats Flown on Cosmos 936: A Cosmic Ray Experiment. Aviat. Space and Environ. Med. 51:556, 1980.

23. Philpott, D. E., A. Fine, F. D'Amelio, K. Kato and R. Corbett. The Effects of Hypokinesia on the Heart: Ultrastructure and Biochemical Observations. J. Cell Biol. 95:359a, 1982.

24. Philpott, D. E., A. Fine, K. Kato, R. Egnor, L. Cheng and M. Mednieks. Microgravity Changes in Heart Structure and Cyclic AMP Metabolism. Suppl. to The Physiologist 28:(6),S209, 1985.

25. Philpott, D. E., K. Kato and M. Mednieks. Ultrastructure and Cyclic AMP MediatedChanges in Heart Muscle Under Altered Gravity Conditions. J. Mol. Cell Cardiol. 19:(IV), S61, 1987.

26. Philpott, D. E., I. A. Popova, K. Kato, J. Stevenson, J. Miquel and W. Sapp. Morphological and Biochemical Examination of Cosmos 1887 rat heart tissue: Part I - ultrastructure. FASEB J. 4:73-78, 1990.

27. Popovic, V., Antiorthostatic Hypokinesia and Circulation in the Rat. Physiologist. 24:15-16, 1981.

28. Rohlenko, K. D., and P. Ya. Mul'diyarov. Ultrastructure of the Myocardium of Rats Flown aboard the Cosmos 936 Biosatellite. Kosmich. Biol. i Aviakosmich. Med. 1:77-82, 1981.

29. Romanov, V. S. Quantitative Evaluation of Ultrastructural Changes in Rat Myocardium During Prolonged Hypokinesia. Space Biol and Aerospace Med. 10, 74, 1976.

30. Rouslin, W., J. MacGee, A. R. Wessellman, R. J. Adams and S. Gupte. Mitochondrial Cholesterol in Myocardial Ischemia. J. Mol. Cell Cardiol. 12:1475, 1980.

31. Shidlovskaya, T. Y., Intensity of Lipid Peroxidation in Hypokinetic Rat Tissue. Kosmich. Biol. i Aviakosmich. Med. 19: 45-48, 1985.18.

32. Shtykhno, Yu. M. and V. I. Udovichenko. Vest. Akad. Med. Nauk SSSR. 2:68-71, 1978.

33. Sohal, R. S., S. C . Sun, H. L. Colcolough, and G. E. Burch. Ultrastructural Changes of the Intercalated Disc in Exercised Hearts. Lab. Invest. 18:(1)49-53, 1968.

34. Taylor, I. M. and N. A. Shaikh. Ultrastructure Changes of Ischemic Injury Due to Coronary Artery Occlusion in the Porcine Heart. J. Mol. Cell. Cardiol. 16:79, 1984.

35. Tzagoloff, A. Mitochondria. Plenum Press, New York, 244, 1982.

36. Weibel, E.R. Stereological Principles for Morphometry in Electron Microscopy Cytology. Int. Rev. Cytol. 26:235, 1969.

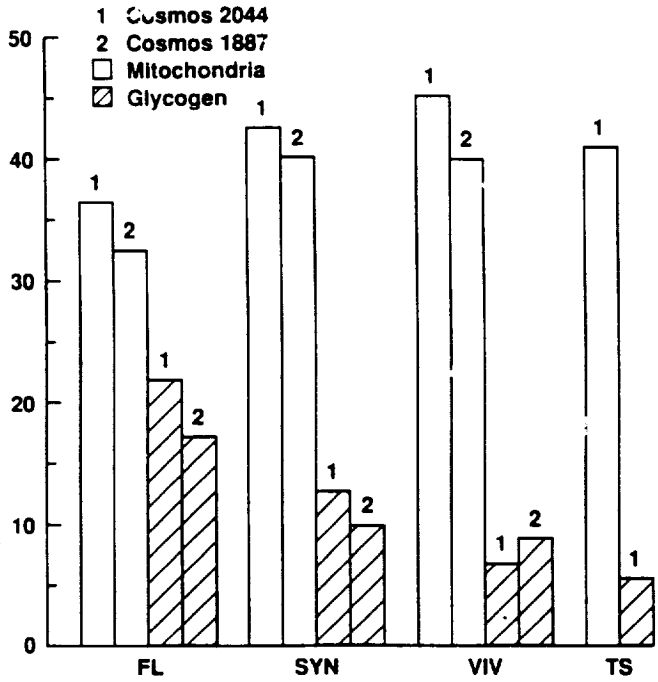

Figure 1. Comparison of mitochondria (MIT) and glycogen (GLY) content in the left ventricle of rats after vivarium, (VIV), synchronous, (SYN), flight, (FL), from Cosmos 2044 and Cosmos 1887 and tail suspension, (TS), carried out only with Cosmos 2044.

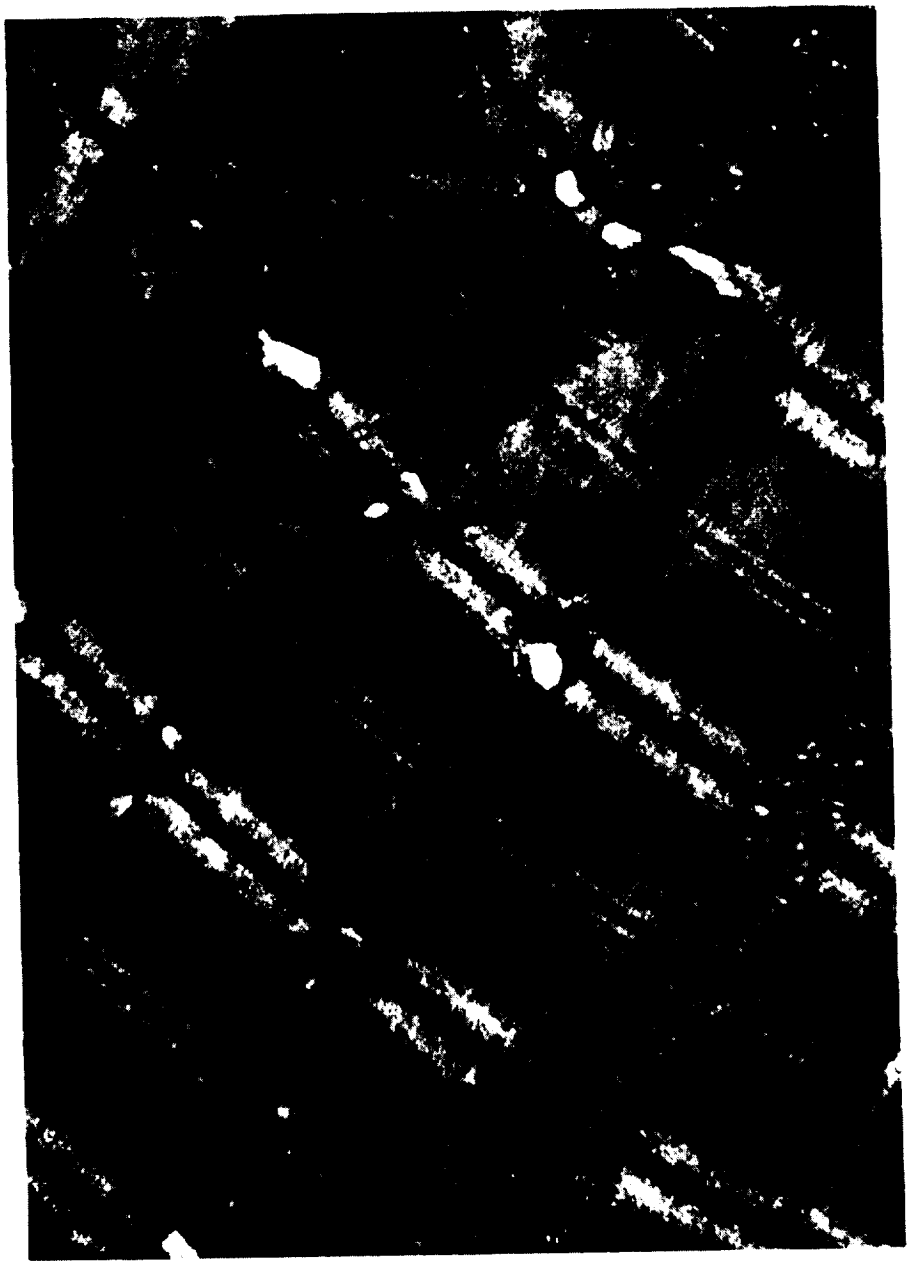

Figure 2. Vivarium control, left ventricle. All micrographs are from rat heart left ventricle Cosmos 2044. Note excellent preservation. 16,500X

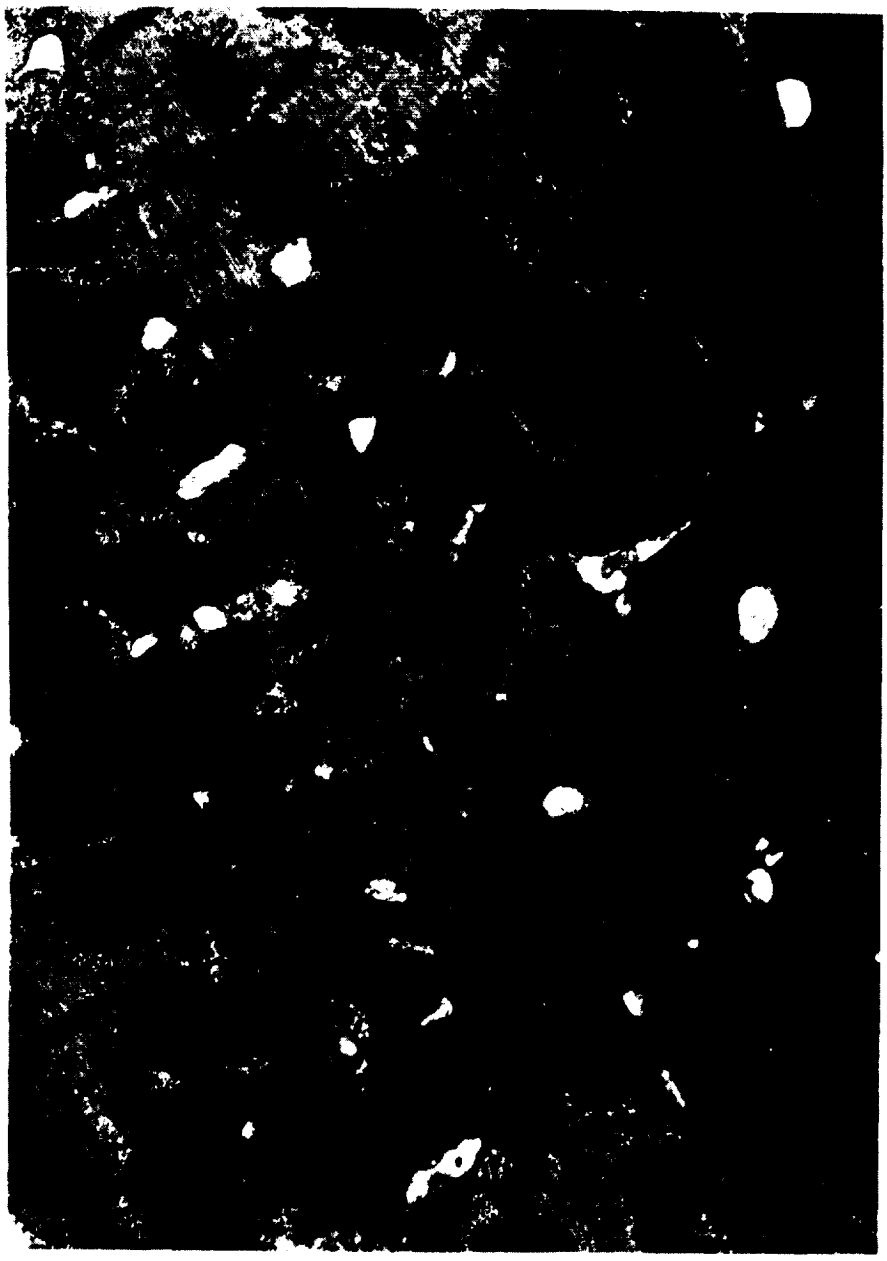

Figure 3. Synchronous control. Similar to vivarium, however some increase in glycogen is visible. 11,700X.

Figure 4. Flight. Note increase in glycogen and edemtous appearance. 16,500X.

Figure 5 Flight. Note increase in glycogen especially around the nucleus and the presence of lipid and residual (dense) bodies. 15,750X.

Figure 6. Tail suspension. Note glycogen and loose appearance of the tissue and residual bodies. 16,500X.

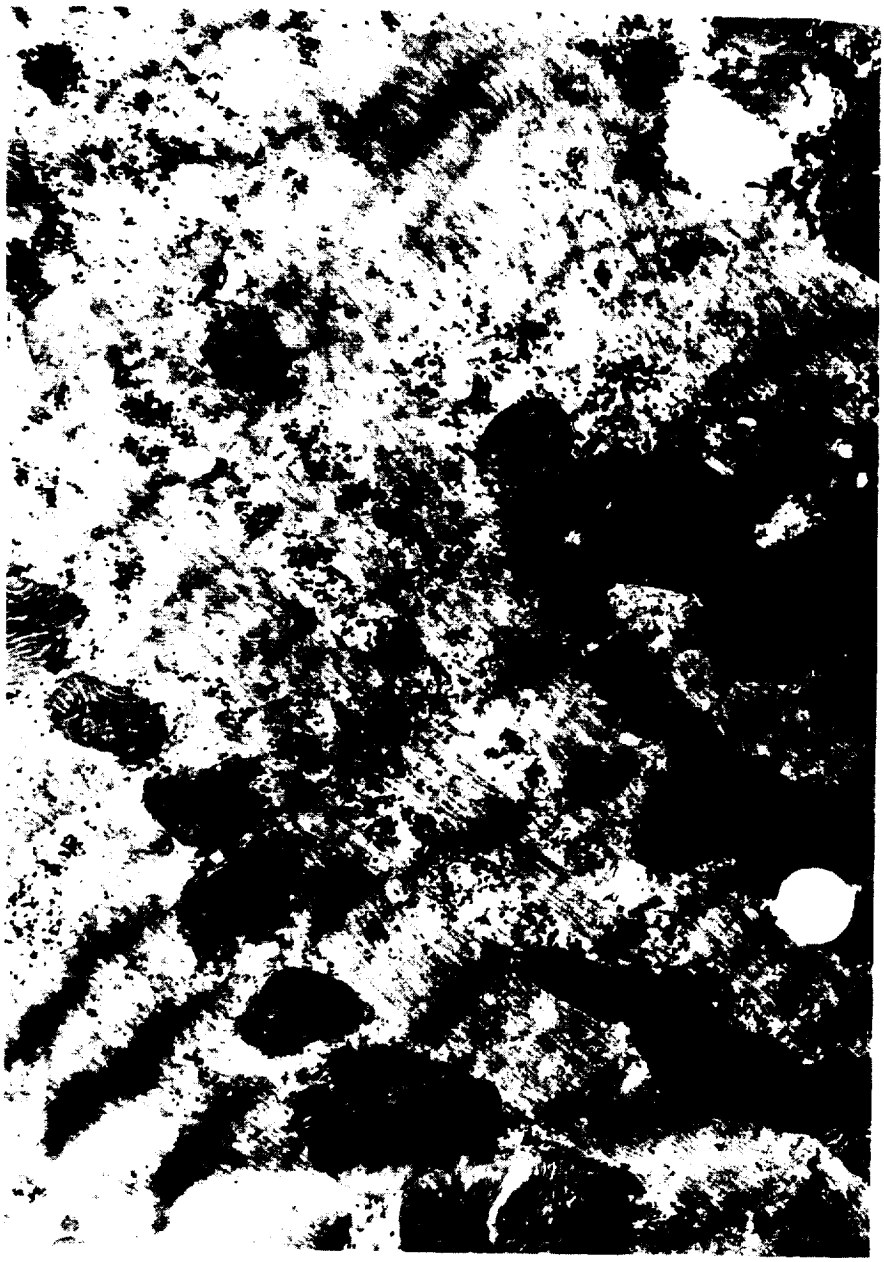

Figure 7. Flight. Supercontraction, disorganization of filaments, glycogen and lipid visible in this affected myofibril. 27,500X.

Figure 8. Cross section of flight tissue. Note the missing myofilaments. 78,500X.

Figure 9. Flight cross section. Note the normal appearance of an unaffected flight specimen. 50,000X.

Figure 10. Flight. Note light staining mitochondria in the center of the micrograph. 42,500X.

EXPERIMENT K-7-13

PART II: CARDIAC MORPHOLOGY AFTER CONDITIONS OF MICROGRAVITY ON COSMOS 2044

M.A. Goldstein, J.P. Schroeter, R.J. Edwards, and I.A. Popova

SUMMARY

Light microscope and electron microscope studies were performed on cardiac muscle from four groups of rats flown on COSMOS 2044. Average cross-sectional area of myofibers was measured by video analysis of the light microscope images of both papillary and ventricular muscle samples from all animals. The comparison of all four groups showed a decrease in cross sectional area in flight, tail suspension and synchronous control groups compared to the vivarium group and a significant decrease in flight compared to synchronous control At the electron microscope level, general morphological features similar to those observed in samples from the previous COSMOS 1887 flight were observed. Endothelial cell surfaces of capillaries with extended projections and elongated marginal folds were observed in papillary muscle from all groups, but seemed most pronounced in the flight group. Stereological analysis of papillary muscle samples revealed normal mitochondrial volume density values for the vivarium group, increased values for the tail suspension and flight groups and reduced values for the synchronous group. Mitochondrial to myofibril ratios showed the same trend. Microtubule numbers per sq. um. in papillary muscle of flight, tail suspension and vivarium groups were very low compared to reported normal adult values for rat. Optical diffraction studies of cross-sectional electron micrographs revealed A band $d_{1,0}$ values that were normal and Z spacings that were close to the Z spacings observed for the basketweave form of the lattice. High magnification images of the Z band showed some loss of ordering in the Z lattice in samples from all four groups.

INTRODUCTION

Reported changes in cardiac morphology after exposure to microgravity include increase in the number of lipid droplets and the amount of glycogen, a loss of microtubules and a significant decrease in volume density in the mitochondria (Philpott et al., 1985). A previous study of rat hearts after 120 days of restraint showed heart mass decrease of 4.26% (Kovalenko et al, 1971). Studies of induced hypokinesia also showed reduced heart function accompanied by a clear decrease in mass (Mailyan et al., 1970). A more recent stereological evaluation of rats under hypokinesia showed a decreased ratio of muscle to connective tissue in the myocardium and myocardial atrophy (Nepomnyashchikh et al., 1985). The effect of prolonged microgravity on ventricular heart muscle tissue in rats was assessed in the COSMOS 1887 mission after a flight of 12 1/2 days (Philpott et al., 1990). In the present COSMOS 2044 mission after a flight of 14 days, ventricular muscles from rats of similar strain but greater age and size were studied. In addition to the flight, synchronous control and vivarium groups, a tail suspension group was studied and papillary muscles as well as left ventricular muscles were analyzed.

The purpose of the cardiac morphology studies was 1) to compare papillary muscle and ventricular muscle; 2) to determine if there is a change in heart cell size in rat hearts exposed to microgravity; and 3) to assess concomitant ultrastructural changes. Cross-sectional areas of heart cell profiles in light microscope sections were measured for papillary and ventricular muscle samples. Electron microscopy was used to correlate general morphological features in the cardiac cells and in the capillaries with features observed in the larger samples taken for light microscopy. Stereological analysis and optical diffraction techniques were used for quantitative electron microscopy studies.

MATERIALS AND METHODS

Animals

Twenty male specific-pathogen-free rats of Czechoslovakian Wistar origin (Institute of Endocrinology, Bratislava, Czechoslovakia) were flown in the COSMOS 2044 Biosputnik for 14 days. Flight housing, feeding and recovery conditions were as described in the mission description of this technical report. Cardiac tissues from rats numbered 6-10 in each of four groups (flight, synchronous control, tail suspension, and vivarium) were used in the cardiac morphology project.

Preparation of Muscles

After sacrifice of each rat, the heart was removed from the chest and dissected through the right ventricle and septum to expose the left ventricular papillary muscles. Papillary muscles with an underlying strip of ventricular tissue were cut out and placed on silastic mounts and pinned to rest length with insect pins. A strip of ventricular tissue was also excised from the left ventricle and left unpinned. Specimens were placed in 2% glutaraldehyde in 100mM PIPES buffer at pH 7.0 at a temperature of 20° for 2 hours and then transferred to fresh fixative and chilled to 4° for transport to Moscow

For post-flight processing muscles were cut crosswise to the long axis of the muscle and pieces of tissue were rinsed in 100mM PIPES buffer for 8 rinses of 15 minutes each for a total of 2 hours at room temperature. Post-fixation in 1% osmium in 100mM PIPES buffer at room temperature for 60 minutes was followed by a wash in 100mM PIPES. The tissue was transported in 100mM PIPES buffer at 4° to Ames Research Center and then to Baylor College of Medicine.

Tissue samples were rinsed in fresh buffer and dehydrated in ethanol. One mm cubes of the most superficial fibers were oriented and embedded in LX-112 resin in flat silastic molds (Goldstein et al, 1986). Twenty-one blocks of papillary and 21 of ventricular muscle were embedded for each animal in all four groups. Each block was given a code number so that all microscopy and data analyses were done on coded samples.

Papillary muscles from a group of five Sprague-Dawley 200-250gm rats were dissected in the same manner as COSMOS samples and fixed by immersion in the same fixatives and buffers for the same prolonged times. This group was used to assess the effects of the dissection times, the immersion fixation and the modified fixation procedures necessary for the COSMOS mission.

Light Microscopy

Semi-thin sections (0.5 to 1u) were stained with methylene blue-azure II and were examined with the light microscope to determine quality of fixation and proper orientaion. We examined seven blocks of papillary muscle and seven blocks of ventricular muscle of each rat in all four groups. The blocks that showed the most damage at the light microscope level and showed shortening of the myofibrils, we did not examine further at the electron microscope level.

Measurement of Cross-Sectional Area of Myofibers

Two cross-sections were taken at random from each animal. Care was taken to use a section of similar thickness on each slide. Quantitative evaluation of the material was carried out using the JAVA 13 Video Analysis software. Each and every muscle cell profile (range 25-99), projected through a 40x objective from the Nikon microscope to the same defined area on the video screen, but only those profiles wholly within this area were outlined with a hand- driven mouse. The area and

perimeter of muscle cell profiles were calculated and scaled against a calibration in microns and square microns and averaged for each image. The image was saved and printed on a Sony Video printer and the averaged values were entered in a data table.

Statistical Analysis

The two types of tissue (papillary and ventricular)were considered separately in all of the analyses. A histogram of range and distribution of cross-sectional areas for each of two blocks (slides) for each animal from all groups was generated. After visual inspection of the data, and consultation with our statistician, we decided to use an analysis of variance because of the limited number of animals in each group and the variability. The first method, Pooled Method, was to pool the raw data from both slides, and to express mean area, range and number of cells. The second method, Averaged Method, was to average the two means, two ranges, etc. Data tables and histograms for each of these methods were compared for two types of muscle. The Kruskall-Wallis method, which uses analysis of variance on the ranks of the means rather than the original means, was applied to both the Pooled and the Averaged groups.

Electron Microscopy

For electron microscopy at least two cross sections and two longitudinal sections, selected at random for optimal orientation and uniformity of preservation, were examined for both muscle types (papillary and ventricular) for each animal in all groups. Thin sections (40-120nm) were cut with a diamond knife on a Porter-Blum MT-2B ultramicrotome and longitudinal sections were taken from blocks with the muscle fibers parallel to the knife edge. Sections were stained with uranyl acetate in 50% ethanol and lead citrate and examined in a Philips 201 or a JEOL JEM 200CX electron microscope. The microscopes were calibrated with a Fullam carbon grating for each group of negatives.

Mitochondrial and Myofibril Measurements

One cross sectional block was chosen at random from each animal in all groups. Ten to twelve fields within the cell and away from the nucleus were photographed at 10,000X for each block. Five fields chosen at random were enlarged to 30,000X and stereological measures on these prints were made using a grid overlay. Each grid square covered 0.25 sq. um. The number of points (formed by intersection of the horizontal and vertical grid lines) within the muscle cell P_T, and the number of points within or touching mitochondria in the fiber area P_M, were counted. The fractional cell, volume occupied by mitochondria is P_M/P_T. The ratio of mitochondria/myofibrils is $P_M/(P_T - P_M)$, since mitochondria and myofibrils are closely packed in non-nuclear regions of the cardiocyte.

Microtubule Numbers per Cross-Sectional Area

The same 100 electron micrographs at 30,000X used for stereological measures were also used to count microtubules in an area = 48 sq. um. Values for all five micrographs were averaged and these averages were used to compute a group mean for each group of five animals.

Optical Diffraction

Optical diffraction analysis was carried out as reported previously (Goldstein et al, 1986) on papillary muscle samples only. Z band and A band data were collected from one or two animals in each group from cross sections and a few measurements were taken from longitudinal sections for comparison.

RESULTS

Light Microscopy - General Morphology

Variability in tissue appearance both from block to block and animal to animal within each experimental group for the papillary muscles was assessed. At least seven blocks from all animals in all groups were examined. Since in all cases the most superficial fibers were examined, it was possible to see a gradient from the surface of the muscle to the interior of the sample with the greatest mitochondrial damage appearing toward the center. In all samples there was heterogeneity among the myofibers, but only rarely and only in the synchronous group was severe shortening and misalignment of cells observed. We saw no changes suggestive of necrotic tissue. Similar results were obtained from examination of a total of 69 light microscope slides of ventricular tissue samples from all rats in all four groups.

Cross-sectional area of myofibers

Typical cross-sectional profiles of papillary muscle used for determination of average cross-sectional area of myofibers are shown in Figure 1. Similar profiles from ventricular muscle are shown in Figure 2. There is a weak overall difference among the four groups with respect to the means ($p= 0.1176$) shown by the ANOVA for papillary muscles (see Statistics Table 1). A significant difference is shown for the flight (red) group versus the synchronous (yellow) group in both the Pooled method and the Averaged method ($p=0.03$) (see Statistics Tables 1 - 4, especially 1A and 3A). Histograms of the individual muscle samples by group show a downward trend from vivarium (green) to synchronous (yellow) to tail suspension (blue) to flight (red) (see Figures 9-18).A 19% decrease in mean value of the flight group compared to vivarium and a 21% decrease in mean value of flight group compared to the synchronous control group was observed. The flight group had the smallest standard deviations.

Ultrastructural Observations

A variation in tissue response was observed in all animals in all groups including the group of smaller rat heart muscles fixed in our laboratory as a ground-based control for the dissection and fixation. Normal looking tissue was seen in all groups. (See Figures 3-5,7). Cellular changes similar to those observed in ischemic damage showed a range from minor mitochondrial blebbing to edema and severe fiber shortening. The greatest amount of tissue damage was seen in the synchronous group for both papillary muscle and ventricular muscle. However, in this group no necrotic tissue was seen. Supercontraction, which produced ridges in the sarcolemma and displaced mitochondria into large clumps, was observed. Severe shortening, to the point that thick filaments were deformed due to the compression of the sarcomeres, was pronounced in ventricular samples from the tail suspension and flight groups. However, the M bands were not disrupted, so the integrity of the contractile apparatus was not likely to be affected. Like other changes such as the mitochondrial changes, the response is heterogeneous and suggests that any possible damage is focal and likely to be reversible. The endothelial cell projections within capillaries seemed most pronounced in the flight group but were observed to a lesser extent in the other groups.

Mitochondrial fractional volume and mitochondria/myofibril ratio

Table 5 presents the results of the stereological analysis of rat papillary muscles from all animals from all groups. The analysis of variance for the mitochondrial fractional volume showed differences among the groups but not within the groups ($F = 3.41$, $df = 3, 16$, $p = 0.04$). The Bonferroni technique showed the flight-synchronous pair ($p=0\ 06$) contributed most significantly to the overall difference. A similar analysis for the mitochondrial/myofibril ratios also showed

differences among the groups (F = 3.19, df = 3, 16, p = 0.05) and again the primary contributor was the flight-synchronous pair.

Mitochondrial number per cross-sectional area

Microtubule numbers in a region corresponding to 48 sq. u., on each of the micrographs in the flight, tail suspension, and vivarium groups used for the mitochondrial fractional volumes, were counted. See Figure 6). The average number per micron squared for each group was F = 0.07, T = 0.07 and V = 0.09 and S = 0.08..

Optical Diffraction Analysis

Optical diffraction studies of cross-sectional electron micrographs reveals A band $d_{1,0}$ values that were normal (F = 1,0 33.6nm, T = 33.2nm, S = 31.1nm, V = 30.1nm) and Z spacings that were close to the Z spacings observed for the basket- weave form of the lattice (F = 26.5nm, T = 25.2nm, S = 30.7nm, V = 26.7nm). High magnification images of the Z band showed some loss of ordering in the Z lattice in samples from all four groups but the basketweave lattice form could be seen in some images (see Figure 8).

DISCUSSION

The current study presents additional data to indicate that space flight of only two weeks affects cardiac morphology. The significant decrease in myofiber cross-sectional area in the papillary muscles of the flight group rats compared to those of the synchronous control group suggests some mass loss in hearts. The overall morphology of the tissue suggests adequate preservation and no major damage to cardiac tissue from the flight group compared to the other three groups.

The reduction in average cross-sectional area of muscle cells and the larger number of small fibers for a given region (see histograms of profile size in Figures 3 and 4) is consistent with an overall mass loss in the cardiac cells, particularly in the flight group. The 19% decrease in the mean value of the flight group compared to the vivarium group is much greater than that reported for studies of hypokinetic or restrained rats (3, 4).

Three aspects of experimental design could affect measured cell response at the electron microscope level. Decapitation precedes opening of the chest cavity and can affect the heart. Dissection of the heart without preperfusion of fixative allows frozen samples to be taken from hearts simultaneously but results in ischemic changes during further dissection, particularly in mitochondria. The number of animals per group, five, is smaller than that for most quantitative morphological studies.

The variation in flight and synchronous groups in appearance of cells, such as amount of mitochondrial damage, fiber shortening, capillary endothelial cell changes and edema, suggests ischemic changes during dissection and shows the usual heterogeneity of this response. (9). Similar but less pronounced mitochondrial changes were seen in our laboratory control group as well as in the vivarium group from COSMOS. The observed gradient of damage from surface to interior suggests further ischemia during the diffusion of the chemical fixative. Nevertheless, since all quantitative studies were done on the most superficial fibers, some valid conclusions can be drawn.

No significant difference in mitochondrial fractional volume or volume density was observed in either the flight group or the tail suspension group compared to the vivarium group for the papillary muscles. The trend toward higher values in fractional volumes as well as in mitochondria/myofibril ratios for the experimental groups is consistent with a proportional decrease in myofibril mass in these two groups. These results are in contrast to previous studies of ventricular tissue (1, 2) and the results for ventricular tissue in COSMOS 2044 (10) which show a significant decrease in mitochondrial density in flight rats. The mean values reported for each group of papillary muscles in

the present study are quite different from those reported previously for ventricular tissue. Nevertheless, the mean values for the mitochondrial fractional volume in papillary muscles in the vivarium, tail suspension and flight groups are in the range of mean values (0.34 - 0.37; 0.33 - 0.34; and 0.31) reported for control rat hearts in three studies of hypertrophy (11-13).

The mean values for microtubule number per micron squared are very low compared to the mean value of 0.25 reported for normal adult heart (14). Given the small number of animals, the small sample size and the difficulties with fixation, it is not possible to say if the reduction of this important cytoskeletal component is related to the variable ischemia. The low values in all four groups are suggestive of this, since mitochondrial changes indicative of ischemia were seen in all four groups. Nevertheless, loss of microtubules may parallel the myofibril mass loss and its significance in the flight group may be obscured by the methods for obtaining the heart tissue.

The normal A band and Z band spacings seen with optical diffraction suggest that the remaining myofibrils are well-ordered and functional. The subtle loss of ordering seen in many of the Z bands is suggestive of a further progression of damage to the myofibrils in a very early stage.

The interpretation of these mitochondrial, cytoskeletal and myofibril changes observed at the EM level in the flight group is difficult. The effects of microgravity are combined with the effects of re-entry. The observed mitochondrial changes in the synchronous group, exposed to conditions that mimic re-entry compared to the vivarium group, while not significant, are opposite in direction to the experimental groups, Also, stress-induced changes during re-entry could be aggravated by ischemia during specimen preparation.

The addition of a tail suspension group for comparison adds a new dimension to these studies of cardiac morphology. The observed loss of hind limb skeletal muscle mass partially mimics the skeletal muscle atrophy seen with microgravity and the head down tilt mimics the blood redistribution seen in the early phase of adaptation to microgravity. Both of these effects of microgravity can influence heart function. If a major function of the heart is to pump blood to muscles operating under a gravitational load, will less heart cell mass be required to sustain a diminishing skeletal muscle mass that has less strength? It is intriguing that in all parameters measured the tail suspension group falls consistently between the flight group and the vivarium group. Another correlation that should be examined in future cardiac studies is the possible correlation between amount of atrophy and degree of necrosis and time in microgravity. Riley et al (15) have observed in soleus muscles flown one week a 29% atrophy and 1% necrosis, and in soleus muscles flown 12.5 days on COSMOS 1887 a 38% atrophy and 6.8% necrosis. The observed decrease of 19% in the present study of heart may be close to the limit of compensated adaptation. If further mass decrease is accompanied by increasing necrosis, the irreversible loss of heart cells could have profound effects for animals and humans in prolonged flight.

SUMMARY AND CONCLUSIONS

These results suggest possible future directions for research in this area. First of all, the current study with five animals in each group was small for a quantitative morphological analysis. The study needs to be repeated to confirm the data and to allow a better statistical analysis. Secondly, the greater age of these rats and their greater size (350gms) meant papillary muscles were much larger than expected and only the superficial fibers of these and the ventricular samples could be analyzed. Rats in the 200- 250gm range would be more comparable to those for existing data on normal morphology, for stereological analysis and from tail suspension studies. Third, a concern for the ischemic damage that occurs in the minutes of dissection and the additional time for diffusion of fixative at temperatures below 22°C is a limitation in this study but is outweighed by the advantage of correlating biochemical data on adjacent tissue. These biochemical findings should be integrated with the morphological data and their functional significance determined. Fourth, the comparison of

findings from papillary and ventricular samples should be continued, since orientation of cells in the papillary muscle can facilitate the quantitative analyses and correlation of biochemical data from the ventricle should be made with adjacent ventricular tissue. Fifth, a measure of capillary number per cross-sectional area of papillary muscle in the four groups would also be helpful in assessing the adaptation to microgravity and would correlate with other parameters used for conditions of atrophy or hypertrophy.

We conclude that cardiac morphology is affected by space flight and that a continuing concern for a compensated adaptation of the heart to microgravity is warranted.

ACKNOWLEDGMENTS

The authors wish to thank Dr. A. S. Kaplansky and the Soviet Cosmos recovery and dissection teams. We are grateful to Richard Grindeland, James Connolly, and Marilyn Vasques for help in planning and performance of a complicated task. We thank Elizabeth Lacefield and David Ohlmer for technical assistance. We also thank the following students for help in data collection: Agustin Avilar-Sakar, Jonathan Cheng, Marselle Guerra, Laura Scholten, Erika Smith and James Smith. This study was funded by NASA grant NAG2-603 and by funds from the NASA COSMOS 2044 Parts Program.

REFERENCES

1. Anversa, P., A.V. Loud, and L. Vitali-Mazza. Morphometry and Autoradiography of Early Hypertrophic Changes in the Ventricular Myocardium of Adult Rat. Lab. Invest. 35 (5): 475-483, 1976.

2. Anversa, P., A.V. Loud, F. Giocomelli, and J. Wiener. Absolute Morphometric Study of Myocardial Hypertrophy in Experiment Hypertension. II. Ultrastructure of Myocytes and Interstitium. Lab. Invest. 38 (5): 597-609, 1978.

3. Baranski, S., M. Kujawa, and A. Kaplanski. Ultrastructural Qualitative and Quantitative Evaluation of Cytoplasmic Structures of Heart Muscle of Rats Living Aboard Biosputnik Kosmos 936. The Physologist 23: S38-S39, 1980.

4. Cartwright, J. Jr., and M.A. Goldstein. Microtubules in the Heart Muscle of the Postnatal and Adult Rat. J. Mol. Cell. Cardiol. 17: 1-7, 1985.

5. Goldstein, M.A., L.H. Michael, J.P. Schroeter, and R.L. Sass. The Z-band Lattice in Skeletal Muscle Before, During and After Tetanic Contraction. J. Musc. Res. Cell Motil. vol. 7, 1986, pp. 527-536.

6. Goldstein, M.A. Ultrastructure of the Ischemic Myocardium. Cardiovascular Research Center Bulletin, 18, pp.1-33, 1979.

7. Grindeland, R.E., M.F. Vasques, R.W. Ballard and J. P. Connolly, COSMOS 2044 Mission Overview. J. Appl. Physiol., in press, 1990.

8. Kovalenko, Ye A., V.L. Popkov, and E.S. Mailyan. Kosm. Biol. Med. vol. 4, pp. 3-8, 1971.

9. Mailyan, E.S., L.I. Grinberg, and Ye.A. Kovalenko. Adaptatsiva K Myshechnoy Deyatel'nosti I Gipokinezii 1971, pp. 111-113, Novosibirsk.

10. Nepomnyashchikh, L.M., L.V. Kolesnikova and G.I. Nepomnyashchikh. Myocardial Tissue Organization in Rats under Hypokinesia (a stereological investigation). Arkh. Anat. Gistol. Embriol., vol. 88, pp. 57-62, 1985.

11. Page, E., P.I. Polimeni, R. Zak, J. Earley, and M. Johnson. Myfibrillar Mass in Rat and Rabbit Heart Muscle. Circ. Res. 30: 430-439, 1972.

12. Philpott, D.E., A. Fine, K.Kato, R. Egnor, L.Cheng and M. Mednieks,: Microgravity Changes in Heart Structure and Cyclic AMP Metabolism. Physiologist (Suppl.) vol. 28, S209, 1985.

13. Philpott, D.E., I.A.Popova, Kato, K, J.Miquel, W.Sapp and J.Stevenson. Ultrastructural Alterations in Rat Hears after COSMOS 2044 Compared to Cosmos 1887. J. Appl. Physiol. in press, 1990.

14. Philpott, D.E., I.A.Popova, Kato, K, J.Miquel, W.Sapp and J.Stevenson. Morphological and Biochemical Examination of COSMOS 1887 Rat Heart Tissue: Part I - Ultrastucture. FASEB J. 4: 73-78, 1990.

STATISTICS TABLE 1 (Papillary Pooled Method)

This table presents the results of the Kruskal-Wallis oneway analysis of variance of the area of the two pooled blocks across the four groups.*

VARIABLE	CHI-SQUARE WITH 3 DEGREES OF FREEDOM	P-VALUE
Pooled Mean	5.880	0.1176
Pooled Range	8.120	0.0436
Pooled Number of Cells	4.706	0.1947

* For each of the two papillary blocks for each rat the area of each cell in the block was calculated. Then the mean and range were computed for the pooled cells for the two blocks for each rat. That is the two blocks were considered as though they formed a single block.

STATISTICS TABLE 1A (Papillary Mean for Pooled Method)

Since the Pooled Mean in Table 1 is borderline significant across the four groups, this table gives the comparison of the groups in pairs. The entries in each cell are the chi-square with 1 degree of freedom (top) and the p-value (bottom).

	RED	YELLOW	BLUE
Yellow	4.811 0.0283		
Blue	1.844 0.1745	1.320 0.2506	
Green	2.455 0.1172	0.098 0.7540	0.884 0.3472

STATISTICS TABLE 1B (Papillary Range for Pooled Method)

Since the Pooled Range in Table 1 is significant across the four groups, this table gives the comparison of the groups in pairs. The entries in each cell are the chi-square with 1 degree of freedom (top) and the p-value (bottom).

	RED	YELLOW	BLUE
Yellow	3.938 0.0472		
Blue	0.884 0.3472	0.884 0.3472	
Green	6.818 0.0090	0.535 0.4647	2.455 0.1172

STATISTICS TABLE 2 (Ventricle Pooled Method)

This table presents the results of the Kruskal-Wallis oneway analysis of variance of the area of the two pooled blocks across the four groups.*

VARIABLE	CHI-SQUARE WITH 3 DEGREES OF FREEDOM	P-VALUE
Pooled Mean	0.164	0.9831
Pooled Range	4.056	0.2554
Pooled Number of Cells	0.557	0.9061

* For each of the two ventricle blocks for each rat the area of each cell in the block was calculated. Then the mean and range were computed for the pooled cells for the two blocks for each rat. That is the two blocks were considered as though they formed a single block.

STATISTICS TABLE 3 (Papillary Averaged Method)

This table presents the results of the Kruskal-Wallis oneway analysis of variance of the area of the averaged blocks across the four groups.*

VARIABLE	CHI-SQUARE WITH 3 DEGREES OF FREEDOM	P-VALUE
Averaged Mean	6.291	0.0983
Averaged Range	8.291	0.0404
Averaged Number of Cells	4.706	0.1947

* For each of the two papillary blocks for each rat the area of each cell in the block was calculated. Then the mean and range were computed for each block. The number of cells for each block was also recorded. The pairs of statistics were then averaged to get a single value for each rat (i.e. the Averaged Mean is the average of the two means).

STATISTICS TABLE 3A (Papillary Averaged Mean)

Since the Averaged Mean in Table 3 is borderline significant across the four groups, this table gives the comparison of the groups in pairs. The entries in each cell are the chi-square with 1 degree of freedom (top) and the p-value (bottom).

	RED	YELLOW	BLUE
Yellow	4.811 0.0283		
Blue	2.455 0.1172	0.273 0.6015	
Green	3.153 0.0758	0.011 0.9168	1.844 0.1745

TABLE 3B (Papillary Averaged Range)

Since the Averaged Range in Table 3 is significant across the four groups, this table gives the comparison of the groups in pairs. The entries in each cell are the chi-square with 1 degree of freedom (top) and the p-value (bottom).

	RED	YELLOW	BLUE
Yellow	3.938 0.0472		
Blue	0.884 0.3472	0.535 0.4647	
Green	5.771 0.0163	1.844 0.1745	3.153 0.0758

STATISTICS TABLE 4 (Ventricle Averaged Method)

This table presents the results of the Kruskal-Wallis oneway analysis of variance of the area of the averaged blocks across the four groups.*

VARIABLE	CHI-SQUARE WITH 3 DEGREES OF FREEDOM	P-VALUE
Averaged Mean	0.570	0.9033
Averaged Range	3.854	0.2776
Averaged Number of Cells	0.557	0.9061

* For each of the two ventricle blocks for each rat the area of each cell in the block was calculated. Then the mean and range were computed for each block. The number of cells for each block was also recorded. The pairs of statistics were then averaged to get a single value for each rat (i.e. the Average Mean is the average of the two means).

TABLE 5: MITOCHONDRIAL FRACTIONAL VOLUME AND MITOCHONDRIA/MYOFIBRIL RATIO

ANIMAL NO.	FRACTIONAL VOLUME	MITOCHONDRIA/ MYOFIBRIL
	Flight (red)	
F6	0.42 +- 0.01*	0.72 +- 0.03
F7	0.35 +- 0.02	0.51 +- 0.06
F8	0.36 +- 0.03	0.57 +- 0.08
F9	0.35 +- 0.02	0.54 +- 0.05
F10	0.36 +- 0.02	0.56 +- 0.04
	Group mean 0.37 +- 0.04	0.58 +- 0.05
	Tail suspension (blue)	
T60.	42 +- 0.02	73 +- 0.05
T70	35 +- 0.05	56 +- 0.12
T80.	35 +- 0.02	55 +- 0.04
T90.	27 +- 0.02	37 +- 0.03
T100.	37 +- 0.02	59 +- 0.04
	Group mean 0.35 +- 0.03	0.56 +- 0.06
	Vivarium (green)	
V6	0.33 +- 0.02	0.51 +- 0.05
V7	0.36 +- 0.04	0.60 +- 0.11
V8	0.39 +- 0.05	0.69 +- 0.17
V9	0.40 +- 0.02	0.67 +- 0.04
V10	0.24 +- 0.02	0.33 +- 0.03
	Group mean 0.34 +- 0.03	0.56 +- 0.08
	Synchronous (yellow)	
S6	0.20 +- 0.01	0.25 +- 0.02
S7	0.35 +- 0.02	0.53 +- 0.04
S8	0.21 +- 0.02	0.30 +- 0.04
S9	0.31 +- 0.02	0.45 +- 0.03
S10	0.28 +- 0.03	0.39 +- 0.06
	Group mean 0.27 +- 0.03	0.38 +- 0.06

* Standard error of the mean

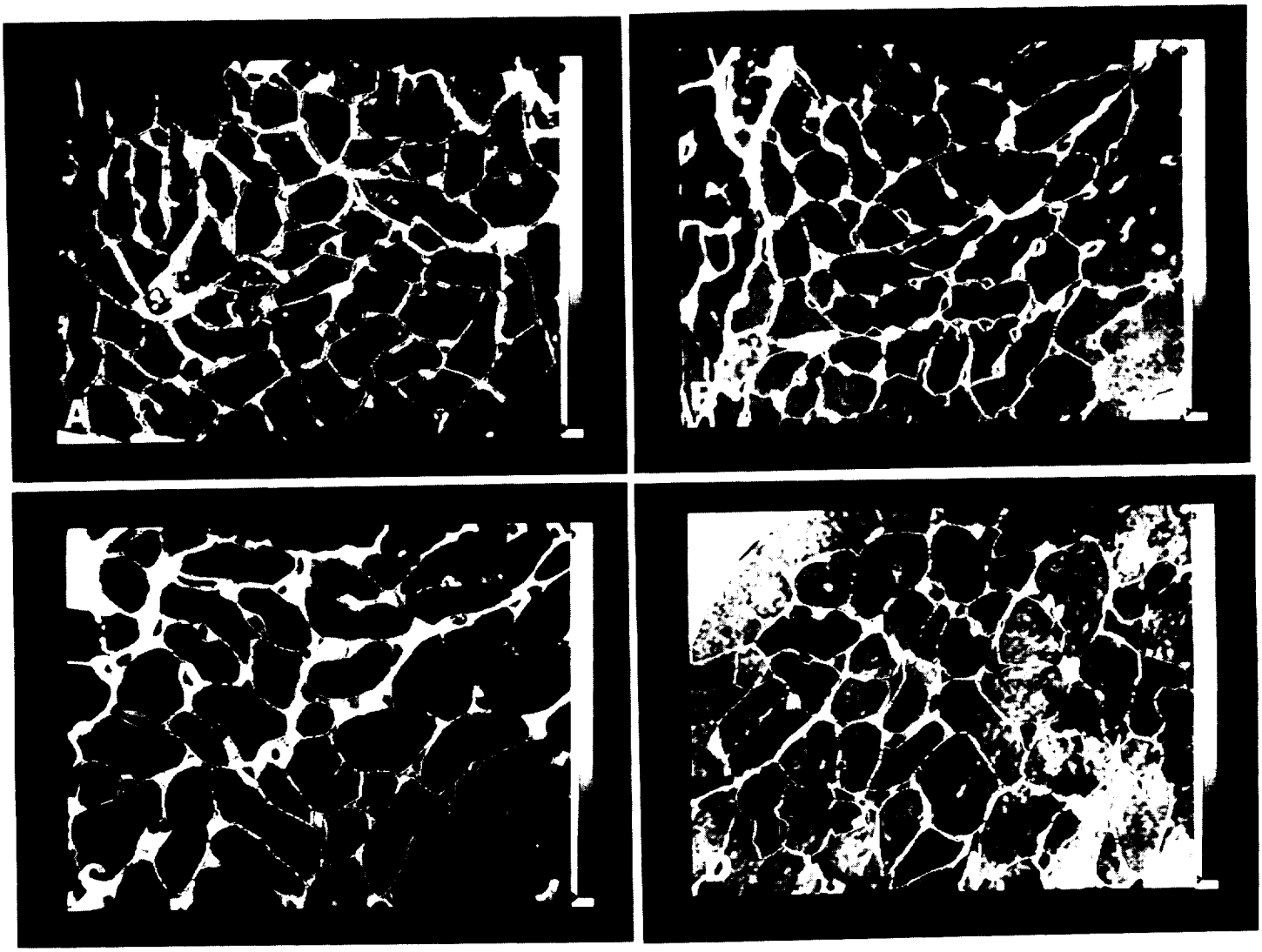

Figure 1. A-D Papillary muscle cross-sectional profiles used for determination of average cross-sectional area of myofibers.

A. Papillary muscle sample from rat F6 from flight group.
B. Papillary muscle sample from rat T7 from tail suspension group.
C. Papillary muscle sample from rat S9 from synchronous group.
D. Papillary muscle sample from rat V8 from vivarium group.

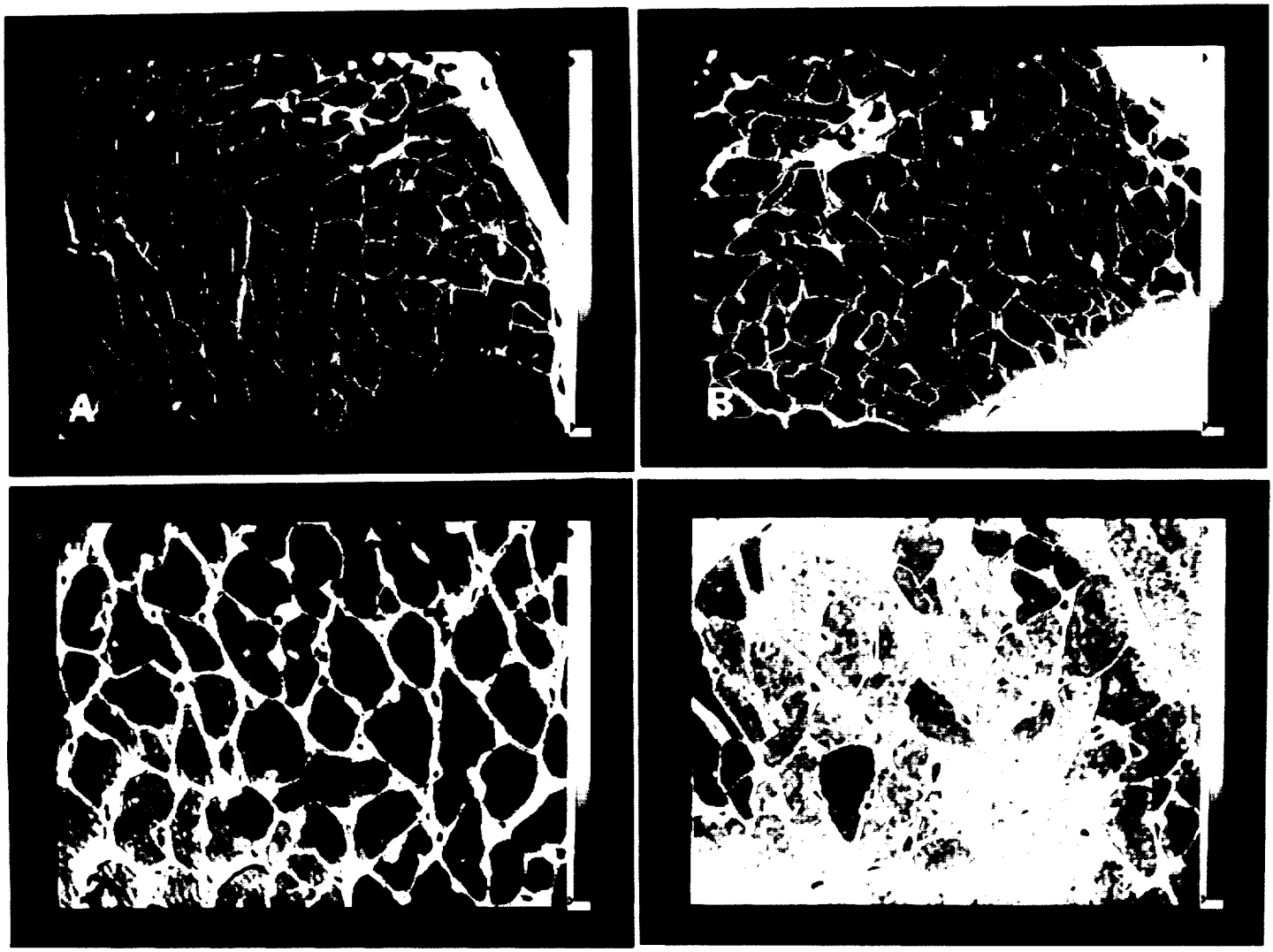

Figure 2. A-D Ventricular muscle cross-sectional profiles used for determination of average cross-sectional area of myofibers.

A. Ventricular muscle sample from rat F7 from flight group.
B. Ventricular muscle sample from rat T9 from tail suspension group.
C. Ventricular muscle sample from rat S6 from synchronous group.
D. Ventricular muscle sample from rat V7 from vivarium group.

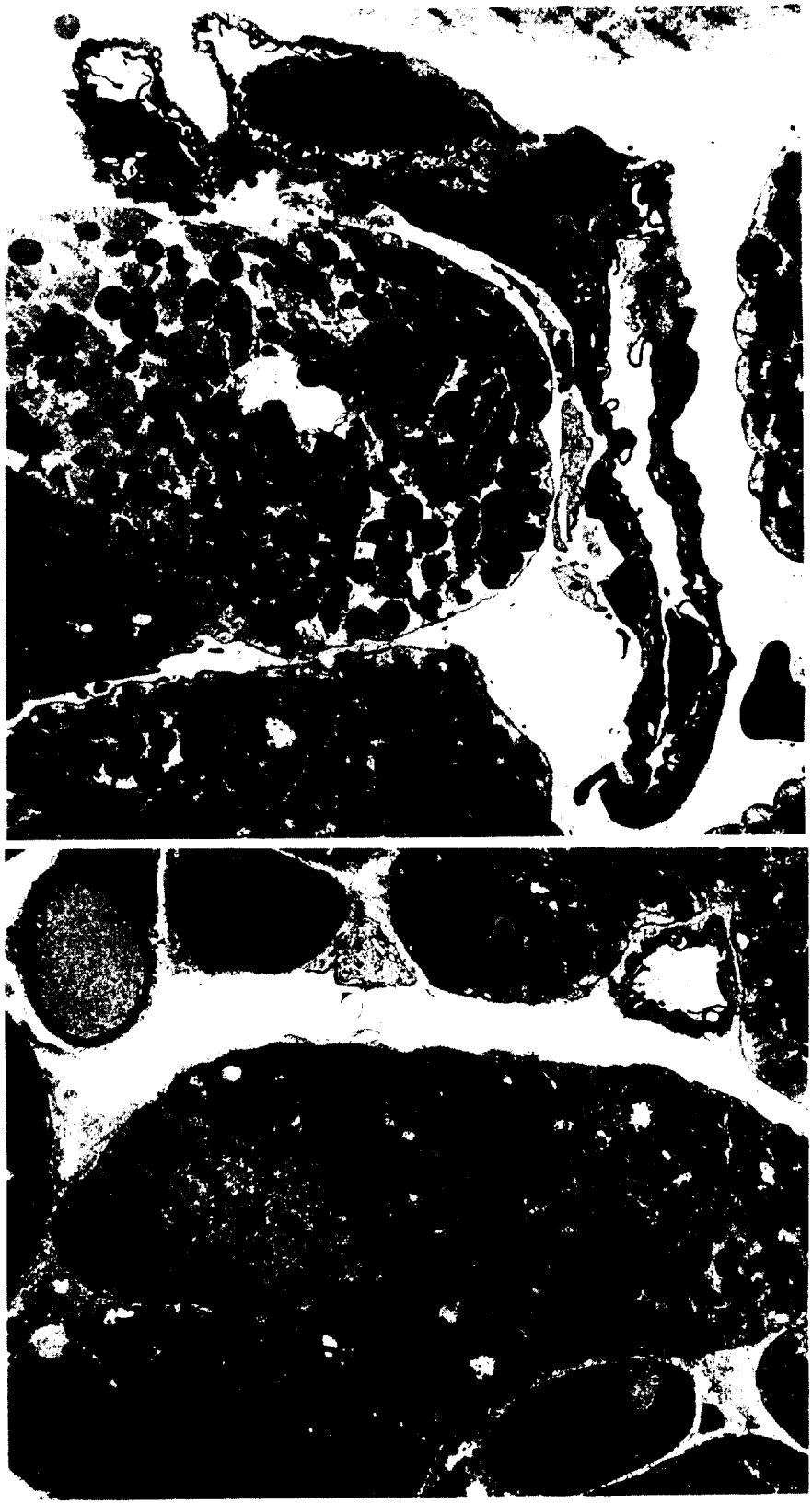

Figure 3. A-B Electron micrographs of oblique sections of ventricular muscle X6000.

A. *Note elaborate wavy protections from endothelial surfaces within the capillaries. Some capillary damage is evidenced by the red blood cell, free in the extracellular space. Overall morphology in this example from rat F6 is typical of that seen in the flight group and in the other three groups of rats.*
B. *A few but smaller projections from endothelial surfaces within the capillaries are seen. Mitochondrial damage seen in this example from rat S9 is typical of that seen in the synchronous group and was observed in all groups. Note heterogeneity in adjacent cells as in Figure 3A.*

Figure 4. Electron micrograph of longitudinal section of papillary muscle from rat F7 in the flight group. Note projections from endothelial cell surfaces within the capillary. The variation in mitochondrial morphology seen in both of these cells was frequently observed in the rat hearts from all four groups. The uniformity of sarcomere length, lateral registration of myofibrils and the well-ordered banding patterns of the sarcomeres are seen in papillary muscles pinned at rest length. X10,000.

Figure 5. Electron micrograph of longitudinal section of papillary muscle from rat T6 in the tail suspension group. Morphology is similar to that seen in all four groups. X10,000.

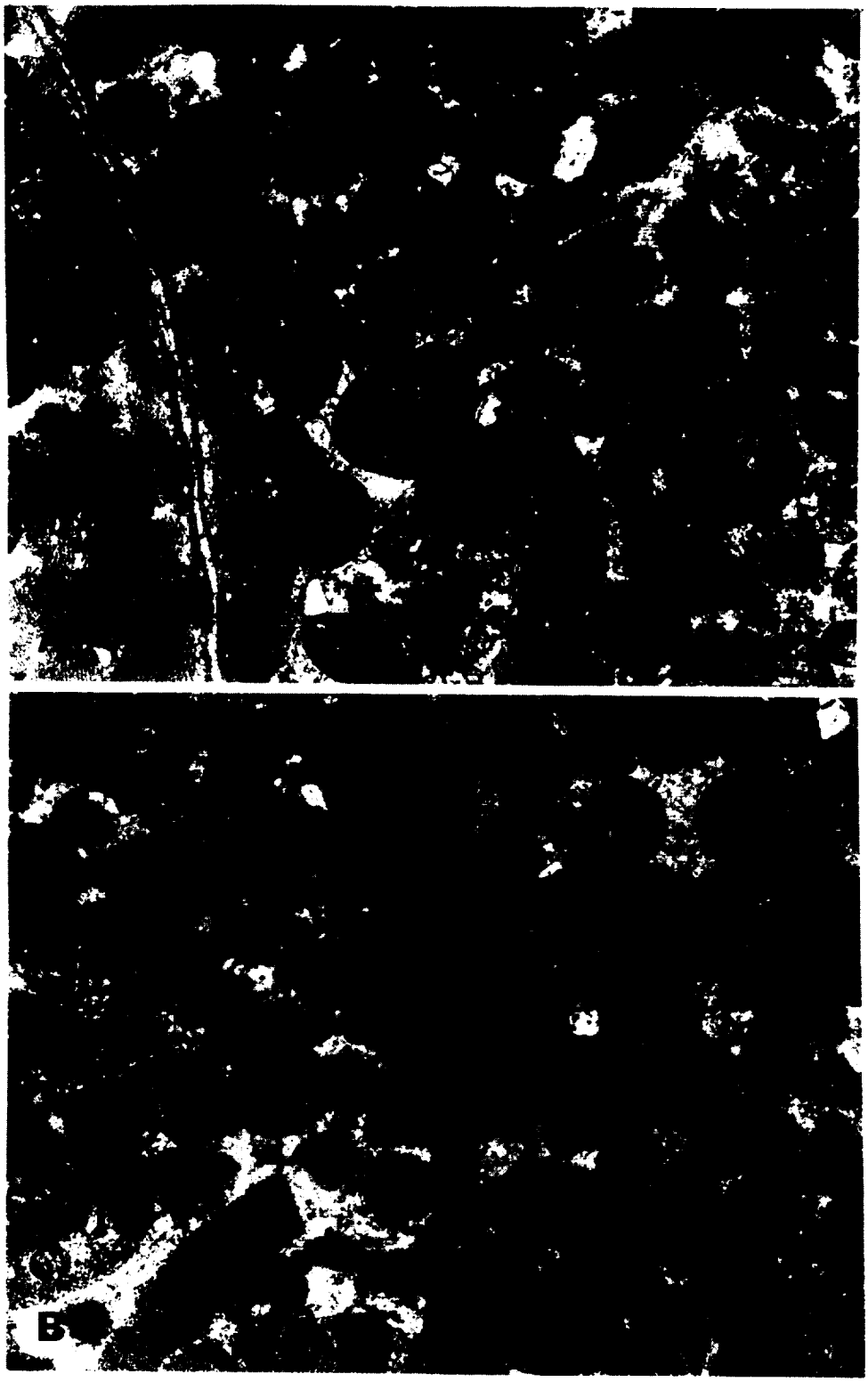

Figure 6. A-B Electron micrographs of cross sections of papillary muscles used for mitochondrial fractional volume measurements are shown at reduced magnification. X17,000.

A. Mitochondria are intact mostly, but some blebbing is seen in this example from rat F7 in the flight group.
B. Similar morphology is seen in this example from rat V10 from the vivarium group.

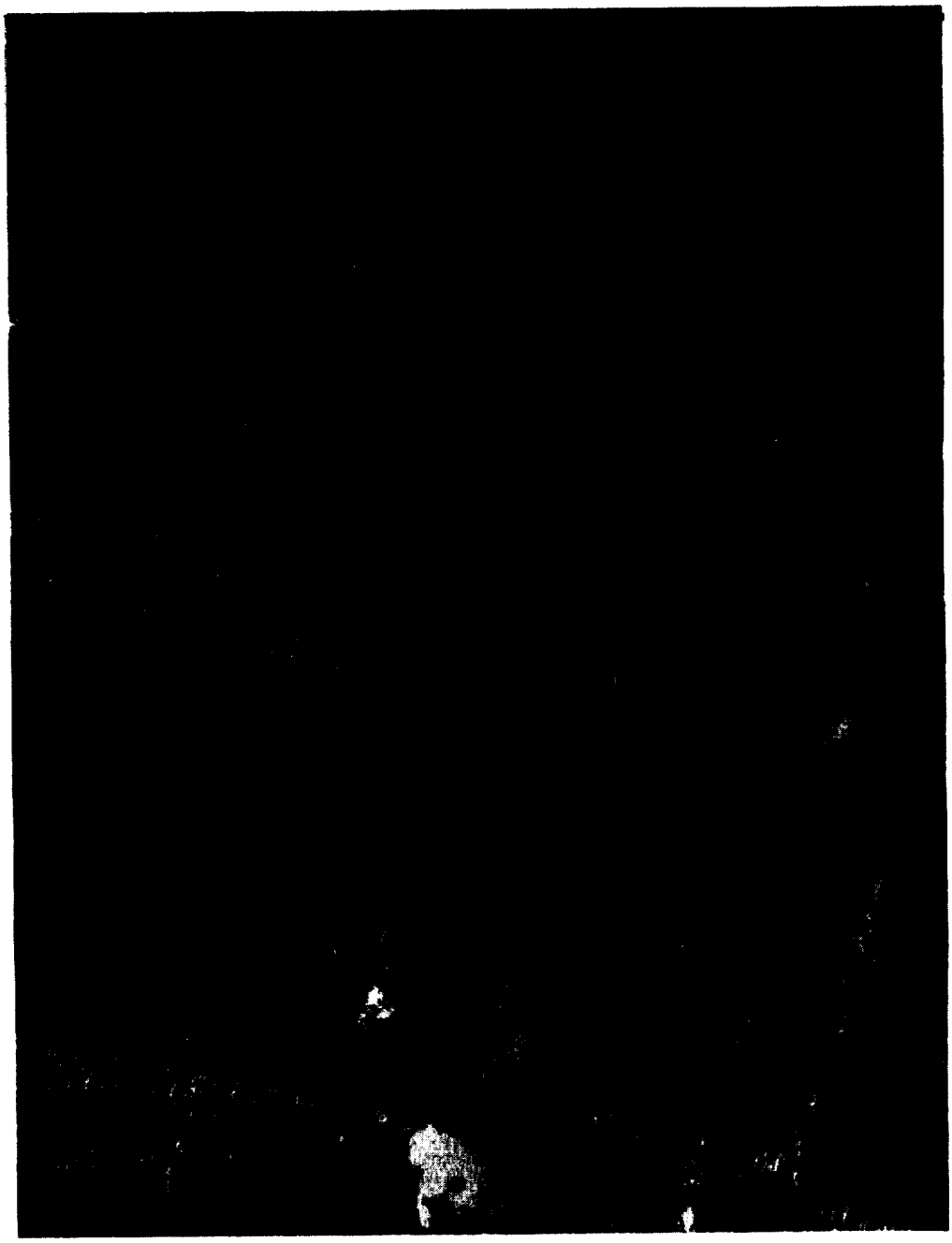

Figure 7. Electron micrograph of longitudinal section of papillary muscle from rat F7 in the flight group used for optical diffraction of Z and A bands. X40,000.

Figure 8. Electron micrograph of cross section of papillary muscle from rat T8 in the tail suspension group used for optical diffraction of Z and A bands. X40,000.

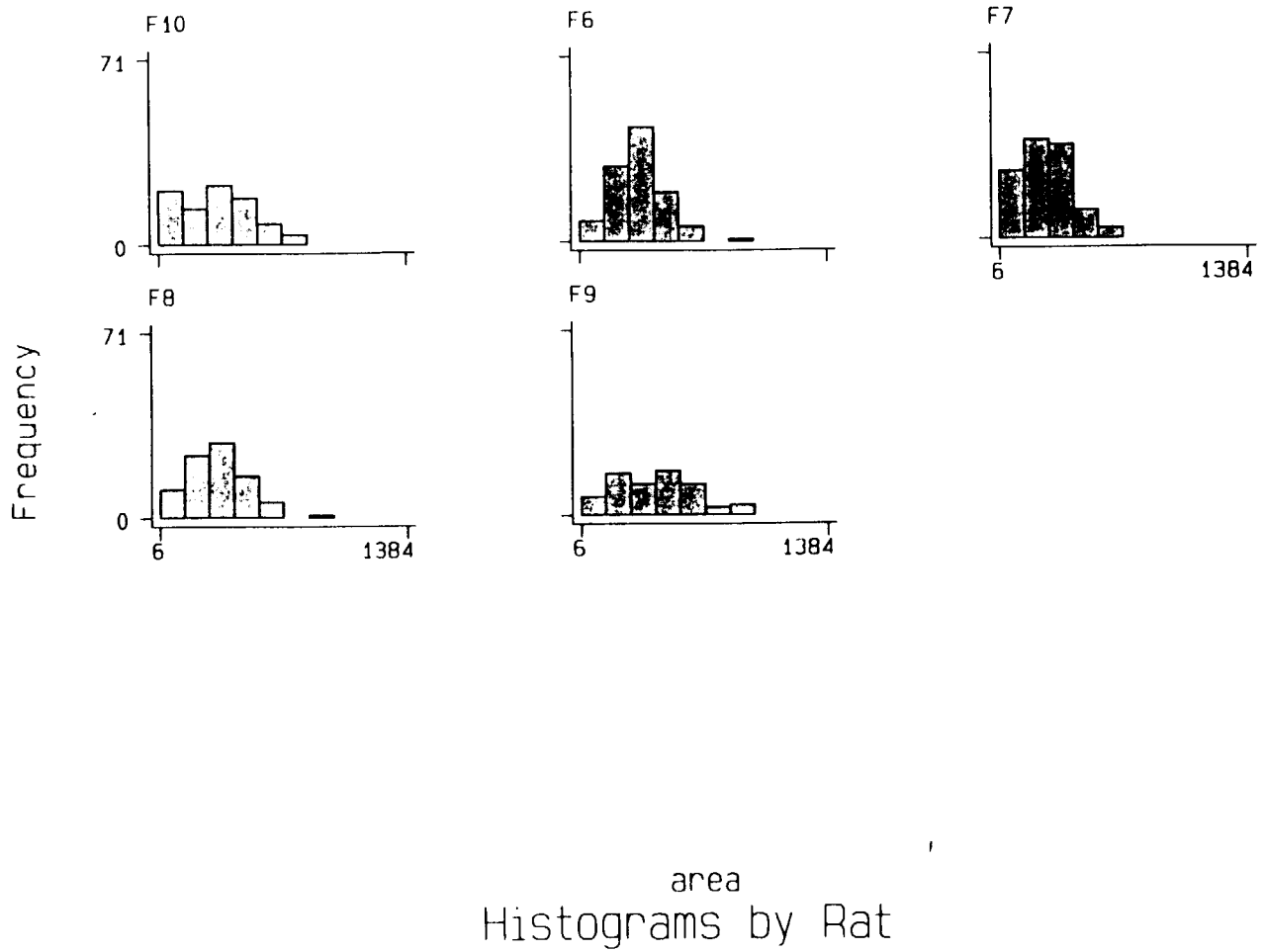

Figure 9. Red papillary pooled. (Histograms of myofiber cross-sectional area for papillary and ventricular muscles from all rats in all four groups.)

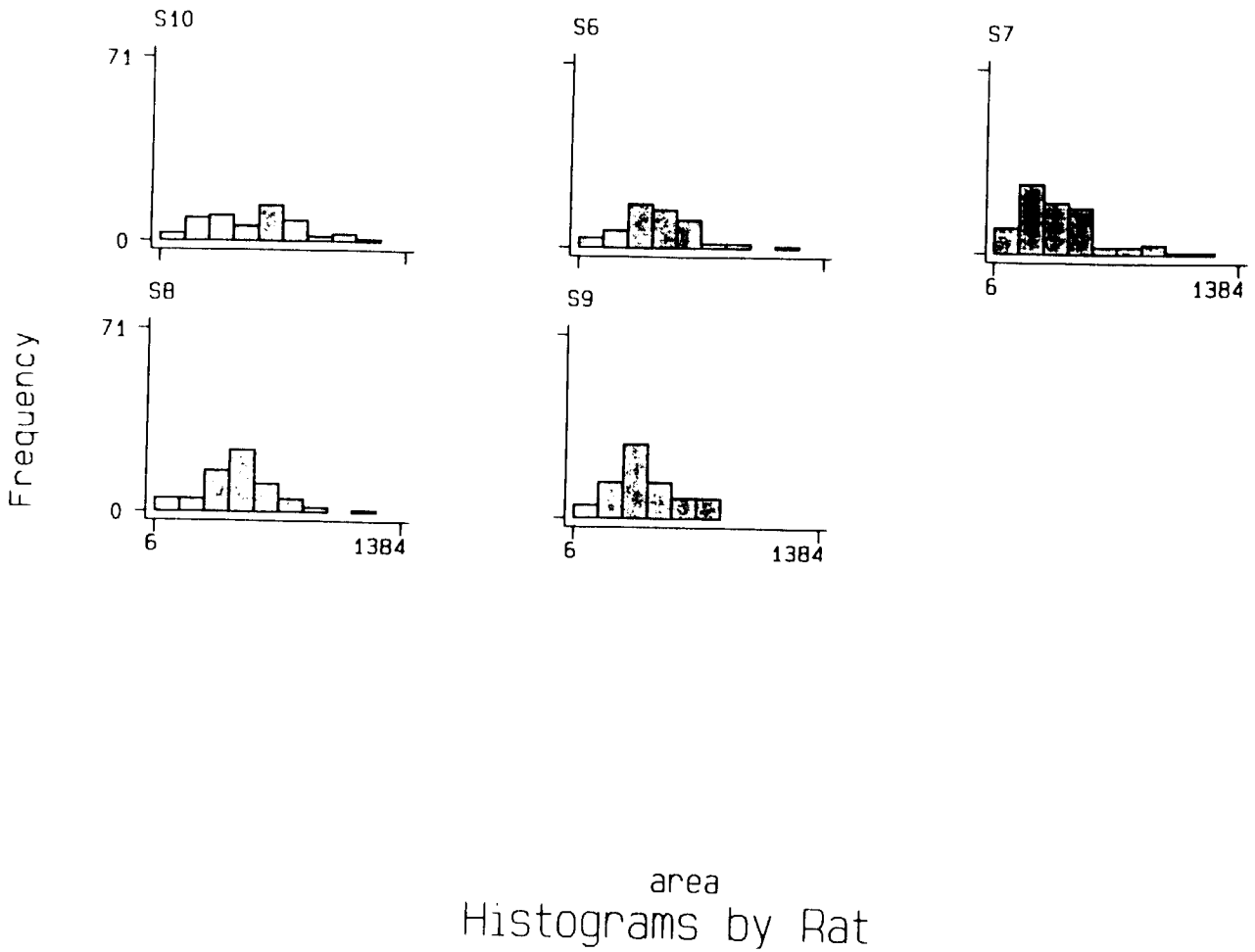

Figure 10. Yellow papillary pooled. (Histograms of myofiber cross-sectional area for papillary and ventricular muscles from all rats in all four groups.)

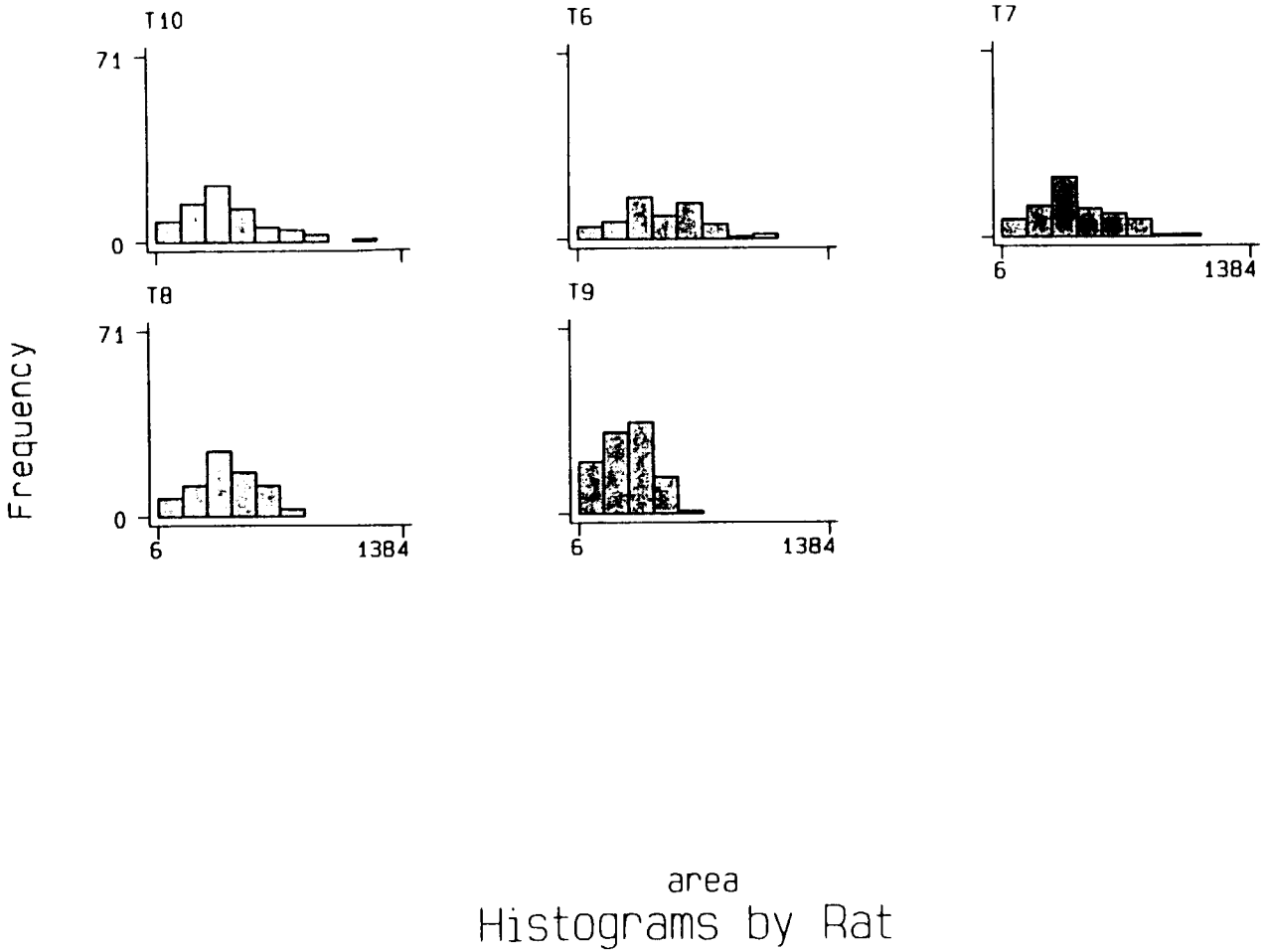

Figure 11. Blue papillary pooled. (Histograms of myofiber cross-sectional area for papillary and ventricular muscles from all rats in all four groups.)

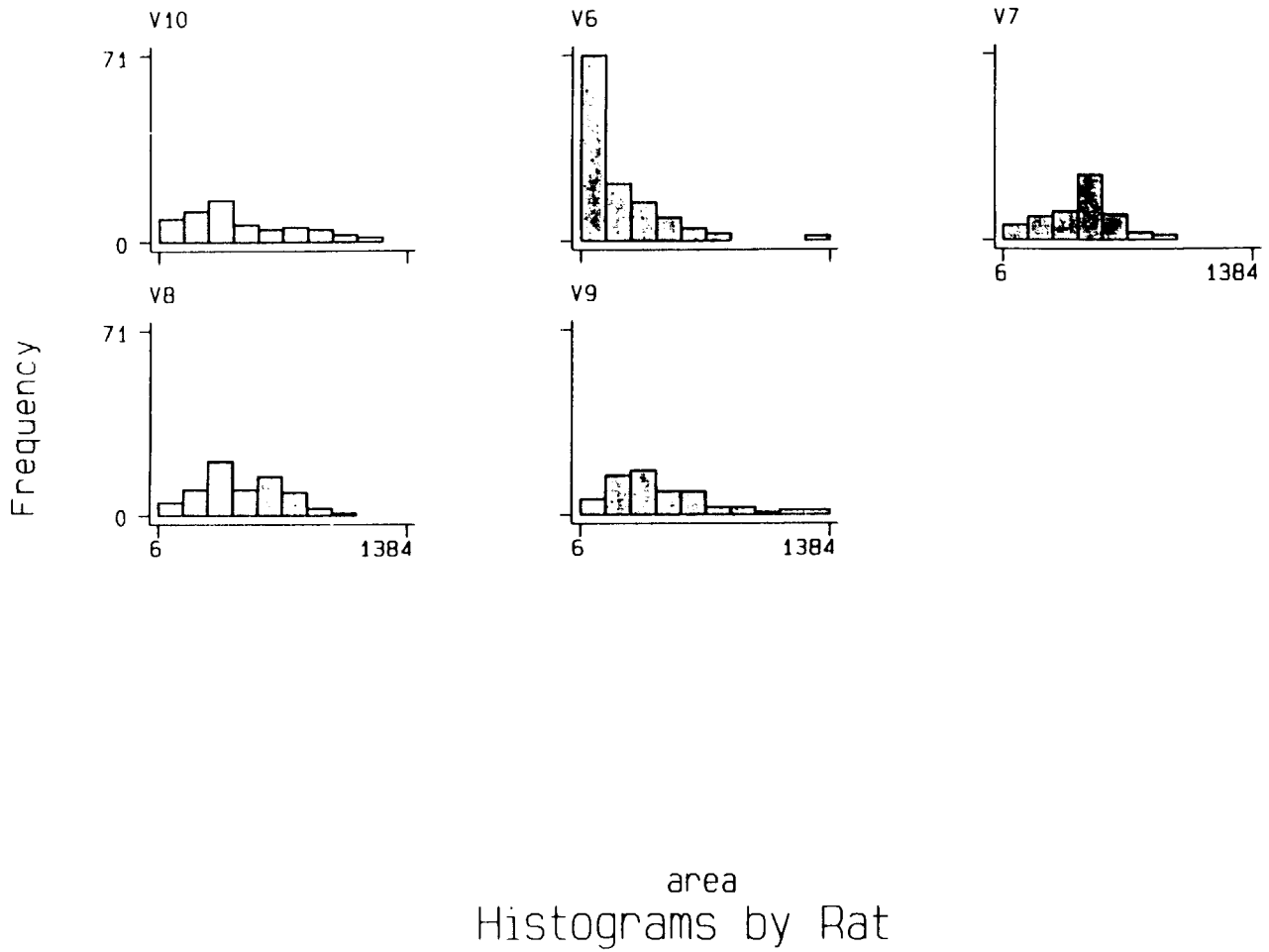

Figure 12. Green papillary pooled. (Histograms of myofiber cross-sectional area for papillary and ventricular muscles from all rats in all four groups.)

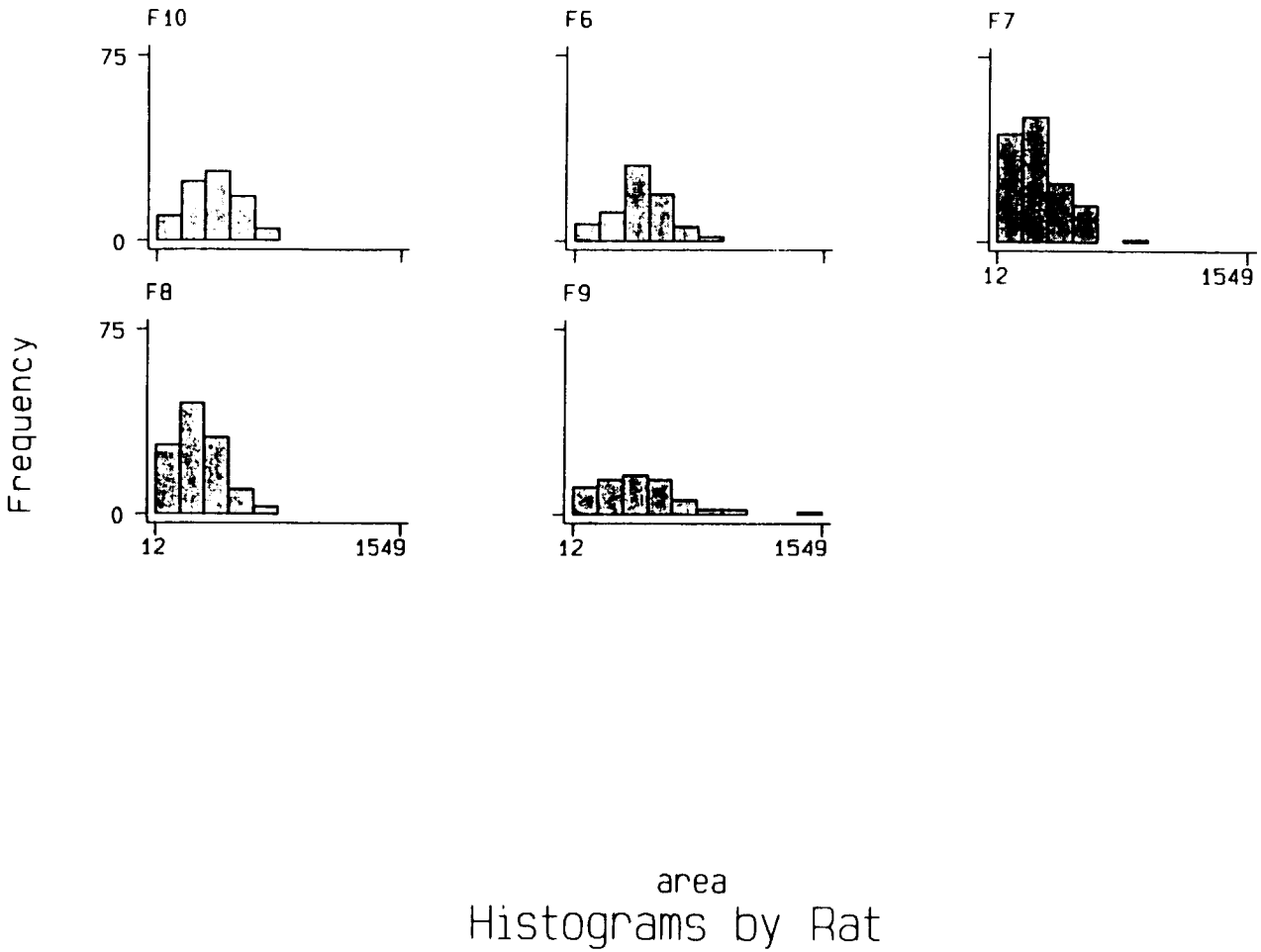

Figure 13. Red ventricle pooled. (Histograms of myofiber cross-sectional area for papillary and ventricular muscles from all rats in all four groups.)

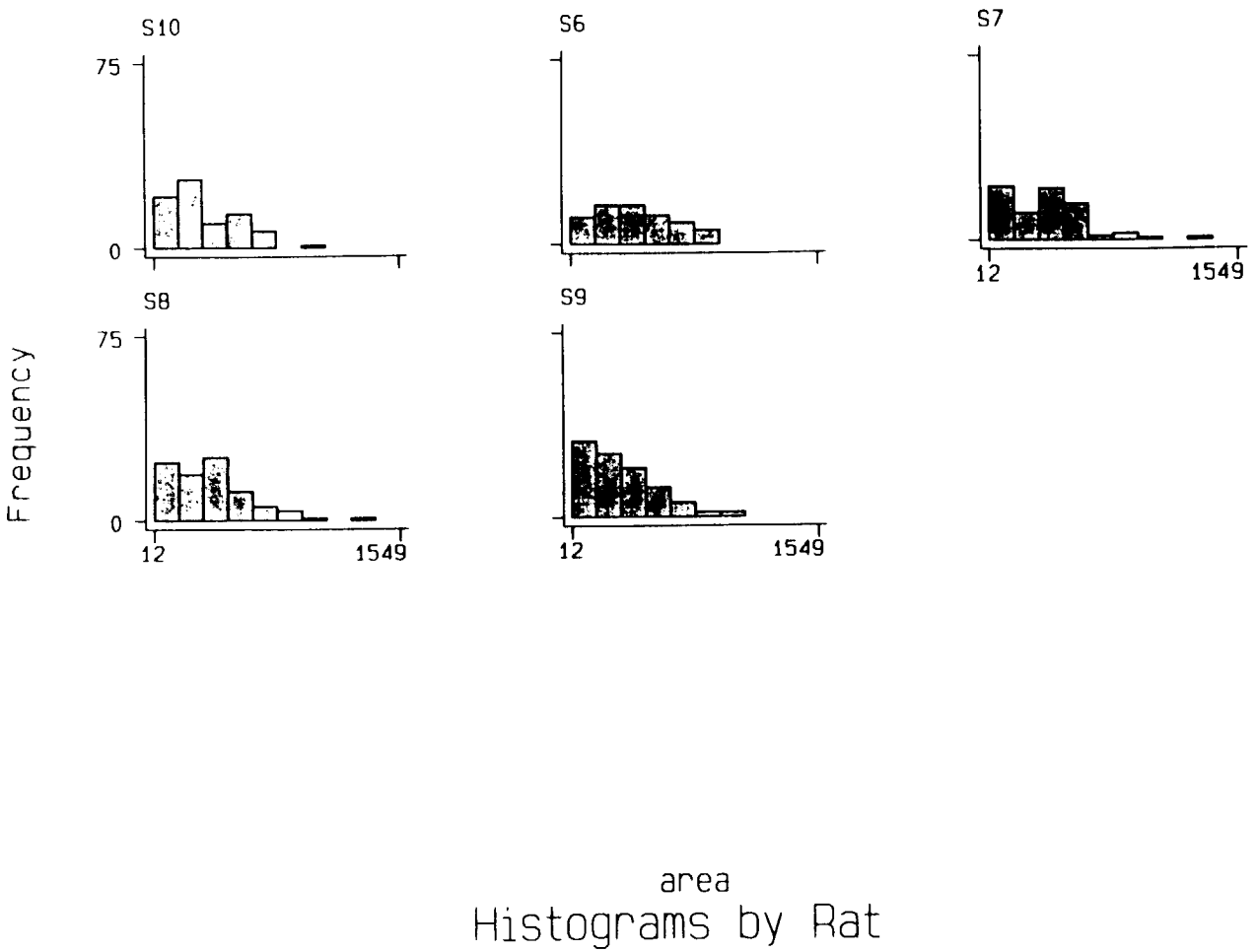

Figure 14. Yellow ventricle pooled. (Histograms of myofiber cross-sectional area for papillary and ventricular muscles from all rats in all four groups.)

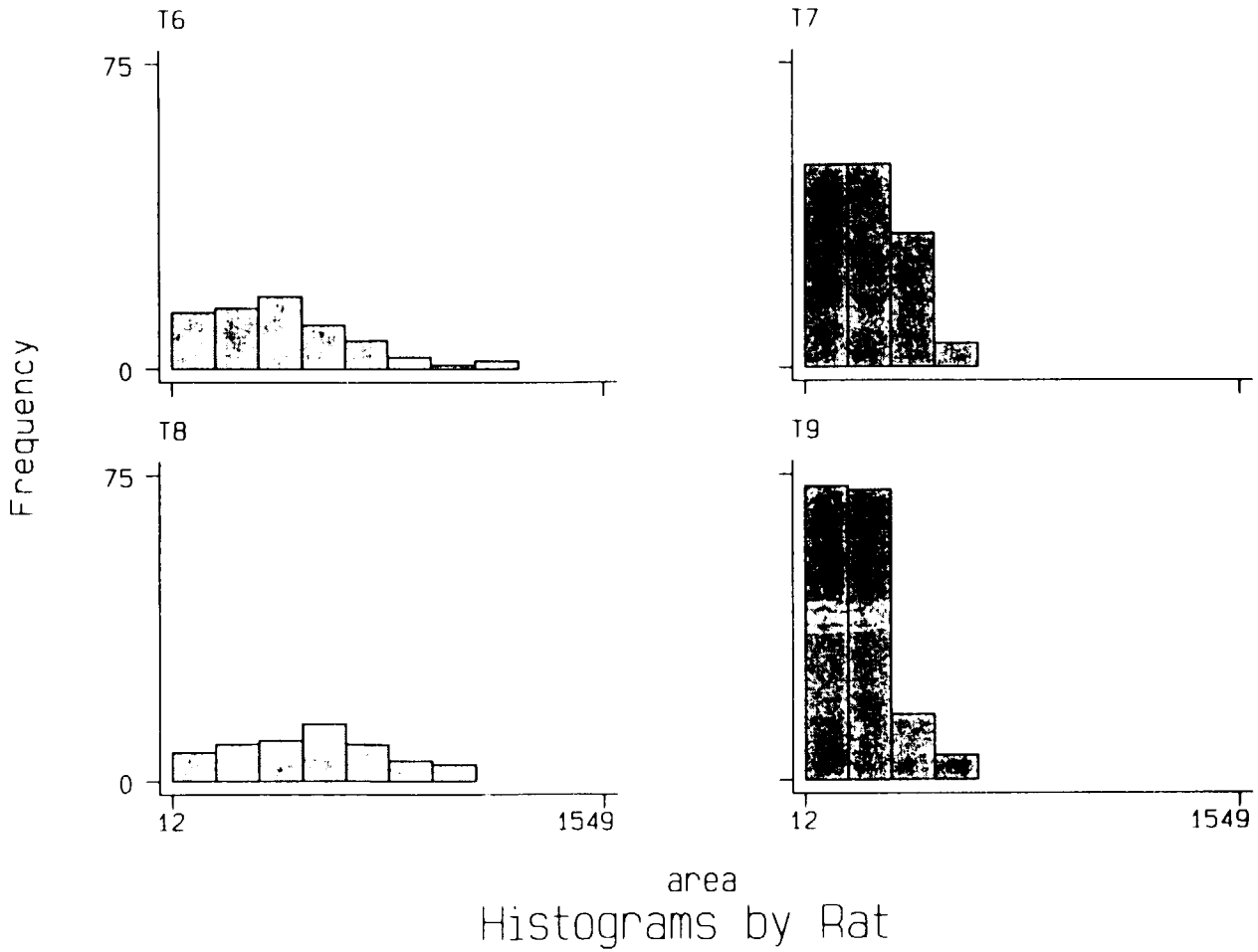

Figure 15. Blue ventricle pooled. (Histograms of myofiber cross-sectional area for papillary and ventricular muscles from all rats in all four groups.)

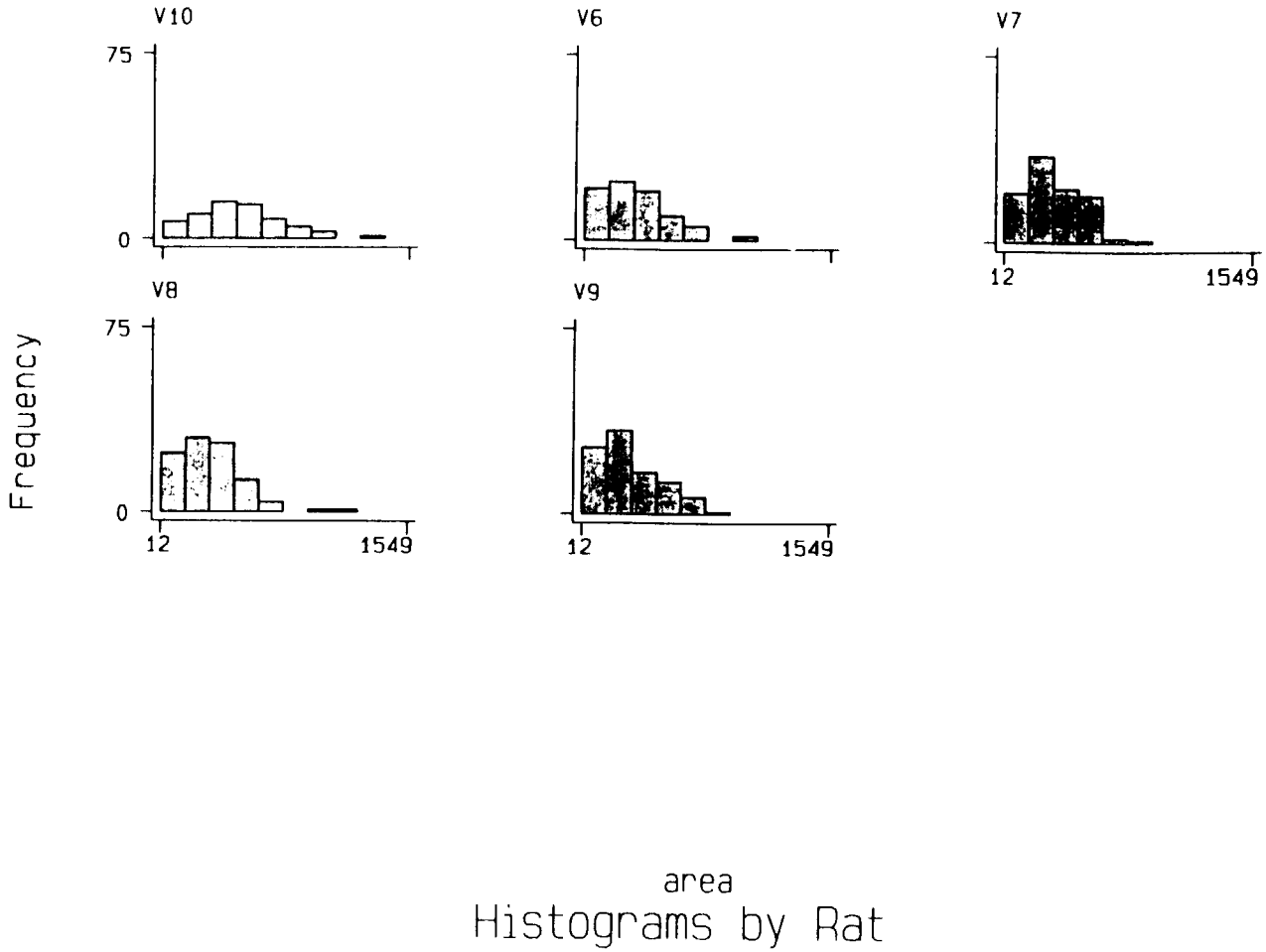

Figure 16. Green ventricle pooled. (Histograms of myofiber cross-sectional area for papillary and ventricular muscles from all rats in all four groups.)

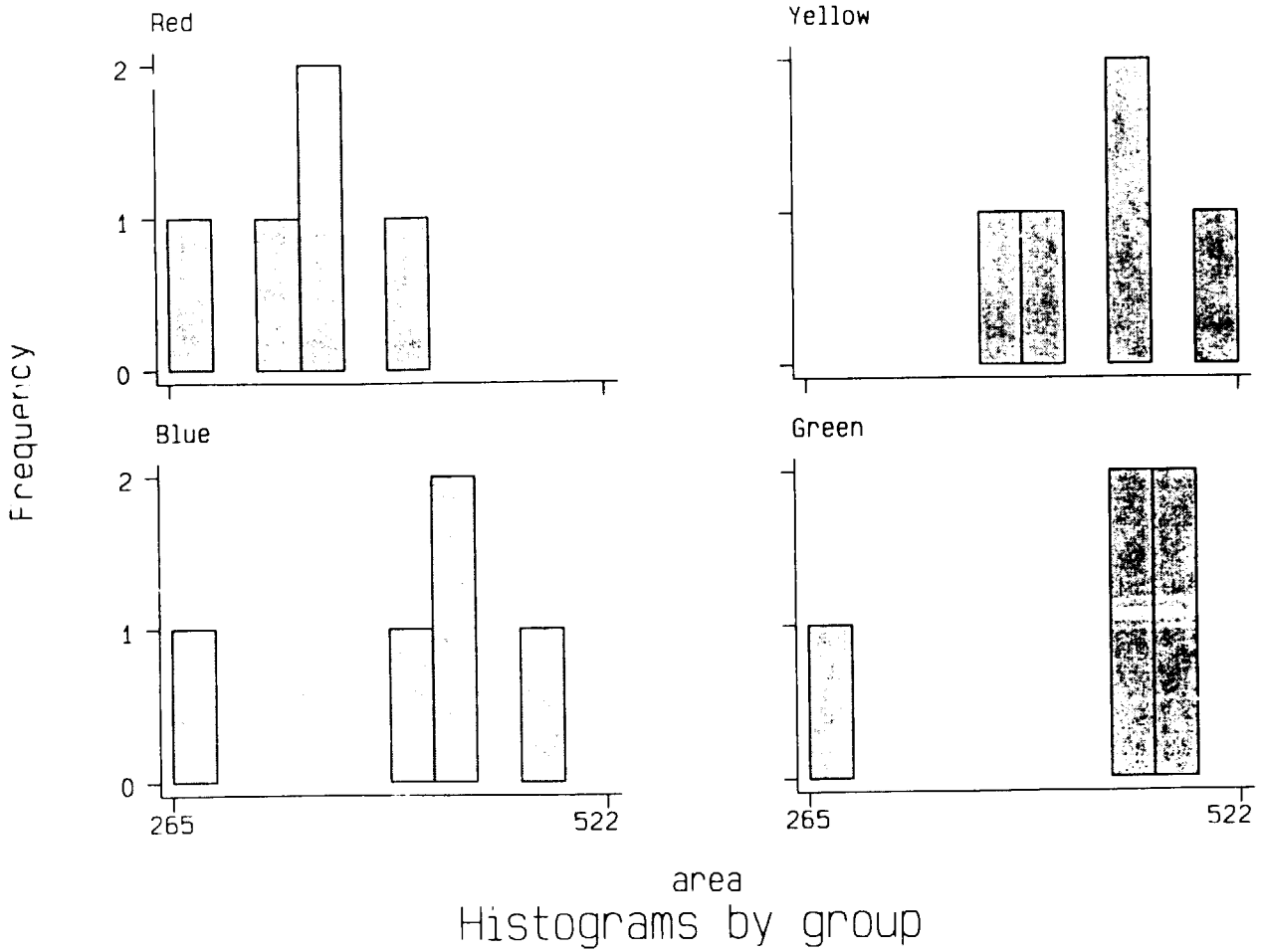

Figure 17. Papillary averaged. (Histograms of myofiber cross-sectional area for papillary and ventricular muscles from all rats in all four groups.)

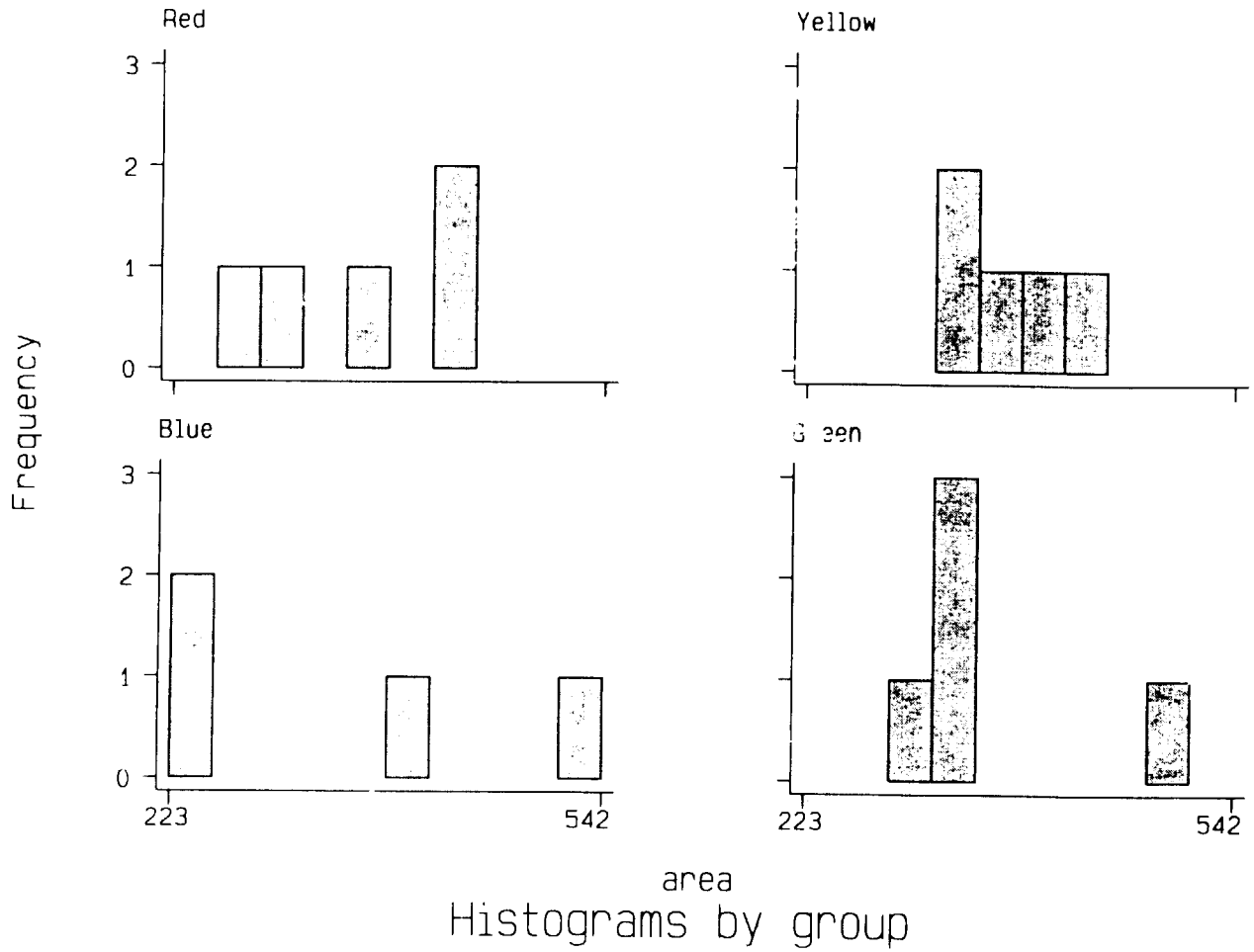

Figure 18. Ventricle averaged. (Histograms of myofiber cross-sectional area for papillary and ventricular muscles from all rats in all four groups.)

EXPERIMENT K-7-13

PART III: CYCLIC AMP RECEPTOR PROTEIN DISTRIBUTION IN HEART MUSCLE OF RATS FLOWN ON COSMOS 2044

M.I. Mednieks, I. Popova and R.E. Grindeland

SUMMARY

Cyclic AMP binding protein activities, as measured by photoaffinity labeling of regulatory (RI and RII) subunits of cyclic AMP-dependent protein kinase, were decreased in heart tissue of rats flown on Cosmos 2044. Densitometric analyses showed a significant decrease of RII in the particulate cell fraction extract (S2), $p<0.05$ in all cases, when vivarium controls (V) were compared with tissue samples of flight (F) animals. Photoaffinity labeling of the soluble fraction (S1) was unaffected by spaceflight or any of the simulation conditions. This was previously observed in heart muscle of rats flown on the U.S. Space Lab-3 and on the Soviet Cosmos 1887 missions. A decrease in either the number or affinity of the R subunits for cyclic AMP apparently results from some aspect of space flight. The proteins of the S2 fraction constitute the minor (~10%) component, while the RI subunit label in the soluble fraction, S1, (containing most of the cell proteins) was unchanged, by spaceflight, synchronous or simulation conditions. A negative correlation resulted upon comparing controls with flight, synchronous and tail-suspended animals when incorporation of total counts due to azido labeling was based on body weights. No changes were seen when total label was calculated on the basis of adrenal gland weights. Factors which influence the body weight changes, therefore, in the experimental groups of animals, may alter hormonal responses. Conversely, changes in a relatively minor aspect of cyclic AMP-mediated reactions may have a metabolic effect on an organismal level.

INTRODUCTION

The effects of actual or simulated travel in space on the cardiovascular or other systems have been investigated in order to determine if measurable changes can be noted, and if such changes might influence the health or performance of the individual (3,4,6,15,27,30). The present study was undertaken in order to gain insight into a specific biochemical mechanism which may be associated with cardiac changes that experimental animals and possibly humans undergo as a consequence of travel in space.

Several physiologic changes attributed to space travel conditions in experimental animals and in humans may be associated with changes in circulating levels of catecholamine hormones (1,11,20). There are two general types of such responses, involving second messenger-mediated receptor-effector cascades. The first, immediate responses involve cytoplasmic protein phosphorylation by several kinases and frequently having Ca^{++} as a second messenger are generally transient in nature (1,9,11,21). The later effects appear to be longer lasting, may involve gene regulation and have longer or unknown recovery periods (7,12,13). The later reaction is mediated most likely by cyclic AMP, occurs in the nuclear , chromatin bound compartment, may have physiologic consequences, is therefore of practical concern (2,10,19,30). Cyclic AMP-receptor reactions in the cell particulate fraction were investigated in this study.

Sequential cellular events occur as a consequence of stimulation of cardiac muscle tissue by (catecholamine or peptide) hormones, pharmacological agents, or chemical analogs of either group of compounds. Receptor binding at the cell's surface is followed by activation of adenylate cyclase in the plasma membrane resulting in increased intracellular cyclic AMP. The

extracellular signal is propagated by activation of cyclic AMP-dependent protein kinase (cAPK; E.C. 2.7.1.37). The ensuing intracellular signal processing is then a function of the distribution and activity of cAPK or its subunits (22). The basic steps in activation of cAPK by cyclic AMP are binding to the regulatory (R) subunits, holoenzyme dissociation resulting in the freeing of the catalytic (C) subunit: for phosphorylative activity. These steps can be represented by the following equation:

$\pi R_2C_2 + 4$ cAMP (or analog) ————> $R_2{\bullet}(cAMP)_4 + 2C\pi$

where R_2C_2 is the catalytically inactive holoenzyme and R•cAMP represents regulatory subunits with occupied cyclic AMP binding sites. Two isotypes (I and II) of cAPK have been found which have identical C subunits, but differing R subunits, RI having a relative electrophoretic mobility (Mr) of approximately 48-50 kdal and RII an Mr of 52-56 kdal (16,22). The specificity of R subunits of cAPK as the cyclic AMP-receptor or cyclic AMP-binding proteins (16,22,23) was exploited in this experimental design. An isotopically labeled 8-azido analog of cyclic AMP ([^{32}P]8-N_3-cAMP) served as a high resolution, radioactive probe to identify soluble (cytoplasmic) and particulate (membrane-associated/organellar) R subunits among all the other cellular proteins that are present (14,26).

Tissue samples from the Cosmos flight 2044 were tested with respect to cellular compartmentalization and cyclic AMP-receptor activity of the R proteins. *The fundamental finding of this study is the apparent decrease of cAPK RII in an extract of a particulate subcellular fraction.* This is consistent with previous results that were obtained using tissues from rats flown on SL-3 and Cosmos 1887 (8,25).

MATERIALS AND METHODS

Cell Fractionation

Tissue collection and animal handling was carried out by the Soviet dissection team, headed by Dr. A.S. Kaplansky. Heart ventricle pieces from animals numbered 6-10, were provided for this study. Protocols were essentially as described previously (8,25). Animal handling was in compliance with World Health Organization guidelines and according to the principles stated in the Declaration of Helsinki of the Guiding Principles in the Care and Use of Animals. Animals were killed at timed intervals, the tissues removed and frozen at -80°C (storage and shipping were also at that temperature). In addition to the flight (F) and in-house, vivarium (V) control groups, there was a synchronous (S) a tail-suspended (T) control group of rats which were housed in identical cages, fed space flight diets and underwent the same vibration, impact, noise and conditions of ground transport as did the flight group of rats.

The strategy employed in sample preparation for cyclic AMP-receptor studies was somewhat modified from that used in similar experiments of Space Lab 3 and Cosmos 1887 missions. Tissue homogenates in addition to the subcellular fractions were azido-labeled and analysed for total cyclic AMP-binding analysis. Colour and number coding, with record keeping by two individuals, was maintained until the first numerical and electrophoretic results of azido labeling experiments became available. All subsequent analyses were carried out on samples labeled with group and animal numbers.

Heart (left ventricle) tissue pieces from individual animals were weighed and a 0.25 M sucrose, 0.05 M Tris, pH 7.5 buffer (STEM) containing 0.06 M EDTA, 0.005M $MgCl_2$, 0.001M benzamidine and phenylmethylsulfonyl fluoride (PSMF) was added to make a 15% (w/v) homogenate. Benzamidine and PMSF (μM) were included in subsequent buffers as well. The tissue pieces were disrupted using an Ultra-Turrax T25 (Jahnke and Kunkel Co.,

W. Germany) probe at the number 6 setting with two 30 second bursts. The homogenates were diluted 3 fold and strained through gauze to remove connective and unbroken tissue components. Unless otherwise stated, these and all subsequent operations using the tissue homogenates or subcellular fractions were carried out at 4°C.

The homogenates were centrifuged at 1x kG for 10 min and the supernatant solution was removed, centrifuged 20 min at 10 xkG and designated the soluble (S_1) fraction. The first (10 x kG) particulate fraction was suspended in one half the volume of the original homogenate in STEM buffer containing 0.40 M NaCl. The samples were mixed using a vortex mixer at the maximum setting, allowed to stand for 30 min, mixed again and centrifuged at 10 kG for 20 min. The supernatant fraction of this centrifugation, referred to as the particulate fraction extract, (S_2), was saved for analysis. A flow chart outlining the steps in obtaining the cell fractions is shown in Fig 1. Each of the fractions were divided into two aliquots - the first for immediate testing, and the second stored at -80°C for a repetition analysis. Protein content of the S_1 and S_2 fractions of individual samples in each group (5) was determined.

Photoaffinity Labeling

Photoaffinity labeling was carried out using a method modified from Hoyer et al. (14) as described by us previously (24). Briefly, duplicate aliquots of each S_1 and S_2 fraction containing 50-100 µg total protein for S1 and for S2 were used in each incubation. The cell fractions were then incubated with 5 µCi each, of [^{32}P]-8-azido cyclic AMP (8-N_3-cAMP) in a buffer with a final concentration of 0.25 M KCl, 0.002M Tris, pH 7.6 and 0.001M EDTA for 30 min at 4°C in the dark. To test for labeling specificity, duplicate incubations were carried out using 10^{-3} M cyclic AMP for cold competition. Photolysis was carried out using a UV lamp (Mineralite Co., San Gabriel, CA) at a wavelength of 250 nm for 5 min at a distance of 5 cm. The S_1 and S_2 cell fraction samples were then treated with activated charcoal, centrifuged and the supernatant diluted with water, shaken with G-25 Sephacryl and concentrated to 1/2 the original volume using Minicon concentrators (Amicon Corp., Danvers, MA). The chromatography steps were omitted when the whole homogenates were labeled. Aliquots were prepared for electrophoresis by adding sample buffer of 20% glycerol, 0.2% ß-mercapto ethanol and 0.1% bromphenol blue as an indicator dye and heating to 90 °C, for 5 min.

Total incorporation of the labeled analog was measured by taking duplicate aliquots of individual sample homogenates representing 0.1 mg of the original heart tissue and adding trichloroacetic acid to make a total concentration of 5% and allowing a precipitate to form overnight in the cold. The precipitates were collected, washed, solubilized, dialyzed and duplicate aliquots were counted using a liquid scintillation counter.

Electrophoresis and Autoradiography

Polyacrylamide gel electrophoresis (PAGE) in the presence of sodium dodecyl sulfate was carried out using a conventional size as well as a mini-gel apparatus (Hoeffer Instruments, San Francisco, CA). Standard procedures, described previously (18,23), were employed in the electrophoretic separations. The proteins were then transferred to nitrocellulose by electroblotting (31). The nitrocellulose membranes were stained with 0.1% Amido Black and 0.05% Coomassie blue dye to determine the protein banding patterns. Autoradiography was carried out by exposing either dried gels or electroblots to X-ray film (X-OMAT, Kodak/DuPont, Nutley, N.J.) to detect the radioactively labeled protein bands. Colored protein molecular weight markers (Rainbow Markers, Amersham Corp., Arlington Heights,

IL) were used to determine relative mobilities of standard proteins and to identify the radioactively labeled R subunits (rabbit skeletal muscle RI and beef heart RII, Sigma Co., St. Louis MO). The initial experiments were repeated using separate, stored aliquots of the homogenates and S_1 and S_2 cell fractions to ensure that the results were repeatable. Densitometric analyses of electrophoretic protein banding patterns, areas and peak heights of autoradiographic bands were carried out using a Hoeffer Densitometer, GS-300 and HSI software for data reduction adapted to the Macintosh. Statistical analyses were carried out using the t-test and analysis of variance in the STATWORKS program for tabulated data.

RESULTS

Protein Concentration and Banding Patterns

Electrophoretic separation under denaturing conditions was carried out in order to examine the protein banding patterns of the flight animal heart tissue and to compare them to those of simulation and control rat hearts. No significant differences could be established in protein banding patterns when each individual soluble and particulate fraction of flight animals were compared to the synchronus or control group. Representative banding patterns of the soluble, S_1 cell fraction samples for F and V animal groups is shown in Fig. 2.

Densitometric analyses revealed individual variations (from animal to animal) in protein bands in either S_1 or S_2, but no consistent differences among the flight animal tissues, the tissues of the rats from simulation experiments and the control group. Electrophoretic protein banding patterns also differ between the soluble and particulate cell fractions. Integration of a specified number of peaks resulted in comparable total areas within the normal range (not shown). Relative to each other, the individual peak heights nevertheless did vary from animal to animal. No consistent pattern, however, was seen that could be significantly correlated with the flight or with either of the control groups. Various parameters in respect to heart protein were calculated (Tables 1 and 3.) In themselves, the banding patterns of the soluble or particulate fractions of either the vivarium or synchronous controls were not different from those of the flight animals (not shown). This is consistent with our earlier observations (8,27).

It was expected that protein concentrations would be within a 10% error limit. Protein concentrations of the soluble fraction and of the extracted particulate fraction (S_1 and S_2 respectively) were determined by colorimetric measurements and by densitometric analysis integrating peak areas of the individual banding patterns, in order to check the consistency of the preparations. Table 1 shows that protein concentrations were essentially the same in the majority of samples (within experimental error). Additionally, no significant variation was found between groups (Table 1, see p values at the bottom), indicating that overall protein synthesis was unaffected by flight or simulation. Comparative densitometric banding pattern peak analysis carried out using both Cosmos 1887 and 2044 might yield information on sample data to focus into the region of RI and RII, but was beyond the scope of this study.

Cyclic AMP-Receptor Protein Activity

The binding of an isotopically labeled azido analog of cyclic AMP to its receptor protein (cAPK R subunits) was determined by photoaffinity labeling followed by electrophoretic separation of RI and RII and determination of their relative covalently-linked cyclic AMP analog. In order to compare the compartmental distribution between flight tissues and control, photoaffinity labeling with 8-N_3- cAMP of S_1 and S_2, soluble cell fractions and the particulate fraction extracts, respectively, was undertaken to determine the cellular distribution of cAPK R subunits.

Significant differences in photoaffinity labeling were consistently found in the S_2 or particulate fraction extracts: less azido cAMP is bound to flight than to control animal R subunits (Fig. 3A). Banding pattern analysis demonstrated first, that essentially equal amounts of total protein were reacted with the 8-azido analog and second, that the label matched the relative mobility of R subunits. Thus, while the banding pattern exhibits no difference between flight and control tissues, the autoradiogram shows a substantially reduced binding to RII in the F group, compared to the controls. Note also that both control and flight tissue samples show a faster moving autoradiographic label - presumably a proteolytic degradation product. Similar observations were previously made by us in studying cAMP-binding protein distribution in other tissues after chronic stimulation with isoproterenol (23).

No significant differences were found in 8-N_3 cAMP label of the soluble fractions (Fig. 3B). Label is incorporated in the S_1 fraction, mainly in RI, as has been demonstrated in other studies regarding the species and compartmental distribution of R subunits of cAPK in rat heart (2,27). Additionally, there is also no difference between the groups in terms of total binding of the cAMP analog in the S1 fraction (Table 2), or binding normalized to either rat body weight or adrenal gland weight (Tables 2, 4 and 5). The R subunit in the cytosol of the rat heart is predominantly from the type I isozyme, although in some preparations a small amount (<10% of RI) of azido-labeled RII bands were observed.

An autoradiogram of combined sample of S2 fractions consisting of all the individual sample aliquots in equal protein concentration are shown in Fig. 4. There is qualitatively visible reduction in the label of the F group, indicating that the decrease in S2 RII is still present when a combined sample or average effects are considered. The lane labeled C, was a sample of heart ventricle from a rat killed the previous day and the tissue frozen at -80^{o} overnight. This was included to demonstrate that storage and shipment of the tissue did not alter the overall R subunit azido labeling reactions. A decrease of a slower moving (presumably RII isoform) was seen in the C sample. A summary of RI and RII distribution is shown in Table 6.

Total Azido Labeling and Comparisons with Other Parameters

Total 8-N_3cAMP bound to proteins, shown in Tables 2-6, demonstrated the difference between cytoplasmic and particulate cell fraction R subunit content. Generally, the cytoplasmic fraction proteins were more extensively 2 to 4 fold) labeled than the particulate fraction proteins. The particulate cell fraction aliquots had a lower protein content, and greater variability of the counts was seen between individual aliquots. The results in Tables 2 and 4, show a significant difference between flight and control groups of the S2 fraction, whereas no differences between any of the groups were seen in any S1 measurements. A correlation with body weight also became evident between cyclic AMP-receptor binding of the S2 group and every treatment group when compared to the vivarium control (Table 4). An identical correlation was found when the same comparison was made to total heart proteins (Table 2). Interesting to note was the failure of any significant correlation with adrenal gland weights Table 5).

DISCUSSION

The hormonal milieu of tissues exerts a regulatory role and translates information of environmental influences as a biochemical signal to be processed on a molecular level, but the ultimate effects are expressed on the organismal level of organization. Such agonist-induced desensitization of the beta-adrenergic receptor-linked adenylate cyclase and the corresponding intracellular signal processing events have been extensively reviewed (7,9).

Many hormones act on responsive cells by activating second messenger pathways. Of these the cyclic AMP (and the calcium) pathways change cellular activity through specific protein kinases (20). By phosphorylating cytoplasmic and nuclear proteins, kinases generally coordinate cellular activity (16). Biosynthesis of specific proteins is known to be modulated in cardiac as well as in other cell types (13,21). Consequently, the relative cellular disposition of cyclic AMP-dependent protein kinase may be an index of such events in heart muscle. The results of this study appear to be related to these phenomena and should be further investigated from the molecular biology standpoint.

The basic signal processing of beta-adrenergic stimulation is by the adenylate cyclase system via cyclic AMP-mediated intracellular events. Indices of these events are measures of cyclic AMP-dependent protein kinase activity and distribution. While catalytic activity measurements are difficult in frozen tissues, the photoaffinity labeling of cAPK R subunits can be reliably carried out and used to determine relative amounts and cellular distribution of these proteins. This method of labeling cAPK R subunits using both a photoaffinity and an immunological probe was applied to heart muscle tissue of rats from the Cosmos 1887 flight.

Tissues from each individual animal were homogenized separately and were subsequently analyzed on an individual basis. This procedure was adopted so that subtle differences between experimental and control groups would not be missed by examining only a combined sample. Conversely, a single tissue piece with extreme variability may impart a disproportionately great effect. When individual samples were examined, extreme differences could be explained by some special condition in one animal, e.g. flight animal #10 showed an atypical protein banding pattern and a reduced protein concentration (Table 1, flight sample 5)

Rat heart ventricular tissue fractionation and R subunit labeling revealed a normal (compared to control) distribution of R subunits in the soluble, but a decrease in R subunit label in the particulate cell fractions. Interpretation of these data must necessarily be conservative. While photoaffinity labeling is more successful than attempting enzyme reactions in frozen tissues, this method has a relatively low efficiency, therefore, only those R subunits whose binding sites are unoccupied are labeled.

Although the electrophoretic and autoradiographic determination of R subunit presence and distribution may not represent all the binding sites, the flight particulate fraction contains markedly diminished or absent label in the cell fractions in animals from the Cosmos flight (Fig. 3A). The R subunits in the particulate fraction are mainly RII with some RI, and occasionally a faster moving fragment. These fragments are probably products of proteolysis. This might also explain the increase of total counts in the synchronous simulation samples indicating that more label per total protein may be present due to increased protein degradation, but not necessarily due to increased/decreased amounts of intact RII. Alternatively, a change in tissue levels of cyclic AMP may reduce site occupancy by the photoaffinity probe. Third, no precise controls are available to compare results between flights (e.g., SL-3 to Cosmos 1887). Variability in individual protein banding patterns, however, is sufficiently noticeable so that this information may be of future use. Data compiled from previous flights could be compared with those from subsequent ones. Nevertheless, changes in the heart muscle under space conditions are likely, and those seen in the experimental animals may be of value in understanding problems of the human heart.

ACKNOWLEDGEMENTS

Expert technical support by Mrs. Nancy Ciletti and Ms Khang M. Bui is gratefully acknowledged, as is the work of Ms. Pat Grabovac in managing the administrative logistics of this project.

REFERENCES

1. Axelrod, J. and T. Reisine. Stress Hormones: Their Interactions and Regulation. Science. 224:452-459, 1984.

2. Bhalla, R.C., R.C. Gupta and R.V. Sharoa. Distribution and Properties of cAMP-Dependent Protein Kinase Isozymes in the Myocardium of the Spontaneously Hypertensive rat. J. Mol. Cell Cardiol. 14:33-39, 1982.

3. Blomquist, G, J. H. Mitchell and B. Saltin. Effects of Bed Rest on the Transport System in Hypogravic and Hypodynamic Environments. (RH Murphy and M McCally, eds) NASA SP-269, Washington DC, 1969.

4. Bonder-Petersen, F., Y. Suzuki, T. Saduoto and N.J. Christensen. Cardiovascular Effects of Simulated Zero Gravity in Humans. Acta Astronautica. 10:657-661.5, 1983.

5. Bradford, M.M. A Rapid and Sensitive Method for Quantitation of Microgram Quantities of Protein Utilizing the Principle of Protein Dye Binding. Anal. Biochem. 72:248- 254, 1976.

6. Bungo, M.W. and P.C. Johnson. Cardiovascular Examination and Observations of Deconditioning During the Space Shuttle Orbital Flight Test Program. Aviat. Space Env Med 54:1001-1002, 1983.

7. Clark, R.B. Desensitization of Hormonal Stimuli coupled to Regulation of Cyclic AMP levels. Adv. Cyc. Nuc. Prot. Res. 20:151-200, 1986.

8. Cosmos 1887 Mission Description. Reports on U.S. Experiments Flown on the Soviet Biosatellite COSMOS 1887. J.P. Connolly, R.E. Grindeland and R.W. Ballard (eds), pp 1-50. NASA Technical Memorandum 102254, Moffett Field, CA, 1990.

9. Fan, T.H.M. and S.P. Benarjee. Age-related Reduction of Beta Adrenoceptor Sensitivity in Rat Heart Occurs by Multiple Mechanisms. Germatology. 31:373-380, 1985.

10. Grindeland, R.E, I. Popova and M.F. Vasques. Cosmos 1887 Mission Overview; Effects of Microgravity on Rat Body and Adrenal weights and Plasma Constituents. FASEB J., 1990.

11. Harden,T.K. Agonist Induced Desensitization of the ß-adrenergic Receptor-linked Adenylate Cyclase. Pharm. Revs. 35:5-30, 1983.

12. Heigler, S., T. Reisine, V.Y.H. Hook and J. Axelrod. Somatostatin Inhibits Multireceptor Stimulation of Cyclic AMP Formation and Corticotropin Secretions in Mouse Pituitary Cells. Proc. Natl. Acad. Sci. U.S.A. 79: 6502-6506, 1982.

13. Houge, G, O.K. Vintermyr and S.O. Doskeland. The Expression of cAMP-dependent Protein Kinase Subunits in Primary rat Hepatocyte Cultures. Cyclic AMP down-regulates its Own Effector System by Decreasing the Amount of Catalytic Subunit and Increasing the mRNA's for the Inhibitory (R) Subunits of cAMP-dependent Protein Kinase. Mol. Endocrinol. 4:481-488, 1990.

14. Hoyer, P., J. Owens and B.Haley. Use of Nucleotide Photoaffinity Probes to Elucidate, Molecular Mechanisms of Nucleotide-Regulated Phenomena. Ann. NY Acad. Sci. 346:280-301, 1980.

15. Karapu, V.Y. and A.I. Ferents. Effects of Hypokinesia and Physical Loading on Cardiac Myocyte Ultrastructure. Arkhiv Anatomia,GistologiiI Embyologii NASA TM-76179, 28-37.17, 1979.

16. Keely, S.L., J.D. Corbin and C.R. Park, Regulation of Adenosine 3',5'-monophosphate-dependent protein kinase. J. Biol. Chem. 250:4832-4840, 1975.

17. Kvetnansky, R. and R.A. Tigranayan. Epinephrine and Norepinephrine Concentrations in Rat Cardiac Ventricles and Atria after Flight Abroad Cosmos-1120 Biosatellite. Kosnicheskaya Biologiya I Aviakosmicheskaya Meditsina 16:(4)87-89, 1982.

18. Laemmli, U.K. Cleavage of Structural Proteins During the Assembly of the Head of Bacteriophage T4. Nature. 227:680-685, 1970.

19. Lefkowitz, R.J., M.R. Wessels and Stadel, J. Hormones, Receptors and Cyclic AMP. Their Role in Target Cell Refractoriness. Cell. Reg. 17:205-230, 1980.

20. Lefkowitz, R.J. and M.G. Caron. The Adrenergic Receptors. Adv. in Second Messgner and Phosphorylation Res. 24:1-8, 1990.

21. Lindeman, J.P. and A.M. Watanabe. Phosphorylation of Phospholamban in Intact Myocardium. Role of Ca^{+}-calmodulin-dependent mechanisms. J. Biol. Chem. 260:4516-4525, 1985 .

22. Lohmann, S.M. and U.Walter. Regulation of the Cellular and Subcellular Concentrations and Distribution of Cyclic Nucleotide-dependent Protein Kinases. Adv Cyc Nuc. Prot. Phos. Res. 18:63-117, 1984.

23. Mednieks, M. I, and A. R. Hand. Cyclic AMP-dependent Protein Kinase in Stimulated Rat Parotid Gland Cells: Compartmental Shifts After in vitro Treatment with Isoproterenol. Eur. J. Cell Biol. 28:264-271, 1982.

24. Mednieks, M.I., and A. R. Hand. Nuclear cAMP-dependent Protein Kinase in Rat Parotid Acinar Cells. Exp. Cell. Res. 149:45-55, 1983.

25. Mednieks, M.I., and A.R. Hand. Salivary Gland Ultrastructure and Cyclic AMP-dependent Protein Kinase Reactions in Space Lab-3 rats. Am J Physiol (Reg Int Comp Physiol. 21) 252:R233-239, 1987.

26. Mednieks, M.I., R.A. Jungmann and A.R.Hand. Immunogold Localization of the type II Regulatory Subunit of Cyclic AMP-dependent Protein Kinase. Monoclonal Antibody Characterization and RII Distribution in Rat Parotid Cells. J. Histochem. Cytochem. 37:339-346, 1989.

27. Mednieks, M.I., A.S.Fine , J. Oyama and D.E. Philpott. Cardiac Muscle Ultrastructure and Cyclic AMP Reactions to Altered Gravity Conditions. Am. J. Physiol. (Reg. Int. Comp. Physiol.: 21) 252:R227-232, 1987.

28. Musacchia, X.J, D.R. Deavers, G.A. Meninger and T.P. Davis. A Model for Hypokinesia: Effects on Muscle Atrophy in the Rat. J. Appl. Physiol. Respirat. Environ. Physiol. 48:479-486, 1980.

29. Popovic, V. Antiorthostatic Hypokinesia and Circulation in the Rat. The Physiologist. 24:15-16, 1981.

30. Sandler, H. Cardiovascular Responses to Weightlessness and Prolonged Bed Rest. In: A Critical Review of the U.S. and International Research on Effect of Bed Rest on Major Body Systems. (Nicogossian AE and Lewis CS, eds). Washington DC, NASA, 3-80, 1982.

31. Towbin, H, T. Stahelin and J. Gordon. Electrophoretic Transfer of Proteins from Polyacrylamide Gels to Nitrocellulose Sheets: Procedure and Some Application. Proc. Natl. Acad. Sci. USA 76:4350-4354, 1979.

TABLE 1

S1 Heart protein [HP] ug/ml

	Vivarium	Flight	Synchronous	Tail suspension
6	21.5	31.0	30.0	28.0
7	29.0	19.0	37.0	36.5
8	19.0	38.0	34.0	36.0
9	31.0	37.0	42.5	47.5
10	52.0	34.0	38.0	52.5
mean	30.5	31.8	36.3	40.1
s.e.	5.8	3.4	2.1	4.4

S2 Heart protein [HP] ug/ml

	Vivarium	Flight	Synchronous	Tail suspension
6	5.75	4.50	5.40	2.80
7	5.10	3.40	5.22	3.80
8	3.48	4.85	3.70	4.95
9	4.45	3.60	3.82	3.62
10	3.98	5.12	3.42	4.20
mean	4.55	4.29	4.31	3.87
s.e.	.40	.34	.41	.35

T-test

versus	Flight	Synchronous	Tail suspension
Vivarium	NS	NS	NS
Flight	-	NS	NS
Synchronous	-	-	NS

NS=not significant (for S1 and S2 values)

TABLE 2

S1 cAMP binding [cA] cpm/ug [HP]

	Vivarium	Flight	Synchronous	Tail suspension
6	31060.0	34170.3	34647.3	57867.7
7	12992.4	47193.7	20656.8	22659.1
8	37621.4	20165.8	36968.8	37142.2
9	31189.4	16579.4	17252.6	17799.4
10	20781.3	20470.9	36636.3	20573.1
mean	26728.9	27716.0	29232.4	31208.3
s.e.	4366.7	5720.8	4248.8	7456.3

S2 cAMP binding [cA] cpm/ug [HP]

	Vivarium	Flight	Synchronous	Tail suspension
6	8636.4	14415.6	9514.5	16979.9
7	12278.1	17681.9	20410.4	18285.0
8	13723.3	22333.8	24246.4	14055.6
9	4103.0	19358.7	21999.5	20047.8
10	17610.4	13562.2	20037.9	26022.8
mean	11270.2	17470.4	19241.7	19078.2
s.e.	2297.1	1610.4	2542.4	1992.8

T-test

versus	Flight		Synchronous		Tail suspension	
	S1	S2	S1	S2	S1	S2
Vivarium	NS	<.06	NS	<.05	NS	<.05
Flight	-	-	NS	NS	NS	NS
Synchronous	-	-	-	-	NS	NS

NS=not significant

TABLE 3

S1 [HP]/g body weight (bw)

	Vivarium	Flight	Synchronous	Tail suspension
6	.0597	.0934	.0845	.0798
7	.0794	.0569	.1028	.1000
8	.0528	.1111	.1133	.1150
9	.0861	.1095	.1417	.1475
10	.1405	.0994	.1206	.1522
mean	.0840	.0940	.1130	.1190
s.e.	.0150	.0100	.0090	.0140

S2 [HP]/g body weight (bw)

	Vivarium	Flight	Synchronous	Tail suspension
6	.0160	.0136	.0152	.0080
7	.0140	.0102	.0145	.0104
8	.0097	.0142	.0123	.0158
9	0110	.0106	.0127	.0112
10	.0120	.0150	.0108	.0122
mean	.0130	.0130	.0130	.0120
s.e.	.0010	.0010	.0010	.0010

T-test

versus	Flight	Synchronous	Tail suspnsion
Vivarium	NS	NS	NS
Flight	-	NS	NS
Synchronous	-	-	NS

NS=not significant (for S1 and S2 values)

TABLE 4

S1 cAMP binding [cA]/g body weight (bw)

	Vivarium	Flight	Synchronous	Tail suspension
6	86.28	102.31	97.60	164.86
7	35.60	141.30	57.38	62.08
8	104.50	58.96	123.23	118.66
9	86.64	49.05	57.51	55.28
10	56.16	59.86	116.30	59.63
mean	73.84	82.30	90.40	92.10
s.e.	12.32	17.37	14.09	21.58

S2 cAMP binding [cA]/g body weight (bw)

	Vivarium	Flight	Synchronous	Tail suspension
6	23.99	43.42	26.80	56.92
7	33.64	52.94	56.70	50.09
8	38.12	65.30	80.82	44.91
9	11.40	57.27	73.33	93.32
10	47.60	39.66	63.62	75.43
mean	30.95	51.72	60.25	64.13
s.e.	6.19	4.64	9.32	8.94

T-test

versus	Flight		Synchronous		Tail suspension	
	S1	S2	S1	S2	S1	S2
Vivarium	NS	<.05	NS	<.05	NS	<.05
Flight	-	-	NS	NS	NS	NS
Synchronous	-	-	-	-	NS	NS

NS=not significant

TABLE 5

S1 cAMP binding [cA]/mg adrenal weight (aw)

	Vivarium	Flight	Synchronous	Tail suspension
6	730.82	813.58	769.94	1042.66
7	328.92	1048.75	409.04	467.20
8	874.92	485.92	739.38	781.94
9	751.56	352.75	304.68	355.99
10	466.99	470.59	796.44	388.17
mean	630.64	634.32	603.50	607.19
s.e.	100.54	128.84	102.88	132.45

S2 cAMP binding [cA]/mg adrenal weight (aw)

	Vivarium	Flight	Synchronous	Tail suspension
6	203.20	343.23	211.43	305.94
7	310.84	392.93	404.17	377.01
8	319.15	538.16	484.93	295.91
9	98.87	411.89	385.96	400.96
10	395.74	311.77	435.61	490.99
mean	265.56	399.66	384.42	374.16
s.e.	51.74	38.91	46.39	35.46

T-test

versus	Flight	Synchronous	Tail suspnsion
Vivarium	NS	NS	NS
Flight	-	NS	NS
Synchronous	-	-	NS

NS=not significant (for S1 and S2 values)

TABLE 6

Distribution of cAPK R subunits

S1 fraction

	Vivarium	Flight
mean	7659.8	6842.8
s.e.	698.2	1503.3

T-test p value not significant

S2 fraction

	Vivarium	Flight
mean	7761.8	4892.7
s.e.	914.2	845.3

T-test p value <0.04

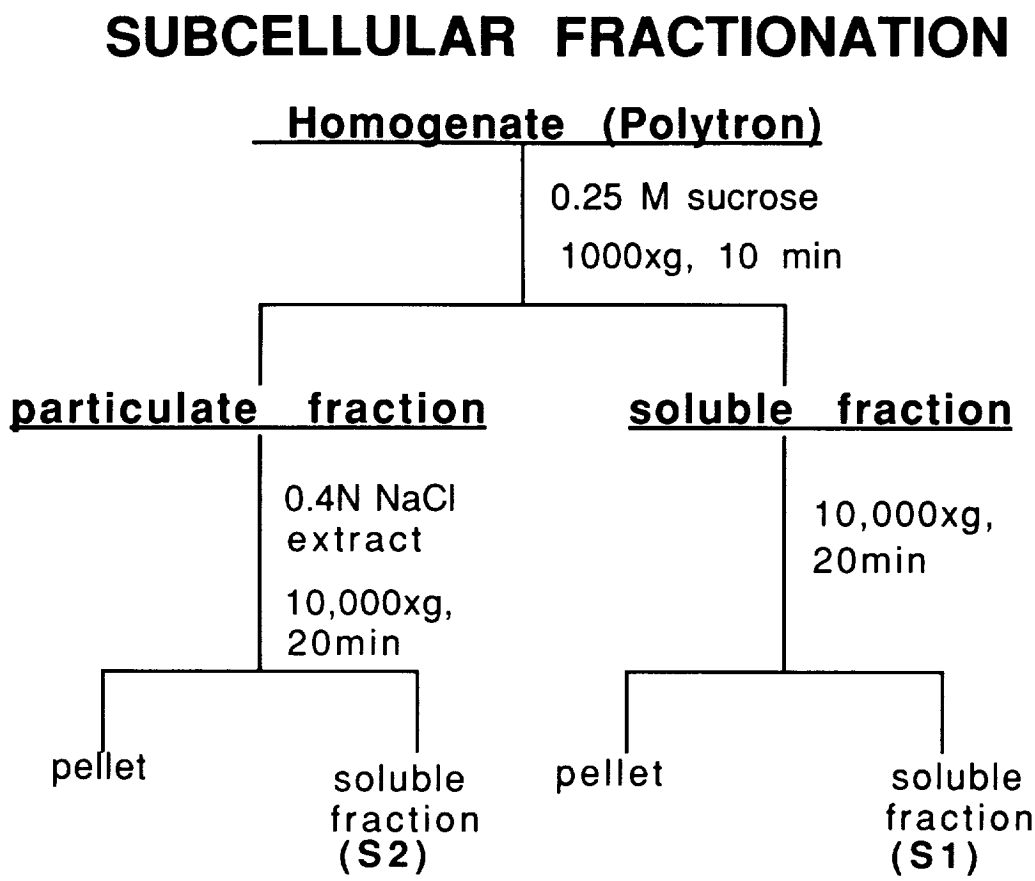

Figure 1. Flow chart showing the subcellular fractionation steps of the homogenate for obtaining the soluble and particulate fraction extracts which were used for the photoaffinity experiments.

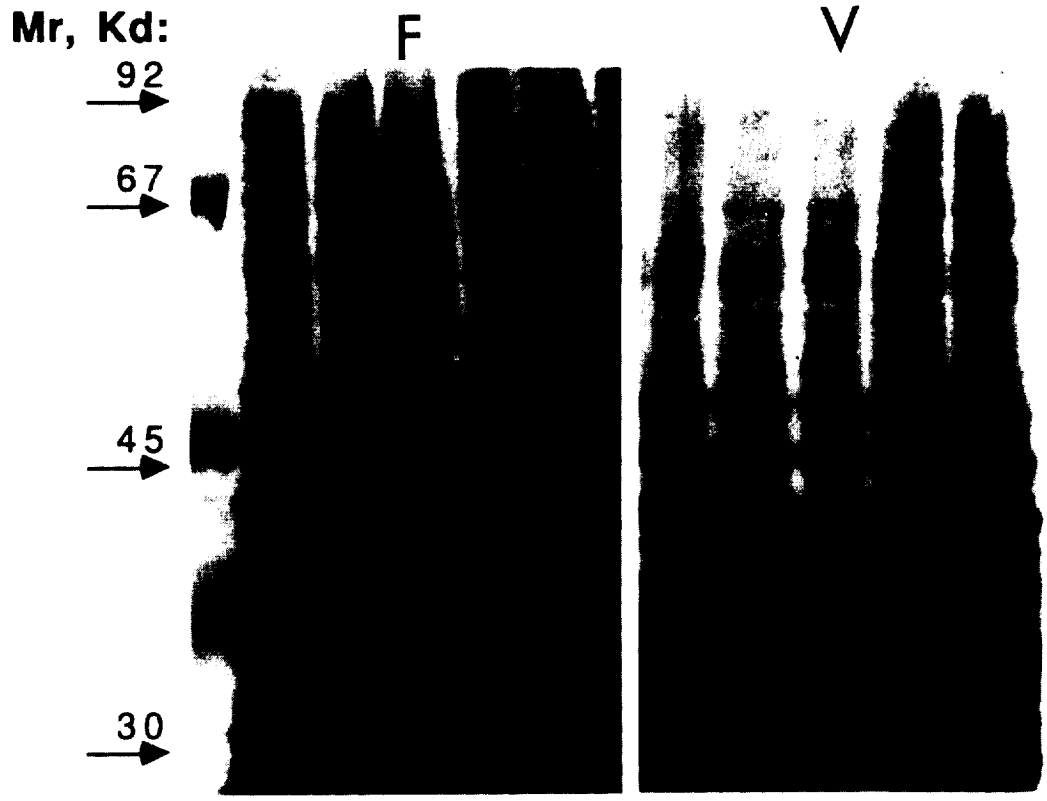

Figure 2. Electrophoretic banding patterns of the SI fraction of the flight (F) and control (V) group of samples. Equivalent protein concentrations were loaded in each lane, left to right corresponding to samples 6-10 in each group. The first lane preceding the V group contained protein standards having the indicated relative mobility (Mr) of protein sizes in kd.

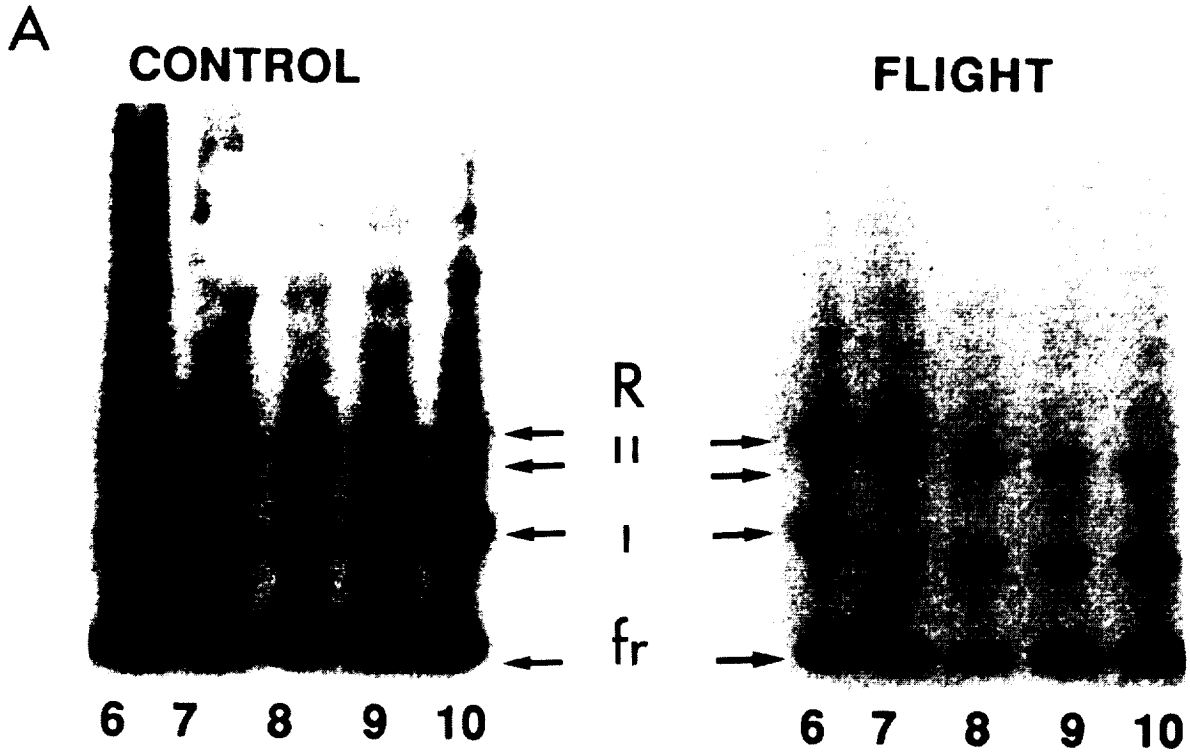

Figure 3(a). Autoradiography of (a), S2 cell fractions of flight (F) and ground control (V) group heart tissue samples. Photoaffinity labeled cell fraction aliquots were purified to remove unreacted 8-N_3-cAMP and proteolytic peptide fragments as described in Methods. The relative mobilities of RI and RII were identified by comparison with those of commercially available standard proteins. Rf refers to a probable degradation product of the relative mobility of 36 kd.

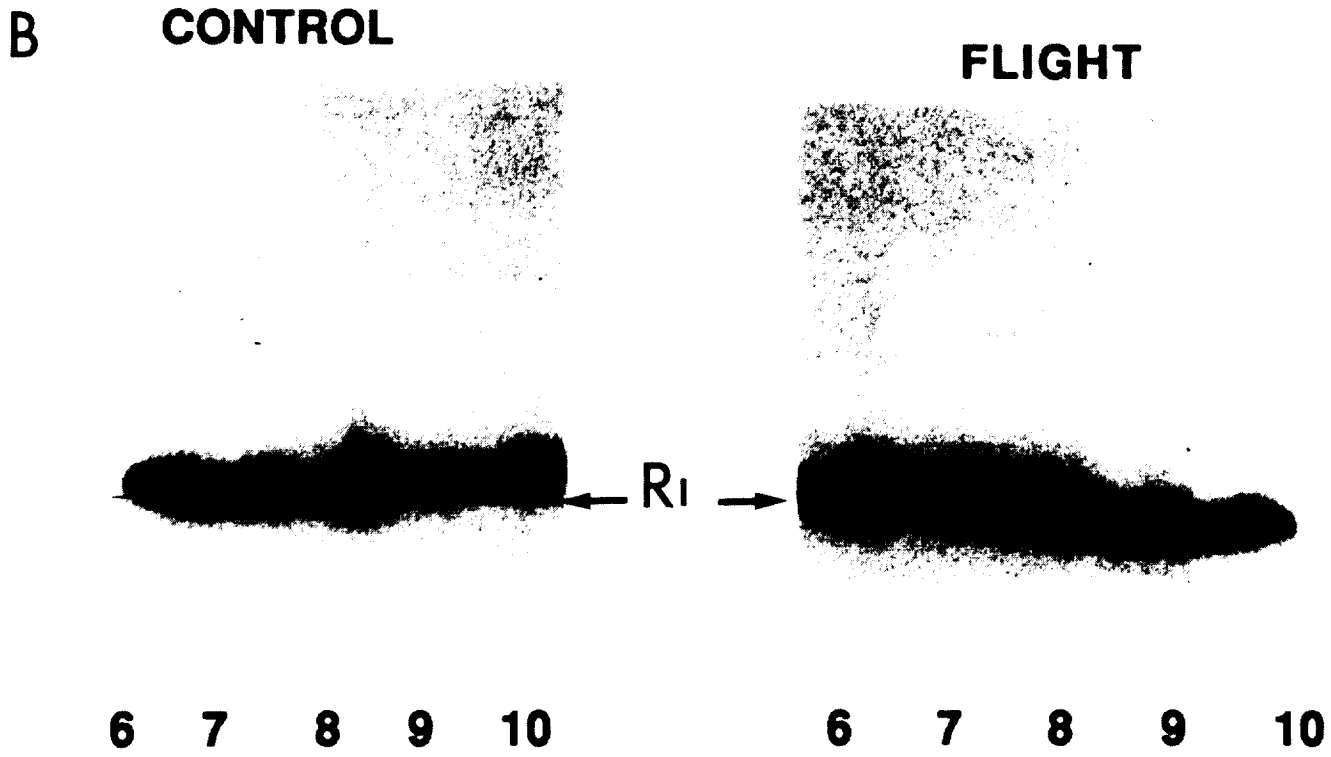

Figure 3(b). Autoradiography of (b), S1 cell fractions of flight (F) and ground control (V) group heart tissue samples. Photoaffinity labeled cell fraction aliquots were purified to remove unreacted 8-N_3-cAMP and proteolytic peptide fragments as described in Methods. The relative mobilities of RI and RII were identified by comparison with those of commercially available standard proteins. Rf refers to a probable degradation product of the relative mobility of 36 kd.

Figure 4. Autoradiography of cyclic AMP-receptor activity in the particulate cell fraction of samples from the vivarium (V), synchronous (S), tail-suspended (T) and flight (F) groups when samples 6–10 were combined in equal amounts, azido labeled, purified as described in Methods, separated by electrophoresis and the R subunits visualized by autoradiography. Group designations are on top of the lanes, R subunit relative mobilities on the left ordinate. The lane labeledC is a sample from an animal whose heart tissue was taken on the previous day.

EXPERIMENT K-7-13

PART IV: ALTERED MYOSIN EXPRESSION IN RAT VENTRICULAR MUSCLE DURING EXPOSURE TO MICROGRAVITY

D.B. Thomason, V. Organov, E. Ilyina-Kakueva, F.W. Booth, and K.M. Baldwin

INTRODUCTION

Microgravity, as a consequence of spaceflight, is known to produce cardiovascular deconditioning (Henry et al., 1974; Michel et al., 1974). This decrease in cardiovascular function is accompanied by a reduction in the number of cardiac microtubules, a disruption of the cardiac cytoskeletal pattern, and a decrease in cardiac contractility (Groza et al.,1983; Mednieks et al., 1987; Philpott et al., 1990). These changes may result, at least in part, from a regulation of cardiac muscle gene expression at the level of translation. Ground-based studies that simulate the absence of weightbearing locomotor activity have shown that protein synthesis rapidly decreases in the rat heart (Thomason et al., 1989). Furthermore, this rapid down-regulation of protein synthesis appears to result from the protein synthesis machinery (the polysomes) responding to an intracellular signal that slows nascent polypeptide chain elongation (unpublished data). However, little is known about the possible role of transcriptional regulation in the control of gene expression in the heart during spaceflight. The purpose of this study was to examine the potential role of transcriptional regulation of myosin expression during the 14 days of weightlessness experienced by the rats on the COSMOS 2044 mission.

MATERIALS AND METHODS

Frozen ventricular muscle samples from flight and synchronous control rats #6 through 10, collected as per mission description, were powdered in liquid nitrogen. Approximately 20 mg was reserved for myosin protein isoform analysis and the remainder used for RNA extraction and mRNA analysis, all as described elsewhere (Thomason et al., 1986; Thomason et al., 1989). Briefly, myosin protein isoforms were extracted in pyrophosphate buffer and electrophoresed on native polyacrylamide gels; the protein isoform profile was determined from these gels. Total RNA was extracted from the frozen, powdered muscle with the guanidinium isothiocyanate-cesium chloride method (Maniatis et al., 1982). Varying amounts of total RNA (3, 5, 7, 9 μg) from each sample were electrophoresed on an RNA denaturing gel, the gel dried, and probed with a [^{32}P]-labelled oligonucleotide probe specific for the ß-myosin heavy chain mRNA. The gel was washed under low-stringency conditions and exposed to X-ray film to develop an image. The film image was subsequently scanned densitometrically.

Statistical differences between the flight and control groups were determined by an analysis of covariance for ß-myosin heavy chain mRNA expression and covariance mapping of composite densitometric scans.

RESULTS AND DISCUSSION

No differences between the flight and control groups were observed in the myosin protein isoform profile of the cardiac muscle samples (results not shown). These data indicate that a myosin protein isoform shift, either as a result of changes in hemodynamic functional demand or hormonal status, is not readily apparent during short-term spaceflight.

ß-Myosin heavy chain mRNA expression also was not statistically different between the flight and synchronous control groups, though the flight group tended toward a greater level of expression (Figure 1). These data are consistent with the ground-based data from soleus muscle, where a decreased rate of myofibrillar protein synthesis is accompanied by a tendency toward greater levels

of expression of ß-myosin heavy chain mRNA (Thomason et al., 1989). These data may indicate a post-transcriptional stabilization of mRNA.

Despite the lack of a statistical difference in the amount of ß-myosin heavy chain mRNA expressed per unit of total RNA, there is a difference in the relationship between the amount of ß-myosin heavy chain expressed and other RNA species that partially co-react with the oligonucleotide probe (primarily the 18S and 28S rRNA). This relationship is best seen with covariance mapping of composite scans of the X-ray film image formed by the probe binding, as described in the following paragraphs.

The principle of covariance mapping is a general technique that establishes the likelihood of occurrence of two events separated by distance, time, frequency, intensity, or any other measurable quantity. The technique has been applied to areas as diverse as ion fragmentation analysis and angular diameter of stars (Frasinski et al., 1989). In this particular application we sought to determine the relationship between the ß-myosin heavy chain mRNA species and other RNA species that co-react with the oligonucleotide probe under low-stringency conditions. To obtain the data for the covariance map, full-length densitometric scans of the image formed on X-ray film by the probed gel were obtained for each sample. The data for each scan, actually 320 discrete optical density measurements equally spaced along the length of the gel, can be notationally represented as a data vector such as X_i or Y_i , where i ranges from 6 to 10 to represent animals #6 through #10; each data point in the vector can be represented as $X_i(x)$ or $Y_i(y)$. To calculate the covariance, C, for each point x in X versus each point y in Y, one performs the following calculation:

$$C(x,y) = \frac{1}{N}\sum_{i=6}^{10} X_i(x)\ Y_i(y) - \left[\frac{1}{N}\sum_{i=6}^{10} X_i(x)\right]\left[\frac{1}{N}\sum_{i=6}^{10} Y_i(y)\right]$$

In this case, N=5, as there are five sample data sets from each group (flight and control). The covariance matrix thus generated is a 320x320 array. In the case where X=Y, the covariance matrix is the autovariance. *The larger the value C(x,y), the greater correlation between the data points X(x) and Y(y).* This is shown graphically in Figures 2, 3,and 4. These figures are color coded such that areas of blue (and black) represent the least correlation and areas of red the greatest correlation.

Figure 2 is the autovariance map of the composite scans from the synchronous control heart RNA lanes. We have noted pertinent RNA species on the scans: myosin heavy chain mRNA (MHC), 28S rRNA, and 18S rRNA. There is a diagonal symmetry because of the identity of the two data sets (X=Y), and a strong correlation along the diagonal because features that appear in one set of scans also appear in the other set. Also, note the relatively strong correlation between the myosin heavy chain and the rRNA species, and among the rRNA species. These features are altered in the autovariance map of the scans from the flight heart RNA lanes (Figure 3). In this case there is a much stronger correlation between the myosin heavy chain mRNA and 28S rRNA species than in control hearts, and relatively little correlation with the 18S rRNA species. The differences between the flight and control animals are clearly seen in the covariance map of these two sets of data (Figure 4). Clearly, there are features of the RNA identified by the oligonucleotide probe that are present or absent in one data set and not the other.

Collectively, these data indicate that, on a relative basis, an analysis of the myosin protein isoform profile or the ß-myosin heavy chain mRNA content reveals no differences between flight and synchronous control hearts. In part this may be artifactual because, on a relative basis, many other species of contractile protein and RNA may also be changing in content. This is demonstrated by

the covariance mapping analysis of the RNA, where there are clearly features identified by the oligonucleotide probe that are different among the flight and control hearts. Therefore, the cardiovascular deconditioning that is observed as a result of long-term spaceflight may begin early during the exposure to microgravity as a change in transcriptional regulation of gene expression.

REFERENCES

1. Frasinski, L. J., K. Codling, P. A. Hatherly. Covariance Mapping: A Correlation Method Applied to Multiphoton Multiple Ionization. Science. 246:1029-1031.

2. Groza, P., R. Vrancianu, M. Lazar, R. M. Baevski, and V. L. Funtova. Systolic Time Intervals After a Seven-Day Orbital Flight. Physiologie. 20:45-52, 1983.

3. Henry, W. L., S. E. Epstein, J. M. Griffith, R. E. Goldstein, and D. R. Redwood. Effect of Prolonged Space Flight on Cardiac Function and Dimensions. In: The Proceedings of the Skylab Life Sciences Symposium. National Aeronautics and Space Administration, Houston, NASA TM X-58154. Vol II.974:711-722, 1974.

4. Maniatis, T., E. F. Fritsch, and J. Sambrook. Molecular Cloning (a Laboratory Manual). Cold Spring Harbor Laboratory, Cold Spring Harbor. 1982.

5. Mednieks, M. I., A. S. Fine, J. Oyama,and D. E. Philpott. Cardiac Muscle Ultrastructure and Cyclic AMP Reactions to Altered Gravity Conditions. Am. J. Physiol. 252:R227-R232, 1987.

6. Michel, E. L., J. A. Rummel, C. F. Sawin, M. C. Buderer, and J. D. Lem. Results of Skylab Medical Experiment M171 - Metabolic Activity. In: The Proceedings of the Skylab Life Sciences Symposium. National Aeronautics and Space Administration, Houston, NASA TM X-58154. Vol II:723-762, 1974.

7. Philpott, D. E., I. A. Popova, K. Kato, J. Stevenson, J. Miquel, and W. Sapp. Morphological and Biochemical Examination of Cosmos 1887 Rat Heart Tissue: Part I-Ultrastructure. FASEB J. 4:73-78, 1990.

8. Thomason, D. B., K. M. Baldwin, and R. E. Herrick. Myosin Isozyme Distribution in Rodent Hindlimb Skeletal Muscles. J. Appl. Physiol. 60:1923-1931, 1986.

9. Thomason, D. B., R. B. Biggs, and F. W. Booth. Protein Metabolism and ß-Myosin Heavy Chain mRNA in Unweighted Soleus Muscle. Am. J. Physiol. 257 (Regulatory Integrative Comp. Physiol. 26):R300-R305, 1989.

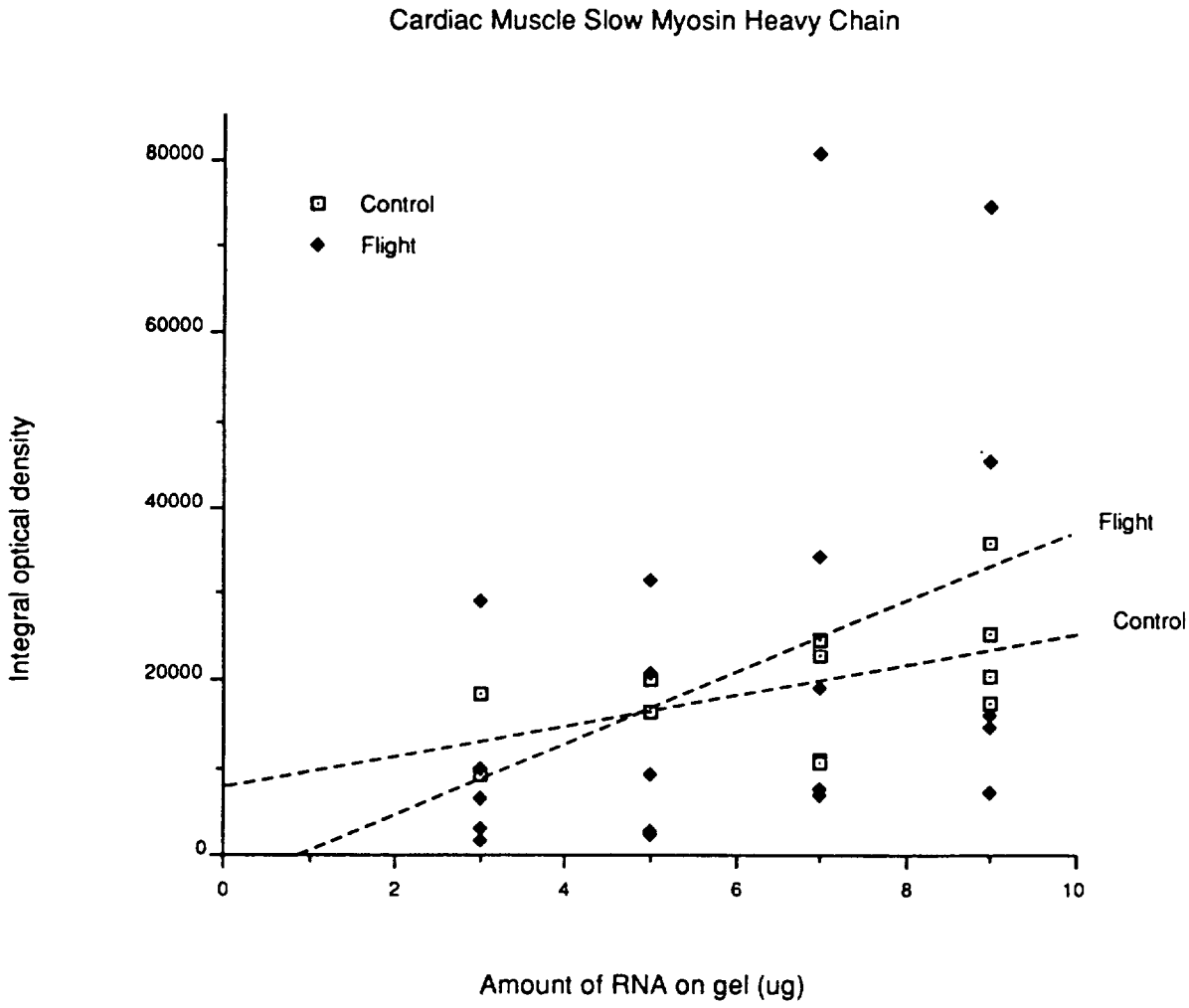

Figure 1. Analysis of covariance of the amount of [^{32}P]-labeled oligonucleotide probe bound to the ß-myosin heavy chain mRNA band in RNA denaturing gels reveals no statistical difference between the synchronous control and flight hearts. Different amounts of total RNA extracted from the hearts were electrophoresed on an RNA denaturing gel, the gel was dried, and hybridized with the probe. Following a low-stringency wash, X-ray film was exposed to the gel for 48 hours. The image formed was densitometrically scanned and the optical density integrated for the band corresponding to the myosin heavy chain mRNA.

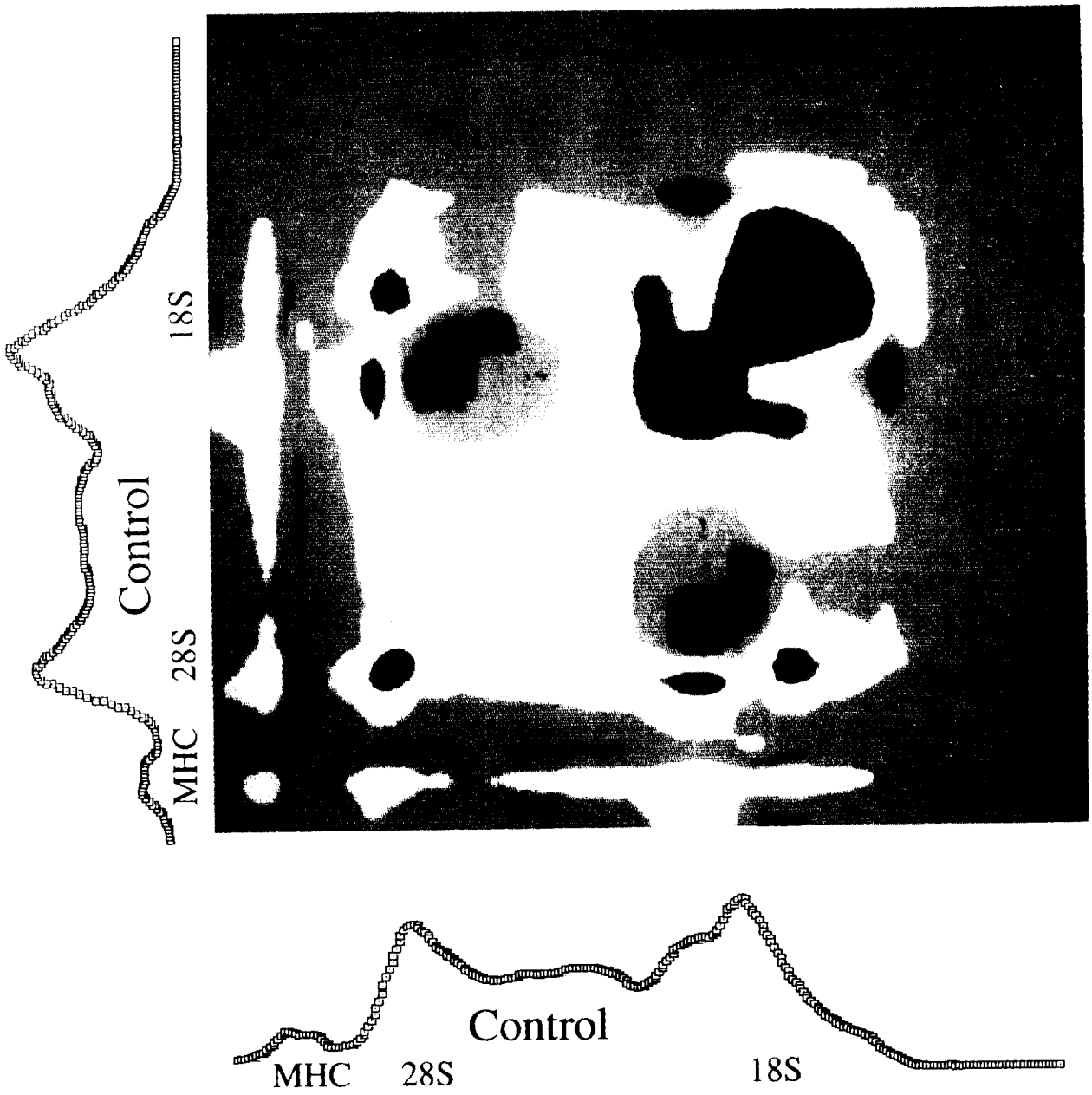

Figure 2. Covariance mapping of the scans for the synchronous control heart RNA. The low-stringency wash of the oligonucleotide probe from the RNA denaturing gel allowed for some cross-reactivity of the probe with other RNA species. Major features identified in the scans are ß-myosin heavy chain mRNA (MHC), 28S rRNA (28S), and 18S rRNA (18S). Features which show a strong correlation are designated in red, whereas features with little or no correlation are blue or black. See text for further explanation.

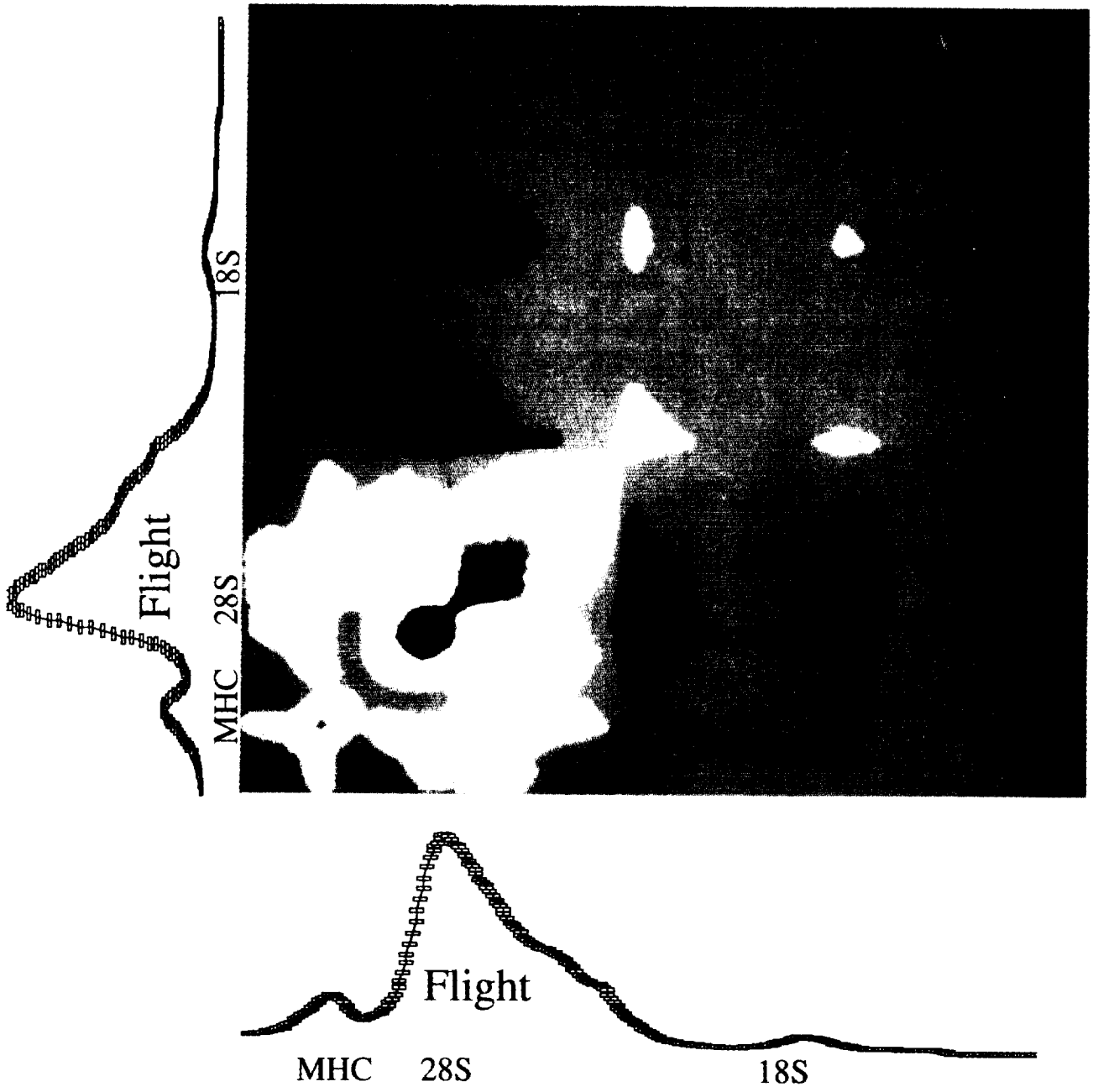

Figure 3. Covariance mapping of the scans for the flight heart RNA. The features of this map are marked according to the legend of figure 2.

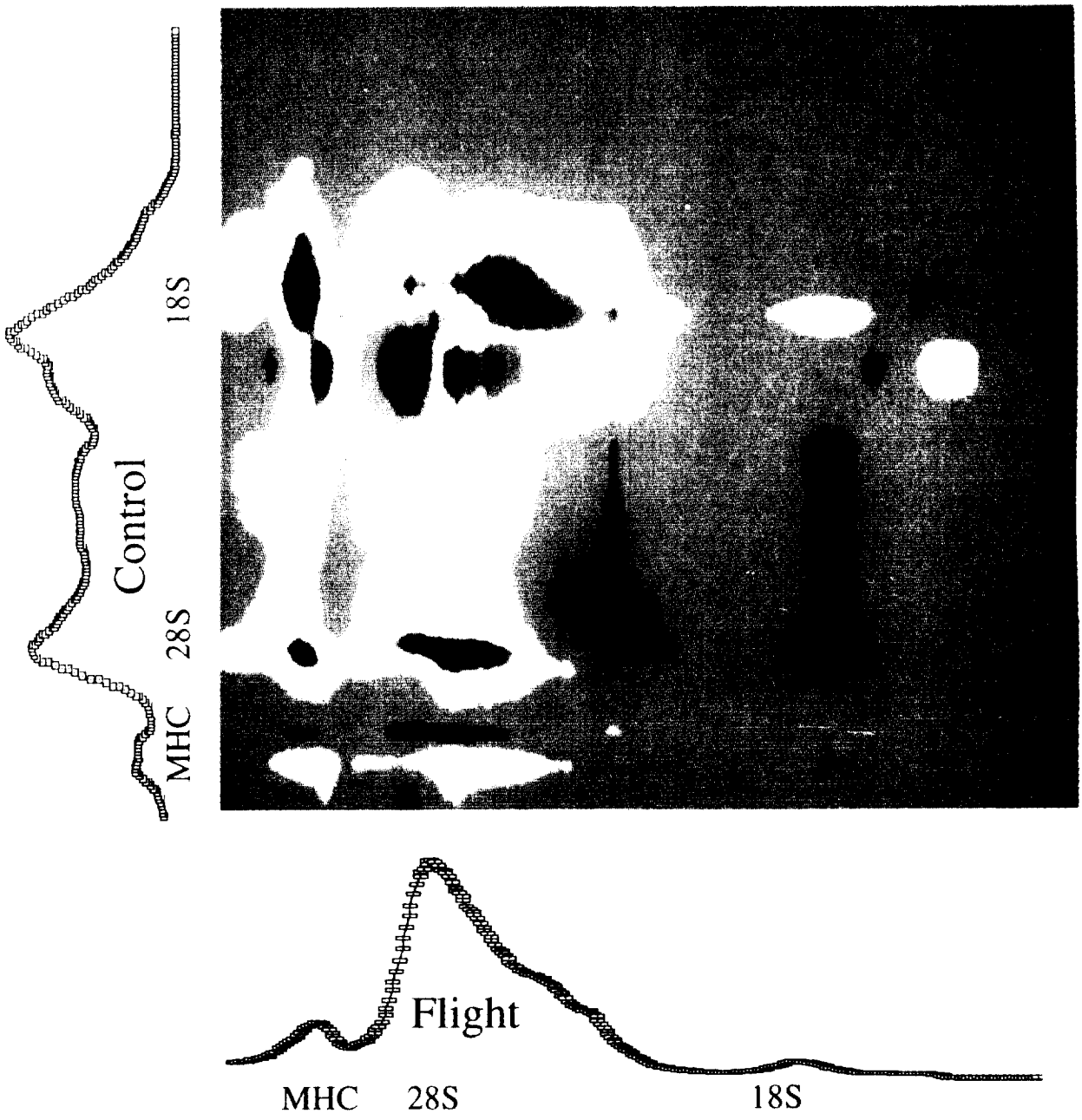

Figure 4. Covariance mapping of the scans for synchronous control versus flight heart RNA. As with the previous two figures, the strong areas of correlation that are indicated in red show that despite the lack of a statistical difference in the relative expression of ß-myosin heavy chain mRNA (figure 1), other species of RNA have changed in the flight hearts.

EXPERIMENT K-7-14

HEPATIC FUNCTION IN RATS AFTER SPACE FLIGHT

PART I: ANALYSES OF SELECTED PARAMETERS OF CARBOHYDRATE, AMINIOACID, LIPID, AND XENOBIOTIC METABOLISM IN LIVER AND SERUM

Principal Investigator:

A. Merrill
Department of Biochemistry
Rollins Research Center
Emory University School of Medicine
Atlanta, Georgia

Co-Investigators:

J. Hargrove
Department of Nutrition
University of Georgia
Athens, Georgia

R. Mullins
E. Wang
R. LaRoque
E.T. Morgon
H.L. Bonkovsky
Department of Biochemistry, Pathology,
Pharmacology, and Medicine
Emory University School of Medicine
Atlanta, Georgia

I.A. Popova
Institute of Biomedical Problems
USSR Ministry of Health
Moscow, USSR

PART II: HEPATIC FUNCTION AFTER SPACE FLIGHT

Co-Investigators:

S.M. Cormier
R.N. Racine
Department of Biology
University of Louisville
Louisville,Kentucky

I.A. Popova
Institute of Biomedical Problems
USSR Ministry of Health
Moscow, USSR

460

PART I: ANALYSES OF SELECTED PARAMETERS OF CARBOHYDRATE, AMINO ACID, LIPID, AND XENOBIOTIC METABOLISM IN LIVER AND SERUM, FROM RATS FLOWN ON COSMOS 2044

A. H. Merrill, Jr., I.A. Popova, E. Wang, R, E. Mullins, R. LaRoque, J. L. Hargrove, E.T. Morgan, and H.L. Bonkovsky

SUMMARY

Liver and plasma samples from rats flown aboard Cosmos 2044 were analyzed for hepatic protein, glycogen and lipids as well as the activities of a number of key enzymes involved in metabolism of these compounds and xenobiotics. The major differences between the flight group versus the synchronous control were elevations in: microsomal protein, liver glycogen content, tyrosine aminotransferase, and tryptophan oxygenase; and, reductions in sphingolipids and the rate-limiting enzyme of heme biosynthesis, delta-aminolevulinic acid synthase. These results support the hypothesis that spaceflight alters liver function; however, the results with samples from Cosmos 2044 differed notably from those from Spacelab 3 (Merrill, et al., J. Physiol. 252:R222-R226, 1987) and Cosmos 1887 (Merrill, et al., FASEB J. 4:95-100, 1990), presumably due to the conditions of spaceflight and/or the post-flight recovery period for Cosmos 2044.

INTRODUCTION

Animals returning from spaceflight typically exhibit multiple changes in blood and tissue biochemistry. While these have been investigated most extensively in muscle and bone, early studies of rats flown on Cosmos biosatellites suggested that liver function is also altered (1-6). This has been supported by subsequent analyses of liver samples from rats flown aboard Spacelab 3 (7) and Cosmos 1887 (8). Overall, it appears that there are significant changes in hepatic protein, glycogen, lipids, and some of the key hepatic enzymes of the metabolic pathways for these compounds during spaceflight and/or the post-flight recovery period (1-8).

For the most recent flights, another vital function of liver--the metabolism of various hormones, drugs, and xenobiotics--has been examined by measuring components of the mixed function oxidase system that utilizes cytochrome P_{450} as the terminal electron acceptor. For rats flown aboard Spacelab 3 (7), the amounts of cytochrome P_{450} were significantly lower than for the controls, and livers from rats on Cosmos 1887 (8) exhibited decreases in the amount of microsomal cytochrome P_{450} and the activities of aniline hydroxylase and ethylmorphine N-demethylase, two cytochrome P_{450}-dependent enzymes. These findings suggests that xenobiotic metabolism is altered by spaceflight.

Since liver is basically a central "clearing house" for the metabolism of most nutrients, drugs, and other foreign compounds (plant toxins, pesticides, and other substances generally referred to as xenobiotics), further study of the effects of spaceflight on this organ appeared warranted with samples from Cosmos 2044. Described in this report are additional data from analyses of liver and serum samples from rats flown on Cosmos 2044. They generally support the hypothesis hepatic metabolism is affected by spaceflight and/or the post-flight period; however, differences in the results obtained with these samples and those from the preceding flights may indicate that some of the biochemical changes occur during the post-flight recovery period.

462

MATERIALS AND METHODS (EXPERIMENTAL PROCEDURES)

Experimental Animals

The conditions of the spaceflight and the handling of the animals have been presented in the overall project descriptions. As soon as possible after the rats were killed, the livers were removed, immediately frozen, and stored at -80°.

Tissue Preparation

The liver samples were thawed, homogenized, and centrifuged following fairly standard protocols to yield a microsomal fraction and a high-speed (cytosolic) fraction as described previously (7,8). We have found this procedure to recover microsomes in approximately 78% yield with little contamination with markers of other subfractions (9). Aliquots of the original homogenate, microsomes, and cytosol were stored at -80° until assayed. Individual aliquots were used for each assay to minimize losses of activity during freezing and thawing.

Analytical Methods

Total protein was assayed using a modification of the method of Lowry (10) with bovine serum albumin as the standard. Liver glycogen was quantitated using the method of Johnson and Fusaro (11) and rabbit liver glycogen (Sigma Type III) as the standard. DNA was quantitated by the method of Fiszer-Szafarz et al. (12) using calf thymus DNA as the standard. Lipids were extracted as described before (7) using essentially the method of Bligh and Dyer (13) and analyzed for triglycerides and cholesterol using the COBAS Analyzer. Phospholipids were quantitated by assaying the amount of organic-solvent soluble phosphate, and the total sphingolipids were estimated by analysis of the sphingosine content after acid hydrolysis (14). Free sphingosine was quantitated by high-performance liquid chromatography (15).

Most of the enzyme assays were conducted as described previously (7). HMG-CoA reductase was assayed as described by Shapiro et al. (16) as modified (7,8). Serine palmitoyltransferase was assayed using [^{3}H]serine (9,17). Cytochrome P_{450} was measured spectrophotometrically (18), and by standard assays of testosterone metabolism and by immunochemistry (19-22). Tyrosine aminotransferase (23), tryptophan oxygenase (24), and alanine aminotransferase (25) were assayed as described. Other enzymes were analyzed by a COBAS Bio-centrifugal Analyzer. The serum analyses were also conducted using the COBAS Analyzer calibrated with certified clinical standards.

RESULTS

General Effects of Spaceflight on Liver

There were virtually no differences between the body weights and liver weights of the flight and synchronous rats (see Table 1). This was confirmed by similar DNA values and amounts of total and cytosolic liver protein. There were, however, small differences in the amount of microsomal protein, as well as differences between these groups and the vivarium and tail suspension controls. As has been seen before, the major difference was in the level of hepatic glycogen, which is higher for the flight group than for the synchronous control and the vivarium and tail suspended animals (Table 1). This study also noted a slight reduction in hepatic sphingolipids.

Liver enzymes of rats after spaceflight

Most of the enzymes assayed were identical in the flight and synchronous groups, although there were some differences from the vivarium or tail suspended groups (Table 1).

Cytochrome P_{450} was assayed by both mass amount and by diagnostic assays. All failed to detect significant differences, in contrast to the lower levels previously observed in the flight group (7,8). To further test the absence of differences in cytochrome P_{450}, two isozymes were examined by Western blot analyses and these, too, were not significantly different. All together, these findings indicate that under the conditions of Cosmos 2044 there were no apparent alterations in cytochrome P_{450} and related activities.

HMG-CoA reductase was also surprisingly constant among the groups, even though this enzyme has previously been seen to be over 2-fold higher for the flight rats versus both vivarium and synchronous controls (8). This correlated with the lack of a difference in hepatic cholesterol, although serum cholesterol was slightly higher for the flight group (Table 2). Serine palmitoyltransferase was not lower for the flight group even though there was a slight reduction in liver sphingolipids.

The significant differences between the flight group and synchronous controls ($p<0.05$) occurred with tyrosine aminotransferase and tryptophan oxidase, both of which were elevated. These data suggest that the animals from this Cosmos flight were exposed to a short-term stressor that elevated the activity of TAT, but not alanine aminotransferase. The other major difference was in the activity of delta-aminolevulinate synthase, which was significantly lower in the flight group. This would imply that heme synthesis was reduced in the flight group, although limiting heme would have been expected to affect the level of cytochrome P_{450}.

Effects of Spaceflight on Serum Components

As another index of the overall biochemical status of these animals, a standard profile of serum components was obtained (TABLE 2). Serum glucose was elevated, in agreement with the high hepatic glycogen. In addition, the levels of BUN, creatinine, AST/GOT, and lactate dehydrogenase were elevated in the flight group--suggestive of a catabolic state (perhaps due to muscle and/or liver trauma). There were very slight decreases in calcium, and these were probably real since serum phosphate was elevated significantly. The flight animals were somewhat hypercholesterolemic, although this was not also seen as elevated triacylglycerols.

DISCUSSION

The results obtained from these analyses that were most consistent with previous spaceflights were the high glycogen content of liver in the flight group (with high blood glucose), the fact that these animals were hypercholesterolemic, and the elevation in various blood parameters (BUN, creatinine, etc.) that are indicative of muscle or liver trauma in the flight animals. Elevated hepatic glycogen remains one of the most reproducible derangements of spaceflight, and has persisted despite different regimes of feeding and fasting as well as short (hours) to long (several days in Cosmos 1887) delays in the removal of the liver post-spaceflight (1-8). The glycogen deposition is visible biochemically and histochemically (see the related morphological studies), and represents a fundamental alteration of regulation at the level of substrate availability and/or the control of key enzymes or transporters.

It warrants mention that one of the new findings of this study--that is, that delta-aminolevulinate synthase is reduced in flight animals--may be related to the elevated glucose and glycogen. It has long been known that glucose can suppress the activity of this enzyme when added to cells in culture. If de novo heme synthesis is reduced for an extended period of time, one can speculate that there would be a reduction in cytochrome P_{450}, as has been seen in earlier flights (7,8), since cytochrome P_{450} accounts for a major portion of the heme synthesized in liver. Thus, we would like to present the working hypothesis that one of the earliest biochemical changes in liver during spaceflight (or the post-flight recovery period) is an alteration in glucose homeostasis and that this

results in other metabolic changes, such as an altered heme synthesis and, ultimately, reductions in various heme-dependent systems represented by cytochrome P_{450}.

We conclude that rats undergoing spaceflight and post-flight recovery have significant alterations in liver function but that the magnitude of the differences may be affected by the time after landing. Because the liver functions to regulate the supply, distribution, and deposition of numerous compounds that are either required by other organs or that can be toxic to them, these findings imply that long-term adaptation to weightlessness and/or the post-flight recovery process could be complicated by impaired hepatic function. This idea should continue to be evaluated in future work.

ACKNOWLEDGEMENTS

The authors are grateful to Dr. A. S. Kaplansky and the Soviet dissection team for preparation of these samples, and thank Richard E. Grindeland and Marilyn Vasques for help during these studies. This work was supported by the National Aeronautics and Space Administration.

REFERENCES

1. Abraham, S., C.Y. Lin, H.P. Klein, C. Volkmann, R.A. Tigranyan, and E.G. Vetrova. Studies of Specific Hepatic Enzymes Involved in the Conversion of Carbohydrates to Lipids in Rats Exposed to Prolonged Spaceflight Aboard Cosmos 1129. Physiologist. 23(6)Suppl.:S55-S58, 1980.

2. Abraham, S., C.Y. Lin, C. Volkmann, and H.P. Klein. Biochemical Changes in Rat Liver After 18.5 days of Spaceflight. Proc. Soc. Exp. Biol. Med. 172:334-339, 1983.

3. Ahlers, I., E. Misurova, M. Praslicka, and R.A. Tigranyan. Biochemical Changes in Rats Flown on Board the Cosmos 690 Biosatellite. Life Sci. Space Res. 14:185-188, 1976.

4. Arlotto, M. P. and A. Parkinson. Identification of Cytochrome P-450a (P450IIA1) as the Principal Testosterone 7-Alpha-Hydroxylase in Rat Liver Microsomes and Its Regulation by Thyroid Hormones. Arch. Biochem. Biophys. 270:458-471, 1989.

5. Belitskaya, R. A. Carbohydrate and Lipid Content of Rat Liver Tissue Following a 22-Day Spaceflight. Space Biol. Aerospace Med. 4:97-99, 1977.

6. Bensadoun, A. and D. Weinstein. Assay of Proteins in the Presence of Interfering Materials. Anal. Biochem. 70:241-250, 1976.

7. Bligh, E. A. and W.J. Dyer. A Rapid Method of Total Lipid Extraction and Purification. Can. J. Biochem. 37:911-917, 1959.

8. Civen, M. and W.E. Knox. The Independence of Hydrocortisone and Tryptophan Induction of Tryptophan Pyrrolase. J. Biol. Chem. 234:1787-1792, 1959.

9. Fiszer-Szafarz, B., D. Szafarz,and A.G. De Murillo. A General, Fast, and Sensitive Micromethod for DNA Determination: Application to Rat and Mouse Liver, Rat Hepatoma, Human Leukocytes, Chicken Fibroblasts, and Yeast Cells. Anal. Biochem. 110:165-170, 1981.

10. Gaver, R. and C.C. Sweeley. Methods for Methanolysis of Sphingolipids and Direct Determination of Long-Chain Bases by Gas Chromatography. J. Am. Oil Chem. Soc. 42:294-298, 1965.

11. Granner, D. K., G.M. Tomkins. Tyrosine Aminotransferase (Rat Liver). Methods Enzymol. 17B:633-637, 1970.

12. Johnson, J. A. and R.M. Fusaro. Use of Purified Amyloglucosidase for the Specific Determination of Total Carbohydrate Content of Rat Liver Homogenate in a Single Step. Anal. Biochem. 98:47-52, 1979.

13. Koop, D. R., C. L. Laethem, and D. J. Tierney. The Utility of P-Nitrophenol Hydroxylation in P-450IIE1 Analysis. Drug Metab. Rev. 20:541-551, 1989.

14. Merrill, A. H., Jr., E. Wang, D.P. Jones, and J.L. Hargrove. Hepatic Function in Rats After Spaceflight: Effects on Lipids, Glycogen, and Enzymes. Amer. J. Physiol. 252:R222-R226, 1987.

15. Merrill, A. H., Jr., M. Hoel, E. Wang, R.E. Mullins, J.L. Hargrove, D.P. Jones, and I.A. Popova. Altered Carbohydrate, Lipid, and Xenobiotic Metabolism by Liver from Rats Flown on Cosmos 1887. FASEB J. 4:95-100, 1990.

16. Merrill, A. H., Jr., E. Wang, R.E. Mullins, W.C.L. Jamison, S. Nimkar, and D.C. Liotta. Quantitation of Free Sphingosine in Liver by High-Performance Liquid Chromatography. Anal. Biochem. 171:373-381.

17. Merrill, A. H., Jr., D.W. Nixon, and R.D. Williams. Activities of Serine Palmitoyltransferase (3-Ketosphinganine Synthase) in Microsom. 1985.

18. Morgan, E. T., RC. MacGeoch and J.A. Gustafsson. Sexual Differentiation of Cytochrome P-450 in Rat Liver. Evidence for a Constitutive Isozyme as the Male-specific 16 Alpha-Hydroxylase. Mol. Pharmacol. 27: 471-479 1985.

19. Nemeth, S., L. Macho, M. Palkovic, N. Skottova, and R. Tigranyan. Metabolic Changes in Rats Subjected to Spaceflight for 18.5 Days in the Biosatellite Cosmos 936. Adv. Space Res. 1:219-224, 1981.

20. Omura, T., R. Sato. The Carbon Monoxide Binding Pigment of Liver Microsomes. I. Evidence for its hemoprotein Nature. J. Biol. Chem. 239: 2370-2378; 1964

21. Shapiro, D. J., J.L. Nordstrom, J.J. Mitschelen, V.W. Rodwell, and R.T. Schimke. Microassay for 3-Hydroxy-3-Methylglutaryl-CoA Reductase in Rat Liver and in L-Cell Fibroblasts. Biochim. Biophys. Acta. 370 369-377, 1974.

22. Segan, H. and T. Matsuzwa. Meth. Enzymol. 17A:153-159, 1967.

23. Waxman, D. J., J. J. Morrissey, and G. A. LeBlanc. Hypophysectomy Differentially Alters P-450 Protein Levels and Enzyme Activities in Rat Liver: Pituitary Control of Hepatic NADPH-Cytochrome P-450 Reductase. Mol. Pharmacol. 35:519-525, 1989.

24. Williams, R. D., E. Wang, and A.H. Merrill, Jr. Enzymology of Long-Chain Base Synthesis by Liver: Characterization of Serine Palmitoyltransferase in Rat Liver Microsomes. Arch. Biochem. Biophys. 228:282-291, 1984.

25. Yakovleva, V. I. About Dynamic Changes of the Lipid Content in the Rat Liver During Bioflight in "Cosmos-605" and "Cosmos-782". Arch. Anat. Histol. Embryol. 10:39-44, 1977.

TABLE 1

LIVER ANALYSES (Mean ± S. E.) N = 5

	Vivarium	Synchronous	Flight	Tail Suspension
Liver weight, g	363± 1.8	343 ± 6.3	337.6 ± 1.8	339.2 ± 8.5
Liver weight, g	10.11 ± 0.19	10.22 ± 0.44	9.98 ± 0.16	8.23 ± 0.25
Liver Components:				
Liver protein				
mg/g liver	226.2 ± 5.4	207.2 ± 2.9	195.6 ± 4.4	236.7 ± 3.2
g/liver	2.29 ± 0.08	2.12 ± 0.12	1.95 ± 0.06	1.95 ± 0.07
g/100 g BW	0.63 ± 0.02	0.62 ± 0.02	0.58 ± 0.03	0.57 ± 0.01
Microsomal protein				
mg/g	10.9 ± 0.70	8.1 ± 0.32	10.5 ± 0.29	9.5 ± 0.63
mg/ 100 g BW	30.4 ± 2.3	24.0 ± 0.8	30.9 ± 1.0	23.1 ± 1.4
Cytosolic protein, mg/g liver	115.2 ± 4.0	118.8 ± 5.0	106.2 ± 3.6	118.0 ± 4.5
DNA mg/g liver (not corrected for extraction)	1.10 ± 0.05	1.09 ± 0.03	1.01 ± 0.02	1.06 ± 0.02
Glycogen, mg/g liver	15.3 ± 2.0	23.0 ± 2.1	51.6 ± 4.4	<2.7 ± 1.0
Total phospholipids, µmol/g liver	30.4 ± 0.5	35.2 ± 0.4	30.2 ± 2.1	27.5 ± 0.3
Triglycerides, mg/g liver	15.85 ± 1.5	11.95 ± 0.7	12.57 ± 1.5	8.64 ± 1.2
Cholesterol, mg/g	1.66 ± 0.1	1.72 ± 0.05	1.50 ± 0.04	1.90 ± 0.08
Total sphingolipids, µmol/g liver	0.85 ± 0.03	0.70 ± 0.03	0.56 ± 0.03	1.05 ± 0.06
Free sphingosine, nmol/g liver	7.0 ± 0.21	5.9 ± 0.15	5.2 ± 0.13	7.56 ± 0.17
LIVER Enzymes				
HMG CoA reductose (U/mg)	4.23 ± 0.35	4.01 ± 0.25	3.44 ± 0.30	4.15 ± 0.58
U/g liver	44.06 ± 4.16	32.31 ± 2.08	35.7 ± 2.95	40.2 ± 6.67
Serine Polmitoyltransferaaasse U/mg	28.0 ± 2.10	30.83 ± 3.16	29.20 ± 2.83	38.69 ± 4.86
U/g liver	301.3 ± 22.8	247.1 ± 22.8	303.3 ± 25.3	355.8 ± 24.4
Tyrosine Aminotransferase U/mg	5.2 ± 0.95	6.1 ± 0.9	9.1 ± 0.9	10.2 ± 1.2
Alonine Aminotransferase	1.44 ± 0.41	2.1 ± 0.21	1.4 ± 0.42	1.86 ± 0.42
Tyrosine Oxygenase (u/mg)	0.0129 ± 0.003	0.0096 ± 0.003	0.0182 ± 0.0058	0.0323 ± 0.011

TABLE 1 cont'd

	Vivarium	Synchronous	Flight	Tail Suspension
Delta-Aminolevulinate Synthase (n mol /mg / h)	0.144 ± 0.022	0.135 ± 0.18	0.052 ± 0.008	0.123 ± 0.008
Cytochrome p450 and p420				
n mol / mg	2.40 ± 0.07	2.51 ± 0.16	2.09 ± 0.12	2.58 ± 0.08
n mol / g liver	26.11 ± 1.94	20.48 ± 1.93	22.01 ± 1.78	24.80 ± 2.22
Cytochrome p450				
n mol / mg liver	0.87 ± 0.03	0.93 ± 0.05	0.91 ± 0.07	0.87 ± 0.09
n mol / g liver	9.48 ± 0.71	7.50 ± 0.52	9.54 ± 0.89	8.45 ± 1.07
Testosterone Hydroxylases, p mol / min / mg				
16 - Alpha	1880 ± 370	1980 ± 300	1770 ± 560	1090 ± 500
7 - Alpha	250 ± 40	230 ± 50	210 ± 40	280 ± 120
6 - Alpha	1200 ± 160	870 ± 260	1150 ± 310	1080 ± 400
2 - Alpha	1810 ± 360	1780 ± 290	1600 ± 430	1090 ± 540
17 - Oxidation	880 ± 120	870 ± 200	790 ± 200	510 ± 230
P - 450H Content (Western blot) % syn	114 ± 21	100 ± 13	92 ± 11	52 ± 12
P - 450j Content (Western blot) % sync	ND	100 ± 50	183 ± 45	228 ± 108
NADPH - Cytochrome C Reductase n mol cytc reduced /mg / min	114 ± 5	97 ± 16	99 ± 19	86 ± 14

TABLE 2

SERUM ANALYSES

		Basal	Vivarium	Synchronous	Flight	Tail Suspension
Cholesterol	(mg / dl)	60 ± 1.7	53.2 ± 2.7	78 ± 5.2	91.6 ± 2.6	61.6 ± 5.1
Triglycerides	(mg / dl)	-	58.9 ± 2.6	99.3 ± 10.9	83.8 ± 7.1	33.6 ± 1.6
Ca ++	(mg / dl)	10.7 ± 0.15	11.0 ± 0.97	11.2 ± 0.04	10.9 ± 0.15	10.7 ± 0.97
BUN	(mg / dl)	12.4 ± 0.88	14.4 ± 0.67	21.2 ± 1.07	34.8 ± 4.82	18.8 ± 1.21
Creatinine	(mg / dl)	0.64 ± 0.04	0.56 ± 0.04	0.64 ± 0.04	0.92 ± 0.12	0.44 ± 0.04
AST / GOT	(U / liter)	128.2 ± 21.6	143.2 ± 12.0	179.6 ± 7.0	287.6 ± 12.5	150.4 ± 6.2
Alkaline Phophatase	(U / liter)	674.8 ± 150.7	253.6 ± 23.8	196.4 ± 13.6	205.6 ± 10.6	114.4 ± 5.4
Lactate Dehydrogenase	(U / liter)	88.8 ± 118.3	7 05.2 ± 66.7	708.8 ± 46.9	889.2 ± 8.7	577 ± 5.0
Albumin	(g / dl)	2.88 ± 0.04	2.72 ± 0.04	3.08 ± 0.04	3.04 ± 0.13	2.68 ± 0.04
Total Protein	(g / dl)	6.48 ± 0.13	6.12 ± 0.13	6.84 ± 0.13	6.68 ± 0.22	5.84 ± 0.10
Phosphate	(mg / dl)	6.05 ± 0.32	7.24 ± 0.10	6.64 ± 0.26	8.24 ± 0.44	7.1 ± 0.44
Potassium	(meq / dl)	7.0 ± 0.19	7.12 ± 0.25	7.2 ± 0.15	7.72 ± 0.41	6.96 ± 0.27
Glucose	(mg / dl)	142.8 ± 5.4	133.6 ± 5.3	121.6 ± 1.19	188 ± 18.56	110.8 ± 3.65

EXPERIMENT K-7-14

PART II: HEPATIC FUNCTION IN RATS AFTER SPACE FLIGHT

S. M. Cormier, R. N. Racine, I. A. Popova

SUMMARY

Hepatic tissue from flight, synchronous, vivarium and tail suspended rats as examined by light microscopy and computer-assisted image analysis. Glycogen levels in flight rats were found to be significantly elevated over controls. Lipid was also higher, but not significantly different. Hepatocytes appeared to be larger in flight animals due to area attributed to glycogen. Sinusoids were less prominent in flight animals compared to controls. The Kupffer cell population appeared to be reduced per total area and may represent changes in immune function of the liver. Alterations in the storage of glycogen and number of Kupffer cells suggests an important effect of space flight on the function of the liver that may have important implications for long-term space flight.

INTRODUCTION

Research from previous space flights has shown marked differences in hepatic glycogen (Abraham et al., 1978, 1981; Hargrove and Jones, 1985; Kraft, 1990; Merrill, 1990) and lipid (Loginov et al., 1979) levels; however, the findings have been somewhat contradictory in some instances. Abraham et al. (1978, 1981) and Merrill et al. (1985) reported no significant change in total lipid measured gravimetrically; whereas, Loginov et al. (1979) reported an increase as observed microscopically. Merrill et al. (1990) reported that total phospholipids were significantly reduced in the livers of flight animals while triglycerides, cholesterol and total sphingolipids were the same as controls; serum cholesterol was significantly increased and serum triglycerides were elevated but not significantly. Glycogen levels have been reported to be 2-30 times higher in flight animals when measured biochemically (Abraham et al., 1978, 1981; Hargrove and Jones, 1985; Merrill et al., 1987, 1990), but Loginov et al (1979) reported no remarkable microscopic difference whereas Kraft (1990) concluded that the extensive vacuolization observed in flight livers was glycogenic in origin. There are several factors that could contribute to these discrepancies, including the method of measurement and differences in the flight protocols.

The accumulation and distribution of glycogen and lipid in the liver has been linked to a number of factors including biotransformation of xenobiotics, stress, diet, carcinogenesis, and hormonal effects (Hrudan, 1979; Cherrington and Vranic, 1986). Both weightlessness (Abraham et al., 1978) and stress (Abraham et al., 1981; Loginov et al., 1979) may play a role in altering liver metabolism in space. Of particular interest is a report in which flight animals that were centrifuged to simulate gravity did not show an increase in glycogen or enzymatic shifts that were seen in a synchronous flight group. This suggests that weightlessness and not stress was the key exogenous factor (Abraham et al., 1978). The effects of stress and subsequent alteration of circulating hormones may still be important, especially during take-off and recovery (Abraham et al., 1981; Loginov et al., 1979).

In addition to weightlessness, changes in detoxification mechanisms are suspect since a report from Spacelab 3 indicated a 50% decrease in the overall level of cytochrome P-450 (Hargrove and Jones, 1985) and a reduction was again seen after Cosmos 1887 (Merrill et al., 1990). Some factors that could alter detoxification processes include cell death or elevated or depressed enzyme synthesis. The occurrence of cell death can be identified directly or inferred from reparative characteristics such as reduced nuclear: cytoplasmic ratios and a higher mitotic index. Evidence to

date based on labeling with tritiated nucleotides does not seem to indicate an increase in hepatocyte DNA synthesis and therefore replacement of lost cells (Loginov et al., 1979). Kraft (1990) reported that no mitoses were observed in any liver sections. Alternatively, reduced levels of detoxifying enzyme systems including mixed function oxidases might be due to reduced m-RNA or protein synthesis (Tyson and Green, 1987).

Hepatic toxicity and fluid redistribution can also cause the loss or reduction of certain cell types such the immunologically competent Kupffer cells, swelling of sinusoids or the Space of Disse, and accumulation of material in bile ducts or within the extracellular space (Tanikawa, 1979). Experiments using the suspended rat model have shown that the macrophage population in spleen is reduced (G. Sonnenfeld, pers. communication). However, it is not known if the Kupffer cell population, fixed macrophages in the liver, is reduced in the suspended rat or following extended space flight. It would be valuable to know if there is a depression or loss of Kupffer cells of the liver since this would further compromise the immune system.

Lipid and glycogen can be conveniently measured morphometrically (Weibel, 1979) in semi-thin sections and then compared with other morphological alterations that may suggest possible causes of shifts in storage products. Since dietary effects were held relatively constant, alterations in lipid or glycogen storage due to space flight may indicate important metabolic alterations in liver function associated with weightlessness, detoxification, stress, or endocrine function. Our study uses morphometric techniques to examine glycogen and lipid levels in flight animals and compare these finding to ground controls and the tail suspended rat. The latter model simulates many of the effects of weightlessness (Thomason and Booth, 1990).

MATERIALS AND METHODS

Five male rats of Czechoslovakia-Wistar origin were used in each group (flight (F), synchronous (S), vivarium (V), tail suspension (T)). They weighed between 300 and 400 g and were 109-131 days old at sacrifice. The F animals were flown for almost 14 days and maintained on a cycle of 16 h of light and 8 h of dark. They were fed a paste diet of 55 g/day and given water *ad libitum.* The F and S groups received their food four times daily while the V and T groups received the entire amount once each day. More specific details of the flight, housing, feeding, recovery and tissue harvest are described elsewhere in these technical reports (Grindeland et al, this issue).

At necropsy, the caudate lobe of each liver was removed and cut into small pieces. Approximately 2/3 of the pieces were immersed in cold (4°C) fixative consisting of 3% glutaraldehyde in 0.1M phosphate buffer at pH 7.4 and the remaining pieces were placed in cold (4°C) Rossman's fixative (picric acid, methanol, formalin). The tissues were kept at 4°C until brought to Moscow. About 36 hours after harvest, the tissues fixed in glutaraldehyde were washed two times (one hour each) in 0.1M cacodylate buffer with 5mM calcium chloride (pH 7.4). The flight samples were accidently washed in 0.1M pipes buffer (pH 7.4). After washing, the samples were cut into smaller pieces and treated with osmium tetroxide (1%) in cacodylate buffer for two hours. The samples were washed two times (15 min each) in cacodylate buffer and then stored in the buffer at 4°C. The samples in Rossman's fixative were washed two times (1 hour each) in absolute ethanol, cut into smaller pieces and stored in 95% ethanol at 4°C. The samples were then shipped to Louisville, Kentucky for further processing.

For plastic sections (Epon), the fixed tissues were rinsed in a 95% ethanol two times for 15 minutes each followed by four rinses in anhydrous, methanol-free, ethanol for thirty minutes each for a total of two hours. The tissues were briefly rinsed in acetone, placed in a 1:1 acetone-resin mixture, and allowed to infiltrate with resin overnight in a desiccator at room temperature. The mixture was removed and pure resin with catalyst added for three, two-hour periods while being rotated. Following the infiltration the tissue was positioned in BEEM capsules and cured at 70° C for 48 hours. Semi-thin (1.0μm) plastic sections were stained for glycogen with Periodic acid-

Schiff reagent (PAS) according to the method of Ferey et al. (1986). Another section from the same rat was stained with toluidine blue and analyzed for lipid (Cormier et al., 1989).

For paraffin sections, the tissues were dehydrated through a graded series of ethanols to xylene and embedded in paraffin. Paraffin sections (5 μm) were stained with either PAS to assess glycogen or with hematoxylin and eosin (H & E) to assess general tissue architecture.

Twenty-five areas were enumerated for each specimen and the average percent area calculated (Richmond et al., 1988). The area for each compartment (lipid, glycogen, nucleus, fluid-filled space) was measured using standard morphometric techniques with area in the measured field as equivalent to volume (Weibel, 1979). We report the results of the area analyses. Analyses were performed using a Zeiss-IBAS 2000 image analysis system equipped with a microscope with a monochrometer.

For glycogen analysis, one slide was read for each rat at a wavelength of 586 nm using a reference area of 0.06297 mm^2. For lipid, slides were read at 454 nm using a reference area of 9842 μm^2.. When possible slides of two tissue samples were read because the osmium fixation of the tissues was extremely poor--only the extreme outer edge was properly fixed. Since it was not possible to read two slides for each rat and the quality was so variable, the slide with the highest fat count was used in the analysis.

Kupffer cells, hepatocyte nuclei and fluid-filled spaces were measured at 575 nm from 5 μm paraffin sections stained with hematoxylin and eosin. The reference area for these analyses was 9842 μm^2. Hepatocyte nuclear area and calculation of diameter were measured only for round profiles in the plane of focus. The nuclei of Kupffer cells and polymorphonucleocytes were excluded from this analysis. The fluid-filled areas of the liver were measured based on grey levels and included sinusoidal spaces and the Space of Disse. It also included some space that resulted from the extraction of glycogen during processing so that those samples with the most glycogen will be overestimated. The mean total area of a hepatocyte was calculated by subtracting the total fluid filled space from the reference area and dividing by the number of hepatocyte nuclei in the reference area. The cytoplasm of a hepatocyte (i.e., parenchymal component) was estimated by subtracting the hepatocyte nuclear area from the total hepatocyte area. Because the flight group had the most glycogen, their cytoplasm is probably underestimated.

Kupffer cells were estimated independently along with polymorphonucleocytes which could not be separately identified. Kupffer cells were discriminated by a denser grey level and elliptical form.

Differences for each compartment were statistically evaluated with one-way ANOVA using the STATGRAPHICS computer program (STSC, Inc., Rockville, MD).

Since measurements of glycogen were made on sections that were 5μm thick using transmitted light, the measured area is biased to a higher level than if the surface alone were measured. Lipid was measured using 1μm thick sections and therefore is less biased but not a perfect measure of area. The analysis tends to decrease the difference between groups while overestimating the area. These factors must be considered when comparing lipid and glycogen that are determined biochemically (e.g., Merrill et al., this issue). Lipid values presented here are from lipid depots forming droplets and do not account for free lipid or lipid associated with membranes.

RESULTS

Hepatic tissue from all the groups embedded in paraffin and stained with hematoxylin and eosin were similar in appearance, having lobules of hepatocytes arranged in cords (Fig. 1). Hepatocytes were cuboidal in shape with a central nucleus having both heterochromatin and euchromatin. The hepatic cytoplasm in the F group was vacuolated due to the removal of glycogen. The T group had

very evenly stained hepatocytes due to the absence of glycogen. Hepatocytes from the T group were also smaller than the other groups. Sinusoids of all groups were lined with endothelial cells and Kupffer cells. The diameter of sinusoids and the Space of Disse varied from sample to sample, but the T group appeared to have more dilated sinusoids and the F group the least dilated. (Fig. 2). The visual observation is in direct opposition to the findings by image analysis. The T group also had evidence of edema near hepatic venules and other small vessels.

No differences were seen in the ductular system. The number of Kupffer cells did not appear to vary greatly among treatment groups, but F seemed to have less and T seemed to have more. An extensive evaluation of the tissues could find no evidence of mitoses in any of the groups. So, no mitotic index could be computed.

Paraffin embedded tissue stained with PAS showed marked differences between the four groups. The S and V controls had similar patterns of glycogen deposition (Fig. 3). PAS positive staining granules were concentrated near the central vein. Hepatocytes near the hepatic artery, vein and hepatic ducts and at the margins of the lobules had less glycogen. The S group had more PAS positive granules than the V group. PAS positive material was heavily deposited in the hepatocytes of the F group (Fig. 4). The distribution of glycogen appeared more uniform, but this may have been due to the extensive deposition of material. In striking contrast, the T group was almost devoid of glycogen (Fig. 5). Rather than clumps, as in other groups, only individual glycogen granules could be discerned. Again the pattern of deposition was highest near the central vein and became scanty near the margins of the lobule.

Epoxy resin embedded hepatic tissue stained with toluidine blue and PAS confirmed the findings of the paraffin embedded material. However, the quality of the osmification of these samples was poor. The osmium tetroxide did not diffuse more than 30μm into the S, V, and T groups. However, the quality of the F group was better preserved with osmium reaching the center of many samples. Toluidine blue-stained samples revealed the presence of lipid deposits within the hepatocytes. No pattern of deposition was observed; however, the F group appeared to have more lipid than the other three groups.

Morphometric examination clearly showed the marked increase in the amount of glycogen in the flight animals compared to the controls (Table 1). The S control had more glycogen than the V control and almost no glycogen could be found in the tail-suspended animals. Th ANOVA was highly significant ($F = 18.88$, $df = 3, 16$, $P<0.0001$) but *a posteriori* multiple range tests (Tukey HSD) could only distinguish the F rats from the other three groups. S, V, and T rats were considered similar despite the apparent differences (Fig. 6). The small sample sizes and large variation made it difficult to detect differences between groups. There were no significant differences for lipid (Table 2) but the ANOVA ($F = 2.781$, $df = 3,15$, $P > 0.07$) indicates that with a larger sample size the differences might have been significant. As with the glycogen, $F > S > V > T$ (Fig. 7).

Although F and S rats were fed similarly, F consumption was 45g/day and S consumption was 54g/day (no consumption data were provided for V and T). In addition, the F group was the heaviest at time of loading but at time of sacrifice was the lightest (Table 3). The V rats were the only group significantly heavier than all the others. The liver weights for F rats were also less than S and V, but the T rats were the only group significantly lighter than the others. All weight data were provided by R. Grindeland (pers. communication). Data from Cosmos 1887 are also included for comparison.

The morphometric analysis of cell architecture also revealed differences between F rats and controls (Tables 4 and 5). The nuclear diameters were significantly larger ($F = 10.631$, $df = 3,16$, $P = 0.0004$) as was the nuclear area ($F = 10.244$, $df = 3,16$, $P = 0.0005$) (Fig. 8.). The number of nuclei was also significantly different ($F = 4.591$, $df = 3,16$, $F = 0.0168$) but post hoc tests

could only distinguish F rats from T rats. The total hepatocyte area was not found significant by ANOVA ($F = 3.148$, $df = 3,16$, $P = 0.0541$) however, the post hoc test did distinguish F rats from T rats. Since the total hepatocyte contains the nucleus and the glycogen, two parameters significantly larger in F rats, we subtracted these values to determine the cytoplasmic (i.e., parenchymal) area (Table 5). As can be seen in Fig. 9, the F and S rats are now almost identical and no differences were found to be significant ($P > 0.4$).

An analysis was also performed to determine the number of Kupffer cells in the fluid-filled sinusoidal spaces between hepatocytes (Table 6). An ANOVA was not quite significant ($F = 2.833$, $df = 3, 16$, $P = 0.0714$) but the trend clearly shows that T rats had the most and F rats the least (Fig. 10). Further transformation of the data showed that all groups had about the same number of Kupffer cells per hepatocyte but the F rats had the least number per unit of fluid-filled space and V rats had the most. Although the latter data look dramatically different, the ANOVA was not ($P = 0.2521$).

DISCUSSION

The results of the Cosmos 2044 liver studies generally confirm the findings of the Cosmos 1887 study (Kraft, 1990). Glycogen was extremely elevated in the Flight rats compared to controls. Lipid was detected in our study but no significant differences were found among groups. No evidence of mitotic activity was found in either study.

In contrast with Cosmos 1887, the liver weights of F rats were less than controls. Body weight gain was similar for S rats for the two missions (11.9% vs. 11.7%) while weight gain for the F rats was much less for Cosmos 2044 (3.1% vs. 5.2%). Food consumption also differed between the two flights. The F and S rats in Cosmos 1887 both ate about 50g/day while in Cosmos 2044, the F rats only ate 45g/day and the S rats ate 54g/day. Interestingly, the actual liver weights were almost identical for the two missions although Cosmos 1887 was more variable. The results of Cosmos 2044 sheds doubt on Kraft's (1990) explanation of the increased liver size in Cosmos 1887 F rats. Kraft had attributed the increased size to the parenchymal component rather than the increased nuclear and vacuolated area. The Cosmos 2044 F rats had an increase in glycogen and total hepatocyte size but not an increased liver weight. The parenchymal size was almost the same for F and S rats (Fig. 9). It would seem that the increased weight of livers in the 1887 flight may be due to increased glycogen, rather than other cellular organelles or cytoplasm.

The mean nuclear diameters were also smaller for all groups in Cosmos 2044 compared to Cosmos 1887 and no differences were found among the 1887 groups. The method of measurement may account for these differences. Kraft measured perimeters to compute diameters while we measured areas to compute our diameters. The area measurement has less error associated with it for deviations from a perfect circle.

Mandel et al. (1990) have shown immune suppression in flight and suspended rats. The liver also has a very active immune and detoxification function. Kupffer cells lining the sinusoid were reduced from controls in F rats from the Cosmos 2044; whereas the T group was elevated. These differences were not significant with five rats. Also, the number of Kupffer cells may be limited by available sinusoidal space. The competency of the Kupffer cells should be examined by challenging the liver or isolated Kupffer cells to ingest labeled bacteria.

Microscopic inspection showed the F group to have compressed sinusoids when compared with S, V, and T groups. Computer assisted image analysis produced conflicting data that indicated the large amount of extracted cytoplasmic areas as sinusoidal area. This is particularly problematic for the F group that had large glycogen deposits. This would tend to increase the size of the hepatocytes in the F group and decrease the size in the T group.

Flight vs Synchronous

Based on the appearance of liver sections, the S group appears to provide the best control for space flight. This group had similar surroundings, handling and the same controlled feeding regime as the F group. However, the S group did not control for weightlessness. The stress of take off and landing, while simulated in the S rats, may not have accurately reflected the experience of the F rats. Stress on landing may have elevated the corticosterone levels since the F group had the highest of all four groups albeit not statistically different (R. Grindeland, pers. communication). When there was a delay between landing and time of sacrifice, as occurred in the Cosmos 1887, corticosterone levels were near normal. Circulating glucose levels were also higher in the flight than the other groups and may be due to changes in hormone levels. Unfortunately insulin and glucagon levels were not measured for these animals. Changes in hormone levels can rapidly release stored glycogen. The difference between S and F cannot be due to stress of flight because the flight had more, not less glycogen than the other groups. We can only conclude that some other, chronic factor of space flight altered the metabolic storage or use of hepatic glycogen and possibly lipid stores.

The presence of high glycogen stores in flight animals seems contradictory to the observed lower growth in the F rats. The F rats did not eat as much. There is no reason to believe that the flight rats were not sated based on food availability. High glycogen in the liver can be attributed to increased deposition or to reduced accessibility of hepatic glycogen.

A number of factors could alter the metabolism and catabolism of glycogen including hormone levels, hormone receptor availability, enzyme synthesis and catabolism, availability of precursors and blood circulation. Merrill et al. (1990) have reported increased levels of glycogen as did Abraham et al. (1981) who also reported no differences for activities for glycogen synthetase (GS) and phosphorylase (GP), enzymes necessary for glycogen metabolism. However, Abraham at al. (1978) did show reduced levels[1] in the blood seem to argue against a problem with reduced glycogen availability. However, there are other sources of glucose including amino acids available from the breakdown of muscle mass (Merrill et al., 1990). Elevated blood glucose may also be a temporary response to the stress of landing and not a chronic condition of space.

This analysis still does not answer the question regarding the physiological condition of the liver and why space flight would alter the glycogen and perhaps the lipid stores within the liver. Although not significantly different, a continued pattern of increased lipid deposition might be a critical factor in longer space flights. In-flight measurements may need to be done to separate the effect of landing from space flight. Some basic measurements of hormone levels, insulin, and glucagon may also be valuable.

Flight vs.Tail Suspension

The suspended rat (tail or whole-body) has been used as an earth-based model of weightlessness and found to be useful for muscle studies (Thomason and Booth, 1990). Our results suggest that the model, as carried out in this study, may not be appropriate for internal organs. The most dramatic difference was seen in the amount of glycogen. Unfortunately, the feeding regimen of the T rats was not the same as the F rats. The V rats, which had the same feeding schedule as the T rats, also had lower amounts of glycogen. However, both of these groups were not statistically different from the S rats, which did follow the F feeding schedule. It is clear that true

[1]GP activity in F animals in an earlier mission. Elevated glucose.

weightlessness did have a dramatic effect on liver glycogen that was not mimicked by the tail suspension model. Furthermore, there was some slight indication of pathological change in the T rats, such as edema. The liver also weighed considerably less than the other groups. Body weight gain was larger than both F and S so food consumption was probably normal (we did not receive food consumption data for V or T).

Although evidence of edema was seen in T animals, the image analysis of sinusoidal spaces was lowest for the T group. This conflict of evidence could be resolved by injecting suspended rats with trypan blue or carbon black. Exclusion of the dye from the space of Disse and the extracellular spaces would demonstrate no edema.

Hepatocytes of the T group were smaller than the other groups. The sinusoidal spaces were not significantly different from the other groups. The difference due to nuclear size was minor. Whereas, the cytoplasm (hepatocytic area nuclear area) was significantly smaller. When the area attributed to glycogen is subtracted from the cytoplasmic compartment, there is no significant difference between the four groups. Therefore, the smaller size of the livers of the T rats is probably due to glycogen loss. Extrapolation to the liver itself would suggest that the smaller liver in the T group was due to a reduced amount of glycogen.

Synchronous vs. Vivarium

Although not shown significantly different due to the small sample size, the glycogen levels in the S group appeared greater than the V rats. Two factors may be responsible here, a capsule effect or the method of feeding. Glycogen levels have been shown to be altered by fasting for relatively short times and are dependent on feeding regime (Babcock and Cardell, 1974). It is unclear if the V rats had access to food at all times or if they were fasted before time of sacrifice. We assume they had access to food given the greatest weight gain in the V group. It would seem that the temperature differential or the new environment of the simulation altered the deposition or accessibility of glycogen. A slight temperature increase would reduce energy loss; however, too warm a temperature can stress an animal and actually increase energy loss. It is more likely that glycogen storage was increased due to changes in handling and the novelty of the situation.

CONCLUSIONS

The results of this study confirm that space flight alters metabolic activity of the liver in rats. The specific factor of space flight that alters liver functions and the physiologic processes involved remain to be identified. In order to determine if endocrine function is altering glycogen storage, subsequent space flights should include measures of circulating glucagon and insulin and hormone receptors. The effect of stress on blood glucose level could be monitored in real time by periodically measuring glucose in urine. Other metabolites and other hormones might also be measured in urine. Tracer studies with radio-labeled rats might also be considered.

Evaluation of hepatic-immune function also warrants examination. However, more animals would be needed to demonstrate an effect.

The tail suspension model, as performed in this study, was a poor model for weightlessness. For almost all parameters the greatest difference was between the flight and tail-suspended samples. The protocols for this model need improvement.

Metabolic studies would also be enhanced if all groups were given the same feeding regimen.

ACKNOWLEDGEMENTS

We wish to thank Dr. A. S. Kaplansky and the Soviet Cosmos recovery and dissection team for their heroic efforts in obtaining the samples for this study. Dr. Richard Grindeland provided able assistance in Moscow and was responsible for inviting us to participate in this study. Dr. Kathy Klueber, University of Louisville Analytical Electron Microscopy Laboratory, provided technical assistance in the preparation of histological slides. J. H. and H. W. Carter, Wood Hudson Cancer Research Laboratory, Inc. were responsible for the morphometric analyses. This research is supported by NASA grant NAG 2-626.

REFERENCES

1. Abraham, S., H.P. Klein, C.Y. Lin, C and Volkmann. The Effects of Space Flight on Some Liver Enzymes Concerned with Carbohydrate and Lipid Metabolism in the Rat. In: Final Reports of U.S. Experiments Flown on the Soviet Satellite Cosmos 939. Eds: S. N. Rosenzweig and K.A. Souza. NASA Tech Mem 78526, Ames Research Center, Ca., 78-134 , 1978.

2. Abraham, S., H.P. Klein, C.Y. Lin, C. Volkmann, R.A. Tigranyan, and E.G. Vetrova. Studies of Specific Hepatic Enzymes and Liver Constituents Involved in the Conversion of Carbohydrates to Lipids in Rats Exposed to Prolonged Space Flight. In: Final Reports of U.S. Rat Experiments Flown on the Soviet Satellite Cosmos 1129. Eds: M.R. Heinrich and K.A. Souza. NASA Tech Mem 81289, Ames Research Center, Ca., 35-100, 1981.

3. Babcock, M. B. and R.R. Cardell. Hepatic Glycogen Patterns in Fasted and Fed rats. Am. J. Anat. 140:299-338, 1974.

4. Cherrington, A.D. and M. Vranic. In: Hormonal Control of Gluconeogenesis, Vol. I. Ed: N. Kraus-Friedmann. CRC Press, Inc., Boca Raton, Fl., 15, 1986.

5. Cormier, S. M., R.N. Racine, C.E. Smith, W.P. Dey, and T.H. Peck. Hepatocellular Carcinoma and Fatty Infiltration in the Atlantic Tomcod, *Microgadus tomcod* (Walbaum). J. Fish Dis. 12:105-116, 1989.

6. Ferey, L., P. Herlin, J. Marnay, A. Mandard, R. Catania, P. Lubet, R. Lande, and D. Bloyet. Pararosaniline or Acriflavine-Schiff Staining of Epoxy Embedded Tissue After Periodic Acid Oxidation in Ethanol: A Method Suitable for Morphometric and Fluorometric Analysis of Glycogen. Stain Technol. 61:107-110, 1986.

7. Grindeland, R. E., M.F. Vasques, R.W. Ballard, and J.P. Connolly. Cosmos 2044 Mission Description, this isssue..

8. Hargrove, J. L. and D.P. Jones. Hepatic Enzyme Adaptation in Rats After Space Flight. The Physiologist. 28:S-230, 1985.

9. Hrudan, Z. In: Liver Carcinogenesis. Eds: K. Lapis and J.V. Johannessen. Hemisphere Publ. Co., Washington, D.C., 233, 1979.

10. Kraft, L.M. Morphometric Study of the Liver. In: Final Reports of the U.S. Experiments Flown on the Soviet Biosatellite Cosmos 1887. Eds: J.P. Connolly, R.E. Grindeland, and R.W. Ballard. NASA Tech. Mem.102254, Ames Research Center, Ca., 281-290, 1990.

11. Loginov, A.S., L.I. Aruin, V.V. Ul'yanova, V.S. Gorodinskaya, and V.I. Yakovleva. Morphologic Changes in the Stomach and Liver of Rats. In: The Effects of Dynamic Factors of Space Flight on Animal Organisms. Ed: A.M. Genin. NASA Tech. Mem. 75692, Washington, D.C., 195-198, 1979.

12 Mandel, A. D., G. Sonnenfeld, W. Berry, G. Taylor, S.R. Wellhausen, I. Konstantinova, A. Lesnyak, and B. Fuchs. Effect of Space Flight on Levels and Function of Immune Cells. In: Final Reports of the U.S. Experiments Flown on the Soviet Biosatellite Cosmos 1887. Eds: J. P. Connolly, R. E. Grindeland, and R. W. Ballard. NASA Tech. Mem. 102254, Ames Research Center, Ca., 471-480, 1990.

13. Merrill, A. H., E. Wang, and J.L. Hargrove. Hepatic Enzymes of Sphingolipids and Glycerolipid Biosynthesis in Rats from Spacelab 3. The Physiologist. 28:S-229, 1985.

14. Merrill, A. H., E. Wang, D.P. Jones, and J.L. Hargrove. Hepatic Function in Rats After Space Flight: Effects on Lipids, Glycogen, and Enzymes. Am. J. Physiol. 252:R222-R226, 1987.

15. Merrill, A. H., M. Hoel, E. Wang, R.E. Mullins, J.L. Hargrove, D.P. Jones, and I.A. Popova. Altered Carbohydrate, Lipid and Xenobiotic Metabolism by Liver from Rats Flown on Cosmos 1887. FASEB J. 4:95-100, 1990.

16. Richmond, R. E., M.A. Pereira, J.H. Carter, H.W.Carter, and R.E. Long. Quantitative and Qualitative Immunohistochemical Detection of Myc and Src Oncogene Proteins in Normal, Nodule, and Neoplastic Rat Liver. J. Histochem. Cytochem. 36:179-184, 1988.

17. Thomason, D. B. and F.W. Booth. Atrophy of the Soleus Muscle by Hindlimb Unweighting. J. Appl. Physiol. 68:1-12, 1990.

18. Tyson, C.A. and C.E. Green. Cytotoxicity Measures: Choices and Methods. In: The Isolated Hepatocyte: Use, Toxicology and Xenobiotic Biotransformations. Eds: E.J. Rauckman and G.M. Padilla. Academic Press, Orlando, Fl., 119-158, 1987.

19. Tanikawa K. Ultrastructural Aspects of the Liver and Its Disorders. Igaku Shoin, Tokyo, 1979.

20. Weibel, E. R. Stereological Methods, Vol. 1: Practical Methods for Biological Morphometry. Academic Press, N. Y., 1979.

TABLE 1

PERCENT GLYCOGEN FOUND IN HEPATOCYTES

Group	N	Mean	S.E.	Min.	Max.
Flight	5	28.47	5.178	13.8	41.32
Synchronous	5	11.04	2.320	4.08	18.64
Vivarium	5	3.13	1.457	0.03	7.35
Tail Suspended	5	0.08	0.026	0.03	0.13

TABLE 2

PERCENT LIPID FOUND IN HEPATOCYTES

Group	N	Mean	S.E.	Min.	Max.
Flight	5	5.84	1.257	2.73	9.04
Syncronous	5	4.27	0.482	2.42	5.03
Vivarium	4	3.20	0.626	1.71	4.74
Tail Suspended	5	2.90	0.526	1.53	4.26

TABLE 3

COMPARISON OF MEAN BODY WEIGHTS AND LIVER WEIGHTS

	COSMOS 2044			COSMOS 1887		
	At Launch	At Sacrifice		At Launch	At Sacrifice	
Group	Body	Body	Liver	Body	Body	Liver
Flight	321	338	9.98	294	303	9.96
	(2)[a]	(2)	(0.18)	(3)	(2)	(1.41)
Synchronous	307	343	10.22	312	349	8.86
	(3)	(7)	(0.49)	(5)	(6)	(0.19)
Vivarium	298	363	10.11	-[b]	342	8.86
	(1)	(2)	(0.21)	-	(8)	(0.30)
Tail Suspension	298	339	8.23	-[c]	-	-
	(12)	(10)	(0.28)	-	-	-

[a] Standard Error.
[b] Not Provided.
[c] Not Included as Part of Experiment.
All Measurements in Grams.
All Sample Sizes = 5.

TABLE 4

MORPHOMETIRC ANALYSIS OF HEPATOCYTE NUCLEI

Group	Nuclei Number[a]	Mean Nuclear Area (μm^2)	Mean Nuclear Diameter (μm)
Flight	9.86 (0.952)[b]	51.19 (1.322)	8.01 (0.107)
Synchronous	12.62 (0.862)	43.45 (0.901)	7.36 (0.073)
Vivarium	12.52 (1.146)	46.62 (0.875)	7.65 (0.067)
Tail Suspended	16.27 (1.756)	44.02 (1.251)	7.42 (0.098)

[a] Represents the Average Number of Nuclei Observed in a Reference Area of 9842 μm^2
[b] Standard Error
All Sample Sizes = 5

TABLE 5

TOTAL HEPATOCYTE AREA AND AMOUNT OF CYTOPLASM AFTER REMOVAL OF NUCLEAR AND GLYCOGEN AREAS

Group	Hepatocyte Area (μm^2)	Cytoplasm	
		Minus Nucleus	Minus Glycogen
Flight	842.80 (67.399)[a]	791.60 (66.467)	572.31 (79.527)
Synchonous	692.22 (70.809)	648.76 (71.203)	579.15 (72.203)
Vivarium	749.38 (87.484)	702.76 (87.379)	679.92 (84.132)
Tail Suspended	542.42 (54.101)	498.40 (53.656)	497.96 (53.534)

[a] Standard Error
All Sample Sizes = 5

TABLE 6

MORPHOMETRIC ANALYSIS OF KUPFFER CELLS

Group	Number / Reference Area	Number / Hepatocyte	Number / Unit Valcuolar Space
Flight	5.75 (0.308)[a]	0.60 (0.050)	3.38[b] (0.436)
Synchronous	6.58 (0.557)	0.53 (0.050)	5.95 (0.988)
Vivarium	6.67 (0.373)	0.55 (0.072	12.82 (5.609)
Tail Suspended	8.72 (1.307)	0.54 (0.052)	9.83 (3.691)

[a] Standard Error
[b] x 10^{-5}
All Sample Sizes = 5

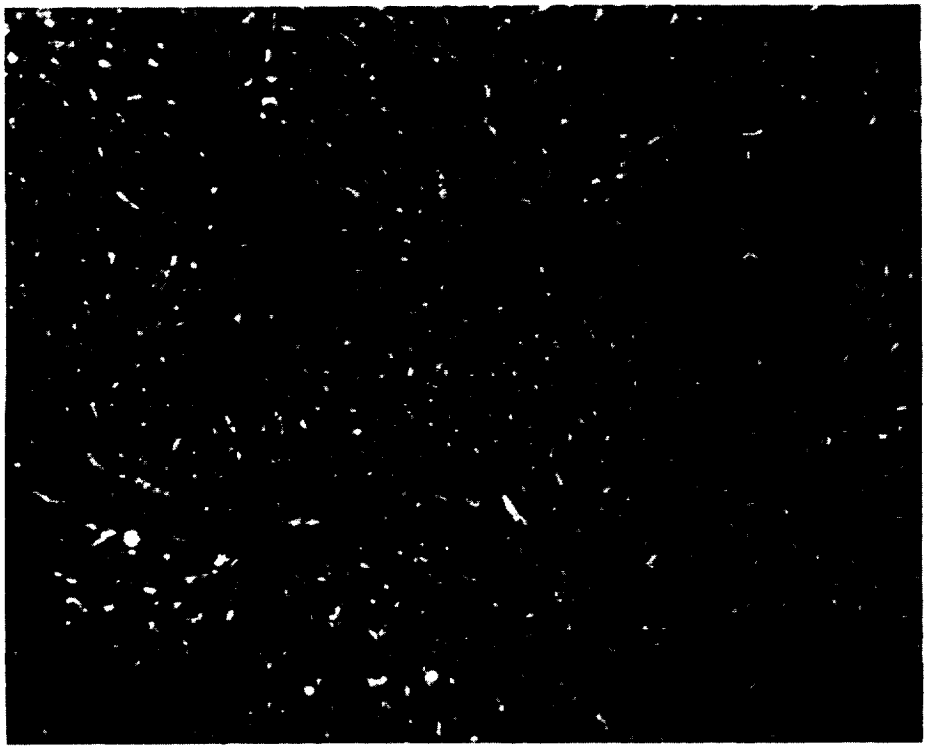

Figure 1. Flight rat (#9), paraffin embedded, H & E stained. Sinusoids are compressed, nuclei have more euchromatin and are larger than controls, cytoplasm is vacuolated. Bar = 100 μm.

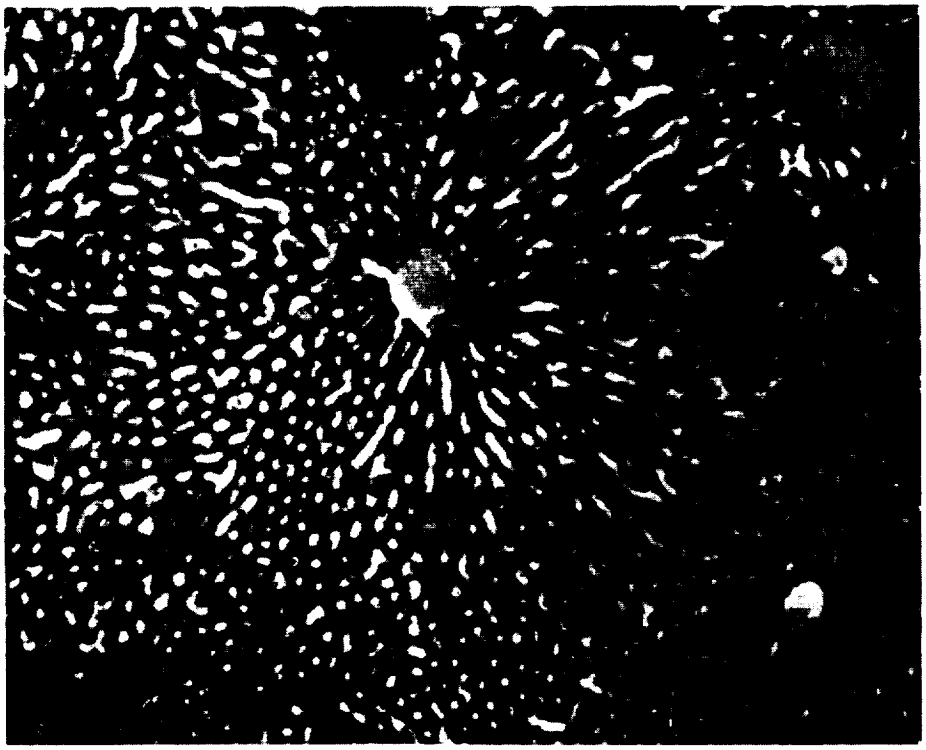

Figure 2. Tail suspended rat (#6), paraffin embedded, H & E stained. Sinusoids and central vein is dilated in this sample. Some of the V and S samples also had dilated sinusoids. Cytoplasm was not vacuolated. Bar = 100 μm.

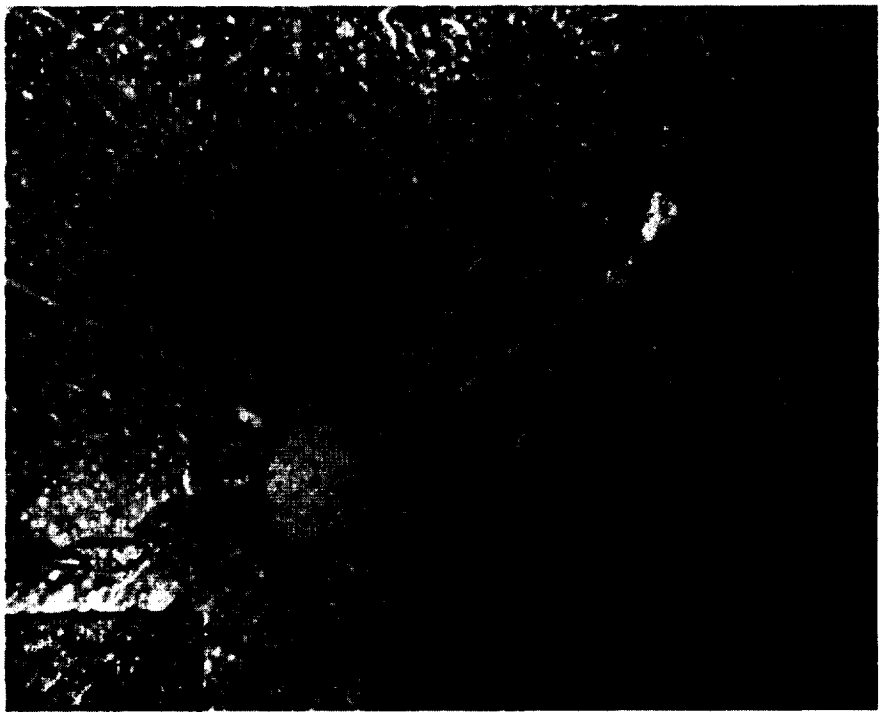

Figure 3. Synchronous rat (#10), paraffin embedded, PAS stained. Darkly stained material is PAS positive granules in hepatocytes. Heaviest deposition in area of central vein. Large circular structure in lower left is hepatic vein. Bar = 100 μm.

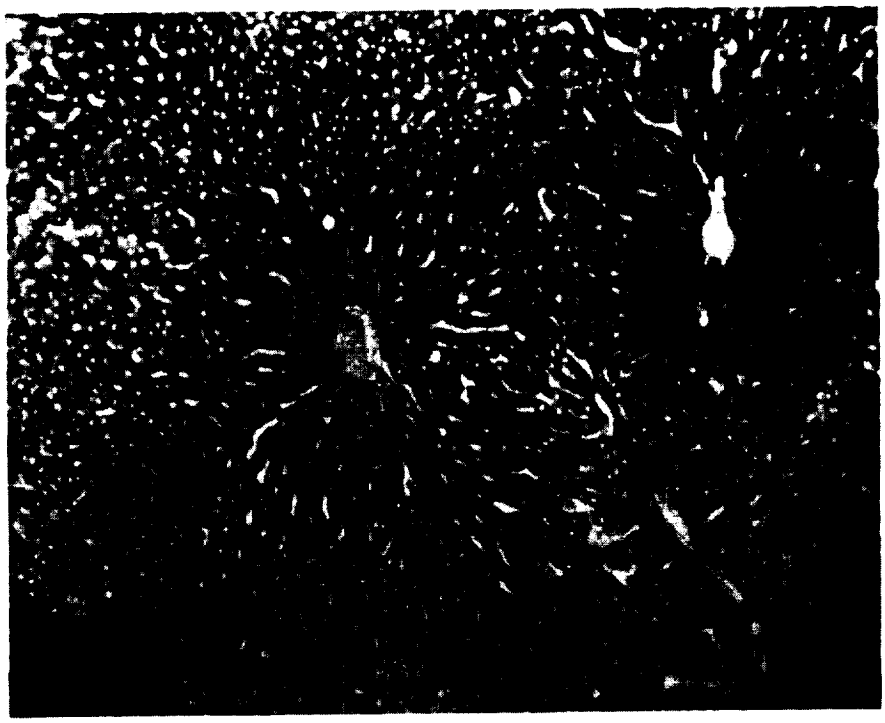

Figure 4. Flight rat (#9), paraffin embedded, PAS stained. A similar pattern of PAS positive granules are present in flight animals. Deposition is heavier than controls. Bar = 100 μm.

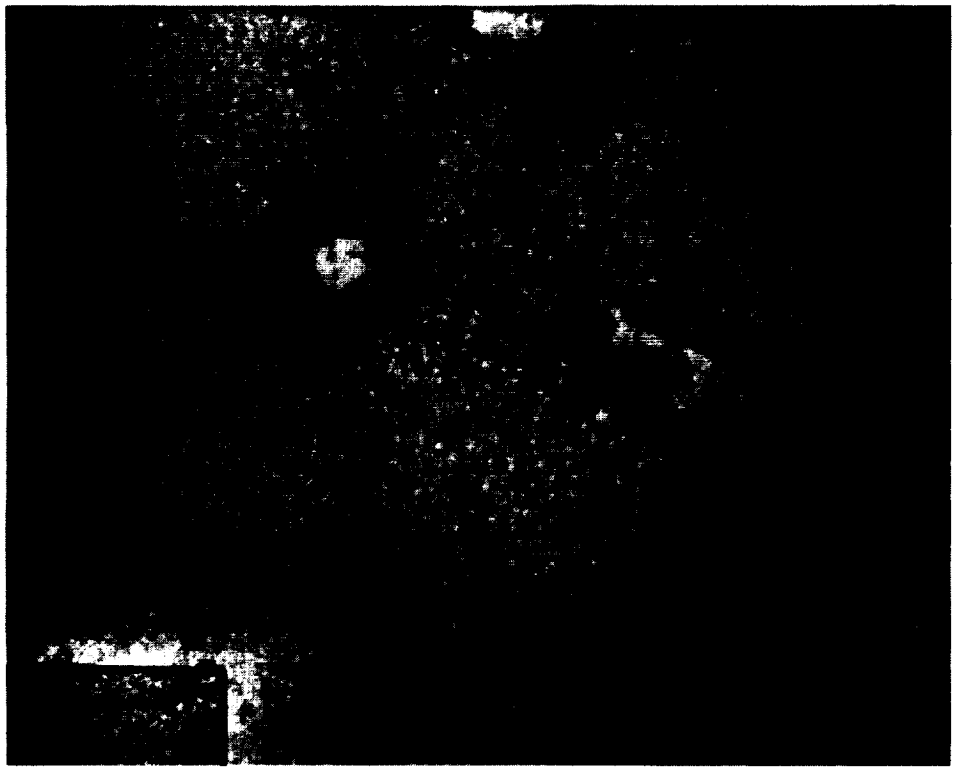

Figure 5. Tail suspended rat (#8), paraffin embedded, PAS stained. Very little PAS positive material is deposited in T samples. Bar = 100 μm.

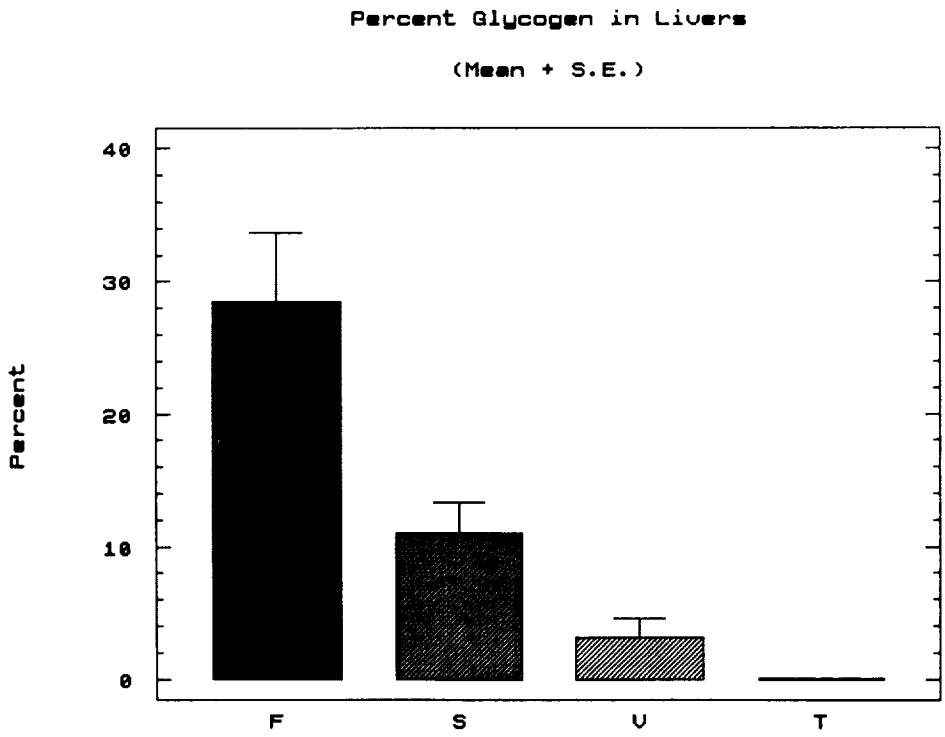

Figure 6. Morphometric analysis of the amount of glycogen found in the livers of F-Flight, S-Synchronous, V-Vivarium and T-Tail Suspended rats.

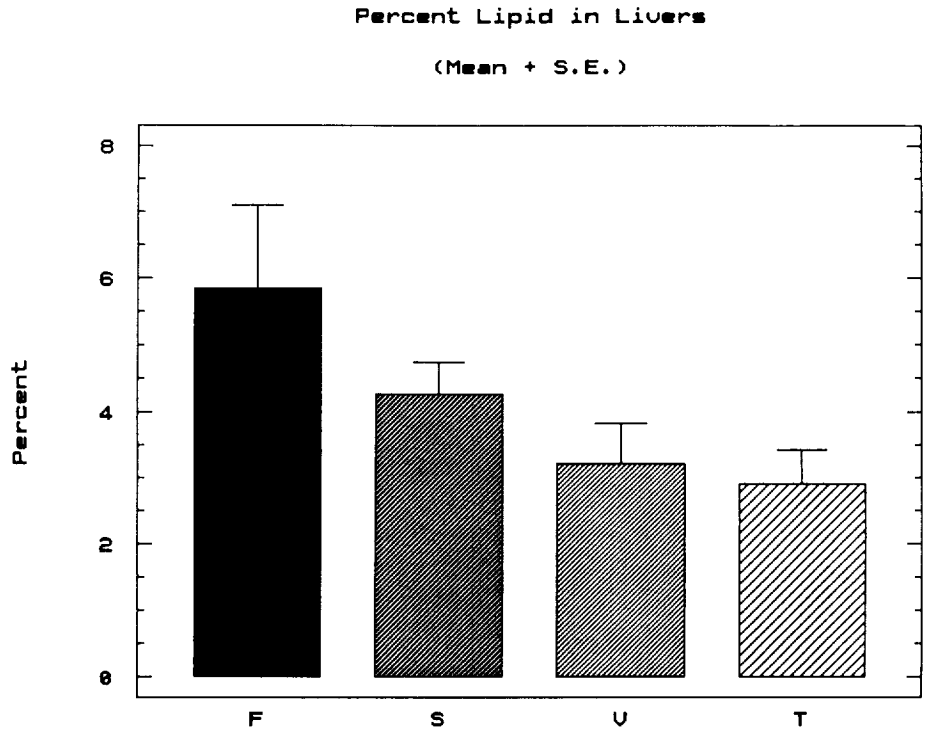

Figure 7. Morphometric analysis of the amount of lipid found in the livers.

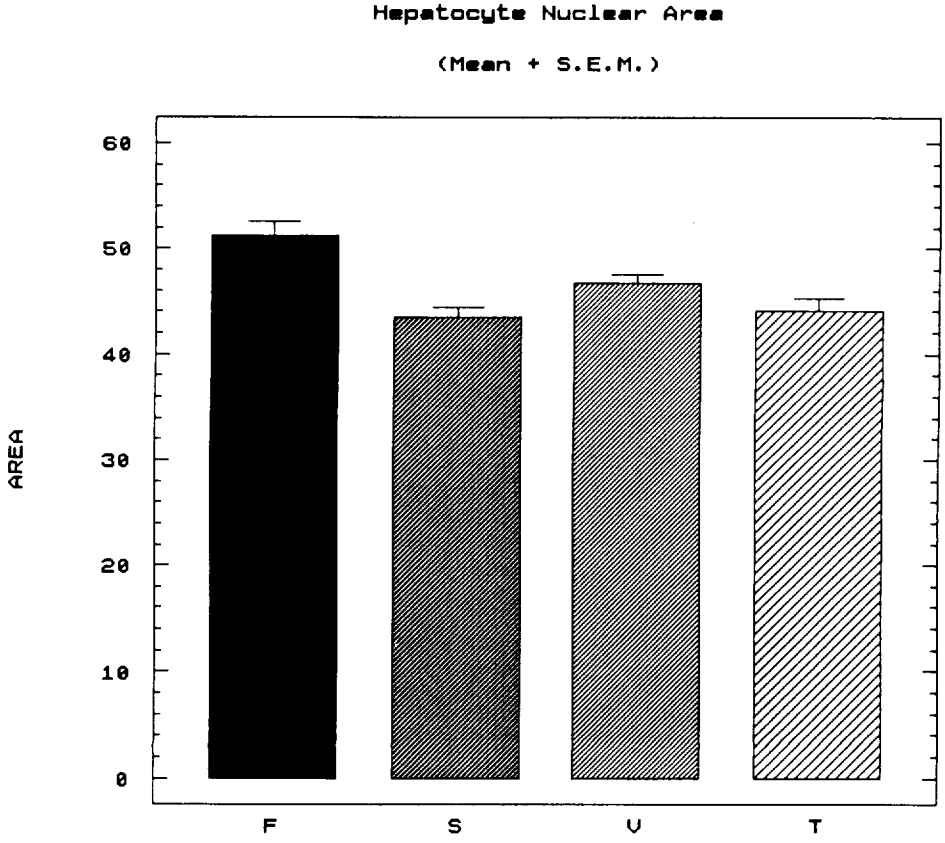

Figure 8. Morphometric analysis of average area of hepatic nuclei. Measurements in μm^2.

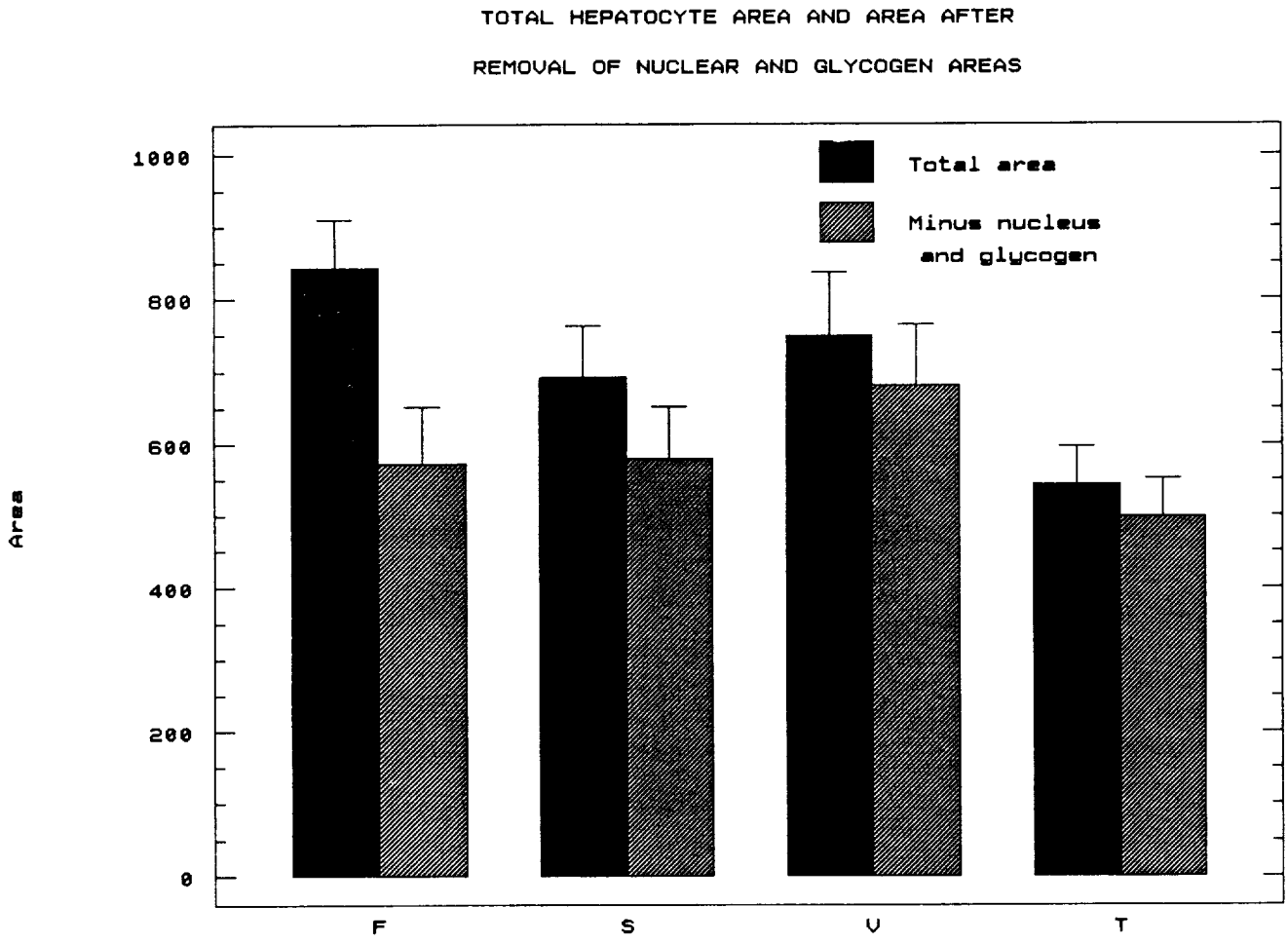

Figure 9. Morphometric analysis of average size of hepatocytes, including nuclei and glycogen deposits. The size was re-computed by removing the area of the nuclei and glycogen to determine the size of the parenchymal component. Measurements in μm^2.

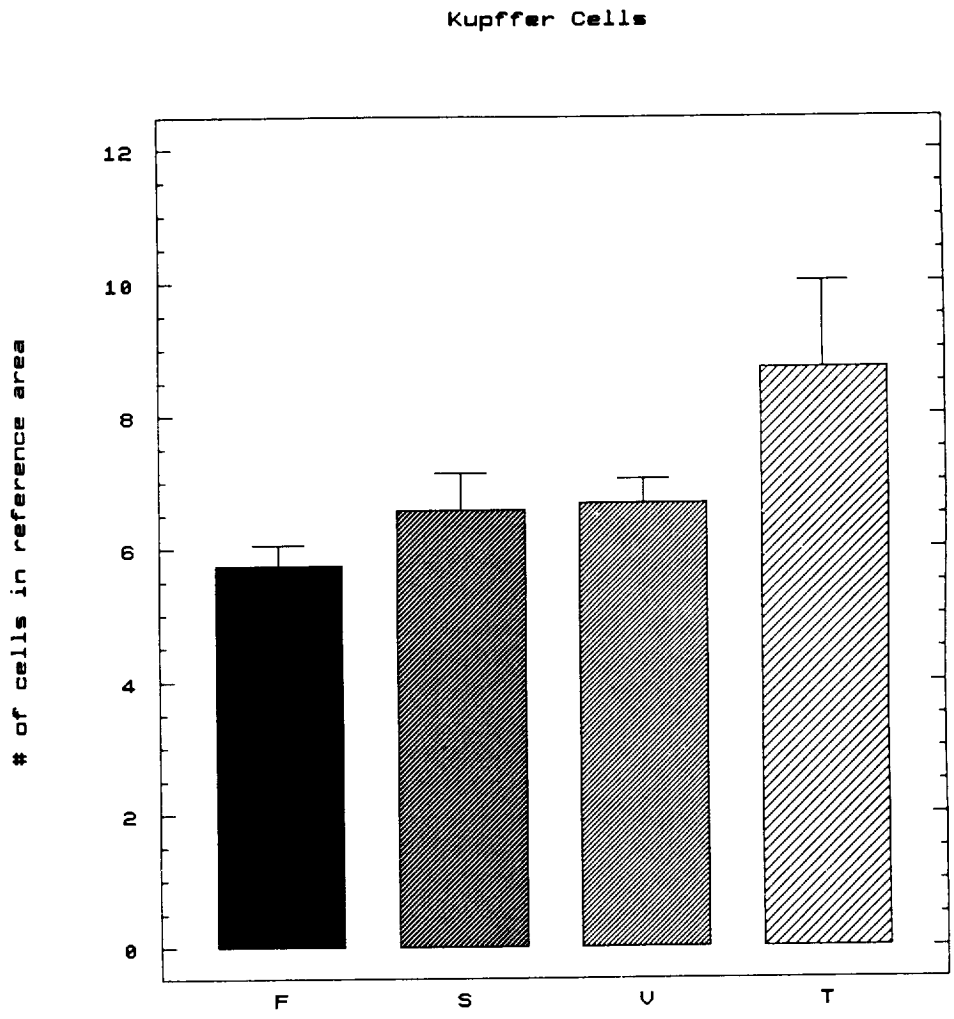

Figure 10. Morphometric analysis of number of Kupffer cells found in the fluid-filled spaces in between hepatocytes. Number was counted in the reference area of 9842 μm^2.

EXPERIMENT K-7-15

HEMATOLOGY STUDIES IN RATS FLOWN ON THE SOVIET BIOSATELLITE COSMOS 2044

Principal Investigator:

R.D. Lange
Department of Medical Biology
University of Tennessee Medical Center in Knoxville
Knoxville, Tennessee

Co-Investigators:

T. B. Driscoll
Baylor College of Medicine
Houston, Texas

L. A. Gibson
A.T. Ichiki
Department of Medical Biology
University of Tennessee Medical Center in Knoxville
Knoxville, Tennessee

N.G. Khrushchov
T. Michurina
N.K. Koltsov Institute of Developmental Biology
Academy of Sciences of the USSR
Moscow, USSR

L.V. Serova
Institute of Biomedical Problems
Moscow, USSR

A. Vacek
Institute of Biophysics
Czechoslovak Academy of Sciences
Brno, Czechoslovakia

EXPERIMENT K-7-15

HEMATOLOGY STUDIES IN RATS FLOWN ON THE SOVIET BIOSATELLITE COSMOS 2044

R.D. Lange, L.A. Gibson, T.B. Driscoll, L. Serova, T. Michurina, A. Vacek, A.T. Ichiki, and N.G. Khrushchov

ABSTRACT

Ten rats were flown on a 14 day flight of Cosmos 2044. Five of the rats had been injured prior to flight and were not used in our studies. Three control groups of rats were studied (basal, vivarium and synchronous) as well as a group of rats which had undergone tail suspension for a period of 14 days.

The hematology studies were carried out by Soviet, Czechoslovak and United States investigators. This report presents the studies of bone marrow cell differential counts, clonal response to the hormone erythropoietin, as well as erythropoietin levels in the plasma.

While some minor differences were found, there were no essential differences in the bone marrow cell differential counts or erythropoietin levels of flight or tail suspended animals as compared to control groups. In studies of colony formation there was a marked increase in the number of CFU-E colonies in flight animals in the bone marrow that was frozen and recultured in the U.S. No such increase was noted in the "fresh" cultures performed in Moscow.

The results of previous studies are discussed; to date, no pattern of erythropoiesis has emerged and the rat may or may not be a valid model to study the decrease in red cell mass that occurs in humans exposed to microgravity.

INTRODUCTION

Astronauts have been found to have a reduction in red cell mass upon returning from microgravity. The reasons for this decrease are unknown but are probably multifactorial with the primary reason being a physiological response to decreased energy requirements in microgravity (Johnson, 1983; Tavassoli, 1982; Talbot and Fisher, 1986).

In a continuing investigation of the pathogenesis of "anemia of space-flight" three red blood cell studies were performed on the material obtained from five rats flown on the fourteen day flight of Soviet Biosatellite Cosmos 2044 together with appropriate controls. The bone marrow cell differentials, clonal bone marrow studies of red blood cell colony formation and plasma erythropoietin (EPO) determinations were performed by U.S. investigators in cooperation with Soviet and Czechoslovakian investigators. The results of these three studies are presented here together with a discussion of previous studies of these three parameters.

MATERIALS AND METHODS

General Flight and Animal Data

The flight information of the Cosmos Biosatellite 2044 is as follows (Ballard and Connally, 1990):

Launch Date	9-15-89
Recovery Date	9-29-89
Mission (Days)	14
Apogee	294 km (159 mi)
Perigee	216 km (117 mi)
Period (minutes)	89.3
Inclination (degree)	82.3

Male Czechoslovakian Wistar rats were obtained from the Institute of Experimental Endocrinology Bratislava, Czechoslovakia.

Five rats had their soleus and gastrocnemius muscles crushed and tibias cut seventeen days before flight and five animals were untreated. The materials for our studies were obtained from uninjured rats.

The rats were divided into five groups: flight, basal controls, synchronous controls, vivarium controls and tail suspended. The body weights at the time of sacrifice of the uninjured rats were as follows:

Group	Weight (grams)
Basal	320.0 + 4
Flight	338.0 + 2
Synchronous	343.0 + 7
Tail Suspended	339.0 + 10

p= 0.05
Flight differs from Basal
Synchronous differs from Basal

Bone Marrow Cell Differentials

Bone marrow smears were made by Soviet scientists at the landing site at Tashkent, fixed in absolute methanol for 10 minutes and sent to the U.S. for staining. The slides were stained for 10 minutes with Wright's stain after which tap water was added for 20 minutes. After rinsing, the slides were stained for 10 minutes with freshly prepared Giemsa stain. (After rinsing and drying, 500 cell differential counts were performed.) The bone marrow cells were classified into the following cell types:

small lymphocytes
large lymphocytes
plasma cells
reticulum cells
mature myeloid cells (metamyelocytes, bands, segmented)
immature myeloid cells (myeloblasts, promyelocytes, myelocytes)
eosinophils
tissue basophils
mature erythroid cells (polychromatophilic and acidophilic normoblasts)

immature erythroid cells (pronormoblasts and basophilic normoblasts)
The myeloid to erythroid ratio was also calculated.

Erythroid Clonal Studies

Bone marrow plugs from the tibias of the rats were flushed into sterile teflon vials containing 10 ml of Iscove's Modified Dulbecco's Media at Tashkent. The tubes were refrigerated at 4° C and sent to Moscow where the marrow was cultured.

The cells were disaggregated, the tubes centrifuged at 800 rpm for 10 minutes and the cells washed twice with Iscove's Modified Media with antibiotics. After the final centrifugation, the supernatant fluid was discarded, and dependent on the size of the pellet, approximately 2 ml of media was added. A cell count was performed after which a dilution was made to give a cell concentration of 4×10^6 viable nucleated cells per ml.

For each tibia a control and three concentrations of erythropoietin were tested. The ingredients of each of the four tubes in mls was:

Ingredient	A	B	C	D
Bone Marrow Cells (4×10^6)	700	700	700	700
L-Glutamine (200mM)	87.5	87.5	87.5	87.5
Erythropoietin* (40mU/ml)	0	44	[1]88	176
Iscove's Modified Media	472.5	428.5	384.5	296.5
Spleen Conditioned Media	700	700	700	700
Pre-Prepared Methylcellulose Mix **	5600	5600	5600	5600

*Erythropoietin Recombinant obtained from Amgen©[1].
**Terry Fox©[2] pre-prepared mix consisted of a pretested mixture of methylcellulose, fetal calf serum and bovine serum albumin in alpha medium.

After thorough mixing, 1ml was pipetted into a sterile 35mm Petri dish and 3 plates were placed in a 100mm Petri dish for determination of CFU-E (colony forming unit -erythroid) colonies. For BFU-E (burst forming unit-erythroid) an additional 35 mm plate filled with water was placed in the 100 mm Petri dish to prevent drying of the cultures. The cultures were incubated at 37° C in a well humidified 7.5% CO_2 incubator. All groups were done in triplicate except for the Vivarium group, which was done in duplicate.

Colonies were scored by the ability of hemoglobin-containing cells to reduce 2,7-diaminofluorene (DAF). A stock solution of stain was prepared by adding 2.5 ml of 90% glacial acetic acid to 0.25 mg of stain. To 150 ml of 2,7- DAF stock solution were added 15 ml of tris HCl buffered saline and 150 ml of 30% H_2O_2. CFU-E were enumerated at 2 days and BFU-E at 7 days.

---

[1]Amgen Biologicals©, 1900 Oak Terrace Lane, Thousand Oaks, Ca, 91320.

[2] Terry Fox Laboratory©, British Columbia Cancer Research Centre, 601 West 10th Avenue, Vancouver, B.C., Canada, V5Z 1L3.

Any cells remaining were frozen and returned to the U.S. where the cultures were repeated. A pellet of the cells was placed in an ice bucket. The freezing mixture, consisting of 10% DMSO and 90% fetal calf serum, was chilled to 4° C and then mixed with chilled cells to give a concentration of 5 x 10^7 cells /ml. The mixture was dispensed into Sarstedt© cryovials in 1 ml aliquots. The vials were placed in a can containing foam and 70% ethanol and the can was placed in a -70° C freezer for approximately 24 hours. The vials were then transferred to a liquid nitrogen dewar flask until shipment to the U.S.

Erythropoietin Radioimmunoassay

Frozen plasma (0.2ml) was used for erythropoietin determinations. A commercial kit obtained from the Incstar© Inc.[1] was utilized and we followed the accompanying directions. The radioimmunoassay detects 5.5 mU/ml of erythropoietin. Normal plasma and laboratory samples containing high levels of EPO were run concurrently with the test plasma. Samples were counted on a Packard Gamma Counter.

An example of the dose response curve is shown in Figure 1.

Statistical Analysis

The statistical analysis was carried out on the IBM PC using the Statgraphics©[2] version 2.6 statistics package. Graphics were created with the Cricket Graph©[3] graphics package on a Macintosh SE computer.

Summary statistics were performed on each data group and a 2-sample analysis was performed to determine any group differences. A non-parametric test to discard outlyers was performed on any groups showing differences on the 2-sample analysis. A summary of differences in non-parametric p-values is given in Appendix E.

RESULTS

In this section we present results of the flight, tail suspended and synchronous control animals. We utilized the synchronous control group since they did not significantly differ from the vivarium or basal controls. We also include an appendix in which the results of all the groups are included.

Bone Marrow Cell Differential Counts

Figure 2 depicts the bone marrow cell differentials of the major cell types of the three animal groups. As shown there was a slight increase in the granulocytic bone marrow cells of flight animals as compared to those of the synchronous controls and the tail suspended animals. There was an increase in immature myeloid cells accompanied by a decrease in small lymphocytes (Appendix A).

As shown in Figure 3 there was no essential difference in the M:E ratio for the three groups of animals.

---

[1] Incstar© Inc., 1951 Northwestern Ave., Stillwater, Mn., 55082.

[2] Statgraphics©, 2115 East Jefferson St., Rockville, Maryland, 20852.

[3] Cricket Graph©, Great Valley Corporate Center, 40 Valley Parkway, Malvern, Pa., 19355.

Clonal Erythroid Studies

Two types of colonies were assessed: CFU-E and BFU-E. The clonal studies were made in Moscow at the N.K. Koltsov Institute of Developmental Biology and were repeated on cells, which had been frozen, at the Department of Medical Biology of the University of Tennessee Medical Center in Knoxville, Tennessee. A summary of results is found in Appendices B and C.

1. Clonal Studies in Moscow

a) CFU-E

The CFU-E colony counts on tibia bone marrow cells are shown in Figure 4. Data without and with 250 mU/ml of erythropoietin are shown. The response to erythropoietin should be noted. There were no significant differences between the flight, tail suspended, and synchronous control animals bone marrow cells.

b) BFU-E
The number of BFU-E colonies per 4 x 10^5 tibial bone marrow cells is depicted in Figure 5. At the 250mU/ml EPO dose, more colonies were formed from cells obtained from synchronous controls as compared to both flight and tail suspended animals as well as cultures set up without erythropoietin when compared to the tail suspended animals.

2. Repeat Clonal Studies in Knoxville

a) CFU-E

The frozen flight cells had a marked increase in the number of colonies formed both with and without added erythropoietin (Figure 6). Because of the number of cells available, only a single plate was prepared.

b) BFU-E

The results are shown in Figure 7 and at the 0 level of erythropoietin there were slightly more colonies formed than from the cells of tail suspended animals.

Erthyropoietin Determinations

The erythropoietin assay data are depicted in Figure 8. While statistically significant differences were found between the tail suspended group and both the flight and synchronous controls, the actual differences were probably not physiologically significant. A summary of results is found in Appendix D.

DISCUSSION

Relatively few hematology studies have been made on animals flown in microgravity. Ellis in 5 pocket mice flown on Apollo XVII reported a decrease in the number of red cell precursors in the bone marrow (Ellis et al., 1975). Ilyin also found a decrease in erythroblastic elements of rats flown on Cosmos 605 (Ilyin et al., 1975) and Gazenko, et al. (Gazenko et al. 1980), have stated that rats flown aboard biosatellites have had a decrease in the number of their red blood cell precursors. However on Cosmos 936 (Shvets et al., 1977 and 1984), there were no statistically significant changes in bone marrow cell composition and on SL-3 we did not find any significant changes in bone marrow cell differentials (Lange et al., 1985, 1987 and 1988). There were no significant differences in the myeloid-erythroid ratios between the flight, control and tail suspended animals in the present studies.

To our knowledge, only one previous clonal study in animals has been reported (Lange et al., 1985, 1987 and 1988). In SL-3 animals, the bone marrow cells of flight animals showed an increased sensitivity to erythropoietin at EPO levels of 0.02 and 1.0 U/ml but not at 0.2 U/ml. In the present studies in cultures made in Moscow there were no significant differences in CFU-E colony number in the different groups. The synchronous controls had an increased number of BFU-E. We were surprised by the marked increase in the number of flight CFU-E in the repeat cultures made in Knoxville. It should be noted that there was a breakdown of the -70 degree Celsius freezer when the flight cells were frozen. It is not known if this could have contributed to the marked increase in the CFU-E colonies formed in the frozen material. Also only one culture could be made because of the cell numbers available.

One other phenomenon was noted in the BFU-E cultures. An unusual number of fibroblast colonies appeared, which made it very difficult to read the plates. These plates had to be read under high power. It should be noted that this was found in all the groups of cells cultured.

Only one previous study of erythropoietin in animals flown in microgravity has been reported (Lange et al., 1985, 1987 and 1988). No difference was found between the erythropoietin levels of flight and control animals. On Cosmos 2044, also no physiological difference was found in the erythropoietin concentrations of flight, tail suspended or control animals.

Cosmos 2044 provided additional studies of erythropoiesis in animals flown in microgravity. The upcoming SLS 1/2 NASA flights will contribute further information and perhaps provide evidence that the rat is a good animal model to study hematopoiesis in microgravity.

ACKNOWLEDGMENTS

We gratefully acknowledge the expert assistance of the NASA investigators as well as the Soviet investigators and technicians of the Institute of Biomedical Problems and the N.K. Koltsov Institute of Developmental Biology. We also would like to thank Dr. Esteban Walker and Paul Wright for statistical advice, Lisa McGinley for assisting in preparing statistical analysis and Mr. F.J. Miller for editorial review.

REFERENCES

1. Ballard, R.W. and J.P. Connolly. U.S./U.S.S.R. Joint Research in Space Biology and Medicine on Cosmos Biosatellites. FASEB. 4:5-9, 1990.

2. Ellis, J.T., L.M. Kraft, C.C. Lushbaugh, G.L. Humason, W.S. Hartroft, E.A. Porta, O.T. Bailey, R.O. Greep, C.S. Leach, T. Laird, R.C. Simmonds, F.S. Vogel, R.L. Dennis, H.R. Brashear, R.V. Talmage, G.A. Harrison, R.L. Corbett, G. Klein, T. Tilbury, K. Suri, and W. Haymaker. The Effects of Cosmic Particle Radiation on Pocket Mice Aboard Apollo XVII: Appendix III. Evaluation of Viscera and Other Tissues. Aviat Space Environ Med. 46 (4 Sec.2): 639-654, 1975.

3. Gazenko, O.G., A.M. Genin, E.A. Ilyin, V.S. Oganov, and L.V. Serova, L.V. Adaptation to Weightlessness and Its Physiological Mechanisms (Results of Animal Experiments Aboard Biosatellites). Physiologist. 23 (suppl 6): S11-S15, 1980.

4. Ilyin, E.A., L.V. Serova, V.V. Portugalov, R.A. Tigranyan, E.A. Savina, M.S. Gayevskaya, Y.I. Kondratyev, A.D. Noskin, V.I. Milyavsky, and B.N. Yurov. Preliminary Results of Examinations of Rats After a 22-Day Flight Aboard the Cosmos 605 Biosatellite. Aviat Space Environ Med. 46:319-321, 1975.

5. Johnson, P.C. In: Current Concepts of Erythropoiesis. Ed: C.D.R. Dunn. John Wiley, New York. 279-300, 1983.

6. Lange, R.D., R.B. Andrews, L.A. Gibson, P. Wright, C.D. Dunn, and J.B. Jones. Hematologic Parameters of Astrorats Flown on SL-3. Physiologist. 28 (Suppl 6): S195-S196, 1985.

7. Lange, R.D., R.B. Andrews, L.A. Gibson, C.C. Congdon, P. Wright, C.D. Dunn, and J.B. Jones. Hematological Measurements in Rats Flown on Spacelab Shuttle, SL-3. Am. J. Physiol. 252:R216-R221, 1987.

8. Lange, R.D., R.B. Andrews, L.A. Gibson, P. Wright, C.D. Dunn, and J.B. Jones. In: Regulation of Erythropoiesis. Eds: E.D. Zanjani, M. Tavassoli, and J.L. Ascensao, J.L. PMA Publishing Corp., NewYork. 455-466, 1988.

9. Shvets, V.N., and N.P. Krivenkova. Morphology of Bone Marrow Cells of Rats on the Cosmos-690 Biosatellite. Kosm. Biol. Aviakosm. Med. 11:75-78, 1977.

10. Shvets, V.N., A. Vatsek, G.I. Kozinets, I.I. Britvan, and V.I. Korol'kov. Hemopoietic Status of Rats Exposed to Weightlessness. Kosm. Biol. Aviakosm. Med. 18:12-16, 1984.

11. Talbot, J.M. and K.D. Fisher. Influence of Space Flight on Red Blood Cells. Fed Proc. 45:2285-2290, 1986.

12. Tavassoli, M. Anemia of Spaceflight. Blood. 60:1059-1067, 1982.

TABLE A

BONE MARROW DIFFERENTIALS
SUMMARY OF RESULTS
(%)

	Vivarium Control	Synchronous Control	Tail Suspended	Flight
Sm. Lymph.	25.52 ± 5.23	26.6 ± 3.86	23.88 ± 2.44	19.76 ± 4.3
Lg. Lymph.	8.52 ± 2.39	7.88 ± 1.91	7.8 ± 0.85	7.04 ± 4.07
Plasma Cells	0.12 ± 0.11	0.04 ± 0.001	0.12 ± 0.11	0.08 ± 0.18
Reticulum Cells	0.48 ± 0.30	0.94 ± 0.87	0.24 ± 0.22	0.2 ± 0.14
Mature Myeloid	23.56 ± 5.12	21.56 ± 3.35	21.04 ± 1.72	28.72 ± 1.97
Immature Myeloid	9.72 ± 2.93	11.16 ± 1.75	8.36 ± 1.15	13.24 ± 1.37
Eosinophils	1.96 ± 0.55	1.40 ± 0.91	2.24 ± 1.55	1.96 ± 1.96
Tissue Basophils	1.04 ± 1.05	0.28 ± 0.30	0.32 ± 0.22	0.16 ± 0.26
Mature Erythroid	25.2 ± 3.79	23.8 ± 4.91	27.92 ± 3.58	24.68 ± 4.63
Immature Erythroid	5.04 ± 1.49	6.96 ± 1.35	8.24 ± 2.23	6.60 ± 2.29

TABLE B

CLONAL ASSAYS: MOSCOW
SUMMARY OF RESULTS
(Average # of Colonies)

CFU-E Group	EPO Dose mU/ML	Mean / S.D.
Flight	0	3.48 ± .71
Flight	250	199.2 ± 134.44
Flight	500	225.6 ± 128.55
Flight	1.0	202.4 ± 147.73
Tail	0	8.24 ± 13.39
Tail	250	270.38 ± 73.19
Tail	500	318.8 ± 66.39
Tail	1.0	376.8 ± 81.39
Synchronous	0	9.36 ± 6.99
Synchronous	250	222.94 ± 74.12
Synchronous	500	242.94 ± 77.79
Synchronous	1.0	255.74 ± 64.522
Vivarium	0	15.6 ± 20.27
Vivarium	250	217.6 ± 25.04
Vivarium	500	224.0 ± 52.78
Vivarium	1.0	285.6 ± 37.32

BFU-E Group	EPO Dose mU/ML	Mean / S.D.
Flight	0	6.83 ± 7.05
Flight	250	22.23 ± 17.34
Flight	500	17.78 ± 12.64
Flight	1.0	17.03 ± 9.39
Tail	0	5.34 ± 2.10
Tail	250	20.0 ± 4.21
Tail	500	26.4 ± 5.73
Tail	1.0	28.54 ± 16.27
Synchronous	0	17.34 ± 4.42
Synchronous	250	54.12 ± 12.26
Synchronous	500	48.0 ± 6.88
Synchronous	1.0	42.56 ± 10.54
Vivarium	0	12.00 ± 1.41
Vivarium	250	29.20 ± 7.43
Vivarium	500	31.6 ± 7.40
Vivarium	1.0	37.6 ± 8.05

TABLE C

CLONAL ASSAYS: KNOXVILLE
SUMMARY OF RESULTS
(Average # of Colonies)

CFU-E Group	EPO Dose mU/ML	Mean / S.D.
Flight	0	43.0 ± 33.84
Flight	250	69.0 ± 70.00
Flight	500	60.0 ± 44.9
Flight	1.0	89.0 ± 120.28
Tail	0	1.67 ± 3.17
Tail	250	8.33 ± 6.57
Tail	500	11.2 ± 6.79
Tail	1.0	9.71 ± 6.60
Synchronous	0	2.57 ± 3.72
Synchronous	250	13.33 ± 4.94
Synchronous	500	17.06 ± 8.75
Synchronous	1.0	16.8 ± 9.82
Vivarium	0	5.33 ± 6.63
Vivarium	250	21.33 ± 10.44
Vivarium	500	17.6 ± 12.26
Vivarium	1.0	16.53 ± 11.79

BFU-E Group	EPO Dose mU/ML	Mean / S.D.
Flight	0	7.00 ± 6.83
Flight	250	6.53 ± 2.88
Flight	500	25.0 ± 23.86
Flight	1.0	27.0 ± 33.68
Tail	0	1.33 ± 1.97
Tail	250	10.93 ± 5.75
Tail	500	6.53 ± 2.87
Tail	1.0	8.67 ± 3.97
Synchronous	0	3.60 ± 1.72
Synchronous	250	14.40 ± 6.33
Synchronous	500	14.0 ± 6.14
Synchronous	1.0	12.4 ± 5.41
Vivarium	0	6.44 ± 6.15
Vivarium	250	16.13 ± 5.78
Vivarium	500	17.87 ± 7.54
Vivarium	1.0	16.0 ± 4.78

TABLE D

ERYTHROPOIETIN
SUMMARY OF RESULTS

Group	Mean/S.D. mU/ML	N
Flight	26.54 ± 0.77	5
Tail	33.16 ± 2.49	5
Synchronous	27.12 ± 1.78	5
Vivarium	39.68 ± 1.05	5
Basal	23.94 ± 3.04	5

TABLE E

SUMMARY OF DIFFERENCES OF
NON-PARAMETRIC P-VALUES

If $p \leq .05$, a difference is noted with italics

1. Bone Marrow Cell Differentials

Group	vs.	Group	Criteria	p value
Tail		Synch	Sm. Lymph	0.249
			Lg. Lymph	0.749
			Plasma	0.270
			Retic	0.135
			Mat. Myel	0.917
			Imm. Myel	0.073
			Eos	0.296
			Tiss. Baso	0.914
			Mat. Eryth.	0.296
			Imm. Eryth.	0.249
Tail		Flight	Sm. Lymph.	0.095
			Lg. Lymph.	0.248
			Plasma	0.473
			Retic	1.0
			Mat. Myel	0.210
			Imm. Myel	*0.012*
			Eos.	0.753
			Tiss. Baso.	0.327
			Mat. Eryth.	0.210
			Imm. Eryth.	0.600
Synch		Flight	*Sm. Lymph*	*0.037*
			Lg. Lymph	0.398
			Plasma	1.0
			Mat. Myel	0.296
			Imm. Myel	0.059
			Eos.	1.0
			Tiss. Baso	0.571
			Mat. Eryth.	0.835
			Imm. Eryth.	1.0

2. Clonal Studies Using 0 & 250 mU/ml Erythropoietin.

a. Studies performed in Moscow.

Flight	Synchronous	CFU-E 0	0.156
Tail	Flight	CFU-E 0	0.667
Tail	Synch	CFU-E 0	0.290
Flight	Synchronous	CFU-E 250	0.403
Flight	Tail	CFU-E 250	0.403
Tail	Synch	CFU-E 250	0.296
Flight	Tail	BFU-F 0	0.709
Tail	*Synchronous*	*BFU-E 0*	*0.012*
Flight	Synchronous	BFU-E 0	0.084
Flight	Tail	BFU-E 250	0.902
Tail	*Synchronous*	*BFU-E 250*	*0.012*
Flight	*Synchronous*	*BFU-E 250*	*0.037*

b. Repeat studies performed in Knoxville.

Flight	Tail	BFU-E 0 RPT	0.079
Tail	*Synch*	*BFU-E 0 RPT*	*0.003*
Synch	Flight	BFU-E 0 RPT	0.369
Flight	Tail	BFU-E 250 RPT	0.959
Tail	Synch	BFU-E 250 RPT	0.095
Synch	Flight	BFU-E 250 RPT	0.686
Flight	*Tail*	*CFU-E 0 RPT*	*0.003*
Flight	*Synch*	*CFU-E 0 RPT*	*0.004*
Synch	Tail	CFU-E 0 RPT	0.446
Flight	*Tail*	*CFU-E 250 RPT*	*0.022*
Flight	Synch	CFU-E 250 RPT	0.091
Tail	*Synch*	*CFU-E 250 RPT*	*0.034*

3. Erythropoietin Assays

Group	vs.	Group	Criteria	p value
Flight		Synch	Epo	1.0
Flight		Tail	*Epo*	*0.011*
Synch		Tail	*Epo*	*0.012*

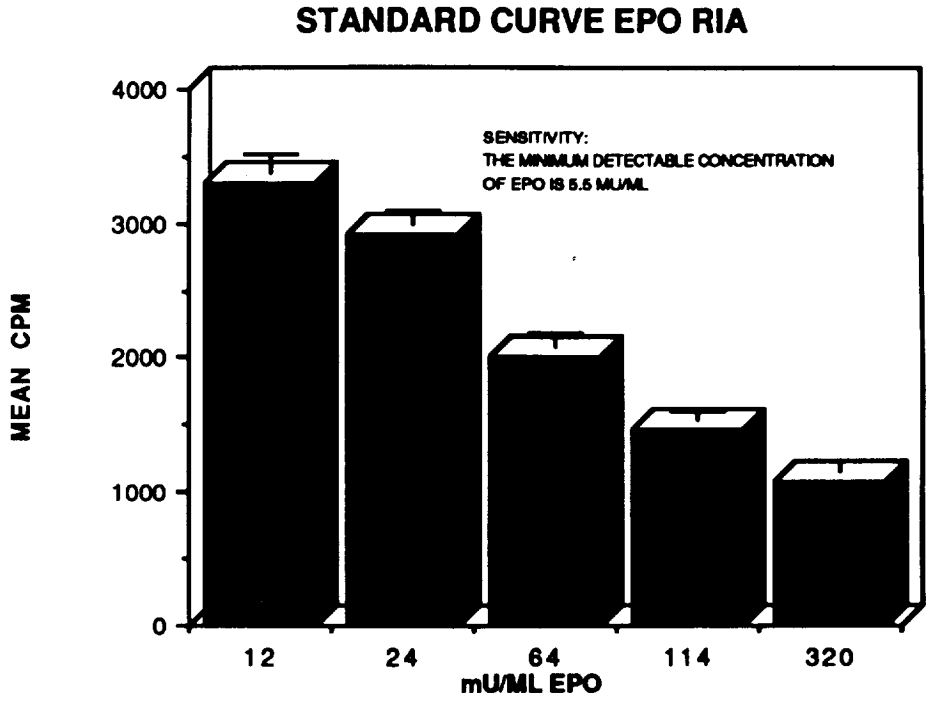

Figure 1. A standard curve of the erythropoietin (EPO) radioimmunoassay. The curve was generated by pre-prepared standard controls provided with the kit. Error bars represent standard deviation.

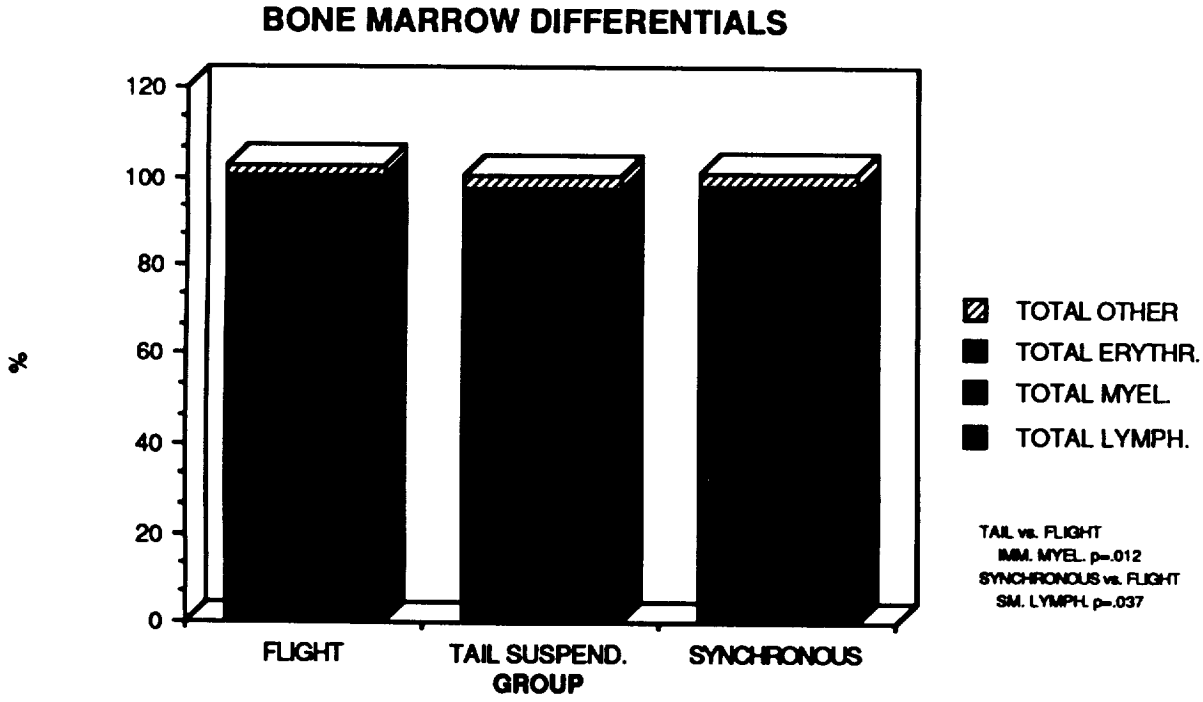

Figure 2. Bone marrow cell differential percentages for flight, tail suspended, and synchronous control rats.

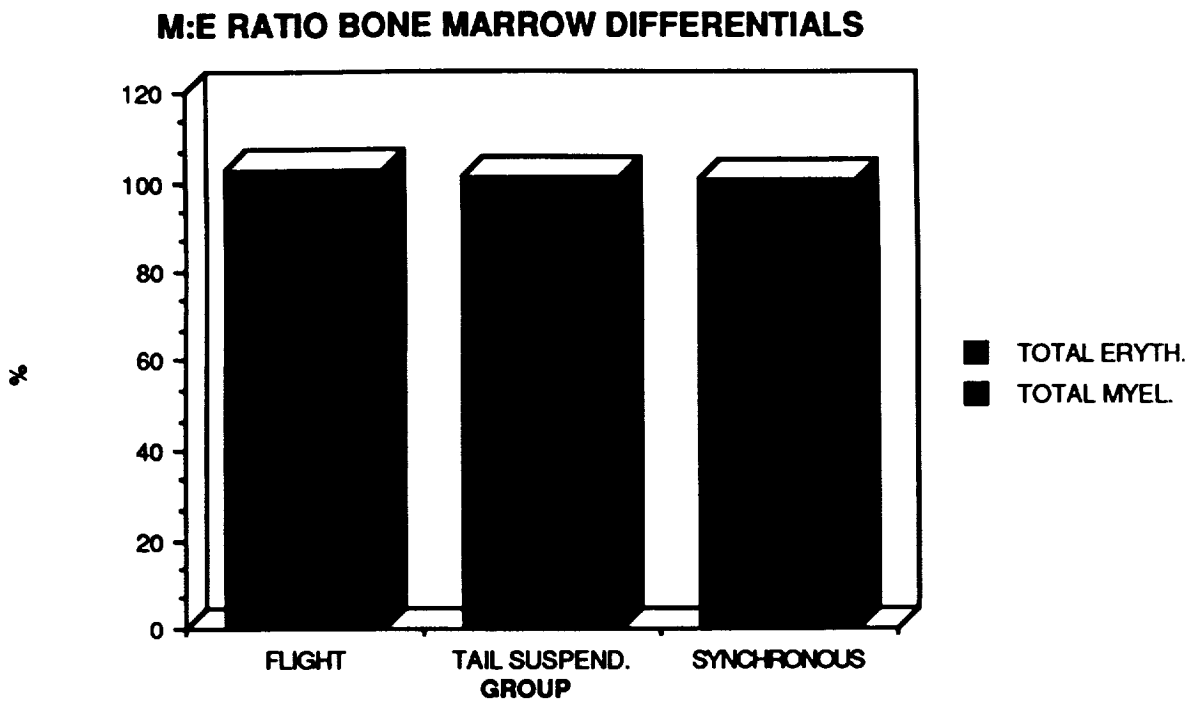

Figure 3. Bone marrow myeloid to erythroid ratios for flight, tail suspended, and synchronous control rats.

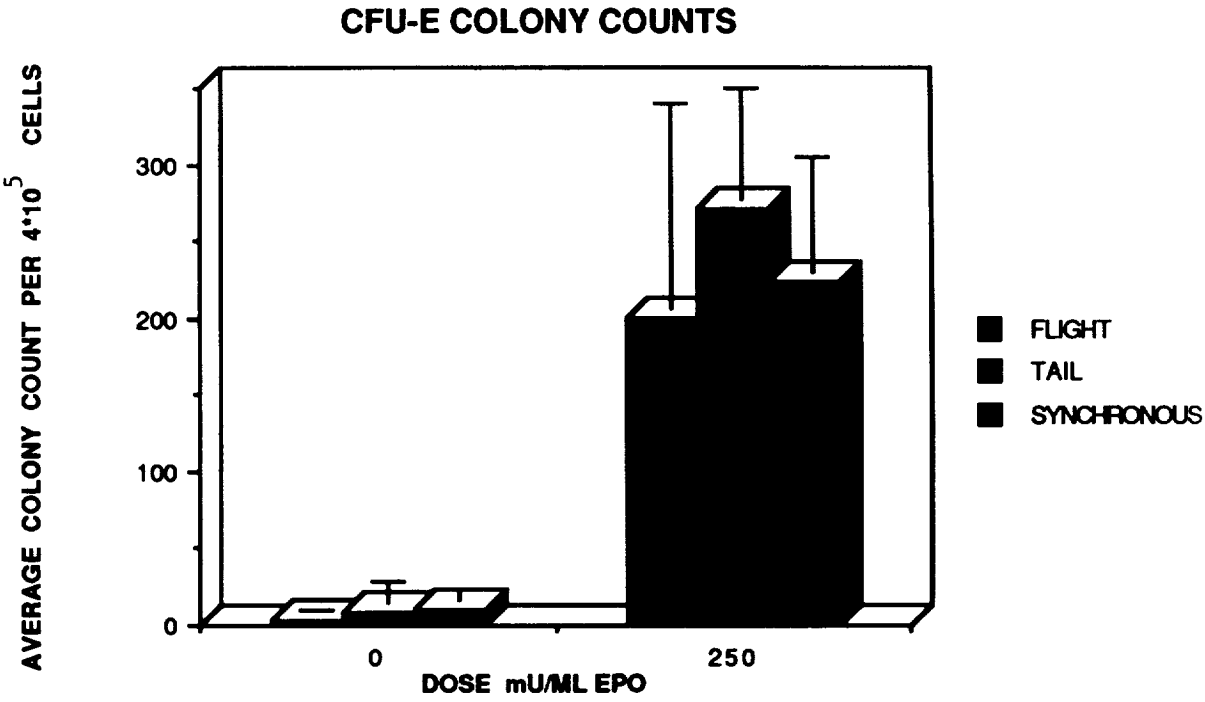

Figure 4. Colony forming unit—erythroid in bone marrow cells cultured in Moscow. Erythropoietin dose in mU/ml given on horizontal axis. Standard deviation represented by error bars in this and the following 3 figures.

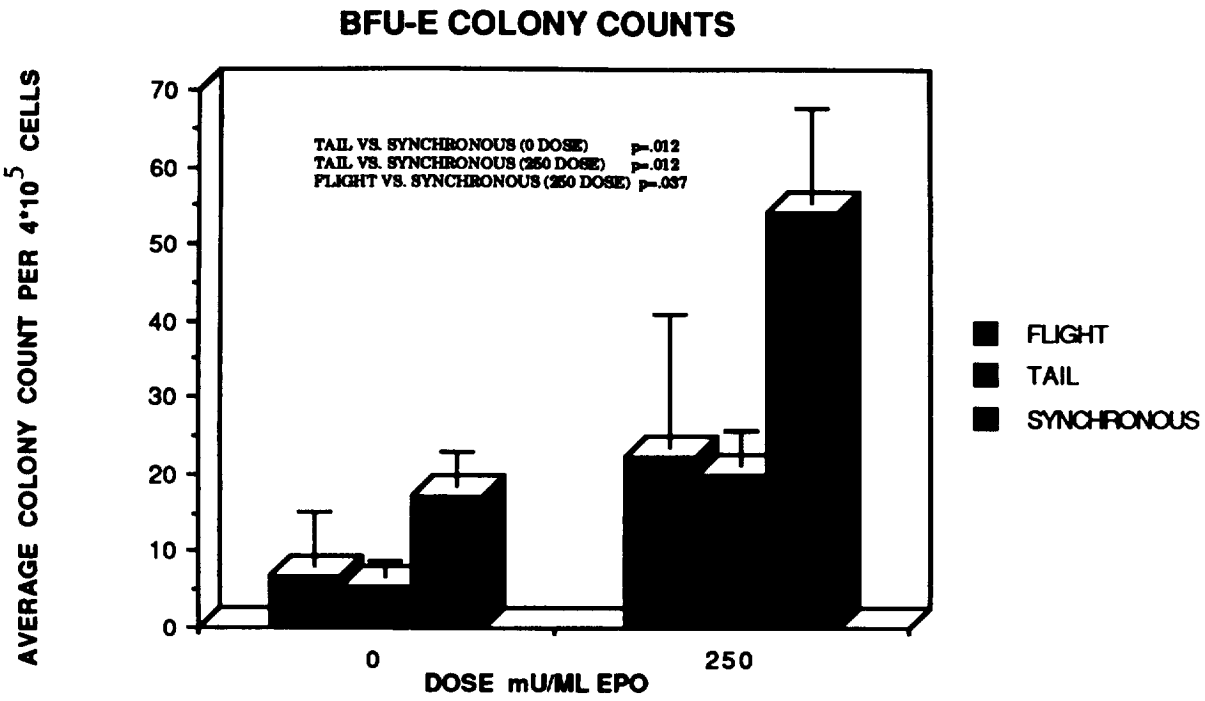

Figure 5. Burst forming unit—erythroid colonies in bone marrow cells cultured in Moscow.

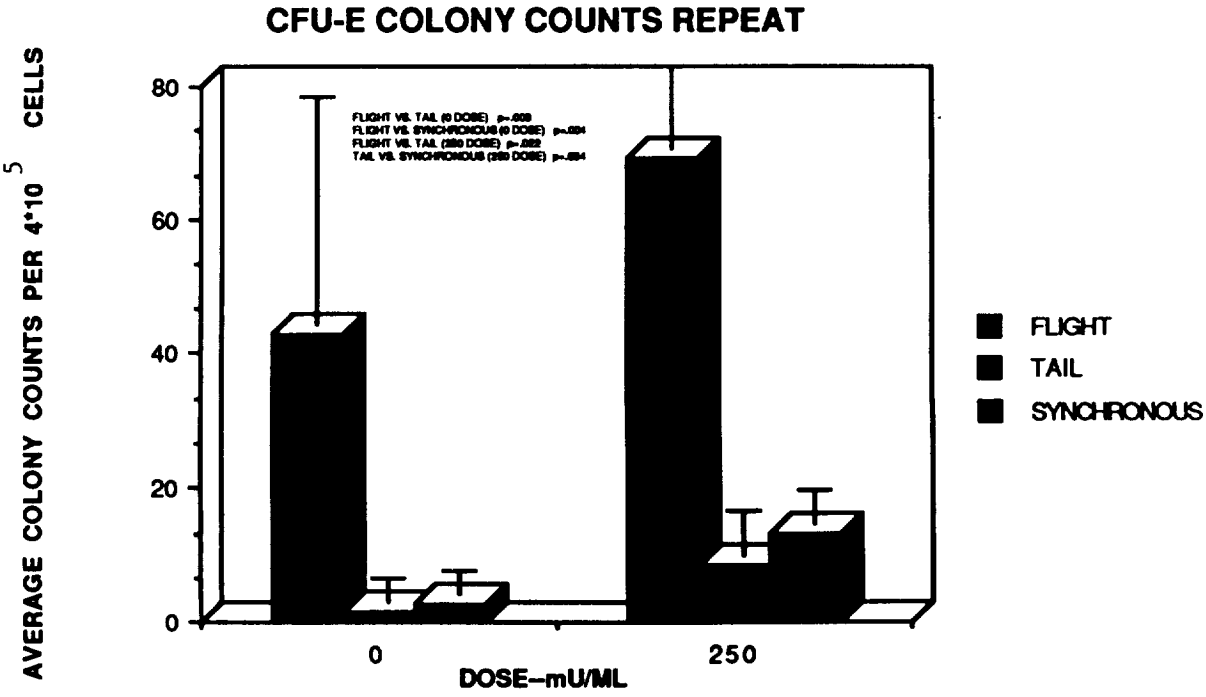

Figure 6. Repeat colony forming unit—erythroid culture results performed in Knoxville laboratory on frozen bone marrow cells.

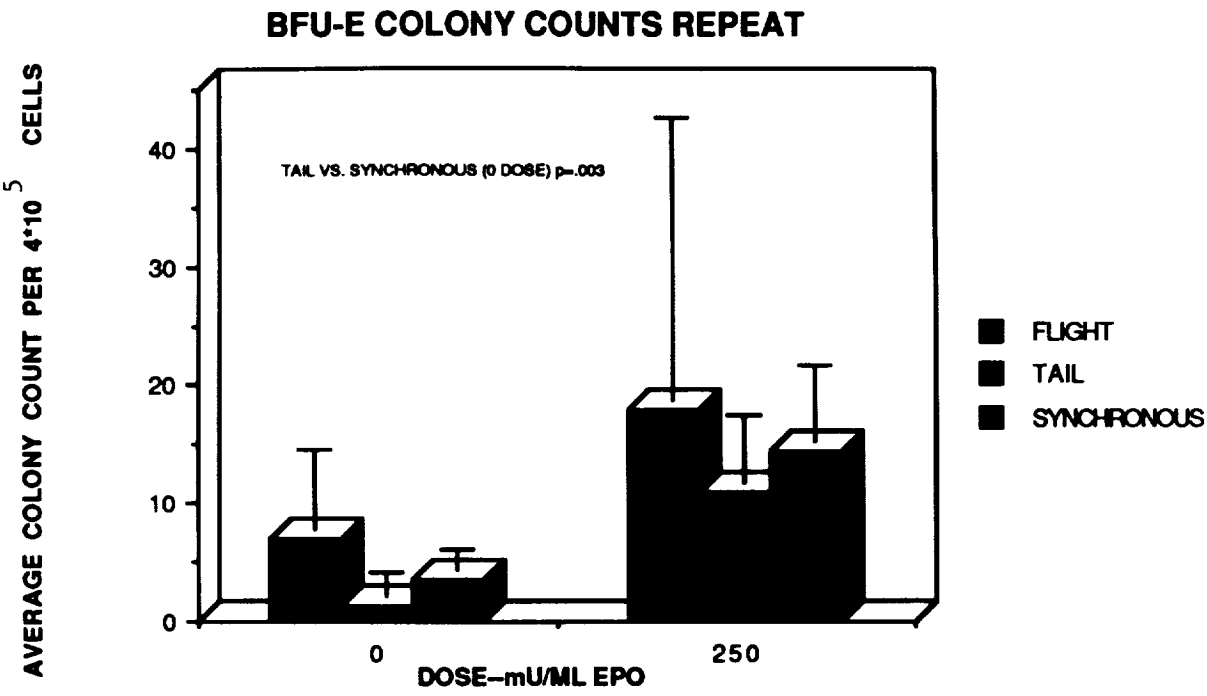

Figure 7. Repeat burst forming unit—erythroid culture results performed in knoxville laboratory on frozen bone marrow cells.

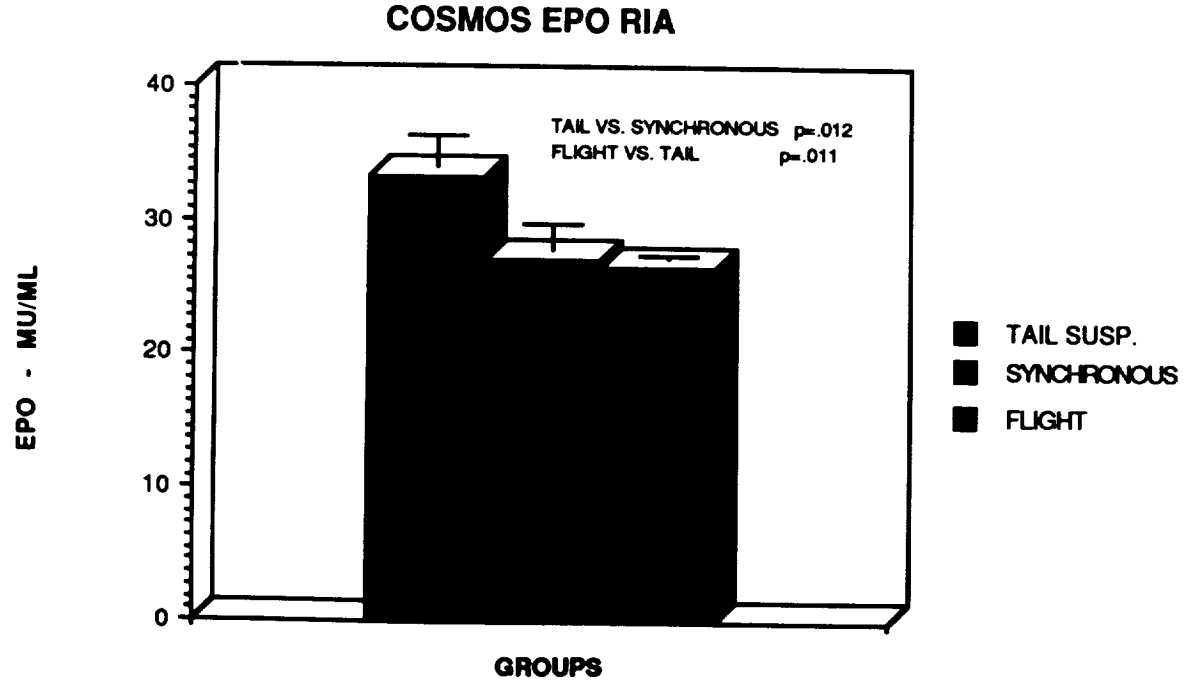

Figure 8. Radioimmunoassay erythropoietin determinations on plasma from flight, tail suspended, and synchronous control rats.

Technical Memorandum 108802 consists of two volumes.

Volume I contains:

- The Mission Description
- U.S. Flight and Ground-Support Hardware
- Rat Studies, Science Reports K-7-01 through K-7-15. (Rat Studies are continued in Volume II).

Volume II contains:

- Rat Studies, Science Reports K-7-16 through K-7-29
- A Comparison of The Physiology of the Spaceflight and the Suspended Rat
- Primate Studies, Science Reports K-7-30 through K-7-35
- Radiation Studies, Science Report K-7-41

C 16

REPORT DOCUMENTATION PAGE

Form Approved
OMB No. 0704-0188

1. AGENCY USE ONLY *(Leave blank)*	2. REPORT DATE	3. REPORT TYPE AND DATES COVERED
	September 1994	Technical Memorandum

4. TITLE AND SUBTITLE
Final Reports of the U.S. Experiments Flown on the Soviet Biosatellite Cosmos 2044 *Volume I: Mission Description, Experiments K-7-01–K-7-15*

5. FUNDING NUMBERS
199-08-12

6. AUTHOR(S)
James P. Connolly, Richard E. Grindeland, and Rodney W. Ballard, Eds.

7. PERFORMING ORGANIZATION NAME(S) AND ADDRESS(ES)
Ames Research Center
Moffett Field, CA 94035-1000

8. PERFORMING ORGANIZATION REPORT NUMBER
A-94031

9. SPONSORING/MONITORING AGENCY NAME(S) AND ADDRESS(ES)
National Aeronautics and Space Administration
Washington, DC 20546-0001

10. SPONSORING/MONITORING AGENCY REPORT NUMBER
NASA TM-108802

11. SUPPLEMENTARY NOTES
Point of Contact: James P. Connolly, Ames Research Center, MS 200-1, Moffett Field, CA 94035-1000; (415) 604-6483
Note: Technical Memorandum 108802 consists of 2 volumes.

12a. DISTRIBUTION/AVAILABILITY STATEMENT
Unclassified — Unlimited
Subject Category 55

12b. DISTRIBUTION CODE

13. ABSTRACT ***(Maximum 200 words)***

Cosmos 2044 was launched on September 15, 1989, containing radiation dosimetry experiments and a biological payload including two young male rhesus monkeys, ten adult male Wistar rats, insects, amphibians, protozoa, cell cultures, worms, plants and fish. The biosatellite was launched from the Plesetsk Cosmodrome in the Soviet Union for a mission duration of 14 days, as planned. The major research objectives were: 1). Study adaptive response mechanisms of mammals during flight; 2). Study physiological mechanisms underlying vestibular, motor system and brain function in primates during early and later adaptation phases; 3). Study the tissue regeneration processes of mammals; 4). Study the development of single-celled organisms, cell cultures and embryos in microgravity; 5). Study radiation characteristics during the mission and investigate doses, fluxes and spectra of cosmic radiation for various types of shielding. American and Soviet specialists jointly conducted 29 experiments on this mission including extensive preflight and postflight studies with rhesus monkeys, and tissue processing and cell culturing postflight. Biosamples and data were subsequently transferred to the United States. The U.S. responsibilities for this flight included development of flight and ground-based hardware, the preparation of rat tissue sample procedures, the verification testing of hardware and experiment procedures, and the postflight analysis of biospecimens and data for the joint experiments. The U.S. investigations included four primate experiments, 24 rat experiments, and one radiation dosimetry experiment. Three scientists investigated tissue repair during flight for a subgroup of rats injured preflight by surgical intervention. A description of the Cosmos 2044 mission is presented in this report including preflight, on-orbit and postflight activities. The flight and ground-based bioinstrumentation which was developed by the U.S. and U.S.S.R. is also described, along with the associated preflight testing of the U.S. hardware.

14. SUBJECT TERMS	15. NUMBER OF PAGES
Cosmos, Biosatellite	529
	16. PRICE CODE: A23

17. SECURITY CLASSIFICATION OF REPORT	18. SECURITY CLASSIFICATION OF THIS PAGE	19. SECURITY CLASSIFICATION OF ABSTRACT	20. LIMITATION OF ABSTRACT
Unclassified	Unclassified		